Development of a non-invasive electrophysiological system for measuring the auditory capability of marine animals

by

Jonathan Murray Lovell

A thesis submitted to the University of Plymouth
in partial fulfilment for the degree of

DOCTOR OF PHILOSOPHY

School of Earth Ocean and Environmental Sciences
Faculty of Science

September 2005

Development of a non-invasive electrophysiological system for measuring the auditory capability of marine animals

Jonathan Murray Lovell

Abstract

The following work describes the development and application of a neurological system to definitively profile the auditory responses of aquatic animals, presented as audiograms showing hearing threshold verses sound frequency. The accuracy of such information is essential for the optimisation of bio-technical devices such as the Acoustic Fish Deterrent (AFD) barrier deployed in the Illinois River to prevent the migration of non-indigenous Asian carp into Lake Michigan, and in the impact assessment of anthropogenic underwater sounds on the hearing of cetaceans and other marine animals.

The ensuing Auditory Brainstem Response (ABR) electrophysiological recording technique developed at the University of Plymouth and described in this thesis is classified by the UK Home Office as being non-invasive, yielding high quality data from vertebrates in the absence of anaesthetics or implanted electrodes. The ABR technique was further refined to allow for the recording of evoked potentials in response to either the sound pressure or particle motion component of an acoustic signal, from animals stationed both at and below the water surface and ranging in size from a few millimetres to nearly a meter in length. The electrophysiological studies have resulted in the publication of three peer reviewed manuscripts, one of which is the first to define hearing for any animal from the order Acipenseriform (sturgeons and paddlefish).

In addition to the development of the electrophysiology system and protocols, the inner ear morphology of the animals tested in this work were studied at the ultrastructural level, along with detailed descriptions of the afferent nerve pathway from the ear to the brain. Current literature shows a paucity of information on consistent and meticulous removal of inner ear parts necessary to identify damage to the ultrastructure that is symptomatic of hearing loss. In order for the acquisition of concise and reliable data, the dissection and preparation technique for Scanning Electron Microscopy (SEM) was refined for each species investigated and has resulted in the publication of a further three peer reviewed manuscripts on inner ear morphology.

Acknowledgments

Much gratitude is extended to Dr Roy Moate and Ron Hill of the (School of Earth Ocean and Environmental Sciences) for their invaluable advice, comment and practical support during many hours of kind and patient assistance, and to Glen Harper and David Bond for their tireless help in the preparation of electron microscopy samples.

Grateful thanks are also due to Dr Mark Pegg and Kevin Irons of the Illinois River Biological Station for their hospitality and help in the acquisition and maintenance of the fish studied in this work; and to Dr Jeremy Nedwell of Subacoustech Ltd for the provision of equipment and technical support. Similarly, my thanks go to Professor Jens Balchen of the Norwegian University of Science and Technology for practical advice in biotechnology and control theory.

Finally, the author owes a great debt to Dr Derek Pilgrim and to Dr Malcolm Findlay, the author's director of studies, whose insight, guidance and encouragement are inestimably responsible for the completion of this work.

Table of Contents

Chapter 4

The hearing abilities of bony generalist fish

Chapter 5

The hearing abilities of cartilaginous generalist fish

Chapter 6

The hearing abilities of crustaceans

Chapter 7

Examination of the cetacean inner ear

Chapter 8

General discussion

List of abbreviations and units

ABR ..... Auditory Brainstem Response

BAFF ..... Bio-Acoustic Fish Fence

EP ..... Evoked Potential

LFA sonar ..... Low Frequency Active sonar

SEM ..... Scanning Electron Microscope

TEM ..... Transmission Electron Microscope

P ..... Absolute pressure in Pascal (Pa)

s ..... Unit of time (seconds)

ms..... Unit of time (milliseconds)

dB ..... Unit of sound pressure (decibels)

dB (re. 1 μPa) ..... Unit of sound pressure (referenced to 1 micro Pascal)

kg ..... Unit of weight (kilograms)

g ..... Unit of weight (grams)

m ..... Unit of length (metre)

mm ..... Unit of length (millimetre)

μm ..... Unit of length (micrometer)

μv ..... Unit of voltage (microvolt)

cc ..... Unit of volume (cubic centimetres)

rho ..... Density of a fluid (kg/m^3)

g ..... Acceleration of gravity (m/s^2)

h ..... Height of fluid above an object (metre)

K ..... Constant

NB: All measurements in this thesis are in metric units

Author's declaration

At no time during the registration for the degree of Doctor of Philosophy has the author been registered for any other University award without prior agreement of the Graduate Committee.

A programme of advanced study financed by ARIA Marine ltd was undertaken, resulting in the development of a system for measuring hearing ability, with application in monitoring the effect of anthropogenic noise pollution in the marine environment.

Relevant scientific seminars and conferences were regularly attended which included a visit to the Norwegian University of Science and Technology, where a presentation was delivered to both undergraduate and postgraduate researchers in the marine biotechnology field. work was often presented; external institutions were visited for consultation purposes and four papers have been published from the body of this work, with a further two currently in review.

External contacts

- Dr. Michel André Laboratori d'Aplicacions Bioacústiques Universitat Politècnica de Catalunya (UPC) Centre Tecnològic de Vilanova i la Geltrú Avda. Rambla Exposició, s/n 08800 Vilanova i la Geltrú Barcelona, Espanya
- Jens G. Balchen Professor Emeritus Institutt for teknisk kybernetikk (Department of Engineering Cybernetics) Norges teknisk-naturvitenskapelige universitet (Norwegian University of Science and Technology) 7491 Trondheim, Norway
- Dr Eulalia Bohigas, Marine Mammal Curator Zoological Park of Barcelona, SA Parc de la Ciutadella, s/n - 08003 Barcelona, Espanya
- Department of fisheries Ghana University
- Dr Paul Jepson. Institute of Zoology, Zoological Society of London, Regents Park, London NW1 4RY
- Dr Jeremy Nedwell. Subacoustech Ltd, Bishops Waltham, Hampshire, UK
- Dr Mark Pegg. Illinois River Biological Station and Forbes Biological Station Illinois Natural History Survey 704 North Schrader Havana, Illinois 62644
- Dr Richard Sabin. Department of Zoology, The Natural History Museum, Cromwell Road, South Kensington, London SW7 5BD
- Dr Hong Yan. Research Station, Institute of Zoology, Academia Sinica, Jiashi, I-Lan 262, Taiwan

Word count of main body of thesis: 45,505

Signed .....

Date 14.2.2006

x

Chapter 1

General introduction

1.1 Introduction

The oceans are virtually transparent to sound and opaque to light and radio waves. At a wavelength of 1 m (1,500 Hz) water is nearly 1,000,000 times more transparent to sound than to radio signals (Pilgrim and Lovell, 2002). This fact underlies the interest currently directed toward acoustical exploration of the oceans. Naturally produced sounds arise from a number of sources, such as breaking waves, heavy rain, volcanic activity, or from marine animals (bio-acoustic sources). Vocalisations such as whale song, along with the grunts and whistles from sonic fish are especially relevant for communication purposes and during predator prey interactions (Myrberg, 1981). There are several types of anthropogenic sources used routinely that produce intense levels of noise, from commercial shipping and powered leisure craft, to deliberately produced signals such as the Low Frequency Active Sonar (LFA) used by the military in anti-submarine warfare, or from the airgun arrays used during a seismic survey of the substrate beneath the seafloor by the petroleum industry. These activities can generate noise levels in excess of 253 dB (re 1 μPa at 1 m) (Engås et al., 1996), and are comparable to the noise levels generated by a seafloor volcanic eruption, which can produce a source level of in excess of 255 dB (re 1 μPa) (Northrop, 1974).

Recent concerns regarding the impact of anthropogenic sounds on fish and other marine animals has prompted a number of studies into the effects of intense noise exposure on the hearing systems of marine mammals (e.g., Costa et al., 2003; Ketten, 1995; Richardson et al., 1995; Todd et al., 1996; Whitlow et al., 1997). Trauma to the auditory system can result in lesions developing along the VIII nerve pathway, or ruptures in the blood vessels surrounding the inner ear (Ketten, 1995). A number of techniques have been developed to investigate gross physiological damage, though despite speculation, concise evidence of inner ear hair cell damage in odontocetiforms exposed to loud noise has yet to be presented. Additionally, several studies of the behaviour of free living fish when exposed

to intense noise have been conducted (e.g. Dalen and Knutsen, 1987; Engås et al., 1996; Pearson et al., 1992; Pickett et al., 1994), and includes the examination of log books from fishing vessels showing a decline in catch rates, when operating within 5 km of a concurrent seismic survey (Lokkeborg and Soldal, 1993).

1.2 The audiogram

Hearing thresholds from any animal possessing the appropriate receptor mechanism are illustrated in an audiogram (Myerberg, 1981), which presents the lowest level of sound that a species can hear as a function of frequency. Both the sensitivity of hearing and the frequency range over which sound can be heard varies greatly from species to species. For man, sound is ultrasonic above 18 to 20 kHz, whilst for many fish species, sounds above 1 kHz are ultrasonic and for a number of odontocetiforms, sounds above 150 kHz are ultrasonic. This diversity in hearing ability between organisms indicates the importance of being able to accurately define hearing thresholds, especially when evaluating the influence of intense underwater sounds on both the physiology and ecology of various marine animals. The intensity of a sound in air is not the same as the intensity in water, primarily because of differences in the way the two measurements are referenced (Urick, 1983). In air, the lowest sound pressure level audible to humans is around 20 micro Pascal, which, on the dB scale is termed 0 dB (re. 20 μPa). However, the sound pressure level in water is referenced to 1 micro Pascal (re.1 μPa); thus the factor for converting 0 dB (re. 20 μPa) in air, into dB water is 20 log (p_{water}/1 μPa) = 20 log (20) = 26 dB (re.1 μPa). The characteristic impedance of water is about 3600 times greater than that of air, thus an equivalent sound intensity between air and water is 10 log (3600) = + 36 dB. By adding together the converted reference intensity (26 dB) with the impedance matching factor (36 dB), an intensity of 0 dB (re. 20 μPa) in air becomes 62 dB (re. 1 μPa) in water.

To pursue an accurate diagnosis of raised hearing thresholds as a result of exposure to intense noise, the audiogram for a normally hearing animal must first be established. Until recently, very little has been documented regarding the hearing abilities of marine animals, with a number of authors purporting that fish and invertebrates are responsive only to strong vibrations and near field disturbances (e.g. Cohen and Dijkgraaf 1961; Larsel, 1967; Wever, 1976). This however is contrary to the findings of Parker (1903) and von Frisch (1938) on fish species, and Lovell et al. (2005a) on the hearing abilities of crustaceans. The hearing frequencies or audiograms for a number of odontocetiformes are well characterised and have been produced using both physiological and behavioural

approaches (see Nachtigall et al., 1995; Kastelein, et al., 2003; Sauerland and Dehnhardt, 1998; Gerstein et al., 1999; Kastelein et al., 2002), though an audiogram for the common dolphin (*D. delphis*) has yet to be produced. The bottlenose dolphin (*T. truncates*) hears frequencies from 100 Hz to 150 kHz (Johnson, 1966; 1967), and the striped dolphin (*Stenella coeruleoalba*) hears frequencies ranging from around 500 Hz to 150 kHz (Kastelein, 2003; Brill et al., 2001), with both producing broadband clicks for echolocation that range in frequency from 20 Hz to around 200 kHz. *P. phocoena* hears frequencies between 300 Hz (Kastelein et al., 2002), up to as high as 190 kHz (Bibikov, 1992; Popov, 1986; Kastelein et al., 2002), and utilises a narrow band high frequency sonar of around 120 to 140 kHz (Busnel and Dziedzic, 1966a). It is feasible that this difference in hearing ability between *T. truncates* and *P. phocoena* is explained by the larger cochlea in the former (Wever et al., 1971; Ketten, 1997). Physiological evidence suggests that the audiogram for *D. delphis* may lie somewhere between the hearing range of *T. truncates* and *P. phocoena*. Therefore, the delineation of hearing ability is of considerable importance as part of an accurate assessment of the impact of anthropogenic sounds on the inner ear physiology of *D. delphis*.

The techniques used to obtain audiograms may require varying degrees of time, surgical and technical expertise, or the use of behavioural paradigms to gain statistically sound data (see Chapter 2 for review of current audiogram production methods). Most of the audiograms for marine animals use units of dB (re. 1 μPa) or dB (re. 1 μBar) to show the lowest Sound Pressure Level (SPL), of the audible frequencies. Figure 1.1 presents published audiograms for both specialist and generalist fish, and shows that they fall into two distinct groups, those that hear a narrow frequency bandwidth (up to 500 or so Hz) known as hearing generalists (closed data points), and those that hear a wide frequency bandwidth (up to 4000 Hz), known as hearing specialists (open data points).

Physiological work on the octavolateralis system shows that some fish can acquire information from a sound source using two systems, the inner ear and the lateral line (Parker, 1909; Popper and Platt, 1993), though sensitivity to sound pressure requires an additional connection between the ear and swim bladder or other air reservoir (Popper and Fay, 1993; Yan et al., 2000). For most fish, the lower frequency range between 10 and 300 Hz is perceptible through the lateral line mechanoreceptors up to a meter or so from the sound source, (Munz, 1989; Popper and Fay, 1993; Coombs and Montgomery, 1999). The limited effective range of a near field signal intended to stimulate the lateral line renders it impracticable for use in large scale acoustic recall projects, though this does not preclude

its use in the design of non physical barriers and acoustic fences (Balchen, 1981). The fish inner ear is capable of detecting sounds within a frequency bandwidth of 30 Hz to around 600 Hz for generalists (Fay, 1988) and up to 4 kHz for pressure sensitive specialists (Hawkins, 1981). The results of a hearing examination are graphed to produce an audiogram or lumen of spectral sensitivity to sound, which graphically illustrates the animal's ability to hear sounds over a range of frequencies and intensities.

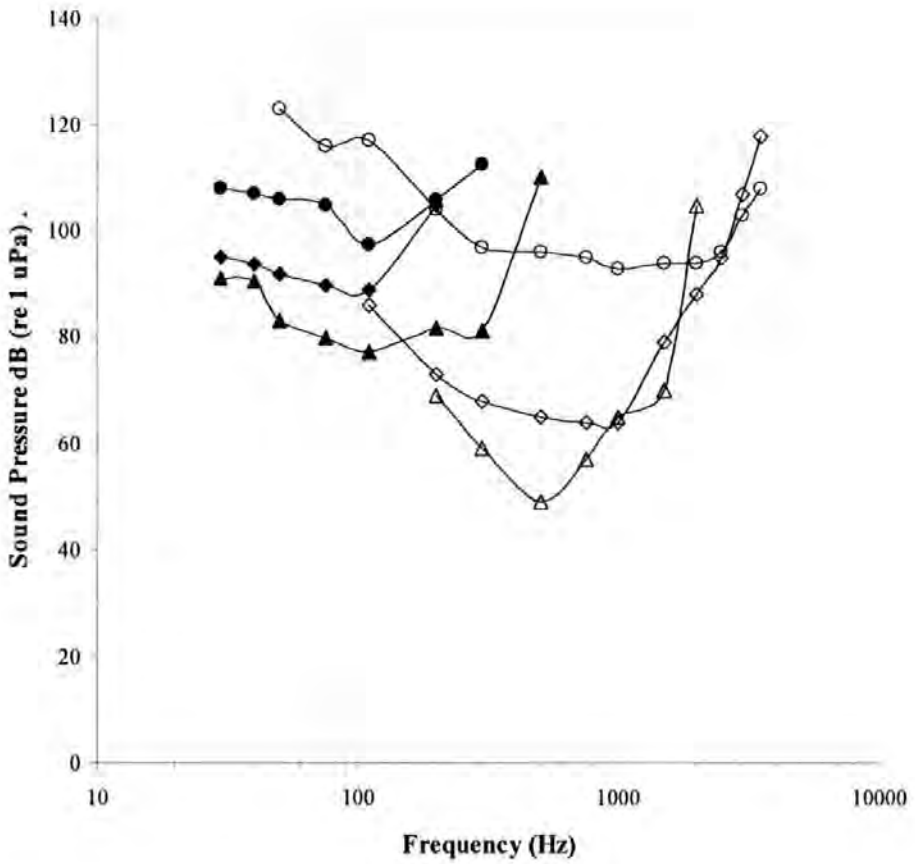

Figure 1.1 Audiograms for a selection of specialist and generalist fish, obtained using different methodologies. Catfish (*I. punctatus*), microphonics (Fay and Popper, 1975) open circles; goldfish (*C. auratus*), ABR (Kenyon et al., 1998) open diamonds; *C. auratus*, behavioural (Yan and Popper, 1971) open triangles; salmon (*S. salar*), behavioural (Hawkins and Johnstone, 1978) closed circles; dab (*L. limanda*), behavioural (Chapman and Sand, 1974) closed diamonds; cod (*G. morhua*), behavioural (Chapman and Hawkins, 1974) closed triangles

The narrow frequency detection capabilities of the hearing generalists is most noticeable when compared to the auditory thresholds of fish with a mechanical connection between the inner ear and swim bladder, such as goldfish (*Carrassius auratus*) and catfish

(*Ictalurus punctatus*). Figure 1.1 shows that thresholds are acquired from *C. auratus* in response to frequencies ranging between 40 Hz to 3000 Hz and from 40 Hz to 4000 Hz for *I. punctatus*. In contrast, the audio capabilities of the generalist fish diminish at around 500 Hz, so they are collectively considered as being sensitive to low frequencies only. An inspection of the audiograms in Figure 1.1 shows the hearing thresholds for *G. morhua*, *S. salar* and *L. limanda*, are positioned between the curves for the specialists *C. auratus* and *P. punctatus*. The Figure presents a considerable difference in the vertical position of the two specialist curves on the Y axis of the audiogram, as the lowest hearing thresholds recorded from *C. auratus* were 49 dB (re 1 μPa) at 500 Hz (Yan and Popper, 1992) and a concise audiogram for *P. punctatus* presents with a lowest threshold of 93 dB (re 1 μPa) at 1000 Hz (Fay and Popper, 1975). Theoretically, thresholds from *I. punctatus* should be considerably lower than thresholds from the generalist fish, though this is not the case in Figure 1.1, casting serious doubt as to the accuracy of the generalist audiograms presented in the Figure.

1.3 The Auditory Brainstem Response

The Auditory Brainstem Response (ABR) electrophysiology recording technique has been used successfully on all major classes of vertebrate (Corwin et al., 1982); a review of audiogram production methodologies is presented in Chapter 2. The non-invasive ABR recording system has been available for clinical use since the early 1970's, and has been used to great effect on non-cooperative subjects, such as children (Warren, 1989) and unconscious patients. The ABR technique developed at the University of Plymouth for this study is classified by the UK Home Office as being completely non-invasive, records far-field of synchronous neural activity in the eighth nerve and brainstem auditory nuclei elicited by acoustic stimuli (Jewett, 1970; Jewett and Williston, 1971; Jacobson, 1985; Kenyon et al., 1998).

The underwater sound projectors, differential (biological) amplifier and stimulus amplifier used in the experiments described in the present study, were obtained from commercial sources. The recording of threshold Auditory Evoked Potentials (AEPs) from fish and crustaceans is usually achieved by placing the subject, electrodes and preamplifier inside a Faraday cage (e.g. Kenyon et al., 1998). However, this precludes the use of the system outside of the laboratory, as the electrodes need to be screened against electrical interference from sources using mains voltage. Thus, the processing software and electrodes (detailed in Chapter 3) had to be developed specifically for this task; screening

would not be necessary on a beach, away from strong electromagnetic sources. Two electrophysiological recording systems were used to acquire the evoked potentials; the first was a Medelec MS 6 mainframe with an AA6 biological amplifier, used when recording under controlled laboratory conditions, and the second was an A-M Systems model 3000 differential amplifier used for recording both under laboratory conditions, and at the Illinois River Field Station. Adaptations in the setup of the specimen and electrode holding equipment is described in detail in the Materials and Methods section in each of the relevant chapters, along with descriptions of the sound projectors and the life support systems used.

1.4 Species selection

As discussed in section 1.2, the hearing abilities of aquatic animals fall into two main groups, the hearing specialists and generalists. In order to fully test the ABR system, a positivist approach to species selection is adopted, this being considered best suited to exploring commonality in neurophysiological studies than the more phenomenological perspective typically gleaned from a single species study; nonetheless, the author is mindful of the excesses of both approaches. Initially, an audiogram for the goldfish (*Carrasius auratus*) from the order Cypriniformes is produced; as this species has been the subject of several audiological investigations (see Chapters 2 and 3). In order to ensure that the recording of evoked potentials is consistent with previously published ABR work on this species, the audiogram is calibrated in accordance with Kenyon et al. (1998). However, an audiogram for *C. auratus* has limited application in a "real world" scenario, thus the hearing abilities of silver carp (*Hypopthalmichthys molitrix*) and bighead carp (*Aristichthysc nobilis*) are also studied, with the findings used to improve the selectivity of an Acoustic Fish Deterrent (AFD) barrier intended to stop the spread of these species through the Illinois River into Lake Michigan. While preventing the spread of *H. molitrix* and *A. nobilis* is critical, it is also important that the AFD system does not affect indigenous species where possible and requires an "in depth" understanding of the hearing abilities of both the target and non-target species. The paddlefish (*Polyodon spathula*) and lake sturgeon (*Acipenser fulvescens*), both from the subclass Chondrostei, in the order Acipenseriformes have been selected as the non-target species, as these fish have a considerable value placed on them by both commercial and recreational fisheries in the geographic area. The morphology of the Acipenseriform inner ear was also studied, along with a Scanning Electron Microscope (SEM) examination of the ultrastructure in the saccule, lagena and utricle from both species.

The inner ear morphology and hearing abilities of the bass (*Dicentrarchus labrax*) is investigated in this study, as it offers an opportunity to test the ABR system on a hearing generalist fish in seawater (an electronically conductive medium). The value placed on this fish by both recreational and commercial fisheries (Pickett et al., 1995) is also a consideration, as commercial interest may make *D. labrax* a suitable candidate in a fish ranching scenario using acoustic recall (e.g. Balchen, 1999) and would require a full understanding of the auditory system in this species. The prawn (*Palaemon serratus*) Phylum Crustacea and Class Eumalacostraca is also tested, as there has been considerable debate as to whether marine invertebrates have the ability to hear sounds or not. This study presents the first audiogram from any animal in the entire phylum, and the acquisition of hearing data from this animal allows for the inclusion of the crustaceans when assessing the impact of anthropogenic sounds on the marine environment.

The inner ears from the common dolphin (*Delphinus delphis*) and the harbour porpoise (*Phocoena phocoena*) are also studied, in conjunction with a SEM examination of the inner ear ultrastructure in the mammalian cochlea and vestibule. In order to assess the dissection and fixation methodologies required for an SEM examination of the inner ear ultrastructure from a large mammal, 12 ears were removed from mature domestic pigs (*Sus scrofa*) during processing for the meat industry, within 1 hour of the animal's death. The use of *S. scrofa* was necessary, owing to the difficulty found when attempting to acquire fresh samples of the cetacean inner ear that had been fixed in the appropriate chemicals for an SEM type examination.

1.5 Significance of the work to bioacoustics and biotechnology

The work presented herein is of significance, given that concise morphological and physiological information on the hearing systems of marine animals is essential for the optimisation of bio-technical devices such as the Acoustic Fish Deterrent (AFD) barrier. Therefore, the intention of this study is to develop a system and protocol that will allow for the acquisition of audiological data from both fish and crustaceans, which can be used in a number of disciplines such as fish ranching (Balchen 1999; Alfredsen 2000), in the development of selective Acoustic Fish Deflection (AFD) barriers, or as a fundamental part of an acoustic impact assessment (Scholik and Yan, 2001, 2002a and 2002b).

It is imperative to investigate the morphology of the inner ear when studying the hearing system of an animal, being especially relevant where the animal is thought to have died as a consequence of intense noise exposure. As previously discussed, a number of techniques have been developed to investigate gross physiological damage, though this form of injury may have been sustained by the animal as it struggles in fishing nets or thrashes about on the shoreline. If caused by intense noise, these signs of trauma would probably manifest at the highest end of the impact scale, whereas more subtle damage to the ears may only show in the ultrastructure and thus be missed when using conventional examination methodologies. Current literature shows a paucity of information on consistent and meticulous removal of inner ear parts necessary to identify damage to the ultrastructure that is symptomatic of hearing loss. As part of this study, methodologies for removal of the inner ear were developed for fish, invertebrates and marine mammals.

The primary aim of this study is therefore to extend human knowledge in the field of audition in aquatic animals, and to develop procedures and technologies that can be applied to the accurate assessment of the impact of anthropogenic sounds on the hearing of cetaceans and other marine animals. In order to achieve this aim, the work is divided into a number of objectives, which includes the refinement of the ABR electrophysiology system and technique to allow for the recording of evoked potentials both above and below the water surface. A further refinement to the system is required to allow for the production of audiograms "in the field" whilst requiring no anaesthetics, as this may preclude the use of the system on animals in the natural environment. Owing to controversy regarding the accuracy of many published audiograms, it is essential that the audiograms produced for each species are both accurate and can be validated using standard neurophysiological indicators. In the case of when the animal is dead (e.g. after a stranding event), the ultrastructure of the inner ear may be the only indicator of hearing loss. In order for the acquisition of concise and reliable data, the dissection and SEM preparation technique needs to be refined for each species investigated, thus minimising potential artefacts prior to an SEM type examination of the ultrastructure in relation to hair cell loss.

Chapter 2

Review of Current Audiogram Production Methodologies

2.1 Introduction

The hearing thresholds of any organism possessing the appropriate receptor mechanism are illustrated in an audiogram (Myerberg, 1981), which presents the lowest level of sound that a species can hear as a function of frequency. Audiograms for marine animals are predominantly expressed in units of sound pressure, or dB (re. 1 μPa) and is the rationale for using them in this study. The techniques used to obtain fish audiograms may require a varying degree of time, surgical and technical expertise, or the use of behavioural paradigms to gain statistically sound data (see for instance, Yan, 1995). Behavioural methods require that fish are trained to react in a specified and measurable way (e.g. a reward based method by seeking food) when a tone at a given frequency is presented; however, in practice, the behavioural method is very time consuming and only effective with species that are easy to train. Conditioning can take up to 3 weeks (feeding 3-4 times per day) to get a stable association between stimulus, response and food reward (Fujiya, 1974; Hughes, 2001; Lovell, 1999 and Russon, 2002). The advantages of the operant (reward based) conditioning methodology is that invasive procedures are not required, and the stimulus equipment can be relatively simple, however, the feeding behaviour of the species under investigation needs to be suited to this type of experiment (Yan, 1995).

The measurement of microphonics from auditory end organs during acoustic stimulation is a technique favoured by a number of authors (e.g. Enger and Andersen, 1967; Fay and Popper, 1975; Fine, 1981). Although results can be obtained more rapidly than from

behavioural paradigms, preparation can often be complex and require invasive surgery to implant the electrodes directly into the nerve (c.f. Enger and Andersen, 1967). The electrode is thus restricted to a specific end organ or region of macula, and the evoked potential does not necessarily represent the whole auditory pathway (Kenyon et al., 1998).

The Auditory Brainstem Response (ABR) technique of measuring hearing thresholds has been successfully applied to both mammalian and non-mammalian vertebrates (Corwin, Bullock and Schweitzer, 1982), Elasmobranchs (Casper et al., 2003), and marine invertebrates (Lovell et al., 2005 a). The ABR is a non-invasive far-field recording of synchronous neural activity in the eighth nerve and brainstem auditory nuclei elicited by acoustic stimuli (Jewett, 1970; Jewett and Williston, 1971; Jacobson, 1985; Kenyon et al., 1998), and waveforms clearly present with similarities between fish and higher vertebrates (Corwin, 1981) and between vertebrates and invertebrates (Lovell et al., 2005a). Electrophysiological studies of the ABR response is used routinely in the clinical evaluation of human hearing (Jacobson, 1985), allowing for the acquisition of thresholds from uncooperative or inattentive subjects and in situations where behavioural methods cannot be readily applied (Kenyon et al., 1998).

The literature review of current audiogram production methodologies has been divided up into three sections. The first section looks at the use of microphonics, or recordings taken directly from the saccular and VIII nerves. The second looks at behavioural methodologies, and includes classical shock conditioning and heart rate suppression to ascertain hearing thresholds. The final section reviews works that use the Auditory Brainstem Response (ABR) technique to measure Auditory Evoked Potentials (AEPs) in both fish and marine mammals.

2.2 Microphonics

Enger and Anderson (1967) conducted a field study of fish audiometry by measuring microphonic potentials from the cod (*Gadus morhua*) and the sculpin (*Cottus scorpious*) in the open sea. Electrode implantation involved a highly complex surgical procedure, and involved drilling small holes in the cranium close to the saccular nerve. A 0.5 mm diameter silver wire was inserted in the hole, and sealed using dental cement. Using this method, the authors recorded microphonics of 70 μv from both cod and sculpin, when stimulating with tone bursts presented from a J9 underwater sound projector driven by a Philips RC oscillator and a Quad II amplifier.

Fay and Popper (1974) recorded microphonic potentials from the ear of the goldfish (*Carrassius auratus*) in a situation where sound pressure and particle displacement could be independently varied. When two transducers positioned facing each other are operated in phase, the water between them is compressed, creating a sound field dominated by pressure and minimal particle displacement. When the transducers are operated out of phase, one compresses the water whilst the other pulls it, creating a field dominated by particle displacement with minimal sound pressure (both modes of sound presentation are discussed further in Chapter 5). The authors also tested the fish with the swim bladder present and after its removal. The fish were tested in a 330 mm diameter PVC cylinder 1500 mm high, located in a soundproof acoustic chamber. A water bag containing the fish was suspended in the middle of the cylinder; air speakers were positioned above and below the bag containing the fish and the stimulus sounds presented using a Dyna 120 amplifier and a 7056 function generator.

In a second series of experiments measuring microphonics, Fay and Popper (1975) recorded potentials from the saccule of the African mouthbreeders (*Tilapia macrocephala*) and the catfish (*I. nebulosus*) using submerged glass insulated tungsten electrodes. The fish were tested in a soundproof acoustic chamber to both acoustic and vibrational stimulation, and for sound reception with the swim bladder filled with water. The test tank was a 250 mm diameter PVC cylinder 200 mm high, filled to a height of 160 mm. The floor of the cylinder was made from 5 mm thick "Rho C" rubber supported by a plastic grating. A loudspeaker with a diameter of 200 mm was suspended facing upwards 250 mm below the test tank in an airtight extension of the cylinder. The sound pressure level required to evoke a 1 μv RMS Auditory Evoked Potential (AEP), was determined using a Clevite Model CH-17T hydrophone positioned adjacent to the fish's ear.

Fine (1981) investigated the mismatch between sound production and hearing in the oyster toadfish (*Opsanus tau*). Anaesthetised fish were and clamped in a tank with the top of the head above the water surface. Single nerve fibres were then isolated from the saccular afferents, and the response to 300 ms tone burst from a speaker in air was measured. The tone bursts were phase-locked, had rise-fall times of 5 ms, and presented to the subject at a rate of 1 burst per second. The stimulus sound and background noise were measured using a Celesco LC34 hydrophone connected to A B&K 2508 amplifier, and wave analyser with a 3Hz filter.

2.3 Behavioural approaches

Popper (1972) used an avoidance conditioning procedure to define auditory thresholds for the carp (*Cyprinus carpio*). In this experiment, the fish were trained to cross a barrier in the middle of tank whenever a pure tone was presented through a loudspeaker mounted in the air, about 100mm from the test tank. The experimental tank was placed in an acoustic chamber to reduce ambient noise, and the experiment tested the hearing of 6 animals ranging in standard length from 50 to 60 mm. When the fish failed to cross the barrier during presentation of the stimulus, it was concluded that that the fish had not heard the sound, and thresholds were determined at the 50 % level using the up-down staircase method.

Offutt (1974) used classical conditioning of heart rate to determine hearing thresholds in the Atlantic cod (*Gadus morhua*). Fish were held in a nylon mesh net, in a tubular tank 530 mm long, and a diameter of 305 mm, positioned lengthwise in a wooden framework. The test tank and all test equipment was housed in an underground concrete room, and the pure tone stimulus sounds were generated by a 410 mm speaker built into the wall of the chamber. ECG's were obtained using an electrode inserted in the pericardial cavity, and a reduction in the heart rate indicated fish had heard signal. Thresholds were determined by the staircase method, with the stimulus attenuated in 2dB steps and a minimum of 10 reversals.

A Field study of hearing in two species of flatfish *Pleuronectes Platessa* (L.) and *Limanda limanda* (L.) was conducted by Chapman and Sand (1974) in Upper Loch Torridon, Scotland, using a PVC frame located 15m below the water surface and 6m from the seabed. A pair of stainless steel electrodes was built into the cage, to administer an electric shock to the subject's tail, and the potentials generated by the cardiac muscles were recorded using a subcutaneous electrode. The conditioning stimulus was a pure tone pulse presented to the fish for 10 seconds, paired with a 6 to 12 V dc electric pulse administered to the fish from the loch shore. The cardiac potentials from the fish were amplified and recorded using a storage oscilloscope, and a hydrophone positioned 10 mm below the head of the fish recorded the sound pressure of the stimulus tone. The sound was presented to the fish through two sound projectors located 0.7 m, and 3 m from the holding cage. In order to condition the fish, the electric shock was administered after presentation of the stimulus sounds. Conditioning using this methodology was repeated until the fish showed an alteration in heart rate after onset of sound but before the shock. Full conditioning was

considered to have occurred when 5 consecutive trials had yielded positive responses. In some experiments a small 34 mm diameter spherical air-filled rubber balloon was placed behind the cranium to simulate the presence of a swim bladder.

Coombs and Popper (1979) conditioned Squirrelfish (*Myripristis kuntee*) and (*Adioryx xantherythrus*) to respond to sound in a 410 x 240 x 170mm Plexiglas tank situated in an anechoic chamber. The stimulus sounds were presented to the fish through two air mounted loudspeakers, which produced a series of 600ms tone bursts with a 5ms rise and fall, followed by 400ms of silence. A shock avoidance technique was used to measure auditory sensitivity, and the fish trained to swim across a barrier on hearing a sound or risk an electric shock. The staircase method was used to determine threshold, and the sound level increased or decreased in 5dB steps depending on the response of the fish during the test.

A behavioural study of hearing in damselfish (*Eupomacentrus dorsopunicans*, *E. mellis*, *E. variabilis*, *E. diencaeus*, and *E. planifrons*) by Myrberg and Spires (1980) looked at hearing in these closely related species. The audiological tests were conducted in a 5m long, 150 mm internal diameter glass tube, divided into two sections, and filled with seawater. The farthest end of the section in which fish was placed had a type J-9 underwater transducer mounted on anti-vibration pads. The second section was filled with sponges to act as sound absorbers, and the entire assemblage was suspended from the floor by rubber bungees attached to a beam above the tube. For some tests, in order to increase ratio between sound pressure and velocity, a 150 mm ø hollow rubber ball was placed at the end of the first tube opposite the speaker. The fish was restrained in a transparent Plexiglas cylinder positioned so the fish was equidistant from the surrounding wall of the glass tube. Little sideways movement was possible, but the fish could easily be moved vertically. Stainless steel rods were located on each side of the restrainer as electrodes for applying a shock to the fish, and the sound pressure was measured by an Aquadyne AQ-12 hydrophone placed in the restrainer below the head of the fish. The fish was stationed either 400 mm or 1.45 m from the speaker face. The fish was conditioned to respond to sound by moving downwards if it detected a tone, and the staircase method was used to determine the threshold (the sound level was varied in 2dB steps). Threshold was determined from the average sound level attained after 50 sound presentations beyond the point where the levels accompanying response and no-response varied by no more than 8dB.

Coombs and Popper (1982) studied the structure and function of the auditory system in 3 specimens of the clown knifefish (*Notopterus chitala*). The association between the ear and anterior projections of the swim bladder were subjected to an anatomical investigation. Auditory sensitivity was determined using an operant conditioning technique, where the fish was trained to cross a barrier in the centre of a tank on hearing the audio cue, in order to avoid being given an electric shock. The sound pressure level was decreased in 5 dB steps following each successful avoidance response, and increased by 5 dB if the fish did not avoid the shock. Two tanks were placed in an anechoic chamber, and the stimulus sound source was a single 203 mm diameter speaker positioned in air, above the test tanks. Vertical particle velocity was also measured with a velocity hydrophone at four positions in the tank.

Hawkins and Myrberg (1983) used cardiac suppression to define the hearing abilities of 43 immature cod (*Gadus morhua*) ranging in length between 210 mm and 470 mm. The fish were anaesthetized in a 1:15000 solution of MS-222 whilst silver electrodes were inserted subcutaneously into the body cavity, in order to detect the electric potentials from the heart. Experiments were performed in a framework immersed in the sea 100 m from the shore, and the top of the framework was located 15 m below the sea surface, and 6 m above the seabed. The test cages contained stainless steel electrodes, which were used to administer a shock on presentation of a sound during conditioning. Two sound projectors were placed on a line from the shore, at right angles to the axis of the cage. The intensity of the stimulus sounds were recorded using a hydrophone and filtered to bandwidth of between 10 Hz to 1000 Hz. For some experiments, a high level of random noise was continuously transmitted from the sound projector and the pure tone stimulus superimposed.

McCormick and Popper (1984) studied auditory sensitivity and psychophysical tuning curves in the elephant nose fish, *Gnathonemus petersi* using a behavioural method. The auditory tests were carried out in tanks located in a chamber which had 150mm thick sand-filled walls. The test fish had to cross a barrier dividing the tank within 10sec of the sound being presented, to avoid being given an electric shock. The sound projector was a 203 mm diameter speaker positioned in the air above the test tank, and the stimulus tones were generated with a 5 ms rise and decay time. The staircase method was used for threshold determination, and the sound level was varied in 5dB steps. The threshold was calculated from the final 8 trials over a 24 hour period. The sound level in the tank was measured with a Clevite hydrophone, at 10 locations, and the median values of the levels was used as

the calibrated value. Particle velocity was also measured at 4 locations using a velocity hydrophone. The ambient sound pressure was found to be well below threshold levels at all frequencies, and tests were also conducted to ascertain if the fish might be influenced by electric fields; it was concluded that this was highly unlikely.

Yan and Popper (1992) defined the auditory sensitivity of the cichlid (*Astronotus ocellatus*) using a non invasive reward based methodology, and present a behavioural audiogram for the goldfish from Yan and Popper (1991). The experiment involved using an automatic feeding device to train 3 *A. ocellatus* to respond to an acoustic cue. A clear plastic tube delivered the food pellets to the fish, feeding tube was clear to allow the fish to receive visual as well as acoustic clues to a feeding event. 2 paddles were suspended from a platform and sent response signals to a PC which controlled food delivery if the correct sequence of paddles were pressed during acoustic stimulation. The experiments were conducted in a soundproof chamber, and the stimulus tones were presented to the fish using an underwater speaker (University Sound UW-30). The fish were trained to peck the O-paddle and then to peck the R-paddle if they detected the stimulus sound; a correct response resulted in the fish obtaining food. Once trained, thresholds were determined from the sound level at which 50% of the trials resulted in a correct responses.

Mann, Lu & Popper (1997) also used a cardiac suppression methodology to determine ultrasonic hearing by the American shad (*Alosa* spp). The experiment involved training 5 fish to reduce their heart rates on presentation of an audible sound; however the experiment was conducted with an active pump system, which may have masked responses to low frequencies.

Casper, Lobel and Yan (2003) studied the hearing sensitivity of the little skate (*Raja erinacea*) using both behavioural and ABR methods (see next section for ABR description). 3 test subjects were conditioned in a tank 1.5 m x 1.08 m x 0.65 m using a 60-s pulsed recording of brown noise (low-passed noise that has a 4 dB drop per octave), played through an underwater speaker 1 m from the skate's head. The fish were trained to associate noise with food provision, and feeding/conditioning events were conducted 3 to 4 times per day for 6 weeks. Conditioning was considered a success if the skate showed response 10 times without the introduction of food. A positive response was acknowledged if skate began swimming on presentation of the stimulus sound, or an increase in the rate of respiration was observed. Following training, audiological tests were conducted using 500 ms pulsed tones emitted from a Lubell Corp. LL-98A projector

positioned 200 mm above bottom of tank, and 1m from the skate. An Interocean Systems Model 902 hydrophone was used to record the sound pressure at a distance of 150 mm above the skate's head. If the skate responded 5 times consecutively, it was deemed to be responding to the sound stimulus at that intensity, so the pulsed tone was attenuated in 5 dB steps until the fish did not respond to the sound (threshold was determined from the lowest sound pressure where a 100 % response could be observed).

2.4 Measurements of the Auditory Brainstem Response

Kenyon, Ladich and Yan (1998) used the ABR audiometric method on goldfish (*Carassius auratus*) and the cichlid (*Astronotus ocellatus*) to generate audiograms. The experiments were conducted in a soundproof booth (2 m x 3 m x 2 m), into which anaesthetised fish were clamped in place using a net mesh and positioned so the top of the head was 1 mm above the water surface. Two electrodes were pressed against the exposed cranium above the medulla, with the reference electrode positioned 5 mm anterior of the recording electrode. Frequencies below 3 kHz were generated using a 300 mm loudspeaker suspended 1 m above the water surface in the holding tank, and for frequencies above 3 kHz, a 120 mm loudspeaker was used. The Sound Pressure Level (SPL) was recorded using a hydrophone placed near the ear of fish; tone bursts and clicks were presented over a range of intensities, in order to obtain evoked potential thresholds defined by visual inspection of two overlaid traces from a repeat test at a particular frequency and intensity. Clicks were 0.1 ms in duration, and presented at a rate of 38.2 clicks per second. The number of cycles in a tone burst was set to get best compromise between stimulus rapidity and peak frequency bandwidth, with bursts gated using a Blackman window function applied to reduce spectral leakage from the signal (e.g. if a 3 Hz sine wave is sampled for .9 seconds, a discontinuity results). In total, eight fish were given Flaxedil (gallamine triethiodode) to immobilise them, whilst three fish remained untreated. The authors reported that thresholds were significantly lower for the Flaxedil treated fish, demonstrating that the restraining methodology allows untreated fish enough gross movement to contaminate the ABR trace.

Ladich and Yan (1998) used the ABR method to study hearing in the paradise fish (*Macropodus opercularis*). The experiments were conducted on an air table located in a soundproof booth (see Kenyon, Laditich and Yan, 1998 for dimensions). During the investigation, Flaxedil immobilised fish were held in place using a net mesh, with just 1 mm of top of head above the water surface. 2 electrodes were pressed against the head,

with the reference electrode positioned 10 mm anterior of the recording electrode. Sound was generated by a loudspeaker suspended 1 m above the surface of the water, with a 300 mm speaker used to generate frequencies below 3 kHz, and a 120 mm speaker was used for frequencies above 3 kHz. The SPL was obtained using a hydrophone (Celesco LC-10) placed in proximity to the ear of the fish. Tones and clicks were presented at various pressure levels to obtain thresholds, which were identified by visual inspection of the averaged ABR traces when superimposed over the first run. Clicks were 0.1 ms in duration, and presented at 38.2 clicks per second, and the number of cycles in each of the tone bursts was programmed to optimise stimulus rapidity and peak frequency bandwidth and gated using a Blackman window.

Yan, (2001) tested a number of hearing specialists including the goldfish (*Carassius auratus*), blue gourami (*Trichogaster trichopterus*), kissing gourami (*Helostoma temminckii*), dwarf gourami (*Colisa lalia*), and a mormyrid (*Brienomyrus brachyistius*) using ABR audiometry. In addition, Yan studied auditory thresholds from the oyster toadfish (*Opsanus tau*), a hearing generalist. The experiments took place in a soundproof booth (see Kenyon, Laditich and Yan, 1998 for dimensions). The fish were sedated with Flaxedil (gallamine triethiodode) and clamped in a mesh net suspended in a tank (see Scholik and Yan, 2002 for dimensions) standing on an air table. The top of the head was positioned 1 mm above water level, and tissue placed on head to prevent it from drying out. The electrodes were pressed against the head, and the reference electrode positioned 5 mm anterior to the recording electrode. Sound was presented to the fish through a speaker suspended 1 m above subject, with a 300 mm speaker used for frequencies below 3 kHz and a 120 mm speaker for frequencies above 3 kHz. Clicks with a duration of 0.1 ms, were presented at a rate of 38.2 clicks per second. The number of cycles in each of the tone bursts was set to get best compromise between stimulus rapidity and peak frequency bandwidth, and gated using a Blackman window. The Sound Pressure Level of the stimulus sounds was obtained using a hydrophone placed near the fish ear, and once the baseline audiogram had been taken, the gas inside the swim bladder was removed using a syringe and needle. The audiogram procedure was repeated with the swim bladder deflated to show that the organ enhanced hearing sensitivity.

Scholik and Yan (2001) studied the effects of underwater noise on auditory sensitivity of the fathead minnow (*Pimephales promelas*) exposed for selected durations. A mesh screen prevented the fish from jumping out of the tub (see Kenyon, Laditich and Yan, 1998 for dimensions); though the fish were free to swim around during noise exposure. The

bandwidth of the noise was limited to between 300 Hz to 4 kHz, and presented at a Sound Pressure Level (SPL) of 142 dB (re 1μPa). The fish were mildly sedated with Flaxedil and the ABR technique used to obtain the threshold values. The experiment was designed to establish hearing thresholds immediately after 24 hours of continuous exposure to the noise, then at 1, 2, 4, 8 and 24 hours after exposure.

In a similar experiment, Scholik and Yan (2002) produced several ABR generated audiograms to ascertain the effects of noise on the auditory sensitivity of the bluegill sunfish (*Lepomis*). Specimens of *L macrochirus* were exposed to white noise presented at 142 dB re 1μPa, and a bandwidth of between 300 Hz to 2000 Hz. The fish were sedated with Flaxedil, and the ABR technique was used to obtain the threshold values after exposure to the noise. The stimulus sounds used to test for threshold shifts were generated using an air mounted transducer, and the evoked response recorded using two cutaneous electrodes held in place using micromanipulators, with the fish placed in a plastic tub (380 mm x 24.5 mm x 145 mm).

Casper, Lobel and Yan (2003) studied the hearing sensitivity on 4 specimens of the little skate (*Raja erinacea*), using ABR audiometry. The fish were immobilised by an injection of d-tubocurarine chloride and suspended in a 380 mm x 245 mm x 145 mm plastic tray, suspended at an angle so the entire body of the skate was immersed. A small portion of the head (near the medulla region), posterior to the eyes, was exposed to the air, and chosen for the primary site for the placement of the electrodes. The plastic tub was placed on a vibration-isolating table, in a sound proof booth (2 m × 3m × 2 m). Tone bursts with a duration of 20 ms, were presented through a Pioneer 300 mm speaker, positioned 1 m above the subject's head. 3000 iterations of the stimulus sound were averaged at each Sound Pressure Level (SPL), which was reduced in 5 dB steps until the threshold was reached. The threshold SPL value was measured with a Celesco LC-10 hydrophone placed where the subject's head was during the audiometric examination.

Akamatsu, Nanami and Yan (2003) defined the hearing abilities of the spotlined sardine (*Sardinops melanostictus*) using the ABR technique. Audiograms were generated from fish stationed in a seawater-filled plastic tub, 280 mm x 200 mm x 35 mm deep, and placed on a vibration isolating table in a soundproof chamber. The stimulus sound was presented through a ceiling-mounted loudspeaker positioned 450 mm above the head of the fish. The stimulus sounds were digitally generated 5-cycle tone bursts, multiplied with a Gaussian function. The sound in the water was monitored with a B&K Type 8103 hydrophone

located adjacent to the subject's head, and the fish restrained using a neoprene rubber sling with stainless steel plates attached to sides. The fish were held horizontally, with the inner ear and anterior end of gas bladder kept at the same depth to ensure equal levels of incident sound pressure on both organs. A small area of skin on the top of the head was exposed above the water line to facilitate in the placement of the electrodes. The potentials were amplified and filtered to a bandwidth of between 50 Hz to 10 kHz. Only 300 stimulus exposures at each frequency were used, thus cutting back on the time it takes to produce the audiogram as it was found to be difficult to sustain life support for the test sardine. The sound level at each frequency tested was varied initially in 6 dB steps, and then in 3 dB steps as the threshold was approached. Water was continually supplied to the mouth of the subject, with the flow maintained by gravity to avoid the noise generated by an electric pump. The electrodes, through which the evoked potential was conducted, were placed along the midline of the skull over the medulla region, with the cables twisted in an effort to reduce the electromagnetic noise generated outside the chamber.

Lugli, Yan and Fine (2003) studied the relationship between ambient noise, hearing thresholds and sound spectra in acoustic communication between two freshwater gobies *Padogobius martensii* and *Gobius nigricans*. A total of 5 fish (2 females, 3 males) were tested to generate the ABR audiograms; in each case the fish was held with the nape of the head just above the water surface, in a 380 mm x 245 mm x 145 mm plastic tub. The stimulus sounds were presented to the fish through a 300 mm Pioneer speaker located 1 m above the subject. The sound used was a tone burst 20 ms in duration, and used for each frequency tested; the sound level in the water was monitored with a Celesco LC-10 hydrophone located adjacent to the head of the fish. During the experiment, the sound level was reduced in 5 dB steps until threshold was reached. Part of the experiment was to study the sound produced by the fish, and how their hearing might be related to the ambient noise in their normal environment (shallow stony streams); a relationship was found between the sound spectrum of the ambient noise and hearing sensitivity.

2.5 Previous uses of ABR in cetacean audiometry

Popov and Supin (1990) studied hearing in the beluga dolphin (*Delphinapterus leucas*), the bottlenose dolphin (*Tursiops truncates*), the Amazon River dolphin (*Inia geoffrensis*), tucuxi dolphin (*Sotalia fluviatilis*) and the Manatee (*Trichechus inunquis*) using the ABR technique. The hearing tests were conducted in either a 4 m x 0.6 m x 0.6 m bath, in a round pool, or in an enclosed sea bay. During the tests, the subject was supported on a

stretcher positioned so only the top of the head with the blowhole and the back, as far as the dorsal fin was out of the water. The Auditory Evoked Potentials (AEPs) were recorded using 0.4 mm to 0.6 mm diameter subcutaneous needle electrodes inserted into the skin at depths of between 3 mm to 5 mm (see also: Popov, Ladygina and Supin, 1986). The record electrode was placed on the dorsal head surface 60 mm to 90 mm caudal from the blowhole, and the reference electrode placed on the back near to the dorsal fin. The potential difference between the two electrodes was fed to a biological amplifier (gated between 5 Hz to 5000 Hz) and the signal averaged to reveal the AEP. The stimulus sounds used in the audiological tests were clicks, square enveloped noise or ramped tone bursts of frequencies of between 5 kHz to 160 kHz, generated using piezo-ceramic transducers with diameters of 20 mm, 30 mm and 50 mm. The array was stationed 300 mm below the water surface, at distances of between 1 m to 2 m anterior of the subject's head.

In a second series of experiments using the ABR technique on odontocetiforms, Bibikov (1992) studied hearing in the harbour porpoise (*Phocoena phocoena*) using both cutaneous and implanted electrodes. The porpoise was loosely restrained in a bath with dimensions of 2.5 m x 0.6 m x 0.65 m, which had been lined with sound absorbing rubber and filled with seawater. The record electrode used in the first experiment was a 10 mm diameter silver disc placed on the surface of the skin above the muscles overlying the vertex of the head, whilst the second experiment used an implanted electrode. In both experiments, the reference electrode was a subcutaneous needle electrode inserted into the skin close to the dorsal fin, and the AEPs gated between 50 Hz and 4 kHz for the subcutaneous electrode and 200 Hz to 5 kHz for the surface electrode.

André et al. (2002) found evidence of deafness in a young stranded female striped dolphin, *Stenella coeruleoalba*, which cancelled her possibility to process correctly any acoustic information. The experiments took place in a large seawater pool, with the dolphin held in a stretcher made from a sound transparent fabric, stationed at a depth of 40 to 50 cm in the centre of the pool. This allowed the body of the dolphin to remain under the water, while the dorsal part of the head and the blowhole stayed above the surface. The stimuli used during the study were sinusoidal amplitude-modulated tones, generated using a function generator and amplified using a B&K 2713 amplifier driving a piezoceramic transducer (B&K 8104 hydrophone). Tone bursts were presented for a duration of 20 ms, at a rate of 20 s -1. The stimulating transducer was placed in front of the dolphin, at a distance of 1 m from the head and a depth of 20 cm, with stimulus intensity specified in units of dB (re. 1 μPa) RMS. The evoked potentials were recorded using 1-cm disk electrodes secured at the

body surface inside 6-cm suction cups. The active electrode was placed at the head vertex, just behind the blowhole, with the reference electrode placed on the back (both electrodes were above the water surface). The recorded potentials were digitised using an A/D converter and averaged over 1000 sweeps of 30 ms, using a standard personal computer. The analysis of the results from the experiment suggests that the dolphin had great difficulty processing acoustic stimulus, and most likely explains the cause of the stranding.

2.6 Chapter discussion

Over the last 100 years, a number of approaches have been used to generate audiological data from aquatic animals, reward based training paradigms or the administration of an electric shock are used to generate conditioned responses during acoustic stimulation (e.g. Offutt, 1974; Chapman and Sand, 1974; Coombs and Popper, 1979; Myrberg and Spires, 1980; McCormick and Popper, 1984; Mann, Lu & Popper, 1997). As discussed at the beginning of the Chapter, the sound field can be difficult to calibrate if the fish are free swimming and training can take several weeks for a stable association between the stimulus and response to develop (Yan and Popper, 1992; Yan, 1995). Results from the measurement of microphonics from the auditory end organs during acoustic stimulation are obtained more rapidly than from behavioural paradigms (e.g. Enger and Anderson, 1967; Fay and Popper, 1975; Fine, 1981). However, preparations can be complex and require invasive surgery to implant the electrodes directly into the nerve (c.f. Enger and Anderson, 1967). The electrode is thus restricted to a specific end organ or region of macula, and the recorded evoked potential does not necessarily represent the response of the whole auditory pathway (Kenyon et al., 1998).

Although ABR has been used successfully in the clinical evaluation of human hearing (Jacobson, 1985), controversy still exists regarding audiological information acquired from generalist fish species. A number of recently published experiments using ABR show that generalist fish hear sounds above 1000 Hz (e.g. Kenyon et al., 1998; Scholik and Yan, 2001; Casper, Lobel and Yan, 2003); however, it is generally recognised that generalist fish do not hear sounds above a frequency of 500 to 600 Hz (e.g. Wolf, 1967; Chapman, 1973; Fine, 1981; Fay, 1988). Therefore, based on the review of the literature, it is clear that a number of important questions remain unanswered. As discussed by Kenyon et al., (1998), thresholds from fish which had not been administered an anaesthetic were considerably higher than thresholds from anaesthetised fish. It is considered here, that in order to record accurate AEPs without the application of anaesthetics, the specimen

holding and electrode positioning system needs to be adapted to minimise voluntary muscular movement. Particular attention is also focused on the EP recording system and the development of a versatile specimen cradle and electrode clamp to allow for underwater recording from fish and other aquatic animals with body length from a few millimetres up to a meter, in both marine and fresh water. The ABR system must be further refined so underwater sound fields dominated by particle motion or sound pressure can be generated to stimulate the fish ear, rather than the air mounted transducers used in previous ABR type experiments. The results of this work are discussed in the following chapters, involving "in depth" studies of the form and function of the hearing system in specialist and generalist bony fish, cartilaginous generalist fish and decapod crustaceans. In addition to this, the morphology of the cetacean ear is examined, and a technique developed for removing and preparing it for SEM examination using a large mammal (*S. scrofa*) as a surrogate.

Chapter 3

The hearing abilities of specialist fish

3.1 Introduction

This part of the thesis relates to testing of the hearing thresholds of specialist fish, beginning with the goldfish (*Carrasius auratus*), tested in order to validate both the audio stimulation system and the accuracy of the electrophysiological recording technique. *C. auratus* is especially good as a validation species, as a number of ABR generated audiograms have been published for this fish (see Kenyon et al., 1998; Yan et al., 2000 and several other studies discussed in Chapter 2.). To this end, *C. auratus* was stimulated with tone bursts presented through an air mounted transducer, and the sound field calibrated in accordance with Kenyon et al. (1998). The second series of experiments described in this chapter look at the hearing abilities of silver carp (*Hypopthalmichthys molitrix*) and bighead carp (*Aristichthysc nobilis*). The work presented herein is of significance, given that concise physiological information on the hearing ability of *H. molitrix* and *A. nobilis* is not known. As discussed in Chapter 1, the audiograms are required to improve the selectivity of an Acoustic Fish Deterrent (AFD) barrier intended as a freshwater management strategy to stop the spread of these species through the Illinois River into Lake Michigan. The audiograms for *H. molitrix* and *A. nobilis* were acquired using submerged transducers (a setup not previously attempted in an ABR investigation of fish hearing). An additional challenge was forthcoming when testing *A. nobilis*, as some of the fish used in the experiment were approaching 750 mm in length, and weighed nearly 6.75 kg.

3.2 Materials and methods

4 specimens of *C. auratus* with fork lengths of 59 mm (3.6 g), 69 mm (9.7 g), 71 mm (12.3 g) and 72 mm (12.7 g) were kept in a 200 litre freshwater tank. Water quality was maintained by an Eheim type 2013 biological filter with a flow rate of 390 litres per hour, which provided aeration by spraying filtered water back into the tank via the filter outlet

pipe located 60 mm above the water surface. In all of the experiments, the ambient water was kept at a temperature of 12 ° C. When under experimental protocols, the goldfish were provided with 14 hours of light per day from a fluorescent tube controlled by a mains timer switch, and fed on a pellet feed at a rate of 1.6 g per day. Twelve specimens of *H. molitrix* ranging in length between 137 mm (25 g) to 392 mm (700 g) were kept in four 200 litre freshwater tanks. Twelve specimens of *A. nobilis* ranging in length between 545 mm (2.8 kg) to 740 mm (6.75 kg) were kept in two 2.5 m x 1 m x 0.5 m tanks The water temperature in the holding tanks and test tank ranged between 18.2 and 18.6 ° C over a 24 hour period, and when not under experimental protocols, the fish were provided with 16 hours of light per day.

3.2.1 Method of recording audiograms

The ABR measurements of hearing thresholds were made using a proprietary control and analysis programme named "Brainwave", and written in LabView 7. The amplified electrophysiological signal from the auditory cortex of the subjects under investigation was fed via screened cables to an A-M Systems model 3000 differential amplifier with the band pass filters filter set between 0.3 kHz to 5 kHz. The filtered "real time" signal of neural activity was inputted via a BNC interface block, to an American Megatrends PC with a CPU speed of 950 MHz and 128 MB of RAM fitted with a National Instruments AT-M 1.0 digital to analogue card. The signal was recorded prior to, during and after stimulation with a single tone burst, then digitised at a sample frequency of 10 000 bits per second and stored in the programme memory buffer. This process was repeated after a 25 ms pause in the programme, and the subsequent digitised recording was averaged against the previous recording; this was then repeated for a further 1000 to 2000 iterations of a particular tone and intensity. The effect of averaging on the raw signal causes random electrophysiological noise to reduce in intensity by the $\sqrt{n}$. whilst activity associated directly with the tone burst increases with each successive sample by n. Thus, the ratio between the Auditory Evoked Potentials and random neurological waveforms alter by the $^{\sqrt{n}}/_{n}$ and allows for the amplification of very small electro potentials against a relatively noisy background.

A block diagram of the equipment used to provide audiometric measurements from *H. molitrix* and *A. nobilis* is shown in Figure 3.1.a, and the equipment schematic used to test *C. auratus* is presented in Figure 3.1.b and c. For *C. auratus*, amplification of the sound was achieved using a Pioneer type SA-420 amplifier and a 200 mm Eagle L032

loudspeaker with a frequency response range of 40 Hz to 18000 Hz. Additionally, the loudspeaker was placed inside a Faraday cage 1 m above the test tank and connected to a centralised earth point located in an adjacent room where the PC, amplification, and analysis equipment was set up. Connecting wires were fed through a 100 mm port in the partitioning wall. The sound field in the experimental water tank holding *H. molitrix* and *A. nobilis* was generated by means of two Fish Guidance Systems Ltd. Mk II 15-100 Sound Projectors; with the stimulus sound amplified using a Tandy 250W power amplifier. These faced each other at a distance of 200 mm; the inner ear of the fish during measurements was arranged on the axis connecting the centres of the two projectors.

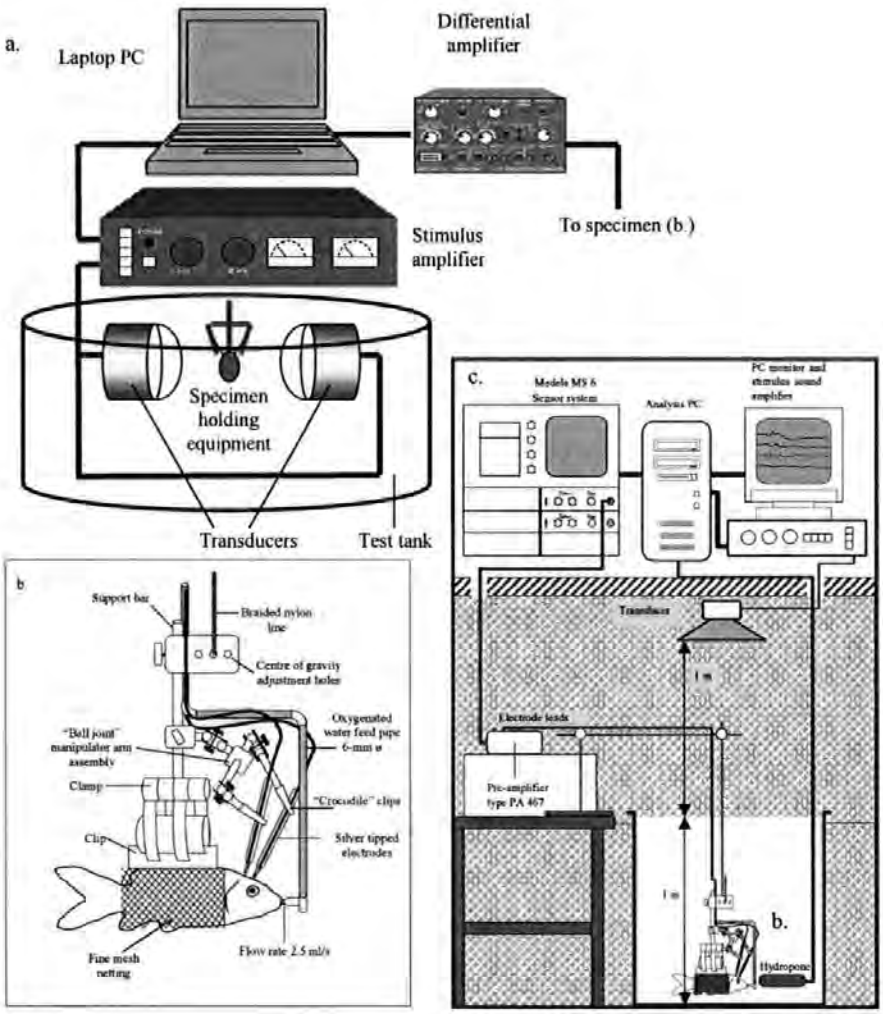

Figure 3.1.a and **b.** Schematic of the ABR audiometry system used to test *H. molitrix* and *A. nobilis*, and **Figure 3.1.b** and **c**, schematic of the ABR system used to test *C. auratus*

The procedure used to acquire the acoustically evoked potentials was approved by the University of Illinois, United States (Institutional Animal Care and Use Protocol #04271) and the United Kingdom Home Office 11.03.03.

The test subjects were placed into a flexible cradle formed from a soft nylon mesh rectangle saturated with freshwater for the small fish, and a clear rubber coated 1 mm gauge wire mesh for fish over 0.5 kg weight, presented in Figure 3.2 with a specimen of *H. molitrix*. Oxygenated water kept at a temperature of 18 °C was gravity fed at an adjustable flow rate of between 5 millilitres per second for the small fish, to 25 millilitres per second for the large, and directed toward the gills through a soft rubber mouth tube. The small fish were first placed lengthwise and centrally on a 160 mm x 120 mm rectangle of fine nylon netting, which was wrapped firmly around the body and tail, and the two sides of the net were held together using a clip. The clip was placed in a retort stand clamp fitted with ball joint electrode manipulator arms, and the aerated water pipe. During the procedure to position the electrodes the specimen and clamp were suspended over the test tank, and aerated water was supplied to the fish. The attachment of the electrode manipulation assembly to the cradle holding the fish has not been attempted in any previous ABR type investigations. The principle advantage of this over the conventional setup used by Kenyon et al. (1998) and the subsequent experiments by Yan, where the electrodes are held in place using micromanipulators, is that the entire system can be easily moved or suspended at any desired depth. Although gross muscular activity was minimised by the supporting cradle, the design allows some flexibility between the electrode and fish, so slight movements had little overall effect on the ABR trace.

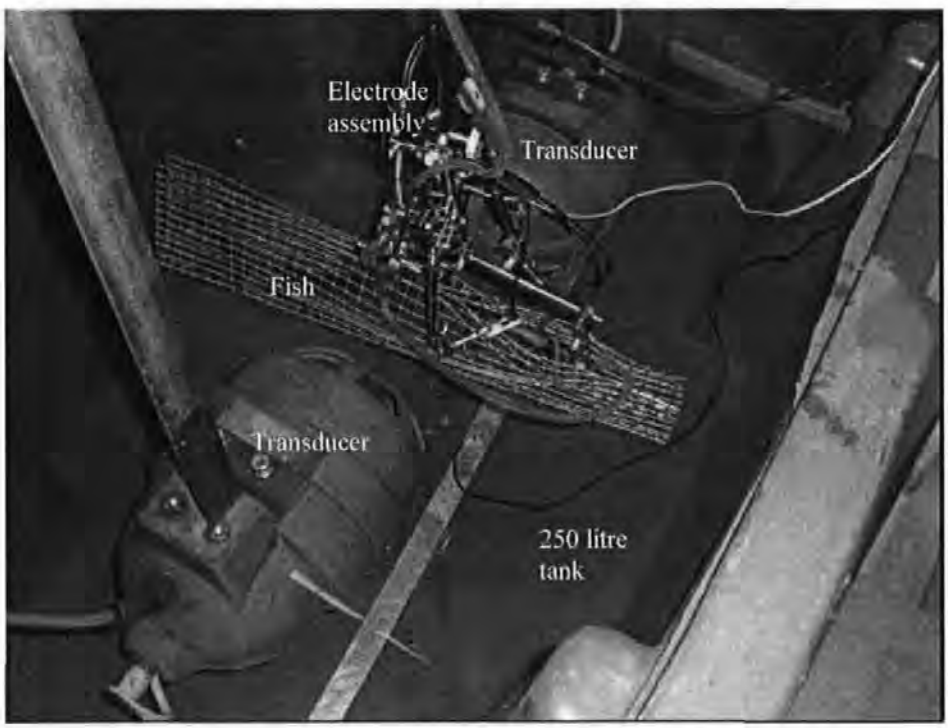

Figure 3.2. Photograph of a 0.5 kg *H. molitrix* during the audiological test

The electrophysiological response to acoustic stimulation was recorded using the two sub-cutaneous electrodes presented in Figure 3.3, which were connected to the differential preamplifier by 1 m lengths of screened coaxial cable with an external diameter of 1.5 mm. The outer insulating layer of the coax was removed 15 mm from the end where the electrode tip was to be fixed, and the screening layer removed 10 mm from the cable end. The inner insulating material was then trimmed by 2 mm, and the exposed inner wire (0.5 mm diameter) was tinned with silver solder and joined to a 10 mm length of silver wire (0.25 mm diameter), tapered to a fine point. The assemblage was pushed through a 100 mm glass pipette with an internal diameter of 4 mm, until 0.4 mm of the silver wire was exposed. The remaining space inside the pipette was filled with a clear epoxy resin, and then trimmed to expose 0.3 mm of silver tip through which the AEP could be conducted. The impedance of the electrodes, both between the outer shielding and inner core, and the silver tip and differential amplifier, were tested using an M 205 precision digital multimeter. The impedance between the tip and pre-amplifier was found to be 0.2 Ω for both electrodes, and an open circuit was recorded between the outer shielding and inner core.

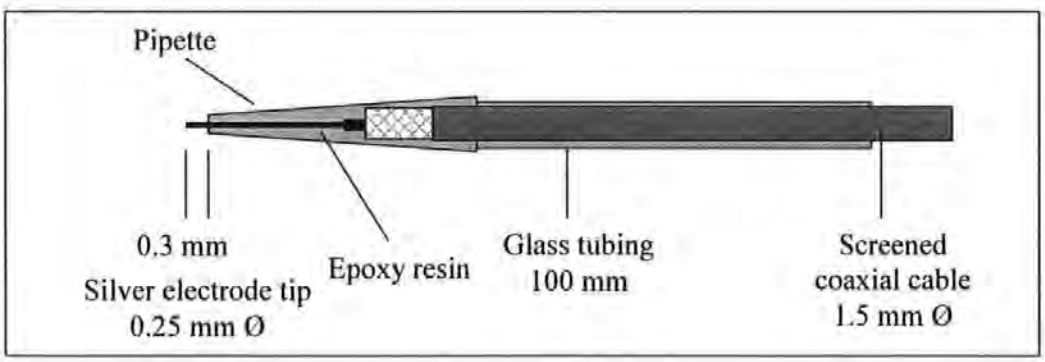

Figure 3.3 Schematic of the electrodes used to record the evoked potentials

Stimulus sound was presented to the specialist fish at sound pressures initially not exceeding 145 dB (re. 1 μPa). The electrophysiological response of the fish to acoustic stimulation was recorded using two cutaneous electrodes, which were positioned on the cranium of the fish adjacent to and spanning the VIII nerve. The reference electrode was positioned centrally on the head above the medulla, and the record electrode was located 5 mm anterior of this point. The evoked response was amplified and digitised to 12 bits resolution and recorded. This process was repeated between 500 to 2000 times (at threshold) and the response averaged to remove electrical interference caused by neural activities other than audition, and the myogenic noise generated by muscular activity.

Each measurement was repeated twice; this aids in separating the evoked response, which is the same from trace to trace, from the myogenic noise, which varies in two successive measurements. After the averaging process, the evoked potential could be detected, following the stimulus by a short latency period of one millisecond.

During the audiological assessment of *H. molitrix* and *A. nobilis* the projectors were driven with load resistors placed between the amplifier and projector. The reason for this was that due to the sensitive hearing of carp only relatively low levels of sound were required to cause an acoustic brainstem response. The full output of the amplifier was only required when measuring the hearing of the less sensitive generalist fish such as the Paddlefish and Sturgeon (see Chapter 5). The stimulus tones presented to *H. molitrix* and *A. nobilis* were calibrated using an insertion calibration, where the sound level is recorded in the absence of the fish, with the hydrophone stationed where the inner ear of the fish would be. The insertion method measurements were made using a Bruel and Kjaer Type 8104 Hydrophone (serial number 2225715) calibrated and traceable to International Standards, and the signal from the hydrophone was amplified by a Bruel and Kjaer Type 2365 Charge Amplifier (Serial Number 1079556). In case there was any non-linearity of the signal, calibrations were made at every frequency and Sound Pressure Level (SPL) used for a measurement, totalling some 660 individual calibrations. These calibrated levels were then applied to the threshold defined by the ABR measurement to provide calibrated audiograms with pressure levels traceable to International Standards. In fact, no evidence of non-linearity was detected, other than at the very highest levels of sound, which was not required in any case for measuring audiograms. Comparisons in the relative power change between each frequency at each pulse length were made by calculating the signal RMS, the results of which are presented in Figure 3.4.

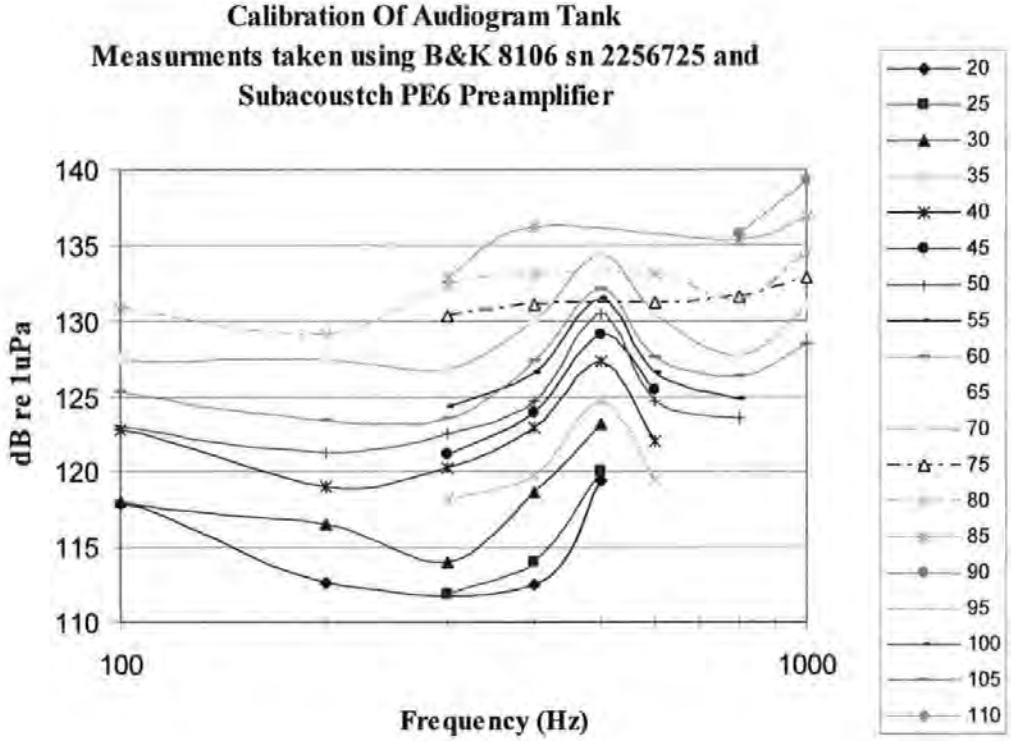

Figure 3.4 Calibration markers for the stimulus sound recorded in the holding tank using a B&K hydrophone (legend shows the arbitrary units of gain used)

3.3 Results

3.3.1 Audiogram for *C. auratus*

Figure 3.5 shows evoked potentials from the test *C. auratus* in response to a 500 Hz tone burst averaged over 1000 sweeps. The sweep is a recording of the neural generation of waveforms over a user defined time span termed the sweep velocity, which in the case of the recording in Figure 3.5 is 25 ms in duration. The recording shows a period prior to, during and after stimulation of the inner ear; the period of c. 3.3 ms prior to the onset of the AEP is accounted for by the time it takes for a sound generated in air to reach the fish located 1 m from the transducer (indicated by the dashed vertical line in Figure 3.5). Additional waveform generation by other neural activities combined with muscular movements ensure that recordings have to be repeated over 1000 to 2000 presentations before clear results can be obtained (Kenyon et al 1998; Yan et al 2000). The recorded wave forms resulting from each sweep are averaged together and produce a recognisable ABR waveform, which is then repeated and overlaid on the first run, to show that the evoked potentials are repeatable.

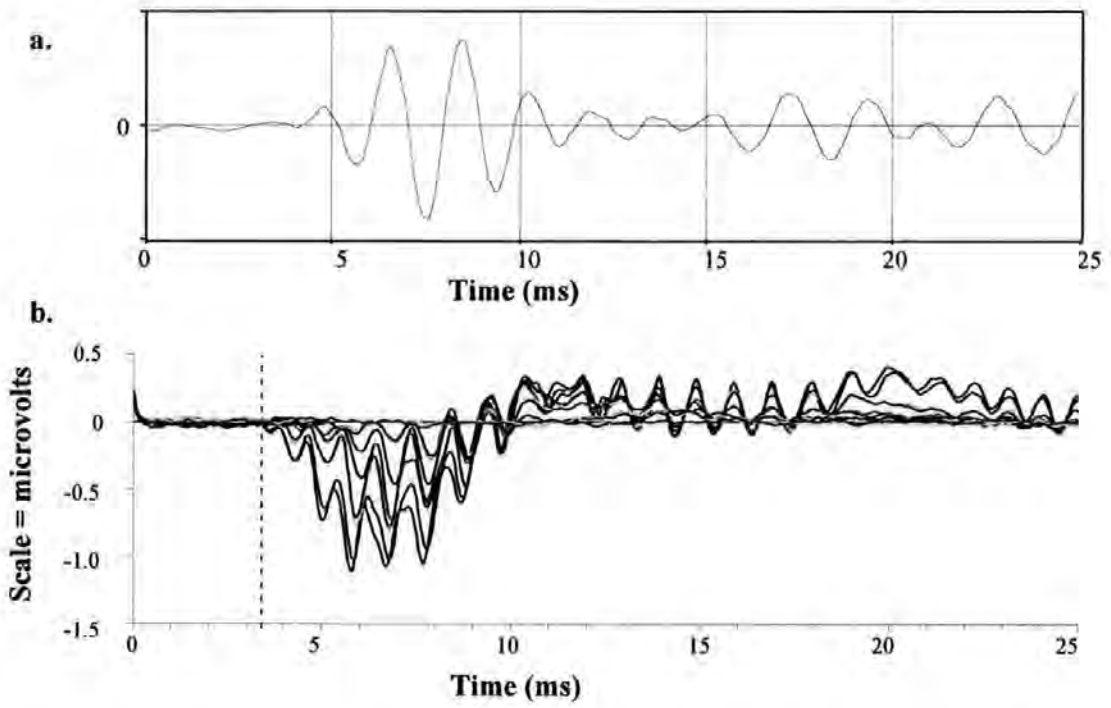

Figure 3.5 a. The 500 Hz pulse recorded underwater using the hydrophone. **b.** Overlaid evoked potentials from the test fish *C. auratus* in response to the 500 Hz tone burst. The hatched line shows the time taken for the sound to reach the fish positioned 1 m from the transducer and attenuated in 5 dB steps then 2 dB steps as threshold is approached

The waveforms represent vertex positive components issuing from the neural centres situated along the auditory pathway to the midbrain (Overbeck and Church 1992). The frequency and intensity of the tone burst influences the latency of the evoked response (hatched line in Figure 3.5) (Corwin et al., 1982; Kenyon et al., 1998), as does the metabolic state of the organism (Corwin et al., 1982). The increase in the latency of the evoked potential in response to decreasing stimulus intensity is often used to verify that the averaged waveform is a product of auditory stimulation rather than a transient generated at the electrode tip (Kenyon et al., 1998).

Figure 3.6 shows evoked potentials from the auditory brainstem of *C. auratus*, to a range of tone bursts averaged over 1000 stimulus presentations per frequency tested. The sweep and sound stimulation are triggered synchronously with one another, though the onset latency of the response is also dependant on the distance the sound has to travel to reach the inner ear.

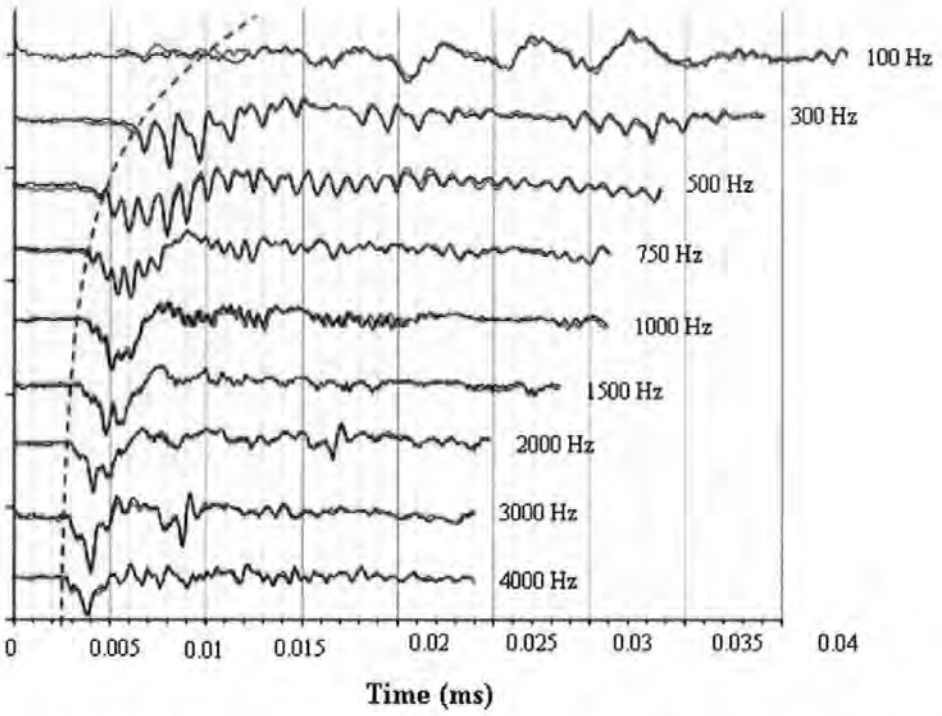

Figure 3.6. Auditory brainstem response of *C. auratus* to a range of tone bursts. The hatched line shows a reduction in response latency with increasing frequency (note, y-axis scale bars are cropped for presentation so have no units)

The waveforms in Figure 3.6 show a characteristic latency decrease with increasing frequency, in agreement with the findings of Corwin et al (1982) and Kenyon et al. (1998). For *C. auratus* the latency from the arrival of a 500 Hz tone at the ear, to the onset of the first sinusoid of the response was 3.7 ms at 15 dB (re. 1 µPa) above threshold, whilst for the remaining frequencies the waveforms were taken 10 dB (re. 1 µPa) above threshold. For the 750 Hz tone, the latency was 1.8 ms, the 1000 Hz tone was 1.4 ms, the 2000 Hz tone 1.1 ms and the 3000 Hz tone was 0.8 ms. Latency changes with variations in frequency and sound pressure are used to verify that a series of waveforms are evoked potentials, and not a stimulus artefact contaminating part of the ABR trace. An increase in airborne sound intensity can produce substantial stimulus artefacts, which potentially have an adverse effect on an ABR trace, and become more pronounced as intensity increases (Kenyon et al 1998).

The waveforms presented in Figures 3.7 through 3.10, are the results of a complete audiological assessment of *C. auratus*, and were found to be consistent (in both onset latency and general waveform shape) with the results of Kenyon et al. (1998), and Yan et al. (2000). The Figure shows Evoked Potentials (EPs) averaged from *C. auratus*, in response to frequencies presented in steps from 100 Hz to 4 kHz. The EPs are arranged

sequentially, in order of descending stimulus intensity. The sequential arrangement of the waveforms prevents the use of a scale bar in the y-axis, as each of the waveforms are from separate graphs and the y-axis scale bars have been cropped for presentation purposes. The sound pressure values displayed alongside the corresponding waveform are presented in units of dB (re. 1 μPa), determined using the calibration factors described by Kenyon et al. (1998).

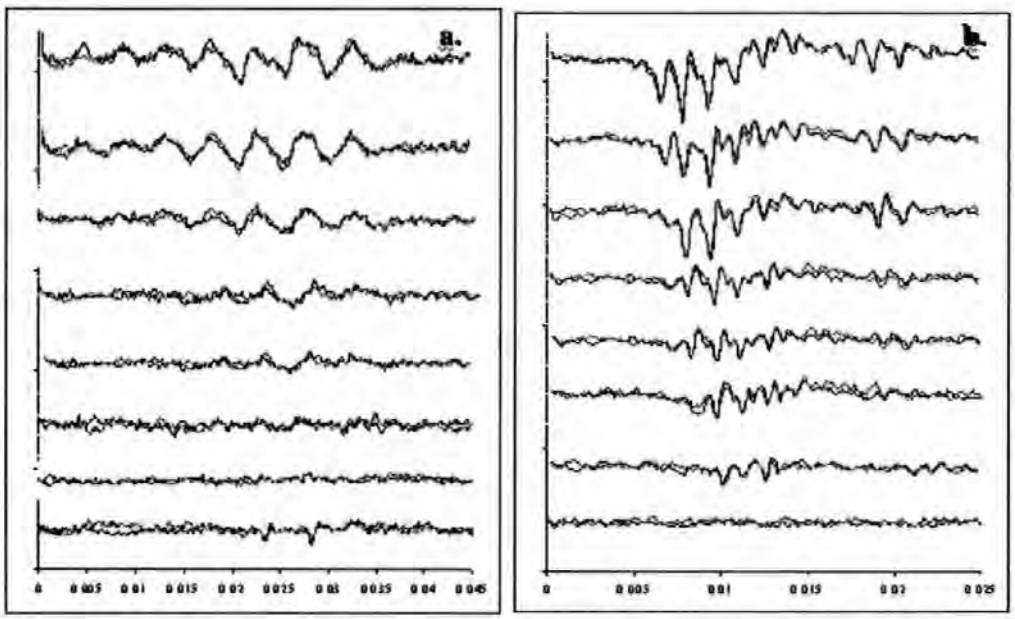

Figure 3.7 ABR response from *C. auratus* in response to **a.** a 100 Hz tone, and **b.** a 300 Hz tone burst. x-axis = time (s), y-axis scale bars are cropped for presentation so have no units

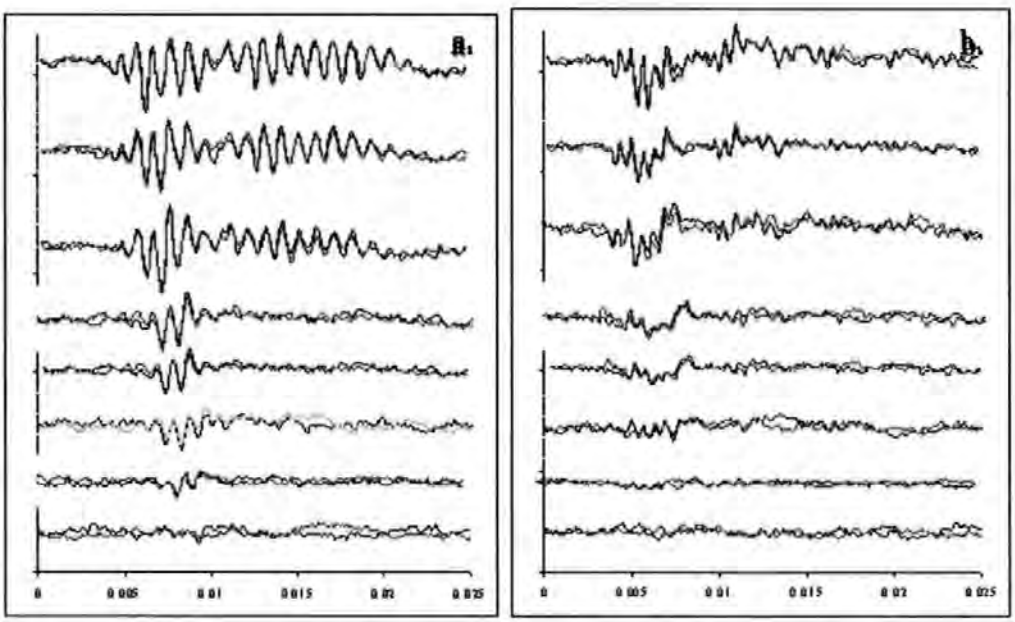

Figure 3.8 ABR response from *C. auratus* in response to **a.** a 500 Hz tone, and **b.** a 750 Hz tone burst. x-axis = time (s), y-axis scale bars are cropped for presentation so have no units

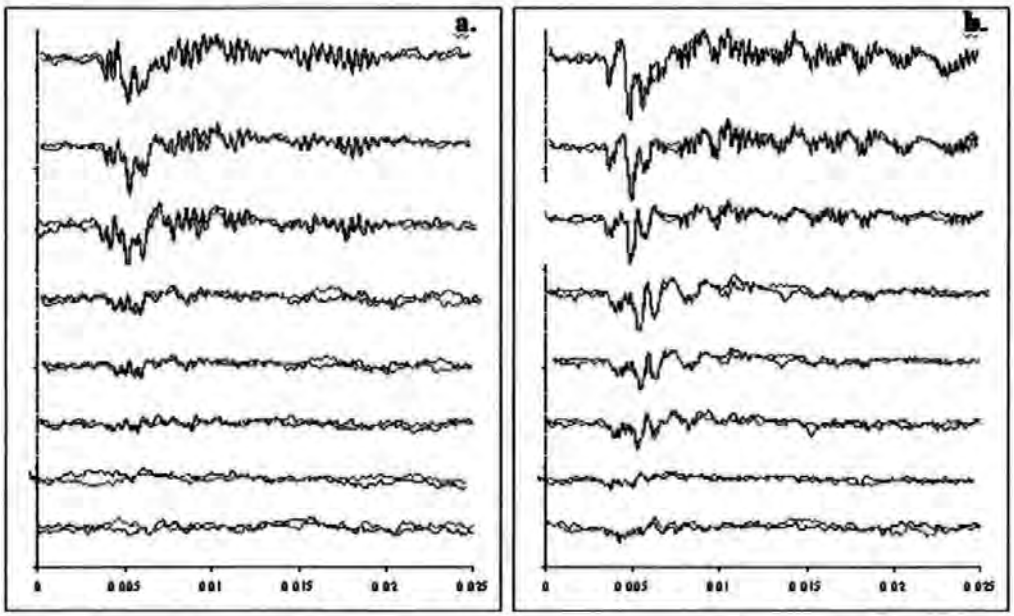

Figure 3.9. ABR response from *C. auratus* in response to **a.** a 1000 Hz tone, and **b.** a 1500 Hz tone burst. x-axis = time (s), y-axis scale bars are cropped for presentation so have no units

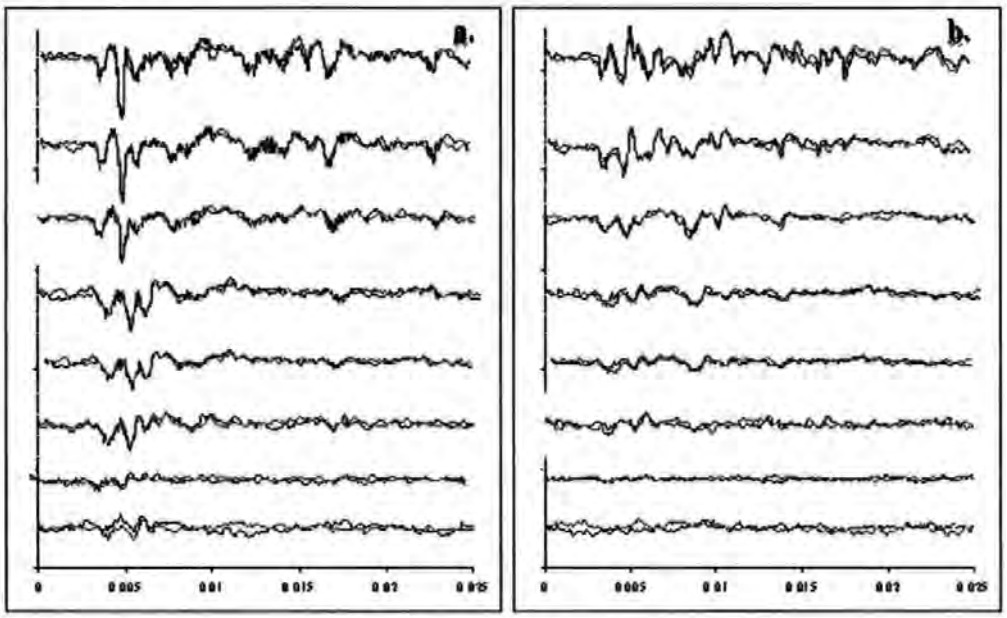

Figure 3.10. ABR response from *C. auratus* in response to **a.** a 2000 Hz tone, and **b.** a 3000 Hz tone burst. x-axis = time (s), y-axis scale bars are cropped for presentation so have no units

At each tone burst frequency the Inter Peak Latency (IPL) becomes shorter with decreasing stimulus intensity, in accordance with the findings of Overbeck and Church (1992). The evoked potentials presented in Figure 3.7 through 3.10, show an increase in latency with decreasing stimulus intensity. This phenomenon can only be observed when traces are arranged sequentially (Weber 1983), and are often used to validate ABR recordings, as

artefacts will not show any variation in latency. The audiogram presented in Figure 3.11 shows the intensity of tone bursts required to generate threshold evoked potentials from *C. auratus* (Figures 3.7 through 3.10), with sound pressures calibrated in accordance with Kenyon (1996). The audiogram for *C. auratus* by Kenyon, et al. (1998) has been included for comparison.

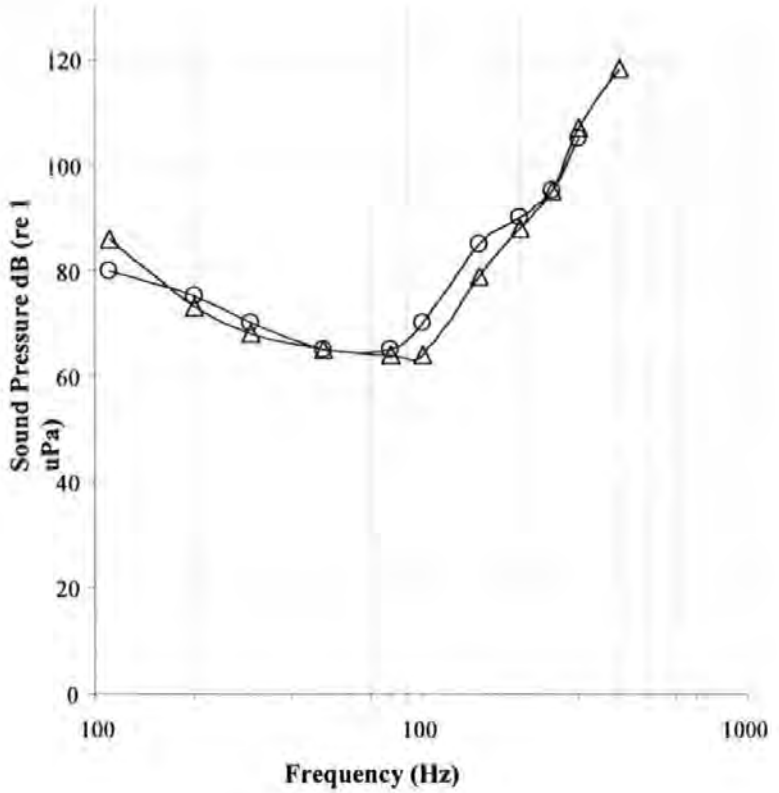

Figure 3.11. ABR generated audiogram for *C. auratus* from Kenyon et al. (1998) (triangles), and the audiogram produced in this study using the calibration factors defined by Kenyon (1996) (circles)

3.3.2 The function of the swim bladder in acoustic detection

Auditory perception by fish varies between species (Popper and Fay, 1993; Yan et al 2000), with most falling into the category of being either a hearing specialist or generalist. Specialists such as *C. auratus*, *H. molitrix* and *A. nobilis* have a connection between the swim bladder and inner ear, and are responsive to the sound pressure component of an acoustic signal measured here in units of dB re 1μPa. Generalists lack this connection and rely on the shear forces generated by a phase differential between the dense otolith and less dense surrounding medium to stimulate the sensory ciliary bundles found in the inner ear (Hawkins and MacLennan 1976; Yan 2000). Members of the superorder Otophysi (carp,

catfish etc) possess a series of bones or Weberian ossicles that couple the swim bladder with the inner ear. In a pressure field the swim bladder expands and contracts, and the motion is transmitted mechanically to the inner ear via the ossicles (von Frisch 1938; Fay and Popper 1974; Finneran and Hastings 2000). This system allows specialists to detect a wider bandwidth of frequency with greater sensitivity, when compared to generalist fish (Popper and Fay, 1993; Yan et al 2000). Other specialists include the Clupeiforms, with the herring *(Clupea harengus)* (Blaxter, Denton and Grey, 1981), and American shad (*Alosa*) (Popper, 1997) having been most thoroughly examined in respect of audition. These fish have a connecting sinus between the bullae, a hollow bone sphere located in the cranium of all Clupeids (Figure 3.12.a) and the swim bladder, indicating hearing specialisation. When sound waves reach the gas filled lower half of the bulla, vibrations occur in the bulla membrane (Figure 3.12.b) causing the sound energy to be transported along an elastic thread connected to the macula of the utricle (Blaxter et al, 1981). This specialisation of the inner ear mechanism offers an indication of the diversity of the hearing system between teleosts, since the primary auditory detection area for the Clupeids, is for example, within the utricle, rather than the saccular receptors common to the Otophysans and many other teleost orders.

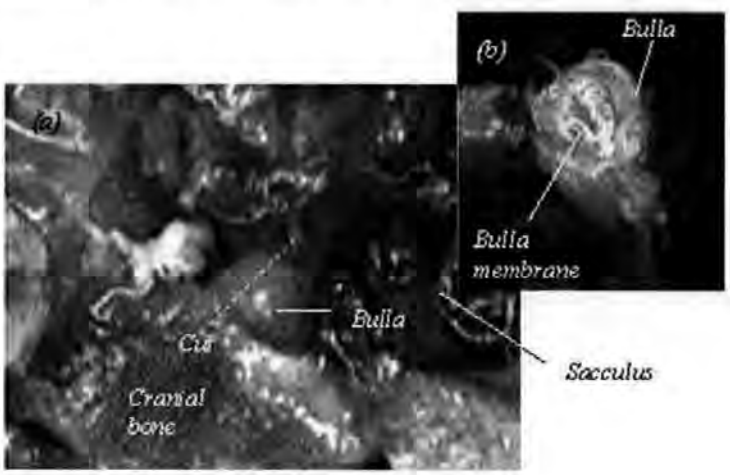

Figure 3.12. (a) Inner ear, bulla and (b) bulla membrane of the specialist allis shad (*Alosa alosa*) (Lovell, 1999)

For species with no specialised linkage between the swim bladder and inner ear, signals generated by fluctuations in the pressure field are subjected to substantial attenuation as they pass through flesh and bone from the swim bladder to the inner ear (Popper and Fay 1993; Yan et al 2000). The only published field study of fish audiometry using an electrophysiological approach was conducted by Enger and Andersen (1967), in a comparative study of audition in the cod (*Gadus morhua*) and the sculpin (*Cottus*

scorpious) in the open sea. After a series of experiments conducted mostly in the acoustic near field, that involved a highly complex surgical procedure to implant the electrodes, the authors conclude that the swim bladder of teleosts is essential for hearing in the acoustic far field. However, for species with no specialised mechanical linkage between the swim bladder and inner ear, signals generated by fluctuations in the pressure field are subjected to substantial attenuation as they pass through flesh and bone from the swim bladder to the inner ear (Popper and Fay 1993; Yan et al 2000).

It has been demonstrated (Yan et. al., 2000), that the removal of gas from the swim bladder of the generalist oyster toadfish (*Opsanus tau*) does not have any impact on hearing thresholds with the fish positioned at 2-5 mm below the water surface (e.g. Yan et. al., 2000). On the other hand, complete removal of gas from the swim bladder of *C. auratus*, a hearing specialist with a mechanical coupling between inner ear and swim bladder resulted in the significant elevation of hearing thresholds (Yan, et al., 2000). The initial volume of a swim bladder positioned at the water surface, at standard atmospheric pressure (Sleigh & MacDonald, 1972), can be calculated from the body mass (Yan et. al., 2000).

Figure 3.13 shows the ratio between Body Mass (BM) and the volume of the swim bladder (SB) from *C. auratus*. The amount of body volume that must be taken up by gas in order to achieve neutral buoyancy is dependent upon whether the fish is in fresh or marine water.

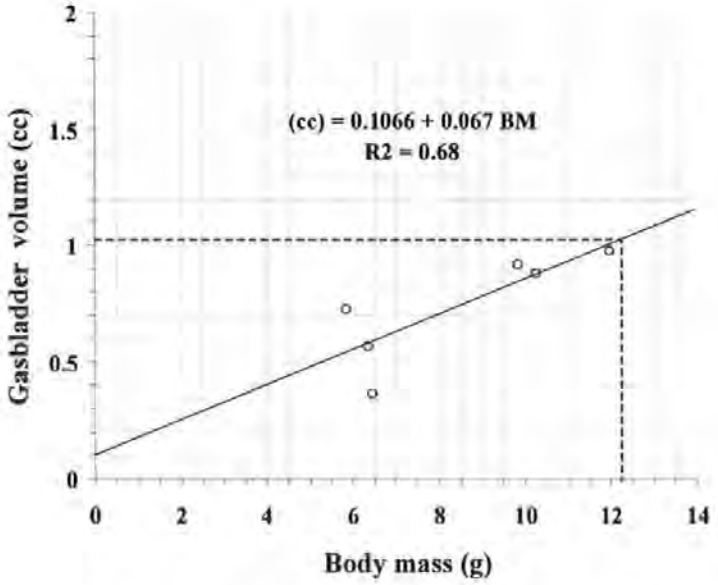

Figure 3.13. Swim bladder volume as a function of Body mass for *C. auratus*, (redrawn from Yan et. al., 2000). The hatched lines show the intersection between body mass and the volume of the swim bladder from a 12.3-g *C. auratus* used in this experiment

This is due ostensibly to the water density difference between the two environments; thus freshwater fish require a proportionally larger swim bladder than do marine fish to maintain neutral buoyancy. According to Figure 3.13, the volume of the swim bladder from *C. auratus*, at the water surface, is 11 % of the body volume.

At constant temperature, the volume of a gas varies inversely with absolute pressure, while the density of a gas varies directly with absolute pressure.

For any gas at a constant temperature, Boyle's Law is:

$$\mathbf{PV = K}$$

Where: P = absolute pressure, V = volume, and K = constant.

The formula that gives the pressure (p) exerted on an object submerged in a fluid is:

$$\mathbf{p = r * g * h}$$

Where: (rho) is the density of the fluid, g is the acceleration of gravity, and h is the height of the fluid above the object.

The pressure of fresh water exerted on an object submerged at a depth of 1 m (not accounting for atmospheric pressure) is:

$$\text{pfluid} = r * g * h = (999 \text{ kg/m3})\ (9.8 \text{ m/s2})\ (1 \text{ m})$$

$$= 9.79 \text{ kPa}$$

Calculation of the Swim Bladder Volume (SBV) with a loading of 9.79 kPa on a 12 g BM *C. auratus* under atmospheric pressure + 1-m of fresh water is:

$$(1.03 \text{ cc})(101.325 \text{ kPa})/(101.325 \text{ kPa} + 9.79 \text{ kPa})$$

$$\mathbf{= 0.94 \text{ cc at } 1 \text{ m} = 9 \text{ \% reduction in SBV}}$$

At a constant temperature, the volume of gas in the swim bladder varies inversely with absolute pressure, while the density varies directly with absolute pressure, in accordance

with Boyle's Law. The effect of this law is of importance to fish, as it defines the relationship between pressure and volume i.e., changes in depth = changes in the volume of the swim bladder. Figure 3.14 shows the relationship between the swim bladder volume of a 12-g *C. auratus*, and its relative depth in the water column.

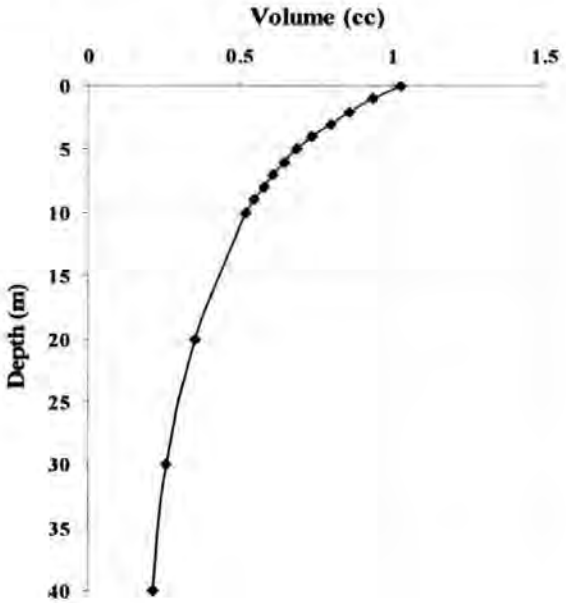

Figure 3.14. The relationship between depth in freshwater, and the volume of the swim bladder from a 12-g *C. auratus*, over a range of depths in the water column up to 40-m

The Auditory Evoked Potentials (AEPs) presented in Figure 3.15, are in response to a 500 Hz, four-cycle tone burst, presented to a 7.9 g *C. auratus*. The fish was first positioned on the water surface, and then lowered to a depth of 1 m. The stimulus sounds were presented in air, and measured with the fish at the water surface using an AZ 8928 digital sound level meter (giving results comparable to Kenyon et al., 1998). The tone bursts were presented initially at 90 dB (for frequencies of below 1000 Hz), and attenuated in 5 dB steps. Threshold responses from *C. auratus* were determined visually from the sequentially arranged waveforms for each frequency tested, in accordance with Kenyon et al (1998).

When two replicates of waveforms showed opposite polarities, or are dissimilar (see 60 dB in Figure 3.15.a, and 65 dB in 3.15.b), it is considered below threshold (c.f. Kenyon et al., 1998). The SPL of the tone bursts at threshold, for frequencies ranging from 300 Hz, to 3000 Hz, were recorded using a hydrophone which had been calibrated at the water surface using the sound pressure meter. The results of the audiological investigation are presented in the form of an audiogram or limn of spectral sensitivity (Figure 3.16), and reveals that the sound pressure levels required to evoke threshold AEPs, at each of the frequencies

tested. The start amplitude and attenuation steps were presented identically to the fish, when stationed both at the surface and at 1 m. The curves show that the response thresholds increased by between 5 to 10 dB over the range of frequencies tested.

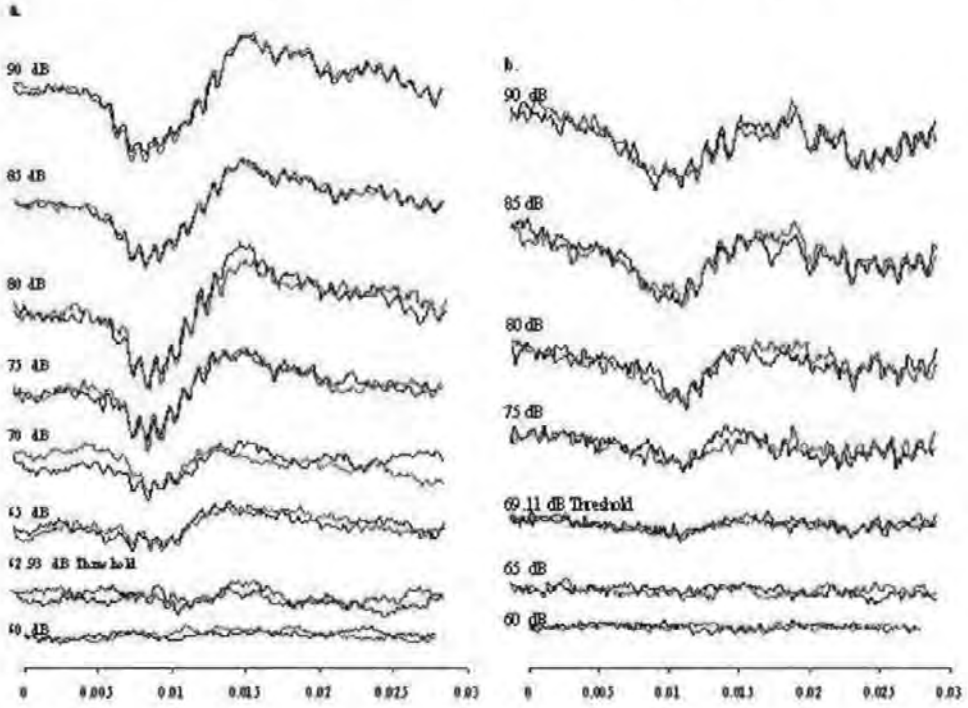

Figure 3.15 Auditory Evoked Potentials in response to a 500 Hz four cycle tone burst presented to *C. auratus*, positioned (a.) on the water surface, (b.) at a depth of 1 m, with the stimulus sounds presented in air

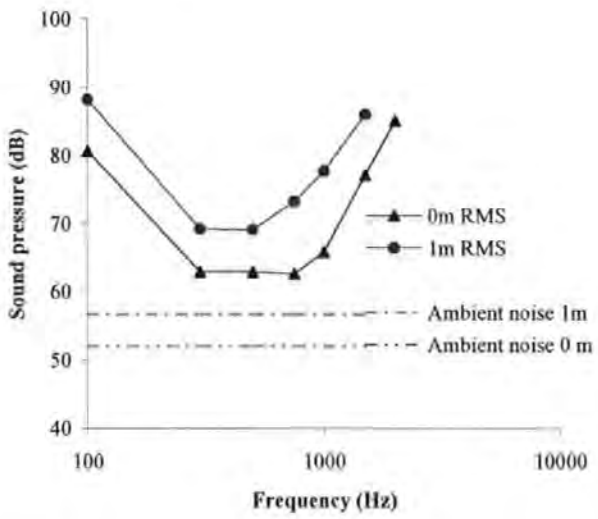

Figure 3.16 Stimulus intensities required to evoke threshold responses from *C. auratus*, with the fish on the water surface, and at a depth of 1 m

Threshold responses were not obtained at 1 m for frequencies above 1500 Hz, as the reflectivity of the water surface and rapid attenuation of the higher frequencies meant that the sounds would need to be presented at intensities outside of the operational range of the loudspeaker (in this experiment the sound was presented in air) and amplifier.

3.3.3 Audiogram for Silver carp (*Hypopthalmichthys molitrix*)

The ABR generated audiogram for the silver carp (*H. molitrix*) was produced in Illinois USA, using the equipment setup described in Figure 3.1. Figure 3.17 illustrates a typical set of acoustic brainstem responses to sound pressure at an insonification frequency of 500 Hz. The Figure presents traces acquired as the sound pressure level was successively atenuated; it may be seen that the responses vary from strong response to the sound to no discernible response. The lowest pressure of sound at which a response occurred was taken to be the auditory threshold.

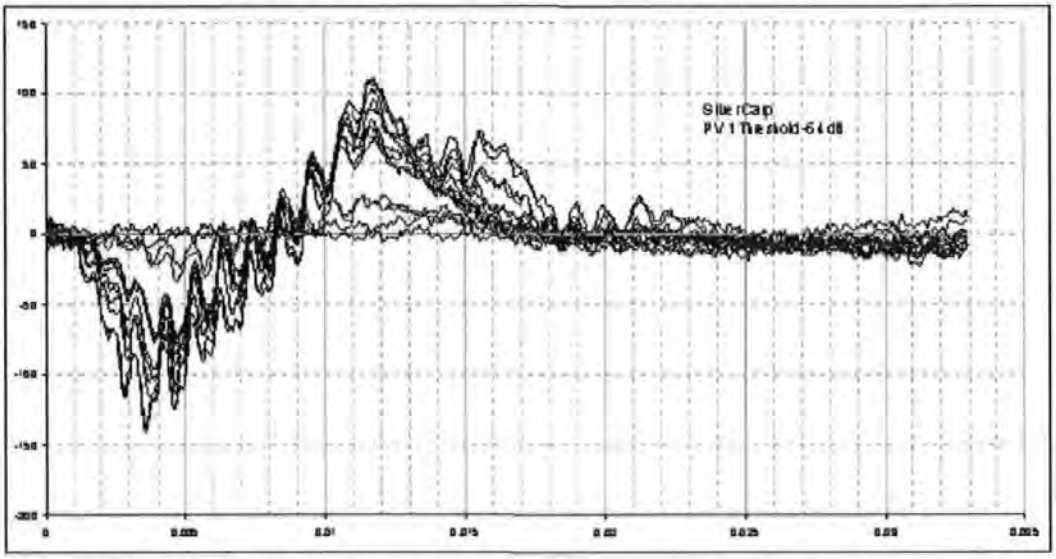

Figure 3.17 A typical set of acoustic brainstem responses to sound pressure for the Silver Carp (*H. molitrix*) at an insonification frequency of 500 Hz. x-axis = time (s), y-axis = Microvolts * 100

Figure 3.18 presents the audiogram found by visual inspection of the ABR traces from *H. molitrix*. The audiogram indicates the sound pressure level in dB (re. 1 μPa) at the threshold of hearing. It may be seen that the hearing is most sensitive (has the lowest threshold of hearing) at frequencies between about 500 Hz and 3 kHz, where the maximum hearing sensitivity is of the order of 105 dB (re. 1 μPa). At the higher frequencies, the hearing reduces sharply in sensitivity; the sensitivity also reduces more gradually for lower frequencies. It may be noted that the background noise level is lower than the recorded

thresholds of hearing, and hence it may be concluded that the audiograms are uncontaminated by background noise, and both *H. molitrix* and *A. nobilis* follow a similar Gaussian profile.

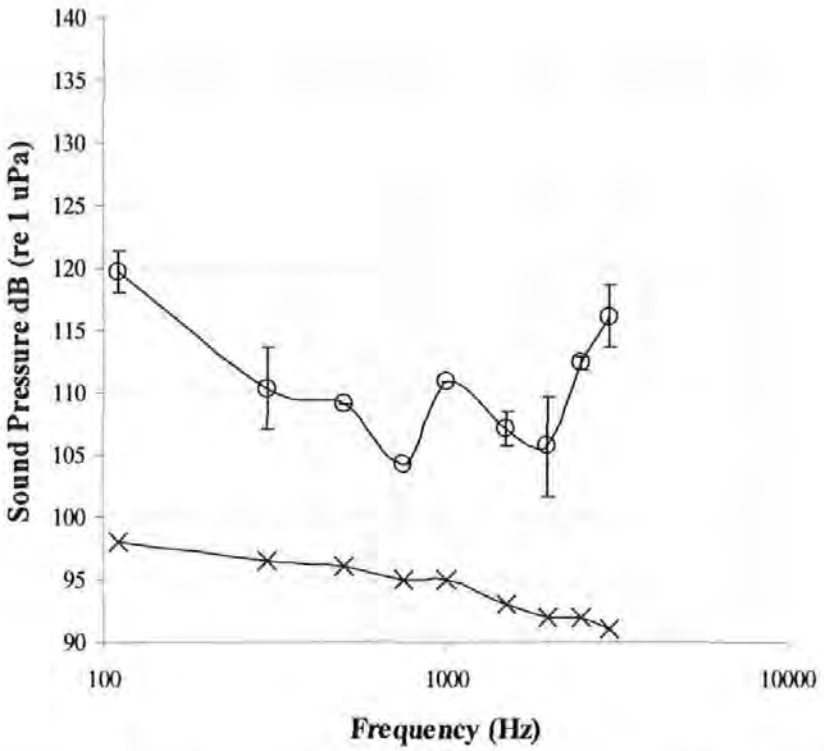

Figure 3.18. The audiogram (sound pressure level at threshold of hearing in units of dB (re. 1 μPa) of the Silver Carp (*H. molitrix*), the lower line (x) represents the ambient noise level in the test tank. Y error bars show the standard deviation of the data

3.3.4 The audiogram of the Bighead Carp (*Aristichthys nobilis*)

The ABR generated audiogram for the bighead carp (*A. nobilis*) was also produced in Illinois USA, as part of the AFD barrier project. Figure 3.19 illustrates a typical set of acoustic brainstem responses from *A. nobilis* to sound pressure at an insonification frequency of 500 Hz. The form of the traces is similar to that of *H. molitrix*, however the threshold of hearing was found to be at generally slightly lower levels of sound.

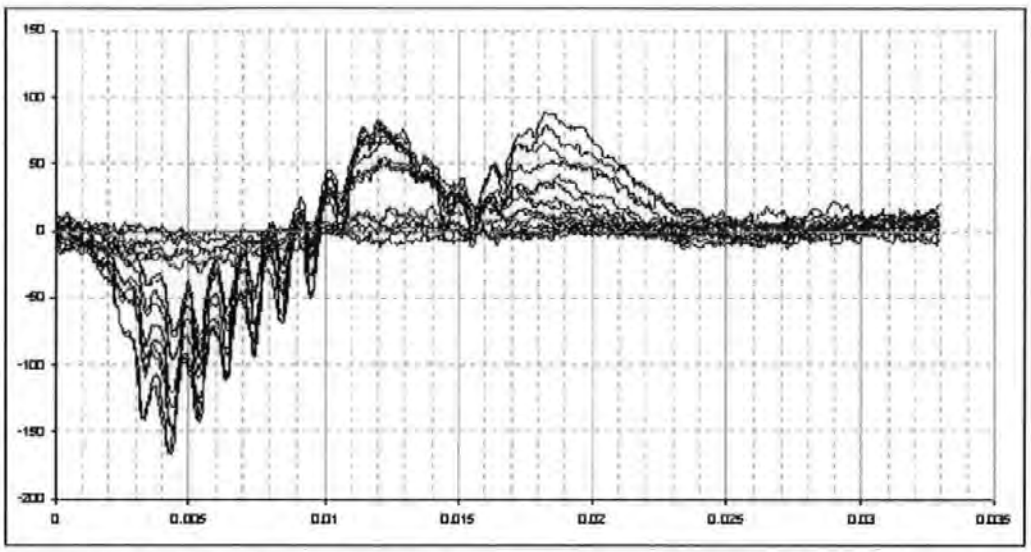

Figure 3.19 A typical set of ABR waveforms to sound pressure for the Bighead Carp (*A. nobilis*) at an insonification frequency of 500 Hz. x-axis = time (s), y-axis = Microvolts * 100

Figure 3.20 presents the audiogram in units of sound pressure (dB re 1 μPa) determined by visual inspection of the ABR traces from *A. nobilis* at the threshold of hearing. The hearing peaks in sensitivity at a frequency of about 1500 Hz, where *A. nobilis* has its lowest threshold of hearing, at a sound pressure level of about 106 dB re 1 μPa.

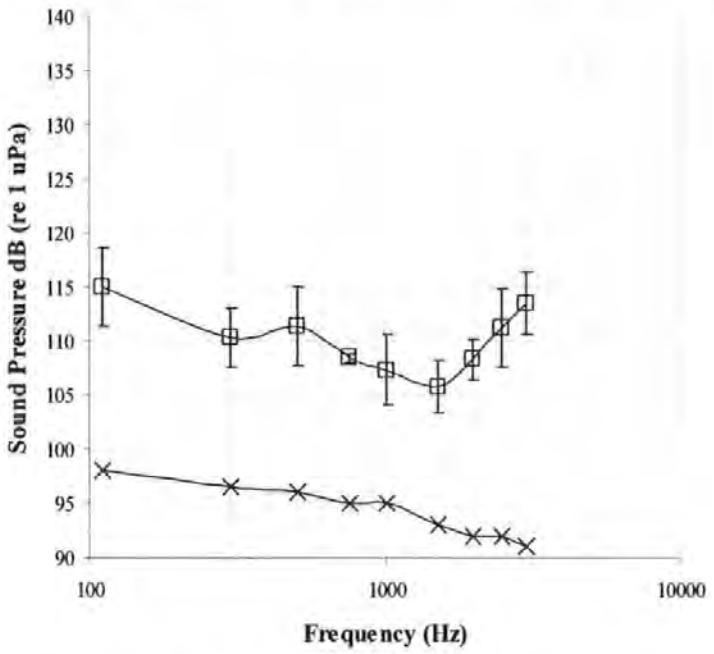

Figure 3.20 The audiogram (sound pressure level at the threshold of hearing in dB (re. 1 μPa)) for the Bighead Carp (*A. nobilis*), the lower line (x) represents the ambient noise level in the test tank. Y error bars show the standard deviation of the data

3.4 Chapter discussion and conclusions

The comparability of the goldfish audiograms produced in this study, with published works (e.g. Kenyon et al., 1998), provides a benchmark for the accuracy of the ABR system when measuring AEP's from fish with the transducer fixed in air. However, ABR has not previously been used in conjunction with submerged transducers and brings into question auditory data from other established methodologies, which do not faithfully emulate the transmission of sound sources integral to the AFD barrier or other device used as part of a management strategy.

The hearing thresholds of silver carp (*H. molitrix*) and bighead carp (*A. nobilis*) are presented in an audiogram as the lowest levels of sound pressure as a function of frequency that evoked a repeatable threshold response. The audiograms produced for the two Asian carp species is comparable in frequency bandwidth (though with slightly higher thresholds), to the audiogram for the specialist channel catfish (*I. punctatus*) produced by Fay and Popper (1975) in an electrophysiological study of fish audition using an air mounted transducer. Figure 3.21 presents the audiograms of both *H. molitrix* and *A. nobilis*, which are presented along with the audiogram for *I. punctatus* from Fay and Popper (1975).

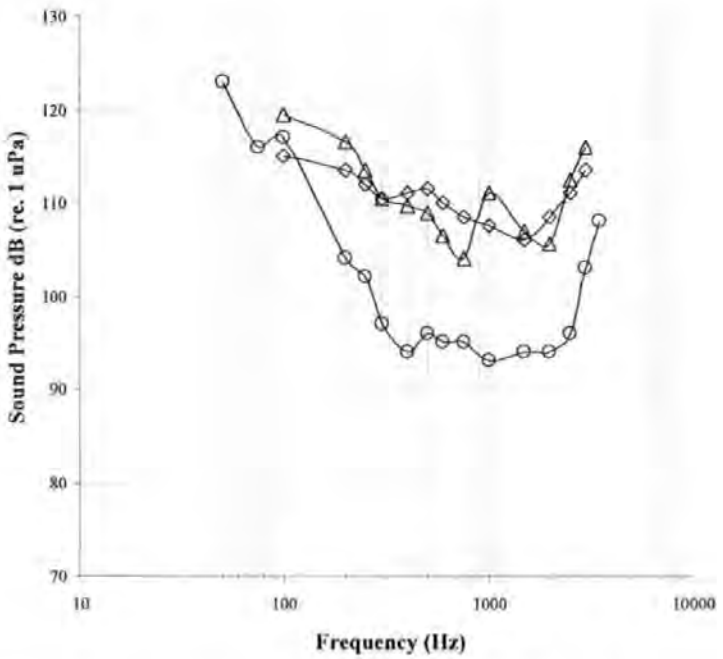

Figure 3.21 Comparison of the audiogram for *I. punctatus* (Popper and Fay (1975) (circles), and the calibrated audiograms (B&K hydrophone) for *H. molitrix* (triangles) and *A. nobilis* (diamonds)

Figure 3.21 shows that hearing thresholds from *H. molitrix* and *A. nobilis* are moderately higher than thresholds obtained from *I. punctatus*. It is probable that the higher thresholds recorded is, in part, due to the hearing of the two carp species being more acute than the lowest level of sound that the submerged transducers used in this study can consistently generate. In an attempt to stabilise the sound field at low intensities, the projectors were driven with load resistors placed between the amplifier and projector. To counter this problem, a number of published studies of specialist fish hearing (c.f. Fay and Popper, 1975, Kenyon et al., 1998), have used air mounted transducers to generate underwater sound fields below the threshold of hearing. However, in this instance, the use of submerged transducers is the most appropriate stimulus generating methodology (rather than air mounted transducers), as the sound field in the test tank is produced using the same type of transducer as is used in the AFD barrier. Thus, the sound transmission methodology is arguably closely representative of sources used in aquatic management strategies, thereby providing a more reliable approach to the acquisition of auditory information for practical "field" applications.

The experiment described in section 3.4.4 shows that in *C. auratus*, hearing thresholds elevate with increasing loading on the swim bladder. This effect has, in part, been demonstrated by Yan, et al. (2000), who found an increase in thresholds after removal of gas from the organ, however, this is the first time that the effect of pressure loading on the swim bladder has been measured by increasing the depth of the fish in the experimental tank. In the present experiment, the goldfish was lowered to a depth of 1 m, in a 200 l tank, and gives a more realistic effect of swim bladder loading on the sensory pathway. The subsequent water pressure loading on the swim bladder at this depth (in fresh water), is known to reduce the volume of the organ by 9 %, in accordance with Boyle's law. This reduction in the GBV was found to have a small, but measurable affect on threshold AEP's recorded from *C. auratus*, which increased by approximately 5 dB when the fish was positioned at a depth of 1 m from the water surface (resulting in a swim bladder volume reduction of 9 %). It was found (Yan et. al., 2000), that the complete removal of gas from swim bladder of *C. auratus* resulted in a 60 dB elevation in the hearing thresholds. It is concluded, that accurate and comparable threshold AEP's can be obtained from various sized fish, stationed both at the water surface and at least 1 m below it, and that the subsequent reduction in swim bladder volume has a small but measurable effect on the hearing abilities of *C. auratus*, again confirming the accuracy of the ABR system. It is known that the acquisition of concise auditory information from generalist fish using

behavioural methods is often challenging (Kenyon et al., 1998); thus, it remains to be shown if the ABR system used in this study is capable of recording threshold responses from generalist fish. As has already been mentioned, generalists have a narrower bandwidth and higher thresholds of hearing than the specialists, and the performance of the system at higher stimulus intensities is explored in the next chapter.

Chapter 4

The hearing abilities of bony generalist fish

4.1 Introduction

As discussed in the previous chapter, specialist fish hear sounds ranging in frequency between 50 Hz or so, to as much as 5000 Hz, at intensities of around 65 dB (re 1 μPa), which they detect through a mechanical coupling between the swim bladder and inner ear. Generalist fish lack this coupling, and are considered as having considerably higher hearing thresholds, and a narrower frequency detection bandwidth than the specialists. This Chapter sets out to examine the morphology of the inner ear, and determine the hearing abilities of the European sea bass (*Dicentrarchus labrax*). This species has been selected to represent bony generalist fish in this study, due principally to there being no concise auditory data for this species in the literature, even though it is an important fish to both recreational and commercial fisheries (Pickett, et al., 1995). The distribution and polarisation of the afferent receptors found in the otolithic end organs are also investigated using Scanning and Transmission Electron Microscopy (SEM and TEM), to show that *D. labrax* has an ear that conforms to the standard configuration of generalist fish. Several authors (e.g. Platt & Popper, 1984; Popper, 1981; Yan et al., 1991) have used the Scanning Electron Microscope (SEM) to study surface detail of the inner ear ultrastructure, and this was the approach adopted here. In the second series of experiments described in this Chapter, the hearing abilities of *D. labrax* in a sound field dominated by sound pressure are defined using ABR audiometry, using air mounted transducers and a setup similar to Kenyon et al., (1998), with the exception that the fish and recording equipment are not in faraday conditions. The acquisition of comparable results from *D. labrax* with published audiograms for generalist fish (c.f. Casper et al., 2003; Kenyon et al., 1998) will allow for the assessment of the accuracy of the system outside of controlled conditions, when using relatively loud stimulus sounds compared to the audiological tests of the specialist fish.

4.2 Materials and methods

4.2.1 SEM preparation

Six fresh *D. labrax* heads taken from individuals ranging in size from 70 mm (9 g) to 200 mm (90 g) were acquired locally from the commercial fishing sector, and trimmed to small blocks containing both ears. The cranial cavity was then opened dorsally and the brain removed by dissection and aspiration. Chilled fixative (2.5% glutaraldehyde in 0.1 M cacodylate buffer with 3.5% sodium chloride) was perfused into the sacculi, and vented through a small incision in the chamber wall, located well away from the needle entry point and macula. The ears and surrounding tissue were subsequently immersed in chilled fixative for 48 hours prior to dissection of the pars inferior from the remaining cranium. The sacculi and integral macula was washed from the surface of the sagitta using a pipette and a small quantity of excess fixative. The otolith capsules were then dehydrated through a graded ethanol series ranging from 35% through 50%, 70% and 90% to absolute ethanol, prior to desiccation using the critical point drying method described by Platt (1977). Fully desiccated otolith capsules were subsequently mounted on a specimen stub using a carbon tab, and coated with c. 8 nm of gold in an Emitech K 550 sputter coater (working at approximately 5 x 10^{-6} Torr). Finally, the processed specimens were investigated and photographed using a JOEL JSM 5600 scanning electron microscope operated at 15 kv, and a 15 mm working distance.

The orientation of an inner ear hair cell is defined by drawing a line using the JOEL software, from the shorter ciliary bundles towards the longer kinocilium. This procedure was applied and repeated across the surface of the macula at 100-micron intervals, or when there was an abrupt change in hair cell orientation. The line dividing cells with opposing orientations were mapped using a 1000 x magnification electron micrograph montage in accordance with Platt (1977). Images of the ultrastructure were captured using the JOEL software, which saved the micrographs in a bitmap format. The micrographs were then examined using the image analysis software, "ImageJ", which was calibrated using scale markers provided by the JOEL software. Measurements of the ultrastructure were made by drawing a line across an area of interest using the ImageJ drag tool. The software then calculates the number of pixels in the selection and displays either point to point or area data as text, which was entered into an Excel spreadsheet for further analysis. Measurements of hair cell dimensions (height, width etc) unless otherwise stated, are averages taken from at least 12 observations within a similarly orientated cell cluster.

4.2.2 ABR methodology

The procedure used to acquire the evoked potentials was approved by the United Kingdom Home Office. Specimens of *D. labrax* were placed into a flexible cradle formed from plastic mesh and a soft foam rectangle saturated with seawater (see Figure 1.a and b. for photograph of the experimental equipment). Oxygenated seawater kept at a temperature of 18° C was gravity fed to *D. labrax* at an adjustable flow rate of 6 millilitres per second. The water was held in an aerated reservoir positioned in an adjacent room, and fed to the front of the foam "cradle" through a 10 mm diameter plastic tube. Water was able to flow around the fish and vent through an aperture positioned at the rear of the foam cradle; thus the fish was able to ventilate its gills by simply opening and closing its mouth. The foam cradle was placed in a second tank L. 450 mm x W. 300 mm x D. 200 mm, and supported using a clamp to keep the nape of the fish's head 1mm above the surface of the water. The experimental tank was placed on a table with vibration inhibiting properties, located in an underground anechoic chamber L. 3 m x W. 2 m x H. 2 m. After the hearing assessment, the fish were relocated to a holding tank for observation, prior to being returned to a non-experimental aquarium.

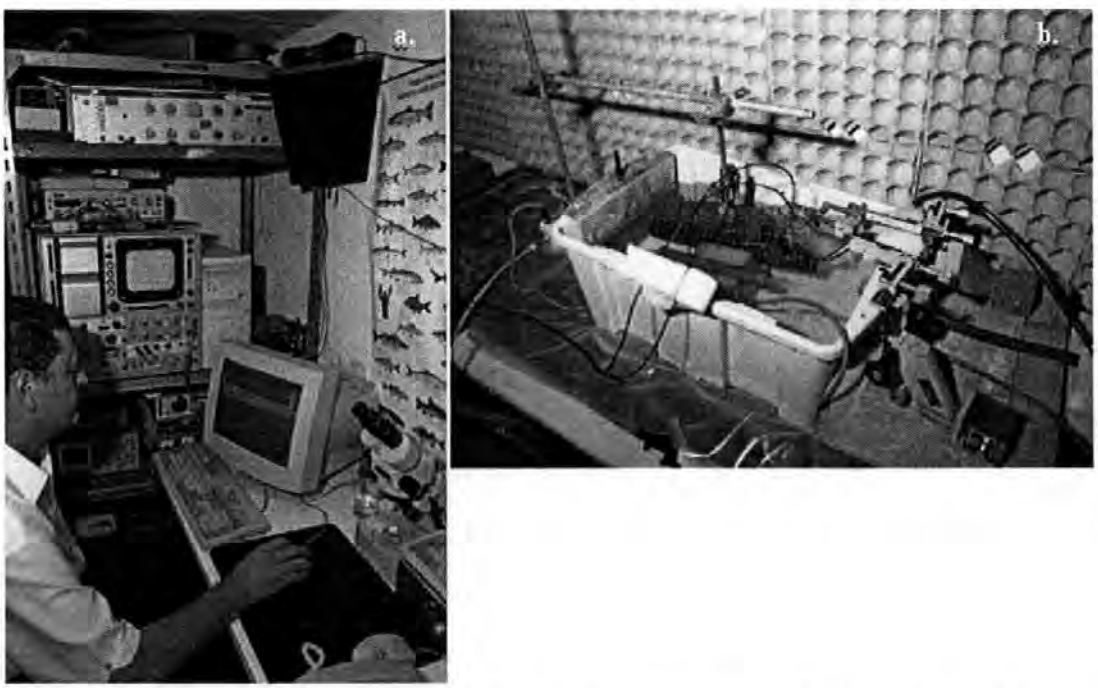

Figure 4.1.a The ABR control room in Plymouth, and **b.** the specimen and one of the test tanks located in an adjacent room

The stimulus sound was generated using a PC and presented to the fish (Figure 4.1.b), at initial sound pressures not exceeding 150 dB re 1 μPa (determined using the Bruel and

Kjaer hydrophone detailed in Chapter 3). Amplification of the sound was achieved using a Pioneer type SA-420 amplifier and a 200 mm Eagle L032 loudspeaker with a frequency response range of 40 Hz to 18 kHz. Additionally, the transducer was placed inside a Faraday cage and connected to a centralised earth point located in an adjacent room where the PC, amplification, and analysis equipment was set up. Connecting wires were fed through a 100 mm port in the partitioning wall. The electrophysiological response of the fish to acoustic stimulation was recorded using the two cutaneous electrodes described in Chapter 3.

4.3 Results

4.3.1 Anatomy of the hearing system of the bass (*D. labrax*)

Skin attached to the roof of the mouth was removed along with the eyes and any additional flesh, producing a clear unobstructed view of the lower cranium and saccular chambers (detailed in Figure 4.4). The bone ridge separating the eyes and continuing between the saccular chambers was cut and pulled away from the head, revealing a continuation of the divide between the left and right chamber. In *D. labrax*, the separation is especially prevalent, and extends near to the ventral plate of the cranial cavity. The head was trimmed to a small block containing both ears, and the cranial cavity was opened dorsally and the brain removed by dissection and aspiration. Chilled fixative (2.5% glutaraldehyde in 0.1 M cacodylate buffer with 3.5% sodium chloride) was perfused into the sacculi, and vented through a small incision in the chamber wall located well away from the needle entry point and macula. The ears and surrounding tissue were subsequently immersed in chilled fixative for 48 hours prior to dissection of the inner ear from the cranium.

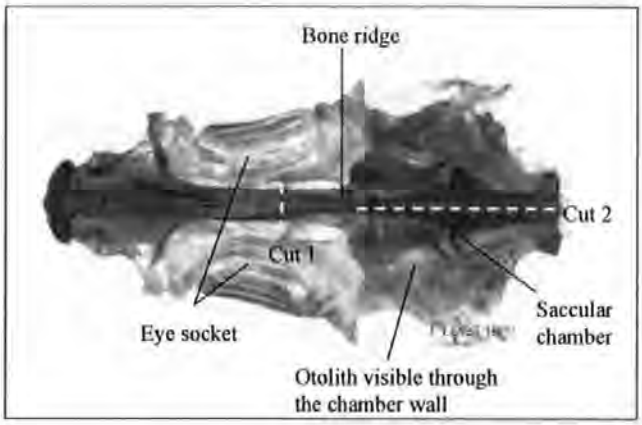

Figure 4.4. The skull of *D. labrax* (*Dicentrarchus labrax*) showing the saccular chamber and location of the initial preparation cuts (adapted from Lovell 1999)

Close inspection of the cranial cavity and inner ear of *D. labrax* did not reveal any evidence of a connection Weberian or otherwise between the swim bladder or other ancillary air reservoir and the inner ear, showing that *D. labrax* is a hearing generalist, reliant on the phase differential between the otolith and sensory macula to stimulate sensory ciliary bundles.

The left ear (Figure 4.5) was dissected in two parts from the remaining cranium and placed into a clear glass dish containing chilled fixative and photographed to reveal the gross morphological layout, prior to SEM preparation. The three canals protruding at right angles from the labyrinth of the pars superior, are known collectively as the semicircular canals (Retzius 1881). Endolymph circulates freely through the canals, all of which institute from either the anterior or posterior ampulla of the utricle. Inside the ampulla is a saddle shaped cristae that partially covers the floor of the organ, which is made up of exceptionally long sensory ciliary bundles and a gelatinous cupula. The cupula and sensory ciliary bundles occlude the ampulla, and movement of endolymph deforms the cupula stimulating the embedded sensory ciliary bundles (Platt and Popper 1981).

The cristae are sensitive to angular accelerations and function in the maintenance of equilibrium and orientation (Romer and Parsons, 1977), though the utricular otolith (lapillus) may also participate in sound reception in some species (Blaxter et al 1981; Popper 1983). The anterior and posterior canals connect to the utricle via the anterior and posterior ampullas, rising with angularity to combine at the apex of the sinus superior. The sinus superior descends vertically into a central region of the vestibule near the endolymphatic duct (Retzius 1881). The external canal however, is positioned horizontally

and paired with anterior and posterior ampullas. The three canal configuration is common to all jawed fish, whilst lampreys have two canals and hagfish have only one (Romer and Parsons, 1977).

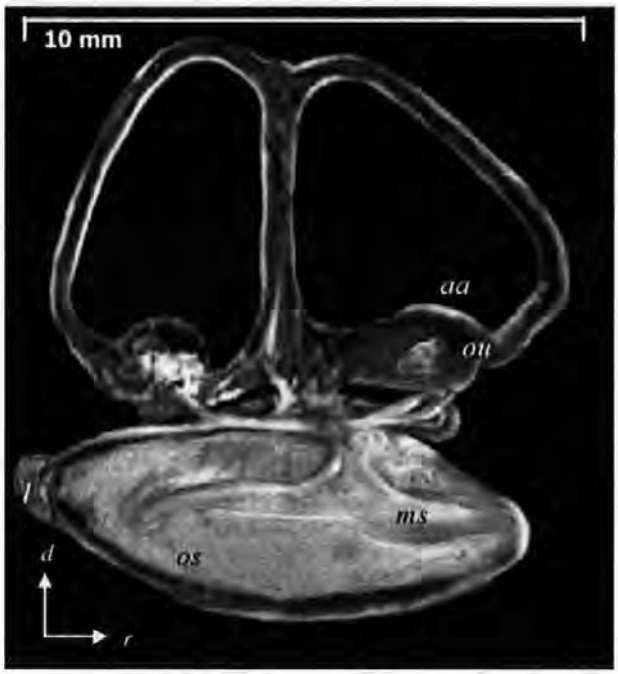

Figure 4.5. Composite of the dissected inner ear from *D. labrax, aa* - anterior ampulla, l – lagena, *ms* – macula of the saccule, *os* – otolith sagitta, *ou* – otolith utricle (lapillus).

In vertebrates, the VIII nerve institutes from the end-organs of the inner ear, and terminates in the octavolateralis area of the medulla (Northcutt, 1981; Bell, 1981; Lovell 1999). This is in agreement with Figure 4.6 which shows the gross anatomical layout of the brain and the peripheral pathway of VIII nerve ganglion from *D. labrax*, dissected by the author as part of an earlier work. Apical hair bundles protrude from the macula and contact the otolith within the medial sulcus depression, and are often surrounded by a gelatinous otolith membrane (Platt and Popper, 1981). Transduction from mechanical to electrochemical energy is dependant on shear forces bending the stereocilia toward or away from the kinocilium, and results in the opening of membrane channels prompting an increase in the flow of sodium (Na^+) and potassium (K^+) outward across the cellular membrane (Platt and Popper 1981).

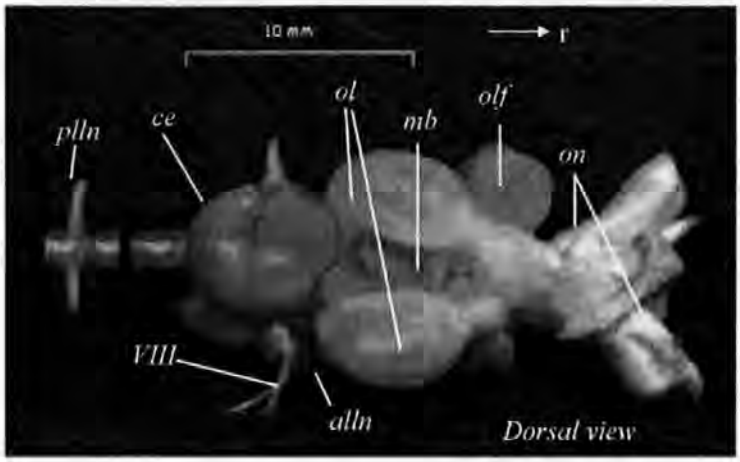

Figure 4.6 Gross anatomy of the brain from *D. labrax*, showing the VIII octavel nerve terminating in the acousticolateralis area of the medulla, *alln* - anterior lateral line nerve, *ce* - cerebellum, *mb* – midbrain, *ol* - optic lobe, *olf* - olfactory lobe, *on* - optic nerve, *plln* - posterior lateral line nerve, *VIII* - octaval nerve (from Lovell 1999)

Many specialist fish have saccular ciliary bundles orientated vertically in two diametrically opposed quadrants (Popper, 1980), whereas most generalists have ciliary bundles orientated both horizontally and vertically in four to six quadrants (Popper and Fay 1993).

The ability of fish to directionally locate the source of a sound has been demonstrated (Sand 1973; Enger, 1976), who theorised that ciliary bundles in generalists have an axis of maximal sensitivity to vibration. Scanning electron microscopy has revealed that there is evidence of a correlation between the morphological polarisation of the saccular receptors and the magnitude of the electrophysiological response to a sound vector (Popper and Fay 1993).

4.3.2 Results of EMC study of hair cell polarities in the ear of *D. labrax*

The view of the saccular macula from the left ear of *D. labrax* (Figure 4.7) was scanned at a magnification of x 50, and annotated to show the overall orientation of the ciliary bundles found in each quadrant as viewed perpendicular to the macula surface. The four quadrants were sub-divided into five sectors and studied at magnification factors of between 1000 x and 5000 x. Detail of the ciliary bundles and their respective orientations can be seen in Figures 4.8 through 4.11, which were scanned at a magnification of 5000 x. Cells of similar bundle size and orientation occupied large areas of the epithelia, often separated

from cells with alternate orientation and size by a narrow transitional zone. Several micrographs, each of between four to ten cells, were taken within each of the larger regions, away from the transitional zones. The polarisation of ciliary bundles in the saccular macula are depicted by the white arrows in Figure 4.7, and reveal that *D. labrax* possesses a standard orientation pattern in common with other hearing generalist fish from the order Perciformes (Platt and Popper 1981; Popper and Fay 1993). The saccular ciliary bundles are divided into four discrete orientation groups (Figures 4.8 through 4.11), with ciliary bundles in each group orientated in the same direction. The polarisation of ciliary bundles in the rostral locus or ostium of the macula are divided into two regions, with caudally-orientated hair cell groups on the dorsal half of the macula, and rostrually-orientated groups on the ventral portion. Ciliary bundles on the caudal locus of the saccular macula are orientated dorsally in the dorsal region and ventrally in the ventral region.

Figure 4.7. Orientation of ciliary bundles on the left ear saccular epithelium of *Dicentrarchus labrax*, orientated horizontally 1 and 2, and vertically 3 and 4 in diametrically opposed quadrants; showing that *D. labrax* is a hearing generalist with standard orientation ciliary bundles.

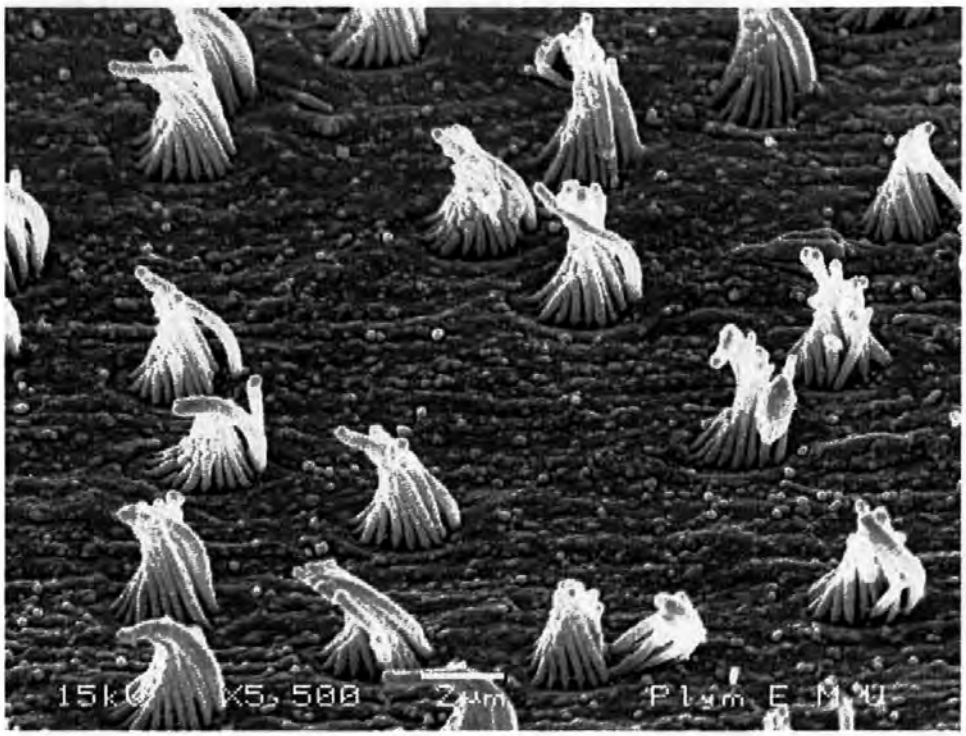

Figure 4.8. Scanning electron micrograph showing the ciliary bundles from quadrant 1

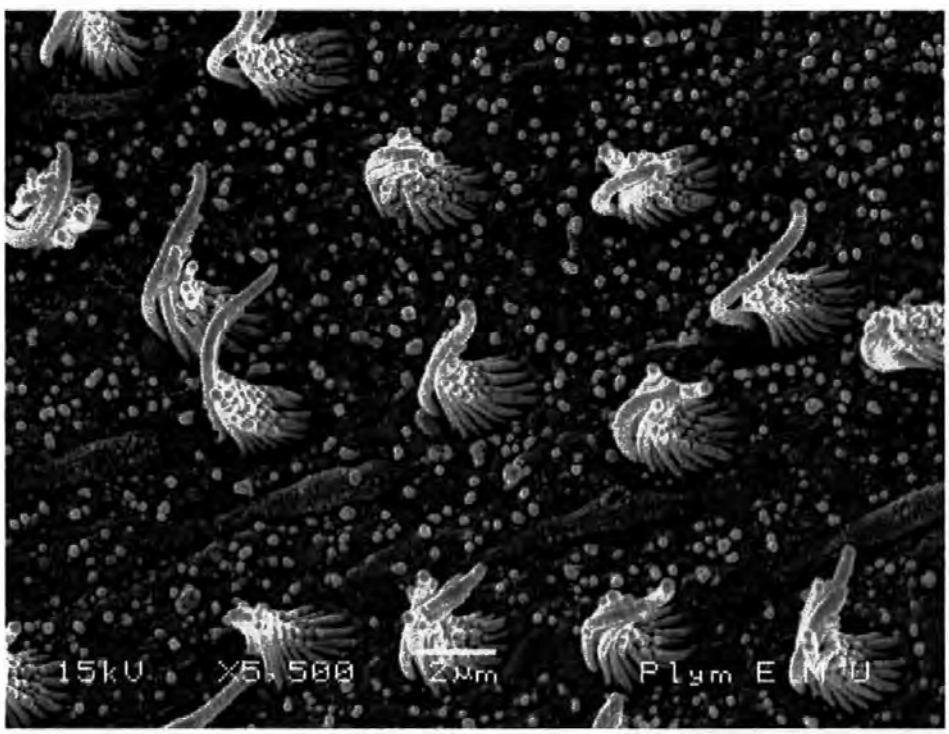

Figure 4.9 Scanning electron micrograph of ciliary bundles from quadrant 2

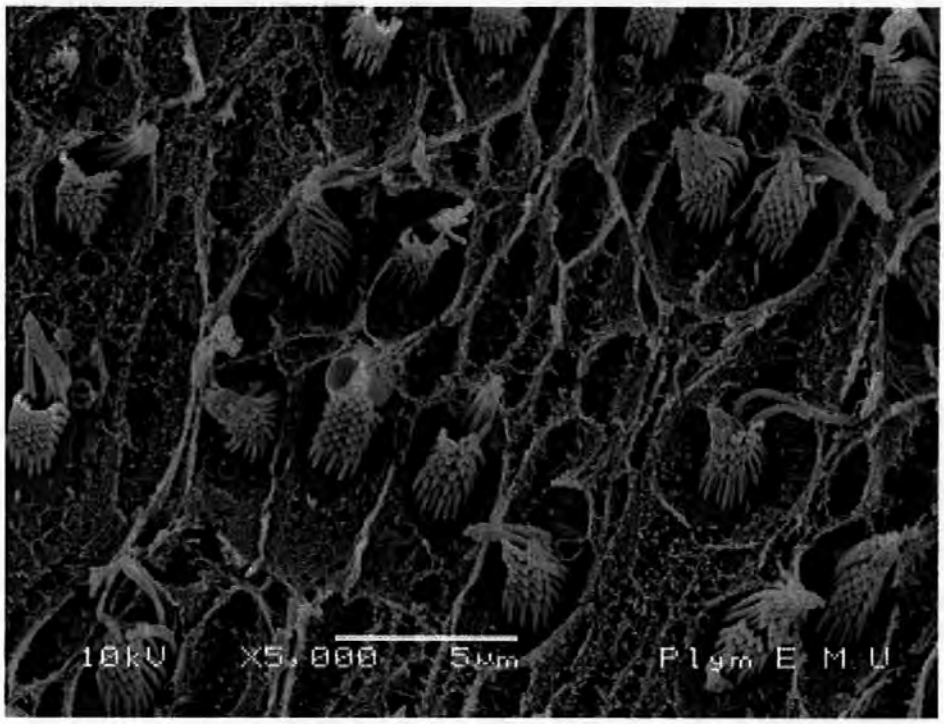

Figure 4.10 Ciliary bundles from quadrant 3

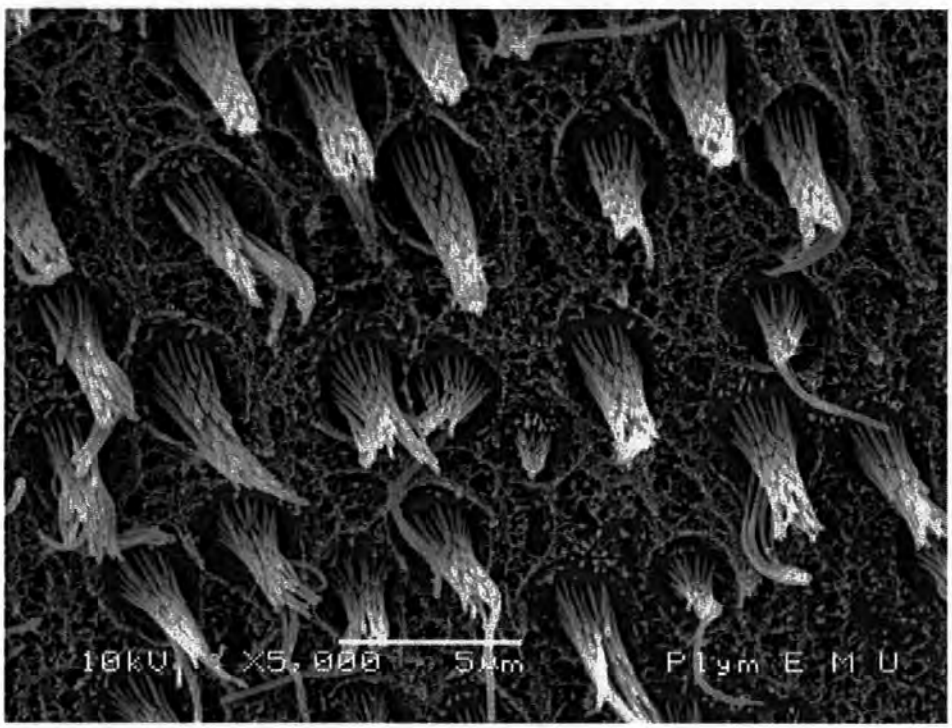

Figure 4.11 Ciliary bundles from quadrant 4

The saccular macula from three *D. labrax* with fork lengths of 170 mm (90 g) 126 mm (53 g) and 72 mm (9.4 g) were examined by EMC, and measurements of the macula and ciliary bundles were calculated by using the ImageJ software. Figure 4.12 shows the outline of

the regions of the macula bearing ciliary bundles from both the left and right ears of the three fish.

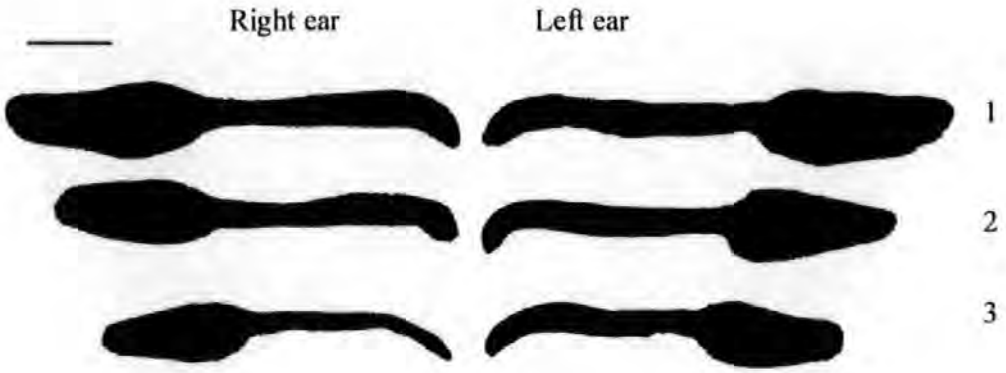

Figure 4.12 Outline of the saccular macula from the left and right ears taken from *D. labrax* with fork lengths of (1) 170 mm, (2) 126 mm and (3) 72 mm (Bar = 1 mm)

The total area of macula from each fish is presented in table 4.1, and was found to be 3.073 mm^2 for the right ear, and 3.219 for the left ear of the 170 mm fish, 2.415 mm^2 for the right and 2.555 mm^2 for the left ear of the 126 mm fish, and 1.58 mm^2 for the right and 1.722 mm^2 for the left ear of the 72 mm fish.

Table 4.1. Results generated by the ImageJ software of the macula area for the left and right ears of the three sizes of fish

	Right ear		Left ear	
Fish length (mm)	Area (mm^2)	Perimeter (mm)	Area (mm^2)	Perimeter (mm)
170	3.073	12.743	3.219	13.065
126	2.415	11.183	2.555	11.677
72	1.572	9.542	1.722	9.803

In order to test the hypothesis that the numbers of ciliary bundles increases with age, measurements of the spacing between ciliary bundles in the dorso-rosteral quadrant of the macula in both x and y coordinates were made. These data were fed into a one-way ANOVA, the results of which are shown in tables 4.2 and 4.3.

Table 4.2. Results of the One-way ANOVA used to test for similarity in receptor cell spacing along the x axis from 3 sizes of fish. Measurements in μm

Analysis of the Variance in the distance between ciliary bundles along the X axis					
Source	DF	SS	MS	F	P
C1	2	7.70	3.85	1.80	0.181
Error	33	70.40	2.13		
Total	35	78.10			
				Individual 95% CIs For Mean	
				Based on Pooled StDev	
Level	N	Mean	StDev	---+---------+---------+---------+---	
1	12	6.233	1.180	(----------*----------)	
2	12	7.287	2.020	(----------*----------)	
3	12	6.402	0.963	(----------*----------)	
				---+---------+---------+---------+---	
Pooled StDev =		1.461		5.60	6.40 7.20 8.00

The P value of 0.181 given by the ANOVA in Table 4.2 suggests that the distance between cells on the dorso-ventral (x) axis, remains constant throughout the development of *D. labrax* from fingerling to the juvenile stages of the life cycle.

Table 4.3. Results of the One-way ANOVA used to test for similarity in receptor cell spacing along the y axis from the 3 sizes of fish. Measurements in μm

Analysis of Variance in the distance between ciliary bundles along the y axis					
Source	DF	SS	MS	F	P
C1	2	19.38	9.69	3.71	0.035
Error	33	86.27	2.61		
Total	35	105.65			
				Individual 95% CIs For Mean	
				Based on Pooled StDev	
Level	N	Mean	StDev	-+---------+---------+---------+-----	
1	12	6.583	2.297	(--------*--------)	
2	12	6.361	1.185	(--------*--------)	
3	12	4.928	1.078	(--------*--------)	
				-+---------+---------+---------+-----	
Pooled StDev =		1.617		4.0	5.0 6.0 7.0

The P value of 0.035 (Table 4.3) shows that there is some evidence that the ciliary bundles will acquire more lateral spacing along the y axis as *D. labrax* grows, though distortions occurring during the critical point drying process may have a slight influence on the y axis results.

The length of the kinocilia from cells in each quadrant of the sensory area were measured using the ImageJ software, the summaries of the measurements from each quadrant are presented in Table 4.4.

Table 4.4. Summaries of average kinocilia lengths from each of the four quadrants of the saccular epithelium from a 126 mm *D. labrax* (measurements in μm)

Quadrant	1	2	3	4
Mean	3.613	3.849	2.429	3.197
SD	0.332	0.605	0.528	0.553
Min	3.214	3.278	1.674	2.214
Max	4.267	4.85	3.292	3.819

The lagena is the second of the end organs found in the pars inferior, and in *D. labrax* it is approximately 1/30th the size of the saccule. The lagena is attached to the caudal end of the saccule, and lays almost perpendicular to the horizontal plane of the fish. It contains an otolith known as the asteriscus (star shaped) (Figure 4.13.a) and is similar in size and form to the associated macula (Figure 4.13.b).

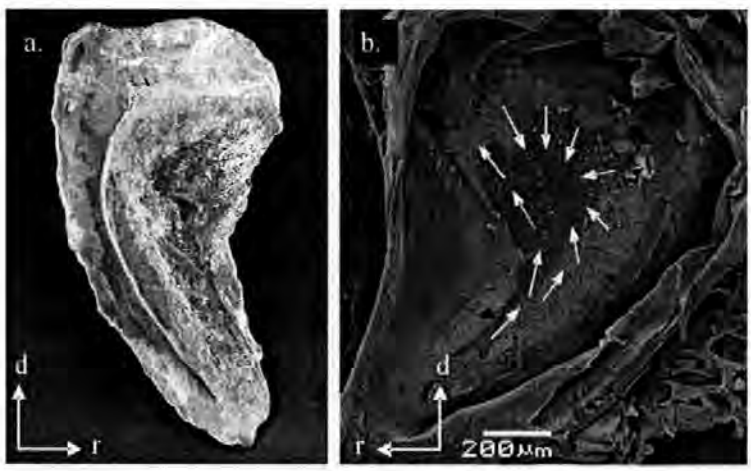

Figure 4.13 The lagena otolith (a.) and macula (b.) from *D. labrax*

Figure 4.14 shows the relative positions of the lagena ciliary bundles across the surface of the lagena macula. The hair cells divide into two regions, with caudal hair cell polarities becoming increasingly opposed, relative to the rosteral receptors as the dorsal extremities of the macula are approached (shown by the white arrows in Figure 4.13.b and 4.14). The two regions were sub-divided into 14 sectors and studied at magnification factors of between 1000 x and 5000 x. Detail of the ciliary bundles and their respective orientations can be seen in the inserts of Figure 4.14, which were scanned at a magnification of 5000 x. Cells of similar bundle size and orientation occupied large areas of the epithelia, with the

rosteral/caudal regions separated in the centre of the macula by a region sparsely populated by ciliary bundles with indeterminate polarisations.

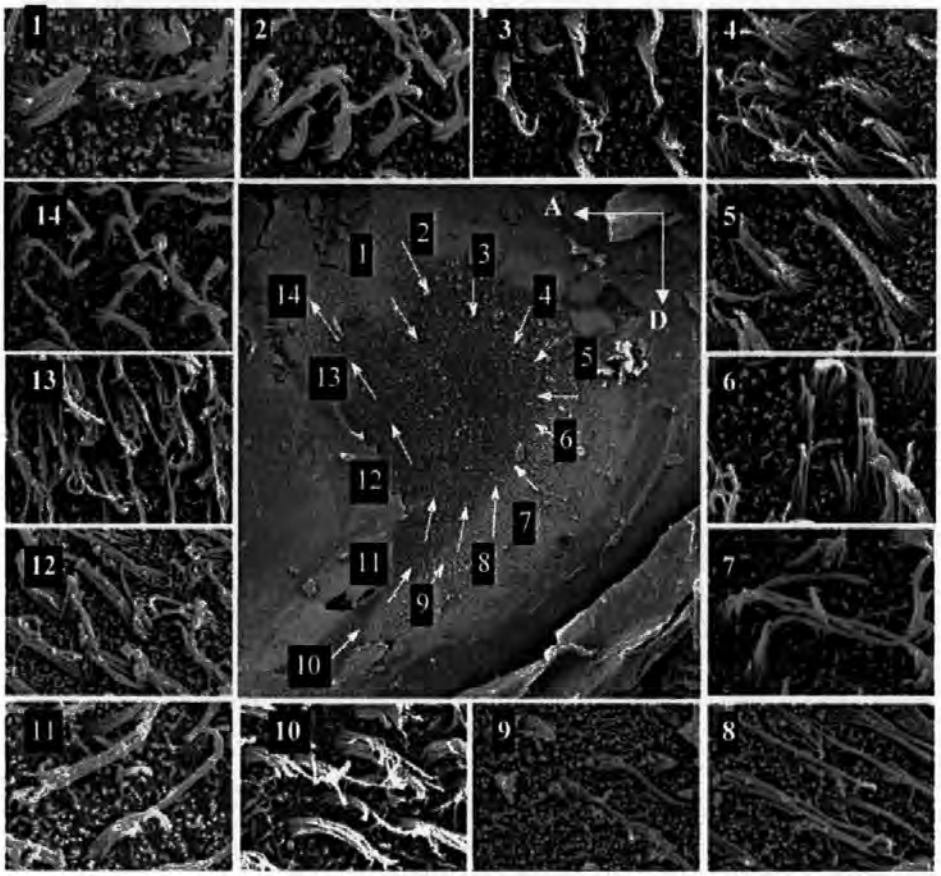

Figure 4.14 The orientation of ciliary bundles on the macula of the lagena from *D. labrax*. The annotations A (Anterior) and D (Dorsal) represent the orientation of the organ relative to the fish

The utricle is located behind the anterior ampulla, in the ventral rostral region of the pars superior, detailed in Figure 4.15. It is a small chamber containing an otolith known as the lapillus (small rock), and the macula, which is innervated by one of the rami extending from the acousticus region eighth nerve (VIII in Figure 4.15).

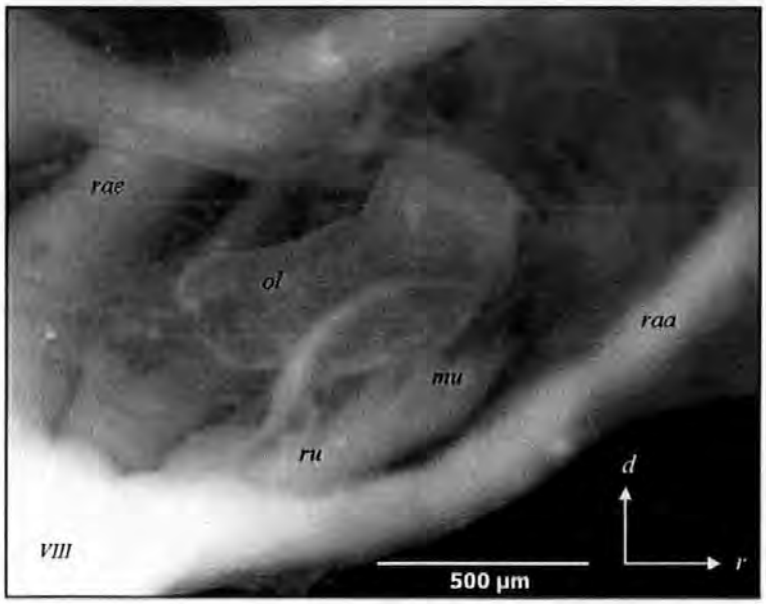

Figure 4.15 Digital photograph of the utricle from *D. labrax* taken using a camera and trinocular microscope. mu – macula of the utricle, ol otolith lapillus, raa ramus of the anterior ampulla, rae ramus of the ampulla external, ru ramus of the utricle, VIII eighth nerve (annotations after Retzius 1881)

The greatest densities of ultrastructural ciliary bundles were found along the horizontal plane of the utricular macula in *D. labrax* (detailed in Figure 4.16), as opposed to the near vertical arrangement of the saccular and lagena macula. The second major difference between the utricle and the other end organs is the partial envelopment of the utricular otolith by the sensory macula, rather than the macula being intimately located in the medial sulcus of the sagitta or following one side of the asteriscus.

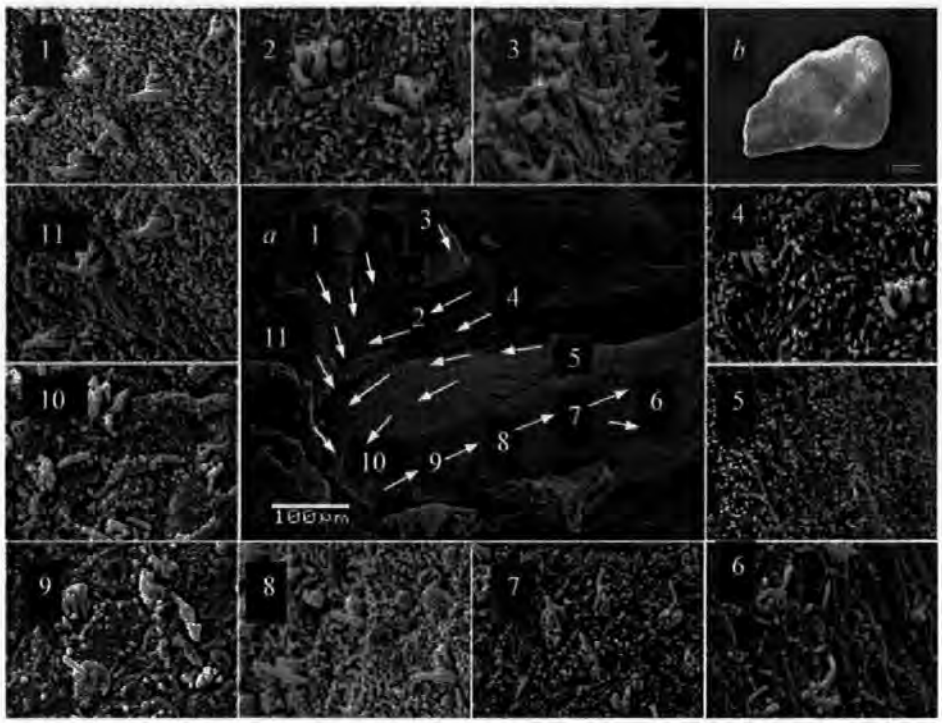

Figure 4.16. The orientation of ciliary bundles on the macula of the utricle from *D. labrax* (insert a.) and the utricular otolith (insert b.)

The thickness and height of the apical ciliary bundles compared to the kinocilium provides an index for distinguishing regional variations in ciliary bundles across the macula surface. Ciliary bundles are referenced by comparing the length of the kinocilia (*e.g.* K8 µm), relative to the first stereocilia (*e.g.* s4 µm) (Platt and Popper 1983). The ciliary bundles shown in Figure 4.17.a proliferate in a narrow band at the margins of the saccular epithelia, and exhibit a long kinocilia with short stereocilia. With an index of K8s4, these cells were the longest identified on the saccular macula of *D. labrax*. Figure 4.17.b shows K2s0.5 ciliary bundles proliferating in the caudal ventral region of the utricular macula, and the shortest receptors found in the inner ear of *D. labrax*. The caudal locus of the saccular macula is predominated by extensive proliferations of K6s5 ciliary bundles (Figure 4.18.a), and the osteum of the saccule is predominated by K6s4 hair cell (Figure 4.18.b). Figure 4.19 shows K8s7 ciliary bundles from the medial caudal region of the lagena macula, and exhibited the longest stereocilia to kinocilia ratio found in the inner ear of *D. labrax*.

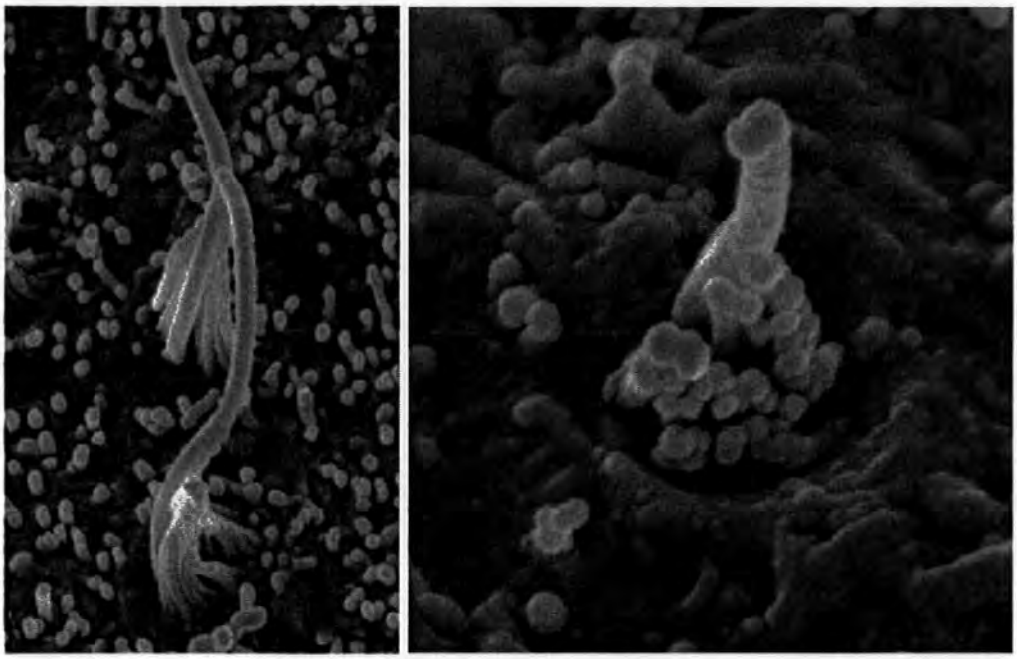

Figure 4.17.a K8s4 Ciliary bundles proliferating in a narrow band at the margins of the saccular epithelia from *D. labrax*, **(b)** K2s0.5 hair cell from the caudal region of the utricle viewed at a magnification of 11 000 x.

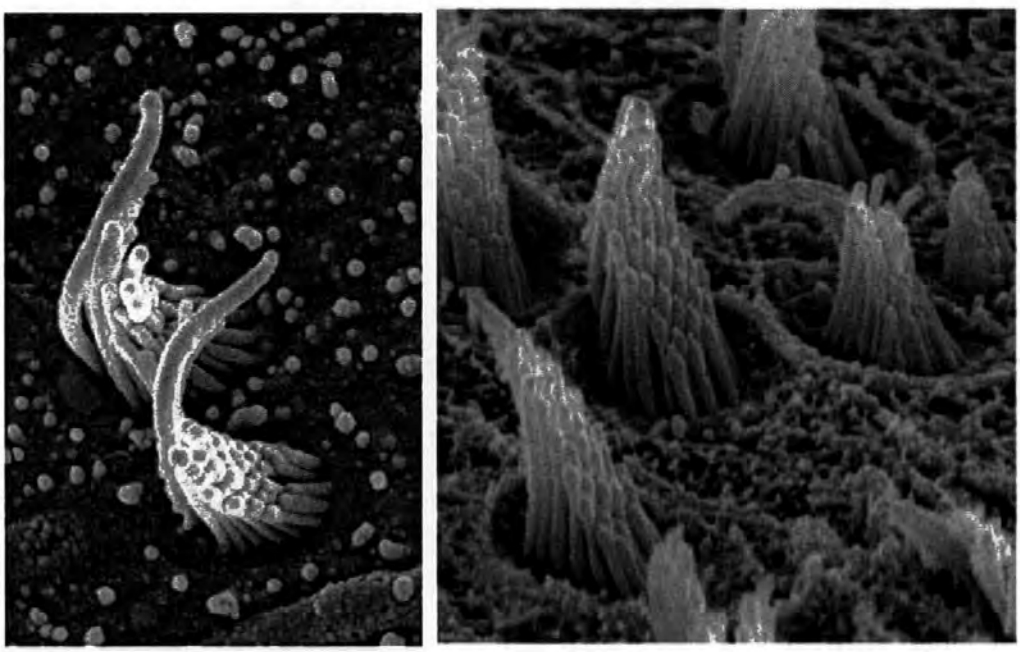

Figure 4.18.a. K6s4 ciliary bundles proliferating in a central region of the osteum of the saccule from *D. labrax* **(b)** K6s5 ciliary bundles proliferating in the caudal ventral locus of the saccule viewed at a magnification of 11 000 x

Figure 4.19 K8s7 ciliary bundles proliferating in the medial caudal region of the lagena macula from *D. labrax* viewed at a magnification of 11 000 x.

Whilst there is marginal variation in the length of the kinocilia located on the saccular epithelia in *D. labrax*, there was not sufficient variability in the lengths to distinguish regional variation except between the perimeter and central ciliary bundles.

4.3.3 Audiogram for *D. labrax*

Threshold responses from *D. labrax* were determined visually from the sequentially arranged waveforms for each frequency tested, in accordance with Kenyon et al (1998). Figure 4.20 shows ABR waveforms evoked from *D. labrax* in response to a. 75 Hz, b. 100 Hz, and c. 200 Hz, and Figure 4.21 shows waveforms evoked from a. 300 Hz, b. 400 Hz and c. 500 Hz tone bursts averaged over 1000 sweeps of 80 ms. The tone bursts were presented initially at 10 dB re 1 μPa above threshold and attenuated in steps of 4 dB re 1 μPa ordinarily, and 2 dB re 1 μPa as the hearing threshold was approached. When two replicates of waveforms showed opposite polarities, it was considered as being below threshold (cf. Kenyon et al. 1998).

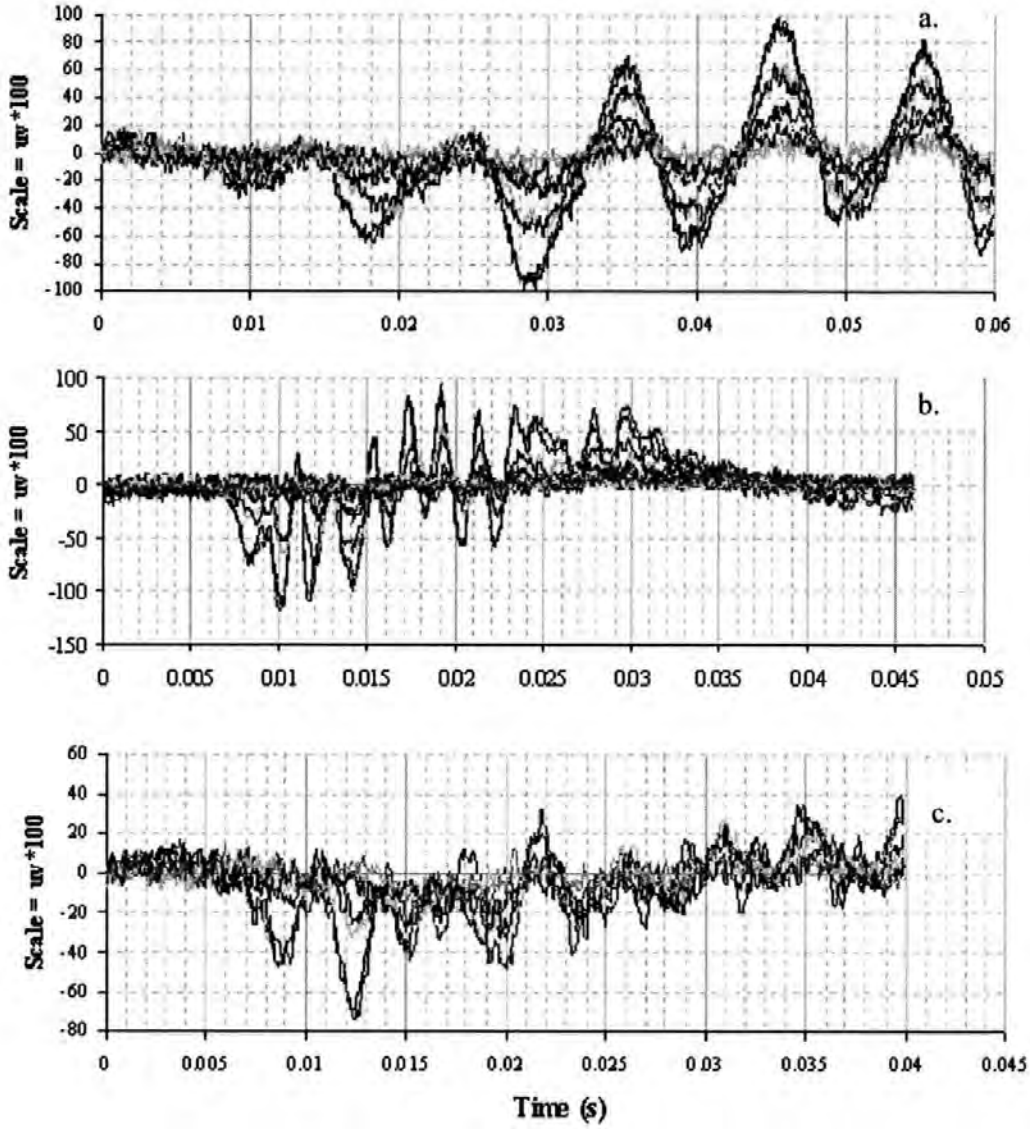

Figure 4.20 Overlaid ABR response from *D. labrax* to a sound of **a.** 50 Hz, **b.** 100 Hz, and **c.** 250 Hz, averaged over 1000 sweeps

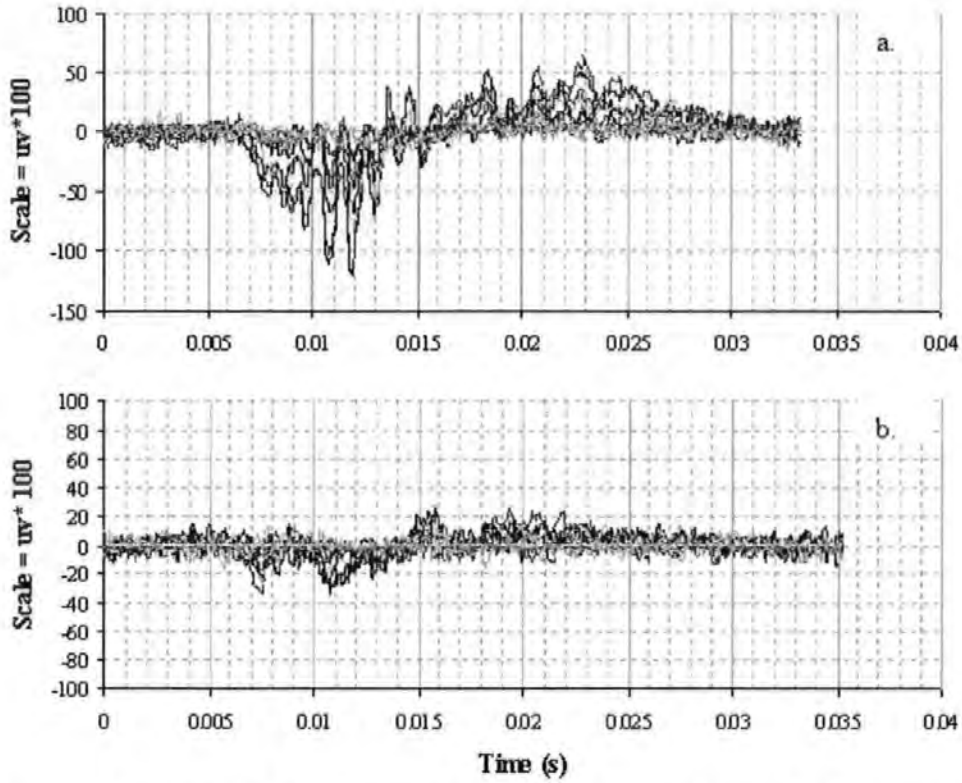

Figure 4.21 Overlaid ABR responses from *D. labrax* to a sound of **a.** 500 Hz, and **b.** 750 Hz, averaged from 1000 sweeps

The intensity of the signal required to generate threshold evoked potentials from *D. labrax* were correlated with the respective frequencies and presented in the audiogram in Figure 4.22.

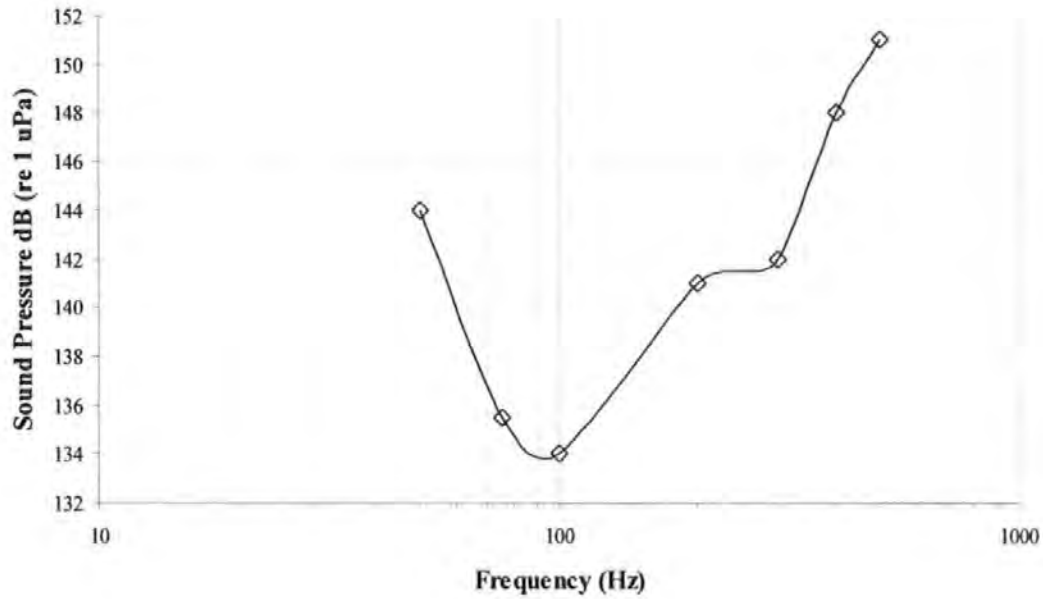

Figure 4.22 ABR generated audiogram for *D. labrax* (data from Figures 4.20 and 4.21)

4.5 Chapter discussion and conclusions

The vertebrate ear is divided into two functionally separate regions, the pars superior and pars inferior (after Retzius, 1881); with the pars superior (semi circular canals and utricle) mediating postural responses and the pars inferior mediating acoustic responses (von Frisch 1938; Jenkins, 1981; Platt and Popper 1981; Popper and Platt, 1993). The pars inferior comprises two fluid filled pouches, the saccule and lagena (Retzius, 1881); with each pouch containing a crystalline calcium carbonate otolith (Carlström, 1963). It is generally accepted that the saccule and lagena of the pars inferior are the primary acoustic receptor organs in most fish species (Fay 1981), though there is probably considerable functional overlap between all three of the otolith organs (Popper and Fay 1993). Fish lacking adaptations that enhance hearing (commonly called hearing generalists) have ciliary bundles orientated both horizontally and vertically in four to six quadrants (Popper and Fay 1993). It is apparent from analysis of the SEM data presented here that *D. labrax* possesses standard orientation ciliary bundles, in common with many hearing generalist species. These findings are in agreement with studies of other Perciform hearing generalists. For example the polarisations of saccular ciliary bundles from the perch (*Perca flavescens*) are divided into four groups; anterior, posterior, dorsal, and ventral with respect to the axis of the fish (Platt and Popper, 1981). This is in contrast with specialist sensory receptor patterns such as those found in the Ostariophysi (Otophysi), which have saccular ciliary bundles orientated vertically in only two diametrically opposed quadrants (Popper, 1980). Bi-directional receptor patterns are often associated with adaptations that enhance hearing and can even extend to other end-organs, such as those found in the clupeid utricle (Blaxter, Denton and Gray 1981; Popper and Platt, 1979). The examination of the afferents in the saccule of *D. labrax* demonstrates the applicability of the dissection and preparation methodologies required for SEM type examinations of the hair cells in the fish ear, and has resulted in the publication of a manuscript on the subject (see appendix 1).

Fish have the ability to determine the direction and distance of a disturbance in the acoustic free field (Schuijf and Hawkins 1983; Hawkins and Sand 1977; Hawkins 1993). Hawkins and Sand (1977) theorise that ciliary bundles in generalists have an axis of maximal sensitivity to vibration. The directional characteristics (excitation or inhibition) of afferent nerves have been qualitatively correlated with anatomically defined patterns of hair cell orientations on the macula of the saccule (Fay 1997). The sleeper goby (*Dormitator latifrons*) detects the spatial location of sound using arrays of ciliary bundles in the

otolithic organs that are oriented specifically along the sound propagation axis (Lu and Popper 1998). The saccular and lagenar epithelia of *D. latifrons* are oriented perpendicular to the horizontal plane of the fish, while the utricular epithelium lies on the horizontal plane. A similar inner ear organisation was also observed in *D. labrax*, and shows that the bass ear is also morphologically capable of being a 3 dimensional sound detector.

The P value of 0.181 given by the ANOVA in Table 4.2 indicates that the distance between cells on the dorso-ventral (x) axis, remains constant throughout the development of *D. labrax* from fingerling to the juvenile stages of the life cycle. However, the P value of 0.035 (Table 3.3) shows that there is some evidence to suggest that the ciliary bundles will acquire more lateral spacing along the y axis as *D. labrax* grows. The test was confirmed by counting the numbers of cells found proliferating in comparable areas of macula, and found to be 51 cells per 0.002 mm^2 for the large fish, 48 for the medium, and 67 for the small. It is well known that in lizards and birds, regions having longer ciliary bundles detect lower-frequency signals while shorter bundles detect higher frequencies (Popper and Fay 1993). Indirect evidence in fish raises the possibility of a similar correlation, as the region of the macula responsive to lower frequencies in *C. auratus* is the region containing the taller kinocilia (Sugihara and Furukawa, 1989), suggesting a parallel with the gradient of ciliary bundle length and frequency responses found in higher vertebrates.

The thickness and height of the apical ciliary bundles compared to the kinocilium provides an index for distinguishing regional variations in ciliary bundles across the macula surface (Platt and Popper 1981). The length of ciliary bundles and the ratio between the kinocilia and first steriocilia (Figures 4.17 through 4.19), shows slight regional variation across the sensory surface of the three otolithic end organs found in *D. labrax*. The ciliary bundles shown in Figure 10.a proliferate in a narrow band at the margins of the saccular epithelia, and exhibit a long kinocilia with short stereocilia. With an index of K8s4, these cells were the longest identified on the saccular macula of *D. labrax*, confirming the report by Barber and Emerson (1980), who found the more centrally located receptor cells on the saccular macula generally have longer stereocilia and shorter kinocilia than the peripheral cells. K6s5 ciliary bundles proliferate in the ventral region of the caudal locus of the saccular macula, and shorter ciliary bundles (K6s4) were found to proliferate in the central region of the osteum. Theoretically, K6s4 ciliary bundles are more responsive to high frequency components of an acoustic signal than the K6s5 ciliary bundles. The smallest hair cell populations (k2s0.5) were found on the macula of the utricle (Figure 4.17.b).

The study of the inner ear physiology of *D. labrax* shows that this fish possesses the sensory apparatus necessary to detect and localise sound in the open environment, albeit with generalist hearing abilities. The generalist configuration of the ear indicates that the hearing of *D. labrax* is restricted to a narrow bandwidth from around 50 Hz to 500 Hz. This finding was corroborated by the results of the ABR investigation.

The lowest hearing thresholds for *D. labrax* were obtained from frequencies of between 50 Hz to 400 Hz, and the intensity of sound required to evoke the lowest threshold response was 134 dB (re 1 μPa) at 100 Hz. The increase in the airborne sound intensity required to evoke responses from *D. labrax*, which are comparable in μv values to those obtained from *C. auratus*, can produce substantial stimulus artefacts. These potentially have an adverse effect on an ABR trace, and become more pronounced as intensity increases (Weber 1983). This phenomenon was not observed during this ABR investigation, even though the equipment and fish were not placed in a faraday cage during the audiological test. The results are comparable to the sound pressure audiogram produced for a generalist fish by Casper et al. (2003), confirming that the ABR system developed here functions with precision outside of an electronically controlled environment. The next chapter tests the ABR system on two species of generalist cartilaginous fish using submerged transducers, generating fields of sound pressure and particle motion in a variety of situations where external factors (e.g. radio interference) cannot be precisely regulated.

Chapter 5

The hearing abilities of cartilaginous generalist fish

5.1 Introduction

In order to test the ABR methodology on cartilaginous fish, the Paddlefish (*Polyodon spathula*) and the Lake sturgeon (*Acipenser fulvescens*) from the subclass Chondrostei, in the order Acipenseriformes (sturgeons and paddlefishes) were selected. This choice was based on two rationales, the first being the direct application of an audiogram in the development of the non-physical barrier discussed in Chapter 1; and the second, the paucity of data regarding hearing ability from any fish in this order. Concern regarding the spread of *H. molitrix* and *A. nobilis* through the Illinois River has prompted the development of an Acoustic Fish Deterrent (AFD) system. As discussed in Chapter 3, the application of this technology has resulted in a need to understand the auditory physiology of fish other than the target species, in order to minimise the effect of the AFD barrier on the ecology of indigenous fish populations. In this Chapter, both the structures involved in sound reception and the hearing abilities of the paddlefish (*Polyodon spathula*) and the lake sturgeon (*Acipenser fulvescens*) from the subclass Chondrostei, in the order Acipenseriformes (sturgeons and paddlefishes) are studied, using a combination of morphological and physiological approaches. The equipment and methodology used to generate the ABR audiograms in this Chapter follows the protocols set out in Chapter 3, used for measuring the hearing abilities of the two Asian carp species.

It is known that the directional responses of afferents in the fish ear are a function of the hair cell polarities and the orientation of the epithelium in space (Fay and Edds-Walton, 1997; Edds-Walton and Fay, 2002; Lu and Popper, 2001). In both *P. spathula* and *A. fulvescens*, the hair cells are aligned in both the horizontal and vertical planes and provide evidence of directional hearing ability in these species. The detection and localisation of a sound source is of considerable biological importance to many fish species; the pallid

sturgeon (*Scaphirhynchus albus*) and shovelnose sturgeon (*S. albus*), are both known to produce a range of sounds during the breeding season (Johnston & Phillips, 2003). Sounds are often used by fish to assess the suitability of a potential mate or during territorial displays (Nordeide & Kjellsby, 1999), and during predator prey interactions (Myrberg, 1981).

Materials and Methods

In order to concisely identify the frequency and intensity of sounds audible to paddlefish, twelve specimens of *P. spathula*, of mixed sex, and ranging in size from 160 mm (58 g) (measured from the tail fork to the anterior of the jaw) to 230 mm (163 g) were stimulated with sounds ranging in the frequency domain between 100 Hz to 1500 Hz. In addition, twelve mixed sex specimens of lake sturgeon, ranging in size from 230 mm (61.8 g) (fork length) to 280 mm (95.4 g), were also stimulated in a similar manner. The procedure used to acquire the acoustically evoked potentials and inner ear samples was approved by the University of Illinois, United States 15.11.04 (protocol # 04271). The water temperature in both the holding tanks and test tank ranged between 18.2 and 18.6 ° C over a 24 hour period, and when not under experimental protocols, the fish were provided with 16 hours of light per day.

5.2.1 Preparation of the saccule prior to SEM examination

The preparation methodology employed in this study was based on techniques used by Platt (1977), and the fish dispatched using the conventional protocol set out by the University of Illinois. The cranium containing the inner ears from *P. spathula* and *A. fulvescens* were trimmed to small blocks and immersed in chilled fixative (2.5% glutaraldehyde in 0.1 M cacodylate buffer with 3.5% sodium chloride), and delivered to the Plymouth EM unit within 72 hours post removal. The ears and surrounding tissue were subsequently immersed in a watch glass containing 30 % ethanol; then, working under a MEIJI binocular microscope, the end organs were dissected and the otoliths removed. The dissected capsules were dehydrated through a graded ethanol series ranging from 35% through 50%, 70% and 90% to absolute ethanol, prior to desiccation using the critical point drying method. Fully desiccated capsules were subsequently mounted on a specimen stub using a carbon tab, and coated with c. 8 nm of gold in an Emitech K 550 sputter coater (working at approximately 5 x 10^{-6} Torr). The processed specimens were investigated and photographed using a JEOL JSM 5600 scanning electron microscope operated at 15 kv,

and a 15 mm working distance. The eucentric stage holding the specimen was aligned for 'planar' image acquisition, and each sample was examined by adjusting the position of the stage in x and y coordinates only. All measurements were carried out on a PC using the analySIS® (Soft Imaging System GmbH) program. The distance between cell bases of the closest neighbour was measured using arbitrary distance and the length of the ultrastructure was measured using polygon length, both measurements were recorded in micrometers. Statistical calculations were carried out using Statgraphics plus 5.1 professional edition program, and an analysis of variance (ANOVA) was also used to test for similarity in the distances between neighbouring hair cell bases from *P. spathula* and *A. fulvescens*.

5.2.2 ABR methodology

The ABR measurements of hearing thresholds were made using a control and analysis program, which both generated the stimulus signals, and captures and analyses the response (refer to Chapter 3 for additional information). The stimulus used was a pulsed 4 cycle tone burst, which was presented to the fish at a given frequency and intensity. ABR recordings require no invasive procedural work, as measurements are taken in the electro-physiological far field using two cutaneous electrodes placed against the skin above the ear and medulla spanning the VIII nerve; the application of this methodology results in significant stress reduction during the hearing assessment (Kenyon et al., 1998). The ABR trace is formed by averaging peak potentials arising from centres in the auditory pathways from the periphery of the VIII nerve to the midbrain (Corwin et al., 1982; Overbeck and Church, 1992). Attenuated waveforms are considered as being below the threshold of hearing when two overlaid recordings, made at the same frequency and intensity, do not present with similarities or are in opposition (e.g. Kenyon et al., 1998).

The procedures used to acquire the acoustically evoked potentials were approved by the University of Illinois, United States 15.11.04, and a schematic of the equipment used to acquire the audiometric measurements is shown in Figure 5.1.

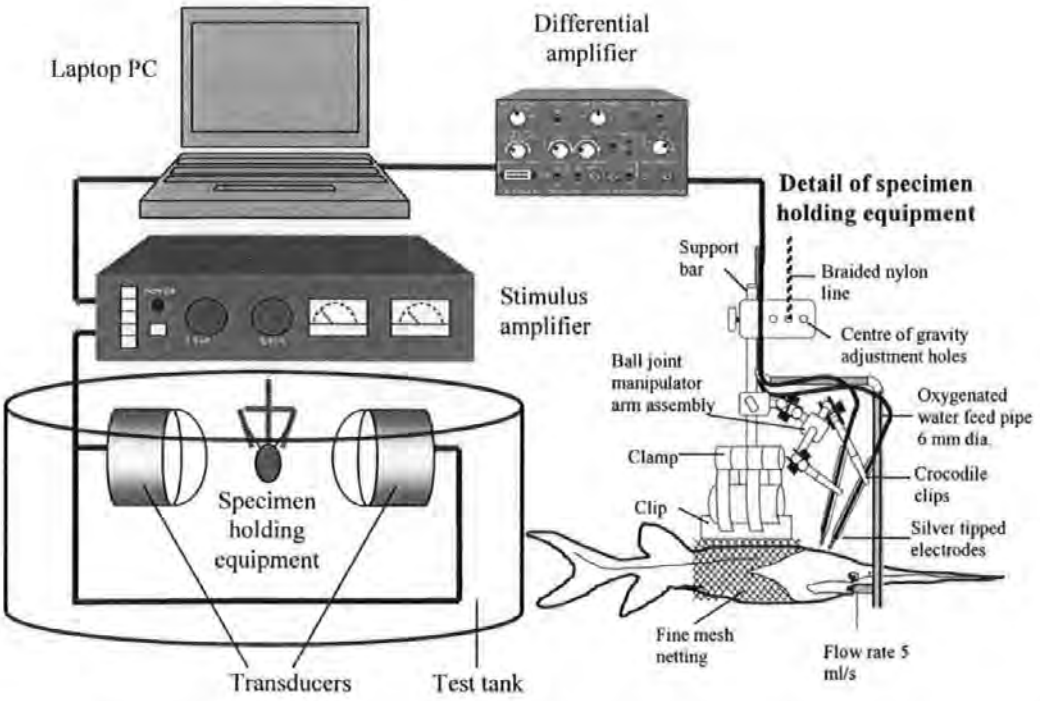

Figure 5.1. Schematic of the ABR setup and detail of the clamp used to hold the fish in position, and manipulate the electrodes during the audiological tests

Small fish (below 230 mm) were first placed lengthwise and centrally on a 160 mm x 120 mm rectangle of fine nylon netting, which was wrapped firmly around the body and tail, and the two sides of the net were held together using the clip. The clip was placed in a retort stand clamp fitted with ball joint electrode manipulator arms and the aerated water supply pipe (detailed in Figure 5.1). Large fish (above 250 mm) were placed in a clear rubber coated 1 mm gauge wire mesh cradle shown in Figure 5.2. A reservoir of oxygenated water was positioned 1 m above the experimental tank, and kept at a temperature of 18° C; water was gravity fed at an adjustable flow rate of between 5 millilitres per second for the small fish, to 12 millilitres per second for the large, and directed toward the gills through a soft rubber mouth tube with a diameter of 6 mm.

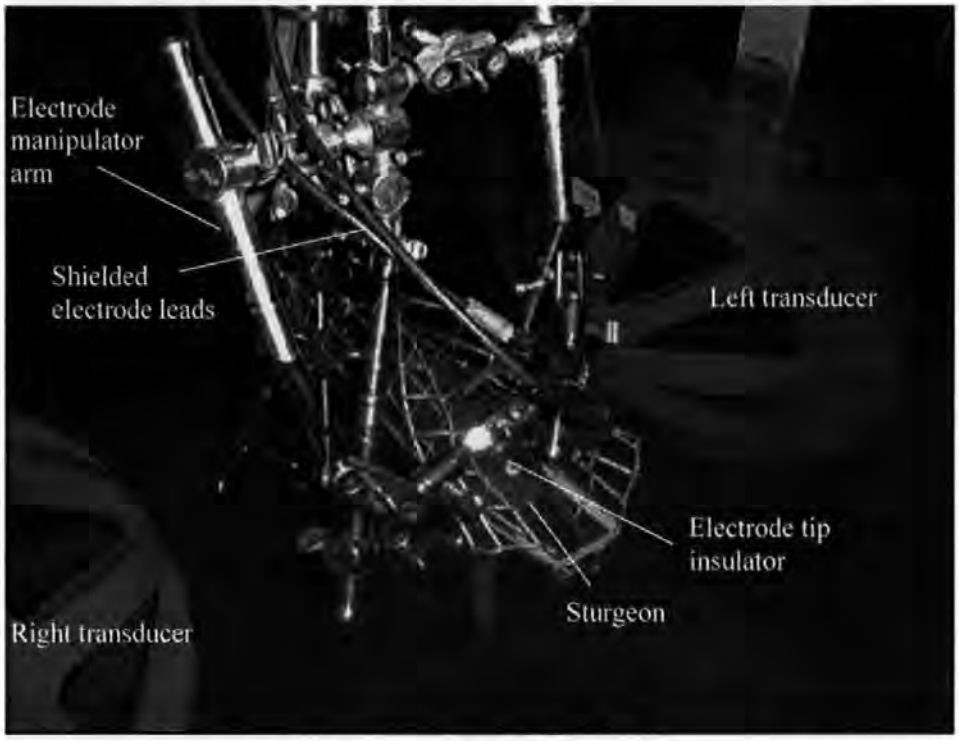

Figure 5.2. The transducers, electrode holding and fish restraining device used during the audiological examination. The record electrode tip insulator is identified above the head of the fish

The Evoked Potential (EP) was recorded using two cutaneous electrodes connected to the differential amplifier by 1 m lengths of screened coaxial cable with an external diameter of 1.5 mm. The outer insulating layer of the coax was removed 15 mm from the end where the electrode tip was to be fixed, and the screening layer removed 10 mm from the cable end. The inner insulating material was then trimmed by 2 mm, and the exposed inner wire (0.5 mm diameter) was tinned with silver solder and joined to a 10 mm length of silver wire (0.25 mm diameter), tapered to a fine point. The assemblage was pushed through a 100 mm glass pipette with an internal diameter of 4 mm, until 0.4 mm of the silver wire was exposed. The remaining space inside the pipette was filled with a clear epoxy resin, and then trimmed to expose 0.3 mm of silver tip through which the Auditory Evoked Potential (AEP) could be conducted. The impedance of the electrodes, both between the outer shielding and inner core, and the silver tip and differential amplifier, were tested using an M 205 precision digital multimeter. The impedance between the tip and pre-amplifier was found to be 0.2 Ω for both electrodes, and an open circuit was recorded between the outer shielding and inner core. Using the anatomical information from *A. fulvescens* (Figure 5.3 b) as a guide, the record electrode was placed 6 mm anterior of the reference electrode which was positioned centrally above the medulla. The dermal elements of the skull are ossified in *A. fulvescens*, making electrophysiological recordings

difficult, as there was no fleshy skin on the head for the electrode to push against and create a good connection. This resulted in the 0.3 mm silver tip being almost entirely exposed to the ambient water, which can substantially attenuate the evoked potential. To resolve this issue, silicone tip insulators were used to create a seal around the electrode tip and fish, preventing the ambient water from contacting the electrodes. These adaptations can be clearly seen on the record electrode in Figure 5.2, which shows a specimen of *A. fulvescens* held in place during the audiological test. Stimulus sounds were presented to the fish using submerged transducers at sound pressures initially not exceeding 150 dB re 1 μPa. The evoked response was amplified and digitised to 12 bits resolution and recorded. This process was repeated 2000 times and the response averaged to remove electrical interference caused by neural activities other than audition and the myogenic noise generated by muscular activity. Each measurement was repeated twice; this aids in separating the evoked response, which is the same from trace to trace, from the myogenic noise, which varies in two successive measurements. After the averaging process, the evoked potential could be detected following the stimulus by a short latency period of approximately a millisecond.

5.2.3 The sound field

In this experiment, submerged projectors were used to generate the stimulus sounds; previous ABR type investigations have used a domestic hi-fi loudspeaker positioned above the experimental water tank to create the insonifying sound field (e.g. Kenyon et al., 1998; Yan, et al., 2000). The audiological assessment of *P. spathula* and *A. fulvescens* involved two identical sound projectors, set up facing each other with the fish on the axis of symmetry between the two. Where the projectors are driven in phase, it is possible to create a region between them of high sound pressure, and low particle velocity, and when driven out of phase, the transducers create an area associated with high particle motion and minimal sound pressure. Previous studies of fish audiometry using the ABR technique have not separated sound pressure from particle motion, using submerged transducers to generate the sound field.

The stimulus sound signal was generated by a laptop computer running the ABR software, and amplified using a Tandy 250 W power amplifier. The sound field in the experimental water tank was generated by means of two Fish Guidance Systems Ltd. Mk II 15-100 Sound Projectors. These faced each other at a distance of 200 mm, and the inner ear of the fish during measurements was arranged on the axis connecting the centres of the two projectors. The projectors were driven directly from the amplifier, and the stimulus tones

presented to the fish were calibrated using the insertion calibration technique. In this method, the intensity of the sound is recorded in the absence of the fish, with the hydrophone positioned where the inner ear of the fish would be. The measurements were made using a Bruel and Kjaer Type 8104 calibrated Hydrophone, and the signal amplified by a Bruel and Kjaer Type 2365 Charge Amplifier (see back of appendix 3 for certification).

5.3 Results

5.3.1 Gross anatomy

Representative specimens of *P. spathula* and *A. fulvescens* were dissected to facilitate the correct positioning of the electrodes, and to facilitate removal of the inner ear from specimens selected for the SEM investigation. Figure 5.3.a illustrates a dissected paddlefish and shows the internal organs and location of the brain and Figure 5.3.b shows the position of the cranial cavity and brain from the sturgeon.

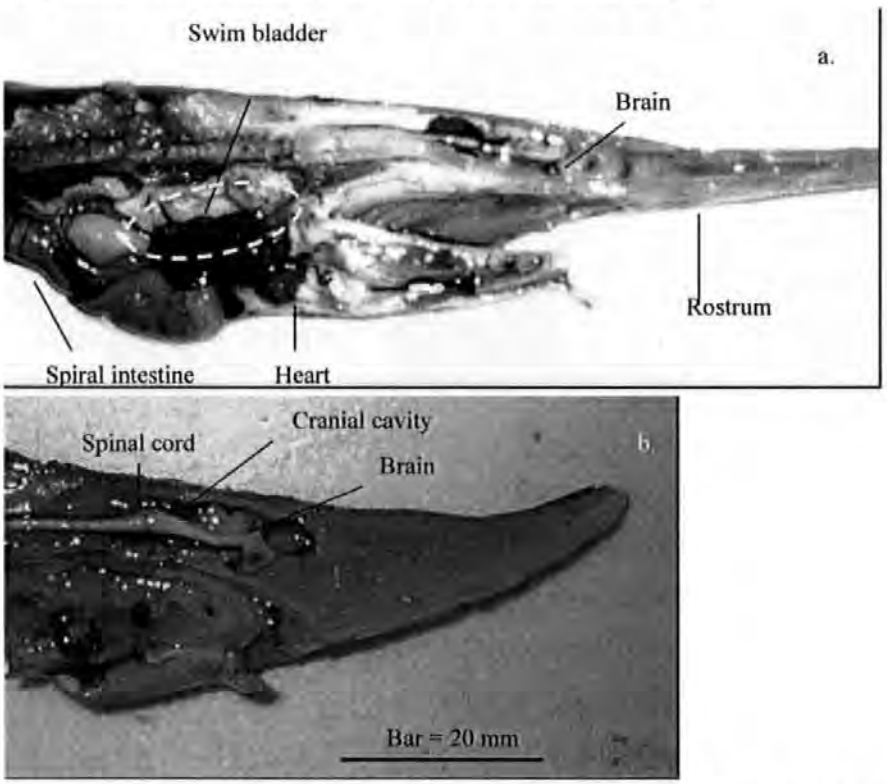

Figure 5.3.a. Dissected paddlefish showing the internal organs and location of the brain, revealing that *P. spathula* possesses a well developed swim bladder. **5.3.b.** Dissected head of the sturgeon (*A. fulvescens*), showing the cranial cavity, brain and spinal cord (Bar = 20 mm)

Figure 5.4 illustrates the left ear and peripheral auditory nerves from *P. spathula*; the saccule (*s*) and lagena (*l*) are situated in close proximity to one another, and the two otoliths that can be seen in the figure are similar in size. The peripheral nerves innervating the saccule and lagena (*rs*) share a pathway with the nerves from the posterior ampulla (*pa*); the peripheral nerve bundle projects forward, and connect with the utricular nerve and ramulus anterior ampulla (*raa*) to form the VIII octavel nerve. In both species, there is no internal division between the saccule and lagena, thus the pars inferior consists of just one fluid filled pouch.

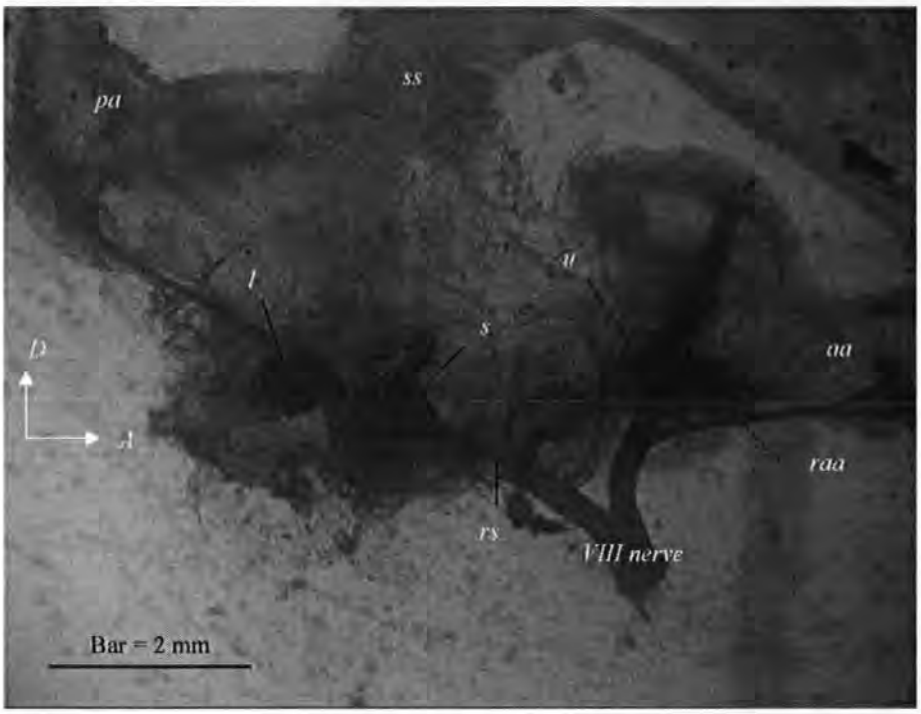

Figure 5.4. The left ear and VIII nerve from *P. spathula*; *aa.* anterior ampulla , *pa.* posterior ampulla, *l.* lagena, *raa.* ramus anterior ampulla, *s.* saccule, *ss.* sinus superior, *u.* utricle. The annotations D (dorsal) and A (anterior) show the orientation of the ear in the fish. Bar = 2 mm

5.3.2 Electron microscopy

Figure 5.5 a. shows the saccule and lagena from a 200 mm (90 g) *P. spathula*, and 5.5 b. from a 260 mm (90 g) *A. fulvescens*; Figure 5.5 c. shows the utricle from *P. spathula* and 5.5 d. from *A. fulvescens*. The micrographs have been annotated to show the macula area (hatched lines), and the hair cell polarisations are indicated by white arrows. The area of the saccule and lagena macula was both found to be 0.36 mm^2 for *P. spathula*, and 0.44

mm^2 and 0.42 mm^2 respectively for *A. fulvescens*. The utricular macula had an area of 0.63 mm^2 in *P. spathula*, and 0.64 mm^2 for *A. fulvescens*.

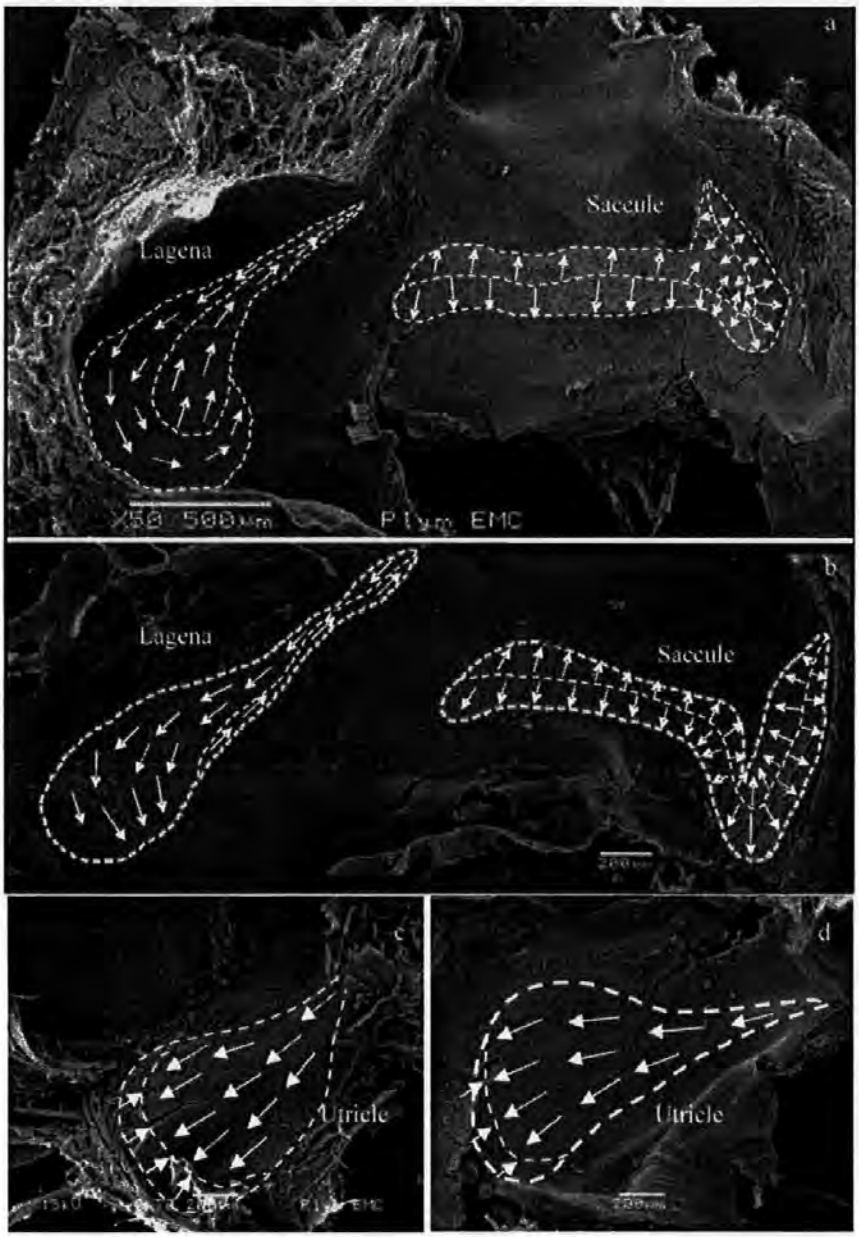

Figure 5.5. Electron micrographs of the right inner ear end organs annotated with arrows to show hair cell polarisations across the sensory surface. **a.** the saccule and lagena from a 200 mm (90 g) *P. spathula*, **b.** the saccule and lagena from a 260 mm (90 g) *A. fulvescens*, **c.** the utricle from *P. spathula*, and **d.** from *A. fulvescens*

The topographic data from the saccule shows that caudal hair cells are orientated on the dorsal and ventral axis, whereas the anterior hair cells are orientated on the anterior posterior axis with respect to the fish. As Figures 5.5.a and 5.5.b show, the four quadrant (standard) receptor configuration from both *P. spathula* and *A. fulvescens* is caused by a 90° curve in the macula, rather than the hair cells changing polarity relative to the adjacent

perimeter, as would be expected in a number of generalist fish species. This feature is clearest in Figure 5.5.b, and shows that the hair cell polarisations from both *P. spathula* and *A. fulvescens* can still be considered as being arranged in a standard configuration.

Figure 5.6 shows electron micrographs of the three otoliths associated with the inner ear end organs of *P. spathula*. The saccular otolith (Figure 5.6.a) is known as the sagitta or arrowhead, the lagena otolith (Figure 5.6.b) is the asteriscus (star shaped), and the utricular otolith (Figure 5.6.c) is the lapillus (small rock).

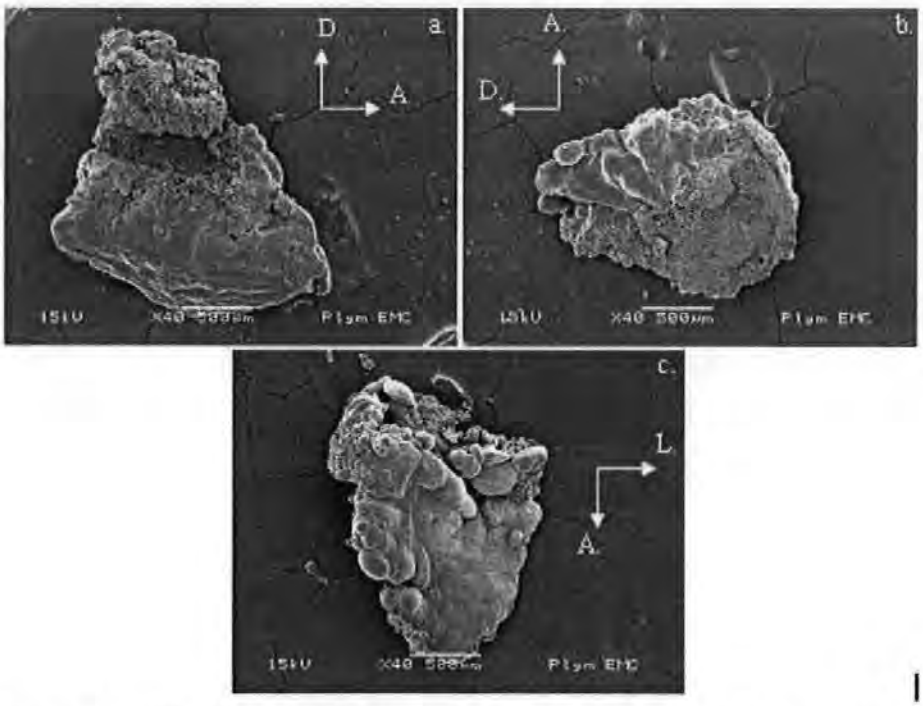

Figure 5.6. The three otoliths from the ear of *P. spathula*. **a.** The saccular otolith known as the sagitta or arrowhead, **b.** the lagena otolith or asteriscus (star shaped), and **c.** the utricular otolith or lapillus (small rock). The arrows annotated D. (dorsal), A. (anterior), and L. (left) show the orientation of the otolith if it were in the fish

Each of the micrographs in Figure 5.6 uses the same scale, showing that the three otoliths are similar in overall size, with the area of the sagitta recorded at 2.5 mm^2, the asteriscus at 1.8 mm^2 and the lapillus at 2 mm^2. High powered images of the hair cells from the saccule, lagena and utricle from *P. spathula* and *A. fulvescens* are presented in Figure 5.7, which show similarities in ultrastructural features between both fish.

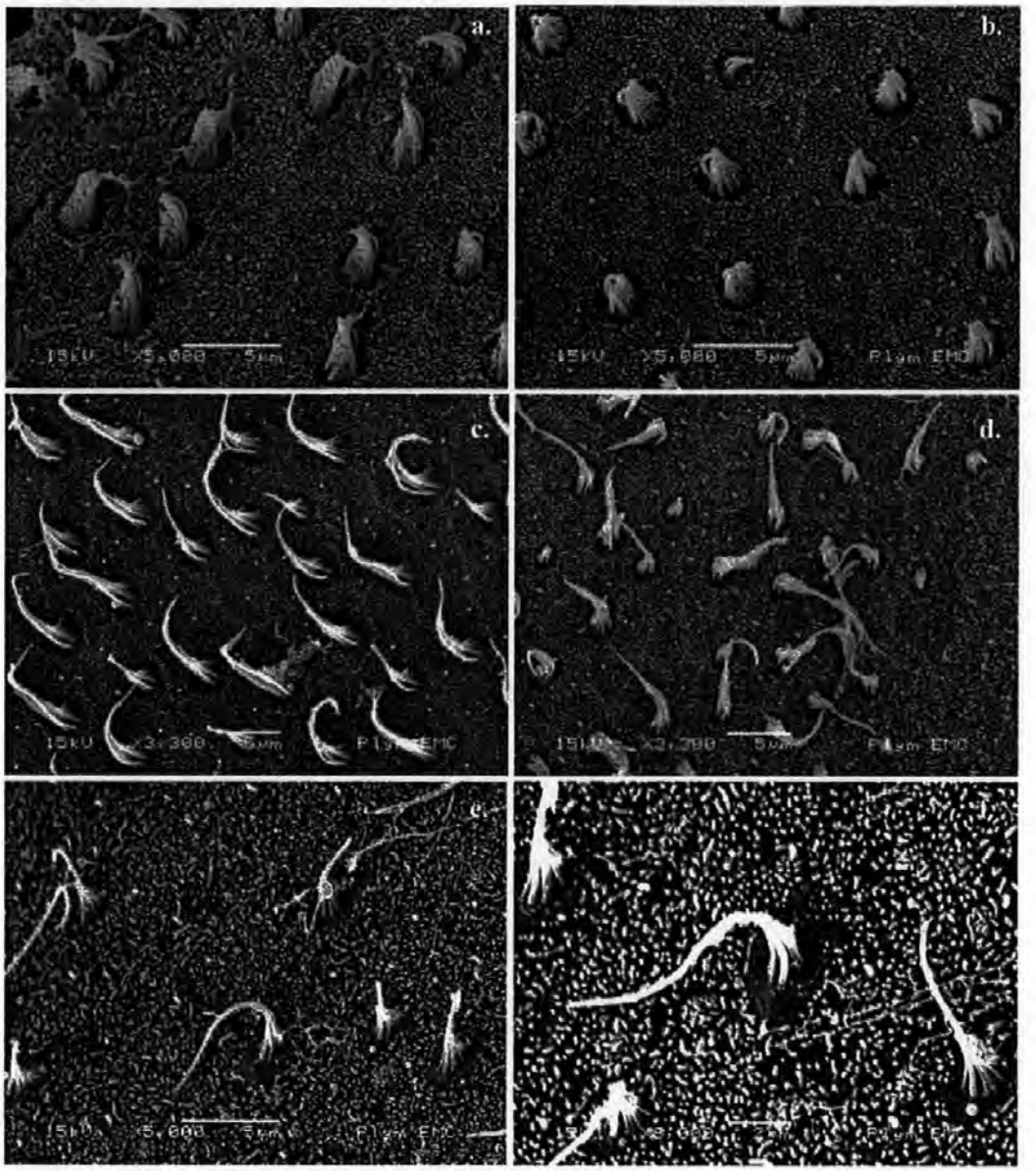

Figure 5.7. Saccular hair cells from **a.** *P. spathula*, and **b.** *A. fulvescens*. Lagena hair cells from **c.** *P. spathula*, and **d.** *A. fulvescens*. Utricular hair cells from **e.** *P. spathula*, and **f.** *A. fulvescens*.

The hair cells on the saccule from both species (Figures 5.7.a and b) have up to 40 stereocilia partially surrounding a single kinocilium 3 μm in length, positioned close to the anterior of the cell. Each hair cell is buttressed by what appear to be support cells, which present with small centrally placed microvillus like structure, in evidence on both inferior maculae. The hair cells on the lagena (Figures 5.7.c and d) have long stereocilia (up to 6 μm in length), and partially surround a 9 μm kinocilium. Both the longest and shortest hair cells were found proliferating on the utricular macula, which presents with kinocilium lengths of between 12 to 15 μm around the perimeter, down to as short as 1.3 μm in the central (striola) region (Figures 5.7.e and f). The number of hair cells proliferating on each

end organ was approximated from at least 12 observations taken from around the macula from a 200 mm *P. spathula*, and a 260 mm *A. fulvescens*. The numbers of hair cells on the saccular macula was approximately 4600 from *P. spathula*, and 6800 from *A. fulvescens*. In the order of 3600 hair cells were found on the lagena macula of *P. spathula*, and 5000 on the lagena of *A. fulvescens*, and approximately 8000 hair cells were found on the utricular maculae from both species.

5.3.3 Electrophysiology

Figure 5.8 illustrates the auditory evoked potentials from *P. spathula* in response to tone bursts at frequencies of 100 Hz, 200 Hz, 250 Hz, 300 Hz and 500 Hz, in response to both sound pressure and particle motion. Higher frequencies were tested (up to 1500 Hz), but on close analysis of the resultant waveforms, no stimulus matching response could be distinguished, so they were rejected. Each of the waveform sets recorded from stepped amplitudes from a particular frequency have been overlaid, revealing a latency change in response to the attenuation in the intensity of the sound. Above threshold EP waveforms in both Figures are presented with a blue colour coding, whilst below threshold recordings are orange or red. At each frequency, the ABR waveforms evoked by the tone bursts typically consisted of a series of four to eight rapid negative peaks, followed by a slow positive deflection. The onset latency of the centre or largest sinusoid of the ABR response varied with frequency, ranging from 7.3 ms after stimulus onset at 100 Hz to 5 ms at 500 Hz. As the sound pressure levels approached threshold, 2000 sweeps were required to distinguish ABRs from the background electronic noise.

The left column in Figure 5.8 shows waveforms recorded from *P. spathula* in response to a 4 cycle tone burst ranging in frequency from 100 to 500 Hz, presented in a sound field dominated by particle motion, whilst the right column presents waveforms recorded in a sound field dominated by Sound Pressure.

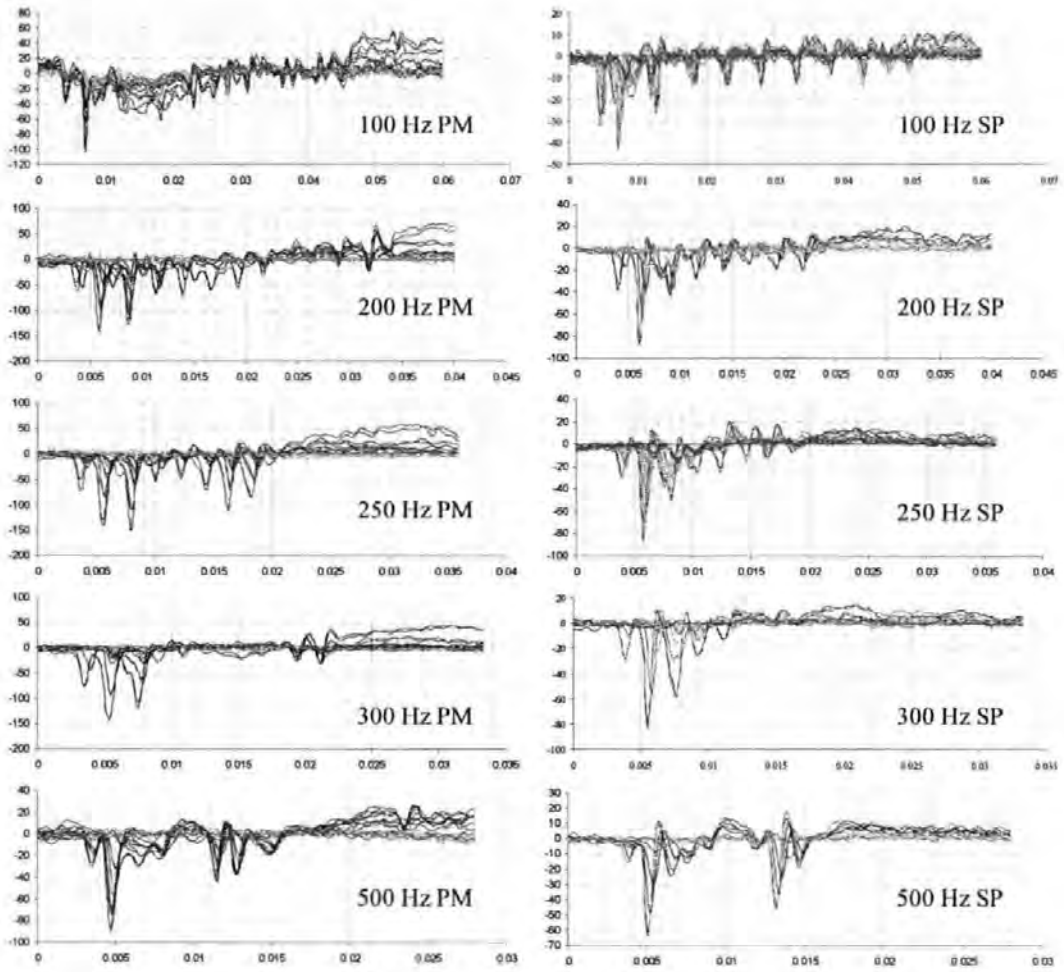

Figure 5.8. Averaged waveforms evoked from *P. spathula* in response to four cycle tone bursts of 100 Hz to 500 Hz, attenuated in 5 dB steps, with the sound fields dominated by either particle motion or sound pressure (y axis scale = microvolts * 100, x axis scale = time (s))

As can be seen in Figure 5.8, the waveforms are similar at each frequency and presentation mode (sound pressure or particle motion), though there is a slight increase in the duration of the evoked potentials by 1 to 2 ms when stimulating in a sound field dominated by particle motion. Also, the particle motion waveforms above 100 Hz are followed by smaller responses with similar characteristics, possibly the result of reflected sound waves. These responses to "echoes" are not present in the sound pressure results except at 500 Hz, which appears to evoke a very similar response from the two stimulus modes. Figure 5.9 presents waveforms from *A. fulvescens* recorded under identical conditions to *P. spathula*, though as previously discussed, the heavily ossified cranium of *A. fulvescens* effectively reduced the contact area between the electrode and fish, resulting in a reduction in the EP quality.

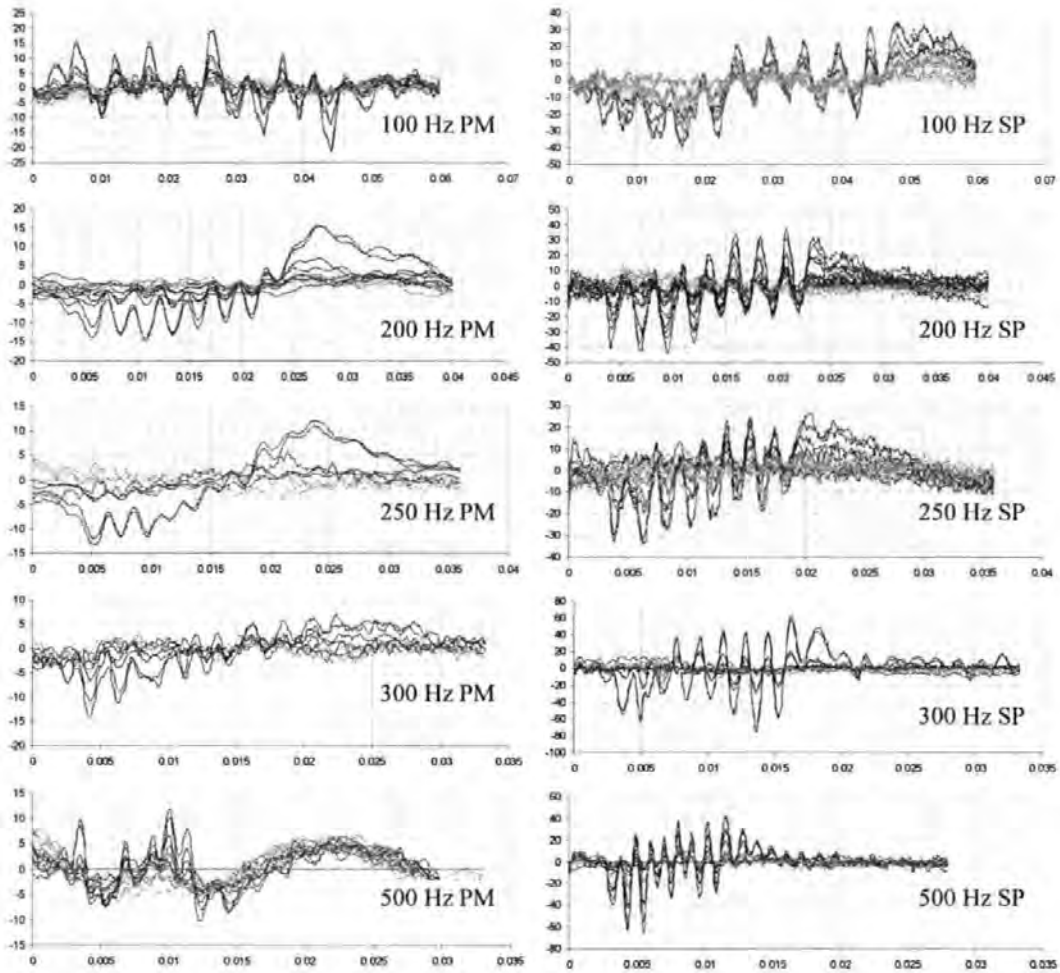

Figure 5.9 Averaged waveforms evoked from *A. fulvescens* in response to tone bursts of 100 Hz to 500 Hz, attenuated in 5 dB steps, with the sound fields dominated by either particle motion or sound pressure (y axis scale = microvolts * 100, x axis scale = time (s))

In Figure 5.9, the evoked potentials from *A. fulvescens* are similar in overall shape to the waveforms recorded from *P. spathula*, presented in Figure 5.8; however, they are noticeably lower in amplitude. This is especially evident in the particle motion waveforms (left column in Figure 5.9), and is attributed to the reduced contact area between the electrode tip and cranium. Although present, the waveforms following the initial response (the "echoes") are also considerably lower in intensity than those recorded from *P. spathula*, and again reflect the difficulties encountered when recording AEPs from *A. fulvescens*. The Inter Peak Latency (IPL) observed clearly in the *P. spathula* waveforms are not so pronounced in *A. fulvescens*, though are clearest in the 100 Hz sound pressure results; however, the absence of a sharp AEP peak has a considerable effect on the lucidity of the IPL at all frequencies tested.

Figure 5.10 shows ABR waveforms evoked from a 300 Hz tone burst, presented initially at 150 dB (re 1 μPa), and attenuated in steps of between 8 to 4 dB ordinarily, then in 2 dB

steps as the hearing threshold was approached. When two replicates of waveforms showed opposite polarities, as seen in the traces for the results at 130 dB in Figure 5.10, the response was considered as being below threshold (cf. Kenyon et al., 1998).

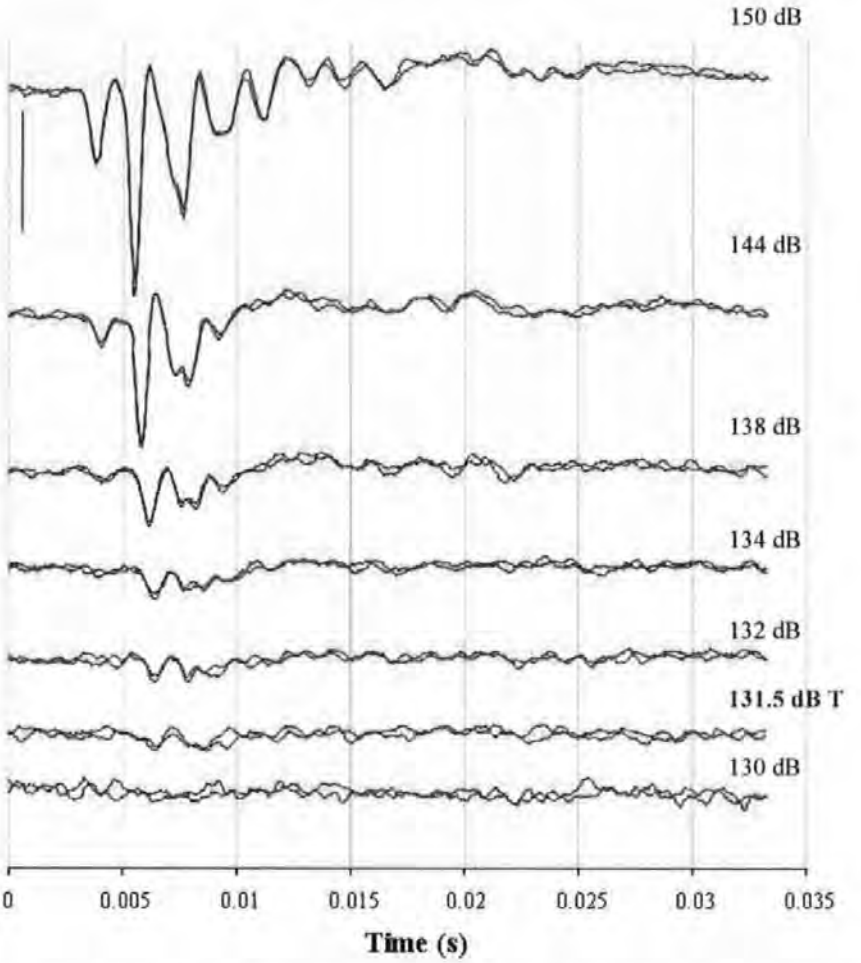

Figure 5.10. ABR waveforms from *P. spathula* in response to a 300 Hz tone burst attenuated in sequential steps. Averaged traces of two runs (2000 sweeps each), for each intensity are overlaid and arranged sequentially. Bar = 0.5 μv

All threshold responses were measured in this way, with each audiogram produced using the sequential ABR waveform data (e.g. Figures 5.8 and 5.9), acquired from frequencies of 100 Hz to 500 Hz. The individual audiograms acquired from the populations of P. spathula and A. fulvescens were combined to create an average composite audiogram (Figure 5.11), using both the mean and standard deviation data generated by the statistical analysis software.

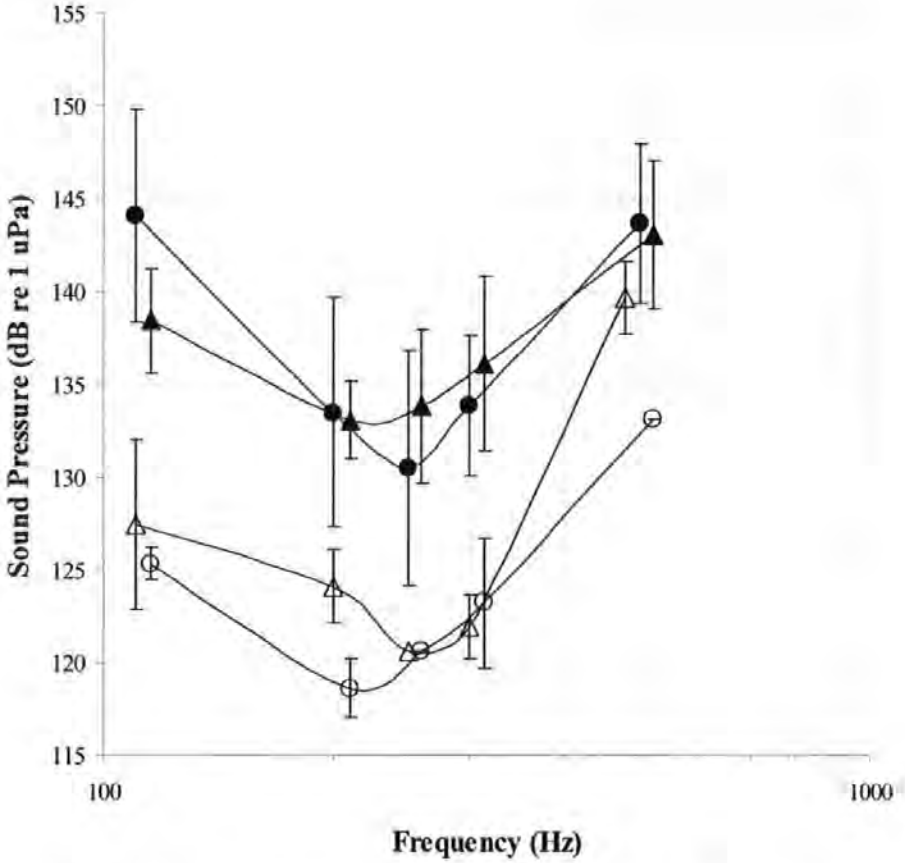

Figure 5.11 Audiograms for *A. fulvescens* (closed circles = maximum sound pressure; open circles = maximum particle motion), and for *P. spathula* (closed triangles = maximum sound pressure; open triangles = maximum particle motion). The audiograms were generated using the sequential ABR waveform data presented in Figures 2 and 3, acquired from frequencies between 100 Hz to 500 Hz (error bars show the standard deviation of the threshold responses and are separated by 5 to 20 Hz for ease of viewing)

The audiograms follow a Gaussian profile, determined by calculating the lowest intensity stimulus sounds (recorded underwater using the hydrophone located adjacent to the fish ear) that evoked a repeatable ABR response (e.g. 131.6 dB in Figure 5.10). The lowest hearing thresholds with the sound field dominated by sound pressure (transducers driven in phase) was 130.5 dB (re 1 µPa) at 250 Hz for *P. spathula*, and 133 dB (re 1 µPa) at 200 Hz for *A. fulvescens*. Lower thresholds were recorded when the sound field was dominated by particle motion (transducers driven out of phase), and the lowest response was 120.7 dB (re 1 µPa) at 250 Hz for *P. spathula*, and 118.2 dB (re 1 µPa) at 200 Hz for *A. fulvescens*. The standard deviation for P. spathula show that the response from this fish varies by approximately 12.5 dB in the pressure dominated sound field, possibly due to the fish being insensitive to sound pressure. The differences in the intensity required to evoke

threshold responses from tone bursts presented in either sound pressure or particle motion dominated sound fields, are presented in Table 5.1 for *P. spathula* and Table 5.2 for *A. fulvescens*.

Table 5.1 Mean hearing thresholds from *P. spathula*, in units of dB (re. 1 µPa) with the sound field dominated by sound pressure and particle motion

Hz	Threshold dB/SP	Threshold dB/PM	Mean Dif dB (SP/PM)	Calc. t	p
100	144.1	126.4	17.7	10.4	**<0.001**
200	133.5	124.5	9.0	3.6	**<0.009**
250	130.5	120.7	9.8	5.21	**<0.001**
300	131.6	122.3	9.3	6.7	**<0.001**
500	143.6	139.2	4.4	3.5	**<0.005**

Table 5.2 Mean hearing thresholds from *A. fulvescens*, in units of dB (re 1 µPa) with the sound field dominated by sound pressure and particle motion

Hz	Threshold dB/SP	Threshold dB/PM	Mean Dif dB (SP/PM)	Calc. t	p
100	138.4	125..6	12.9	17.8	**<0.001**
200	133.1	118.2	14.9	26.1	**<0.001**
250	133.8	120.7	13.1	11.0	**<0.001**
300	136.1	124.1	12.0	8.0	**<0.001**
500	143.5	137.3	5.7	4.7	**<0.001**

As can be seen in the table, the disparity between the responses from *P. spathula* and *A. fulvescens* to sound pressure and particle motion generally decrease as the higher frequencies are approached. The results of the ABR examination using the two stimulation modes were compared statistically by a set of paired t-tests for each frequency. In tables 5.1 and 5.2, the p-values associated with t are low (< 0.05), thus there is evidence of a difference in means across the paired observations of hearing ability from each species and stimulus mode. Additionally, the standard deviation values are smaller in each case for the particle motion condition, tending towards confirmation of the hypothesis that the particle

motion component of the sound field is more important to generalist fish than the sound pressure component.

5.4 Chapter discussion and conclusions

The fish inner ear is divided into two regions, the pars superior and the pars inferior (Retzius, 1881). The former responds primarily to movements of the body and postural changes, while the latter responds to both gravistatic and acoustic stimuli (Jenkins, 1981; Popper & Platt, 1993). The examination of the inner ears from *A. fulvescens* and *P. spathula* revealed similar inner ear morphology between these two fish, in both the size of the three otoliths and the pathway taken by the VIII nerve. In bony fish, the pars inferior usually comprises two fluid filled pouches, the saccule and lagena, with each pouch containing a crystalline calcium carbonate otolith (Carlström, 1963). However, in *P. spathula* and *A. fulvescens*, there is no internal division between the saccule and lagena, thus, in these species, the pars inferior consists of just one fluid filled pouch.

The saccule is considered to be the major auditory organ in most bony fish species and in sharks and rays (Corwin, 1983). Though fish from the order Acipenseriformes are principally cartilaginous, they evolved from fish that were originally bony (Nelson, 1984). The morphology of the inner ear supports this hypothesis, as both *P. spathula* and *A. fulvescens* have three otolithic organs and associated sensory epithelia comparable to that of many bony fish with generalist hearing abilities. For fish to locate the source of a sound in both the horizontal and vertical planes, they rely on the stimulation of ciliary bundles oriented specifically along the sound propagation axis (Lu & Popper, 1998). In *P. spathula* and *A. fulvescens* the saccule bears hair cells orientated in two opposing quadrants, rather than the usual four quadrant (standard) arrangement found in most generalist fish species (Popper & Fay 1993). However, the topographic data from the saccule shows that caudal hair cells are orientated on the dorsal and ventral axis, whereas the anterior hair cells are orientated on the anterior posterior axis with respect to the fish. The four quadrant configuration is common to a number of generalist fish (Popper & Fay,

1993); but in the case of *P. spathula* and *A. fulvescens*, it is caused by a 90° curve in the macula, rather than the hair cells changing polarity relative to the adjacent perimeter. The shape and polarisation of the hair cells of the lagena macula in *P. spathula* is similar to the arrangement found in other teleost fish (see Lovell et al., 2005 b; Popper & Fay, 1993), though in *A. fulvescens* the macula was longer and more narrow, with fewer dorsally orientated hair cells restricted to a narrow band running along the upper anterior margin.

This is the first time that fish from the order Acipenseriformes have been assessed in an ABR audiological examination, so by testing both *P. spathula*, and *A. fulvescens*, it allows for a comparative analysis of the results between both species. The twelve specimens of *A. fulvescens* and twelve specimens of *P. spathula* were stimulated with sound ranging in the frequency domain between 100 Hz to 1500 Hz (only up to 500 Hz has been included on the audiogram), presented in a sound field dominated by either sound pressure or particle motion, at levels of between 156 dB to below 120 dB (re 1 μPa). Statistical analysis of each frequency tested was also performed using a t-test, and compared the means of threshold responses from *P. spathula* and *A. fulvescens*. The results presented in tables 5.1 and 5.2 show a statistical similarity at all frequencies from 250 Hz and upwards (in the pressure dominated sound field), giving a p value greater than 0.05, whilst 100 Hz and 200 Hz were found to have p values less than 0.05, and are therefore not statistically similar between these two fish; *A. fulvescens* hears slightly better at low frequencies than *P. spathula*. The statistical analysis of the thresholds of hearing in a sound field dominated by particle motion was found to be statistically similar between both species, at all frequencies tested (in some cases, e.g. 250 Hz and 500 Hz, there was very little to distinguish between individuals).

Overall, the audiograms for *P. spathula* and *A. fulvescens* (presented in Figure 5.11), show similar sensitivity to frequency and general hearing abilities between Acipenseriform fish, with the lowest hearing thresholds acquired from frequencies in a bandwidth of between 200 Hz to 300 Hz, and higher thresholds at 100 Hz and 500 Hz. This is in contrast with the usual generalist audiograms, many of which show that the lowest thresholds are obtained from frequencies at or below 100 Hz, such as the results of the ABR audiogram for the Italian freshwater gobies *Padogobius martensii* and *Gobius nigricans* by Lugilli et al. (2003), or the behavioural audiogram for the cod (*Gadus morhua*) by Chapman and Hawkins (1973). The lowest hearing thresholds with the sound field dominated by sound pressure (transducers driven in phase) was 131 dB (re 1 μPa) at 250 Hz for *P. spathula*, and 133 dB (re 1 μPa) at 200 Hz for *A. fulvescens*; whilst the lowest hearing thresholds

with the sound field dominated by particle motion (transducers driven out of phase) was 200 Hz, 119 dB (re 1 µPa) for *P. spathula*, and 120 dB (re 1 µPa) at 250 Hz for *A. fulvescens*. Worthy of note here, is the similarity of the sound pressure audiograms from both *P. spathula* and *A. fulvescens* to an ABR generated audiogram for the little skate *Leucoraja erinacea* by Brandon et al., (2003). The pallid sturgeon (*Scaphirhynchus albus*) and shovelnose sturgeon (*S. albus*) are known to produce a wide variety of sounds ranging from squeaks and chirps of around 1000 Hz to 2000 Hz, to low frequency knocks and moans ranging in frequency between 90 Hz to 400 Hz (Johnston & Phillips, 2003). Comparisons of the sounds produced by these fish with the audiogram for *A. fulvescens*, reveals that the knocks and moans produced during the breeding season appear to fall well within the optimum range of audible frequencies, whilst the squeaks and chirps may fall outside of this range.

It is known that the frequency and intensity of a tone burst effects the latency of the evoked response (Corwin et al., 1982; Kenyon et al., 1998), as does the metabolic state of the organism (Corwin et al., 1982). The latency of the evoked potentials from *P. spathula* can be observed in Figure 5.12, and are in response to the second sinusoid of the 300 Hz tone burst presented in Figure 5.8. The sound was presented initially at 156 dB (re 1 µPa), and attenuated in 5 dB steps, and the arrows positioned at 0.3 ms intervals represents the response issuing from the auditory pathway to the midbrain. The increase in the latency of the evoked potential in response to decreasing stimulus intensity is often used to verify that the averaged waveform is a product of auditory stimulation rather than a transient generated at the electrode tip (Kenyon et al., 1998). Thus, the Inter-Peak Latency (IPL) cannot be accounted for acoustically, as transients and other artefacts directly associated with the stimulus sound would occur at the same time regardless of sound amplitude.

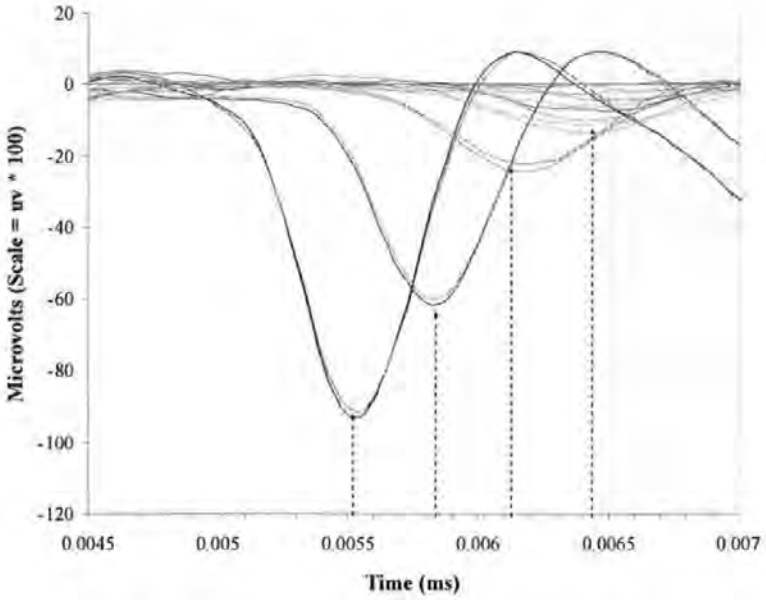

Figure 5.12. Auditory Evoked Potentials (AEPs) from *P. spathula* in response to the second sinusoid of a 300 Hz 4 cycle tone burst presented initially at 150 dB (re 1 μPa), and attenuated in accordance with Figure 5.10. The arrows show the peak of the AEP, which occurs with an Inter-Peak Latency (IPL) of approximately 0.3 ms for each of the amplitudes tested (averaged over 2000 iterations per waveform set)

It may be concluded from the evidence presented both from this Chapter, and Chapters 3 and 4, that the system and protocols described here can be used with relative ease and minimal discomfort to the subject, to generate reliable and accurate audiological information from both generalist and specialist fish. As discussed, the shape and amplitude of the recorded waveforms presented in this study compare well with published ABR type investigations, and confirms the suitability of the system for the specific objective of measuring hearing ability. It now remains to build on current understanding of hearing in marine animals, and provide useful information on the hearing ability of the crustaceans, a sub-phylum of animals that are considered to be deaf and only capable of feeling strong vibrations transmitted directly through a solid (see Cohen and Dijkgraaf, 1961). Many invertebrate animals posses balance organs that function similarly to the vertebrate ear, and in the next Chapter, it is hypothesised that this organ should also provide the crustacean central nervous system with auditory data, contrary to the current literature.

Chapter 6

The hearing abilities of crustaceans

6.1 Introduction

The previous three Chapters have investigated hearing in both specialist and generalist bony fish, and in two species of cartilagionous fish, demonstrating the flexibility of the system when testing a diverse range of species. In this chapter, the mechanism of sound reception and the hearing abilities of the prawn (*Palaemon serratus*), are studied using a combination of anatomical, electron microscopic and electrophysiological approaches, and reveal that *P. serratus* is responsive to sounds ranging in frequency from 100 Hz to 3000 Hz. It is the first time that the Auditory Brainstem Response (ABR) recording technique has been used on marine invertebrates, and the acquisition of hearing ability data from the present study adds valuable information to the inclusion of an entire sub-phylum of animals when assessing the potential impact of anthropogenic underwater sounds on marine organisms. Work was pursued to acquire auditory evoked potentials from *P. serratus*, using two subcutaneous electrodes positioned in the carapace close to the supraesophageal ganglion and the statocyst (a small gravistatic organ located below the eyestalk on the peduncle of the bilateral antennules). The morphology of the statocyst receptors, and the statocyst nerve pathways to the brain have also been studied, revealing that *P. serratus* possesses an array of sensory hairs projecting from the floor of the statocyst into a mass of sand granules embedded in a gelatinous substance.

The fundamental measure of the hearing ability of any organism possessing the appropriate receptor mechanism is its audiogram, which presents the lowest level of sound that the species can hear as a function of frequency. The statocyst of *P. serratus* is shown here to be sensitive to the motion of water particles displaced by low frequency sounds ranging from 100 Hz up to 3000 Hz, with a hearing acuity similar to that of a generalist fish. Also, recorded neural waveforms were found to be similar in both amplitude and shape to those acquired from fish and higher vertebrates, when stimulated with low frequency sound, and complete ablation of the electrophysiological response was achieved by removal of the statocyst.

It is known that several crustacean species produce sound; for example, the pistol shrimp (*Alpheus spp*) produces a loud click by rapid closure of a specially adapted claw (Schmitz and Herberholz 1998). The spiny lobster (*Palinurus vulgaris*) and the rock lobster (*P. longipes*) make alarm sounds by drawing the base of the antenna across scale like ridges below the eyestalks; Patek, 2001; Meyer-Rochow et al., 1982). Additionally, *P. longipes* has been shown to take longer emerging from a hide, when feeding was preceded by a white noise (Meyer-Rochow et al., 1982). The female cricket (*Gryllus bimaculatus*) has the ability to localise and respond to male chirp sounds (Hedwig & Poulet, 2004; Schildberger & Hörner, 1988), using specially adapted acoustic receptors (tympanum), located in the forelegs below the knee (Huber & Thorson, 1985). On hearing the chirp, a receptive female will orientate itself toward the sound using a behavioural response known as phonotaxis (Schildberger & Hörner, 1988).

The ability of an organism to orientate itself in the 3-D marine environment requires the presence of a suitable gravity receptor. These receptors occur in many diverse organisms throughout the marine environment, and include cephalopod (Dilly et. al., 1975; Bettencourt & Guerra, 2000), crustaceans (Prentiss, 1901; Schöne, 1971; Rose & Stokes, 1981; Patton & Grove, 1992), and fish (Popper & Platt, 1983; Bretschneider et al., 2001). In crustaceans the statocyst is located either at the anterior end of the animal in the basal segment of each antennule, or posteriorly within the uropods, abdomen or telson, (Farre, 1843; Cohen and Dijkgraaf, 1961; Finley and Macmillan, 2000). It has been well established that the crustacean statocyst functions as an equilibrium organ by initiating corrective movements to maintain the animal's position in the water column, (Cohen and Dijkgraaf, 1961; Sekiguchi and Terazawa, 1997; Finley and Macmillan, 2000; Fraser, 2001), thus swimming activity is highly dependent on statocyst input (Fraser et al., 1987).

In this work, the electrophysiological response of the statocyst in an underwater sound field is studied, using the Auditory Brainstem Response (ABR) recording technique originally developed for use in clinical neurophysiology. Until now, this method of acquiring hearing ability has been applied only in auditory assessments of vertebrates (Corwin et al., 1982), though the presence of afferents in the statocyst, and existence of a neural pathway terminating in the supraesophageal ganglion, indicates that the physiology of *P. serratus* may be suitable for an ABR type investigation. An ABR waveform is acquired by averaging conglomerate responses of peak potentials, arising from nuclei in the auditory pathway during acoustic stimulation (Corwin et al., 1982; Overbeck & Church, 1992; Lovell et al., 2005 A). The sweep records the generation of neural

waveforms over a user-defined time span termed the sweep velocity, and measures activity prior to, during and after stimulation of the receptor organ. Additional waveform generation by neural activities other than those associated with hearing, combined with muscular movements, ensure that recordings have to be repeated over 1000 to 2000 presentations before clear results can be obtained (Kenyon et al., 1998; Yan et al., 2000). The recorded waveforms resulting from each sweep are averaged together and produce a recognisable ABR waveform, which is then overlaid on the first run, to show that the evoked potentials are repeatable.

The nerves associated with the statocyst and the pathways taken to the neuropil of the antennule in the supraesophageal ganglion were examined to provide a detailed description of how acoustic signals are perceived and transmitted by the neuronal pathways. The aim of the present study, therefore, is to examine the morphology of the statocyst receptor array of the prawn (*Palaemon serratus*) using both scanning and transmission electron microscopy (SEM & TEM). Measurements of the electrophysiological response of the statocyst and Central Nervous System (CNS) to acoustic stimuli were also made, and by ablation, it was demonstrated that the evoked response was generated in the statocyst organ.

6.2 Materials and Methods

One hundred specimens of the prawn (*Palaemon serratus*) Phylum Crustacea and Class Eumalacostraca of mixed sex, and ranging in length from 27 mm (0.1 g) to 71 mm (1.9 g) were obtained from wild stock in the South West of England using a dip net. Once captured, the prawns were transferred to a marine tank divided by a fine mesh screen into four equal sized compartments of 50 litres each. An Eheim type 2013 biological filter with a flow rate of 390 litres per hour maintained water quality and provided aeration by spraying filtered seawater back into the tank via the filter outlet pipe located 60 mm above the water surface. The ambient noise within the holding tank was measured using a hydrophone, and the sound pressure level was calculated to be 102 dB (re 1 μPa), with the Eheim pump active. In all of the experiments, and in the holding tank, the ambient water was kept at a temperature of 18° C and a salinity of 34 psu. When not under experimental protocols, the prawns were provided with 14 hours of light per day from a fluorescent tube controlled by a mains timer switch. Prior to any experimentation the prawns were divided by size into three populations, and fed on a granulated feed at a daily rate of 6 g for the large prawns, 4 g for the medium and 2.5 g for the small.

6.2.1 Preparation methodology for dissection and electron microscopy

The pathway taken by the innervating nerves of the statocyst to the supraesophageal ganglion or brain was revealed by the anatomical investigation of a 54 mm *P. serratus*. The prawn was first immersed in 70% ethanol for 18 hours, to "fix" the specimen prior to the investigation. Exposure of the brain and statocyst was achieved by the dissection and removal of the dorsal-rostral section of carapace, the dorsal cuticle layer of the peduncle, the left eye, and the stomach.

Specimens of *P. serratus* selected for EM examination were denied access to materials that could be used as otoliths, primarily by having no substrate present in the tank. Additionally, uneaten feed and other waste products were removed by ensuring that the return flow of water to the filtration system was strongest at the base of the tank. Particulate matter was drawn by the flow of water through a 5 mm gap under each of the tank divisions, through which the prawns could not pass. The denial treatment was applied to all 100 of the prawns, with the exception of Figure 6.4 which was prepared for EM examination within 48 hours of capture. Moulting was induced in the remaining specimens over a 24 hour period using a method that involved not changing the ambient tank water for 7 days, followed by a sudden change of all the water.

The statocyst capsules were removed by dissection from 12 of the specimens, and placed in a conical dish containing 2.5 ml of 0.9 % sodium chloride. The capsules were opened by making a lateral incision around the statocyst chamber using a fine scalpel. Needlepoint tweezers were used to lift the upper section of the capsule, thus exposing the sand granules and ultrastructure. The sodium chloride solution was removed using a pipette and replaced with a solution of 2.5 % S-Carboxymethyl-L-Cysteine in sodium chloride, which was used to hydrolyse the mucus surrounding the statocyst receptors. The contents of the dish were gently agitated for two minutes, after which the solution was removed and replaced with chilled fixative (2.5% glutaraldehyde in 0.1 M cacodylate buffer with 3.5% sodium chloride). The statocyst capsules were then dehydrated through a graded ethanol series ranging from 35% through 50%, 70% and 90% to absolute ethanol, prior to desiccation using the critical point drying method described by Platt (1977). Fully desiccated statocyst capsules were subsequently mounted on a specimen stub using a carbon tab, and coated with c. 8 nm of gold in an Emitech K 550 sputter coater (working at approximately 5 x 10^{-6} Torr). Finally, the processed specimens were investigated and

photographed using a JEOL JSM 5600 scanning electron microscope operated at 15 kv, and a 15 mm working distance. Images of the ultrastructure were captured using the JEOL software, which saved the micrographs in a bitmap format. All measurements were carried out on a PC using the analySIS® (Soft Imaging System GmbH) program. The setae dimensions were measured using polygon length, and measurements were recorded in micrometers (μm). Measurements of setae dimensions (height, width etc) are averages taken from at least 12 observations of a feature within a similarly orientated cluster of cells, with the exception of those in Figure 4 which were taken from 5 observations.

6.2.2 ABR methodology

In order to concisely answer the question of hearing by crustaceans, twelve prawns were stimulated with sound ranging in the frequency domain between 100 Hz to 3000 Hz, presented at sound pressure levels of between 132 dB (re 1 μPa at 1 m) to below 90 dB (re 1 μPa at 1 m). The response of the prawn to acoustic stimulation was measured using a well established audiometry technique, with the results expressed as an audiogram or limen of sound spectral sensitivity. The ABR measurements of hearing threshold were made using a proprietary control and analysis programme, written in a LabView 7 environment. This programme both generated the stimulus signals and captured and analysed the response, and was installed onto the PC shown in Figure 6.1.a. The stimulus used was a sine train (sine wave pulse) which was presented to *P. serratus* at a given frequency and sound pressure level, not exceeding 130 dB (re 1 μPa at 1 m) for each of the frequencies tested. For ABR recordings to be clear, it requires that short duration tone bursts are used, especially for the low frequencies. Kenyon et al. (1998) used a two cycle burst for frequencies between 100 and 300 Hz, a five cycle burst with a 2 cycle attack decay for frequencies between 400 and 3000 Hz. Amplification of the sound was achieved using a Pioneer type SA-420 amplifier and a 200 mm Eagle L032 loudspeaker with a frequency response range of 40 Hz to 18000 Hz. Additionally, the loudspeaker was placed inside a Faraday cage and connected to a centralised earth point located in an adjacent room where the PC, amplification, and analysis equipment was set up. Connecting wires were fed through a 100 mm port in the partitioning wall.

The test subjects were placed in a flexible cradle formed from a soft nylon mesh rectangle saturated with seawater. Oxygenated water kept at a temperature of 18° C was gravity fed at an adjustable flow rate of 3 millilitres per second and directed toward the gills. The

water was held in an aerated reservoir positioned in an adjacent room, and fed to the prawn through a 4 mm diameter plastic tube. The prawn was first placed lengthwise and centrally on an 80 mm x 60 mm rectangle of fine nylon netting, which was wrapped firmly around the cephalothorax and pleon, and the two sides of the net were held together using the clip shown in Figure 6.1.b.

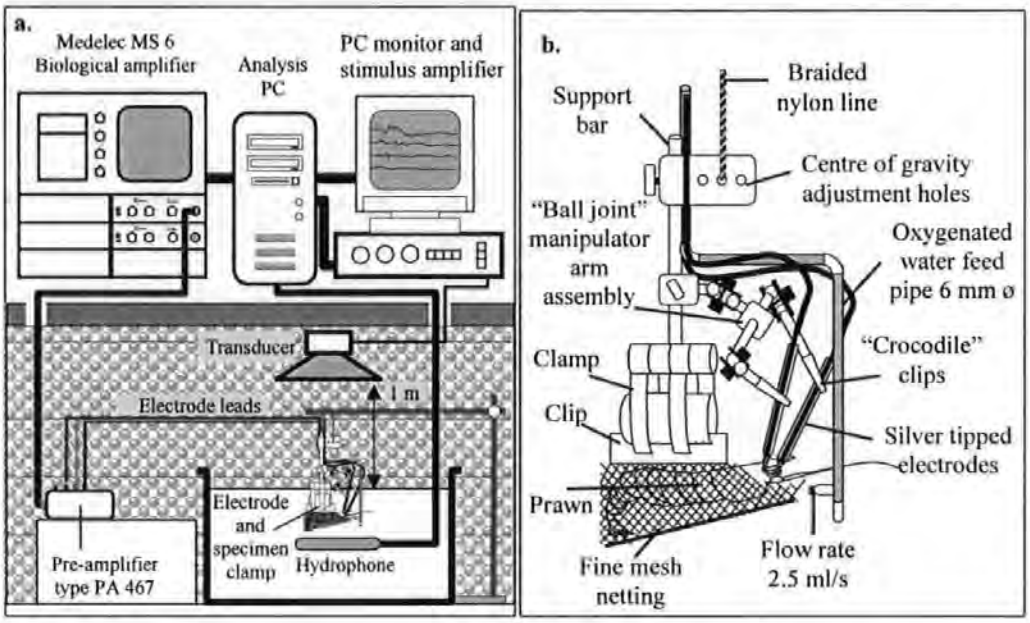

Figure 6.1.a. Schematic of the ABR audiometry system, and **6.1.b.** the clamp used to hold the prawn in position, and manipulate the electrodes during the audiological tests

The clip was placed in a retort stand clamp fitted with ball joint electrode manipulator arms, and the aerated water pipe (detailed in Figure 6.1.b). During the procedure to position the electrodes detailed in Figure 6.2, the specimen and clamp were suspended over a plastic tray, and aerated water was supplied to the prawn. A retort stand and the experimental tank (L. 450 mm x W. 300 mm x D. 200 mm) were placed on a table with vibration inhibiting properties, located in an underground anechoic chamber L. 3 m x W. 2 m x H. 2m. Working under a MEIJI binocular microscope, two small holes were made in the cuticle layer using a lancet, penetrating the carapace to a maximum depth of 0.3 mm. The reference electrode was located behind the supra-orbital spine, close to the neuropil of the antennule, and the record electrode was located in the peduncle close to the statocyst, at the junction between the lateral antennular and statocyst ganglia. The clamp assembly with the specimen and sited electrodes were then suspended from the retort stand positioned over the experimental tank, and the prawn stationed 5 mm below the surface of

the water. After the hearing assessment, the prawns were relocated to a holding tank for observation, prior to being returned to the divided aquarium.

The electrophysiological response of the prawn to acoustic stimulation was recorded using the two sub-cutaneous electrodes (see Figure 3.3 for schematic), which were connected to the MS6 preamplifier by 1 m lengths of screened coaxial cable with an external diameter of 1.5 mm. The outer insulating layer of the coax was removed 15 mm from the end where the electrode tip was to be fixed, and the screening layer removed 10 mm from the cable end. The inner insulating material was then trimmed by 2 mm, and the exposed inner wire (0.5 mm diameter) was tinned with silver solder and joined to a 10 mm length of silver wire (0.25 mm diameter), tapered to a fine point.

The assemblage was pushed through a 100 mm glass pipette with an internal diameter of 4 mm, until 0.4 mm of the gold wire was exposed. The remaining space inside the pipette was filled with a clear epoxy resin, and then trimmed to expose 0.3 mm of silver tip through which the AEP could be conducted. The impedance of the electrodes, both between the outer shielding and inner core, and the silver tip and MS 6, were tested using an M 205 precision digital multimeter. The impedance between the tip and pre-amplifier was found to be 0.2 Ω for both electrodes, and an open circuit was recorded between the outer shielding and inner core. The evoked response was amplified and digitised to 12 bits resolution and recorded. This process was repeated 2000 times and the response averaged to remove electrical interference caused by neural activities other than audition, and the myogenic noise generated by muscular activity.

Each measurement was repeated twice; this aids in separating the evoked response, which is the same from trace to trace, from the myogenic noise, which varies in two successive measurements. After the averaging process, the evoked potential could be detected, following the stimulus by a short latency period of 5 milliseconds or so. The latency is accounted for by the time it takes the sound in air to travel the 1 m to the prawn, plus 1 to 2 milliseconds response latency.

6.2.3 The sound field

The properties of the sound field are especially relevant when comparing the audio capabilities of both pressure sensitive and motion sensitive aquatic animals in the near field. In a small laboratory set-up, the complexities associated with independently

measuring sound pressure and particle motion are compounded by the reflectivity of the tank sides and base. For this reason, a number of experiments have used used air-mounted transducers to successfully generate sounds underwater (e.g. Fay and Popper, 1975; Yan et al., 2000; Akamatsu et al., 2002). The principal advantage of such a system is that as the sound source is located at a distance of 1 m from the air/water interface, the moving part of the transducer does not contact the water and generate near-field displacements. In this situation the pressure and motion of the water adjacent to the fish ear can be considered as being equal (Hawkins 1981). The stimulus tones presented from the loudspeaker to the prawn were calibrated using an insertion calibration. A calibrated Bruel and Kjaer Type 8106 Hydrophone (Serial Number 2256725) was placed in the tank and positioned adjacent to the shrimp cephalothorax region (See Figure 3.4 for calibration markers). The signal from the hydrophone was amplified using a PE6 preamplifier and digitised using a National Instruments DAQ-6062e interface card at a sample rate of 300 kS/s. Figure 6.3 shows the power spectra of the 500 Hz and 1000 Hz stimulus sounds, which were recorded using the hydrophone and analysis software from Figure 6.1a. The onset/decay of 2 cycles was used to reduce spectral side lobes and speaker transients which can be generated by sudden high power transmissions.

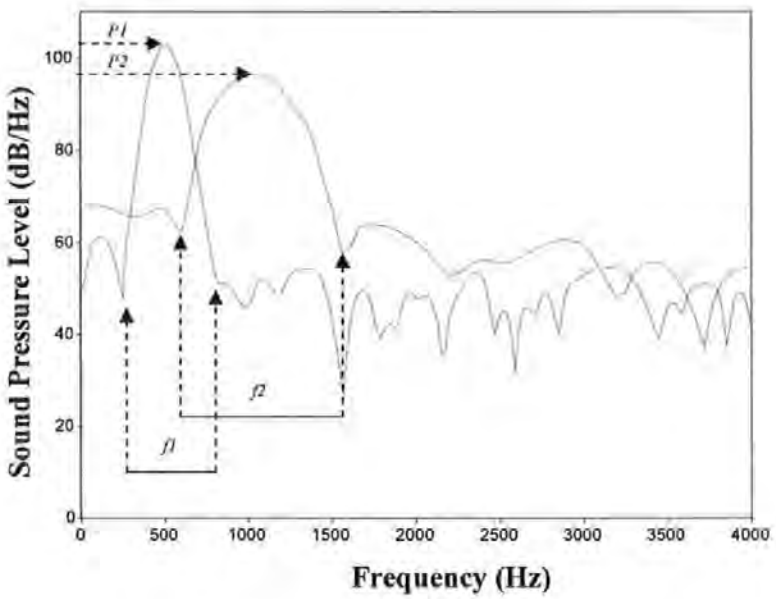

Figure 6.2. Power spectra of the 500 Hz and 1000 Hz tone bursts, recorded underwater using the hydrophone and analysis PC shown in Figure 6.1. The arrows *P1.* and *P2.* show the peak sound pressures, and the bars *f1* and *f2* indicate the overall bandwidth of frequencies generated during the transmission of the two bursts

In case of non-proportionality of the response of the loudspeaker, measurements of the sound pressure were taken for each amplitude and frequency setting used. Consequently, a total of 110 individual calibration measurements were taken in the calibration process.

6.2.4 Ablation

Specimens of *P. serratus* selected for the ablation procedure were first tested for an electrophysiological response to a 500 Hz sound presented at 110 dB (re 1 μPa at 1 m). Removal of the statocyst was achieved by making a circular cut in the cuticle layer above the chamber, and withdrawing the capsule using needle point tweezers (a procedure that took a few seconds). A sham operation (the cuticle layer cut, but the statocyst left in place) was also performed, and the prawns were re-tested 1 hour after cutting around the chamber, prior to removal of the statocyst. The prawns were then placed into an empty compartment of the holding tank and allowed to recover for 24 hours, prior to being retested on the electrophysiology apparatus. The post ablation recovery period was included to give the prawns time to settle after the procedure, as the metabolic state of the organism can have a detrimental affect on the evoked potential (Corwin et al., 1982).

6.3 Results

6.3.1 Innervation of the statocyst

In decapod crusteacea, the lateral antenular and statocyst nerves extend with bi-lateral symmetry from the neuropil of the antennule; a region located centrally in the brain (Prentis, 1901), to the statocyst and tactile bristles of the antennules. The brain of *P. serratus* lies close to the rostral extremities of the carapace, ventral to the eyestalks and posterior to the antennules. On leaving the anterior region of the brain (detailed in Figures 6.3.a and 6.3.b), the lateral antennular ganglion (*gla.*) projects forward and enters the antennule close to the inside edge of the peduncle. From there, the statocyst ganglia branches outward from the main antennular nerve which projects forward to the tactile receptors.

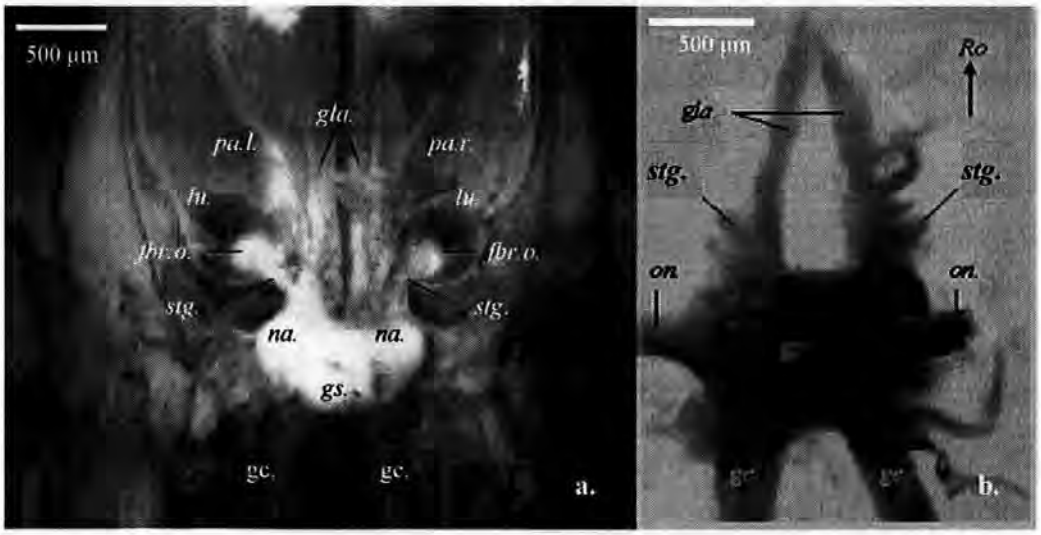

Figure 6.3.a. Dorsal view of the supraesophageal ganglion and lateral antennular and statocyst ganglia from *P. serratus* (with the statocyst capsules and optic neuropil removed). *fbr.o.* peripheral statocyst nerve fibres, *gc.* commissural ganglion, *ga.* antennular ganglion, *na.* neuropil of the antennule, *gs.* supraesophageal ganglion, *stg.* statocyst ganglion, *lu.* lumen of the statocyst, *pa.r,l.* peduncle of the right and left antennule. **Figure 6.3.b.** Dorsal view of the brain and major nerve ganglia dissected from *P. serratus*. *gs.* supraesophageal ganglion, *gla.* lateral antennular ganglion, *stg.* statocyst ganglion, *on.* optic nerve, *gc.* commissural ganglion. *Ro*. Rostral direction.

6.3.2 Scanning electron microscopy

The examination of the complete statocyst (prior to removal of the sand granules) revealed ultrastructural cell projections extending into the mass of sand granules shown in Figure 4.a. The cells project from small apertures in the statocyst floor about 7 µm in diameter; through which the receptor connects to the peripheral fibres of the statocyst ganglion. At a distance of 2 µm from the base, the cell widens and forms a bulb (*rb.* in Figure 6.4.a) which has a diameter of 9 µm at its widest point, and displays a series of longitudinal ridges that run around the bulbous structure. The uppermost portion of the cell base narrows to 0.8 µm, forming a fulcrum point from where a 3.5 µm diameter hair shaft extends 40 µm into the lumen of the statocyst, and contacts with the sand granules (*sg.*).

The overall view of the receptor array and the tips of the cells are precluded from view by the sand and a fine structure, consisting mostly of residuals left by the desiccation process of a gelatinous mucus (*mu.*) that in life surrounds the sand and cell tip. The view of the

statocyst ultrastructure (without sand granules attached) in Figure 6.4.b. (taken perpendicular to the horizontal plane) shows the setae array from a specimen of *P. serratus* denied sand for 7 days post moulting.

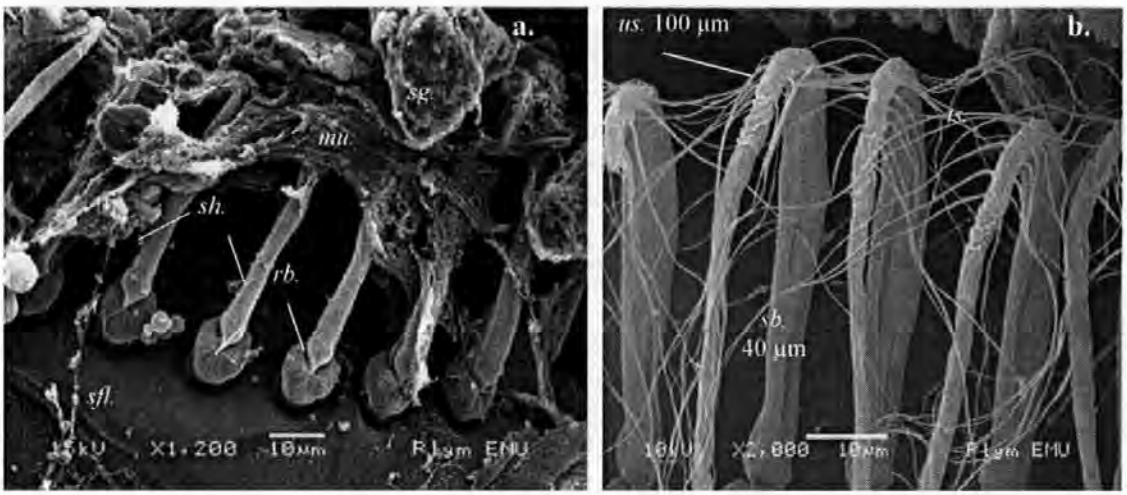

Figure 6.4.a. Receptor cell projections contacting sand granules in the statocyst of *P. serratus*. *mu.* mucus, *rb.* receptor base, *sfl.* statocyst floor, *sg.* sand granule, *sh.* setae shaft, and **Figure 6.4.b.** shows the 40 µm lower setae body (*sb.*), the 100 µm upper tapering sections (*us.*) and thread like strands (*ts.*) found enmeshed with the sand granules, orientated toward a central point. *sb.* cell setae body

The absence of sand granules reveals more than 70 vertical cell projections arranged in a row shaped like a crescent, covering 0.073 mm^2 of statocyst (Figure 6.5.b). Each setae is orientated toward a common central region (*cr*), and the shortest hairs (< 120 µm) were found proliferating in a band running down the left side of the array, whilst the longest hairs (> 170 µm) were found in the right caudal quadrant. The statocyst capsule is elliptical in shape, and the walls (Figure 6.5.b) symmetrically curve inward toward the base, where the receptor cells are located on a mound rising 40 µm from the floor of the capsule. From the crest of the mound, the receptor hairs project upward into the lumen of the statocyst at angles of between 27° and 74° from the horizontal plane. Behind the setaes, in the space between opposing receptors, the mound flattens and forms a plateau (*pl*), which is devoid of any ultrastructure.

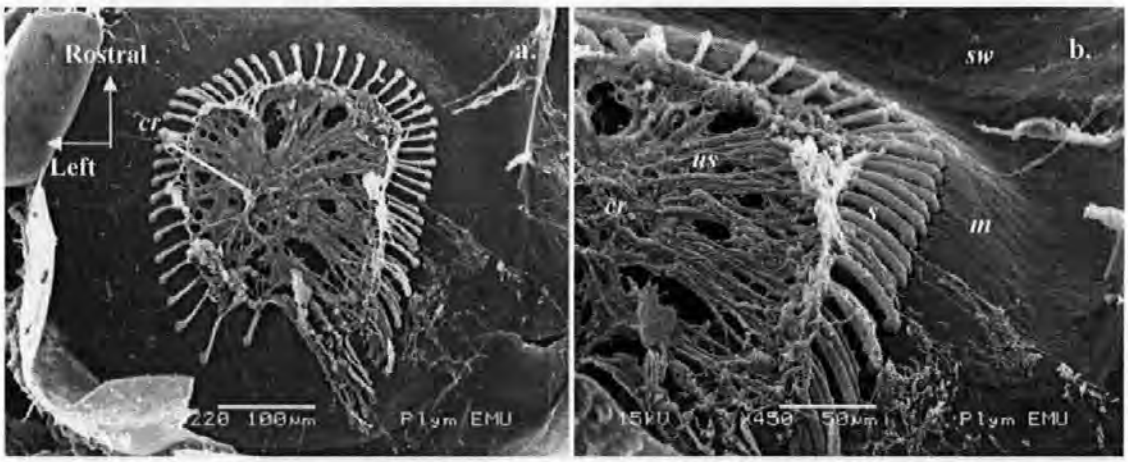

Figure 6.5.a. Dorsal view of the statocyst from a 55 mm prawn denied sand for 7 days post moulting. *cr.* central region, and **Figure 6.5.b.** Lateral view of the statocyst. *cr.* central region, *s.* setae, *m.* mound, *sw.* statocyst wall, *us.* upper tapering section of setae

6.3.3 Transmission electron microscopy (TEM)

The TEM section in Figure 6.6.a shows a cross section through the setae base and structures present in the peripheral nerve bed, from the statocyst of *P. serratus*. Figure 6.6.b shows a cross section through a hair cell from the saccule of the European sea bass (*Dicentrarchus labrax*), which has been included in this section along with the SEM of the setae (Figure 6.6.d) for comparative purposes. The two hatched lines drawn on the prawn setae SEM micrograph presented in Figure 6.6.c shows the locations from where the statocyst TEM sections in 6.6.a. was taken.

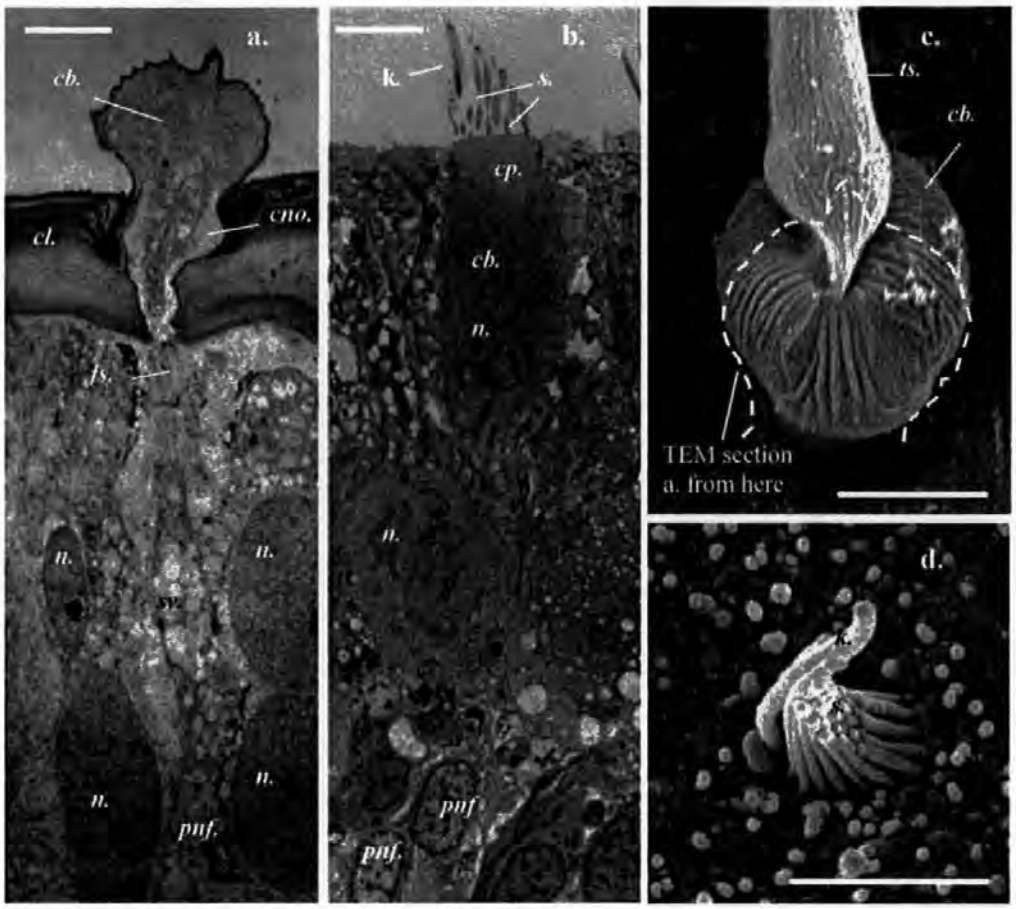

Figure 6.6.a. TEM micrograph of the setae base from the statocyst of *P. serratus*, *fs.* fibrous strands, *cl.* cuticle layer, *cno.* cuticular notch, *n.* neuclei, *pnf.* peripheral nerve fibre, *sv.* synaptic vesicles. **6.6.b.** saccular hair cell and innervating nerve fibres from the ear of *Dicentrarchus labrax* (From Lovell et al., 2005 C), *cb.* cell body, *cp.* cuticular plate, *k.* kinocilia, *n.* nucleus, *pnf.* peripheral nerve fibres, *s.* stereocilia. **6.6.c.** SEM micrograph of the statocyst setae from *P. serratus*, *cb.* cell base *ts.* tapering section, **6.6.d.** SEM micrograph of the ciliary bundles projecting from the epithelial surface of *D. labrax*, *k.* kinocilia, *s.* stereocilia. Bars = 5 μm

The "root" of the statocyst setae is buttressed by supporting cells with large nuclei (*n.*), and fibrous strands (*fs.*) resembling actin filaments, which can be seen extending into the peripheral nerve bed through the cuticular plate. The filaments may help anchor the setae into position, and work in conjunction with a small notch in the cuticle layer (*cno.*) containing part of the lower cell body. The filament strands terminate 15 μm below the cuticle layer, in a region containing rounded structures less than 0.75 μm in diameter, which are thought to be the synaptic vesicles between the setae and the peripheral statocyst nerve fibres (*pnf.*). Close examination of the TEM section through the statocyst setae body

(Figure 6.7.a) reveals that it contains a single nucleus (*n.*) positioned at the top of the cell. The hatched line in the basal region of the cell marks the perimeter of two vesicles, which appear to be associated with the fibres in the cell root. Figure 6.7.b shows the fibrous strands as they terminate in the synaptic vesicles (*sv.*) located 15 μm below the cell base.

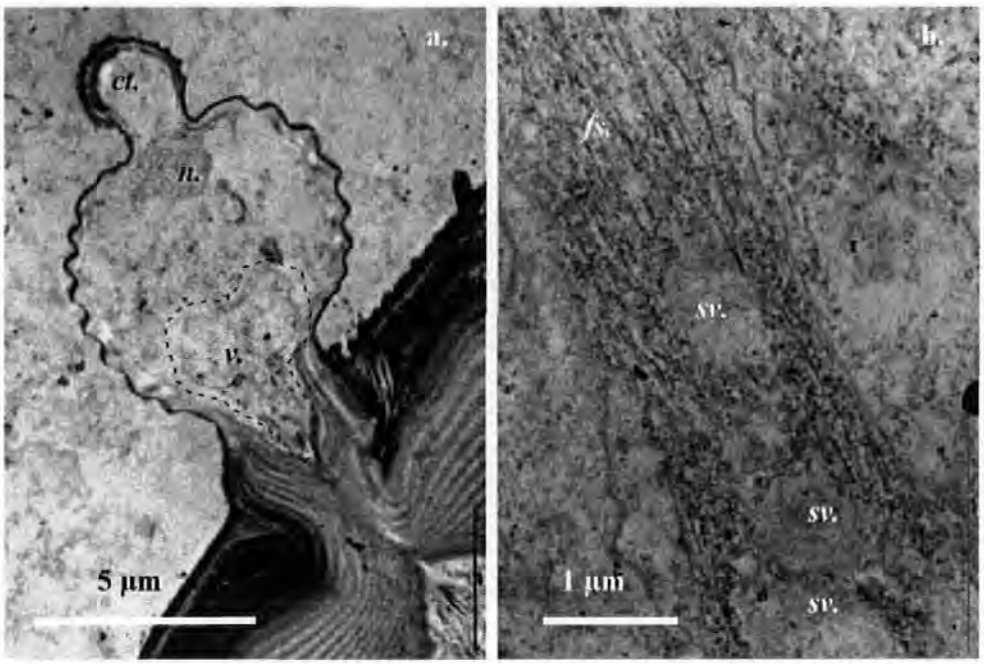

Figure 6.7.a. TEM section through the cell base from *P. serratus*, showing the cell nucleus (*n.*), and the beginning of the angled cell tip (*ct.*), and vesicles (*v.*) which appear to be associated with the fibrous strands (hatched area). **Figure 6.7.b.** shows the fibrous strands (*fs.*) of the cell root, and the synaptic vesicles (*sv.*) located in the peripheral nerve bed.

6.3.4 Electrophysiological response to auditory stimuli

In order to more concisely answer the question of hearing by crustaceans, twelve prawns of mixed sex were stimulated with sound ranging in the frequency domain between 100 Hz to 3000 Hz, presented at sound pressure levels of between 130 dB (re 1 μPa at 1 m) to below 90 dB (re 1 μPa at 1 m). The Auditory Brainstem Response (ABR) recording technique has been successfully applied in the auditory assessments of both mammalian and non-mammalian vertebrates. An ABR waveform is acquired by averaging potentials from nuclei in the auditory pathway during acoustic stimulation. The AEPs presented in Figure 6.7 were recorded using the Medelec MS 6 biological amplifier with subcutaneous electrodes positioned using a jointed clamp assembly, and the prawn held in place using a

fine mesh nylon cradle. The reference electrode was located in proximity to the neuropil of the antennule, and the record electrode located at the junction between the lateral antennular and statocyst ganglia. The acoustically evoked neural waveforms presented in Figure 6.7, were recorded from *P. serratus* in response to tone bursts ranging in frequency from 500 Hz to 3000 Hz, and averaged over 2000 stimulus presentations (100 Hz and 300 Hz have not been included for scaling reasons). The waveforms show a series of peaks contiguous with the stimulus sound.

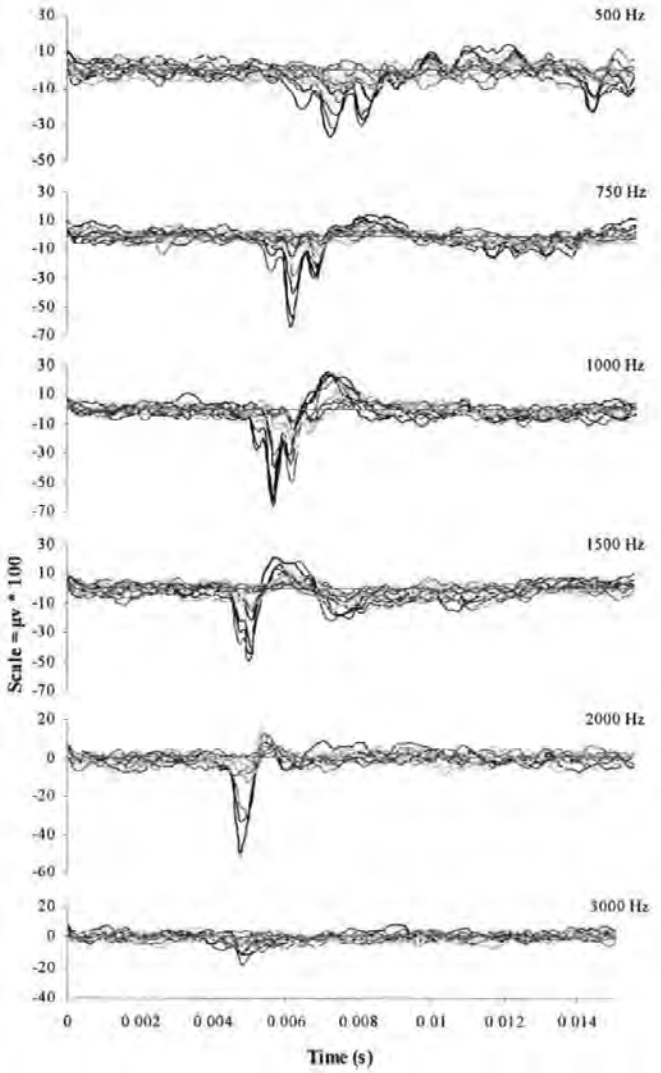

Figure 6.8. Auditory Evoked Potentials from *P. serratus* to tone bursts of 500 Hz, 750 Hz, 1000 Hz, 1500 Hz, 2000 Hz and 3000 Hz, and averaged over 2000 sweeps. The AEP at each amplitude tested has been overlaid, and shows a reduction in the response latency with increasing frequency. Scale: 1 µV = 100

6.3.5 Threshold determination

Threshold responses from twelve, 50 mm to 55 mm (medium) prawns were determined visually from the sequentially arranged waveforms for each frequency tested, in accordance with Kenyon et al (1998). Figure 6.9 shows ABR waveforms evoked from *P. serratus* in response to a 500 Hz tone burst, presented initially at between 120 to 132 dB (re 1 μPa at 1 m), and attenuated in steps of 4 dB (re 1 μPa at 1 m) ordinarily, and 2 dB (re 1 μPa at 1 m) as the hearing threshold was approached. When two replicates of waveforms showed opposite polarities (see 110 dB traces in Figure 6.9), the response was considered as being below threshold (cf. Kenyon et al. 1998).

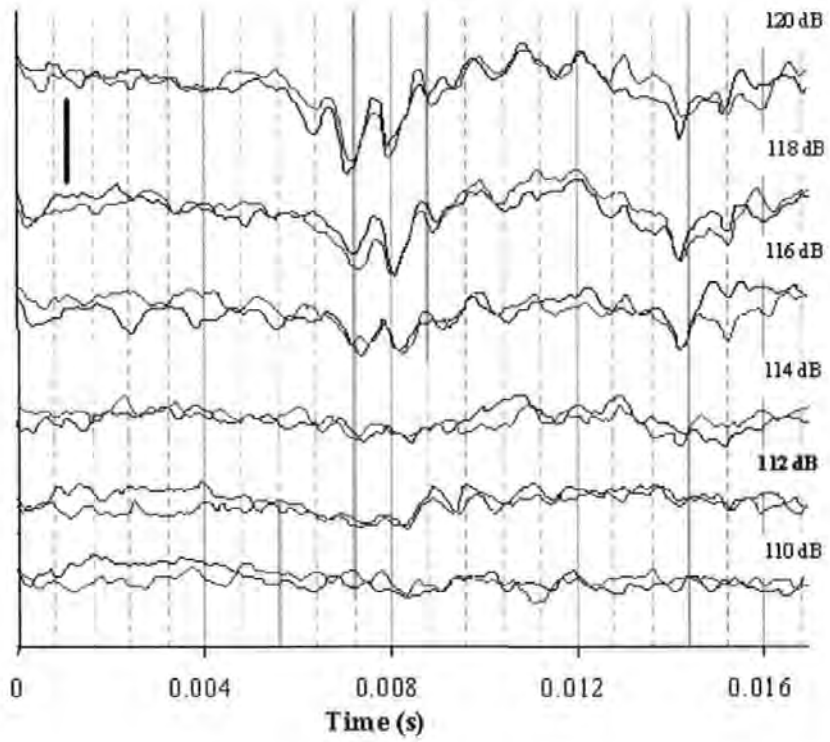

Figure 6.9. ABR waveforms from *P. serratus* in response to a 500 Hz tone burst attenuated in 2 dB steps. Averaged traces of two runs (2000 sweeps each), for each intensity are overlaid and arranged sequentially. Bar = 1 μv

6.3.6 Audiogram for *P. serratus*

The audiogram shown in Figure 6.10 was produced using sequential ABR waveform threshold data, acquired from frequencies of 100 Hz to 3000 Hz, presented in steps of between 200 Hz to 500 Hz. The hearing thresholds of 12 mixed sex *P. serratus* was

measured, and follows a ramp like profile, determined by calculating the lowest intensity stimulus sounds (recorded underwater using the hydrophone located adjacent to the antennule) that evoked a repeatable ABR response (112 dB in Figure 6.9). The profile follows a steady downward gradient to 100 Hz (the lowest frequency tested), and indicates that the "best" frequency in terms of threshold could be below this frequency.

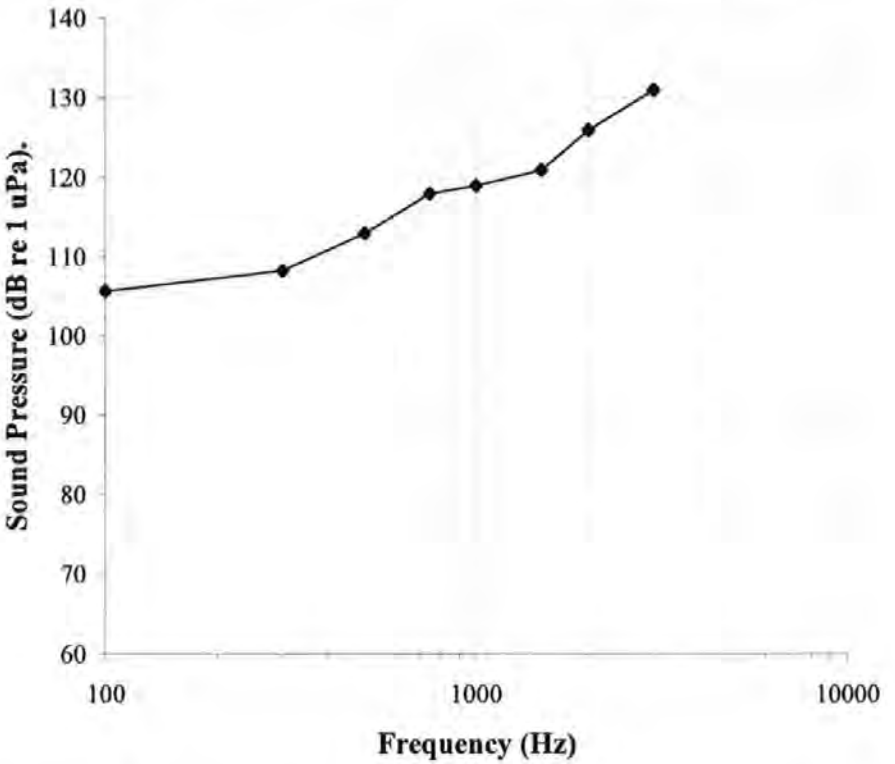

Figure 6.10. Audiogram for *P. serratus*, determined visually from the sequential ABR waveform data, and by calculating the RMS of threshold SPL values of the stimulus sounds, presented at 100 Hz, 300 Hz, 500 Hz 750 Hz, 1000 Hz, 1500 Hz, 2000 Hz and 3000 Hz tone bursts

6.3.7 Ablation

Removal of the statocyst was achieved by making a circular cut in the cuticle layer above the chamber, and withdrawing the capsule using needle point tweezers (a procedure that took a few seconds). Prior to removal of the statocyst, the prawn was re-tested with the cuticle layer cut as a sham operation, revealing that the AEP was no longer present. The sham operation data presented in Figure 6.11 were acquired by re-testing the prawns 1 hour after cutting around the chamber, prior to removal of the statocyst, and shows that the AEP eventually returns.

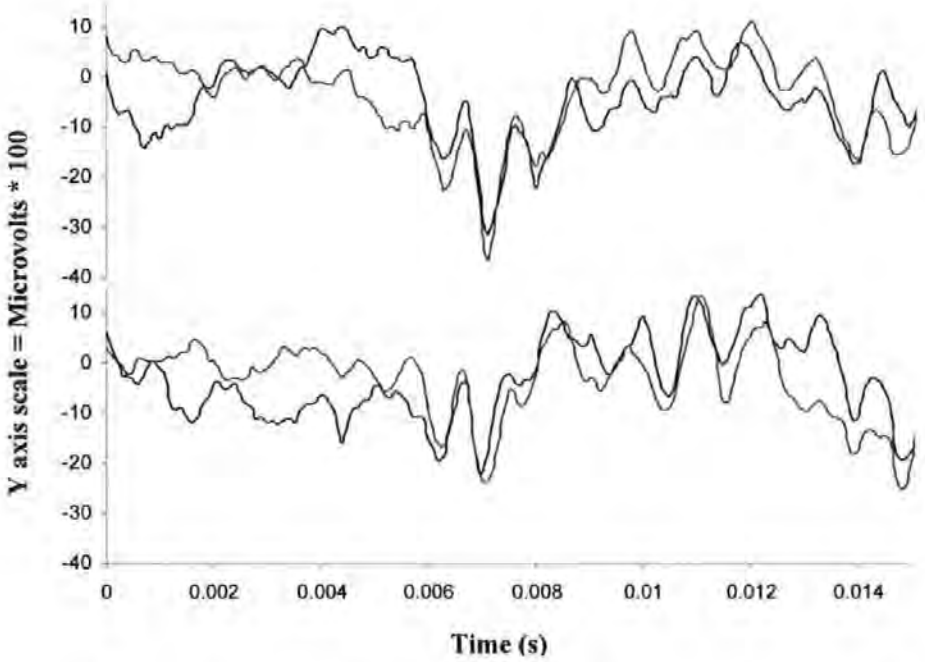

Figure 6.11. ABR waveforms in response to a 500 Hz sound presented 10 dB (re 1 μPa at 1 m) above threshold. Run A was recorded prior to the sham operation, and run B was recorded 1 hour after cutting the cuticle layer covering the statocyst capsule as a sham operation. Y axis scale = μv x 100

On removal of the statocyst, the prawns were placed in the empty fourth compartment of the holding tank, and allowed to recover for 24 hours, prior to being retested on the electrophysiology apparatus. The post ablation recovery period was included to give the prawn's time to settle after the procedure, as the metabolic state of the organism can have a detrimental affect on the evoked potential (Corwin et al 1982).

The evoked potentials shown in Figure 6.12 were recorded from a 45 mm prawn, in response to a 300 Hz tone, presented at an intensity 10 dB above threshold. The first two runs (A and B, with two replicates of each run) were acquired from the prawn prior to the ablation procedure, and the subsequent two runs (C and D, with two replicates of each run) were recorded 24 hours later. The electrodes were removed and replaced between each run, to confirm that the response was consistently repeatable, and to ensure that the absent responses in runs C and D was due to the ablation experiment, and not an extraneous factor associated with electrode placement.

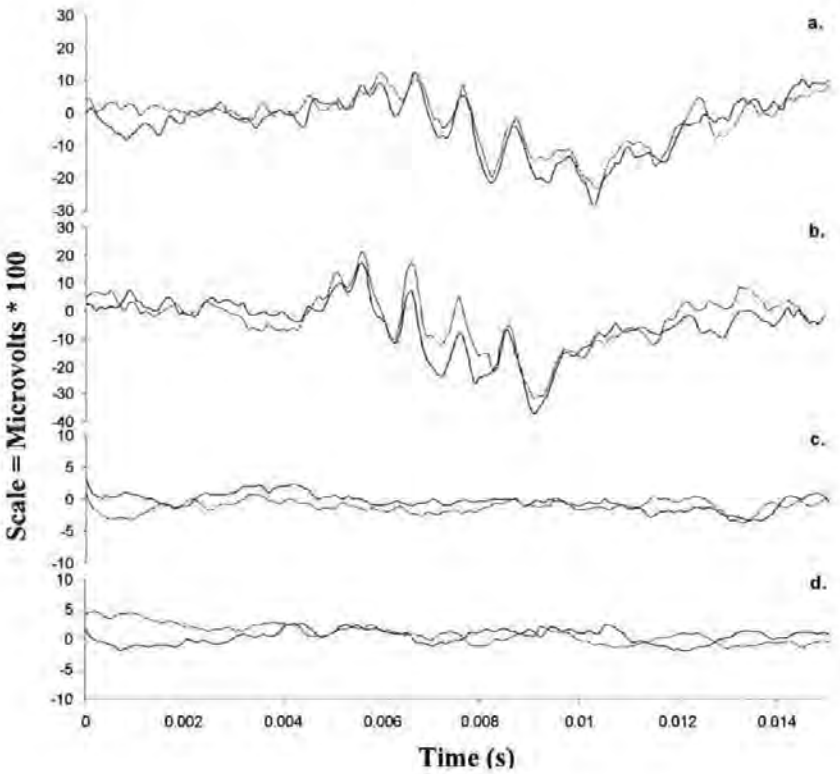

Figure 6.12. Evoked potentials from *P. serratus* to a 500 Hz tone presented 10 dB above threshold and averaged over 2000 sweeps. Runs a. and b. were recorded with the statocyst present; whilst c. and d. were recorded 24 hours after removal of the organ (the electrodes were removed and replaced between each run). Y axis scale = μv * 100

6.4 Chapter discussion and conclusions

The hearing ability of the prawn (*Palaemon serratus*) has been clearly demonstrated by this work using ABR audiometry, and offers conclusive evidence of low frequency sound detection of frequencies ranging from 100 Hz to 3000 Hz by an invertebrate from the sub-phylum crustacea. For hearing in the strictest sense to be attributed to an organism, the physiological response sound should be initiated by a specialised receptor mechanism (Myrberg 1981), shown by this work to be generated in the statocyst. Current literature states that this organ is purely responsive to angular rotations and strong vibrations propagated directly through a solid medium, and is not responsive to sounds propagated in either air or water (Cohen and Dijkgraaf 1961). It is highly probable that Cohen and Dijkgraaf did not find evidence of hearing due to masking of the AEP by neural activities other than audition; and from myogenic noise generated by muscular activity. To produce clear waveforms of an auditory response, it is recommended that AEP recordings be

averaged for at least 1000 to 2000 stimulus presentations (Kenyon et al 1998; Yan et al 2000). The amplitude and shape of the electrophysiological response from *P. serratus* shown in Figures 6.8 and 6.9, bear a remarkable similarity to AEP's generated by fish and higher vertebrates (see Corwin et al., 1982; Kenyon et al., 1998; Yan, 2002).

The two statocyst organs found in *P. serratus* lie adjacent to one another with medial symmetry, in the basal peduncle segment of the antennule. As can be seen in Figures 6.4 and 6.5.a, the statocyst is innervated by the statocyst ganglion, which emanates from a bed of peripheral nerve fibres lying under the mound directly beneath the receptor array (see Figure 6.6.a). The statocyst nerve terminates in the neuropil of the antennule, which is located in the ventral/anterior region of the brain. The dissection of the 54 mm prawn in Figure 6.3.a shows that the total length of the neuronal pathway taken by the statocyst nerve, from the centre of the statocyst organ to the centre of the supraesophageal ganglion is approximately 600 μm. However, the direct distance between the neuropil and the peripheral nerve fibres located below the statocyst, was found to be 500 μm. This is due to the curved pathway taken by the statocyst nerve, which first projects forward with the lateral antennular ganglion along the inside edge of the peduncle for 300 μm. From here, the statocyst ganglion branches away from the antennular ganglion at angles approaching 45 ° either side of the midline, from where it extends for a further 300 μm to the centre of the peripheral statocyst nerve bed.

It is clear from the evidence presented in this chapter, that the perception of sound in the frequency domain by *P. serratus* is similar in range to hearing in generalist fish, which is capable of both hearing and responding to sounds within a frequency bandwidth of 30 Hz to around 400 Hz or so (Fay, 1988), and is reliant on the phase variance between the three otolithic organs and the surrounding flesh to stimulate the sensory hairs of the inner ear (Lu, 2004). The audiogram presented in Figure 6.10 follows a similar ramp like profile to those obtained from the generalist fish, which are considered to detect a best frequency of below 100 Hz (Kenyon et al 1998); however, frequencies below 100 Hz were not tested. It may therefore be concluded that at least one species from the invertebrate sub-phylum of crustacea is sensitive to the motion of water particles displaced by low frequency sounds ranging from 100 Hz up to 3000 Hz.

Chapter 7

Examination of the cetacean inner ear

7.1 Introduction

Growing concern by a number of environmental organisations regarding the use of Low Frequency Active (LFA) sonar and other intense anthropogenic sources by the military and oil industry is stimulating considerable interest in the diagnosis of the existence and extent of hearing loss in marine animals. High intensity low frequency sounds may be particularly damaging to the vestibular (balance) organs of cetaceans and may account for the reported disorientation when these animals strand live, whereas loud midrange to high frequency sounds may damage the ultrastructure in the cochlea.

Concise morphological and physiological information on the hearing systems is critical to the assessment of the potential effect of anthropogenic noise pollution in the marine environment, being especially relevant where an animal is thought to have died as a consequence of intense noise exposure. Trauma to the auditory system can result in lesions developing along the VIII nerve pathway, or ruptures in the blood vessels surrounding the inner ear. A number of techniques have been developed to study gross physiological damage to the inner ear, though these investigations do not necessarily verify the impairment of hearing and balance. In addition, these types of injuries may have been sustained by the animal as it struggles in fishing nets, or thrashes about on the shoreline and thus be unrelated to loud noise exposure. If caused by intense noise, signs of trauma (haematoma and nerve lesions) would probably manifest at the highest end of the impact

scale, whereas more subtle damage to the ears may only show in the ultrastructure and thus be missed when using conventional examination methodologies.

Current literature shows a paucity of information on consistent and meticulous removal of inner ear parts necessary to identify damage to the ultrastructure symptomatic of hearing and balance loss. In addition, the fixing methodology commonly used during autopsy is to fix the ear in formalin, but this chemical does not bind the proteins in the ultrastructure and results in the rapid destruction of the cilia, making the sample unusable for SEM microscopy. It is therefore the purpose of this Chapter to describe work pursued towards dissection and fixation methodologies relevant to an SEM examination of the mammalian inner ear. However, owing to the scarcity of cetacean inner ear samples suitable for SEM microscopy, the inner ear of the domestic pig (*Sus scrofa*) is used to append the dissection and fixation methodologies required to view mammalian ultrastructural hair cells. The periotic bone containing the inner ear from *S. scrofa* is dimensionally similar (though slightly thinner) to the cetacean periotic, and has the considerable advantage of being easy to obtain fresh from commercial sources.

The comparative morphology of the inner ears from the common dolphin (*Delphinus delphis*) and the harbour porpoise (*Phocoena phocoena*) is investigated here, in preparation for a Scanning Electron Microscope study of the cetacean inner ear ultrastructure. The saccule, utricle and semi-circular canals make up the vestibular system, and the scala tympani, scala media and scala vestibuli make up the cochlea (Corti, 1851; Retzius, 1884). Vibrations in the auditory periotic of Odontocetiform animals, caused by sound energy conducted through the mandibular channel oscillate the scala tympani within the inner ear (Whitlow, 1993). It is probable that these oscillations transmit energy to each of the three compartments in the cochlea, through fluid in the scala vestibule, or along the scala media and basilar membrane (the floor of the scala media). The sensory ultrastructure on the organ of Corti in the scala media rests on the basilar membrane and becomes polarised or hyperpolarised by the oscillating motion of the membrane (Ulfendahl et al., 1996). The hair cells convert the sound energy into bioelectric impulses, which travel via the VIII nerve to nuclei in the auditory pathway during acoustic stimulation (Brill, et al., 1988).

7.2 Materials and methods

The common dolphin (*Delphinus delphis*) examined in this study was recovered on the 2nd of February 2005, from Beacon Point in Devon (Ordnance Survey GB grid reading SX674406). The tagged carcass was not designated for collection (autopsy), due to its location at the foot of a steep cliff making access difficult. A brief inspection revealed that the animal was a mature male, approximately 2.4 meters in length, and estimated to have been dead for 10 to 12 days; injury to the front rows of teeth and the jaw indicate that it is highly possible that the animal died as a result of becoming entangled in fishing nets. The mature harbour porpoise (*Phocoena phocoena*) was recovered on the 11th of February 2005 from Andurn Point, near Plymouth Sound, Ordnance Survey GB grid reading SX495492 (NHM reference SW.2005/30). The tagged carcass was 1.47 meters in length and approximately three years of age (Read, 1999) and was not designated for autopsy due to it being in an advanced state of decay. The cause of death was unknown.

The periotic bone containing the inner ears from *D. delphis* and *P. phocoena* were separated from the petrous bone, and washed in 70 % chilled ethanol. Removal of the complete cochlea from the encapsulating periotic bone in *P. phocoena* required two cuts made using a fine cutting wheel, which was stopped short of penetrating to the inner ear canals by approximately 0.4 mm. The weakness in the bone caused by the hemispherical cut allowed for the two halves of the periotic to be gently separated using minimal leverage, thus exposing the internal structure of the ear. The skeletal remains of the cochlea were not removed from the periotic in *D. delphis*; instead it was prepared for the EM study whilst still in the encapsulating bone. A cast of the inner ear cavity was then made by injecting Silicone rubber into the cochlea duct and vestibule, and allowed to cure for 24 hours (Figures 1.a through c). The cast was removed by gently separating the three cut sections of the periotic, and by easing the rubberised impression of the ear from the bone segments; a similar procedure has been used successfully by the author on the elasmobranch ear (Lovell, unpublished). The cast was then washed in 100 % ethanol and processed for a low powered Scanning Electron Microscope (SEM) examination of the surface features.

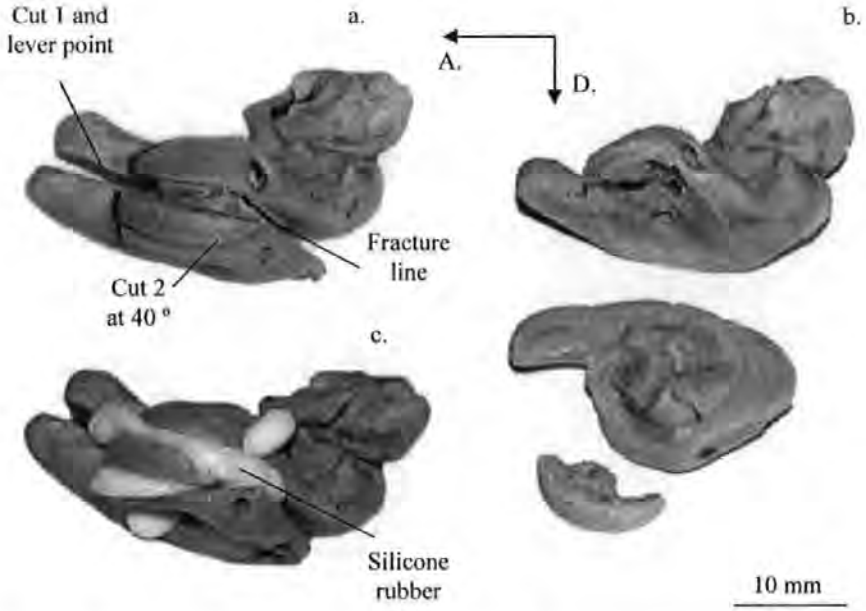

Fig. 7.1 a. Ventral view of the periotic from *P. phocoena* showing the position of the two cuts, **b.** the sections of periotic cut away to free the cochlea, and **c.** the periotic after the silicone injection moulding procedure. The annotations D. (Dorsal), and A. (Anterior) represent the orientation of the periotic in the skull

The use of the Scanning Electron Microscope (SEM) in the examination of the ultrastructure responsible for the mediation of auditory stimuli has been used to considerable effect on lower vertebrates such as fish (Platt 1977; Lovell et al., 2005b), and invertebrates (Lovell et al., 2005a), though no SEM examinations have been conducted on the inner ear ultrastructure from any of the cetacean species. The relative ease and speed with which the auditory periotic can be dissected from behind the mandible of *D. delphis*, indicates that it should be possible to remove the complete inner ear for a Scanning Electron Microscope examination of the hair cells from cetacean carcasses recovered after strandings. It is essential that the periotic is rapidly immersed in chilled fixative (2.5% glutaraldehyde in 0.1 M cacodylate buffer with 3.5% sodium chloride), then refrigerated to inhibit sample decomposition (the sample must not be frozen, as ice crystals will destroy the ultrastructure). In addition to the examination of the cochlea, the other inner ear end organs such as the saccule and utricle should also be assesed, as these organs (in most vertebrate animals), are sensitive to both angular accelerations and low frequency sounds (Popper and Fay, 1993). If either were to become damaged by anthropogenic noise pollution, it may contribute to the reported disorientation experienced by cetaceans which have become stranded live, yet do not present with any obvious signs of injury.

Owing to the extreme care required when processing inner ear tissue for SEM examination of the ultrastructure, it is important to fix the ear immediately after removal from the carcass. Usually, best results are obtained when fixative is injected directly into the canals of the periotic bone, though this approach may be impracticable on a beach or boat. It was therefore decided to test various fixing procedures on easily obtainable domestic mammal inner ears, in this case the pig (*Sus scrofa*). The aim was to find the best way to fix the ears with the minimum of handling outside of controlled laboratory conditions. For SEM, the tissue comprising the inner ear should be fixed in 2.5% glutaraldehyde in 0.1 M cacodylate buffer (with 3.5% sodium chloride for marine animals). Previous studies of the inner ear ultrastructure from lower vertebrates has shown that it is possible to fix the ear whilst in a trimmed block of cranium, and that the fixative will penetrate sufficiently to preserve the ultrastructure. However, the bone surrounding the mammalian inner ear (the periotic) is significantly thicker and denser than the bone surrounding the fish ear. Contained within the periotic is the cochlea, a spiral tube that is coiled approximately two and one-half turns around a hollow central pillar (the modiolus) and the vestibular end organs.

In total, 12 ears were removed from mature domestic pigs (*Sus scrofa*) during processing for the meat industry, within 1 hour of the animal's death. After removal of the first two pairs of ears, a small hole was drilled into the periotic covering the upper tip of cochlea, into which a fine syringe was inserted and fixative injected into the canals below, then the entire periotic was immersed in chilled fixative. The second batch of ears had the bone covering the upper apical tip removed, then immediately immersed in fixative, whilst the final batch were immersed into the fixative with no additional preparation. The periotic bone containing the inner ear was trimmed to a small block and the outer bone layer was removed using a fine cutting wheel. The saccule, utricle and cochlea were dissected from the labyrinth using a fine scalpel, then dehydrated through a graded ethanol series ranging from 35% through 50%, 70% and 90% to absolute ethanol, prior to desiccation using the critical point drying method described by Platt (1977). Fully desiccated end organs were subsequently mounted on a specimen stub using a carbon tab, and coated with c. 8 nm of gold in an Emitech K 550 sputter coater (working at approximately 5 x 10^{-6} Torr). The processed specimens were investigated and photographed using a JEOL JSM 5600 scanning electron microscope operated at 15 kv, and a 15 mm working distance.

7.3 Results

7.3.1 The auditory system from the common dolphin (*D. Delphis*)

The examination of the brain (Figure 7.2.a) revealed a large VIII auditory nerve (Figure 7.2.b), originating at the peripheral end of the nerve in the periotic chamber, and terminating in the medulla. The brain, VIII auditory nerve and auditory periotic bone from the right side of the cranium were removed intact, and the brain weighed using digital precision scales (total weight = 1008 g with the periotic bone absent), then transferred to a large beaker and immersed in 70 % ethanol, prior to fixing in formalin.

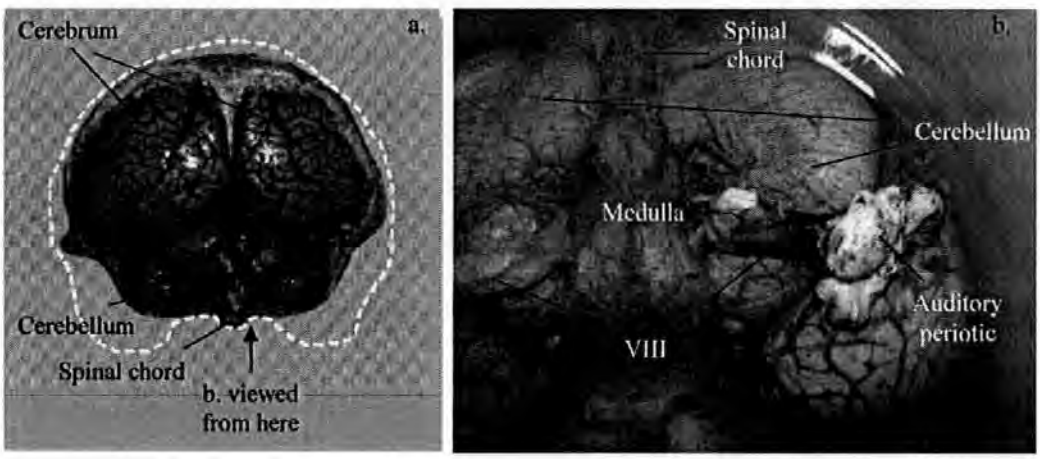

Fig. 7.2.a. Caudal view of the hindbrain and spinal cord from *D. delphis*, **b.** ventral view of the cerebellum and medulla, with the VIII nerve still attached to the auditory periotic containing the inner ear

The skull was then photographed in a number of positions and annotated for reference purposes (Figures 7.3.a through d). The cranium and brain asymmetry in *D. delphis* examined here, was found to be larger in the right hemisphere (especially evident in the nasal passage).

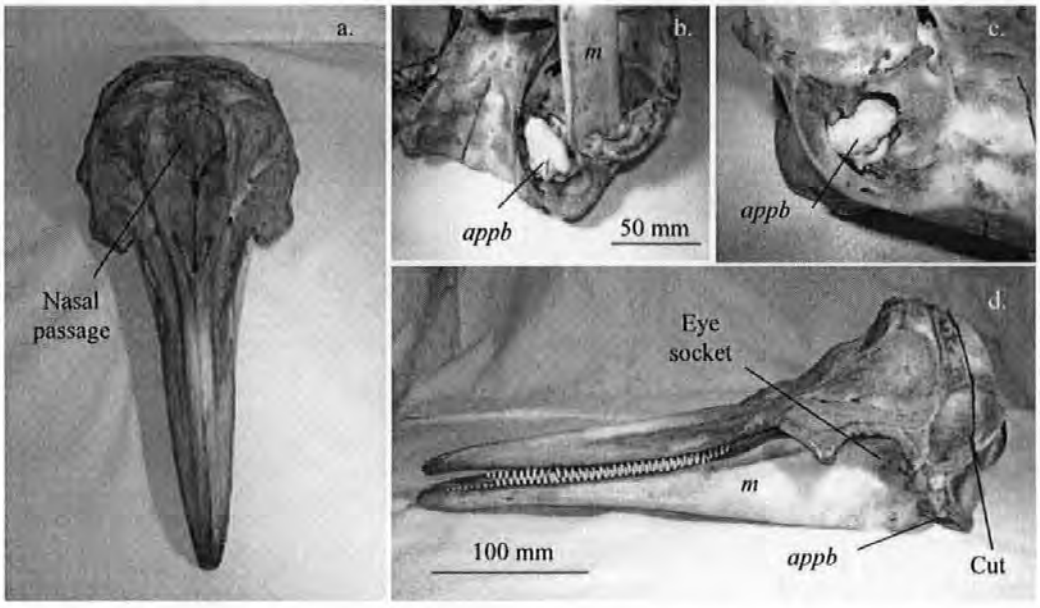

Fig. 7.3. a. Dorsal/anterior view of the skull from *D. delphis* (note there is a slight dominance of the right side). **b.** ventral view of the skull showing position of the auditory periotic and petrous bones (*appb*) and lower mandible (*m*), **c.** endocranial view of the periotic and petrous bones **d.** left side view of the skull showing the position of the periotic and petrous bones relative to the mandible and eye socket

In *D. delphis*, fibrous tissue surrounds the heavily calcified auditory periotic bone (Figures 7.4.a to c) and the thin petrous bone (Figure 7.4.a), which are connected to the skull by a flexible ligament that effectively isolates the inner ear from the skull. Sound enters the ear most efficiently through the mandibular channel in the lower jawbone, which extends back toward the auditory periotic bone.

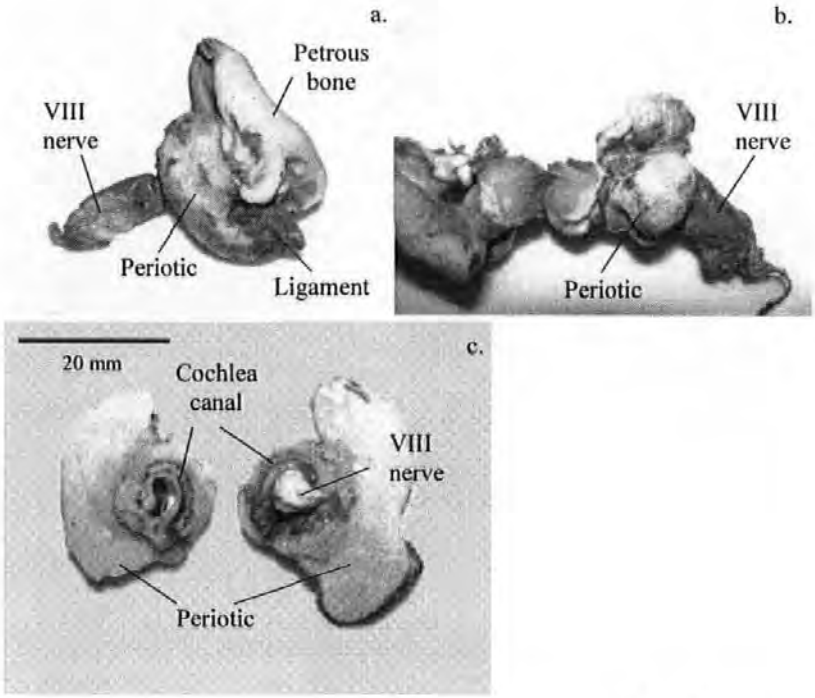

Fig. 7.4.a. The auditory periotic with VIII nerve and the thin petrous bone from *D. delphis*, **b.** dividing the petrous bone from the auditory periotic bone, and **c.** cross section through the periotic capsule containing the inner ear, and peripheral VIII nerve fibres (bar = 20 mm)

Figures 7.5.a and b present the skeletal remains of the cochlea, and shows detail of the bony spiral lamina, scalar tympani and upper portion of the scalar vestibule and peripheral VIII nerve fossa on the inside edge of the lamina.

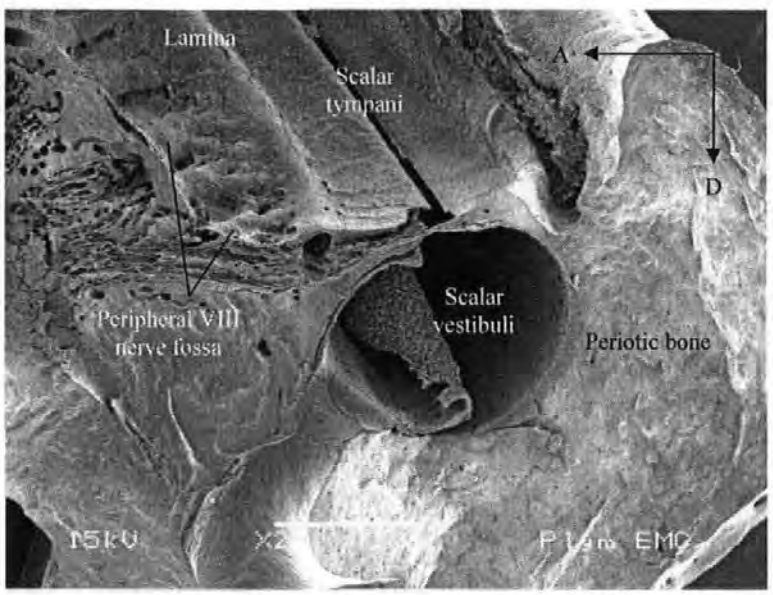

Fig. 7.5. Ventral view of a cross section through the periotic bone from *D. delphis* showing the lower basal section of the cochlea, and the scala vestibuli and scala tympani (the floor of the scala tympani has been removed)

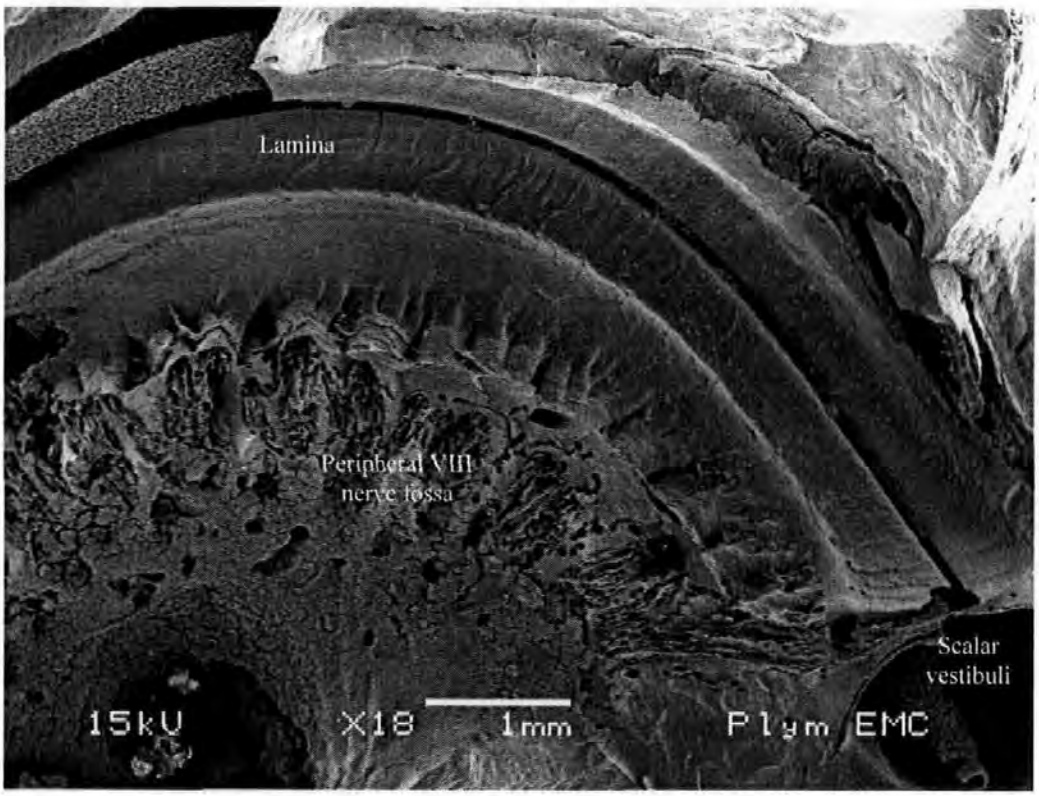

Fig. 7.6. Ventral view of the bony spiral lamina from *D. delphis*

Figure 7.7 and 7.8 presents Electron micrographs of the inner ear cast from *D. delphis*, reproduced by injecting silicone rubber into the auditory periotic bone surrounding the inner ear. This procedure was necessary as the fine internal structure of the ear had decomposed to an extent where it could not be removed by dissection; rather it had to be washed from the chambers within the periotic using 70 % ethanol.

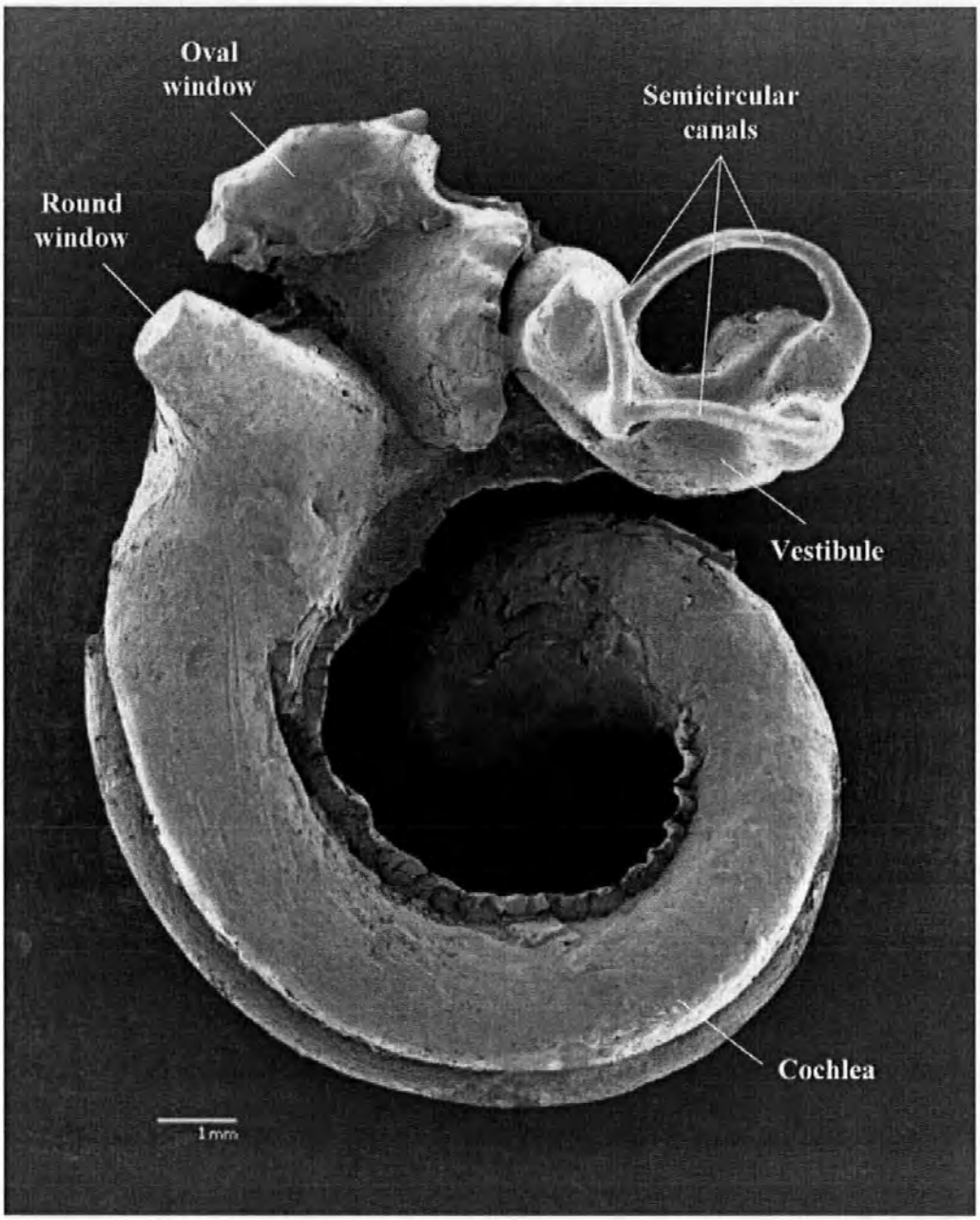

Figure 7.7. SEM micrograph of the left inner ear cast from *D. delphis* (lateral view away from the mid-sagittal plane of the brain). Comparative annotations from Gray (1918)

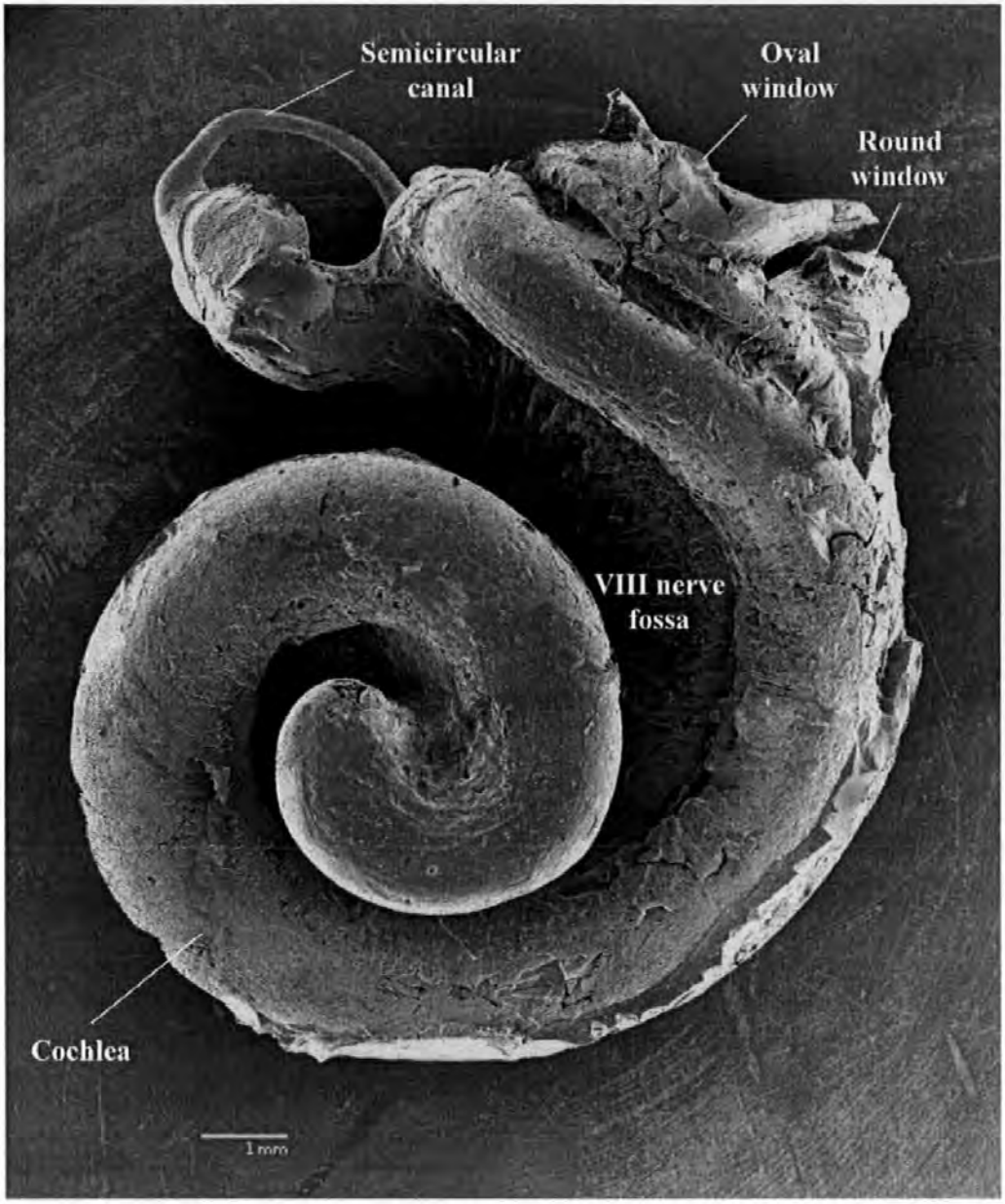

Figure 7.8. SEM micrograph of the left inner ear cast from *D. delphis* (lateral view toward the mid-sagittal plane of the brain)

The length of the cochlea from the upper apical tip to the lower basal segment was calculated to be 30.1 mm, with the vestibule etc, making up the remaining 3 mm of the inner ear (total length 33.1 mm).

7.3.2 Morphological Examination of the Auditory System from the Harbour Porpoise *Phocoena phocoena*

The dissected cochlea from *P. phocoena* was placed in a watch glass containing 70 % ethanol, and photographed using a digital camera and trinocular microscope (Figure 7.9).

The innervated length of the cochlea was measured on a PC using the analySIS® (Soft Imaging System) program, and found to have a length of 21.8 mm; the total length of the sample was calculated to be 24.8 mm, with the saccule and oval window making up the remaining 3 mm. The investigation of the internal dimensions of the periotic bone was conducted to rule out the possibility that some of the organ of Corti still remained in the periotic, or had decomposed and was no longer visible, thus ensuring an accurate measurement of the organ.

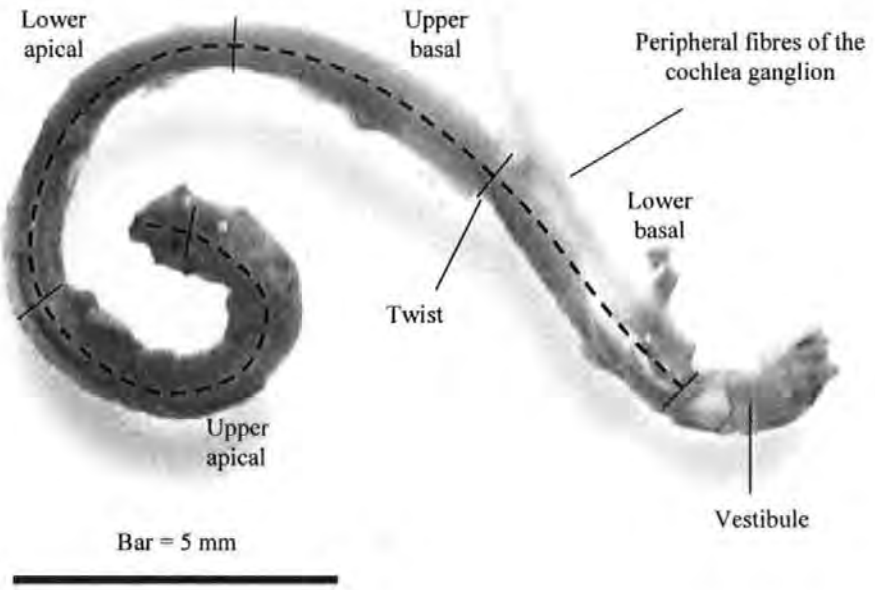

Fig. 7.9. The organ of corti from *P. phocoena*. Total innervated cochlea length: 21.8 mm, total sample length: 24.8 mm

The complete cast of the inner ear from *P. phocoena* in Figures 7.10 and 7.11 presents the complete structure viewed laterally, both toward and away from the mid-sagittal plane of the brain.

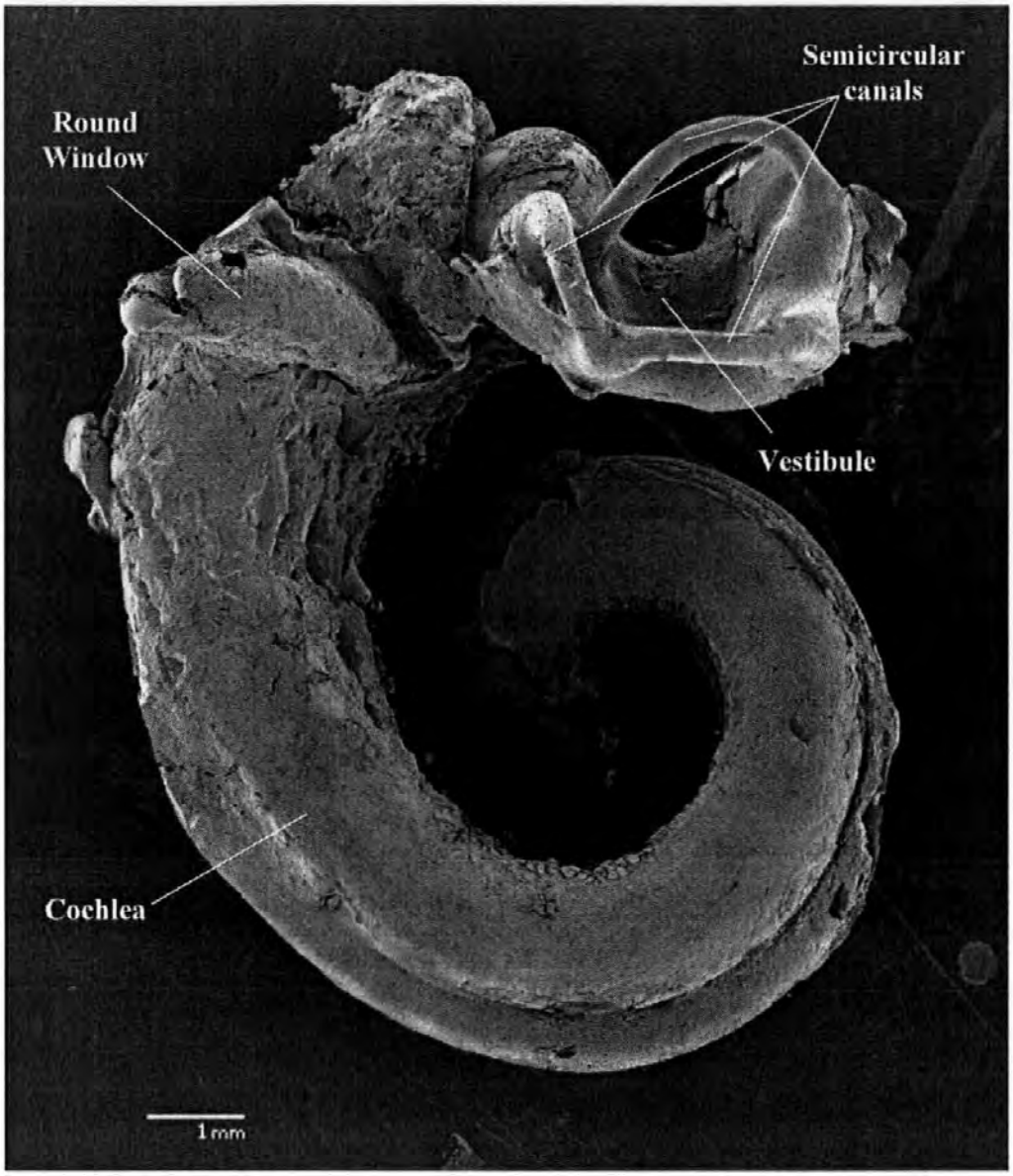

Figure 7.10. SEM micrograph of the left inner ear cast from *P. phocoena* (lateral view away from the mid-sagittal plane of the brain).

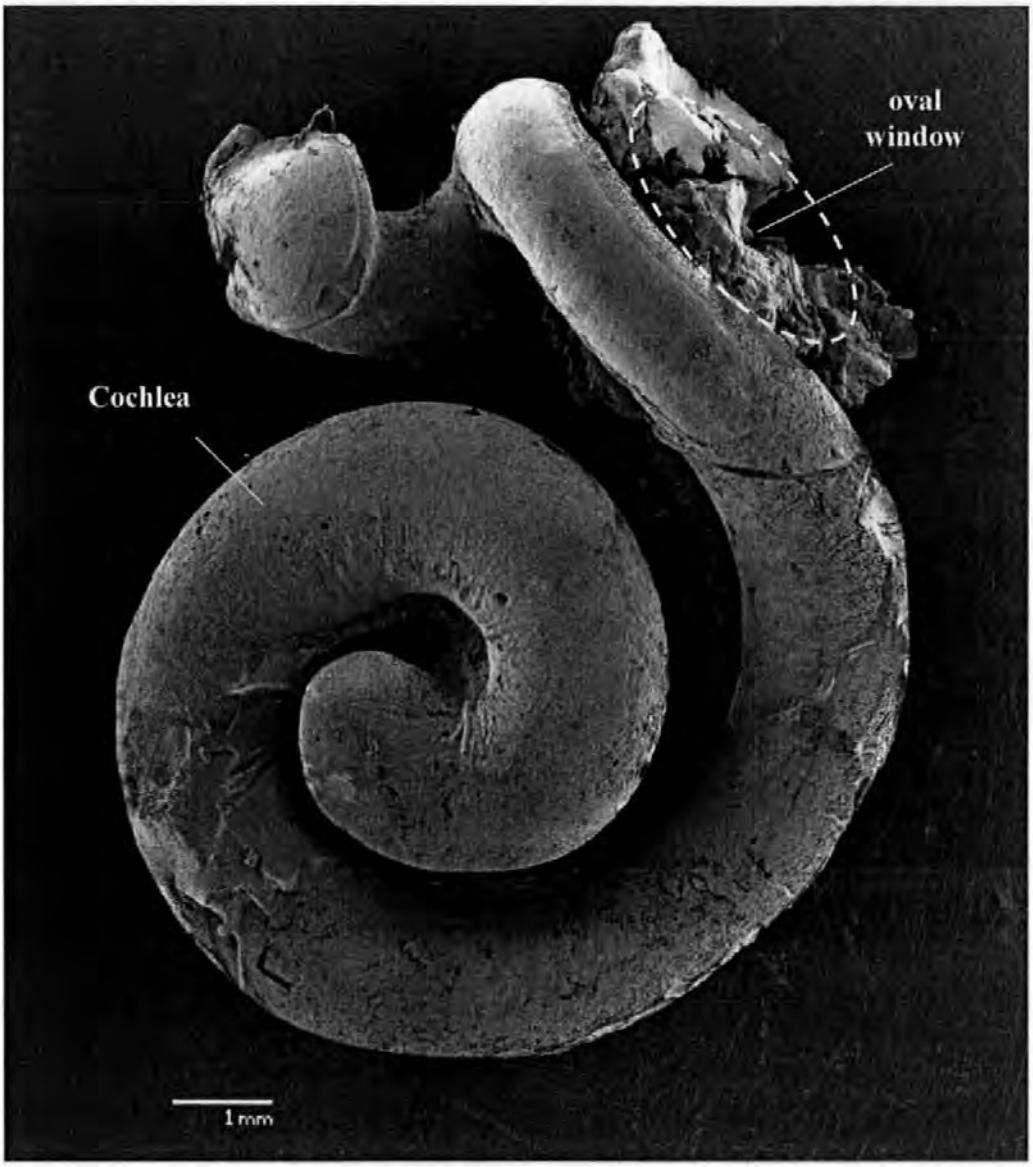

Figure 7.11. SEM micrograph of the left inner ear cast from *P. phocoena* (lateral view toward the mid-sagittal plane of the brain)

7.4 Ultrastructure from the mammalian cochlea

Figure 7.12 presents cochlea hair cells from the domestic pig (*Sus scrofa*) prepared within 1 hour of death and using three distinct methods of introducing the fixative, and a forth where no fixative was used prior to preparation for critical point drying. In Figure 7.12a, a small hole was drilled into the periotic covering the upper tip of cochlea, into which a fine syringe was inserted and fixative injected into the canals below, then the entire periotic was immersed in chilled fixative. In Figure 7.12b, the bone covering the upper apical tip of the cochlea was removed, then the periotic immediately immersed in fixative. In Figure 7.12c, the periotic was immersed into the fixative with no additional preparation, whilst in Figure 7.12d, no fixative was used for the first 48 hours after death.

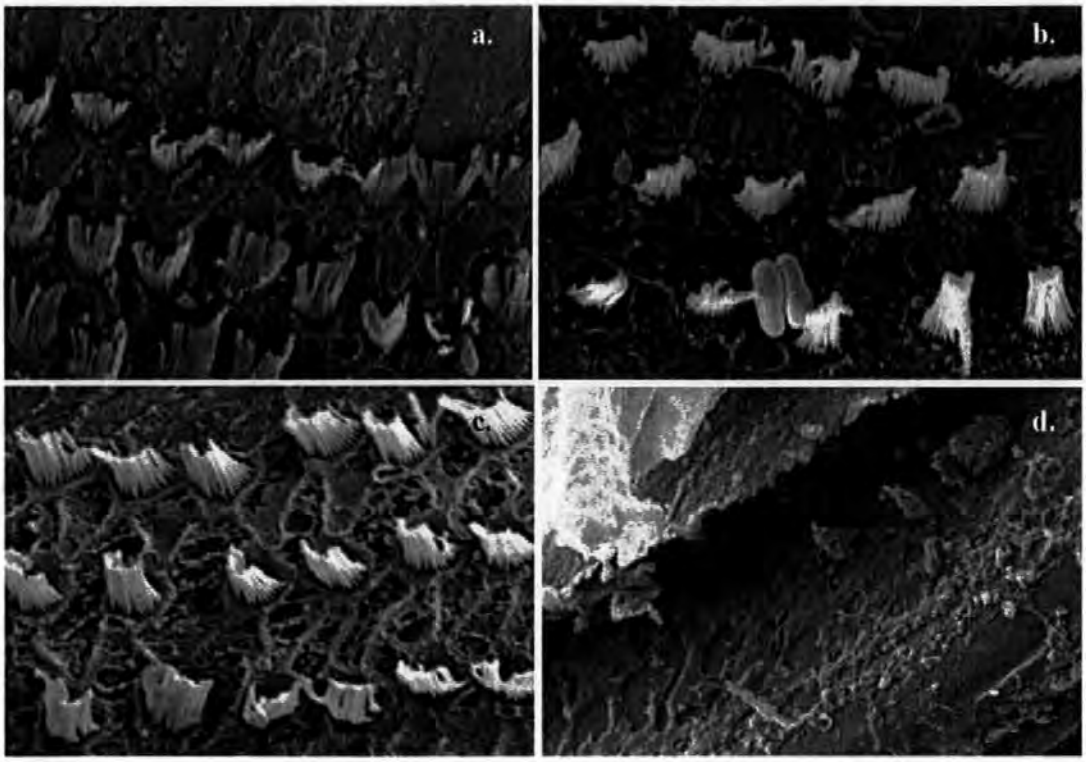

Figure 7.12. Hair cells from the upper basal turn of the cochlea. **a.** fixative injected through a small hole in the upper apical tip, **b.** the bone covering the upper apical tip removed and the ear immediately immersed in fixative, **c.** periotic immersed in fixative complete, and **d.** the cochlea after 48 hours without any fixative

Figures 7.13 through 7.18 show ultrastructural hair cells from the upper apical tip to the lower basal region of the cochlea from *S. scrofa*, fixed in glutaraldehyde 1 hour after death and the periotic immersed in fixative without any additional preparation.

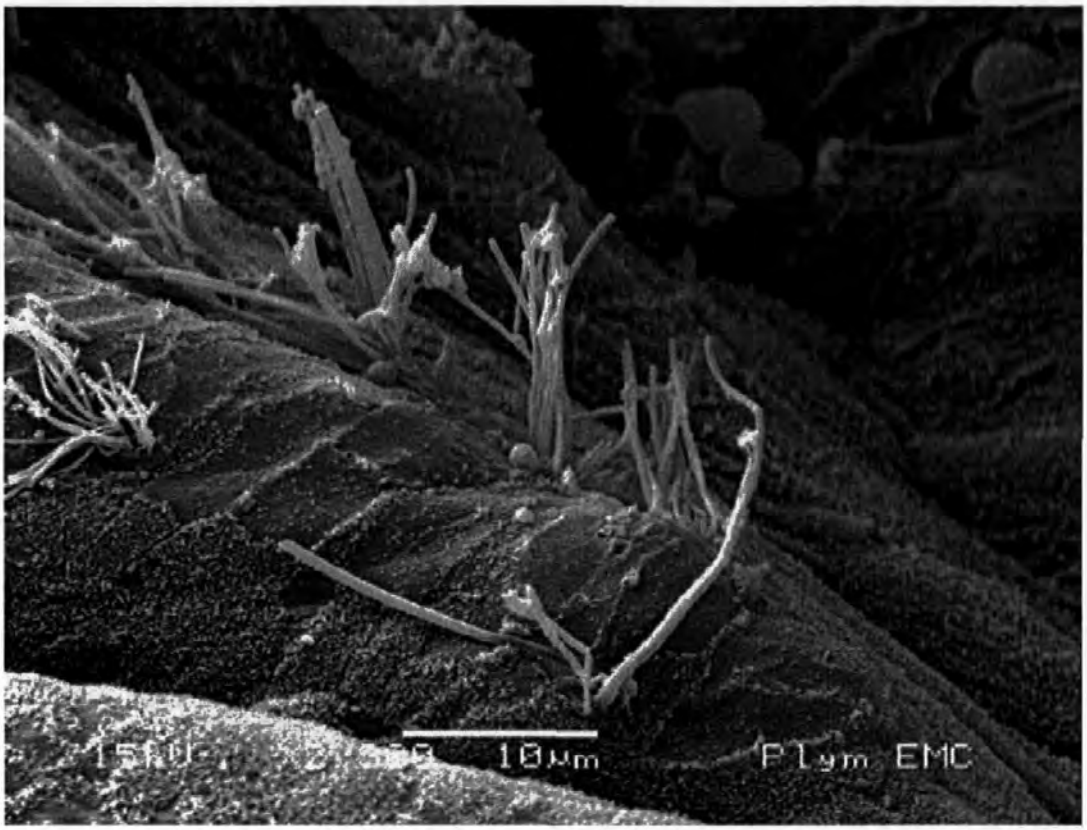

Figure 7.13. long hair cells (10 to 15 µm) from the tip of the upper apical

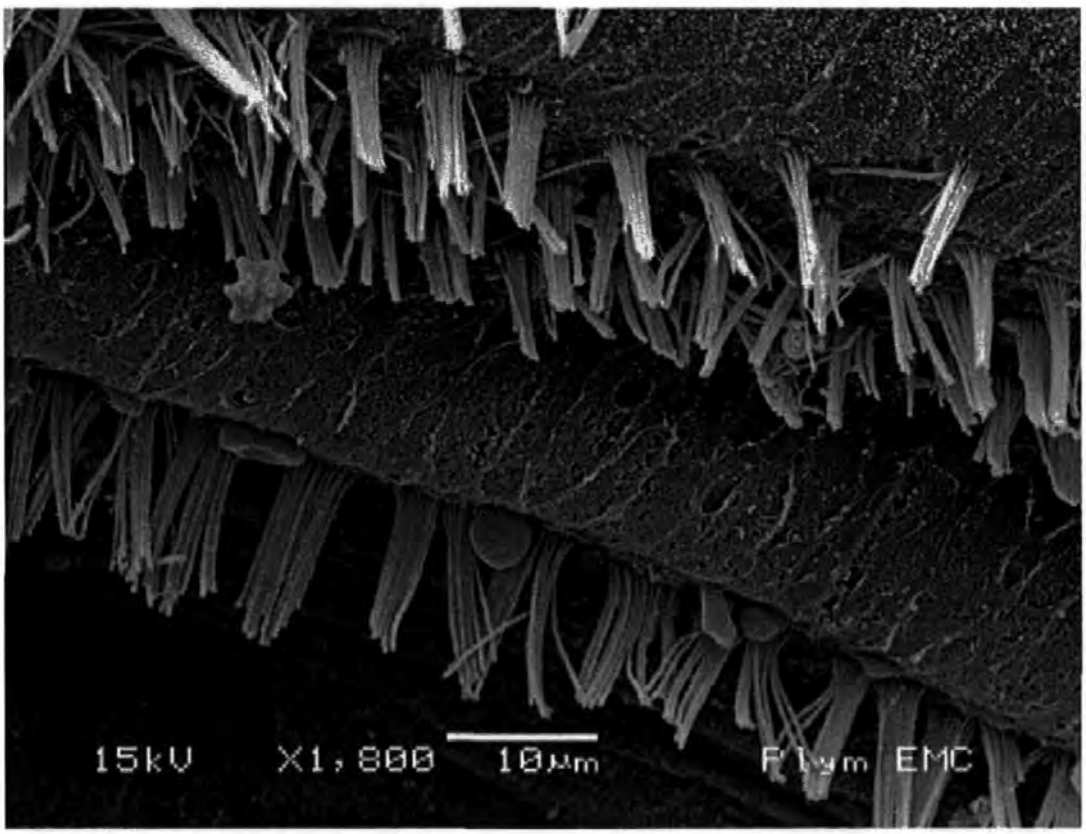

Figure 7.14. long hair cells (8 to 10 µm) from the first half turn of the upper apical

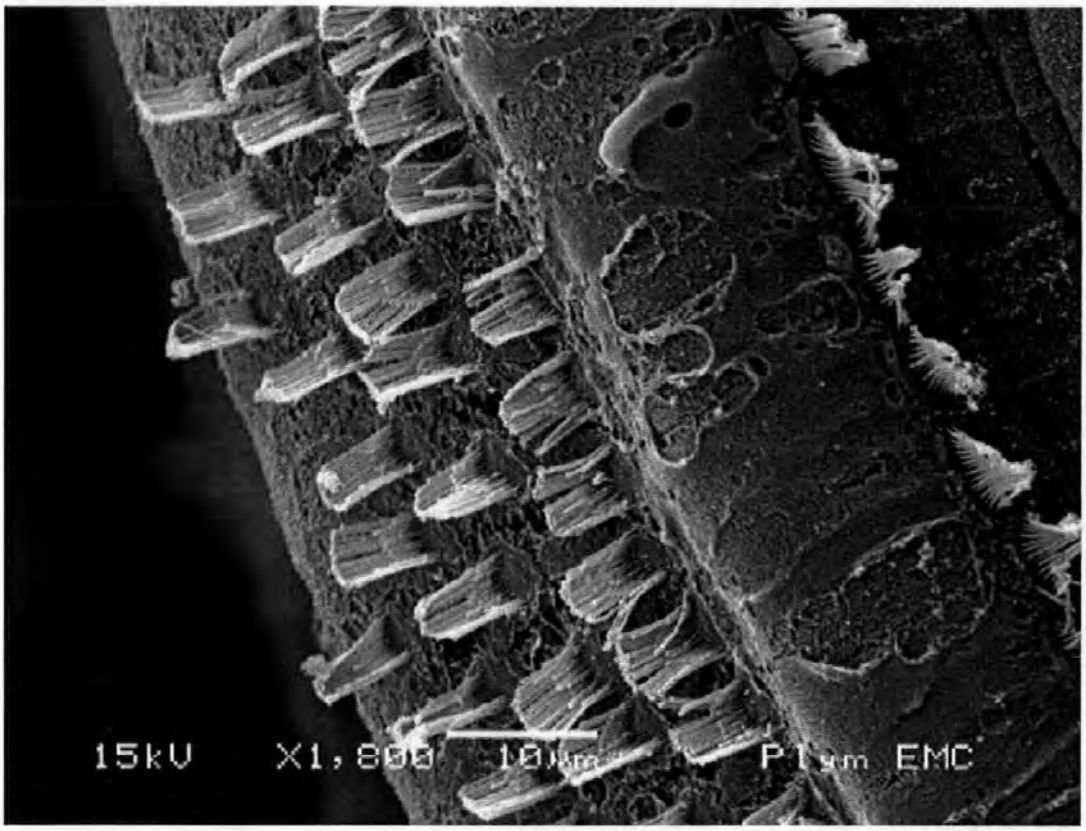

Figure 7.15. Hair cells (6 µm) from the second half turn (1 turn)

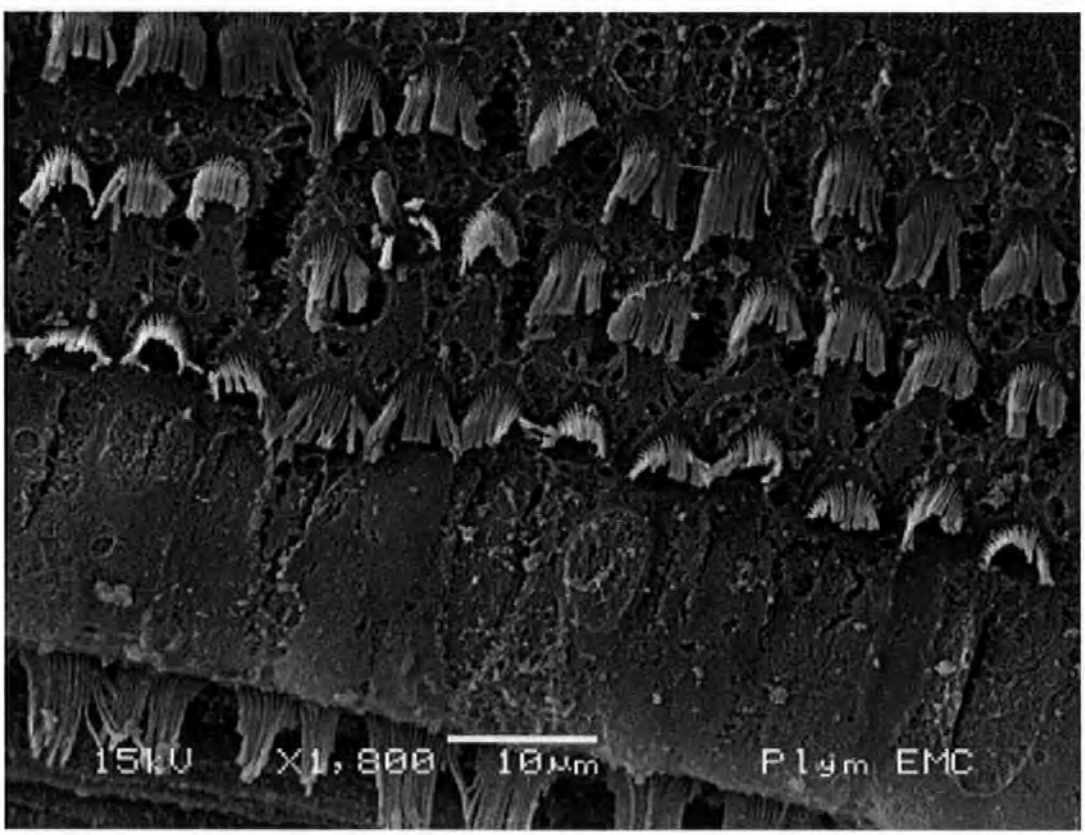

Figure 7.16 Hair cells (6 µm) from the third half turn in the basal region (1 ½ turns)

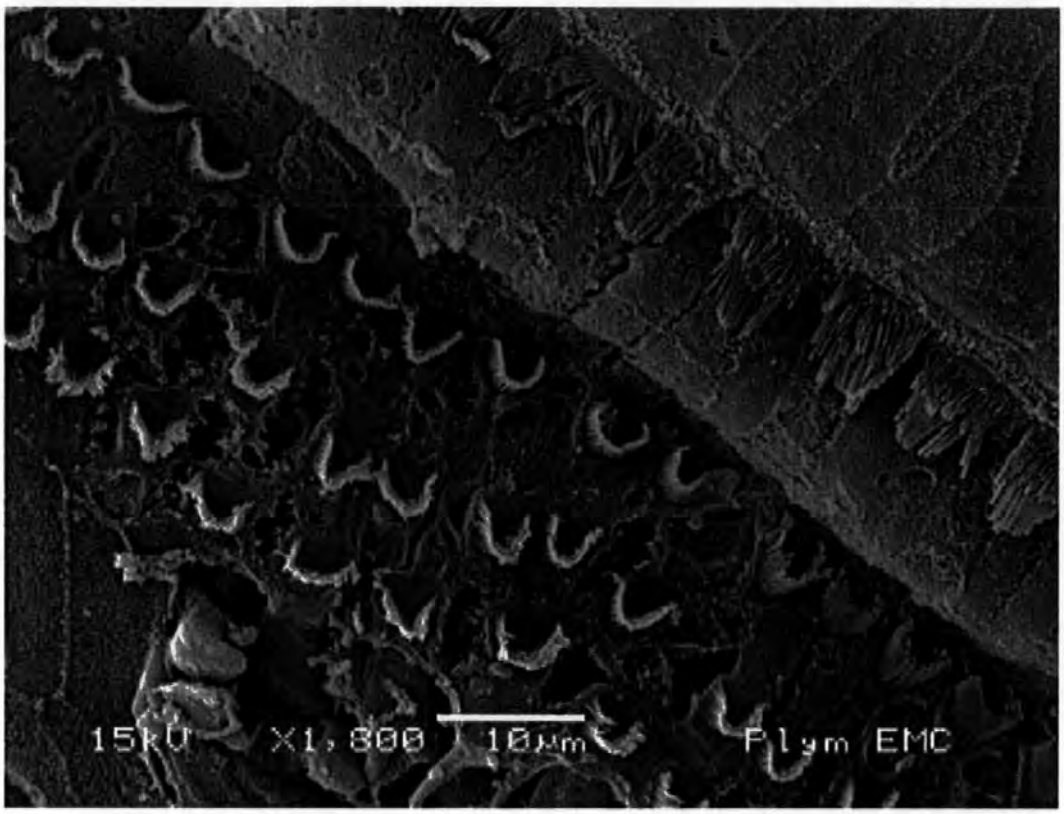

Figure 7.17 . Hair cells (4 µm) from the forth half turn of the lower basal region (2 turns)

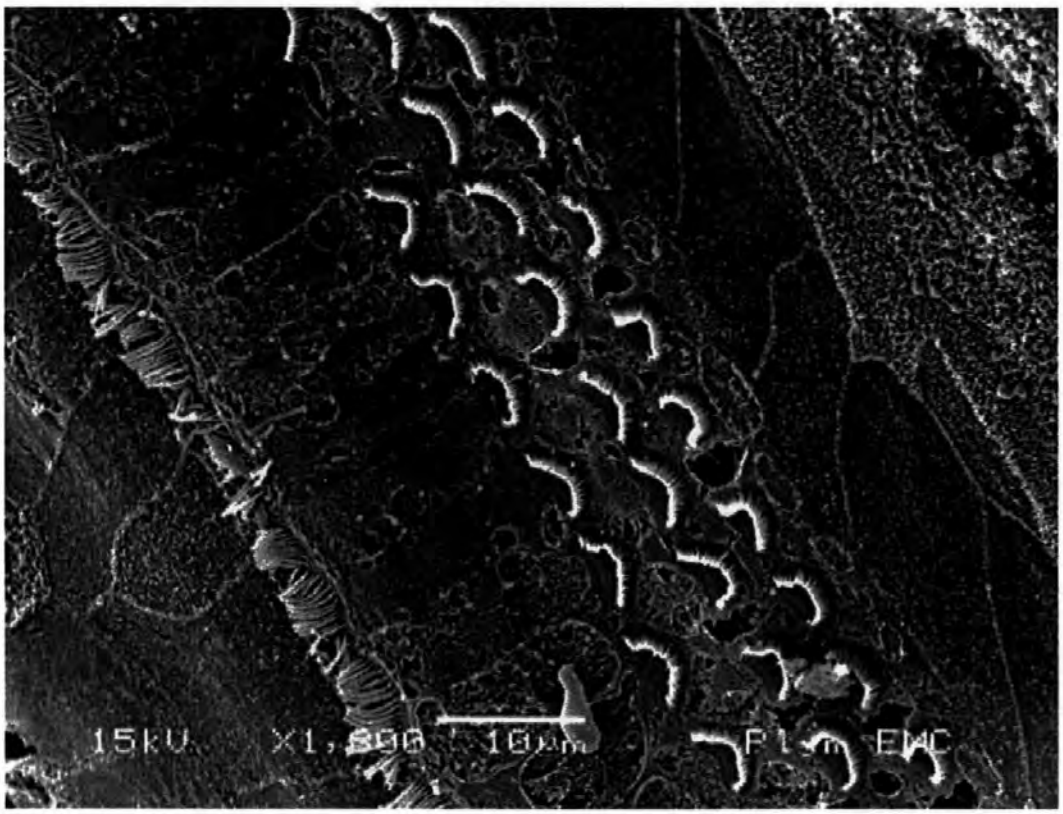

Figure 7.18. Hair cells (3 µm) from the fifth half turn at the end of the lower basal region (2½ turns)

As can be seen in Figures 7.13 through 7.18, there is no evidence of cochlea hair cell damage; thus fixing the entire periotic in glutaraldehyde without any further preparation of the sample will give adequate results for *Sus scrofa*, though the extra thickness of the periotic in the cetaceans may have some additional effect on the sample.

7.5 Ultrastructure from the Mammalian Vestibule

The mammalian inner ear is surrounded by a dense bony capsule, known as the auditory periotic (Figure 7.19). Removal of the bone covering the inner ear reveals the cochlea and membranous labyrinth (*labyrinthus membranaceus*), which is found within the bony cavity of the vestibule and contains the saccule, the utricle and the semi-circular canals, each filled with endolymph (a substance possessing viscous and ionic properties). The anterior part of the inner ear is the cochlea Figures 7.19, while the posterior part is made up of the vestibule containing the saccule, utricle and semicircular canals (Figures 7.19 and 7.20).

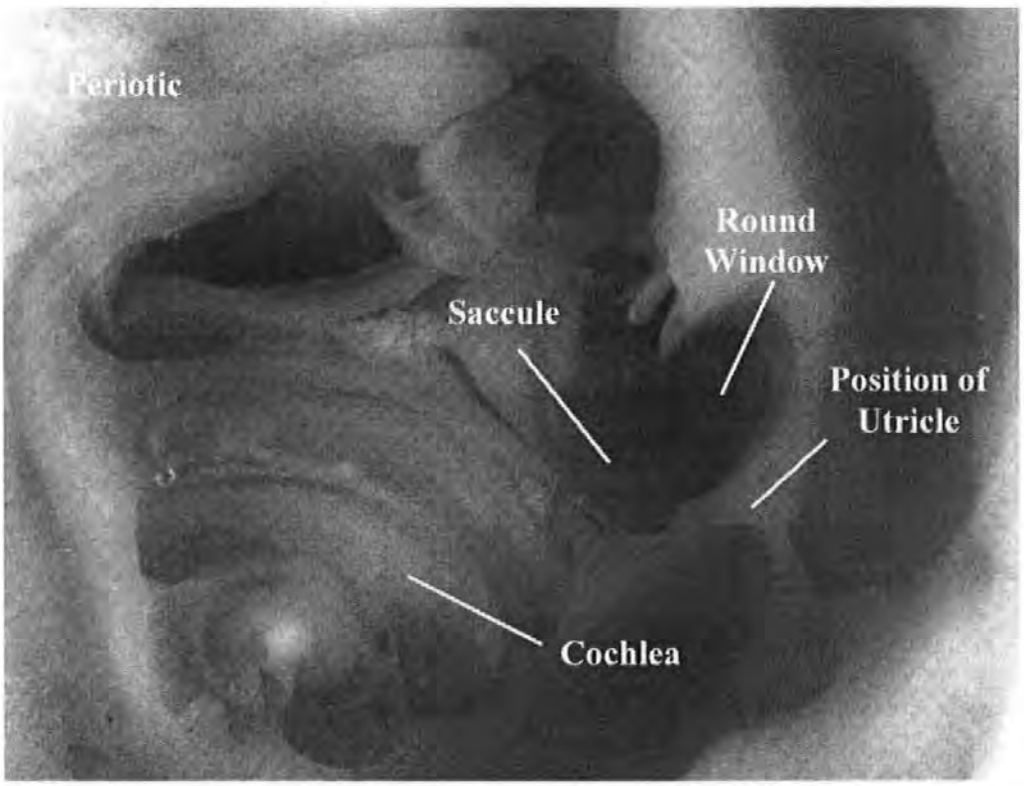

Figure 7.19 The labyrinth of the inner ear from *S. scrofa* with the covering periotic bone partially removed exposing the cochlea and vestibular organs (the saccule and utricle)

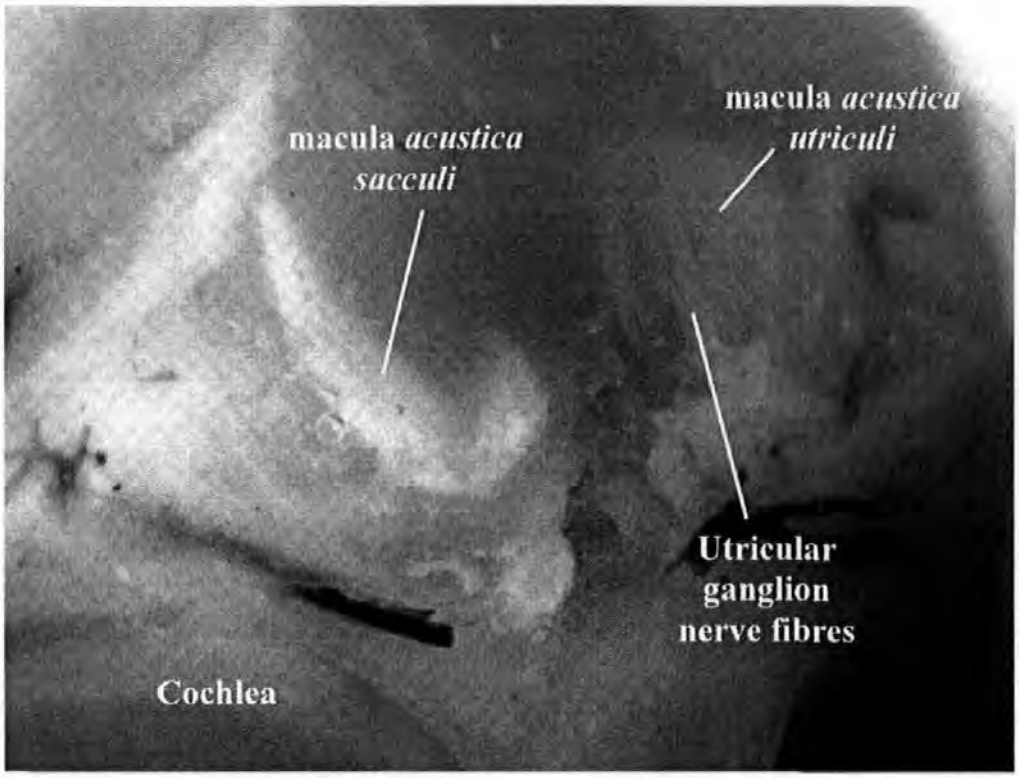

Figure 7.20 The saccule and utricle with the covering bone fully removed prior to preparation for SEM microscopy

The dissection vestibule (Figure 7.20) reveals the saccule and the utricle; the utricle is compressed transversely and occupies the upper and back part of the vestibule, lying in contact with the *recessus ellipticus* (Gray, 1918). The floor and anterior wall of the recess is thickened, forming the macula *acustica utriculi* and innervated by the utricular ganglion of the VIII nerve. The posterior wall of the saccule forms the *ductus endolymphaticus*, which is joined by the *ductus utriculosaccularis* and passes along the *aquæductus vestibuli* ending in the *saccus endolymphaticus*. The cavity of the utricle communicates with the semicircular canal ducts by five orifices, which can be clearly seen in Figures 7.7 and 7.10 from the cetacean ear. The smaller of the two bulbous vestibular sacs is the saccule (Figure 7.21.b), which is fixed to the walls of the labyrinth near to the opening of the cochlea. The cavity is located adjacent to the upper basal turn of the cochlea in proximity to, but not in direct communication with the utricle (Figure 7.21a), and presents with an oval thickening that forms the sensory macula (the *acustica sacculi*).

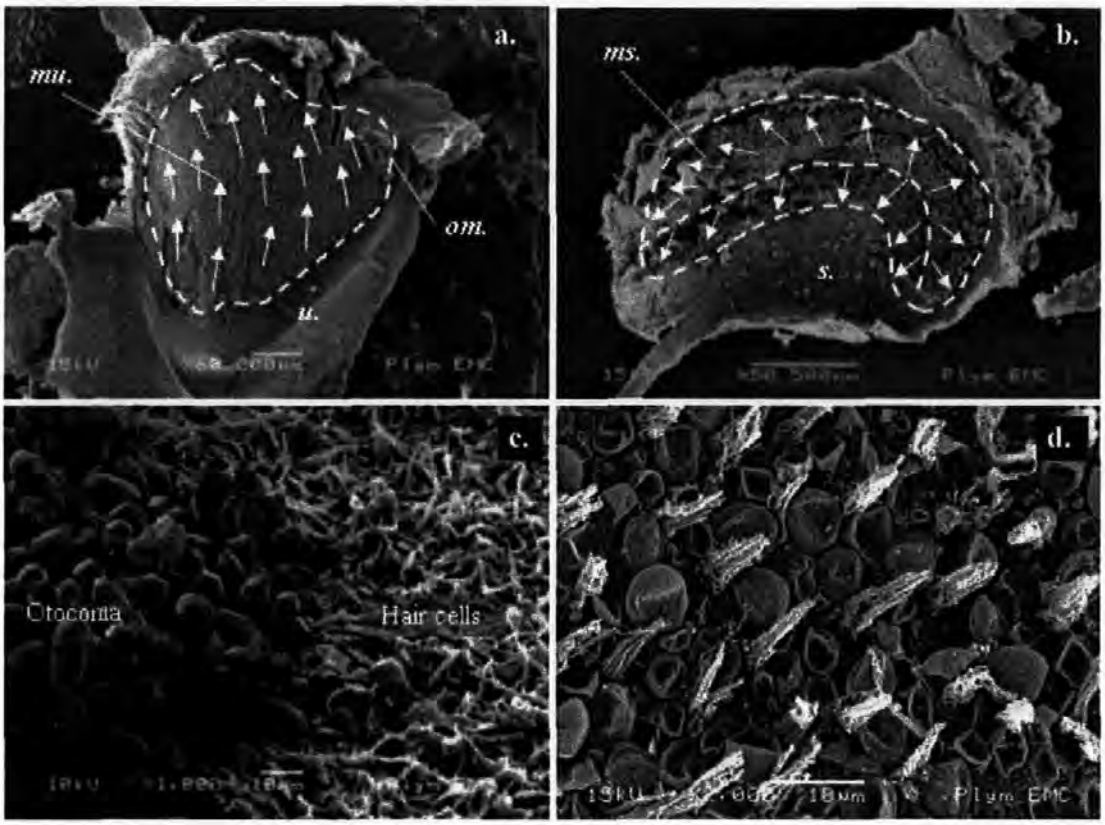

Figure 7.21.a SEM micrograph of the utricle from the domestic pig (*Sus scrofa*); the hatched line defines the perimeter of each sensory macula (*mu.*), **7.21.b.** the saccule (*s.*) and the sensory macula (ms.); the white arrows indicate the polarity of the hair cells across the surface of each macula, **7.21.c.** crystalline calcium carbonate otoconia overlaying the saccular hair cells, **7.21.d.** hair cells from the dorsal quadrant of the saccule after removal of the otoconia

The epithelial surface of the utricle (Figure 7.21.a) and the saccule (Figure 7.21.b), is covered with a thick layer of dense otoconia responsive to accelerational and gravistatic forces. The motion of the otoconia with respect to the ciliary bundles exerts a shearing force detected by the hair cells according to their orientation (Lim, 1984). The utricle is largely horizontal in the head, registering accelerations acting in the horizontal (axial) plane of the head, whilst the saccule registers accelerations in the vertical (parasagittal or coronal) plane. In Figure 7.21.c, some of the otoconia have been removed revealing the underlying hair cells, whilst 7.21.d. shows hair cells from the dorsal quadrant of the saccule after complete removal of the otoconia.

7.6 Chapter discussion and conclusions

A procedure for the fast removal of the complete cochlea and other end organs of the inner ear undamaged has been demonstrated here. However, both cetacean carcass examined in this study were retrieved in an advanced state of decomposition, thus SEM examinations of the ultrastructure within the inner ear was not undertaken as inner ear hair cells are known to deteriorate within a short time after death.

The SEM has been used to considerable effect on lower vertebrates such as fish (Platt 1977; Lovell et al., 2005b), and invertebrates (Lovell et al., 2005a) in the examination of the ultrastructure responsible for the mediation of auditory stimuli, though a review of the literature suggests that no SEM examinations have been conducted on the inner ear ultrastructure from any of the cetacean species. The relative ease and speed with which the auditory periotic was dissected from behind the mandible of *D. delphis*, indicates that it should be possible to remove the complete cetacean inner ear for a Scanning Electron Microscope examination of the hair cells. For this however, it is essential that the periotic is rapidly immersed in chilled fixative (2.5% glutaraldehyde in 0.1 M cacodylate buffer with 3.5% sodium chloride), then refrigerated to inhibit sample decomposition (the sample must not be frozen, as ice crystals will destroy the ultrastructure).

The saccule and utricle are sensitive to both angular accelerations and low frequency sounds (Popper and Fay, 1993). If either were to become damaged by anthropogenic noise pollution, it may contribute to the reported disorientation experienced by cetaceans which have become stranded live, yet do not present with any obvious signs of injury. The examination of both sensory maculae in the vestibule of *S. scrofa* reveals a thick blanket of otoconia which occludes the hair cells from view. The cilia are embedded in the otoconia and cohesion is provided by mucus (the remains of which is evident in Figures 7.21.c and 7.21.d). In order to remove the otoconia and mucus with as little disturbance to the hair cells beneath as possible, S-Carboxymethyl-L-Cysteine was employed to hydrolyse the mucus before fixing the sample. This procedure yielded best results when the solution was 'washed' through the vestibule using a pipette, prior to fixing the sample in the glutaraldehyde.

In *D. delphis* (Figures 7.7 and 7.8) the length of the basilar membrane from the upper apical tip of the cochlea to the round window was calculated to be 30.1 mm, whilst the

basilar membrane from *P. phocoena* (Figure 7.9) had a length of 22 mm. Both the animals investigated in this study were mature individuals (c.f. Read, 1999), thus it is tentatively concluded that the cochlea from *D. delphis* is 8 mm shorter, whilst *P. phocoena* is 16 mm shorter than the 38 mm reported for *T. truncatus* (Wever et al., 1971). All mammalian cochleae appear to function according to the same basic principles; however, the effective frequency range differs between species (Fay, 1988). For example, the range of audible frequencies is about 20 Hz to 16 kHz in the human cochlea, about 300 Hz to 45 kHz in *S. scrofa* (Heffner and Heffner, 1990), about 100 Hz to 150 kHz in *T. truncates* (Johnson, 1966; 1967) and 300 Hz (Kastelein et al., 2002) up to as high as 190 kHz in *P. phocoena* (Bibikov, 1992; Popov, 1986; Kastelein et al., 2002). Table 7.1 presents the outlying frequencies audible to the marine and terrestrial mammals considered here, along with the cochlea length measurements.

Table 7.1 Comparison between cochlea length and audible frequency range

Species	Cochlea Length (mm)	Low (Hz)	High (Hz)
T. truncates	38	100	150000
P. phocoena	22	300	190000
Human	35	20	16000
S. scrofa	32	300	45000

The fundamental measure of hearing ability for any animal possessing the appropriate receptor mechanism is its audiogram (Myerberg, 1981), which presents the lowest level of sound that the species can hear as a function of frequency. The hearing frequencies or audiograms for a number of odontocetiformes are well characterised, and have been produced using both physiological and behavioural approaches (see Nachtigall et al., 1995; Kastelein, et al., 2003; Sauerland and Dehnhardt, 1998; Gerstein et al., 1999; Kastelein et al., 2002), though an audiogram for *D. delphis* has as yet to be produced. The bottlenose dolphin (*T. truncates*) hears frequencies from 100 Hz to 150 kHz (Johnson, 1966; 1967), and the striped dolphin (*Stenella coeruleoalba*) hears frequencies ranging from around 500 Hz to 150 kHz (Kastelein, 2003; Brill et al., 2001), with both producing broadband clicks for echolocation that range in frequency from 20 Hz to around 200 kHz. *P. phocoena* hears frequencies between 300 Hz (Kastelein et al., 2002), up to as high as 190 kHz (Bibikov, 1992; Popov, 1986; Kastelein et al., 2002), and utilises a narrow band high frequency sonar of around 120 to 140 kHz (Busnel and Dziedzic, 1966a). It is feasible that this difference in hearing ability between *T. truncates* and *P. phocoena* is explained by the larger cochlea in the bottlenose dolphin (Wever et al., 1971; Ketten, 1997). The evidence

presented in this study suggests that the audiogram for *D. delphis* may lie somewhere between the hearing range of *T. truncates* and *P. phocoena*. It is to be concluded that the production of an audiogram for *D. delphis* (see chapter 8 for proposal), is of considerable importance for an accurate assessment of the impact of anthropogenic sounds on the inner ear physiology of this animal.

Chapter 8

General discussion

A very important question arises from this study, and primarily concerns the method by which an audiogram is calibrated. As generalist fish are shown here to respond to the motion of the water particles in the sound field, rather than the sound pressure component, it would be prudent to measure the audiogram in units of particle velocity rather than sound pressure. However, the complexities involved in the calibration and maintenance of velocity hydrophones in the dynamic marine environment precludes them from straightforward use in the field (Coates, 1990), with many researchers favouring the use of pressure sensitive hydrophones. In some cases, where an absolute measure is required (e.g. offshore surveying or oceanography), a velocity hydrophone would be used. However, when undertaking comparative work such as the study conducted here, the use of a sound pressure hydrophone is acceptable when testing generalist fish, so long as the sound field in which the auditory assessment is conducted is dominated by particle motion. The ABR generated evoked potentials presented in this study are fundamentally the response of the central nervous system to sound stimulation, and are therefore a quantitative measure of hearing ability regardless of which units are used in the audiogram.

8.1 The audiogram for *C. auratus*

The audiograms presented in Figure 8.1, are from the goldfish (*C. auratus*), and have been produced over the last 30 years using a number of behavioural and physiological approaches (discussed in Chapter 2). The curve bearing the open circles is the result of the ABR examination of hearing in *C. auratus*, from Chapter 3, and was produced following the methodology described by Kenyon et al. (1998). The majority of the curves including the one produced in Chapter 3, follow very similar profiles and appear closely grouped, though the actual threshold values in response to a 500 Hz tone burst, range between 49 dB (re 1 µPa) (Popper and Yan, 1992), to 73.7 dB (re 1 µPa) (Kenyon, et al., 1998). The relative position of the *C. auratus* thresholds from Chapter 3 is slightly higher than the majority (but not all) of the curves presented in Figure 8.1. This is not unexpected, as

behavioural audiograms often yield lower thresholds than physiological audiograms, and is discussed in detail by Yan (1995). It is therefore concluded that the auditory thresholds recorded from *C. auratus* in Chapter 3, are within the range of published audiograms for this species, and validates the electrophysiology system developed to record threshold ABR waveforms for this study.

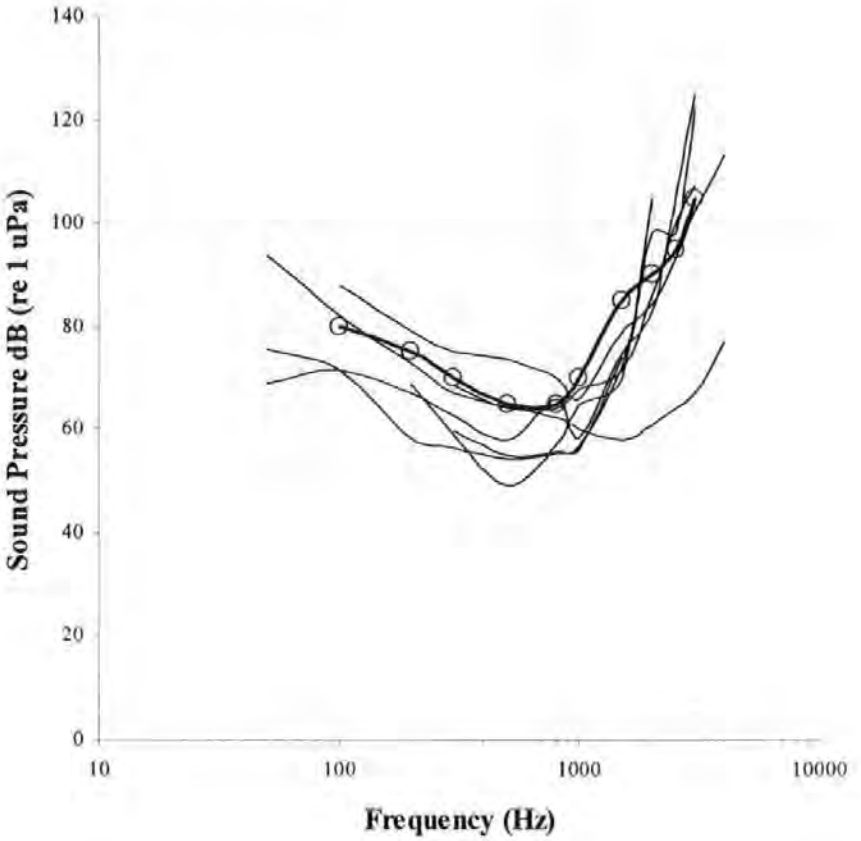

Figure 8.1 Audiograms for *C. auratus* by Chapman & Hawkins (1973), Enger (1966), Jacobs & Tavolga (1967), Kenyon (1998), Popper (1971), Yan (2001), Yan & Popper (1992), and *C. carpio* (Popper, 1972) and the audiogram for *C. auratus* produced in Chapter 3 of this present study (open circles)

8.2 Fish hearing in pressure and motion dominated sound fields

It has been demonstrated in this study, that a sound source positioned underwater and generating a pressure dominated sound field, will stimulate the CNS of a fish in much the same way as a loudspeaker positioned in the air. However, as shown by the results of the ABR investigation in Chapter 5, lower thresholds can be acquired from generalist fish if the sound field is dominated by particle motion. Figure 8.2 presents the audiograms of all the fish tested in this study, and shows that the audiograms fall into 3 main groups. The

lower curves are from *H. molitrix* and *A. nobilis* in response to sound pressure, the middle curves are from *P. spathula* and *A. fulvescens* in response to particle motion, and the high thresholds are from *P. spathula*, *A. fulvescens* and *D. labrax* in a pressure dominated sound field. The profile of the *I. punctatus* audiogram from Fay and Popper (1975) is similar to the audiograms for *H. molitrix* and *A. nobilis*, though it is about 10 dB (re 1 uPa) lower than from the two Asian carp species. This finding is not particularly surprising, as the examination of the numerous goldfish audiograms presented in Figure 8.1, show that the hearing thresholds at 500 Hz vary by over 20 dB (re 1 μPa).

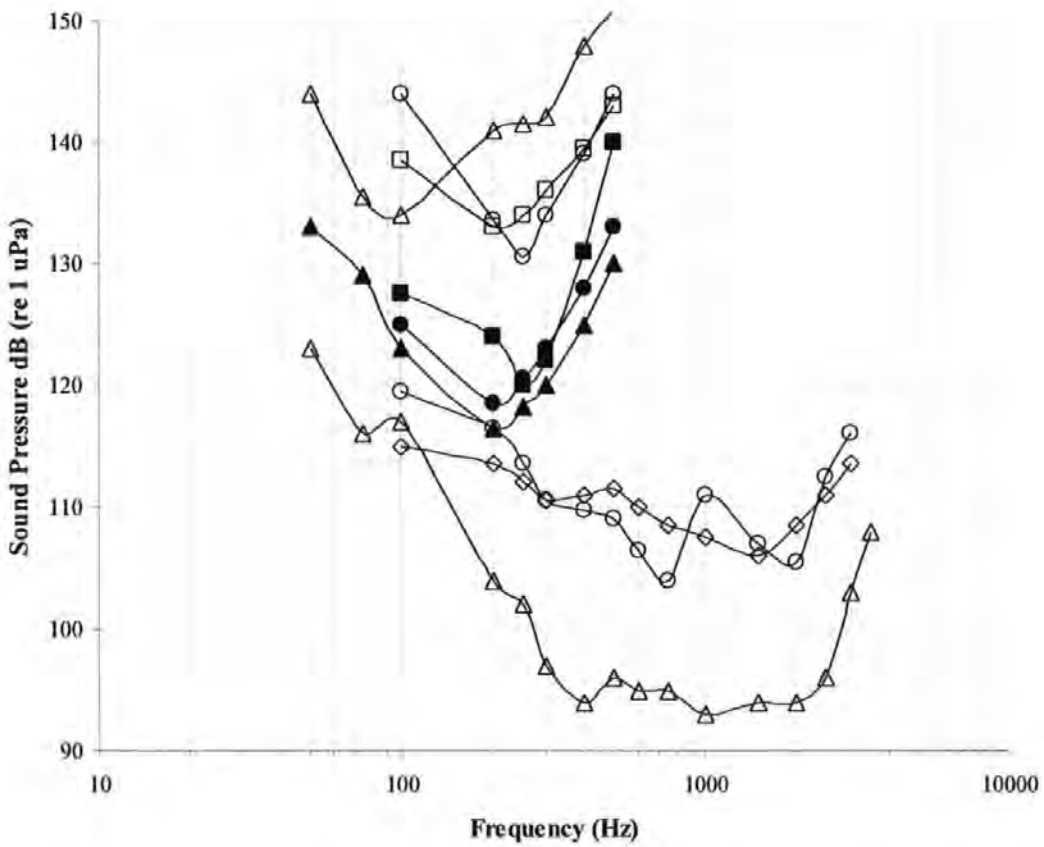

Figure 8.2 Audiograms for all the fish tested in this study, generated using either air mounted or submerged transducers for ABR, and a behavioural approach using an air mounted transducer. *D. labrax* (air), open triangles = ABR sound pressure, closed triangles = behavioural; *P. spathula* (submerged), open circles = ABR sound pressure, closed circles ABR particle motion; *A. fulvescens* (submerged), open squares = ABR sound pressure, closed squares = ABR particle motion; *A. nobilis* (submerged), open diamonds = ABR sound pressure; *H. molitrix* (submerged), open circles (lower set) = ABR sound pressure. The audiogram for the hearing specialist catfish (*I. punctatus*) (air) open triangles (lower set) from Fay and Popper (1975), included for comparative purposes

8.3 Inner ear physiology and hearing

It became very clear during the early stages of this research that no audiological model exists for any of the generalists from the Family Moronidae (sea basses), or any members of the order Acipenseriformes (sturgeons and paddlefish), or from the entire sub phylum of crustacea. It is known that the vertebrate inner ear is divided into two regions, the pars superior and the pars inferior (Retzius, 1881), with the former responding primarily to movements of the body and postural changes, and the latter responding to gravistatic and acoustic stimuli (Jenkins, 1981; Popper & Platt, 1993). However, a single receptor array is all that is found in the statocyst of decapod crustaceans, and this organ detects both gravistatic and acoustic stimuli (see Chapter 6). The audiogram for *P. serratus* (open circles) is presented in Figure 8.3, along with the audiograms for both specialist and generalist fish from Figures 8.1 and 8.2.

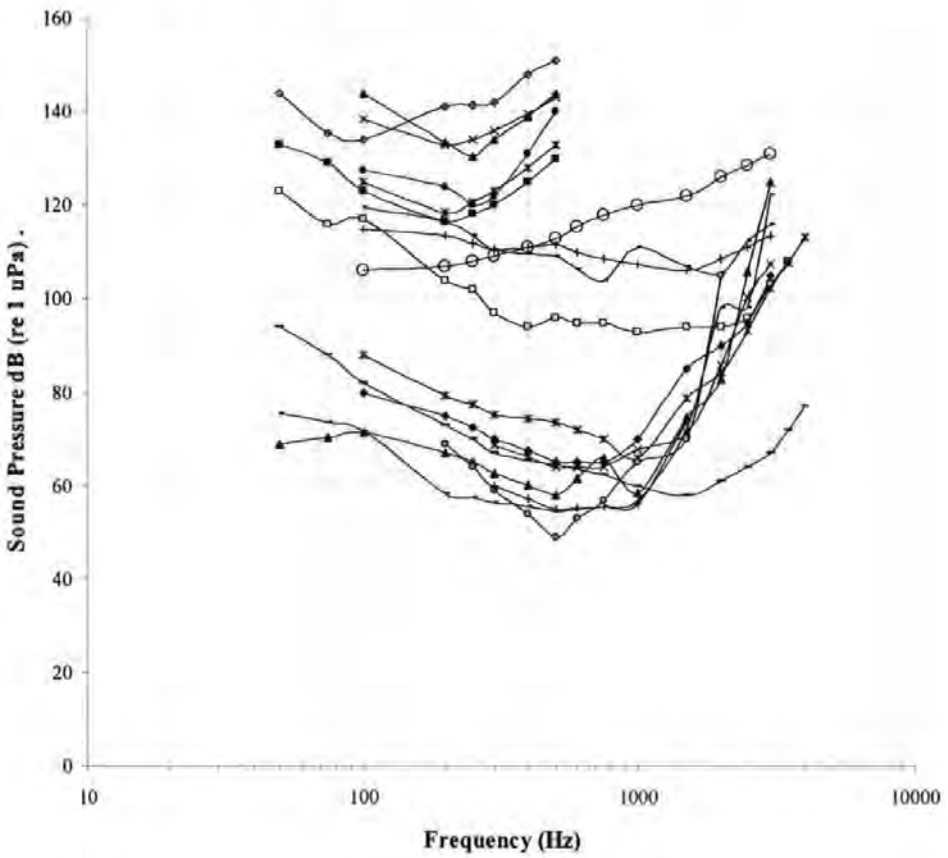

Figure 8.3 The audiogram for *P. serratus* (open circles), presented with the audiograms for both specialist and generalist fish from Figures 8.1 and 8.2

In most bony fish, the pars inferior comprises two fluid filled pouches, the saccule and lagena (Retzius, 1881; Platt & Popper, 1981; Popper & Platt, 1993), with each pouch containing a crystalline calcium carbonate otolith (Carlström, 1963; Popper & Platt, 1993). As discussed in Chapter 6, the statocyst of *P. serratus* contains a dense mass of sand granules known as the statolith, and to all appearances, functions similarly to the fish otolith in response to accelerational and acoustic stimuli. As can be seen in Figure 8.3, the detection thresholds of sounds below 300 Hz by *P. serratus* are better than any of the fish species presented, with the exception of *C. auratus*. Also, the bandwidth of the sounds audible to *P. serratus*, is considerably wider than those identified in the generalist fish species, and are comparable in range (but with slightly higher thresholds) to the audiograms obtained from the Asian carps and the catfish. However, the prawn lacks an air reservoir directly coupled to the ear, as is found in the specialist fish, so another mechanism for this phenomenon needs to be considered. It is possible that the wide range of frequencies audible to *P. serratus* is attributed to the rigidity of the statocyst base and associated receptor cells, which are in direct contact with the dense statolith structure (see Figure 6.4a). The ability to hear frequencies within the bandwidth defined for *P. serratus* would be ecologically beneficial to a number of decapod crustaceans, especially when considering the acoustic energy from the click sound produced by *A. heterochaelis* occupies a bandwidth ranging from 750 Hz to 5000 Hz.

The study of the inner ear morphology of *P. spathula*, *A. fulvescens* and *D. labrax*, undertaken here for the first time, shows that these fish possess the sensory apparatus necessary to detect and localise sound in the open environment; albeit with generalist hearing abilities. The schematics in Figure 8.4.a summarises the association between the hair cells and the sand granule otoliths in *P serratus*, along with the pathway taken by the otic ganglion to the neuropil of the antennule, and Figure 8.4.b represents the ear of the generalist fish examined in this study, and shows the pathway of nervous impulse from the inner ear afferents to the brain (identified during the physiological examinations described in Chapters 4 and 5). The vertebrate inner ear consists of a fluid filled membranous system of contiguous ducts and pouches, containing endolymph, a substance possessing both viscous and ionic properties (Platt and Popper, 1981). In most animals, the flow of Na^+ and K^+ ions across the membrane of the receptor cell afferents causes the potential voltage inside the cell to fall (Hodgkin and Huxley, 1952), and in the fish ear, the potential is transmitted along the VIII nerve to the octavolateralis area of the medulla. This pathway is represented by the schematic in Figure 8.4.b, which shows the receptor array and VIII nerve along and other organs associated with mediating hearing underwater by these

animals. Morphological examination of the inner ear and VIII nerve prior to a "first time" audiological examination of a species is essential, as it reveals the primary positioning of the electrodes, which should be placed extra-cranially, in proximity to the medulla and the peripheral end of the auditory nerve, close to the inner ear.

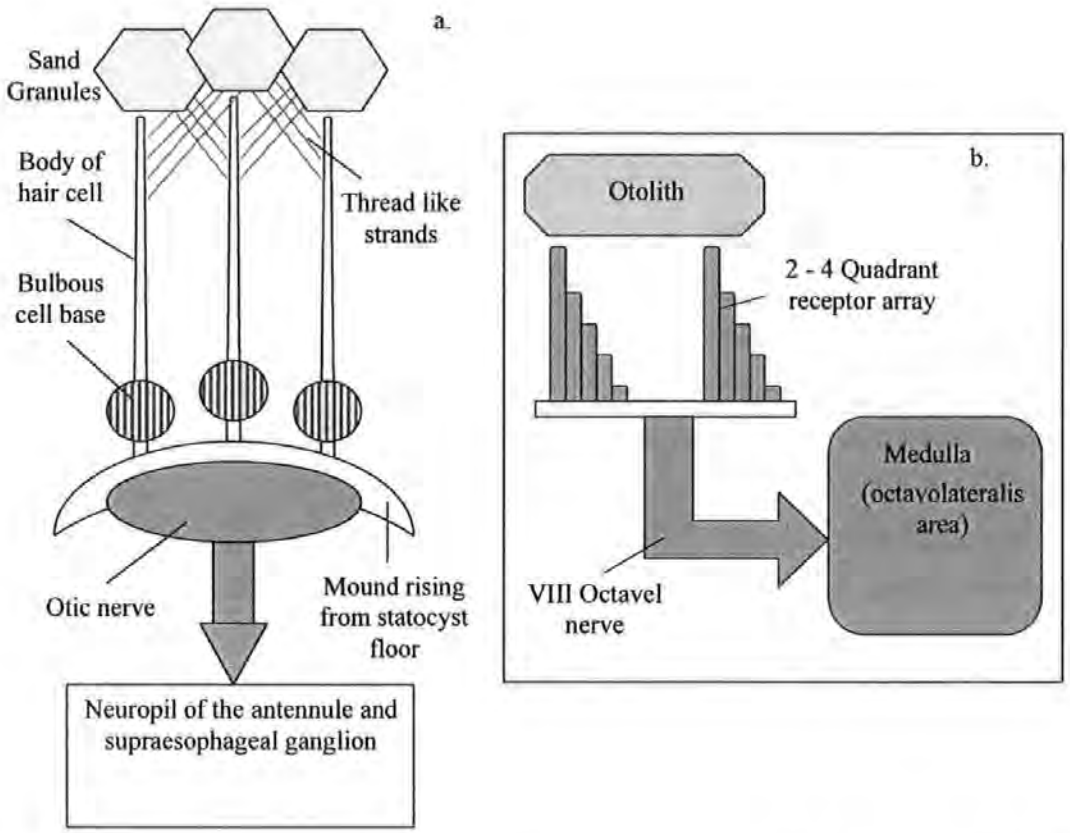

Figure 8.4a Schematic of the statocyst receptor array and nerve pathway to the supraesophageal ganglion from *P. serratus*. **8.4b** Schematic of the generalist fish ear, showing the primary pathway taken by the nervous impulse from the inner ear to the octavolateralis area of the brain, in response to acoustic stimulation

The impedance of fish flesh is nearly identical to that of the surrounding water, thus without the dense otolith, no shear forces would be generated to stimulate the sensory hairs of the generalist fish. Theoretically, a generalist fish lacking an otolith would be unable to detect the motion of the water particles in a sound field, and the same could be said of the crustaceans if the statolith were absent. It is apparent from analysis of the SEM data presented here, that *D. labrax* possesses standard orientation ciliary bundles in common with many hearing generalist species, and is in contrast with the sensory receptor patterns found in the Ostariophysi (Otophysi). These fish have hair cells orientated vertically in two diametrically opposed quadrants (Popper, 1980), a feature also found in amphibians and reptiles (Blaxter, Denton & Gray, 1981; Popper & Platt, 1979). However, the

investigation of the two Acipenseriform fish described in Chapter 5 shows that these fish also have receptors arranged in only two quadrants; though as discussed, the curvature of the macula results in the hair cells occupying four diametric quadrants.

8.4 Directional hearing

The ability to detect and localise the source of a sound is of considerable biological importance to many fish species, and is often used to assess the suitability of a potential mate or during territorial displays (Nordeide and Kjellsby, 1999), and during predator prey interactions (Myrberg, 1981). Experimentation by Schuijf and Hawkins (1983) clearly demonstrate that the cod (*Gadus morhua*), a hearing generalist, has the ability to both directionally locate and discriminate the distance of a sound source in the acoustic free field. Their experiment was conducted using a penned, conditioned cod which would respond to a sound by orientating itself toward the spatial location of the sound source. This knowledge is of considerable benefit to bio-technological systems like AFD barriers and fish ranching, as acoustically conditioned fish are known to have the ability to localise a sound source with considerable precision, even if visibility is poor, or light levels are low (Balchen 1999).

The directionality of water particles during the passage of a wave front divulge important information to the fish's sensory system, allowing it to accurately determine the direction and distance of a disturbance or sound in the acoustic free field (Schuijf & Hawkins, 1983; Hawkins & Sand 1977; Hawkins 1993). The fish achieves this because the directional characteristics of the afferents are qualitatively correlated with anatomically defined patterns of hair cell orientations on the macula of the saccule (Fay & Edds-Walton, 1997). Excitation occurs when stereocilia are bent toward the kinocilium during the passage of a wave front, resulting in the cell becoming depolarised relative to its resting potential (Clegg & Mackean, 1995). Inhibition occurs when the bundle is deflected in the opposite direction, and results in the hyperpolarisation of the cell (Flock & Duvall, 1965). Receptor excitation occurs at a rate of between 1 to 100 spikes per second (Platt and Popper, 1981), and the magnitude of the response is a cosine function of the angle between the direction of the stimulus and the direction at which sensitivity is greatest; thus the receptor array generates inherently directional microphonic potentials (Enger, 1966; Popper, 1983; Sand, 1975). Additionally, the ears of *P. spathula* and *A. fulvescens*, are positioned with a bilateral mirror symmetry, diverging at the anterior end away from the midline of the fish (Sand, 1974; Platt and Popper, 1981). This divergence of the ears can also be seen in

Figure 8.5, which shows the angle of the sagitta in the saccular chamber of *D. labrax*, viewed dorsally perpendicular to the cranium. The production of the image involved removal of the brain by dissection and aspiration, revealing the saccular chambers and relative orientation of both otoliths. The two lines positioned at 340° and 20° from the midline in Figure 8.5, and follow the longitudinal plane of each macula as they diverge outward as the anterior extremities of the fish are approached.

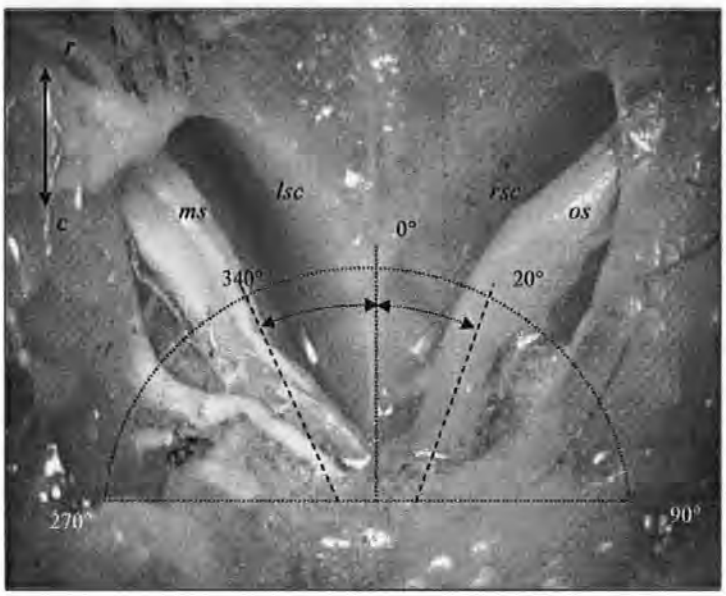

Figure 8.5 Angle of the two sagitta in the saccular chambers from *D. labrax* viewed dorsally, with the brain removed, lsc – left saccular chamber, rsc – right chamber, ms - macula of the saccularis and ramus sacculi, os – otolith sagitta

The macula of the saccule follows the curvature of the otolith, which has an approximate transverse orbital of between 62° and 75° from the horizontal for the right ear, and 105° to 118° for the left ear. Figure 8.6 shows the two bilaterally symmetrical otoliths positioned as they would be found if viewed rostrally through the fish. The image was produced by taking a transverse slice through the saccular chambers, whilst avoiding contact between the scalpel and otoliths.

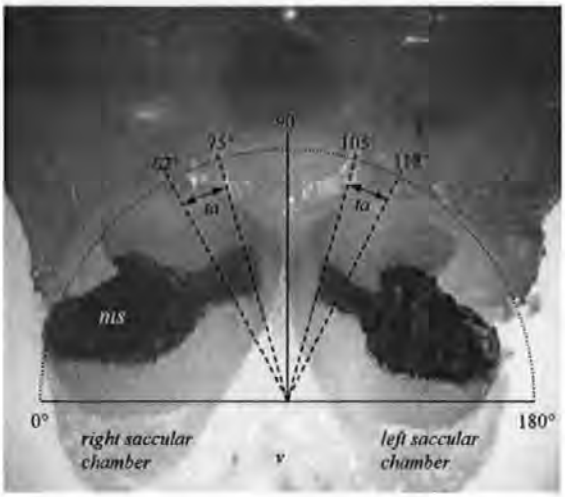

Figure 8. 6 Angle of the two sagitta from the horizontal plane viewed rostrally through the lower cranium of *D. labrax*. ms – medial sulcus, ta – transverse axis of the sagitta

The two angle lines either side of the midline are drawn parallel to the flattest plane of the medial sulcus in contact with the macula, and follow the transverse orbit of the otolith as the head is rotated from the horizontal plane. The shaded area (*ms*) shows the medial sulcus depression, and is the location of the saccular epithelia if it were present in the Figure. This shows that the receptor arrays in the ears of *D. labrax* are positioned in such a way as to be sensitive to the direction of sounds in both the horizontal and vertical planes. The upshot of this is that generalist fish can spatially locate the source of a signal, whereas terrestrial vertebrates efficiently locate the source of a sound only in the horizontal plane (Hawkins and Sand 1977). However some amphibians, reptiles and birds do have ears that act as individual pressure gradient receivers, allowing for both the horizontal and vertical localisation of a sound source (Popper and Fay 1993). The polar diagram in Figure 8.7 shows the recording of microphonic potentials as a function of angle to a sound source in the horizontal plane for the perch (*Perca fluviatilis*). Line a. and b. indicate that maximum directional sensitivity is evoked by acoustic stimuli deviating 20° from the midline (Sand, 1973), thus the perch is most acutely aware of the location of a sound it is swimming toward.

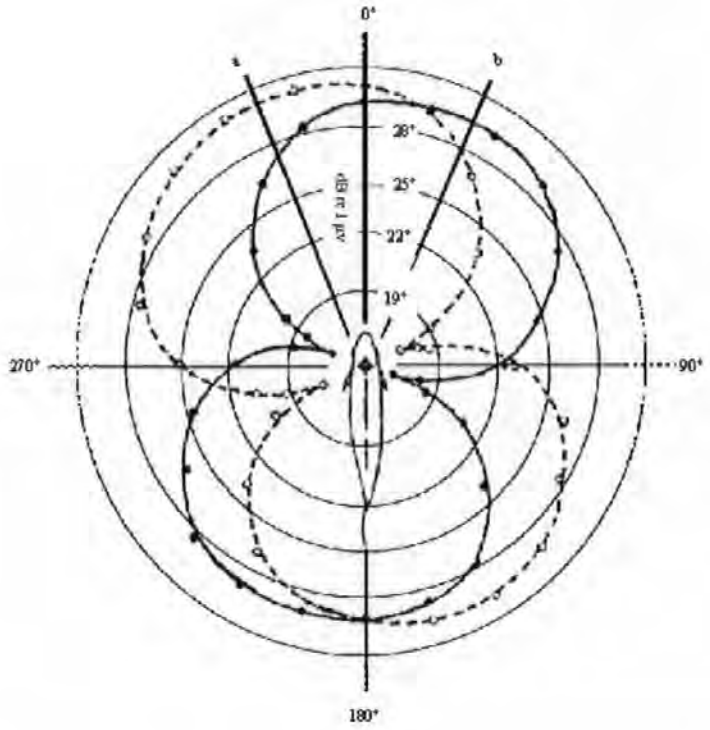

Figure 8.7 Polar diagram showing the recording of microphonic potentials as a function of angle to a sound source in the horizontal plane for a perciform fish (*Perca fluviatilis*) (Redrawn from Sand, 1973) Line a. and b. show the maximum directional sensitivity of *P. fluviatilis*, which is evoked by acoustic stimuli deviating 20° from the midline of the fish

8.5 Application of the carp, sturgeon and paddlefish audiograms

During the experimental work associated with the efficiency of the Acoustic Fish Deflection (AFD) barrier system (Taylor, Pegg and Chick, in press), introduced in Chapters 1, 3 and 5, the barrier was found to be only 50% effective when using sounds in a bandwidth of 20 Hz to 500 Hz. The signal was changed to include higher frequency components, and a substantial increase in efficiency occurred. It was therefore suggested that, in order to achieve the highest possible levels of fish deflection for the non-indigenous carp species, further information concerning the auditory sensitivity of each species was required. The present study provides audiograms for the silver carp (*H. molitrix*) and bighead carp (*A. nobilis*), along with the audiograms for paddlefish (*P. spathula*) and sturgeon (*A. fulvescens*), which have been measured using the Acoustic Evoked Potential (AEP) audiometry method. The second AFD signal tested, had a frequency range of up to 2 kHz, and resulted in the efficiency the barrier increasing to 95%

(Taylor et al., in press). The increase in barrier efficiency is most likely attributed to *H. molitrix* and *A. nobilis* having relatively high frequency hearing abilities; thus, the 2 kHz signal falls into their peak range of hearing, as defined by the audiogram in Figure 8.2. These results demonstrate the importance of matching the sound generated by the AFD system, to the hearing range of the target species if a high efficiency is to be achieved. In addition, this difference in hearing ability between fish species offers a prospective advantage that it may be possible to tailor the system to selectively deflect one species of fish, whilst allowing another to pass.

8.6 The auditory assessment

The hearing of *D. labrax* is now known to be restricted to a narrow bandwidth of between 50 Hz to 500 Hz, and has a best detection frequency of 134 dB (re 1 uPa) at 100 Hz. The Auditory Brainstem Response (ABR) method of acquiring auditory data (introduced in chapter 4), was selected due to it being a non invasive practice. This approach relies on the fact that the electrical potential of the nervous impulse passing along the auditory nerve can be detected by electrodes placed on the skin of the fish. Commonly, anaesthetics are used to immobilise the fish during an ABR examination (see Kenyon et al, 1997), thereby reducing muscular activity which can produce considerably higher amplitude waveforms than does the evoked potential. The procedure developed for this thesis, avoids the use of anaesthetics on the grounds of ethical considerations; instead it utilised natural behavioural responses of the fish in an unfamiliar situation.

While undertaking the ABR measurements, the level of ambient light was kept at a minimum; though a small amount of light was directed at the wall in front of the fish. The soft light appeared to have more of a calming effect on the fish, as opposed to it being in total darkness. Additionally, it was found that fish would become calm if they were placed in a cradle lined with a thin layer of soft micromesh netting saturated in well oxygenated sea water. This combination of low light levels and the adapted cradle provided the fish with an acceptable level of comfort, to the point where auditory evoked potentials could be successfully measured.

8.7 Continued work

8.7.1 Crustacean hearing

As has been shown in this study, *P. serratus* is able to detect sounds from below 100 Hz, to around 3000 Hz, though for completeness, low frequencies need to be tested to find the point where thresholds successively rise with lower frequencies. In addition, it would be of interest to test *P. serratus* in both pressure and motion dominated sound fields, in a similar test as the one conducted on *A. fluviatilis* and *P. spathula*. It has been demonstrated that body size has no influence on the amplitude of the evoked response from *P. serratus* (see appendix ii), though nothing is known of the effect of the moulting cycle on hearing thresholds. Hearing ability has been defined only in this one species, yet as discussed in chapter 6, several crustacean species produce sound using a number of mechanisms (Schmitz and Herberholz 1998; Patek, 2001; Meyer-Rochow et al., 1982).

The investigation of hearing ability and the analysis of sounds produced by crustaceans would prove to be of considerable value in determining the importance of hearing on the ecology of these animals. Although a number of physiological and behavioural experiments have been conducted on fish to assess the impact of noise on the auditory system, none have so far been directed toward the crustaceans, a major link in the oceanic food chain. The long-term effects of intense low frequency sounds on the shrimp hearing ability and ecology is not known, but the data presented here show that there is a need to include crustaceans in such an assessment, in order to gain a more insightful view of the effect of intense noise on the entire marine ecosystem.

8.7.2 The audiogram for a normally hearing common dolphin (*Delphinus delphis*) using the Auditory Brainstem Response (ABR) technique

As previously discussed, ABR shows the response of the entire auditory system and will allow for the diagnosis of hearing damage, even if restricted to the microscopic hair cells or other fine structures of the ear, that may, in all probability, not be found using conventional examination methods. In the proposed ABR audiological investigation of *D. delphis*, surface (cutaneous) electrodes are arranged with the reference electrode positioned

at the vertex of the head and the record electrodes positioned behind each ear. This configuration will enhance the recording of far field AEP's, as the electrodes span the length of the nerve pathway between the cortex, brainstem and ear, thus each ear can be tested independently; a procedure commonly used in human audiological tests.

The ABR measurements of hearing thresholds is made using a control and analysis program, which both generates the stimulus signals and captures and analyses the response. The sound field is generated by a Laptop PC and presented through an array of free standing transducers positioned at least 1 m to 2 m from the head of the subject (see Figure 8.8 for equipment schematic). The array will need to generate tone bursts ranging in frequency from below 50 Hz to in excess of 150 KHz. A low frequency transducer (20 Hz to 3 kHz) has been set up and calibrated, though the high frequency ceramic transducers have as yet to be incorporated in the system. The time it takes to identify thresholds is dependant on the frequency of the tone burst and the recording conditions; high frequencies (above 10 kHz) can be taken to threshold within 3 minutes, whilst lower frequencies take longer (up to 15 minutes at 100 Hz). Figure 8.9 shows the time taken to run two repeat ABR tests for single amplitude at a selected frequency (using a standard setup averaging 500 sweeps of 25 ms). The number of averaged sweeps required to determine threshold is dependant on the setup of the system and recording conditions, as in some instances threshold can be reached in as little as 200 sweeps, up to as many as 2000. The usual protocol is to attenuate the stimulus sound in six equal steps, until the EP waveform is no longer discernable above the averaged ambient electrical noise (about 0.1 μv in ideal recording conditions). In general, it takes just over an hour to complete a full audiological test, though there is no reason why this cannot be broken up into more than one session.

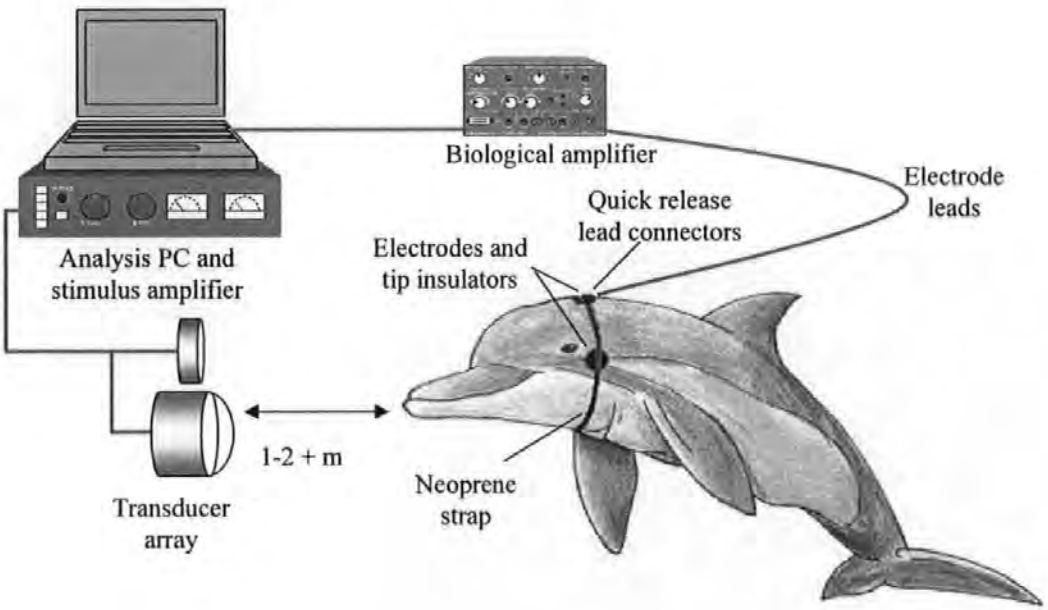

Figure 8.8 Schematic of the non-invasive ABR system

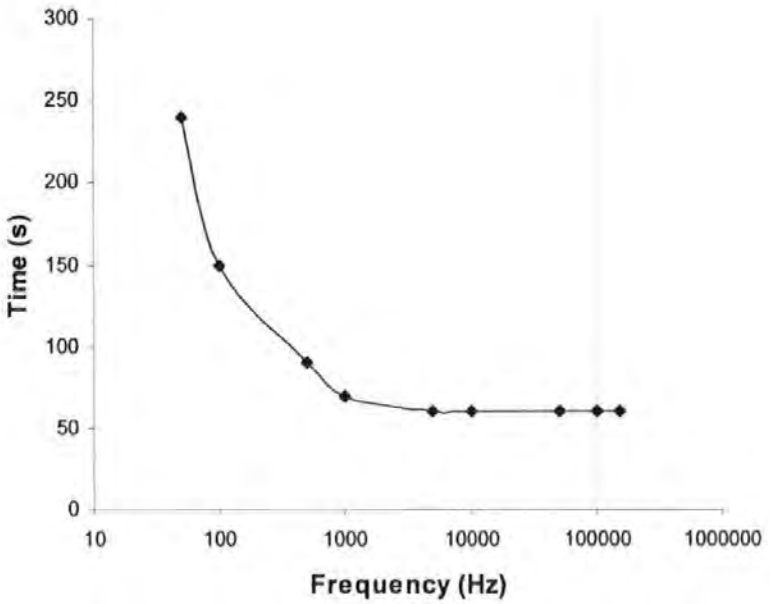

Figure 8.9 Graph showing the time taken to repeat test single amplitudes at a given frequency, averaged from 500 sweeps of 25 ms (using a 4 cycle tone burst)

8.7.3 The interface between the electrode and test subject

When recording Evoked Potentials from *A. fulvescens*, using cutaneous electrodes, it was found that the signal strength from the fish to the biological amplifier was lower than signals recorded from the *P. spathula*. However, the presence of the electrode tip insulators ensured that most of the ambient water did not contact the tip, and allowed for the acquisition of comparable sized waveforms. The reason for this is discussed in Chapter 5, and is mainly attributed to the ossified cranial plates preventing a good seal between the fish and electrodes; soft fleshy skin such as was found on the head of *P. spathula* is best, and probably accounts for the high quality of the ABR traces in Figures 5.8 and 5.10. Though the ABR examinations of *D. labrax* and *P. serratus* were conducted in seawater, the increased electrical conductivity of this medium did not result in high attenuation of the EP. This is because in the test of *D. labrax*, the electrodes and very top of the head were out of the water by 1 mm, and in *P. serratus*, the electrodes were fitted subcutaneously.

When recording Auditory Evoked Potentials (AEPs) from a fish stationed below the surface in seawater using cutaneous electrodes, it was found that substantial attenuation of the evoked potential signal occurred at the tip, and had a profound effect on the quality of the ABR trace. Evoked responses from the tench (*Tinca tinca*) were examined in respect to EP attenuation in water of different salinities, as it is a hearing specialist with a high tolerance to seawater. Therefore, by using this species, it allowed for the direct comparison of neural waveforms that have been recorded with the fish in marine, brackish and fresh water. In order to record high quality AEP's in seawater, it was found that a modification needed to be made at the electrode tip (see Figure 8.10 for schematic). The modification involved fitting a silicone rubber cap to the upper portion of the exposed electrode tip, thus providing an insulated seal between the ambient seawater, and the contact point between the electrode tip and fish.

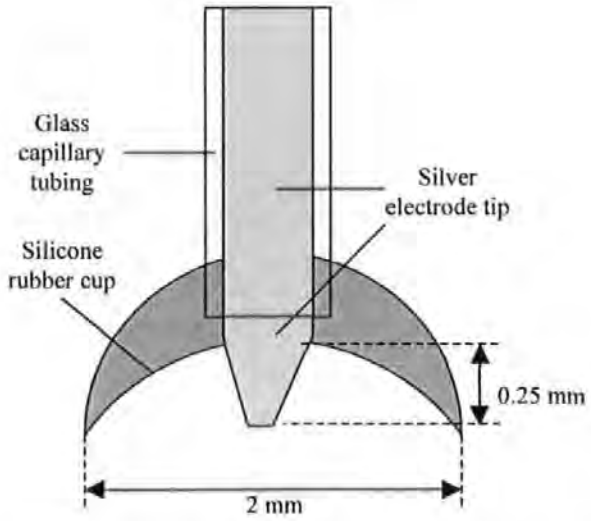

Figure 8.10 Silicone rubber cap fitted to the upper portion of the exposed electrode tip, providing electrical insulation between the ambient seawater, and the contact point between the electrode tip and fish, and was used successfully to preserve the EP signal when testing *A. fulvescens* and *T. tinca*

The Auditory Evoked Potentials in Figure 8.11 show the recordings of neural waveforms from *T. tinca* in response to acoustic stimulation with a 500 Hz tone burst presented initially at 120 dB, and attenuated in 5 dB steps, with the fish in seawater. The first of the waveform sets were acquired with the electrodes and nape of the fish's head above the water surface. The second set was recorded with the fish at a depth of 120 mm, and shows a signal loss of approximately 90 %. The third set were recorded again with the fish at a depth of 120 mm, but on this occasion the electrodes had been fitted with a silicone cup type shield which provided insulation from the seawater, and reduced signal loss at the electrode tip to less than 40 %.

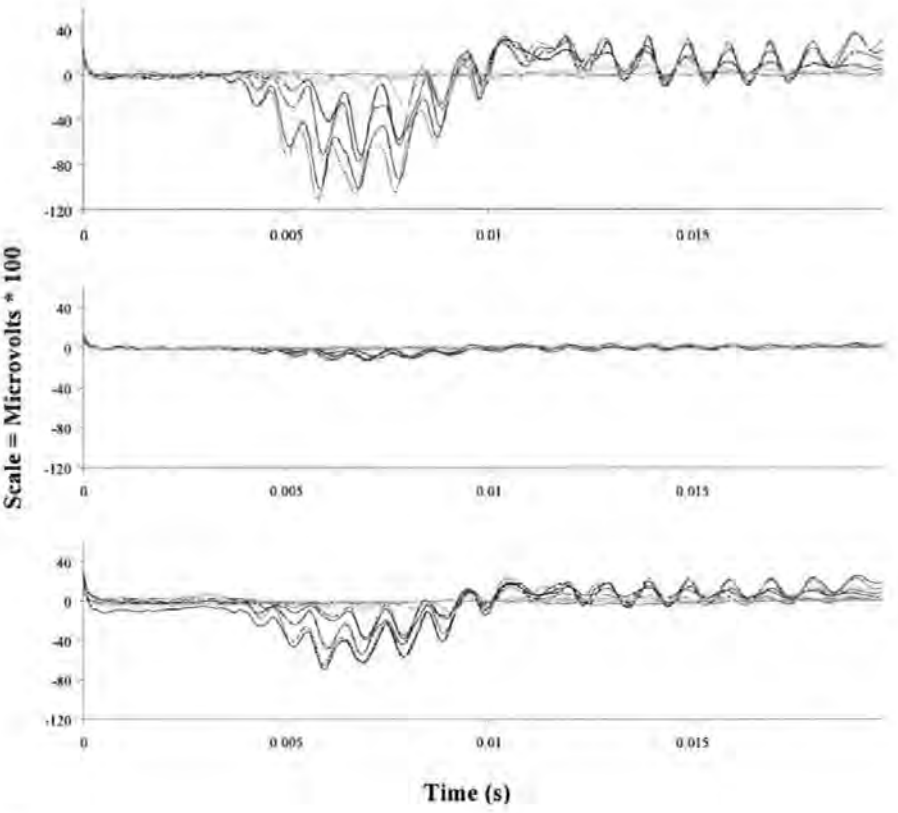

Figure 8.11 Evoked potentials from a hearing specialist tench (*Tinca tinca*), in response to a 500 Hz tone burst, with the fish in seawater. The top set were acquired with the fish at the water surface, the centre set were from a fish positioned 120 mm under the water surface without the modification, and the lower set were acquired from a fish positioned 120 mm below the water surface using the electrode tip insulators

The preliminary results of this experiment shows that the inclusion of the cap has a significant effect on the preservation of the EP in seawater. However, the efficiency of the insulators can be further improved by positioning the cap whilst the fish is briefly immersed in fresh water, thus trapping the less conductive water in the electrode cap, and can result in a less than 10 % loss in the EP signal.

Previous ABR investigations of odontocetiform animals have mainly used sub-cutaneous electrodes that are out of the water during the test, thus reducing AEP attenuation through conduction. AEP responses have been examined in respect of the levels of attenuation in marine, brackish and fresh water (Lovell, unpublished data). It was found that in order to record high quality AEP's in seawater, a modification needed to be made at the electrode tip (see Figure 8.12 for schematic). The modification involved fitting a silicone rubber cap to the upper portion of the exposed electrode tip, thus providing an insulated seal between

the ambient seawater and the contact point between the electrode tip and fish. Figure 4 presents a schematic of the electrode configuration, which uses a rubber sucker disk to provide electrical insulation from the conductive properties of the ambient seawater.

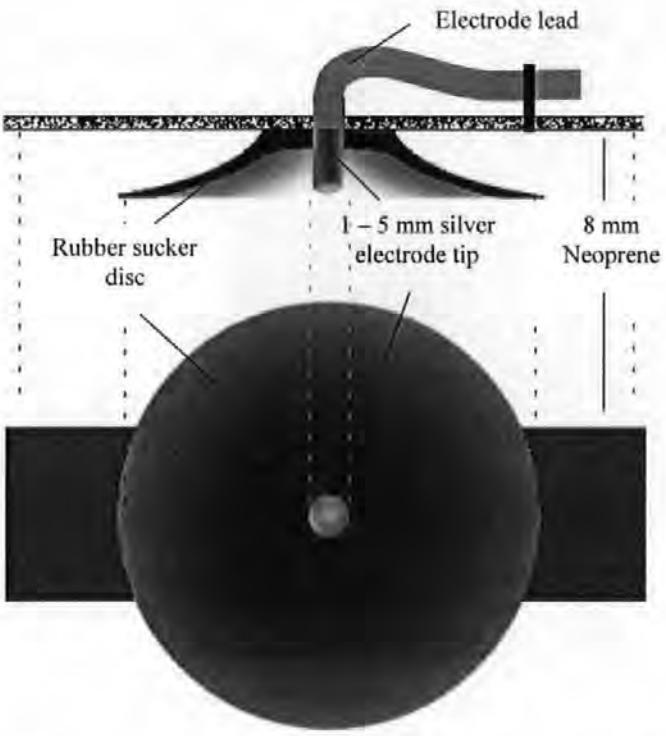

Figure 8.12 The electrode tip configuration with the rubber sucker disk, providing insulation from the conductive properties of the ambient seawater (scale1.5:1)

The electrodes are integrated into a lightweight 20 mm wide strip of 8 mm elasticated neoprene, which is positioned firmly but not tightly around the dolphin's head, about 100 mm posterior of the eyes. The ends of the neoprene strip are held together with Velcro, so the headgear can be easily positioned or removed. It would be of great benefit to include a small hydrophone, to allow for constant monitoring of the sound level during the hearing test, though this has as yet to be incorporated in the prototype.

The ABR response is readily dominated by myogenic noise caused by muscular movement, thus while undertaking the ABR measurements on fish, the subject is held in a cradle and supplied with oxygenated water so it has no need to swim. The ambient light levels are kept low during the assessment since many species react to this by becoming passive, though the proposed system can detect and reject ABR responses that are contaminated by myogenic noise. In order for an ABR assessment of hearing to be conducted on *D. delphis*, protocols will need to be developed that will minimise voluntary

muscular activity during the test. Primarily, this will involve discussions with handlers and others involved in the animals day to day maintenance and welfare, as a psychological approach may be the most appropriate to achieve optimum results.

8.7.4 Summary of short to medium term aims and objectives for future work

- **Develop a working relationship with the organisations and individuals directly responsible for the care and welfare of the dolphins to be assessed in the ABR examination.**

- **Identify the appropriate protocols for minimising voluntary muscular movement during the hearing test**

- **Develop and prototype the non-invasive headgear for *D. delphis*, that can function when submerged in seawater**

- **Add ceramic disks to the transducer array and produce tone bursts of sufficient amplitude from below 50 Hz to above 150 kHz**

- **Refine the ABR electrophysiology system and techniques so the equipment can be used "in the field"**

References

Akamatsu, T., Nanami, T. & Yan, H.Y. (2003). Spotlined sardine *Sardinops melanostictus* listens to 1-kHz sound using its gas bladder. Fisheries Science; 69: 348–354.

Akamatsu T, Okumura T, Novarini N and Yan HY (2002) Empirical refinements applicable to the recording of fish sounds in small tanks. J. Acoust. Soc. Am. Vol. 112, No. 6, December 2002

Alfredsen, J.A., 2000. Effects of conditioning on free-ranging fish: A theoretical and experimental study. *Dr. ing. thesis.* Report 2000:8-W. Department of engineering cybernetics, Norwegian University of science and technology.

Au, W. W. L. (1993). "The Sonar of dolphins". Springer-Verlag, New York, N.Y.

Balchen, JG (1999). "Thirty years of research on the application of cybernetic methods in fisheries and aquaculture technology", *Modeling, Identification and Contro*l vol. 21, pp 1–62.

Balchen, J.G., (1981). Recent progress in the control of fish behaviour. *In* Akashi, H. (ed.) *Proceedings of the eighth triennial world congress of the international federation of automatic control. Kyoto, Japan.* Pergamon press.

Barber VC and Emerson CJ (1980). "Scanning electron microscopic observations on the inner ear of the skate, (*Raja ocellata*)". Cell and Tissue Research (Germany, F.R.), v. 205(2) pp. 199-215

Bell C.C. (1981). Some central connections of medullary octavolateral centers in a mormyrid fish". Ed Tovolga W; Popper A; Fay R. *Hearing and sound communication in fishes.* Springer Verlag. New York pp 383 - 392

Bibikov, N.G. (1992). Auditory brainstem responses in the harbour porpoise (*Phocoena phocoena*). In: 'Marine Mammal Sensory Systems', 197-211. Thomas, J. *et al* (eds). Plenum Press, New York.

Blaxter JHS, Denton EJ and Gray JAB (1981). "Acousticolateralis system in clupeid fishes". Ed's Tovolga W; Popper A; Fay R. *Hearing and sound communication in fishes*. Springer Verlag. New York. pp 39-61

Brill, R.L., Moore, P.W.B. & Dankiewicz, L.A. (2001). Assessment of dolphin (*Tursiops truncates*) auditory sensitivity and hearing loss using jawphones. JASA, 109(4), 1717-1722.

Busnel, R.G., & Dziedzic, A (1966 A). Acoustic signals of the pilot whale *Globicephala melaena* and of the porpoises *Delphinus delphis* and *Phocoena phocoena*. (in K.S. Norris, ed.) Whales, dolphins and porpoises. University of California Press, Berkeley. pp. 607-646

Carlström DA (1963) "Cystallographic study of vertebrate otoliths". Biol. Bull. 125, 441-463.

Casper, B.M., Lobel, P.S. & Yan, H.Y. (2003). The hearing sensitivity of the little skate, *Raja erinacea*: a comparison of two methods. Environmental Biology of Fishes. 68, 371-379.

Chapman, C.J. and Hawkins, A.D., (1973). A field study of hearing in the cod, *Gadus morhua*. *Journal of comparative Physiology* 85, 147-167.

Chapman, C.J. and Sand, O., (1974). Field studies of hearing in two species of flatfish *Pleuronectes platessa* and *Limanda limanda*. *Comp. Biol. Physiol.* 47A, 371-385.

Clegg CJ and Mackean DG (1994) "Advanced Biology: principles and applications". John Murray, London, 448-461pp.

Coates R (1990). "Underwater acoustic systems". Macmillan Publishing, London.

Coombs, S and Montgomery, JC (1999). The enigmatic lateral line system. In Comparative Hearing: Fishes and Amphibians (ed. A. N. Popper and R. R. Fay), pp. 319 -363. New York: Springer-Verlag.

Coombs, S. & Popper, A.N. (1982). Structure and function of the auditory system in the clown knifefish, *Notopterus chitala*. J. Exp. Biol., 97:225-239.

Coombs, S. & Popper, A.N. (1979). Hearing differences among Hawaiian squirrelfish (Family Holocentridae) related to differences in the peripheral auditory system. J. Comp Physiol. A, 132:203-207.

Corwin JT, Bullock TH, Schweitzer J (1982). "The auditory brainstem response in 5 vertebrate classes". Electroencephalogr Clin Neurophysiol 54: 629 - 641

Corwin, J.T., (1981). Audition in elasmobranchs. In: Tavolga WN, Popper AN, Fay RR (eds) Hearing and sound communication in fishes. Springer, Berlin Heidelberg New York, pp 81 - 105

Costa, D.P, Crocker, D.E, Gedamke, J, Webb, P.M, Houser, D.S, Blackwell, S.B, Waples, D, Hayes, S.A. & Le Boeuf, B.J. (2003). The effect of a low-frequency sound source (acoustic thermometry of the ocean climate) on the diving behavior of juvenile northern elephant seals, *Mirounga angustirostris*. Journal of the Acoustical Society of America 113(2):1155-1165.

Dalen J and Knutsen G (1987). "Scaring effects in fish and harmful effects on eggs, larvae and fry by offshore seismic explorations". In: H.M. Merklinger (ed.) Progress in Underwater Acoustics. Proceedings 12th International Congress on Acoustics. Plenum Press, New York: 93-102.

Engås, A., Løkkeborg, S., Ona, E., & Soldal, A.V. (1996). Effects of seismic shooting on local abundance and catch rates of cod (*Gadus Morhua*) and haddock (*Melanogrammus aeglefinus*). Canadian J. of Fisheries and Aquatic Sciences. 53, 2238 - 2249.

Enger P.S. (1976). On the orentation of haircells in the labtrinth of pearch (*Perca fluviatilis*). Eds Schuijf A; Hawkins A.D. *Sound reception in fish*. Elsevier. Oxford. pp 49 - 62.

Enger PS, Hawkins AD, Sand O and Chapman CJ (1973). "Directional sensitivity of saccular microphonic potentials in the haddock". J. Exp. Biol., 59:425-433.

Enger PS & Andersen RA (1967). An electrophysiological field study of hearing in fish. Comp. Biochem. Physiol. 22, 517-525

Enger PS (1965). Acoustic thresholds in *C. auratus* and its relation to the sound source distance. Comp Biochem Physiol 18: 859-868

Fay, R. (1981). Coding of acoustic information in the eighth nerve. Ed Tovolga W; Popper A; Fay R. Hearing and sound communication in fishes. Springer Verlag. New York. pp 189 - 219

Fay, R. R. and A. N. Popper (1975). Modes of stimulation of the teleost ear. J. Exp. Biol., 62:379-387.

Fay, R.R. and Edds-Walton, P.L. (1997). Directional response properties of saccular afferents of the toadfish, (*Opsanus tau*).. Hearing Research 111 (1-2): 1-21

Fay RR (1981). Coding of acoustic information in the eighth nerve. *Hearing and sound communication in fishes*. Eds Tovolga W; Popper A; Fay R. Springer Verlag. New York. pp 189-219.

Fay, R. R. and A. N. Popper. (1980). Structure and function in teleost auditory systems. In: Comparative Studies of Hearing in Vertebrates. Popper, A. N. and R. R. Fay, eds. Springer-Verlag. 42 pp.

Fay, RR. and Popper AN (1975). Modes of stimulation of the teleost ear. J. Exp. Biol., 62:379-387.

Fine, M.L. (1981). Mismatch between Sound Production and Hearing in the Oyster Toadfish. In: Hearing and Sound Communication in Fishes, Tavolga, W.N. et al (eds.), 257-263.

Fraser, P.J (2001). Statocysts in crabs: short-term control of locomotion and long-term monitoring of hydrostatic pressure Biol. Bull. 200: 155-159

Fraser, P. J., Bevengut, M. and Clarac, F (1987). Swimming patterns and the activity of identified equilibrium interneurons in the shore crab, *Carcinus maenas*. J. Exp. Biol. 130:305–330

Frisch, K. von, (1936). UÈ ber den GehoÈ rsinn der Fische. Biol Rev 11: 210 - 246

Gerstein, E.R., Gerstein, L., Forsythe, S.E, & Blue, J.E. (1999). The underwater audiogram of the West Indian manatee (*Trichechus manatus*). JASA, 105(6), 3575-3583.

Hastings M, Popper A, Finneran P, and Lanford P (1996). Effects of low frequency sound on the hair cells of the inner ear and lateral line of teleost fish (*Astronotus ocellatus)*. J. Acoust. Soc. Am 99(3): pp 1759 – 1766.

Hawkins, A.D., 1993. Underwater sound and fish behaviour. *In* Pitcher, T.J. (ed.) *Behaviour of teleost fishes: 2nd edition.* Chapman and Hall, pp 129-169.

Hawkins, A.D. 1986. "Underwater sound and fish behaviour". The Behaviour of teleost fishes. pp. 114-151.

Hawkins, A.D. & Myrberg, A.A. (jnr). (1983). Hearing and sound communication under water. In: Bioacoustics: a comparative approach. B. Lewis (ed.), pp. 347-405. Academic Press, New York.

Hawkins AD (1983), Underwater sound and fish behavior. Ed. Pitcher T.J. *The behavior of teleost fishes*. Croom Helm. London. pp- 114-151.

Hawkins AD (1981). The hearing abilities of fish. Eds Tovolga W; Popper A; Fay R. Hearing and sound communication in fishes. Springer Verlag. New York. pp 109 - 139.

Hawkins, A.D. and Johnstone, A.D.F., (1978). The hearing of the Atlantic salmon, *Salmo salar*. *Journal of fish biology* 13, 655-673.

Hawkins AD, Sand O (1977), Directional hearing in the median vertical plane by the cod. *Journal of Comparative physiology. A*. Vol. 122: page 1 - 8

Hawkins, A.D., and D.N. MacLennan. (1976). An acoustic tank for acoustic studies on fish. In A. Schuijf, and A.D. Hawkins (eds) Sound Reception in Fish. Elsevier, Amsterdam. pp149-169

Higgs DM, Rollo AK, Souza MJ, Popper AN. (2003). "Development of form and function in peripheral auditory structures of the zebrafish (*Danio rerio*)". J Acoust Soc Am. 2003 Feb; 113(2):1145-54.

Hodgkin, A. L. and Huxley, A. F. (1952) A Quantitative Description of Membrane Current and its Application to Conduction and Excitation in Nerve. Journal of Physiology 117: 500-544

Iversen, R.T.B. (1969). Auditory thresholds of the scombrid fish *Euthynnus affinis*, with comments on the use of sound in tuna fishing, FAO Fisheries Rep. No. 62. 3, 849–859.

Jacobs, D.W. and Tavolga, W.N., 1967. Acoustic intensity limens in the *C. auratus*. *Animal behaviour* 15, 324-335.

Jacobson, J.T., (1985). An overview of the auditory brainstem response. In: Jacobson JT (ed) The auditory brainstem response. College-Hill Press, San Diego, pp 3 – 12

Jenkins DB (1981). The utricle in *Ictalurus punctatus*. *Hearing and Sound Communication in Fishes*. Tavolga, WN, Popper AN and Fay RR, Eds. Springer-Verlag, New York.

Jensen JC (1994). Structure and innervation of the inner-ear sensory organs in an otophysine fish, the upside-down catfish (Synodontis-nigriventris David). Acta Zoologica 75 (2): 143-160

Jewett, D.L., (1970). Volume conducted potentials in response to auditory stimuli as detected by averaging in the cat. Electroencephalogr Clin Neurophysiol 28: 609 – 618

Jewett, D.L., Williston, J.S., (1971). Auditory evoked far fields averaged from the scalp of humans. Brain 94: 681 - 696

Johnson, C.S. (1966). Auditory thresholds of the bottlenosed porpoise (*Tursiops truncatus*). U.S. Naval Ord. Test Stn., Tech. Oubl., 4178: 1-28.

Johnson, C.S, (1967). Sound detection thresholds in marine mammals. In W.N. Tavolga (ed), Marine bio-acoustics, vol. 2. Pergamon, Oxford, U.K.

Kalmijn AJ (1988). Hydrodynamic and acoustic field detection. In: Sensory Biology of Aquatic Animals. J Atema, RR Fay, WN Tavolga, eds. Springer Verlag, New York, pp 83-130

Kastelein, R.A., Bunskoek, P., Hagedoorn, M., Au, W.L.W. & de Haan, D. (2002). Audiogram of a harbor porpoise (Phocoena phocoena) measured with narrow-band frequency-modulated signals. JASA, 112(1), 334-344.

Kastelein, R.A., Hagedoorn, M., Au, W.W.L. & de Haan, D. (2003). Audiogram of a striped dolphin (*Stenella coeruleoalba*). JASA, 113(2), 1130-1137.

Kenchington T (1999). "Impacts of seismic surveys on fish behaviour and fisheries catch rates on Georges Bank". Norigs 2000, Nova Scotia

Kenyon, T. N., F. Ladich and H. Y. Yan (1998). "A comparative study of hearing ability in fishes: the auditory brainstem response approach". Journal of Comparative Physiology A. 182: 307-318.

Kenyon TN (1996). Ontogenetic changes in the auditory sensitivity of the bicolor damselfish, *Pomacentrus partitus* (Poey). J Comp Physiol A 179: 553-561

Ketten, D.R. (1995). Estimates of blast injury and acoustic trauma zones for marine mammals from underwater explosions. In: Sensory Systems of Aquatic Mammals, R. Kastelein, J. Thomas, and P. Nachtigall (eds.), DeSpil Publishers, pp. 391-408

Ketten, D.R. (1997). Structure and Function in Whale Ears, Bioacoustics, vol.8, no. 1, pp. 103-136.

Kramer, D. L., Manley, D. & Bourgeois, R. (1983). The effect of respiratory mode and oxygen concentration on the risk of aerial predation in fishes. Canadian Journal of Zoology 61, 653-665.

Ladich, F. & Yan, H.Y. (1998). Correlation between auditory sensitivity and vocalization in anabantoid fishes. J Comp Physiol A 182:737-746.

Larsel O (1967). "The comparative anatomy and histology of the cerebellum from Myxinoids through birds". University of Minnesota Press. Minneapolis.

Larsen ON (1995). Acoustic equipment and sound field calibration. In Klump GM et al (eds.) Methods in comparative psychoacoustics. Birkhäuser Verlag, p. 31-45

Lim DJ (1984). The development and structure of otoconia. In: I Friedman, J Ballantyne (eds). Ultrastructural Atlas of the Inner Ear. London: Butterworth, pp 245-269

Løkkeborg S (1991) "Effects of a geophysical survey on catching success in longline fishing". ICES CM 1991/B:40.

Løkkeborg S and Soldal A (1993) "The influence of seismic exploration with airguns on cod (Gadus morhua) behaviour and catch rates". ICES Mar.Sci.Symp. 196: 62-67.

Lombarte A, Popper AN (1994) Quantitative analyses of postembryonic hair cell addition in the otolithic end organs of the inner ear of the European hake, *Merluccius merluccius* (Gadiformes, Teleostei). J. Comp. Neurol. 345:419-428

Lovell JM (unpublished) "The ethology and physiology of sonic production and reception in marine organisms". *BSc Honours project*.

Lovell, J.M., Findlay, M.M., Moate, R.M., & Yan, H.Y. (2005 A). The hearing abilities of the prawn *Palaemon serratus*. Comp. Biochem. Physiol. A Mol. Integr. Physiol. 140, 89-100.

Lovell, J.M, Findlay, M.M., Moate, R.M., & Pilgrim, D.A. (2005 B). The polarization of inner ear ciliary bundles from a scorpaeniform fish. J. Fish. Biol. 66, 836-846

Lovell, J.M, Findlay, M.M, Harper, G, Moate, R.M & Pilgrim, D.A. (2005 C). The polarisation of hair cells from the ear of the European bass (*Dicentrarchus labrax*). Comp. Biochem. Physiol. A Mol. Integr. Physiol. 141, 116-121

Lovell, J.M., Findlay, M.M., Moate R.M., Nedwell J.R., & Pegg M.A. (in press). The inner ear morphology and hearing abilities of the Paddlefish (*Polyodon spathula*) and the Lake Sturgeon (*Acipenser fulvescens*). Comp. Biochem. Physiol. A Mol. Integr. Physiol.

Lu Z and Popper AN (1998). "Morphological polarizations of sensory ciliary bundles in the three otolithic organs of a teleost fish: fluorescent imaging of ciliary bundles". Hear. Res. 126 (1-2): 47-57.

Lugli, M., Yan, H.Y. & Fine, M.I. (2003). Acoustic communication in two freshwater gobies: the relationship between ambient noise, hearing thresholds and sound spectra. J.Comp.Physiol. A, 189, 309-320.

McCormick, C.A. & Popper, A.N. (1984). Auditory sensitivity and psychophysical tuning curves in the elephant nose fish, *Gnathonemus petersii*. J. Comp. Physiol., 155:753-761.

Myrberg, A.A. Jr & Spires, J.Y. (1980). Hearing in damselfishes: an analysis of signal detection among closely related species. J. Comp. Physiol., 140, 135- 144.

Myrberg AA (1981) "Sound communication and interception in fishes". *Hearing and Sound Communication in Fishes*. Tavolga WN, Popper AN, and Fay RR, Eds. Springer-Verlag, New York.

Nachtigall, P.E., Au, W.W.L., Pawloski, J.L. & Moore, P.W.B. (1995). Risso's dolphin (*Grampus griseus*) hearing thresholds in Kaneohe Bay, Hawaii. In 'Sensory Systems of Aquatic Mammals', 49-53. R.A. Kastelein et al (eds). De Spil Publ., Woerden, Netherlands.

Nordeide JT and Kjellsby E (1999). "Sound from spawning cod at their spawning grounds". ICES Journal of Marine Science. 56: pp 326 – 332.

Northcutt (1981). "Audition and the central nervous system of fishes". Ed Tovolga W; Popper A; Fay R. Hearing and sound communication in fishes. Springer Verlag. New York. pp 331 -356

Northrup, J. (1974). Detection of low-frequency underwater sounds from a submarine volcano in the western Pacific. J. Acoust. Soc. Am. 56(3), 837-841.

Offutt, G.C. (1974). Structures for the detection of acoustic stimuli in the Atlantic codfish, *Gadus morhua*. JASA, 56(2), 665-671.

Overbeck GW and Church MW (1992). "Effects of tone burst frequency and intensity on the auditory brainstem response (ABR) from albino and pigmented rats". Hear Res 59: 129 - 173

Parker, G.H., (1903). The sense of hearing in fishes. Am Nat 37: 185 – 204

Pearson W, Salaski J and Malme C (1992). "Effects of sounds from a geophysical survey device on behaviour of captive rockfish (Sebastes spp.)". Can.J.Fish.Aquat.Sci. 49: 1343-1356.

Pickett G, Eaton D, Seaby R and Arnold G (1994). "Results of bass tagging in Poole Bay during 1992". MAFF laboratory leaflet No 74. Lowestoft.

Pilgrim, D.A. & Lovell, J.M., (2002). A review of current publications dealing with the impact of low frequency sounds upon fish. Report to Devon Sea Fisheries Committee.

Pillay T.V.R (1990) *Aquaculture principles and practices*, Fishing News Books, London.

Platt C and Popper AN (1984). "Variation in lengths of ciliary bundles on hair cells along the macula of the saccule in two species of teleost fishes". Scanning Electron Microsc. Becker, R.P. (ed.). No. 4: pp. 1915-1924.

Platt C and Popper AN (1981). "Fine structure and function of the ear". *Hearing and Sound Communication in Fishes.* Tavolga WN, Popper AN and Fay RR, Eds. Springer-Verlag. New York. pp 3 – 38

Platt C (1977). "Hair cell distribution and orientation in *C. auratus* otolith organs". J. Comp. Neurol. 172, 283

Popper, A.N. and Fay, R.R., (1993). Sound detection and processing by fish: Critical review and major research questions. *Brain behav evol* 41, 14-38.

Popper, A.N. and Platt, C (1993). Inner ear and lateral line. *In* Evans, D.H. (ed.) *The physiology of fishes*. CRC Press, London, pp 99-136.

Popper AN, Hoxter B (1984) Growth of a fish ear: 1. Quantitative analysis of sensory hair cell and ganglion cell proliferation. Hear. Res. 15:133-142 [PubMed]

Popper AN (1983). "Organization of the ear and auditory processing". Fish Neurobiology 1st edition. Eds. Northcutt, R. G. and Davis, R. E., University of Michigan Press, Ann Arbor,

Popper AN and Platt C (1983). "Sensory surface of the saccule and lagena in the ears of ostariophysan fishes". J. Morphol., 176, 121,

Popper AN (1981). "Comparative scanning electron-microscopic investigations of the sensory epithelia in the teleost saccule and lagena". Journal of Comparative Neurology. Wiley-Liss, New York 200 (3): 357-374

Popper A; Fay R. (1981) *Hearing and sound communication in fishes*. Springer Verlag. New York. pp 3 – 38

Popper AN (1980). "Scanning electron microscopic study of the saccule and lagena in several deep-sea fishes". Am. J. Anat, 157(2), 115-136.

Popper AN (1979). "Ultrastructure of the saccule and lagena in a moray eel (Gymnothorax sp.)". J. Morphol., 161, 241,

Popper A.N and Platt C (1979). "The herring ear has a unique receptor pattern". Nature, 280 (5725), 832-833.

Popper AN (1978). "A comparative study of the otolithic organs in fishes". In: Scanning electron microscopy II. Eds Becker RP, Johari O. pp. 405-16.

Popper AN (1977). "A scanning electron microscopic study of the saccule and lagena in the ears of fifteen species of teleost fishes". J. Morphol. 153, 397.

Popper, A. N. and R. R. Fay. (1973). Sound detection and processing by teleost fishes: A critical review. Journal of the Acoustical Society of America, 53:1515-1529.

Popper, A.N. (1972). Pure-tone auditory thresholds for the carp, *Cyprinus carpio*. JASA, 52(6) Part 2, 1714-1717.

Popper, A.N. (1971). The effects of size on the auditory capacities of the goldfish. J Aud Res 11: 239-247

Popov, V.V., Ladygina, T.F. & Supin, A.Ya. (1986). Evoked potentials of the auditory cortex of the porpoise, *Phocoena phocoena*. J. Comp. Physiol., 158:705-711.

Popov, V. & Supin, A. (1990). Electrophysiological studies of hearing in some cetaceans and a manatee. In 'Sensory Abilities of Cetaceans', 405-415. J. Thomas & R. Kastelein (eds). Plenum Press, N.Y.

Protasov, V. R. (1970), *Vision and Near Orientation in Fish*, Israel Program for Scientific Translations.

Retzius G (1881). "Das Gehörorgan der Wirbelthiere". Vol. 1, Das Gehörogan der Fische und Amphibien, Samson and Wallin, Stockholm.

Richardson, W. J., Greene, C. R., Jr., Malme, C. I., & Thomson, D. H. (1995). Effects of Noise on Marine Mammals. Academic, San Diego pp 576.

Ridler, N. and Hishamunda, N., 2001. Promotion of sustainable commercial aquaculture in sub-Saharan Africa. *FAO Fisheries Technical Paper* 408/1. FAO, Rome, Italy.

Romer, A.S., and T.S. Parsons. 1977. The vertebrate body. W.B. Saunders Company. Philadelphia. pp 624

Salaski J, Pearson W and Malme C (1992) Effect of sounds from a geophysical survey device on catch per unit effort in a hook and line fishery for rockfish (*Sebastes* spp). Can. J. Fish. Aquat. Sci. 49, pp 1357 – 1365.

Sand O. (1975), "microphonic potentials as a tool for auditory research in fish". Eds Schuijf A; Hawkins A.D. *Sound reception in fish*. Elsevier. Oxford. pp 27 - 48.

Sand, O. and A. D. Hawkins. (1973). Acoustic properties of the cod swim bladder. J. Exp. Biol., 58:797-820

Sauerland, M. & Dehnhardt, G. (1998). Underwater audiogram of a tucuxi (*Sotalia fluviatilis guianensis*). JASA, 103(2): 1199-1204.

Scholik, A.R., Yan, H.Y., (2001). Effects of underwater noise on auditory sensitivity of a cyprinid fish. Hear. Res. 152, 17-24.

Scholik, A.R., Yan, H.Y., (2002a). Effects of boat engine noise on auditory sensitivity of the fathead minnow, Pimephales promelas. Environ. Biol. Fish. 63, 203-209.

Scholik, A.R., Yan, H.Y., (2002b). The effects of noise on auditory sensitivity of the bluegill sunfish, Lepomis macrochirus. Comp. Biochem. Physiol. A. 133, 43-52.

Schuijf A and Hawkins AD (1983). "Acoustic distance discrimination by the cod". Nature 302: 143 – 144.

Sleigh, M.A. & MacDonald, A.G. (Editors) (1972). The effects of pressure on organisms. Symposium of the Society for Experimental Biology. 1972: 26: xi – xiii

Sugihara I and Furukawa T (1989). "Morphological and functional Aspects of two different types of ciliary bundles in the *C. auratus* Saccule". J. Neurophysiol. 62:1330-1343.

Sylvia, G., M. Morrissey and S. Garcia (1996). "Changing Trends in Seafood Markets: The Case of Farmed and Wild Salmon". Journal of Aquatic Food Products Marketing, Vol. 3(2)

Tateda, Y., Nakazono, A. and Tsukahara, H., 1985. Acoustic conditioning of young Red Sea Bream, *Pagrus major. Report of Fishery Research Laboratory, Kyushu University* 7, 27-36.

Tavolga, WN, Popper AN and R. R. Fay, eds. (1981). Hearing and sound communication in fishes. New York : SpringerVerlag, 608 p.

Tavolga, W.N. (1974). "Signal/noise ratio and the critical band in fishes," J. Acoust. Soc. Am. 55, 1323–1333.

Tavolga, W.N. & Wodinsky, J. (1963). Auditory capacities in fishes. Bull. Am. Mus. Nat. Hist., 126, 177-240.

Taylor, R.M., Pegg M.A., & Chick, J., (In Press). Effectiveness of two bioacoustic behavioral fish guidance systems for preventing the spread of bighead carp to the Great Lakes. North American Journal of Fisheries Management.

Todd, S., S. Stevick, J. Lien, F. Marques, & D. Ketten (1996). Behavioural effects of exposure to underwater explosions in humpback whales (*Megaptera novaeangliae*). Canadian Journal of Zoology, 74(9):1661-1672.

Urick, R.J., (1983). Principles of Underwater Sound. Los Altos, California, Peninsula Publishing.

Von Frisch K (1938). "The sense of hearing in fish". *Nature* 141, 8-11.

Ward PD (2000). "Underwater Sound Propagation on the Atlantic Frontier". Published in Scottish Association of Marine Science Newsletter 21, p14.

Ward P, Donnelly M, Heathershaw A, Jones S (1998) "Acoustic modelling of pulse propagation for environmental impact assessment". Published in *Proceedings of the 4th European Conference on Underwater Acoustics*, 217-222, Ed. A. Alippi, G. B. Canelli, Rome.

Wardle C and Carter J (1997) "Effects of a triple 'G' airgun on fish behaviour". Fisheries Research Services Marine Laboratory, Aberdeen

Warren, M.P. (1989). The auditory brainstem response in pediatrics. Otolaryngol Clin North Am. Jun; 22 (3): 473-500

Wever, E. G., McCormick, J. G., Palin, J. & Ridway, S. H. (1971). The Cochlea of the Dolphin, *Tursiops truncatus*: Hair Cells and Ganglion Cells. Proceedings of the National Academy of Sciences of the United States of America 68: 2908-2912.

Whitlow, W., Au, W., Nachtigall, P. & Pawloski, J. (1997). Acoutic effects of the ATOC signal (75Hz, 195 dB) on dolphins and whales. Journal of the Acoustical Society of America, 101(5) Pt1

Yan, HY (2003). The role of gas-holding structures in fish hearing: an acoustically evoked potentials approach. In "Senses of Fishes" (eds.) G. von der Emede and J. Mogdans. Narosa Publishing House. pp. 189-209.

Yan HY (2002). The use of acoustically evoked potentials for the study of enhanced hearing in fishes. Bioacoustics. 12: pp325-328.

Yan, H.Y. (2001). A non-invasive electrophysiological study on the enhancement of hearing ability in fishes. Proc. I.O.A., Vol 23 Part 4, 15-26.

Yan, H.Y., Fine, M.L., Horn, N.S. and Colon, W.E (2000). "Variability in the role of the gasbladder in fish audition". *The Journal of Comparative Physiology* 186(5), 435-445.

Yan H. Y. (1995). Investigations of fish hearing ability using an automated reward method. In "Methods in Comparative Psychophysics" (eds) G. M. Klump, R. J. Dooling, R. R. Fay, and W. C. Stebbins. Birkhauser Verlag Basel/Switzerland. pp. 263-276.

Yan and Popper (1992). " Auditory sensitivity of the cichlid fish *Astronotus ocellatus* (Culver). J. Comp. Physiol. 171A: 105-109

Yan HY, Saidel WM, Chang JS, Presson JC, Popper AN (1991). "Sensory ciliary bundles of a fish ear: evidence of multiple types based on ototoxicity sensitivity". Proc R Soc Lond B Biol Sci 22; 245 (1313):133-8

Yan H. Y. (1995). Investigations of fish hearing ability using an automated reward method. In "Methods in Comparative Psychophysics" (eds) G. M. Klump, R. J. Dooling, R. R. Fay, and W. C. Stebbins. Birkhauser Verlag Basel/Switzerland. pp. 263-276.

Appendix i

Published peer reviewed manuscripts

Lovell, J.M, Findlay, M.M, Moate, R.M & Yan H.Y (2005 A). The hearing abilities of the prawn (*Palaemon serratus*). Comp. Biochem. Physiol. A Mol. Integr. Physiol. Vol 140/1 pp 89-100

Lovell, J.M, Findlay, M.M, Moate, R.M & Pilgrim D.A. (2005 B). The polarization of inner ear ciliary bundles from a scorpaeniform fish. Journal of Fish Biology 66, pp 836–846

Lovell, J.M, Findlay, M.M, Harper, G, Moate, R.M & Pilgrim, D.A (2005 C). The polarisation of hair cells from the ear of the European bass (*Dicentrarchus labrax*). Comp. Biochem. Physiol. A Mol. Integr. Physiol. Vol 141/1 pp 116-121

Lovell, J.M; Findlay, M.M; Moate, R.M; Nedwell J.R & Pegg, M.A (in Press). The inner ear morphology and hearing abilities of the Paddlefish (*Polyodon spathula*) and the Lake Sturgeon (*Acipenser fulvescens*). Comp. Biochem. Physiol. A Mol. Integr. Physiol.

ELSEVIER

Comparative Biochemistry and Physiology, Part A 140 (2005) 89–100

CBP

www.elsevier.com/locate/cbpa

The hearing abilities of the prawn *Palaemon serratus*

J.M. Lovell[a,*], M.M. Findlay[a], R.M. Moate[b], H.Y. Yan[c]

[a]*School of Earth, Ocean and Environmental Sciences, University of Plymouth, Drake Circus, Plymouth PL4 8AA, United Kingdom*
[b]*Plymouth Electron Microscopy Centre, University of Plymouth, Drake Circus, Plymouth PL4 8AA, United Kingdom*
[c]*Research Station, Institute of Zoology, Academia Sinica, Jiashi, I-Lan 262, Taiwan*

Received 5 August 2004; received in revised form 1 November 2004; accepted 2 November 2004

Abstract

The mechanism of sound reception and the hearing abilities of the prawn (*Palaemon serratus*) have been studied using a combination of anatomical, electron microscopic and electrophysiological approaches, revealing that *P. serratus* is responsive to sounds ranging in frequency from 100 to 3000 Hz. It is the first time that the Auditory Brainstem Response (ABR) recording technique has been used on invertebrates, and the acquisition of hearing ability data from the present study adds valuable information to the inclusion of an entire sub-phylum of animals when assessing the potential impact of anthropogenic underwater sounds on marine organisms. Auditory evoked potentials were acquired from *P. serratus*, using two subcutaneous electrodes positioned in the carapace close to the supraesophageal ganglion and the statocyst (a small gravistatic organ located below the eyestalk on the peduncle of the bilateral antennules). The morphology of the statocyst receptors and the otic nerve pathways to the brain have also been studied, and reveal that *P. serratus* possesses an array of sensory hairs projecting from the floor of the statocyst into a mass of sand granules embedded in a gelatinous substance. It is the purpose of this work to show that the statocyst is responsive to sounds propagated through water from an air mounted transducer. The fundamental measure of the hearing ability of any organism possessing the appropriate receptor mechanism is its audiogram, which presents the lowest level of sound that the species can hear as a function of frequency. The statocyst of *P. serratus* is shown here to be sensitive to the motion of water particles displaced by low-frequency sounds ranging from 100 Hz up to 3000 Hz, with a hearing acuity similar to that of a generalist fish. Also, recorded neural waveforms were found to be similar in both amplitude and shape to those acquired from fish and higher vertebrates, when stimulated with low-frequency sound, and complete ablation of the electrophysiological response was achieved by removal of the statocyst.

Keywords: Crustacean; Sensory system; Hair cell; Evoked potential; Hearing; *Palaemon serratus*

1. Introduction

The oceans are virtually transparent to sound, and opaque to light and radio waves. At a wavelength of 1 m (1500 Hz), water is nearly 1,000,000 times more transparent to sound than to radio signals (Pilgrim and Lovell, 2002). This fact underlies the intense interest currently being directed toward the acoustical exploration of the ocean. Naturally produced sounds arise from a number of sources, such as breaking waves, heavy rain, volcanic activity or from marine animals (bio-acoustic sources). Vocalisations such as whale song, along with the grunts and whistles from sonic fish are especially relevant for communication purposes, and during predator prey interactions (Myrberg, 1981). There are several types of anthropogenic sources used routinely that produce intense levels of noise, such as the Low Frequency Active Sonar (LFA) used by the military in anti-submarine warfare, or from the airgun arrays used during a seismic survey of the substrate beneath the seafloor by the petroleum industry. These activities can generate noise levels in excess of 253 dB (re 1 μPa at 1 m) (Engås et al., 1996), and are comparable to the noise levels generated by a seafloor volcanic eruption, which can produce a source level of in excess of 255 dB (re 1 μPa) (Northrup, 1974). Recent concerns regarding the impact of these anthropogenic

* Corresponding author. Tel.: +44 1752 232411; fax: +44 1752 232400.
E-mail address: j.lovell@plymouth.ac.uk (J.M. Lovell).

1095-6433/$ - see front matter © 2004 Elsevier Inc. All rights reserved.
doi:10.1016/j.cbpb.2004.11.003

sounds on fish and other marine animals has prompted a number of investigations into the effects of intense noise exposure on the hearing systems of marine mammals (e.g., Costa et al., 2003; Richardson et al., 1995; Whitlow et al., 1997). Additionally, several studies of the behaviour of free living fish when exposed to intense noise have been conducted (see Dalen and Knutsen, 1987; Engås et al., 1996; Pearson et al., 1992; Pickett et al., 1994), and includes the examination of log books from fishing vessels operating within 5 km of a concurrent seismic survey (Lokkeborg and Soldal, 1993).

It is known that several crustacean species produce sound; for example, the pistol shrimp (*Alpheus* spp.) produces a loud click by rapid closure of a specially adapted claw (Schmitz and Herberholz, 1998). The spiny lobster (*Palinurus vulgaris*) and the rock lobster (*Panulirus longipes*) make alarm sounds by drawing the base of the antenna across scale like ridges below the eyestalks; Patek, 2001; Meyer-Rochow et al., 1982). Additionally, *P. longipes* has been shown to take longer emerging from a hide, when feeding was preceded by a white noise (Meyer-Rochow et al., 1982). The female cricket (*Gryllus bimaculatus*) has the ability to localise and respond to male chirp sounds (Hedwig and Poulet, 2004; Schildberger and Hörner, 1988), using specially adapted acoustic receptors (tympanum), located in the forelegs below the knee (Huber and Thorson, 1985). On hearing the chirp, a receptive female will orientate itself toward the sound using a behavioural response known as phonotaxis (Schildberger and Hörner, 1988).

The ability of an organism to orientate itself in the 3-D marine environment requires the presence of a suitable gravity receptor. These receptors occur in many diverse organisms throughout the marine environment, and include cephalopod (Dilly et al., 1975; Bettencourt and Guerra, 2000), crustaceans (Prentiss, 1901; Schöne, 1971; Rose and Stokes, 1981; Patton and Gove, 1992) and fish (Popper and Platt, 1983; Bretschneider et al., 2001). In crustaceans, the statocyst is located either at the anterior end of the animal in the basal segment of each antennule, or posteriorly within the uropods, abdomen or telson (Farre, 1843; Cohen and Dijkgraaf, 1961; Finley and Macmillan, 2000). It has been well-established that the crustacean statocyst functions as an equilibrium organ by initiating corrective movements to maintain the animal's position in the water column, (Cohen and Dijkgraaf, 1961; Sekiguchi and Terazawa, 1997; Finley and Macmillan, 2000; Popper et al., 2001).

In this work, we study the electrophysiological response of the statocyst in an underwater sound field, using the Auditory Brainstem Response (ABR) recording technique originally developed for use in clinical neurophysiology. Until now, this method of acquiring hearing ability has only been applied in the auditory assessments of vertebrates (Corwin et al., 1982), though the presence of afferents in the statocyst, and existence of a neural pathway terminating in the supraesophageal ganglion, indicates that the physiology of *Palaemon serratus* is suitable for an ABR type investigation. An ABR waveform is acquired by averaging conglomerate responses of peak potentials, arising from nuclei in the auditory pathway during acoustic stimulation (Corwin et al., 1982; Overbeck and Church, 1992). The sweep records the generation of neural waveforms over a user-defined time span termed the sweep velocity, and measures activity prior to, during and after stimulation of the receptor organ. Additional waveform generation by neural activities other than those associated with hearing, combined with muscular movements, ensure that recordings have to be repeated over 1000–2000 presentations before clear results can be obtained (Kenyon et al., 1998; Yan et al., 2000). The recorded waveforms resulting from each sweep are averaged together and produce a recognisable ABR waveform, which is then overlaid on the first run, to show that the evoked potentials are repeatable.

The nerves associated with the statocyst and the pathway taken to the neuropil of the antennule in the supraesophageal ganglion was examined to provide a detailed description of how acoustic signals are perceived and transmitted by the neuronal pathways. The aim of the present paper, therefore, is to examine the morphology of the statocyst receptor array of the prawn (*P. serratus*) using both scanning and transmission electron microscopy (SEM and TEM). Measurements of the electrophysiological response of the statocyst and Central Nervous System (CNS) to acoustic stimuli were also made, and by ablation, it was demonstrated that the evoked response was generated in the statocyst organ.

2. Materials and methods

One hundred specimens of the prawn (*P. serratus*) Phylum Crustacea and Class Eumalacostraca of mixed sex, and ranging in length from 27 mm (0.1 g) to 71 mm (1.9 g) were obtained from wild stock in the South West of England using a dip net. Once captured, the prawns were transferred to a marine tank divided by a fine mesh screen into four equal sized compartments of 50 L each. An Eheim type 2013 biological filter with a flow rate of 390 L/h maintained water quality and provided aeration by spraying filtered seawater back into the tank via the filter outlet pipe located 60 mm above the water surface. The ambient noise within the holding tank was measured using a hydrophone, and the sound pressure level was calculated to be 102 dB (re 1 μPa), with the Eheim pump active. In all of the experiments, and in the holding tank, the ambient water was kept at a temperature of 18 °C and a salinity of 34 psu. When not under experimental protocols, the prawns were provided with 14 h of light per day from a fluorescent tube controlled by a mains timer switch. Prior to any experimentation the prawns were divided by size into three populations, and fed on a granulated feed at a daily rate of 6 g for the large prawns, 4 g for the medium and 2.5 g for the small.

2.1. Preparation methodology for general dissection and electron microscopy

The pathway taken by the innervating nerves of the statocyst to the supraesophageal ganglion or brain was revealed by the anatomical investigation of a 54-mm *P. serratus*. The prawn was first immersed in 70% ethanol for 18 h, to "fix" the specimen prior to the investigation. Exposure of the brain and statocyst was achieved by the dissection and removal of the dorsal–rostral section of carapace, the dorsal cuticle layer of the peduncle, the left eye and the stomach.

Specimens of *P. serratus* selected for EM examination were denied access to materials that could be used as otoliths, primarily by having no substrate present in the tank. Additionally, uneaten feed and other waste products were removed by ensuring that the return flow of water to the filtration system was strongest at the base of the tank. Particulate matter was drawn by the flow of water through a 5-mm gap under each of the tank divisions, through which the prawns could not pass. The denial treatment was applied to all 100 of the prawns, with the exception of Fig. 4 which was prepared for EM examination within 48 h of capture. Moulting was induced in the remaining specimens over a 24-h period using a method that involved not changing the ambient tank water for 7 days, followed by a sudden change of all the water.

The statocyst capsules were removed by dissection from 12 of the specimens, and placed in a conical dish containing 2.5 mL of 0.9% sodium chloride. The capsules were opened by making a lateral incision around the statocyst chamber using a fine scalpel. Needlepoint tweezers were used to lift the upper section of the capsule, thus exposing the sand granules and ultrastructure. The sodium chloride solution was removed using a pipette and replaced with a solution of 2.5% *S*-Carboxymethyl-L-Cysteine in sodium chloride, which was used to hydrolyse the mucus surrounding the statocyst receptors. The contents of the dish were gently agitated for 2 min, after which the solution was removed and replaced with chilled fixative (2.5% glutaraldehyde in 0.1 M cacodylate buffer with 3.5% sodium chloride). The statocyst capsules were then dehydrated through a graded ethanol series ranging from 35% through 50%, 70% and 90% to absolute ethanol, prior to desiccation using the critical point drying method described by Platt (1977). Fully desiccated statocyst capsules were subsequently mounted on a specimen stub using a carbon tab, and coated with c. 8 nm of gold in an Emitech K 550 sputter coater (working at approximately 5×10^{-6} torr). Finally, the processed specimens were investigated and photographed using a JEOL JSM 5600 scanning electron microscope operated at 15 kV, and a 15-mm working distance. Images of the ultrastructure were captured using the JEOL software, which saved the micrographs in a bitmap format. All measurements were carried out on a PC using the analySIS® (Soft Imaging System) program. The hair cell dimensions were measured using polygon length, and measurements were recorded in micrometers (μm). Measurements of hair cell dimensions (height, width, etc.) are averages taken from at least 12 observations of a feature within a similarly orientated cluster of cells, with the exception of those in Fig. 4 which were taken from five observations.

2.2. ABR methodology

In order to concisely answer the question of hearing by crustaceans, 12 prawns were stimulated with sound ranging in the frequency domain between 100 and 3000 Hz, presented at sound pressure levels from 132 dB (re 1 μPa at 1 m) to below 90 dB (re 1 μPa at 1 m). The response of the prawn to acoustic stimulation was measured using a well-established audiometry technique, with the results expressed as an audiogram or limen of sound spectral sensitivity. The ABR measurements of hearing threshold were made using a proprietary control and analysis programme, written in a LabView 7 environment. This programme both generated the stimulus signals and captured and analysed the response, and was installed onto the PC shown in Fig. 1a. The stimulus used was a sine train (sine wave pulse) which was presented to *P. serratus* at a given frequency and sound pressure level, not exceeding 130 dB (re 1 μPa at 1 m) for each of the frequencies tested. For ABR recordings to be clear, it requires that short duration tone bursts are used, especially for the low frequencies. Kenyon et al. (1998) used a two-cycle burst for frequencies between 100 and 300 Hz, a five-cycle burst with a two-cycle attack decay for frequencies between 400 and 3000 Hz. Amplification of the sound was achieved using a Pioneer type SA-420 amplifier and a 200-mm Eagle L032 loudspeaker with a frequency response range of 40–18,000 Hz. Additionally, the loudspeaker was placed inside a Faraday cage and connected to a centralised earth point located in an adjacent room where the PC, amplification and analysis equipment was set up. Connecting wires were fed through a 100-mm port in the partitioning wall.

The procedure used to acquire the acoustically evoked potentials was approved by the United Kingdom Home Office 11.03.03. The test subjects were placed into a flexible cradle formed from a soft nylon mesh rectangle saturated with seawater. Oxygenated water kept at a temperature of 18 °C was gravity fed at an adjustable flow rate of 3 mL/s and directed toward the gills. The water was held in an aerated reservoir positioned in an adjacent room, and fed to the prawn through a 4-mm-diameter plastic tube. The prawn was first placed lengthwise and centrally on an 80×60 mm rectangle of fine nylon netting, which was wrapped firmly around the cephalothorax and pleon, and the two sides of the net were held together using the clip shown in Fig. 1b.

The clip was placed in a retort stand clamp fitted with ball joint electrode manipulator arms, and the aerated water pipe (detailed in Fig. 1b). During the procedure to position the electrodes detailed in Fig. 2, the specimen and clamp were suspended over a plastic tray, and aerated water was supplied to the prawn. A retort stand and the experimental tank (L 450 mm×W 300 mm×D 200 mm) were placed on a

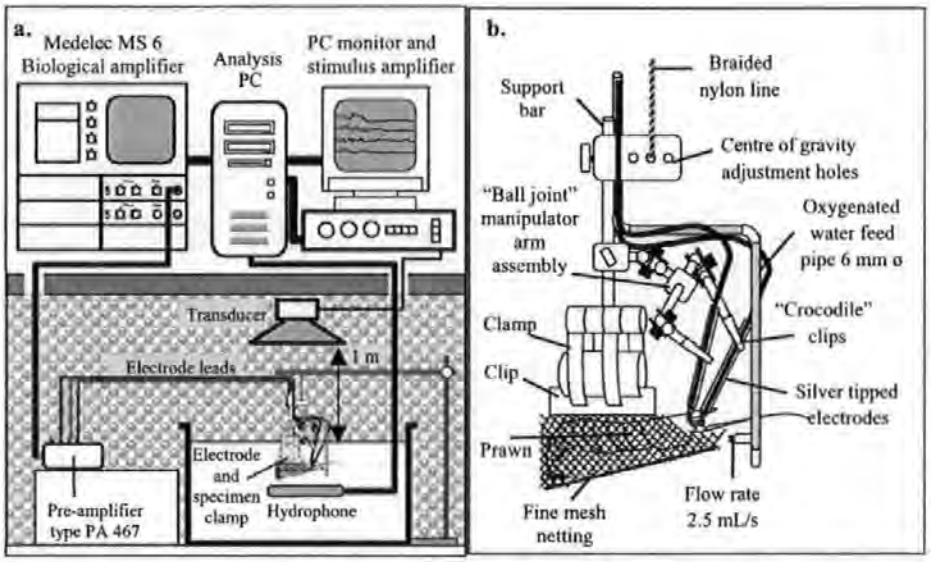

Fig. 1. (a) Schematic of the ABR audiometry system, and (b) the clamp used to hold the prawn in position, and manipulate the electrodes during the audiological tests.

table with vibration inhibiting properties, located in an underground anechoic chamber L 3 m×W 2 m×H 2 m. Working under a MEIJI binocular microscope, two small holes were made in the cuticle layer using a lancet, penetrating the carapace to a maximum depth of 0.3 mm. The reference electrode was located behind the supra-orbital spine, close to the neuropil of the antennule, and the record electrode was located in the peduncle close to the statocyst, at the junction between the lateral antennular and otic ganglia. The clamp assembly with the specimen and sited electrodes were then suspended from the retort stand positioned over the experimental tank, and the prawn stationed 5 mm below the surface of the water. After the hearing assessment, the prawns were relocated to a holding tank for observation, prior to being returned to the divided aquarium.

The electrophysiological response of the prawn to acoustic stimulation was recorded using the two subcutaneous electrodes (Fig. 2), which were connected to the MS6 preamplifier by 1 m lengths of screened coaxial cable with an external diameter of 1.5 mm. The outer insulating layer of the coax was removed 15 mm from the end where the electrode tip was to be fixed, and the screening layer removed 10 mm from the cable end. The inner insulating material was then trimmed by 2 mm, and the exposed inner wire (0.5 mm diameter) was tinned with silver solder and joined to a 10-mm-long silver wire (0.25 mm diameter), tapered to a fine point. The assemblage was pushed through a 100-mm glass pipette with an internal diameter of 4 mm, until 0.4 mm of the gold wire was exposed. The remaining space inside the pipette was filled with a clear epoxy resin, and then trimmed to expose 0.3 mm of silver tip through which the AEP could be conducted. The impedance of the electrodes, both between the outer shielding and inner core, and the silver tip and MS 6, were tested using an M 205 precision digital multimeter. The impedance between the tip and pre-amplifier was found to be 0.2 Ω for both electrodes, and an open circuit was recorded between the outer shielding and inner core. The evoked response was amplified and digitised to 12 bits resolution and recorded. This process was repeated 2000 times and the response averaged to remove electrical interference caused by neural activities other than audition, and the myogenic noise generated by muscular activity. Each measurement was repeated twice; this aids in separating the evoked response, which is the same from trace to trace, from the myogenic noise, which varies in two successive measurements. After the averaging process, the evoked potential could be detected, following the stimulus by a short latency period of 5 ms or so. The latency is accounted for by the time it takes the sound in air to travel the 1 m to the prawn, plus 1–2 ms response latency.

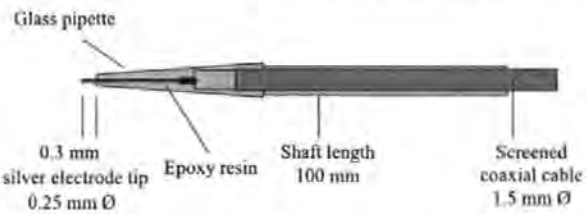

Fig. 2. Schematic of the electrodes used to record the evoked potentials.

2.3. The sound field

The properties of the sound field are especially relevant when comparing the audio capabilities of both pressure-sensitive and motion-sensitive fish in the near field. In a small laboratory set-up, the complexities associated with independently measuring sound pressure and particle motion are compounded by the reflectivity of the tank sides and base. For this reason, a number of experiments have used air-mounted transducers to successfully generate sounds under-

water (e.g., Fay and Popper, 1975; Yan et al., 2000; Akamatsu et al., 2002). The principal advantage of such a system is that as the sound source is located at a distance of 1 m from the air/water interface, the moving part of the transducer does not contact the water and generates near-field displacements. In this situation, the pressure and motion of the water adjacent to the fish ear can be considered as being equal (Hawkins, 1981). The stimulus tones presented from the loudspeaker to the prawn were calibrated using an insertion calibration. A calibrated Bruel and Kjaer Type 8106 Hydrophone (Serial Number 2256725) was placed in the tank and positioned adjacent to the shrimp cephalothorax region. The signal from the hydrophone was amplified using a PE6 preamplifier and digitised using a National Instruments DAQ-6062e interface card at a sample rate of 300 kS/s. In case of non-proportionality of the response of the loudspeaker, measurements of the sound pressure were taken for each amplitude and frequency setting used. Consequently, a total of 110 individual calibration measurements were taken in the calibration process. These calibrated levels were then applied to the threshold defined by ABR measurement to provide calibrated audiograms with pressure levels traceable to International Standards.

2.4. Ablation

Specimens of *P. serratus* selected for the ablation procedure were first tested for an electrophysiological response to a 500-Hz sound presented at 110 dB (re 1 μPa at 1 m). Removal of the statocyst was achieved by making a circular cut in the cuticle layer above the chamber, and withdrawing the capsule using needle point tweezers (a procedure that took a few seconds). A sham operation was also performed, and the prawns were retested 1 h after cutting around the chamber, prior to removal of the statocyst. The prawns were then placed into an empty compartment of the holding tank and allowed to recover for 24 h, prior to being retested on the electrophysiology apparatus. The post ablation recovery period was included to give the prawn's time to settle after the procedure, as the metabolic state of the organism can have a detrimental affect on the evoked potential (Corwin et al., 1982).

3. Results

3.1. Innervation of the statocyst

In decapod crustaceans, the lateral antenular and otic nerves extend with bi-lateral symmetry from the neuropil of the antennule; a region located centrally in the brain (Prentiss, 1901), to the statocyst and tactile bristles of the antennules. The brain of *P. serratus* lies close to the rostral extremities of the carapace, ventral to the eyestalks and posterior to the antennules. On leaving the anterior region of the brain (detailed in Fig. 3a and b), the lateral antennular (*gla.*) and otic ganglia (*go.*) project forward, and enter the antennule close to the inside edge of the peduncle. From there, the otic ganglia branches outward away from the main antennular nerve, which continues to project forward to the tactile receptors.

3.2. Scanning electron microscopy

The examination of the complete statocyst (prior to removal of the sand granules) revealed ultrastructural cell

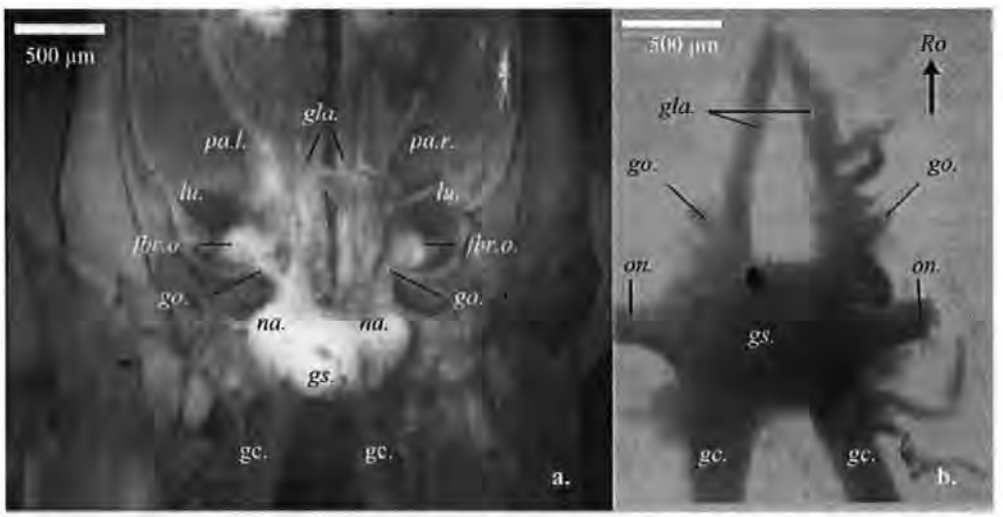

Fig. 3. (a) Dorsal view of the supraesophageal ganglion and lateral antennular and otic ganglia from *P. serratus* (with the statocyst capsules and optic neuropil removed). *fbr.o.* peripheral otic nerve fibres, *gc.* commissural ganglion, *gla.* lateral antennular ganglion, *na.* neuropil of the antennule, *gs.* supraesophageal ganglion, *go.* otic ganglion, *lu.* lumen of the statocyst, *pa.r,l.* peduncle of the right and left antennule. (b) Dorsal view of the brain and major nerve ganglia dissected from *P. serratus*. *gs.* supraesophageal ganglion, *gla.* lateral antennular ganglion, *go.* otic ganglion, *on.* optic nerve, *gc.* commissural ganglion. *Ro.* Rostral direction.

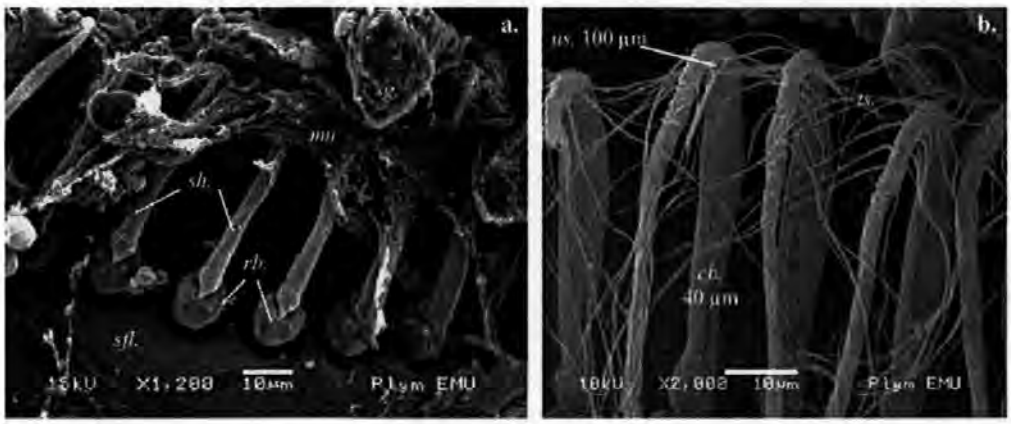

Fig. 4. (a) Receptor cell projections contacting sand granules in the statocyst of *P. serratus*. *mu.* mucus, *rb.* receptor base, *sfl.* statocyst floor, *sg.* sand granule, *sh.* hair cell shaft. (b) The 40 µm lower cell body (*cb.*), the 100 µm upper tapering sections (*us.*) and thread like strands (*ts.*) found enmeshed with the sand granules, orientated toward a central point. *cb.* cell body.

projections extending into the mass of sand granules shown in Fig. 4a. The cells project from small apertures in the statocyst floor about 7 µm in diameter; through which the receptor connects to the peripheral fibres of the otic ganglion. At a distance of 2 µm from the base, the cell widens and forms a bulb (*rb.* in Fig. 4a) which has a diameter of 9 µm at its widest point, and displays a series of longitudinal ridges that run around the bulbous structure. The uppermost portion of the cell base narrows to 0.8 µm, forming a fulcrum point from where a 3.5-µm-diameter hair shaft extends 40 µm into the lumen of the statocyst, and contacts with the sand granules (*sg.*). The overall view of the receptor array and the tips of the cells are precluded from view by the sand and a fine structure, consisting mostly of residuals left by the desiccation process of a gelatinous mucus (*mu.*) that in life surrounds the sand and cell tip. The view of the statocyst ultrastructure (without sand granules attached) in Fig. 4b (taken perpendicular to the horizontal plane) shows the hair cell array from a specimen of *P. serratus* denied sand for 7 days post moulting.

The absence of sand granules reveals more than 70 vertical cell projections arranged in a row shaped like a crescent, covering 0.073 mm^2 of statocyst (Fig. 5b). Each hair cell is orientated toward a common central region (*cr*), and the shortest hairs (<120 µm) were found proliferating in a band running down the left side of the array, whilst the longest hairs (>170 µm) were found in the right caudal quadrant. The statocyst capsule is elliptical in shape, and the walls (Fig. 5b) symmetrically curve inward toward the base, where the receptor cells are located on a mound rising 40 µm from the floor of the capsule. From the crest of the mound, the receptor hairs project upward into the lumen of the statocyst at angles between 27° and 74° from the horizontal plane. Behind the hair cells, in the space between opposing receptors, the mound flattens and forms a plateau (*pl*), which is void of any ultrastructure.

3.3. Transmission electron microscopy

The TEM section in Fig. 6a shows a cross section through the hair cell base and structures present in the

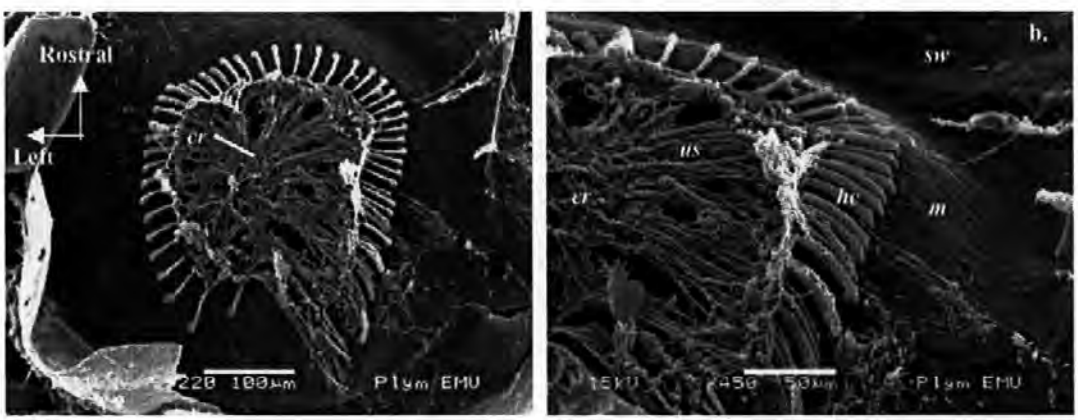

Fig. 5. (a) Dorsal view of the statocyst from a 55-mm prawn denied sand for 7 days post moulting. *cr.* central region. (b) Lateral view of the statocyst. *cr.* central region, *hc.* hair cell, *m.* mound, *sw.* statocyst wall, *us.* upper tapering section of hair cell.

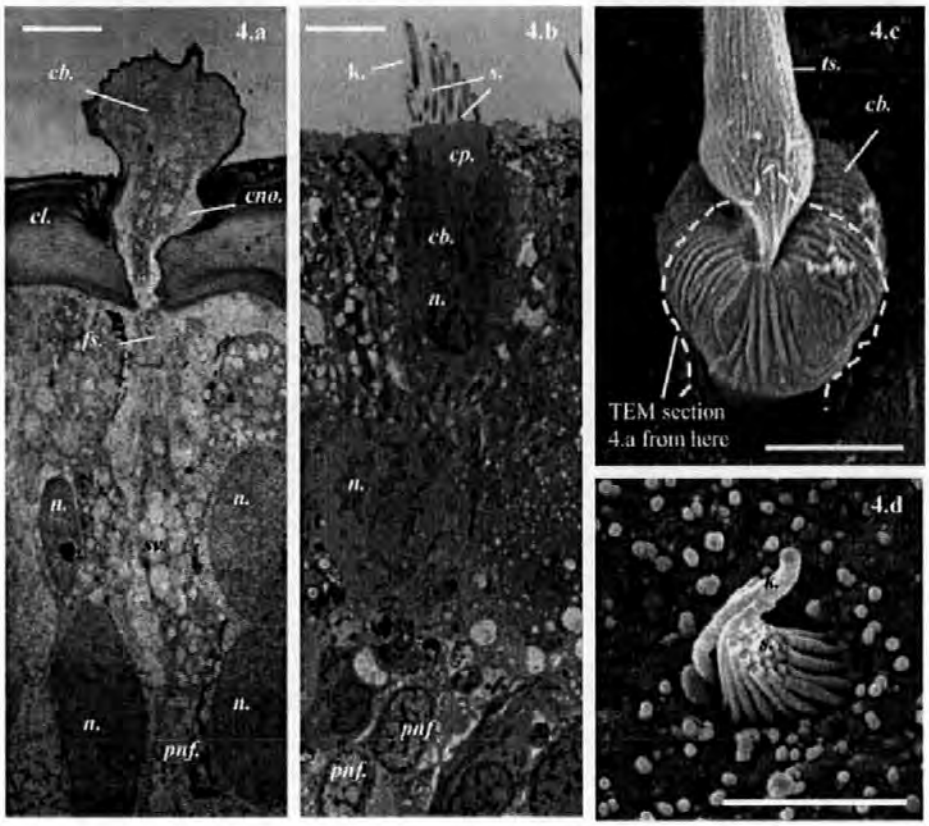

Fig. 6. (a) TEM micrograph of the hair cell base from the statocyst of *P. serratus*, *fs.* fibrous strands, *cl.* cuticle layer, *cno.* cuticular notch, *n.* nuclei, *pnf.* peripheral nerve fibre, *sv.* synaptic vesicles. (b) Saccular hair cell and innervating nerve fibres from the ear of *D. labrax* (from Lovell et al., in preparation), *cb.* cell body, *cp.* cuticular plate, *k.* kinocilia, *n.* nucleus, *pnf.* peripheral nerve fibres, *s.* stereocilia. (c) SEM micrograph of the statocyst hair cell from *P. serratus*, *cb.* cell base *ts.* tapering section. (d) SEM micrograph of the ciliary bundles projecting from the epithelial surface of *D. labrax* (From Lovell et al., in preparation), *k.* kinocilia, *s.* stereocilia. Bars=5 μm.

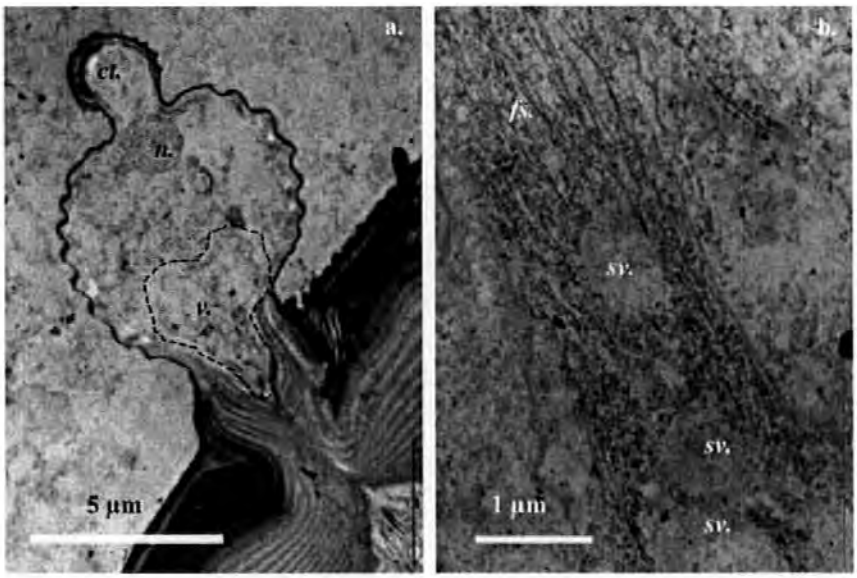

Fig. 7. (a) TEM section through the cell base from *P. serratus*, showing the cell nucleus (*n.*), and the beginning of the angled cell tip (*ct.*), and vesicles (*v.*) which appear to be associated with the fibrous strands (hatched area). (b) Fibrous strands (*fs.*) of the cell root, and the synaptic vesicles (*sv.*) located in the peripheral nerve bed.

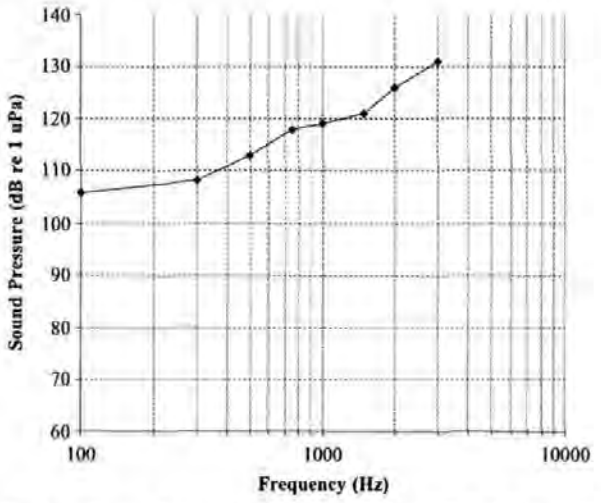

Fig. 8. Audiogram for *P. serratus*, determined visually from the sequential ABR waveform data, and by calculating the RMS of threshold SPL values of the stimulus sounds, presented at 100, 300, 500 750, 1000, 1500, 2000 and 3000 Hz tone bursts.

peripheral nerve bed, from the statocyst of *P. serratus*. Fig. 6b shows a cross section through a hair cell from the saccule of the European sea bass (*Dicentrarchus labrax*), which has been included in this section along with the SEM of the hair cell (Fig. 6d) for comparative purposes. The two hatched lines drawn on the prawn hair cell SEM micrograph presented in Fig. 6c shows the locations from where the statocyst TEM sections in Fig. 6a was taken.

The "root" of the statocyst hair cell is buttressed by supporting cells with large nuclei (*n.*), and fibrous strands (*fs.*) resembling actin filaments, which can be seen extending into the peripheral nerve bed through the cuticular plate. The filaments may help anchor the hair cell into position, and work in conjunction with a small notch in the cuticle layer (*cno.*) containing part of the lower cell body. The filament strands terminate 15 μm below the cuticle layer, in a region containing rounded structures less than 0.75 μm in diameter, which are thought to be the synaptic vesicles between the hair cell and the peripheral otic nerve fibres (*pnf.*). Close examination of the TEM section through the statocyst hair cell body (Fig. 7a) reveals that it contains a single nucleus (*n.*) positioned at the top of the cell. The hatched line in the basal region of the cell marks the perimeter of two vesicles, which appear to be associated with the fibres in the cell root. Fig. 7b shows the fibrous strands as they terminate in the synaptic vesicles (*sv.*) located 15 μm below the cell base.

3.4. Electrophysiological response to auditory stimuli

In order to concisely answer the question of hearing by crustaceans, 12 prawns of mixed sex were stimulated with sound ranging in the frequency domain between 100 and 3000 Hz, presented at sound pressure levels from 130 dB (re 1 μPa at 1 m) to below 90 dB (re 1 μPa at 1 m). The ABR recording technique has been successfully applied in the auditory assessments of both mammalian and non-mammalian vertebrates. An ABR waveform is acquired by averaging conglomerate responses of peak potentials, arising from nuclei in the auditory pathway during acoustic stimulation. The AEPs presented in Fig. 7 were recorded using the Medelec MS 6 biological amplifier with subcutaneous electrodes positioned using a jointed clamp assembly, and the prawn held in place using a fine mesh nylon cradle. The reference electrode was located in proximity to the neuropil of the antennule, and the record electrode located at the junction between the lateral antennular and otic ganglia. The acoustically evoked neural waveforms presented in Fig. 7, were recorded from *P. serratus* in response to tone bursts ranging in frequency from 500 to 3000 Hz, and averaged over 2000 stimulus presentations (100 and 300 Hz have not been included for scaling reasons). The waveforms show a series of peaks contiguous with the stimulus sound.

3.4.1. Threshold determination

Threshold responses from twelve 50–55 mm (medium) prawns were determined visually from the sequentially arranged waveforms for each frequency tested, in accordance with Kenyon et al. (1998). Fig. 6 shows ABR waveforms evoked from *P. serratus* in response to a 500-Hz tone burst, presented initially at between 120 and 132 dB (re 1 μPa at 1 m), and attenuated in steps of 4 dB (re 1 μPa at 1 m) ordinarily, and 2 dB (re 1 μPa at 1 m) as the hearing threshold was approached. When two replicates of waveforms showed opposite polarities (see 110 dB traces in Fig. 6), the response was considered as being below threshold (cf. Kenyon et al., 1998).

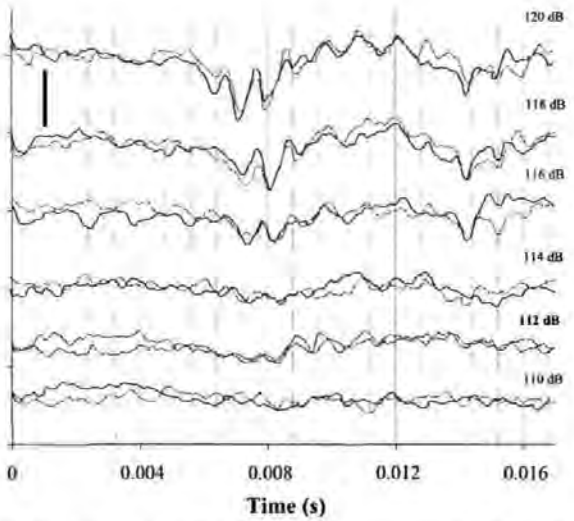

Fig. 9. ABR waveforms from *P. serratus* in response to a 500-Hz tone burst attenuated in 2-dB steps. Averaged traces of two runs (2000 sweeps each), for each intensity are overlaid and arranged sequentially. Bar=1 μv.

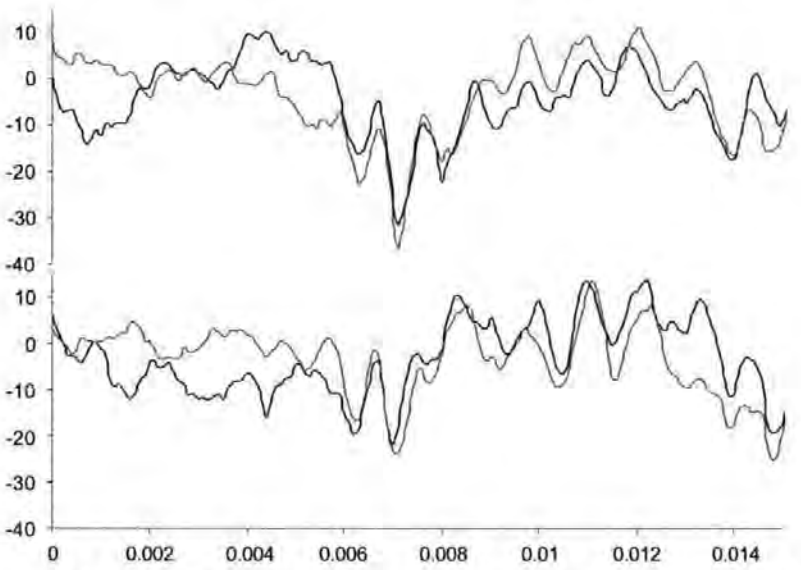

Fig. 10. ABR waveforms in response to a 500-Hz sound presented 10 dB (re 1 μPa at 1 m) above threshold. Run A was recorded prior to the sham operation, and run B was recorded 1 h after cutting the cuticle layer covering the statocyst capsule as a sham operation. *Y* axis scale=μv×100.

3.4.2. *Audiogram for P. serratus*

The audiogram shown in Fig. 8 was produced using sequential ABR waveform threshold data, acquired from frequencies of 100–3000 Hz, presented in steps between 200 and 500 Hz. The hearing thresholds of 12 mixed-sex *P. serratus* was measured, and follows a ramp like profile, determined by calculating the lowest intensity stimulus sounds (recorded underwater using the hydrophone located

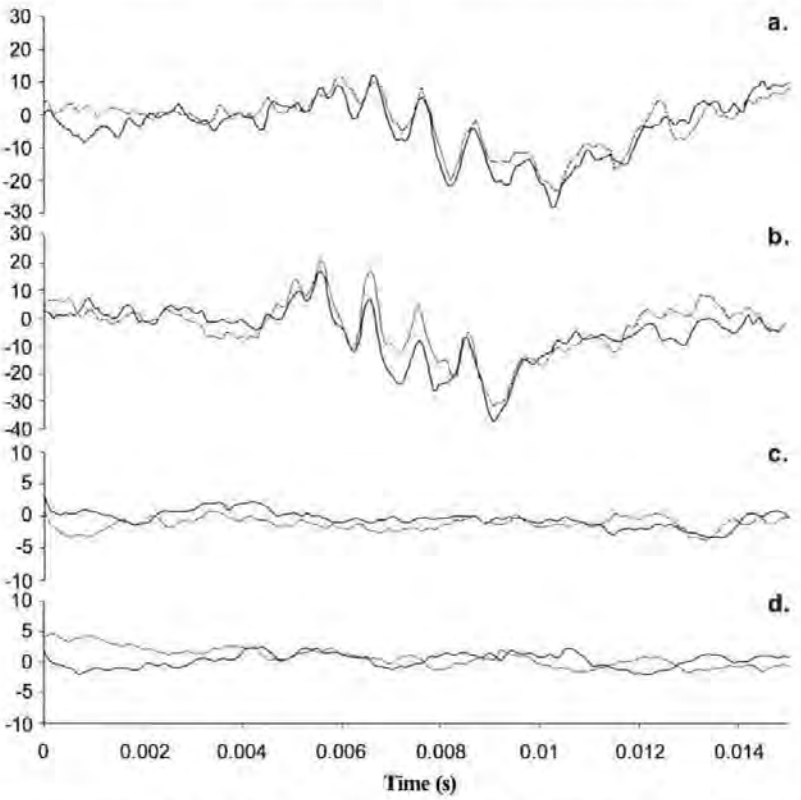

Fig. 11. Evoked potentials from *P. serratus* to a 500-Hz tone presented 10 dB above threshold and averaged over 2000 sweeps. Runs a and b were recorded with the statocyst present, after cutting round the cuticle layer; whilst c and d were recorded 24 h after removal of the organ (the electrodes were removed and replaced between each run). *Y* axis scale=μv×100.

adjacent to the antennule) that evoked a repeatable ABR response (112 dB in Fig. 9). The profile follows a steady downward gradient to 100 Hz (the lowest frequency tested), and indicates that the "best" frequency in terms of threshold could be below this frequency.

3.5. Ablation

Removal of the statocyst was achieved by making a circular cut in the cuticle layer above the chamber, and withdrawing the capsule using needle point tweezers (a procedure that took a few seconds). Prior to removal of the statocyst, the prawn was retested with the cuticle layer cut as a sham operation. This procedure revealed that the AEP was no longer present, and was probably due to an imbalance in the hydrostatic pressure inside the antennule. The sham operation data presented in Fig. 10 were acquired by retesting the prawns 1 h after cutting around the chamber, prior to removal of the statocyst, and shows that the AEP eventually returns.

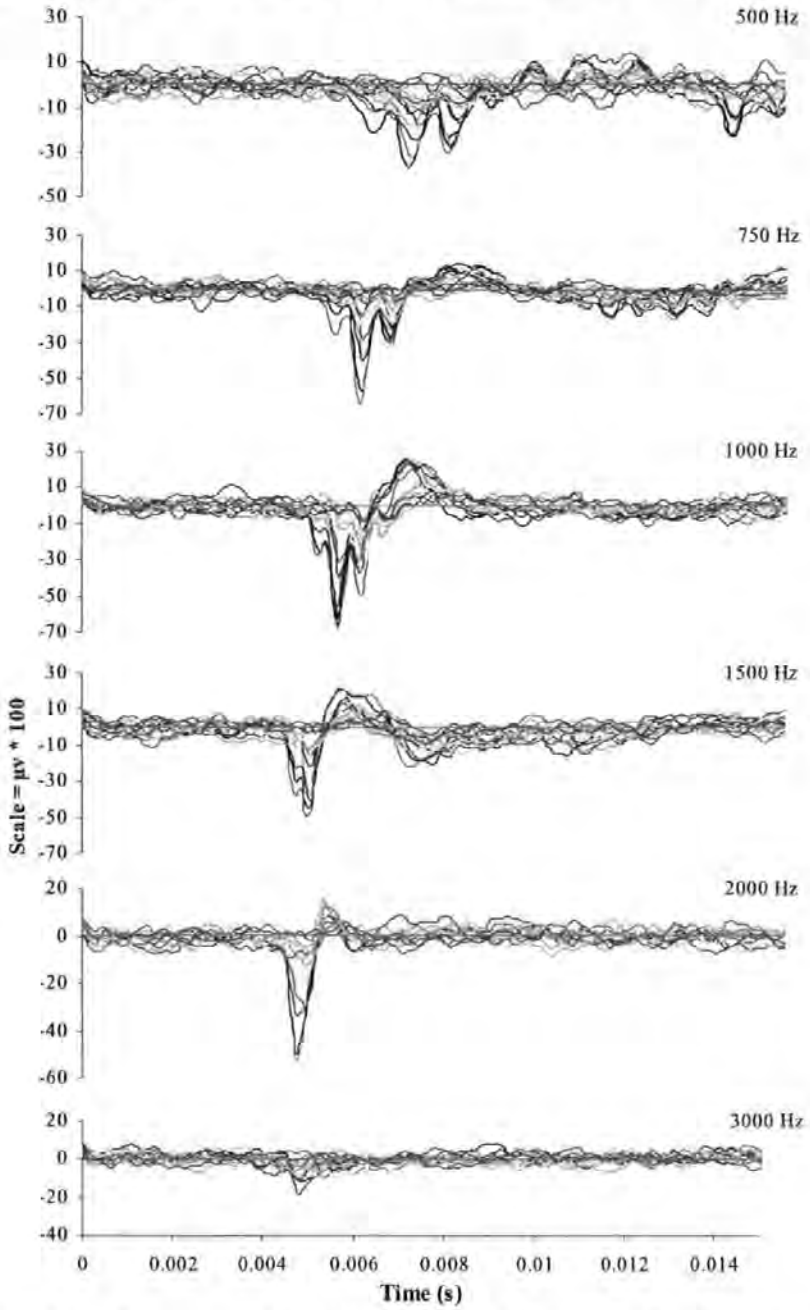

Fig. 12. Auditory evoked potentials from *P. serratus* to tone bursts of 500, 750, 1000, 1500, 2000 and 3000 Hz, and averaged over 2000 sweeps. The AEP at each amplitude tested has been overlaid, and shows a reduction in the response latency with increasing frequency. Scale=µv×100.

On removal of the statocyst, the prawns were placed in the empty fourth compartment of the holding tank, and allowed to recover for 24 h, prior to being retested on the electrophysiology apparatus. The post ablation recovery period was included to give the prawn's time to settle after the procedure, as the metabolic state of the organism can have a detrimental affect on the evoked potential (Corwin et al., 1982). Additionally, the recovery period was included to allow for the equalisation of the hydrostatic pressure within the antennule. The evoked potentials shown in Fig. 11 were recorded from a 45-mm prawn, in response to a 300-Hz tone, presented at an intensity 10 dB above threshold. The first two runs (A and B, with two replicates of each run) were acquired from the prawn prior to the ablation procedure, and the subsequent two runs (C and D, with two replicates of each run) were recorded 24 h later. The electrodes were removed and replaced between each run, to confirm that the response was consistently repeatable, and to ensure that the absent responses in runs C and D was due to the ablation experiment, and not an extraneous factor associated with electrode placement.

4. Discussion

The hearing ability of the prawn (*P. serratus*) has been clearly demonstrated by this work using ABR audiometry, and offers conclusive evidence of low-frequency sound detection of frequencies ranging from 100 to 3000 Hz by an invertebrate from the sub-phylum crustacea. For hearing in the strictest sense to be attributed to an organism, the physiological response sound should be initiated by a specialised receptor mechanism (Myrberg, 1981), shown by this work to be generated in the statocyst. Current literature states that this organ is purely responsive to angular rotations and strong vibrations propagated directly through a solid medium, and is not responsive to sounds propagated in either air or water (Cohen and Dijkgraaf, 1961). It is highly probable that Cohen and Dijkgraaf did not find evidence of hearing due to masking of the AEP by neural activities other than audition; and from myogenic noise generated by muscular activity. To produce clear waveforms of an auditory response, it is recommended that AEP recordings be averaged for at least 1000–2000 stimulus presentations (Kenyon et al., 1998; Yan et al., 2000). The amplitude and shape of the electrophysiological response from *P. serratus* shown in Figs. 9 and 12 bear a remarkable similarity to AEPs generated by fish and higher vertebrates (see Corwin et al., 1982; Kenyon et al., 1998; Yan, 2002).

The two statocyst organs found in *P. serratus* lie adjacent to one another with medial symmetry, in the basal peduncle segment of the antennule. As can be seen in Figs. 4 and 5a, the statocyst is innervated by the otic ganglion, which emanates from a bed of peripheral nerve fibres lying under the mound directly beneath the receptor array (see Fig. 6a). The otic nerve terminates in the neuropil of the antennule, which is located in the ventral/anterior region of the brain. The dissection of the 54-mm prawn in Fig. 3a shows that the total length of the neuronal pathway taken by the otic nerve, from the centre of the statocyst organ to the centre of the supraesophageal ganglion, is approximately 600 μm. However, the direct distance between the neuropil and the peripheral nerve fibres located below the statocyst, was found to be 500 μm. This is due to the curved pathway taken by the otic nerve, which first projects forward with the lateral antennular ganglion along the inside edge of the peduncle for 300 μm. From here, the otic ganglion branches away from the antennular ganglion at angles approaching 45° either side of the midline, from where it extends for a further 300 μm to the centre of the peripheral otic nerve bed. The schematic in Fig. 13 summarises the physiological work and shows the hair cells and the sand granule otoliths, along with the pathway taken by the otic ganglion, to the neuropil of the antennule and supraesophageal ganglion.

It is clear by the evidence presented in this work that the perception of sound in the frequency domain by *P. serratus* is similar in range to hearing in generalist fish, which is capable of both hearing and responding to sounds within a frequency bandwidth of 30 Hz to around 2000 Hz (Bretschneider et al., 2001), and is reliant on the phase variance between the three otolithic organs and the surrounding flesh to stimulate the sensory hairs of the inner ear (Lu, 2004). The audiogram presented in Fig. 8 follows a similar ramp like profile to those obtained from the cichlid *A. ocellatus*, which is considered to detect a best frequency of 100 Hz (Kenyon et al., 1998); however, lower frequencies were not tested. We therefore conclude that at least one species from the invertebrate sub-phylum of crustacea, is sensitive to the motion of water particles displaced by low-frequency sounds ranging from 100 Hz up to 3000 Hz. Although a number of physiological and behavioural experiments have been conducted on fish to assess the impact of noise on the auditory system none have, so far,

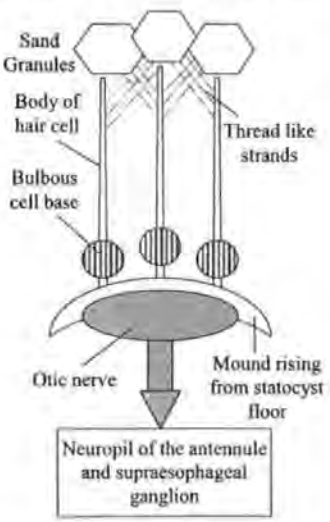

Fig. 13. Schematic of the statocyst receptor array and nerve pathway to the supraesophageal ganglion from *P. serratus*.

been directed toward the crustaceans, a major link in the oceanic food chain. The long-term effects of intense low-frequency sounds on the shrimp hearing ability and ecology is not known, but the data presented here shows that there is a need to include crustaceans in such an assessment, in order to gain a more insightful perspective of the effect of intense noise in the marine ecosystem.

Acknowledgements

The authors would like to thank John Langworthy for the development of the ABR software, and Glen Harper of the Plymouth EMU for his invaluable help with the TEM sectioning.

References

Akamatsu, T., Okumura, T., Novarini, N., Yan, H.Y., 2002. Empirical refinements applicable to the recording of fish sounds in small tanks. J. Acoust. Soc. Am. 112, 3073–3082.

Bettencourt, V., Guerra, A., 2000. Growth increments and biomineralization process in cephalopod statoliths. J. Exp. Mar. Bio. Eco. 248, 191–205.

Bretschneider, F., van den Berg, A.V., Peters, R.C., 2001. In: Kapoor, B.G., Hara, T.J. (Eds.), Sensory Biology of Jawed Fishes. Science Publishers, Enfield, NH, USA. ISBN: 1-57808-099-1.

Cohen, M.J., Dijkgraaf, S., 1961. In: Waterman, T.H. (Ed.), The Physiology of Crustacea, vol. II. Academic Press, New York, pp. 65–108.

Corwin, J.T., Bullock, T.H., Schweitzer, J., 1982. The auditory brainstem response in 5 vertebrate classes. Electroencephalogr. Clin. Neurophysiol. 54, 629–641.

Costa, D.P., Crocker, D.E., Gedamke, J., Webb, P.M., Houser, D.S., Blackwell, S.B., Waples, D., Hayes, S.A., Le Boeuf, B.J., 2003. The effect of a low-frequency sound source (acoustic thermometry of the ocean climate) on the diving behavior of juvenile northern elephant seals, *Mirounga angustirostris*. J. Acoust. Soc. Am. 113, 1155–1165.

Dalen, J., Knutsen, G.M., 1987. Scaring effects on fish and harmful effects on eggs, larvae and fry by offshore seismic exploration. In: Merklinger, H.M. (Ed.), Progress in Underwater Acoustics. Plenum Publishing Corp, pp. 93–102.

Dilly, P.N., Stevens, P.R., Young, J.Z., 1975. Receptors in the statocysts of squid. J. Physiol. 249, 59–61.

Engås, A., Løkkeborg, S., Ona, E., Soldal, A.V., 1996. Effects of seismic shooting on local abundance and catch rates of cod (*Gadus morhua*) and haddock (*Melanogrammus aeglefinus*). Can. J. Fish Aquat. Sci. 53, 2238–2249.

Farre, A., 1843. On the organ of hearing in crustacean. Philos. Trans. 133, 233–242.

Fay, R.R., Popper, A.N., 1975. Modes of stimulation of the teleost ear. J. Exp. Biol. 62, 370–387.

Finley, L., Macmillan, D., 2000. The structure and growth of the statocyst in the Australian crayfish *Cherax destructor*. Biol. Bull. 199, 251–256.

Hawkins, A.D., 1981. The hearing abilities of fish. In: Tavolga, W.N., Popper, A.N., Fay, R.R. (Eds.), Hearing and Sound Communication in Fishes. Springer, Berlin.

Hedwig, B., Poulet, J.F.A., 2004. Complex auditory behaviour emerges from simple reactive steering. Nature 430, 781–785.

Huber, F., Thorson, J., 1985. Cricket auditory communication. Sci. Am. 253, 60–68.

Kenyon, T.N., Ladich, F., Yan, H.Y., 1998. A comparative study of hearing ability in fishes: the auditory brainstem response approach. J. Comp. Physiol., A Sens. Neural Behav. Physiol. 182, 307–318.

Lokkeborg, S., Soldal, A.V., 1993. The influence of seismic exploration with airguns on cod (*Gadus morhua*) behaviour and catch rates. ICES Mar. Sci. Symp. 196, 62–67.

Lu, Z., 2004. Neural mechanisms of hearing in fish. In: von der Emde, G., Mogdans, J., Kapoor, B.G. (Eds.), The Senses of Fishes: Adaptations for the Reception of Natural Stimuli. Narosa Publishing House, New Delhi, India.

Meyer-Rochow, V.B., Penrose, J.D., Oldfield, B.P., Baily, W.J., 1982. Phonoreception in the rock lobster *Panulirus longipes*. Behav. Neural Biol. 34, 331–336.

Myrberg, A.A., 1981. Sound communication and interception in fishes. In: Tovolga, W.N., Popper, A.N., Fay, R.R. (Eds.), Hearing and Sound Communication in Fishes. Springer, Berlin.

Northrup, J., 1974. Detection of low-frequency underwater sounds from a submarine volcano in the western Pacific. J. Acoust. Soc. Am. 56, 837–841.

Overbeck, G.W., Church, M.W., 1992. Effects of tone burst frequency and intensity on the auditory brainstem response (ABR) from albino and pigmented rats. Hear. Res. 59, 129–137.

Patek, S.N., 2001. Spiny lobsters stick and slip to make sound. Nature 411, 153.

Patton, M.L., Gove, R.F., 1992. The response of statocyst receptors of the lobster *Homarus americanus* to movements of statolith hairs. Comp. Biochem. Physiol., A 101, 249–257.

Pearson, W.H., Skalski, J.R., Malme, C.I., 1992. Effects of sounds from a geophysical survey device on behavior of captive rockfish (*Sebastes* spp). Can. J. Fish Aquat. Sci. 49, 1343–1356.

Pickett, G., Eaton, D., Seaby, R., Arnold, G., 1994. Results of Bass Tagging in Poole Bay During 1992. MAFF Laboratory Leaflet, vol. 74. Lowestoft.

Pilgrim, D.A., Lovell, J.M., 2002. A review of current publications dealing with the impact of low frequency sounds upon fish. Report to Devon Sea Fishing Association.

Platt, C., 1977. Hair cell distribution and orientation in goldfish otolith organs. J. Comp. Neurol. 172, 283.

Popper, A.N., Platt, C., 1983. Sensory surface of the saccule and lagena in the ears of ostariophysan fishes. J. Morphol. 176, 121–129.

Popper, A.N., Salmon, M., Horch, K.W., 2001. Acoustic detection and communication by decapod crustaceans. J. Comp. Physiol. 187, 83–89.

Prentiss, C.W., 1901. The otocyst of decapod crustacea: its structure, development and functions. Bull. Comp. Zoo 7, 167–251.

Richardson, W.J., Greene Jr., C.R., Malme, C.I., Thomson, D.H., 1995. Marine Mammals and Noise. Academic Press, San Diego, pp. 576.

Rose, R.D., Stokes, D.R., 1981. A crustacean statocyst with only three hairs: light and scanning electron microscopy. J. Morph. 169, 21–28.

Schildberger, K., Hörner, M., 1988. The function of auditory neurons in cricket phonotaxis. J. Comp. Physiol., A Sens. Neural Behav. Physiol. 163, 621–631.

Schmitz, B., Herberholz, J., 1998. Snapping behaviour in intraspecific agonistic encounters in the snapping shrimp (*Alpheus heterochaelis*). J. Biosci. 23, 623–632.

Schöne, H., 1971. Gravity receptors and gravity orientation in crustacea. In: Gordon, S.A., Cohen, M.J. (Eds.), Gravity and the Organism. University of Chicago Press, Chicago, pp. 223–235.

Sekiguchi, H., Terazawa, T., 1997. Statocyst of *Jasus edwardsii*, *pueruli* (crustacea, palinuridae), with a review of crustacean statocysts. Mar. Freshw. Res. 48, 715–719.

Whitlow, W., Au, W., Nachtigall, P., Pawloski, J., 1997. Acoutic effects of the ATOC signal (75 Hz, 195 dB) on dolphins and whales. J. Acoust. Soc., 101.

Yan, H.Y., 2002. The use of acoustically evoked potentials for the study of enhanced hearing in fishes. Bioacoustics 12, 325–328.

Yan, H.Y., Fine, M.L., Horn, N.S., Colon, W.E., 2000. Variability in the role of the gasbladder in fish audition. J. Comp. Physiol., A Sens. Neural Behav. Physiol. 186, 435–445.

Journal of Fish Biology (2005) **66**, 836–846
doi:10.1111/j.1095-8649.2005.00665.x, available online at http://www.blackwell-synergy.com

The polarization of inner ear ciliary bundles from a scorpaeniform fish

J. M. LOVELL*†, M. M. FINDLAY*, R. M. MOATE‡ AND D. A. PILGRIM*

**School of Earth, Ocean and Environmental Sciences and ‡Plymouth Electron Microscopy Centre, University of Plymouth, Drake Circus, Plymouth PL4 8AA, U.K.*

(Received 7 May 2004, Accepted 3 December 2004)

The polarization of ultrastructural ciliary bundles from hair cells in the inner ear of the sea scorpion *Taurulus bubalis* was studied using a scanning electron microscope, revealing arrays of ciliary bundles with diverse orientations on each of the sensory epithelia. Members of this order are known to produce sound, though results of this study show no significant variation from the standard receptor patterns found in the hearing system of many silent marine teleosts. This is the first time that the ultrastructure of *T. bubalis* has been studied, and this work presents a new set of polarization patterns, which provide anatomical information important in understanding electrophysiological aspects of fish hearing from an ecological perspective.

Key words: fish ear; hair cell; lagena; saccule; Scorpaeniformes; utricle;

INTRODUCTION

The fish inner ear is divided into two regions, the pars superior and the pars inferior (Retzius, 1881). The former responds primarily to movements of the body and postural changes, while the latter responds to both gravistatic and acoustic stimuli (Jenkins, 1981; Popper & Platt, 1993). The pars inferior comprises two fluid filled pouches, the saccule and lagena, with each pouch containing a crystalline calcium carbonate otolith (Carlström, 1963). Of these end organs, the saccule is considered to be the major auditory organ in most teleosts, although there is evidence of a functional overlap between all three otolith organs (Popper & Fay, 1993). For fishes to locate the source of a sound in both the horizontal and vertical planes, they rely on the stimulation of ciliary bundles oriented specifically along the sound propagation axis (Lu & Popper, 1998). It is known (Enger *et al.*, 1973; Hawkins & Sand, 1977; Fay, 1997) that the morphological polarities of sensory hair cells in the otolithic organs are fundamental to the directional hearing capabilities of fishes. In general, azimuths of peak sensitivity tend to lie parallel to the plane of the otolith and sensory epithelium (Enger *et al.*, 1973; Sand & Hawkins, 1973; Fay, 1997).

†Author to whom correspondence should be addressed. Tel.: +44 (0) 1752 232411; fax: +44 (0) 1752 232406; email: j.lovell@plymouth.ac.uk

Examination of the orientation of the ciliary bundles provides evidence of a correlation between the morphological polarization of receptor cells and the magnitude of an electrophysiological response to a sound (Popper & Fay, 1993). Excitation occurs when stereocilia are bent toward the kinocilium during the passage of a wave front, resulting in the cell becoming depolarized relative to its resting potential (Clegg & Mackean, 1994). Inhibition occurs when the bundle is deflected in the opposite direction, and results in the hyperpolarization of the cell (Platt & Popper, 1981). The magnitude of both excitation and inhibition are a cosine function of the angle between the direction of the stimulus and the direction at which sensitivity is greatest (Enger, 1965; Popper, 1983). The detection and localization of a sound source is of considerable biological importance to many fish species, and is often used to assess the suitability of a potential mate or during territorial displays (Nordeide & Kjellsby, 1999), and during predator prey interactions (Myrberg, 1981).

Jensen (1994) used a light microscope to reveal ciliary bundle orientations in the end organs of the upside-down catfish *Synodontis nigriventris* David, along with observations of innervating nerve distributions. Lu & Popper (1998) examined the polarization of ciliary bundles in the end organs of the sleeper goby *Dormitator latifrons* (Richardson) using immunocytochemicals and a confocal imaging technique. Several authors (Barber & Emerson, 1980; Popper, 1981; Yan *et al.*, 1991; unpubl. data), however, have used a scanning electron microscope (SEM) to study surface detail of the inner ear ultrastructure, and Tuset *et al.* (2003) used SEM to study otolith sculpture. This was the approach adopted in the present study for observing both the otolith and ultrastructure.

MATERIALS AND METHODS

The preparation methodology employed in this study was based on techniques used by Platt (1977). Six fresh sea scorpion *Taurulus bubalis* (Euphrasen) heads taken from individuals ranging in size from 91 to 97 mm fork length (L_F) (13·8 to 14·2 g) captured in the Plymouth Sound area of south-west England. Each (with the exception of the 97 mm fish) was trimmed to a small block containing both ears. The 97 mm fish was sectioned along the centre line and photographed, to provide information on the occurrence of gas holding structures (*e.g.* swimbladder) in connection with, or in close proximity to the inner ear. In the remaining specimens, the cranial cavity was opened dorsally and the brain removed by dissection and aspiration. Chilled fixative (2·5% glutaraldehyde in 0·1 M cacodylate buffer with 3·5% sodium chloride) was perfused into the saccule, and vented through a small incision in the chamber wall, located well away from the needle entry point and macula. The ears and surrounding tissue were subsequently immersed in chilled fixative for 48 h prior to dissection of the inner ear from the cranium.

The three otolithic chambers were opened in the regions opposing the macula, on the ventral side of the otolith away from any of the sensory arrays. The incision in the membrane was extended until it was of sufficient size for the macula to be washed from the surface of the otolith, using a pipette and a small quantity of excess fixative. The otolith capsules were then dehydrated through a graded ethanol series ranging from 35 through 50, 70 and 90% to absolute ethanol, prior to desiccation using the critical point drying method described by Platt (1977). Fully desiccated otolith capsules were subsequently mounted on a specimen stub using a carbon tab, and coated with *c.* 8 nm of gold in an Emitech K 550 sputter coater (working at *c.* 5×10^{-6} Torr). Finally, the processed specimens were investigated and photographed using a JOEL JSM 5600 scanning electron microscope operated at 15 kV, and a 15 mm working distance. The orientation of the ciliary bundles in the inner ear was defined by drawing a line from the shorter ciliary

bundles towards the longer kinocilium (Platt, 1977). This procedure was applied and repeated across the surface of the macula at 100 μm intervals, or when there was an abrupt change in ciliary bundle orientation.

RESULTS

The dissection of *T. bubalis*, both in cross-section (Fig. 1) and by removal of the internal organs through a ventral incision into the body cavity did not reveal the presence of a swimbladder in any of the specimens investigated. This finding reflects the benthic lifestyle of *T. bubalis*, and other members of the Cottidae such as the short-horn sculpin *Cottus scorpious* L. which also lacks a swimbladder (Enger & Anderson, 1967). An additional examination of the cranial cavity in the region surrounding the inner ear (Fig. 2) did not reveal the presence of any gas holding structures in close proximity to any of the otolithic end organs. The saccule and lagena were loosely tied to the cranium at the posterior end of the saccular chamber, which facilitated removal of the complete organs for SEM preparation prior to the anatomization of the fish.

THE SACCULE

The saccule of *T. bubalis* is the largest of the inner ear end organs and contains an otolith known as the sagitta or arrowhead (Fig. 3), and the saccular macula (Fig. 4). In *T. bubalis*, the dorsal margin of the sagitta is relatively smooth, and ends with two rounded lobes, with the most forward projecting known as the antirostrum. The sides of the otolith curve down toward the ventral margin, and terminate at the sharply rounded rostrum, and the rounded caudal margin. The excisura lies between the rostrum and antirostrum, and is moderately wide in *T. bubalis*, and has a very shallow excisural notch. The ostio-caudal differentiation is a constriction pushing midway into the colliculum, and divides the depression into the cauda, and the slightly larger ostium. The crista inferior is a low ridge running along the ventral edge of the

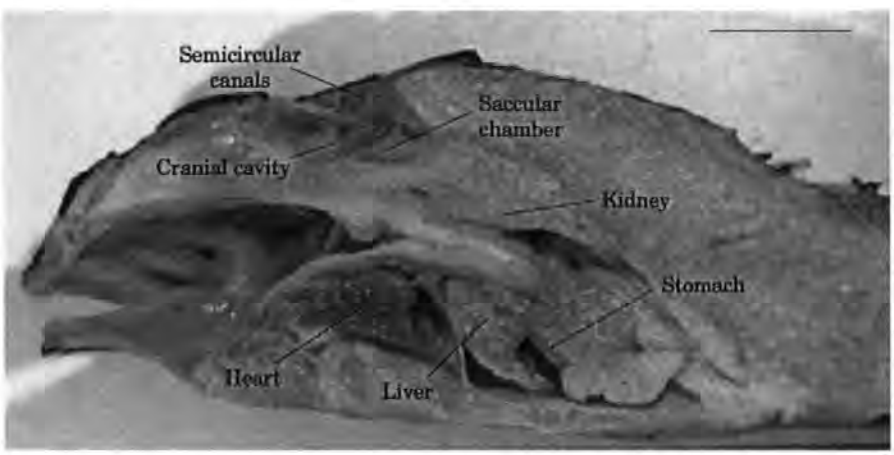

FIG. 1. Cross-section through a 97 mm L_F *Taurulus bubalis*, showing the internal organs and cranial cavity (the brain, saccule and lagena have been removed from the specimen). Bar = 10 mm.

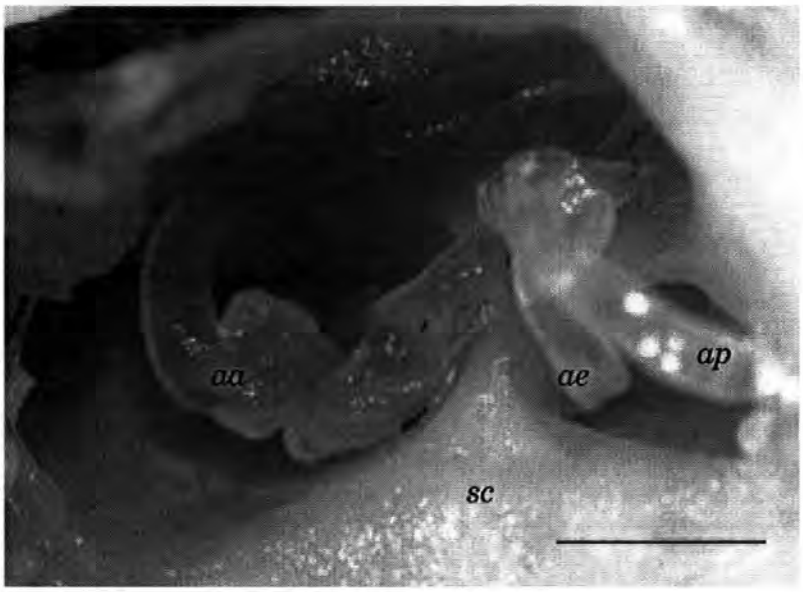

FIG. 2. The semicircular canals and end organs of the pars superior (the sacculus and lagena are not present in the figure as they were removed for SEM preparation). *aa*, anterior ampulla; *ae*, ampulla externa; *ap*, ampulla posterior; *sc*, floor of the saccular chamber (annotations after Retzius, 1881). Bar = 1 mm.

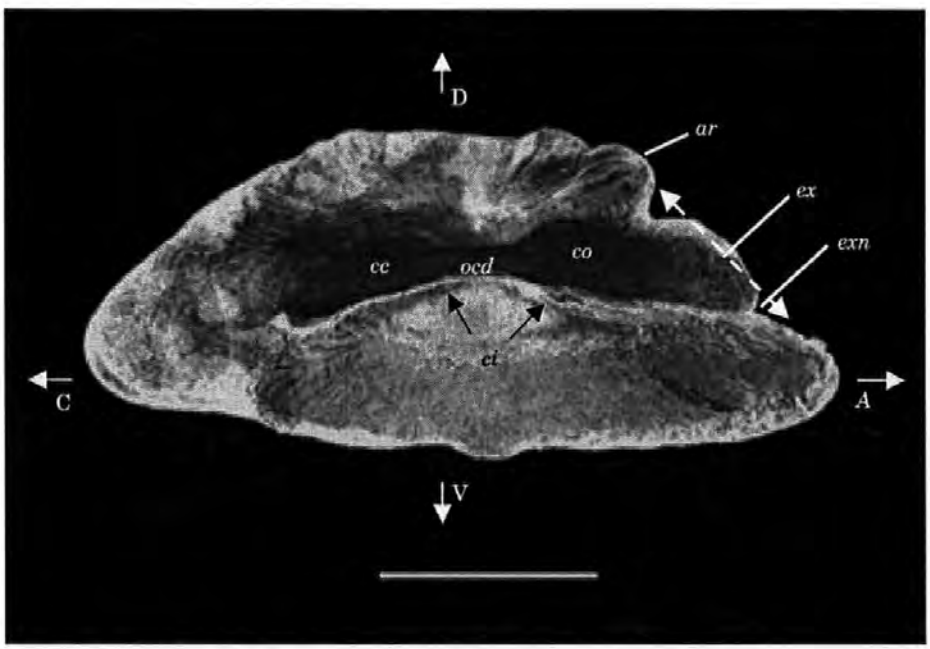

FIG. 3. The sagitta from *Taurulus bubalis*. *ar*, antirostrum; *cc*, colliculi cauda; *co*, colliculi ostium; *ci*, crista inferior; *ex*, excisura; *exn*, excisural notch; *ocd*, ostio-caudal differentiation. Anterior (A), caudal (C), dorsal (D) and ventral (V) represent the orientation of the otolith within the fish. Bar = 1 mm.

colliculum, from mid-ostium to mid-cauda, though it is poorly developed at the extremes (the crista superior was absent from all specimens examined). The macula (Fig. 4) is located in the colliculum or medial sulcus, a depression on the surface of the sagitta, and found here to be similar in shape to the associated epithelium. The low power micrograph of the saccular macula from the left ear of *T. bubalis* has been annotated with white arrows to show the overall orientation of the ciliary bundle proliferations viewed perpendicular to the macula surface. Detail of the ciliary bundles and their respective orientations can be seen in Figs 5, 6 and 7, which were taken at high power. The saccular hair cells from each of the six specimens of *T. bubalis* are divided into four discrete orientation groups, with ciliary bundles in each group orientated in the same overall direction. The ciliary bundles in the rostral locus of the macula (Fig. 5) are divided into two groups, with caudally orientated bundles on the dorsal half of the macula, and rostrally orientated bundles on the ventral portion. The ciliary bundles on the caudal locus of the macula (Fig. 6) are orientated dorsally in the dorsal region and ventrally in the ventral region. Cells of similar bundle size and orientation occupied large areas of the epithelia, separated from cells with alternate orientation and size by a narrow transitional zone; in some regions ciliary bundles immediately switch polarity as can be seen in Fig. 7. By counting the numbers of cells found proliferating in comparable areas of macula from each of the fish investigated, and by measuring the surface area of the macula using the ImageJ graphic analysis software (http://rsb.info.nih.gov/ij/), it was possible to approximate the number of ciliary bundles found in the saccule of *T. bubalis*. The overall hair cell count was calculated to be *c.* 30 000 for a 90 to 100 mm L_F fish, and the average length of the receptors found away from the perimeter in the ostium region of the macula were found to be *c.* 8 μm. This contrasts with the average receptor length of 6 μm found on the macula of the bass *Dicentrarchus labrax* *L.* (J.M. Lovell, M.M. Findlay, G. Harper, R.M. Moate & D.A. Pilgrim, unpubl. data), which was investigated for a related SEM study.

FIG. 4. The saccular macula from the ear of *Taurulus bubalis* (⇨, hair cell polarizations). Anterior (A) and dorsal (D) represent orientation of the organ within the fish. Bar = 500 μm.

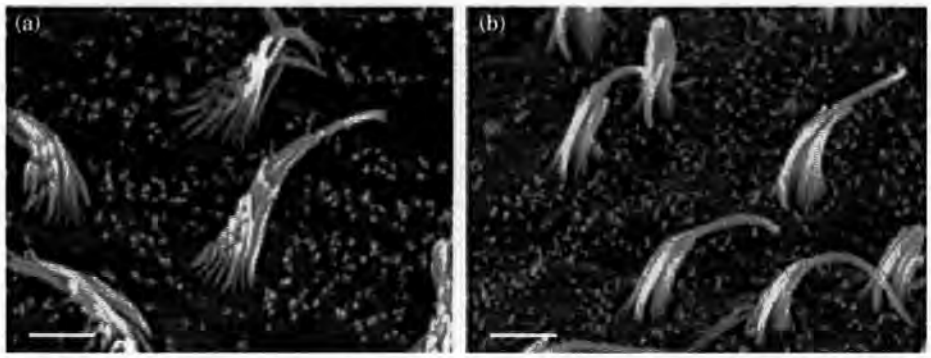

FIG. 5. Ciliary bundles from the osteum of the saccular epithelium: (a) dorsal and (b) ventral quadrant. Bars = 2 μm.

THE LAGENA

The lagena is the second of the end organs found in the pars inferior, and in *T. bubalis* it is *c.* one tenth the size of the saccule, and contains the asteriscus (star shaped) otolith [Fig. 8(a)]. The lagena is attached to the caudal end of the saccule, and the sensory macula [Fig. 8(b)] lies almost perpendicular to the horizontal plane of the fish. The orientation of ciliary bundles proliferating on the lagena epithelia, which are divided into two groups with opposing orientations is shown in Fig. 8(b). The flow is vertical at the ventral end of the macula, with ciliary bundle polarities becoming increasingly horizontal as the dorsal extremities of the macula are approached [shown by the white arrows in Fig. 8(b)]. The two regions were sub-divided into 14 sectors and studied at magnification factors of between ×1000 and ×5000. Detail of the ciliary bundles and their respective orientations can be seen in Fig. 9, which shows cells from a mid ventral region of the macula.

THE UTRICLE

The utricle is located in the anterior ampulla of the pars superior, a small chamber containing an otolith known as the lapillus (small rock) [Fig. 10(a)]

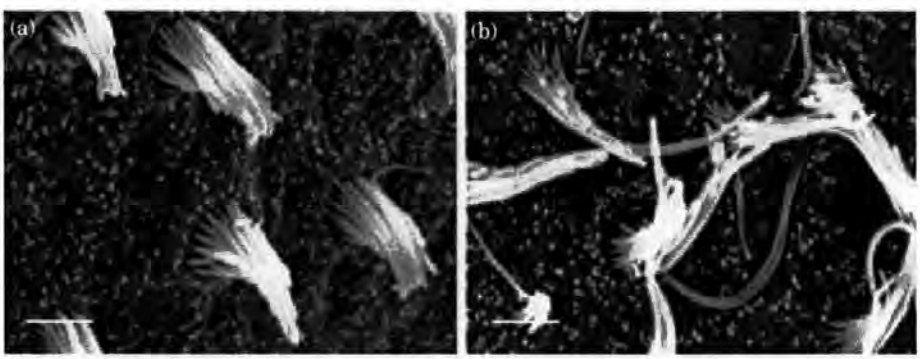

FIG. 6. Ciliary bundles from the caudal locus of the saccular epithelium: (a) dorsal and (b) ventral quadrant. Bar = 2 μm.

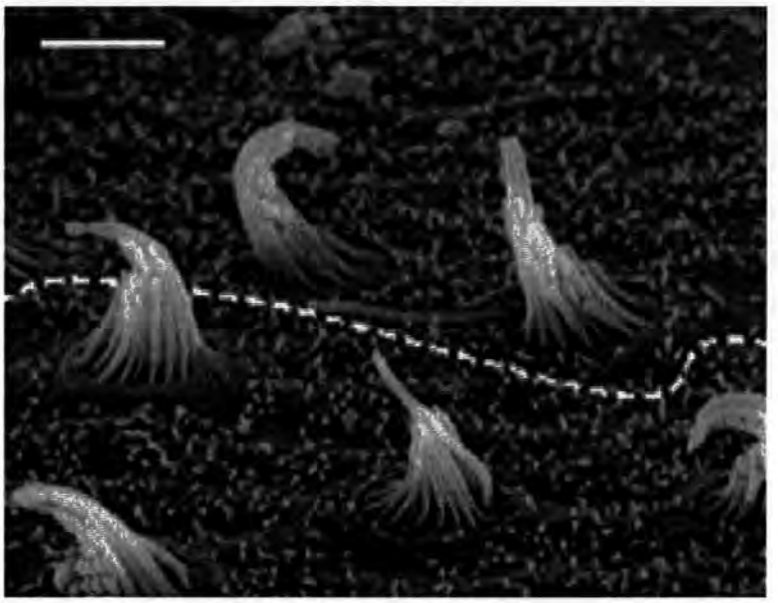

FIG. 7. Ciliary bundles from the osteum with opposing orientations. Bar = 2 μm.

and the macula [Fig. 10(b)]. The greatest densities of ultrastructural ciliary bundles were found to proliferate along the horizontal plane of the utricular macula in *T. bubalis*, as opposed to the near vertical arrangement of the saccular and lagena macula. The polarity of the receptors remained fairly constant across the epithelial surface, with ciliary bundles from a common origin flowing outward across the central (striola) region of the macula [Fig. 11(a)]. The polarization of ciliary bundles along the left perimeter of the

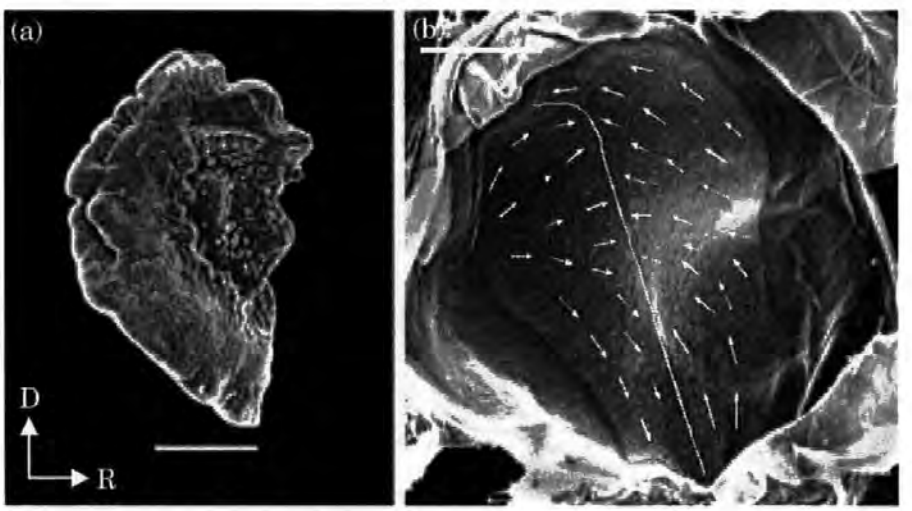

FIG. 8. (a) The otolith asteriscus and (b) the associated lagena epithelium (⇨, ciliary bundle polarizations). D, dorsal margin; R, rostrum. Bars = 200 μm.

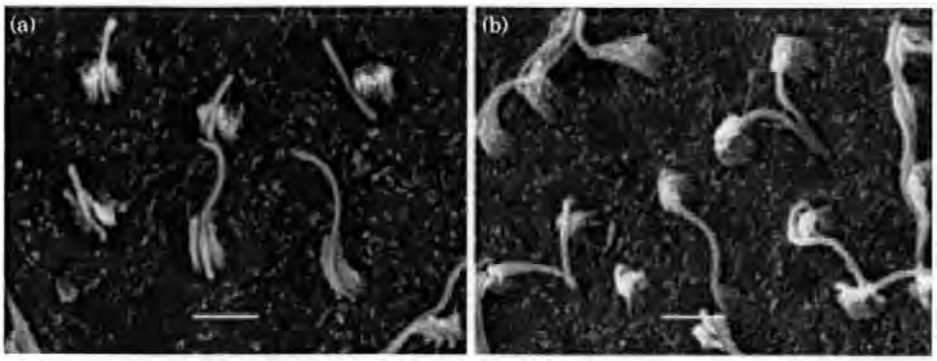

FIG. 9. Ciliary bundles from the lagena epithelia: (a) rostral and (b) caudal quadrant. Bars = 2 μm.

striola became fully opposed in the rostral region of the macula [Fig. 11(b)], extending over halfway down the right side.

DISCUSSION

Fishes possessing a connection between the inner ear and swimbladder are known collectively as hearing specialists (Popper & Fay, 1993, 1999), and are responsive to the sound pressure component of an acoustic signal. Many specialists have an upper hearing response from 3 to 10 kHz (Hawkins, 1981), although it is known that the American shad (*Alosa* spp.) can detect sounds up to 180 kHz (Mann *et al.*, 2001). The hearing system of fishes lacking this connection between the swimbladder and inner ear are known as hearing generalists, and rely on the shear forces generated by a phase differential between the dense otolith and less dense surrounding medium to stimulate the sensory hairs (Hawkins & MacLennan, 1976).

It is known that *C. scorpious* lacks a swimbladder (Enger & Anderson, 1967) and, from the present study this can be said of *T. bubalis*, suggesting that fishes

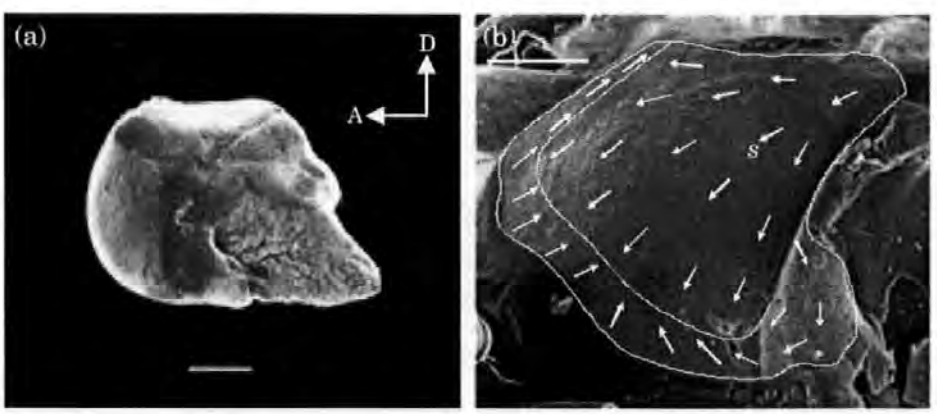

FIG. 10. (a) The otolith lapillus and (b) the utricular epithelium from the left ear of *Taurulus bubalis* (⇨, hair cell polarizations). s, striola. Anterior (D) and dorsal (A) represent the orientation of the otolith within the fish. Bars = 200 μm.

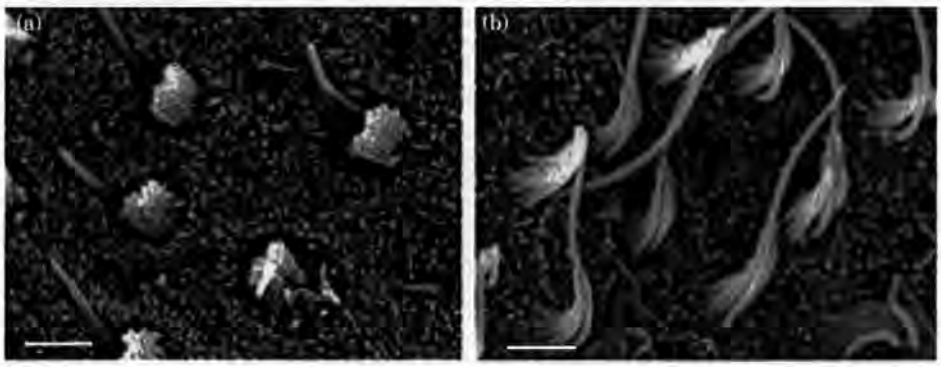

FIG. 11. Utricular ciliary bundles from (a) the central (striola) region and (b) peripheral ciliary bundles. Bars = 2 μm.

belonging to the Scorpaeniformes have generalist hearing abilities, though an audiogram has as yet to be produced for this species. Additionally, the inner ear ultrastructure of the saccule in a generalist fish is orientated both horizontally and vertically in four to six quadrants (Popper & Fay, 1993). It is apparent from analysis of the SEM data presented here, that *T. bubalis* has a standard orientation inner ear configuration, and is comparable to a number of hearing generalist species (Platt & Popper, 1981; Popper & Fay, 1993). Although this polarization pattern occurs frequently in generalists, there exists diversity, as for example the ciliary bundles on the rostral locus of the anguilliform saccular epithelium are orientated anterior, posterior, posterior and anterior (Popper, 1979). This is in contrast with specialist sensory receptor patterns such as those found in the Ostariophysi (Otophysi), which have saccular ciliary bundles orientated vertically in only two diametrically opposed quadrants (Platt, 1977). Bi-directional receptor patterns are often associated with adaptations that enhance hearing and can even extend to other end-organs, such as those found in the clupeid utricle (Popper & Platt, 1979; Blaxter *et al.*, 1981).

This is the first time that the ultrastructure of *T. bubalis* has been studied. This work presents a new set of polarization patterns, which provide anatomical information important in understanding electrophysiological aspects of fish hearing from an ecological perspective.

References

Barber, V. C. & Emerson, C. J. (1980). Scanning electron microscopic observations on the inner ear of the skate, (*Raja ocellata*). *Cell and Tissue Research* **205,** 199–215.

Blaxter, J. H. S., Denton, E. J. & Gray, J. A. B. (1981). Acousticolateralis system in clupeid fishes. In *Hearing and Sound Communication in Fishes* (Tovolga, W., Popper, A., Fay, R., eds), pp. 39–61. New York: Springer Verlag.

Carlström, D. A. (1963). Cystallographic study of vertebrate otoliths. *Biological Bulletin* **125,** 441–463.

Clegg, C. J. & Mackean, D. G. (1994). *Advanced Biology: Principles and Applications.* London: John Murray.

Enger, P. S. (1965). Acoustic thresholds in goldfish and its relation to the sound source distance. *Comparative Biochemistry and Physiology* **18,** 859–868.

Enger, P. S. & Anderson, R. (1967). An electrophysiological field study of herring in fish. *Journal of Comparative Biochemistry and Physiology* **22,** 517–525.
Enger, P. S., Hawkins, A. D., Sand, O. & Chapman, C. J. (1973). Directional sensitivity of saccular microphonic potentials in the haddock. *Journal of Experimental Biology* **59,** 425–433.
Fay, R. R. (1997). Directional response properties of saccular afferents of the toadfish, (*Opsanus tau*). *Hearing Research* **111,** 1–21
Hawkins, A. D. (1981). The hearing abilities of fish. In *Hearing and Sound Communication in Fishes* (Tavolga, W. N., Popper, A. N. & Fay, R. R., eds), pp. 109–133. New York: Springer Verlag.
Hawkins, A. D. & MacLennan, D. N. (1976). An acoustic tank for acoustic studies on fish. In *Sound Reception in Fish* (Schuijf, A. & Hawkins, A. D., eds), pp. 149–169. Amsterdam: Elsevier.
Hawkins, A. D. & Sand, O. (1977). Directional hearing in the median vertical plane by the cod. *Journal of Comparative Physiology A* **122,** 1–8.
Jenkins, D. B. (1981). The utricle in *Ictalurus punctatus*. In *Hearing and Sound Communication in Fishes* (Tavolga, W. N., Popper, A. N. & Fay, R. R., eds), pp. 73–81. New York: Springer-Verlag.
Jensen, J. C. (1994). Structure and innervation of the inner-ear sensory organs in an otophysine fish, the upside-down catfish (*Synodontis-nigriventris* David). *Acta Zoologica* **75,** 143–160.
Lu, Z. & Popper, A. N. (1998). Morphological polarizations of sensory hair cells in the three otolithic organs of a teleost fish: fluorescent imaging of ciliary bundles. *Hearing Research* **126,** 47–57.
Mann, D. A., Higgs, D. M., Tavolga, W. N., Souza, M. J. & Popper, A. N. (2001). Ultrasound detection by clupeiform fishes. *Journal of the Acoustical Society of America* **109,** 3048–3054.
Myrberg, A. A. (1981). Sound communication and interception in fishes. In *Hearing and Sound Communication in Fishes* (Tavolga, W. N., Popper, A. N. & Fay, R. R., eds), pp. 395–425. Berlin, Heidelberg, New York: Springer.
Nordeide, J. T. & Kjellsby, E. (1999). Sound from spawning cod at their spawning grounds. *ICES Journal of Marine Science* **56,** 326–332.
Platt, C. (1977). Hair cell distribution and orientation in goldfish otolith organs. *Journal of Comparative Neurology* **172,** 283.
Platt, C. & Popper, A. N. (1981). Fine structure and function of the ear. In *Hearing and Sound Communication in Fishes* (Tavolga, W. N., Popper, A. N. & Fay, R. R., eds), pp. 3–36. Berlin, Heidelberg, New York: Springer.
Popper, A. N. (1979). Ultrastructure of the sacculus and lagena in a moray eel (*Gymnothorax* sp.). *Journal of Morphology* **161,** 241.
Popper, A. N. (1981). Comparative scanning electron-microscopic investigations of the sensory epithelia in the teleost sacculus and lagena. *Journal of Comparative Neurology* **200,** 357–374.
Popper, A. N. (1983). Organization of the ear and auditory processing. In *Fish Neurobiology* (Northcutt, R. G. & Davis, R. E., eds), pp. 126–178. Ann Arbor, MI: University of Michigan Press.
Popper, A. N. & Fay, R. R. (1993). Sound detection and processing by fish: critical review and major research questions. *Brain Behaviour & Evolution* **41,** 14–38.
Popper, A. N. & Fay, R. R. (1999). The auditory periphery in fishes. In *Comparative Hearing: Fish and Amphibians* (Fay, R. R. & Popper, A. N., eds), pp. 43–100. New York: Springer Verlag.
Popper, A. N. & Platt, C. (1979). The herring ear has a unique receptor pattern. *Nature* **280,** 832–833.
Popper, A. N. & Platt, C. (1993). Inner ear and lateral line. In *The Physiology of Fishes* (Evans, D. H., ed.), pp. 99–136. Ann Arbor, MI: CRC Press.
Retzius, G. (1881). *Das Gehörorgan der Wirbelthiere. Das Gehörogan der Fische und Amphibien*, Vol. 1. Stockholm: Samson & Wallin.

Sand, O. & Hawkins, A. D. (1973). Acoustic properties of the cod swimbladder. *Journal of Experimental Biology* **58,** 797–820.

Tuset, V. M., Lombarte, A., Gonzalez, J. A., Pertusa, J. F. & Lorente, M^{a}J. (2003). Comparative morphology of the sagittal otolith in *Serranus* spp. *Journal of Fish Biology* **63,** 1491–1504. doi: 10.1046/j.1095-8649.2003.00262.x

Yan, H. Y., Saidel, W. M., Chang, J. S., Presson, J. C. & Popper, A. N. (1991). Sensory hair cells of a fish ear: evidence of multiple types based on ototoxicity sensitivity. *Proceedings of the Royal Society of London B* **245,** 133.

ELSEVIER

Comparative Biochemistry and Physiology, Part A 141 (2005) 116 – 121

CBP

www.elsevier.com/locate/cbpa

The polarisation of hair cells from the ear of the European bass (*Dicentrarchus labrax*)

J.M. Lovell[a,*], M.M. Findlay[a], G. Harper[b], R.M. Moate[b], D.A. Pilgrim[a]

[a]*School of Earth, Ocean and Environmental Sciences, University of Plymouth, Drake Circus, Plymouth PL4 8AA, United Kingdom*
[b]*Plymouth Electron Microscopy Centre, University of Plymouth, Drake Circus, Plymouth PL4 8AA, United Kingdom*

Received 12 November 2004; received in revised form 23 February 2005; accepted 15 April 2005
Available online 26 May 2005

Abstract

The polarisation of ciliary bundles on the macula of the saccule in the European bass (*Dicentrarchus labrax* L) has been studied using a scanning electron microscope (SEM). These data show that *D. labrax* possesses ciliary bundles arranged in four dichotomous quadrants with a standard orientation, comparable to hearing generalists from the order Perciformes. The spacing between ciliary bundles was investigated in three size classes of fish, with the results indicating that the addition of receptor cells in the ear of *D. labrax* continues for at least the first 2 years of development. The lengths of the kinocilia from ciliary bundles in each quadrant of the macula were also studied, and found to be of uniform length. In addition, we look at the internal structure of the afferent using transmission electron microscopy (TEM), revealing the nucleated cell body and peripheral nerve fibres of the saccule consistent with other TEM examinations of saccular ultrastructure. This information is required to gain an insight into the inner ear of *D. labrax*, as part of a larger study of the morphology and physiology of the hearing systems of both vertebrate and invertebrate marine animals.

Keywords: Fish ear; Saccule; Hair cell; Cilia; SEM; TEM; *Dicentrarchus labrax*

1. Introduction

The vertebrate inner ear is divided into two regions, the pars superior and the pars inferior (Retzius, 1881). The former responds primarily to movements of the body and postural changes, while the latter responds to both gravistatic and acoustic stimuli (Jenkins, 1981; Popper and Platt, 1993). The pars inferior comprises two fluid-filled pouches, the saccule and lagena (Retzius, 1881; Platt and Popper, 1981; Popper and Platt, 1993), with each pouch containing a crystalline calcium carbonate otolith (Carlström, 1963; Popper and Platt, 1993). Of these end organs, the saccule is considered to be the primary auditory organ in most teleost fish, though there is evidence of a functional overlap between all three otolith organs (Popper and Fay, 1993).

The directional characteristics associated with the motion of water particles during the passage of a wave front divulge important information to the fish's sensory system, allowing it to accurately determine the direction and distance of a disturbance or sound in the acoustic free field (Schuijf and Hawkins, 1983; Hawkins and Sand, 1977; Hawkins, 1993). It is known (Enger et al., 1973; Hawkins and Sand, 1977; Fay and Edds-Walton, 1997b) that the morphological polarities of sensory ciliary bundles in the otolithic organs are fundamental to the directional hearing capabilities of generalist fish. Azimuths of peak sensitivity tend to lie parallel to the plane of the otolith and sensory epithelium (Sand and Hawkins, 1973; Enger et al., 1973; Fay and Edds-Walton, 1997b); excitation occurs when stereocilia are bent toward the kinocilium during the passage of a wave front, resulting in the cell becoming depolarised relative to its resting potential (Clegg and Mackean, 1995). Inhibition occurs when the bundle is deflected in the opposite direction, and results in the hyperpolarisation of the cell (Flock and Duvall, 1965). The ability to detect and localise the source of a sound is of considerable biological importance to many fish species,

* Corresponding author. Tel.: +44 1752 232411; fax: +44 1752 232400.
E-mail address: j.lovell@plymouth.ac.uk (J.M. Lovell).

1095-6433/$ - see front matter © 2005 Elsevier Inc. All rights reserved.
doi:10.1016/j.cbpb.2005.04.010

and is often used to assess the suitability of a potential mate or during territorial displays (Nordeide and Kjellsby, 1999), and during predator–prey interactions (Myrberg, 1981). Jensen (1994) used a light microscope to reveal hair cell orientations in the end organs of the upside-down catfish (*S. nigriventris*), along with observations of innervating nerve distributions. Lu and Popper (1998) examined the polarisation of ciliary bundles in the end organs of the sleeper goby (*Dormitator latifrons*) using immunocytochemicals and a confocal imaging technique. However several authors (e.g. Platt and Popper, 1984; Popper, 1981; Yan et al., 1991) have used the scanning electron microscope (SEM) to study surface detail of the inner ear ultrastructure, and this was the approach adopted here. This paper sets out to address the question of whether the European sea bass (*D. labrax*) has a standard orientation pattern of hair cells in the saccule, in common with many hearing generalists. This information is required to gain an insight on the inner ear structure and configuration of *D. labrax*, as part of a larger study of the morphology and functionality of the hearing systems of both vertebrate and invertebrate marine animals.

2. Materials and methods

2.1. Preparation of the saccule prior to SEM examination

The preparation methodology employed in this study was based on techniques used by Platt (1977). Six fresh bass of mixed sex, ranging in size from 72 mm (9.4 g) to 170 mm (90 g), were obtained from wild stock in the South West of England (ordnance survey GB grid reading SX483539). The fish were delivered "on ice" to the EM unit within an hour of capture, and trimmed to small blocks containing both ears. The cranial cavity was opened dorsally and the brain removed by dissection and aspiration. Chilled fixative (2.5% glutaraldehyde in 0.1 M cacodylate buffer with 3.5% sodium chloride) was perfused into the saccule, and vented through a small incision in the chamber wall, located well away from the needle entry point and macula. The ears and surrounding tissue were subsequently immersed in chilled fixative for 48 h prior to dissection of the pars inferior from the remaining cranium. The saccule capsules were then dehydrated through a graded ethanol series ranging from 35% through 50%, 70% and 90% to absolute ethanol, prior to desiccation using the critical point drying method described by Platt (1977). Fully desiccated capsules were subsequently mounted on a specimen stub using a carbon tab, and coated with ca. 8 nm of gold in an Emitech K 550 sputter coater (working at approximately 5×10^{-6} Torr). The processed specimens were investigated and photographed using a JEOL JSM 5600 scanning electron microscope operated at 15 kV, and a 15 mm working distance. The orientation of an inner ear hair cell is defined by drawing a line using the JEOL software, from the shorter ciliary bundles towards the longer kinocilium. This procedure was applied and repeated across the surface of the macula at 100-μm intervals, or when there was an abrupt change in hair cell orientation. Images of the macula and ultrastructure were saved in a bitmap format, and calibrated measurements were made using the analysis programme ImageJ. All measurements were carried out on a PC using the analySIS® (Soft Imaging System GmbH) program. The distance between bases of the closest neighbour was measured using arbitrary distance and the hair cell length was measured using polygon length, both measurements were recorded in micrometers. The kinocilia were measured from their base to the tip, and total hair cell counts were all completed manually. Statistical calculations were carried out using Statgraphics plus 5.1 professional edition program, and analysis of variance (ANOVA) was used to test whether or not kinocilia length and the distance between cells vary across the macula surface.

2.2. Preparation of the saccule prior to TEM examination

The freshly excised tissue was fixed by placing it into a 2.5% glutaraldehyde in sodium cacodylate buffer (0.1 M pH 7.2) for at least 1 h, then rinsed twice in cacodylate buffer for 15 min each rinse. The saccular chamber was then secondary fixed in a 1% osmium tetroxide in sodium cacodylate buffer (0.1 M pH 7.2) for 1 h. The tissue was then rinsed twice in buffer, then dehydrated in an ethanol series. Once in 100% ethanol, the tissue was placed in increasing concentrations of Spurr's resin until it was fully infiltrated to 100%. The sample was then placed in Beem capsules ready for polymerisation of the resin, which was achieved by placing it in a 70 °C oven overnight in accordance with Glauert (1975). The resulting resin blocks were sectioned using a Reichert–Jung Ultracut and a Micro Star diamond knife. The sections were picked up using 200 mesh thin bar copper grids and stained firstly with a saturated ethanol solution of uranyl acetate and then a second stain of Reynolds lead citrate (15 min each stain) (Lewis and Knight, 1977). The fully processed images were taken with a Jeol 1200 EX II TEM and the images captured with an SIS Mega view III.

3. Results

3.1. Hair cell orientation patterns on the saccule of D. labrax

The view of the saccular macula from the left ear of *D. labrax* (Fig. 1) was scanned at a magnification of ×50 and annotated to show the overall orientation of the ciliary

Fig. 1. Orientation of ciliary bundles on the left ear saccular epithelium of *Dicentrarchus labrax*, orientated horizontally (1 and 2), and vertically (3 and 4) in diametrically opposed quadrants; showing that *D. labrax* is a hearing generalist with standard orientation ciliary bundles.

bundles found in each quadrant, as viewed perpendicular to the macula surface.

The polarisation of the ciliary bundles is depicted by the white arrows in Fig. 1, and reveals that *D. labrax* possesses a standard orientation pattern in common with other hearing generalist fish from the order Perciformes (Platt and Popper, 1981; Popper and Fay, 1993). Detail of the ciliary bundles and their respective orientations can be seen in Figs. 2–5, which were scanned at a high power. The ciliary bundles are divided into four discrete orientation groups, and separated from cells with alternate orientation by a narrow transitional zone. The polarisation of ciliary bundles in the rostral locus or ostium of the macula is divided into two regions, with caudally orientated hair cell groups on the dorsal half of the macula (Fig. 2), and rostrally orientated groups on the ventral portion (Fig. 3). Cells on the caudal locus of the macula are orientated dorsally in the dorsal region (Fig. 4), and ventrally in the ventral region (Fig. 5).

3.2. Surface area and shape of the saccular macula

The saccular macula from three bass with fork lengths of 170 mm (90 g), 126 mm (53 g) and 72 mm (9.4 g) were examined by EMC. Fig. 6 shows the outline of the regions

Fig. 3. Scanning electron micrograph of ciliary bundles from quadrant 2.

of macula bearing ciliary bundles from both the left and right ears.

The total area of the macula was found to be 3.219 mm^2 for the right ear, and 3.073 mm^2 for the left ear of the 170 mm fish, 2.555 mm^2 for the right and 2.415 mm^2 for the left ear of the 126 mm fish, and 1.722 mm^2 for the right and 1.58 mm^2 for the left ear of the 72 mm fish.

3.3. Hair cell spacing and length with increasing age/size

In order to test the hypothesis that the number of ciliary bundles increases with age in *D. labrax*, measurements of the spacing between ciliary bundles in quadrant 2 of the ostium in both x and y coordinates were taken from each size of fish. These data were fed into a one-way ANOVA, which gave an F value of 1.80 and a P value of 0.181, for receptor spacing in the x axis, and an F value of 3.71 and a P value of 0.035 in the y axis. The mean length of the kinocilia across the sensory macula from the 126 mm *D. labrax* was 3.2 μm, though cells in quadrant 3 were observed to be slightly shorter than the overall average. To find if this variation in kinocilia length was significant, the data from each quadrant were fed into

Fig. 2. Scanning electron micrograph showing the ciliary bundles from quadrant 1.

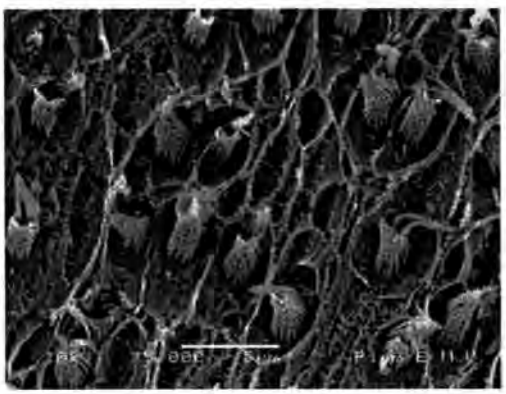

Fig. 4. Ciliary bundles from quadrant 3.

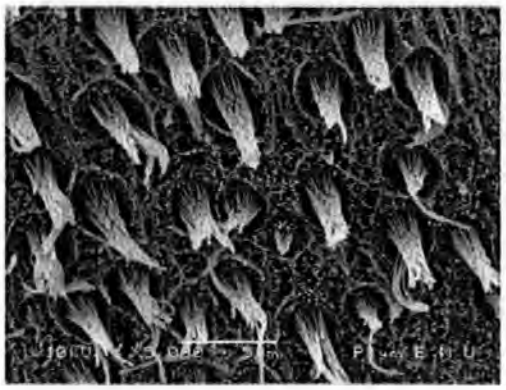

Fig. 5. Ciliary bundles from quadrant 4.

a one-way ANOVA, and gave an F value of 3.34, and a P value of 0.056.

3.4. TEM investigation of the saccular hair cells

The transmission electron micrograph (TEM) section in Fig. 7a shows the complete hair cell from *D. labrax*, sectioned lengthwise from the ciliary bundle at the top of the figure, to the innervating nerves at the bottom. The longest of the cilia with the dark core is the kinocilia, and the shorter hairs are the stereocilia. The peripheral saccular nerve fibres can be seen in an area where the membrane of the axon terminal is in close proximity to the membrane of the neuron. Information travels across the synapse by way of neurotransmitters, which diffuse across the synaptic cleft to the postsynaptic membrane. If sufficient neurotransmitter is secreted, an action potential is generated in the neuron. The crosswise section through the top of the cell (Fig. 7b) shows that the cuticular plate is almost void of obvious structures, except for a number of fine tracts created by actin filaments extending from the cilia base into the cuticular plate. The sides of the receptor cell are buttressed by supporting cellular structures, and the base of the receptor cell sits above two further supporting cells with large nuclei. A high powered micrograph of the section taken through the cuticular plate (Fig. 7c) shows the cilia base and actin filaments (af) that "root" the stereocilia to the hair cell.

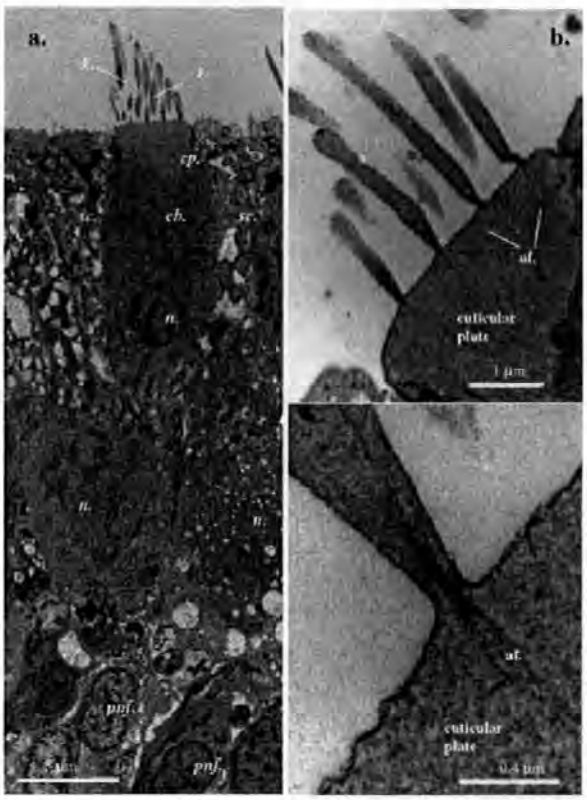

Fig. 7. (a) TEM cross section of a saccular hair cell and innervating nerve fibres from the ear of *Dicentrarchus labrax*. cb., cell body; cp., cuticular plate; k., kinocilia; n., nucleus; pnf., peripheral nerve fibres; sc., support cells; s., stereocilia. (b) Section taken through the cuticular plate, showing internal structures within the cilia and the actin filaments that tie the cilia to the cuticular plate. (c) High powered micrograph of the cilia base and actin filaments (af).

4. Discussion

The study of the saccular hair cells from the bass (*D. labrax*) reveals that this fish has an inner ear configuration

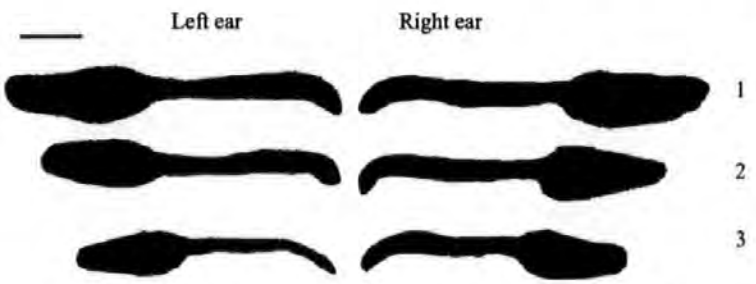

Fig. 6. Outline of the saccular macula from the left and right ears taken from *D. labrax* with body lengths of 170 mm (1), 126 mm (2) and 72 mm (3). Bar=1 mm.

similar to hearing generalist fish, and it is to this group of fish that *D. labrax* most probably belongs. In addition, the TEM examination shows that the internal structure of the saccular hair cell conforms to other published studies of ultrastructure morphology (e.g. Flock and Duvall, 1965). According to Bretschneider et al. (2001), generalists are only responsive to low frequency sounds ranging from around 30 Hz to 2000 or so Hz. However, in a recent ABR investigation of the hearing abilities of two Acipenseriform fish, it was found that an evoked response consistent with the stimulus sound could only be initiated from frequencies up to 500 Hz (Lovell et al., in prep), and (as the experiment used two submerged transducers) it could be demonstrated that the fish were responding to the particle motion component of the sound rather than the pressure. The interaction between the otolith and hair cells in generalist fish is initiated by the motion of the water particles in the sound field, and not the pressure of the sound (Coombs and Popper, 1982; McCormick and Popper, 1984; Lu, 2004).

The study conducted here on the morphology of the saccular macula from three size classes of fish shows that the distance between cells on the rostro-caudal (x) axis, remains constant throughout the development of *D. labrax*, from fingerling to the juvenile stages of the life cycle (shown by the P value of 0.181). However, the P value of 0.035 shows that there is some evidence to suggest that the ciliary bundles may acquire more lateral spacing along the dorso-ventral (y) axis as *D. labrax* grows. The test was confirmed by counting the number of cells found proliferating in comparable areas of macula (51 cells per 0.002 mm^2 for the 170 mm fish, 48 for the 126 mm fish, and 67 for the 72 mm fish). Using these data, it is possible to estimate that the number of ciliary bundles proliferating on the saccular macula of *D. labrax* is approximately 80,000 for the 170 mm fish, 60,000 for the 126 mm fish, and 40,000 for the 72 mm fish. It is therefore concluded that in *D. labrax*, the addition of ciliary bundles continues for at least 2 years post hatching, in agreement with a study of hair cell addition in the saccule of the hake (*Merluccius merluccius*) by Lombarte and Popper (1994).

The one-way ANOVA was also used to test for similarity in the lengths of receptor cells, from all four quadrants of the saccular epithelium of a 126 mm *D. labrax*, and gave a P value of 0.056, showing that the overall length of the kinocilia does not significantly vary between each quadrant. It is known that in lizards and birds, regions having longer ciliary bundles detect lower-frequency signals while shorter bundles detect higher frequencies (Popper and Fay, 1993). Indirect evidence in fish raises the possibility of a similar correlation, as the region of the macula responsive to lower frequencies in goldfish is the region containing the taller kinocilia (Sugihara and Furukawa, 1989), suggesting a parallelism with the gradient of ciliary bundle length and frequency responses found in higher vertebrates. Fish lacking adaptations that enhance hearing (commonly called hearing generalists) have ciliary bundles orientated both horizontally and vertically in four to six quadrants (Popper and Fay, 1993). The directional characteristics (excitation or inhibition) of afferent nerves have been qualitatively correlated with anatomically defined patterns of hair cell orientations on the macula of the saccule (Fay and Edds-Walton, 1997a). It is apparent from analysis of the SEM data presented here that *D. labrax* possesses standard orientation ciliary bundles in common with many hearing generalist species, and is in contrast with the sensory receptor patterns found in the Ostariophysi (Otophysi). These fish have hair cells orientated vertically in two diametrically opposed quadrants (Popper, 1980), a feature also found in amphibians and reptiles (Blaxter et al., 1981; Popper and Platt, 1979).

References

Blaxter, J.H.S., Denton, E.J., Gray, J.A.B., 1981. Acousticolateralis system in clupeid fishes. In: Tovolga, W., Popper, A., Fay, R. (Eds.), Hearing and Sound Communication in Fishes. Springer Verlag, New York, pp. 39–61.

Bretschneider, F., van den Berg, A.V., Peters, R.C., 2001. In: Kapoor, B.G., Hara, T.J. (Eds.), Sensory Biology of Jawed Fishes. Science Publishers, Enfield NH, USA.

Carlström, D.A., 1963. Cystallographic study of vertebrate otoliths. Biol. Bull. 125, 441–463.

Clegg, C.J., Mackean, D.G., 1995. Advanced Biology: Principles and Applications. John Murray, London, pp. 448–461.

Coombs, S., Popper, A.N., 1982. Structure and function of the auditory system in the clown knifefish, *Notopterus chitala*. J. Exp. Biol. 97, 225–239.

Enger, P.S., Hawkins, A.D., Sand, O., Chapman, C.J., 1973. Directional sensitivity of saccular microphonic potentials in the haddock. J. Exp. Biol. 59, 425–433.

Fay, R.R., Edds-Walton, P.L., 1997a. Directional response properties of saccular afferents of the toadfish, (*Opsanus tau*). Hear. Res. 111, 1–21.

Fay, R.R., Edds-Walton, P.L., 1997b. Diversity in frequency response properties of saccular afferents of the toadfish, *Opsanus tau*. Hear Res. 113, 235–246.

Flock, M.B., Duvall, A.J., 1965. The ultrastructure of the kinocilium of the sensory cells in the inner ear and lateral line organs. J. Cell Biol. 25, 1–8.

Glauert, A.M., 1975. Fixation, Dehydration and Embedding of Biological Specimens. North-Holland Publishing Company.

Hawkins, A.D., 1993. Underwater sound and fish behaviour. In: Pitcher, T.J. (Ed.), Behaviour of Teleost Fishes. Chapman and Hall.

Hawkins, A., Sand, O., 1977. Directional hearing in the median vertical plane by the cod (*G. morhua*). J. Comp. Physiol. A. 122, 1–8.

Jenkins, D.B., 1981. The utricle in *Ictalurus punctatus*. In: Tovolga, W., Popper, A., Fay, R. (Eds.), Hearing and Sound Communication in Fishes. Springer Verlag, New York.

Jensen, J.C., 1994. Structure and innervation of the inner-ear sensory organs in an otophysine fish, the upside-down catfish (*Synodontis nigriventris* David). Acta Zool. 75, 143–160.

Lewis, P.R, Knight, D.P., 1977. Staining Methods for Sectioned Material. North-Holland Publishing Company.

Lombarte, A., Popper, A.N., 1994. Quantitative analyses of postembryonic hair cell addition in the otolithic end organs of the inner ear

of the European hake *Merluccius merluccius* (Gadiformes, Teleostei). J. Comp. Neurol. 345, 419–428.

Lu, Z., 2004. Neural mechanisms of hearing in fishes. In: von der Emde, G., Mogdans, J., Kapoor, B.G. (Eds.), The senses of fishes: adaptations for the reception of natural stimuli. Narosa Publishing House, New Delhi, India, pp. 147–172.

Lu, Z., Popper, A.N., 1998. Morphological polarizations of sensory ciliary bundles in the three otolithic organs of a teleost fish: fluorescent imaging of ciliary bundles. Hear. Res. 126, 47–57.

McCormick, C.A., Popper, A.N., 1984. Auditory sensitivity and psychophysical tuning curves in the elephant nose fish, *Gnathonemus petersii*. J. Comp. Physiol. A. 155, 753–761.

Myrberg, A.A., 1981. Sound communication and interception in fishes. In: Tovolga, W., Popper, A., Fay, R. (Eds.), Hearing and Sound Communication in Fishes. Springer Verlag, New York, pp. 395–425.

Nordeide, J.T., Kjellsby, E., 1999. Sound from spawning cod at there spawning grounds. ICES J. Mar. Sci. 56, 326–332.

Platt, C., 1977. Hair cell distribution and orientation in goldfish otolith organs. J. Comp. Neurol. 172, 283–297.

Platt, C., Popper, A.N., 1981. Fine structure and function of the ear. In: Tovolga, W., Popper, A., Fay, R. (Eds.), Hearing and Sound Communication in Fishes. Springer Verlag, New York, pp. 3–36.

Platt, C., Popper, A.N., 1984. Variation in lengths of ciliary bundles on hair cells along the macula of the sacculus in two species of teleost fishes. In: Becker, R.P. (Ed.), Scanning Electron Microscopy, 4, pp. 1915–1924.

Popper, A.N., 1980. Scanning electron microscopic study of the sacculus and lagena in several deep-sea fishes. Am. J. Anat. 157, 115–136.

Popper, A.N., 1981. Comparative Scanning Electron-Microscopic Investigations of the Sensory Epithelia in the Teleost Sacculus and Lagena, J. Comp. Neurol., vol. 200. Wiley-Liss, New York, pp. 357–374.

Popper, A.N., Fay, R.R., 1993. Sound detection and processing by fish: critical review and major research questions. Brain Behav. Evol. 41, 14–38.

Popper, A.N., Platt, C., 1979. The herring ear has a unique receptor pattern. Nature 280, 832–833.

Popper, A.N., Platt, C., 1993. Inner ear and lateral line. In: Evans, D.H. (Ed.), The Physiology of Fishes. CRC Press, Boca Raton, FL, pp. 99–136.

Retzius, G., 1881. Das Gehörorgan der Wirbelthiere. Das Gehörorgan der Fische und Amphibien, vol. 1. Samson and Wallin, Stockholm.

Sand, O., Hawkins, A.D., 1973. Acoustic properties of the cod swimbladder. J. Exp. Biol. 58, 797–820.

Schuijf, A., Hawkins, A.D., 1983. Acoustic distance discrimination by the cod. Nature 302, 143–144.

Sugihara, I., Furukawa, T., 1989. Morphological and functional aspects of two different types of hair cells in the goldfish sacculus. J. Neurophysiol. 62, 1330–1343.

Yan, H.Y., Saidel, W.M., Chang, J.S., Presson, J.C., Popper, A.N., 1991. Sensory hair cells of fish ear: evidence of multiple types based on ototoxicity sensitivity. Proc. R. Soc. Lond., B Biol. Sci. 245, 133–138.

The inner ear morphology and hearing abilities of the Paddlefish (*Polyodon spathula*) and the Lake Sturgeon (*Acipenser fulvescens*)

J .M Lovell[1], M.M Findlay[1], R.M Moate[2], J.R Nedwell[3] and M.A Pegg[4]

[1]School of Earth, Ocean and Environmental Sciences j.lovell@plymouth.ac.uk, [2]Plymouth Electron Microscopy Centre, University of Plymouth, Drake Circus, Plymouth PL4 8AA. [3] Subacoustech Ltd, Bishops Waltham, Hampshire, UK. [4]Illinois River Biological Station and Forbes Biological Station Illinois Natural History Survey 704 North Schrader Havana, Illinois 62644

Abstract

Concern regarding the spread of silver carp (*Hypopthalmichthys molitrix*) and bighead carp (*Aristichthysc nobilis*) through the Illinois River has prompted the development of an Acoustic Fish Deterrent (AFD) system. The application of this technology has resulted in a need to understand the auditory physiology of fish other than the target species, in order to minimise the effect of the AFD barrier on the ecology of indigenous fish populations. To this end, both the structures involved in sound reception and the hearing abilities of the paddlefish (*Polyodon spathula*) and the lake sturgeon (*Acipenser fulvescens*) are studied here using a combination of morphological and physiological approaches, revealing that both fish are responsive to sounds ranging in frequency from 100 Hz to 500 Hz. The lowest hearing thresholds from both species were acquired from frequencies in a bandwidth of between 200 Hz to 300 Hz, with higher thresholds at 100 Hz and 500 Hz. The rationale for studying hearing in *P. spathula* and *A. fulvescens* in particular, is the value placed on them by both the commercial caviar producing industry and by the recreational fisheries sector. The hearing abilities of twelve *P. spathula* and twelve *A. fulvescens* were tested in sound fields dominated by either sound pressure or particle motion, with the results showing that Acipenseriform fish are responsive to the motion of water particles in a sound field, rather than the sound pressure component. In this study, we measure the intensity of the sound field required to evoke threshold responses using a pressure sensitive hydrophone, as pressure dominated sound fields are the most audible acoustic condition for specialists like *H. molitrix* and *A. nobilis* (the target species). The results of the auditory examination clearly show that *P. spathula* and *A. fulvescens* are not sensitive to sound pressure, and will therefore have a significantly

higher deterrent threshold than *H. molitrix* and *A. nobilis* in a pressure dominated sound field.

* Corresponding author. Tel.: +44 1752 232411; fax: +44 1752 232400.
E-mail address: j.lovell@plymouth.ac.uk (J.M. Lovell).

Key words: Fish; Ear; Hearing; Sturgeon; Paddlefish; ABR; Evoked potential; Hair cell

1. Introduction

The spread of the Asian carp species, silver carp (*Hypopthalmichthys molitrix*) and bighead carp (*Aristichthysc nobilis*) through the Illinois River and into the man-made Chicago Canal is causing increasing concern as these non-indigenous species get closer to Lake Michigan. In a work that partners this study, the hearing abilities of the target Asian carp species are defined using the equipment and methodology described here as a benchmark, with the results showing the lowest thresholds were acquired from frequencies in a bandwidth of between 750 Hz to 1500 Hz (Lovell et al., in prep). Trials conducted by the Illinois Natural History Survey (INHS, Havana, Illinois) have shown that 95% effectiveness can be achieved with *A. nobilis* using a Fish Guidance Systems Bio-Acoustic Fish Fence (BAFF) system (Taylor, Pegg and Chick, in press) and further trials are underway with *H. molitrix*. While preventing the spread of these species is critical, it is also important that the noise generated by the barrier does not affect indigenous species where possible. Two species in particular, the paddlefish (*Polyodon spathula*) and the lake sturgeon (*Acipenser fulvescens*) from the subclass Chondrostei, in the order Acipenseriformes (sturgeons and paddlefishes) are of interest in this respect. An ideal acoustic barrier would appear "loud" to the alien carp species and "quiet" to the indigenous species, and therefore have little or no influence on the behaviour of the paddlefish and sturgeon as they pass the barrier. To achieve this level of selectivity, it requires the definition of the potentially affected species hearing thresholds, which can ultimately be used to "fine tune" the sounds generated by the barrier.

The hearing thresholds of any organism possessing the appropriate receptor mechanism are illustrated in an audiogram (Myrberg, 1981), which presents the lowest level of sound

that a species can hear as a function of frequency. Audiograms for marine animals are predominantly expressed in units of sound pressure, or dB (re. 1 μPa) and is the rationale for using them in this study. The techniques used to obtain fish audiograms may require a varying degree of time, surgical and technical expertise, or the use of behavioural paradigms to gain statistically sound data (see, for instance, Yan, 1995). Behavioural methods require that fish are trained to react in a specified and measurable way (e.g. a reward based method by seeking food) when a tone at a given frequency is presented; however, in practice, the behavioural method is very time consuming and only effective with species that are easy to train. The measurement of microphonics from auditory end organs during acoustic stimulation is a technique favoured by a number of authors (e.g. Enger and Anderson 1967; Fay and Popper, 1975; Fine, 1981). Although results can be obtained more rapidly than from behavioural paradigms, preparation can often be complex and require invasive surgery to implant the electrodes directly into the nerve (c.f. Enger and Anderson, 1967). The electrode is thus restricted to a specific end organ or region of macula, and the evoked potential does not necessarily represent the whole auditory pathway (Kenyon et al., 1998). The Auditory Brainstem Response (ABR) technique of measuring hearing thresholds has been successfully applied to both mammalian and non-mammalian vertebrates (Corwin et al., 1982), Elasmobranchs (Casper et al., 2003), and marine invertebrates (Lovell et al., 2005 A). The ABR is a non-invasive far-field recording of synchronous neural activity in the eighth nerve and brainstem auditory nuclei elicited by acoustic stimuli (Jewett, 1970; Jewett and Williston, 1971; Jacobson, 1985; Kenyon et al., 1998), and waveforms clearly present with similarities between fish and higher vertebrates (Corwin, 1981) and between vertebrates and invertebrates (Lovell et al., 2005a). Measurements of the ABR response are used routinely in the clinical evaluation of human hearing (Jacobson, 1985) and allow for the determination of thresholds from uncooperative or inattentive subjects and in situations where behavioural methods cannot be readily applied.

It is known that the directional responses of afferents are a function of the hair cell polarities and the orientation of the epithelium in space (Fay and Edds-Walton, 1997; Edds-Walton and Fay, 2002; Lu and Popper, 2001). In both *P. spathula* and *A.*

fulvescens, the hair cells are aligned in both the horizontal and vertical planes and provide evidence of directional hearing ability in these species. The detection and localisation of a sound source is of considerable biological importance to many fish species; the pallid sturgeon (*Scaphirhynchus albus*) and shovelnose sturgeon (*S. albus*), are both known to produce a range of sounds during the breeding season (Johnston & Phillips, 2003). Sounds are often used by fish to assess the suitability of a potential mate or during territorial displays (Nordeide & Kjellsby, 1999), and during predator prey interactions (Myrberg, 1981). This is the first time that the inner ears of *P. spathula* and *A. fulvescens* have been studied using the Scanning Electron Microscope (SEM), and follows an earlier work by Popper (1978) on the ultrastructure in the ear of the shovel-nose sturgeon (*Scaphirhynchus platorynchus*).

2. Materials and Methods

In order to concisely identify the frequency and intensity of sounds audible to paddlefish, twelve specimens of *P. spathula*, of mixed sex, and ranging in size from 160 mm (58 g) (measured from the tail fork to the anterior of the jaw) to 230 mm (163 g) were stimulated with sounds ranging in the frequency domain between 100 Hz to 1500 Hz. In addition, twelve mixed sex specimens of lake sturgeon, ranging in size from 230 mm (61.8 g) (fork length) to 280 mm (95.4 g), were also stimulated in a similar manner. The water temperature in both the holding tanks and test tank ranged between 18.2 and 18.6 ° C over a 24 hour period, and when not under experimental protocols, the fish were provided with 16 hours of light per day.

2.1 ABR methodology

The ABR measurements of hearing thresholds were made using a control and analysis program, which both generated the stimulus signals, and captures and analyses the response. The stimulus used was a pulsed 4 cycle tone burst, which was presented to the fish at a given frequency and intensity. ABR recordings require no invasive procedural work, as measurements are taken in the electro-physiological far field using two cutaneous electrodes placed against the skin above the ear and medulla; the application of this methodology results in significant stress reduction during the hearing assessment

(Kenyon et al., 1998). The ABR trace is formed by averaging peak potentials arising from centres in the auditory pathways from the periphery of the VIII nerve to the midbrain (Corwin et al., 1982; Overbeck and Church, 1992). Attenuated waveforms are considered as being below the threshold of hearing when two overlaid recordings, made at the same frequency and intensity, do not present with similarities or are in opposition (e.g. Kenyon et al., 1998).

Small fish (below 230 mm) were first placed lengthwise and centrally on a 160 mm x 120 mm rectangle of fine nylon netting, which was wrapped firmly around the body and tail, and the two sides of the net were held together using a "bulldog" clip (Figure 1). The clip was placed in a retort stand clamp fitted with ball joint electrode manipulator arms and an aerated water supply pipe (detailed in Figure 1). Large fish (above 250 mm) were placed in a clear rubber coated 1 mm gauge wire mesh cradle. A reservoir of oxygenated water was positioned 1 m above the experimental tank and gravity fed at an adjustable flow rate of between 5 millilitres per second for the small fish, to 12 millilitres per second for the large, and directed toward the gills through a soft rubber mouth tube with a diameter of 6 mm.

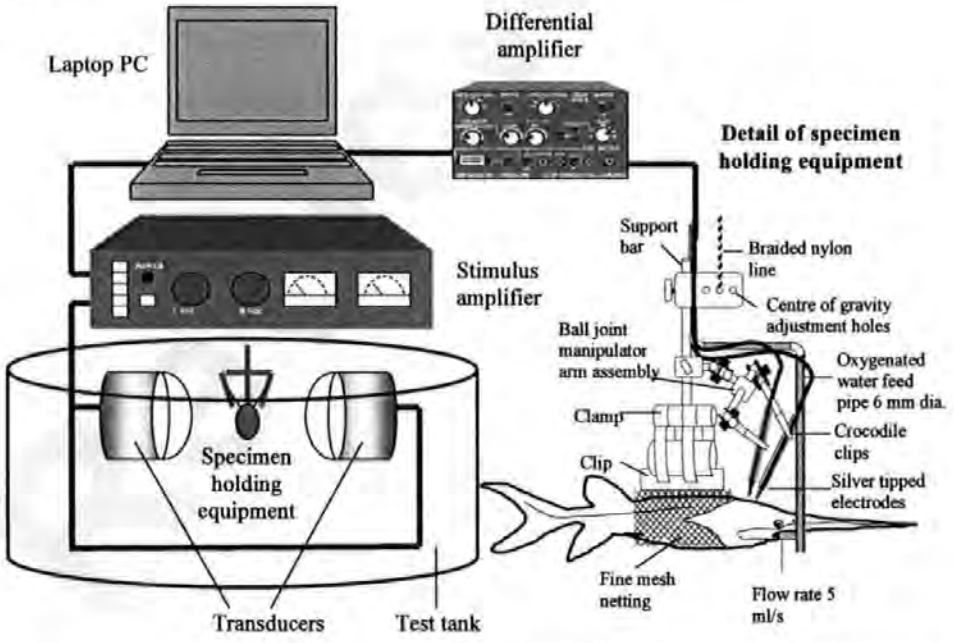

Figure 1. Schematic of the experimental setup and detail of the clamp used to hold the fish in position and manipulate the electrodes during the audiological tests

The electrophysiological response to acoustic stimulation was recorded using two cutaneous electrodes, which were connected to the differential amplifier by 1 m lengths of screened coaxial cable with an external diameter of 1.5 mm. The impedance between the electrode tip and pre-amplifier was found to be 0.2 Ω for both electrodes and recorded an open circuit between the outer shielding and inner core. The record electrode was placed 6 mm anterior of the reference electrode which was positioned centrally against the epidermis above the medulla. The dermal elements of the skull are ossified in *A. fulvescens*, making electrophysiological recordings difficult, as there was no fleshy skin on the head for the electrode to push against and create a good connection. This resulted in the 0.3 mm silver tip being almost entirely exposed to the ambient water, which can substantially attenuate the evoked potential. To resolve this issue, silicone tip insulators were used to create a seal around the electrode tip and fish, thus preventing the ambient water from contacting the electrodes. Stimulus sounds were presented to the fish at sound pressures initially not exceeding 150 dB re 1 μPa and attenuated in 5 dB steps, with a variable attenuation of around 2 dB as threshold was approached. The evoked response was amplified and digitised to 12 bits resolution and recorded. This process was repeated 2000 times and the response averaged to remove electrical interference caused by neural activities other than audition, and the myogenic noise generated by muscular activity. Each measurement was repeated twice; this aids in separating the evoked response, which is the same from trace to trace, from the myogenic noise, which varies in two successive measurements.

2.2 The sound field

In this experiment, we generate the stimulus tones using two Fish Guidance Systems Ltd. Mk II 15-100 sound projectors, submerged to a depth of 200 mm and arranged to face each other at a distance of 200 mm. The fish was also stationed at a depth of 200 mm, with the midline positioned at equal distances from the left and right transducers. Where the projectors are driven in phase, it is possible to create a region between them of high sound pressure, and low particle velocity, and when driven out of phase, the transducers create an area associated with high particle motion and minimal sound pressure; the difference between the two sound fields can be easily measured using a pressure sensitive hydrophone. A similar transducer setup to the one described here was used by Enger and

Anderson (1967), in a comparative study of audition in the cod (*Gadus morhua*) and the sculpin (*Cottus scorpious*). After a series of experiments conducted mostly in the acoustic near field, that involved a highly complex surgical procedure to implant the electrodes, it was concluded that the swim bladder of generalist teleost fish is essential for audition. However, Popper and Fay (1993) are highly critical of these findings, as fluctuations in the swim bladder volume in a pressure field, are subjected to substantial attenuation as they pass through the flesh and bone to the inner ear (see also Yan et al., 2000). A schematic of the equipment used to acquire the audiometric measurements is presented in Figure 1, with the stimulus tones generated by a laptop computer running the ABR software and a Tandy 250 W power amplifier. The projectors were driven directly from the amplifier, and the stimulus tones presented to the fish were measured using a Bruel and Kjaer Type 8104 calibrated Hydrophone, and the signal amplified by a Bruel and Kjaer Type 2365 Charge Amplifier (see Lovell et al., 2005a, for more details). In this method, the intensity of the sound is recorded in the absence of the fish, with the hydrophone positioned where the ears of the fish would be during the experiment.

2.3 Preparation of the saccule prior to SEM examination

The preparation methodology employed in this study was based on techniques used by Platt (1977). Twelve specimens of *P. spathula* and twelve of *A. fulvescens* were anesthetised using MS-222 in a water bath; the fish were dispatched using conventional protocol approved by the University of Illinois Institutional Animal Care and Committee (IACUC) 15.11.04 (protocol # 04271). The cranium containing the inner ears from *P. spathula* and *A. fulvescens* were trimmed to small blocks and immersed in chilled fixative (2.5% glutaraldehyde in 0.1 M cacodylate buffer with 3.5% sodium chloride), and delivered to the Plymouth EM unit within 72 hours post removal. The ears and surrounding tissue were subsequently immersed in a watch glass containing 30 % ethanol; then, working under a MEIJI trinocular microscope, the ear and VIII nerve was dissected from the remaining cranial tissue and photographed. The contrast between the nerves and end organs was optimised for photography by varying the levels of transmitted light from the base of the microscope with the direct light provided by an Olympus fibre optic highlight. The end organs were then dissected and the otoliths carefully removed. Encapsulating tissue was dehydrated through a graded ethanol series

ranging from 35% through 50%, 70% and 90% to absolute ethanol, prior to desiccation using the critical point drying method. Fully desiccated capsules were subsequently mounted on a specimen stub using a carbon tab, and coated with c. 8 nm of gold in an Emitech K 550 sputter coater (working at approximately 5 x 10^{-6} Torr). The processed specimens were investigated and photographed using a JEOL JSM 5600 scanning electron microscope operated at 15 kv, and a 15 mm working distance. The eucentric stage holding the specimen was aligned for 'planar' image acquisition, and each sample was examined by adjusting the position of the stage in x and y coordinates only. All measurements were carried out on a PC using the analySIS® (Soft Imaging System GmbH) program, and the distance between cell bases and the length of the ultrastructure were measured in units of micrometers using the JEOL software. Statistical calculations were carried out using Statgraphics plus 5.1 professional edition program, and an analysis of variance (ANOVA) was also used to test for similarity in the distances between neighbouring hair cell bases from both *P. spathula* and *A. fulvescens*.

3. Results

3.1 Electrophysiology

Figure 2 illustrates the auditory evoked potentials from *P. spathula* in response to tone bursts at frequencies of 100 Hz, 200 Hz, 250 Hz, 300 Hz and 500 Hz, in response to both sound pressure and particle motion. Each of the waveform sets recorded from stepped amplitudes from a particular frequency have been overlaid, revealing a latency change in response to the attenuation in the intensity of the sound. Above threshold EP waveforms in both Figures are presented with a blue colour coding, whilst below threshold recordings are orange or red. At each frequency, the ABR waveforms evoked by the tone bursts typically consisted of a series of four to eight rapid negative peaks, followed by a slow positive deflection. The onset latency of the centre or largest sinusoid of the ABR response varied with frequency, ranging from 7.3 ms after stimulus onset at 100 Hz to 5 ms at 500 Hz. As the sound pressure levels approached threshold, 2000 sweeps were required to distinguish ABR's from the background electronic noise.

The left column in Figure 2 shows waveforms recorded from *P. spathula* in response to a 4 cycle tone burst ranging in frequency from 100 to 500 Hz, presented in a sound field dominated by particle motion, whilst the right column presents waveforms recorded in a sound field dominated by Sound Pressure.

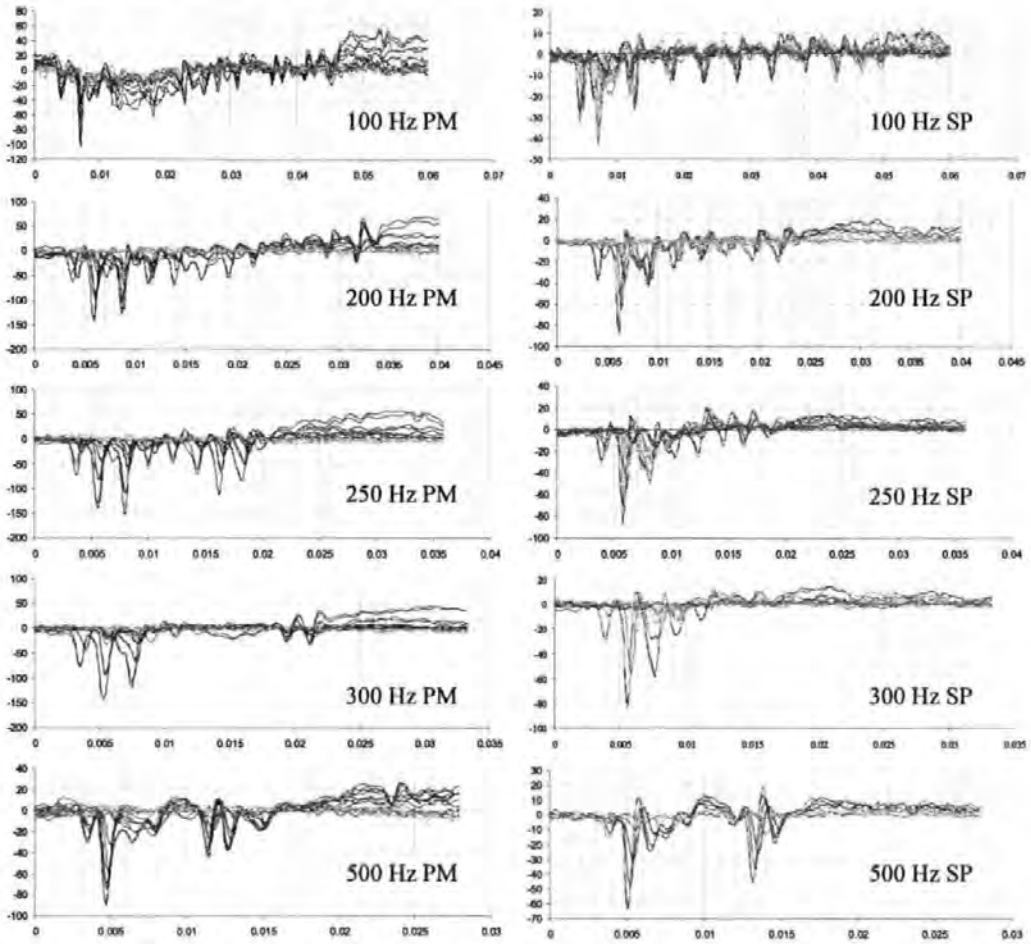

Figure 2. Averaged waveforms evoked from *P. spathula* in response to four cycle tone bursts of 100 Hz to 500 Hz, attenuated in steps of between 6 dB to 0.5 dB as threshold is approached. The waveforms in the left column were recorded with the sound fields dominated by Particle Motion (PM) and the right column in Sound Pressure (SP). The waveforms in blue show above threshold responses, whilst the other colours represent below threshold myogenic noise (y axis scale = microvolts * 100, x axis scale = time (s))

As can be seen in Figure 2, the waveforms are similar at each frequency and presentation mode (sound pressure or particle motion), though there is a slight increase in the duration of the evoked potentials by 1 to 2 ms when stimulating in a sound field dominated by particle motion. Also, the particle motion waveforms above 100 Hz are followed by smaller responses with similar characteristics, which are probably the result of reflected sound waves. These responses to "echoes" are not present in the sound pressure results except at 500 Hz, which appears to evoke a very similar response from the two stimulus modes. Figure 3 presents waveforms from *A. fulvescens* recorded under identical conditions to *P. spathula*, though as previously discussed, the heavily ossified cranium of *A. fulvescens* effectively reduced the contact area between the electrode and fish, thus resulting in a reduction in the EP quality.

In Figure 3, the evoked potentials from *A. fulvescens* are similar in overall shape to the waveforms recorded from *P. spathula*, presented in Figure 2; however, they are noticeably lower in amplitude. This is especially evident in the particle motion waveforms (left column in Figure 3), and is attributed to the reduced contact area between the electrode tip and cranium. Although present, the waveforms following the initial response (the "echoes") are also considerably lower in intensity than those recorded from *P. spathula*, and again reflect the difficulties encountered when recording AEP's from *A. fulvescens*. The Inter Peak Latency (IPL) observed clearly in the *P. spathula* waveforms are not so pronounced in *A. fulvescens*, though are clearest in the 100 Hz sound pressure results; however, the absence of a sharp AEP peak has a considerable effect on the lucidity of the IPL at all frequencies tested.

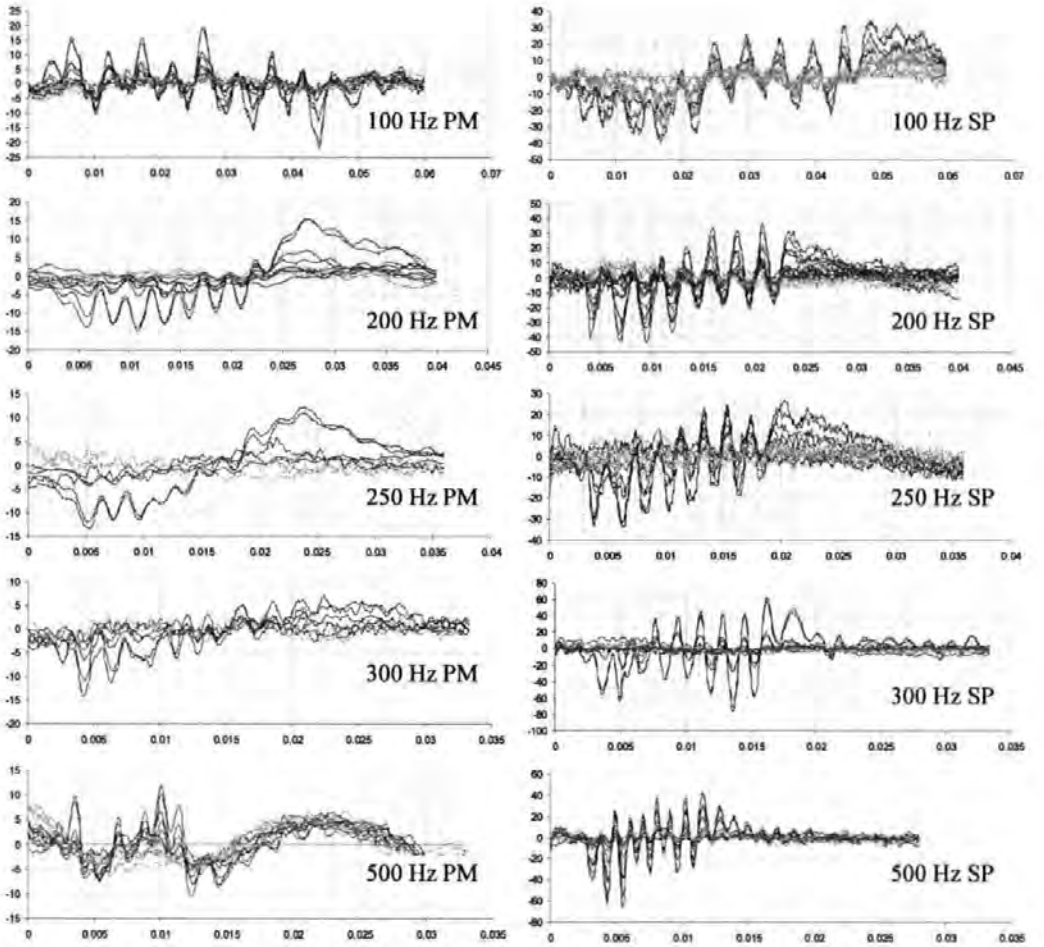

Figure 3. Averaged waveforms evoked from *A. fulvescens* in response to four cycle tone bursts of 100 Hz to 500 Hz, attenuated in steps of between 6 dB to 0.5 dB as threshold is approached. The waveforms in the left column were recorded with the sound fields dominated by Particle Motion (PM) and the right column in Sound Pressure (SP). The waveforms in blue show above threshold responses, whilst the other colours represent below threshold myogenic noise (y axis scale = microvolts * 100, x axis scale = time (s))

Figure 4 shows ABR waveforms evoked from a 300 Hz tone burst, presented initially at 150 dB (re. 1 μPa), and attenuated in steps of between 6 to 4 dB ordinarily, then in 2 dB steps to 0.5 dB as the hearing threshold was approached. When two replicates of waveforms showed dissimilar polarities, as seen in the traces for the results at 130 dB in Figure 4, the response was considered as being below threshold (cf. Kenyon et al., 1998).

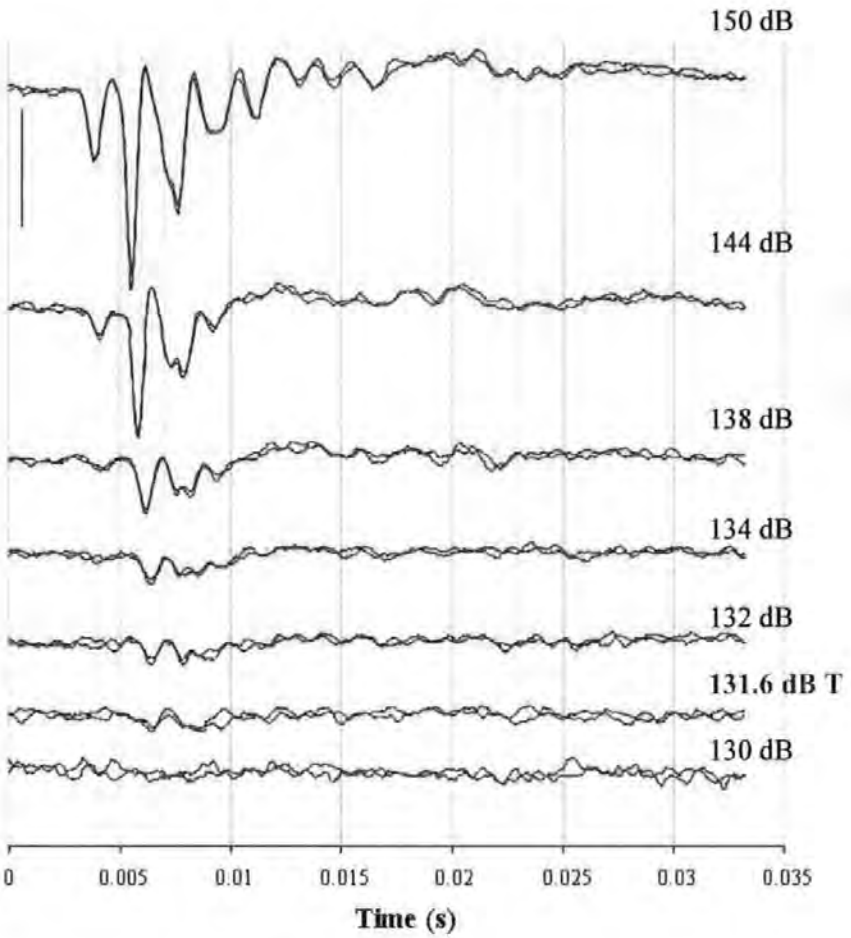

Figure 4. ABR waveforms from *P. spathula* in response to a 300 Hz tone burst attenuated in sequential steps. Averaged traces of two runs (2000 sweeps each), for each intensity are overlaid and arranged sequentially. The T at 131.6 dB represents threshold. Bar = 0.5 μv

All threshold responses were measured in this way, with each audiogram produced using the sequential ABR waveform data (e.g. Figures 2 and 3), acquired from frequencies of 100 Hz to 500 Hz. The individual audiograms acquired from the populations of *P. spathula* and *A. fulvescens* were combined to create an average composite audiogram (Figure 5), using both the mean and standard deviation data.

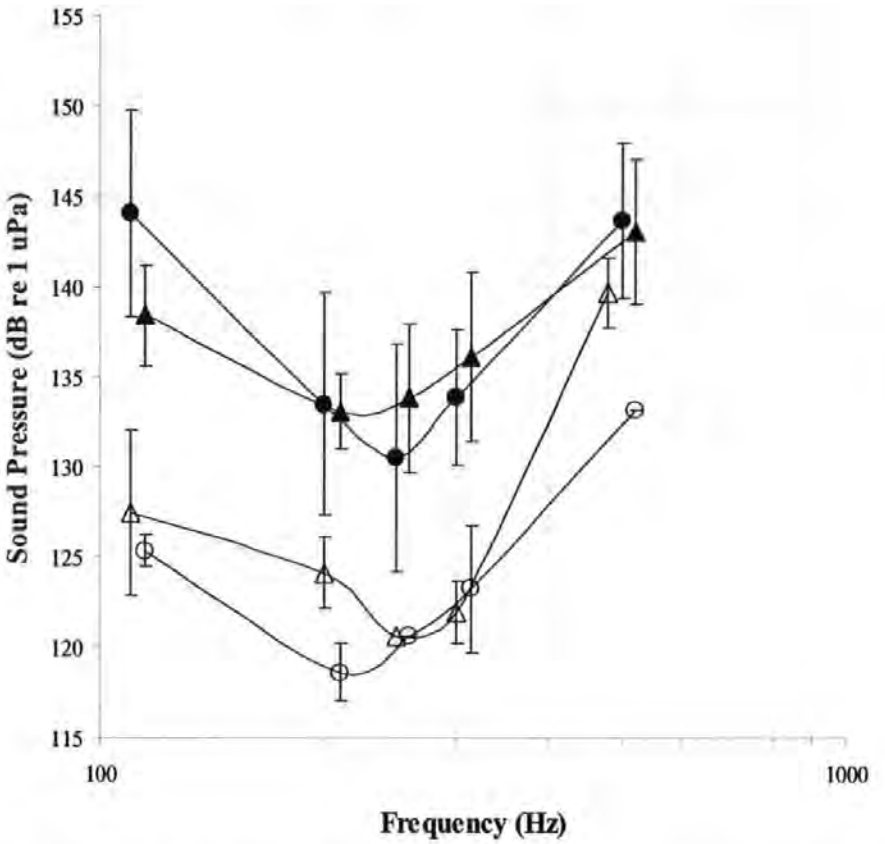

Figure 5. Audiograms for *A. fulvescens* (closed circles = maximum sound pressure; open circles = maximum particle motion), and for *P. spathula* (closed triangles = maximum sound pressure; open triangles = maximum particle motion). The audiograms were generated using the sequential ABR waveform data presented in Figures 2 and 3, acquired from frequencies between 100 Hz to 500 Hz (error bars show the standard deviation of the threshold responses and are separated by 5 to 20 Hz for ease of viewing)

The audiograms follow a Gaussian profile, determined by calculating the lowest intensity stimulus sounds (recorded underwater using the hydrophone located adjacent to the fish ear) that evoked a repeatable ABR response (e.g. 131.6 dB in Figure 4). The lowest hearing thresholds with the sound field dominated by sound pressure (transducers driven in phase) was 130.5 dB (re 1 μPa) at 250 Hz for *P. spathula*, and 133 dB (re 1 μPa) at 200 Hz for *A. fulvescens*. Lower thresholds were recorded when the sound field was dominated by particle motion (transducers driven out of phase), and the lowest response

was 120.7 dB (re 1 μPa) at 250 Hz for *P. spathula*, and 118.2 dB (re 1 μPa) at 200 Hz for *A. fulvescens*.

It is known that the frequency and intensity of a tone burst effects the latency of the evoked response (Corwin et al., 1982; Kenyon et al., 1998), as does the metabolic state of the organism (Corwin et al., 1982). The Inter-Peak Latency (IPL) of the evoked potentials from *P. spathula* can be observed in Figure 6, and are in response to the second sinusoid of a 300 Hz tone burst. The sound pressure recorded at each attenuation follow the sequential steps defined in Figure 4; the arrows positioned at 0.3 ms intervals represent the vertex positive component issuing from the neural centres situated along the auditory pathway to the midbrain (Overbeck and Church., 1992).

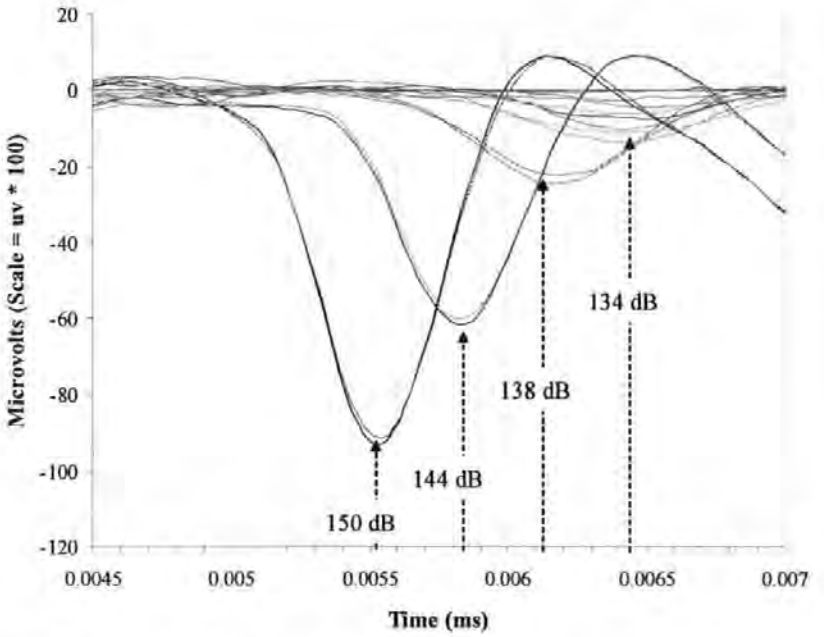

Figure 6. Auditory Evoked Potentials (AEP's) from *P. spathula* in response to the second sinusoid of a 300 Hz 4 cycle tone burst presented initially at 150 dB (re 1 μPa), and attenuated in accordance with Figure 4. The arrows show the peak of the AEP, which occurs with an Inter-Peak Latency (IPL) of approximately 0.3 ms for each of the amplitudes tested (averaged over 2000 iterations per waveform set)

The increase in the latency of the evoked potential in response to decreasing stimulus intensity is often used to verify that the averaged waveform is a product of auditory stimulation rather than a transient generated at the electrode tip (Kenyon et al., 1998). Thus, the Inter-Peak Latency (IPL) cannot be accounted for acoustically, as transients and other artefacts directly associated with the stimulus sound would occur at the same time regardless of sound amplitude. The increase in the latency of the evoked potential in response to decreasing stimulus intensity is often used to verify that averaged waveforms are a product of auditory stimulation rather than a transient generated at the electrode tip (Kenyon et al., 1998).

3.2 Gross anatomy

Figure 7 illustrates the left ear and peripheral auditory nerves from *P. spathula*; the saccule (***s***) and lagena (***l***) are situated in close proximity to one another, and the two otoliths that can be seen in the Figure are similar in size. The peripheral nerves innervating the saccule and lagena (*rs*) share a pathway with the nerves from the posterior ampulla (*pa*); the peripheral nerve bundle projects forward, and connect with the utricular nerve and ramulus anterior ampulla (*raa*) to form the VIII octaval nerve. In both species, there is no internal division between the saccule and lagena, thus the pars inferior consists of just one fluid filled pouch.

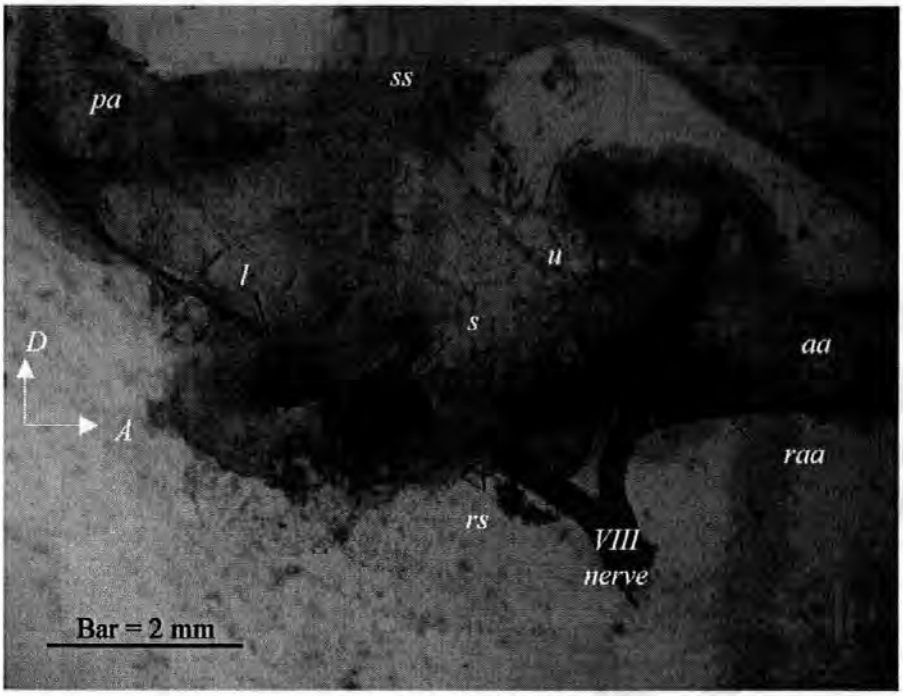

Figure 7. The left ear and VIII nerve from *P. spathula*; *aa.* anterior ampulla , *pa.* posterior ampulla, *l.* lagena, *raa.* ramus anterior ampulla, *s.* saccule, *ss.* sinus superior, *u.* utricle. The annotations D (dorsal) and A (anterior) show the orientation of the ear in the fish. Bar = 2 mm

3.3 Electron microscopy

Figure 8.a shows the saccule and lagena from a 200 mm (90 g) *P. spathula*, and 8.b from a 260 mm (90 g) *A. fulvescens*; Figure 8.c shows the utricle from *P. spathula* and 8.d from *A. fulvescens*. The micrographs have been annotated to show the macula area (hatched lines), and the hair cell polarisations are indicated by white arrows. The area of the saccule and lagena macula was both found to be 0.36 mm^2 for *P. spathula*, and 0.44 mm^2 and 0.42 mm^2 respectively for *A. fulvescens*. The utricular macula had an area of 0.63 mm^2 in *P. spathula*, and 0.64 mm^2 for *A. fulvescens*.

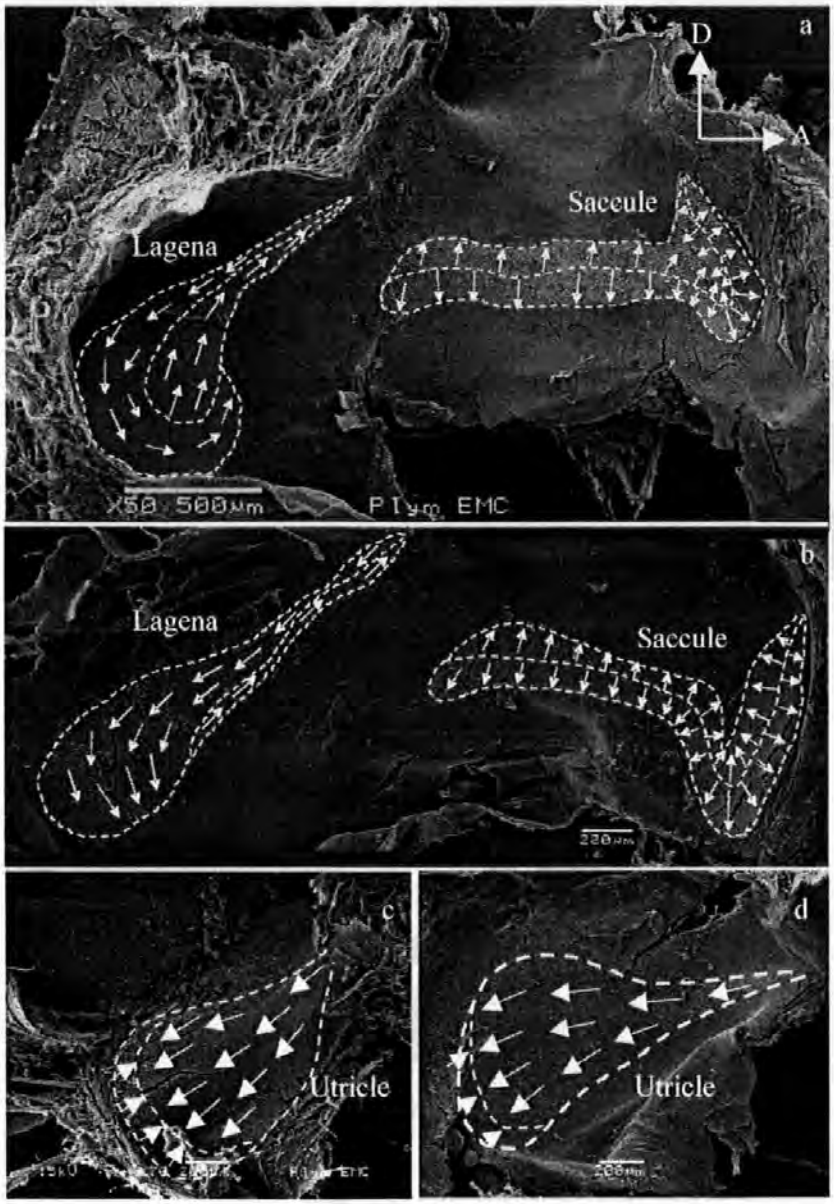

Figure 8. Electron micrographs of the right inner ear end organs annotated with arrows to show hair cell polarisations across the sensory surface. **a.** the saccule and lagena from a 200 mm (90 g) *P. spathula*, **b**. the saccule and lagena from a 260 mm (90 g) *A. fulvescens*, **c.** the utricle from *P. spathula*, and **d.** from *A. fulvescens*. Anterior (A) and dorsal (D) represent orientation of the organ within the fish

The hair cells on the saccular maculae of both species (Figures 9.a and b) are divided into two oppositely oriented groups, with cells on the posterior macula oriented dorsally on the dorsal posterior quadrant and ventrally on the ventral posterior quadrant. The anterior

region of the macula has hair cells orientated toward the anterior and posterior of the fish. Figures 9.c and d present hair cells from the lagena of both species and 9.e and f are from the utricle.

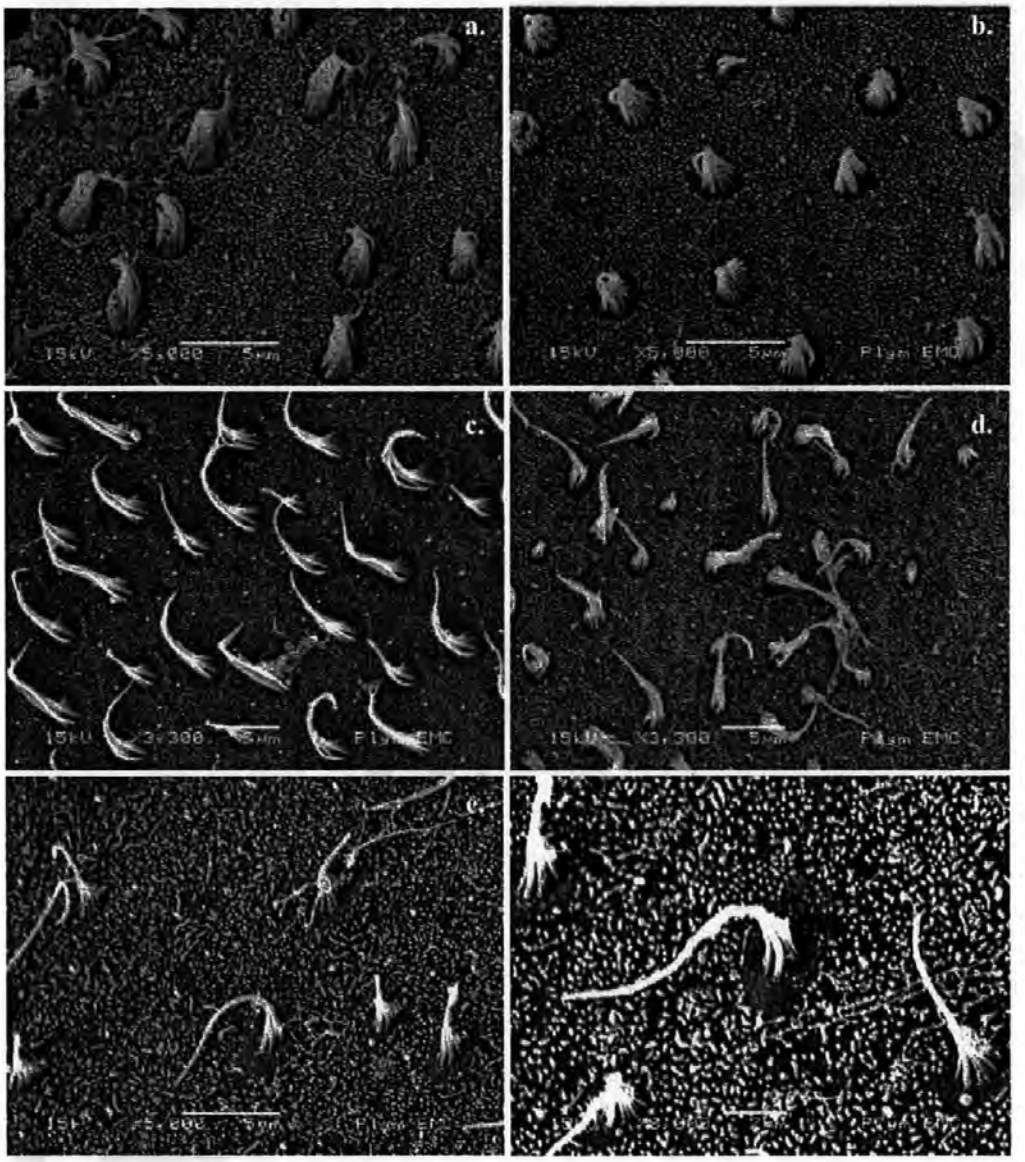

Figure 9. Saccular hair cells from **a.** *P. spathula*, and **b.** *A. fulvescens*. Lagena hair cells from **c.** *P. spathula*, and **d.** *A. fulvescens*. Utricular hair cells from **e.** *P. spathula*, and **f.** *A. fulvescens*.

The hair cells on the saccule from both species (Figures 9.a and b) have up to 40 stereocilia partially surrounding a single kinocilium 3 μm in length, positioned close to the anterior of the cell. Each hair cell is buttressed by what appear to be support cells, which present with small centrally placed microvillus like structure, in evidence on both inferior maculae. The hair cells on the lagena (Figures 9.c and d) have long stereocilia (up to 6 μm in length), and partially surround a 9 μm kinocilium. Both the longest and shortest hair cells were found proliferating on the utricular macula, which presents with kinocilium lengths of between 12 to 15 μm around the perimeter, down to as short as 1.3 μm in the central (striola) region (Figures 9.e and f). The number of hair cells proliferating on each end organ was approximated from at least 12 observations taken from around the macula from a 200 mm *P. spathula*, and a 260 mm *A. fulvescens*. The numbers of hair cells on the saccular macula was approximately 4600 from *P. spathula*, and 6800 from *A. fulvescens*. In the order of 3600 hair cells were found on the lagena macula of *P. spathula*, and 5000 on the lagena of *A. fulvescens*, and approximately 8000 hair cells were found on the utricular maculae from both species.

4. Discussion

The pallid sturgeon (*Scaphirhynchus albus*) and shovelnose sturgeon (*S. albus*) are known to produce a wide variety of sounds ranging from squeaks and chirps of around 1000 Hz to 2000 Hz, to low frequency knocks and moans ranging in frequency between 90 Hz to 400 Hz (Johnston & Phillips, 2003). A comparison of the sounds produced by these fish with the audiogram for A. fulvescens reveals that the knocks and moans produced during the breeding season, fall well within the optimum range of audible frequencies and may serve an ecological purpose to Acipenseriform fish. However, the squeaks and chirps fall well outside of this range and are probably incidental, thus serving no purpose in communication between conspecifics.

This is the first time that fish from the order Acipenseriformes have been assessed in an ABR audiological examination, so by testing both *P. spathula*, and *A. fulvescens*, it allows for a comparative analysis of the results between both species. Twelve specimens of *A. fulvescens* and *P. spathula* were stimulated with sounds ranging in the frequency

domain between 100 Hz to 1500 Hz, though no AEP's were recorded above 500 Hz. Stimulus sounds were presented to the fish at levels of between 156 dB to below 120 dB (re 1 μPa), with the transducers driven either in or out of phase. The phase of the transducers creates a region around the fish with high sound pressure and low particle motion, or high particle motion and low sound pressure. The results of the partner study on audition in the Asian carp (Lovell et al., in prep), show that the range of frequencies and the threshold values of sounds audible to *H. molitrix* and *A. nobilis* compare well with the audiogram for the specialist catfish (*Ictalurus punctatus*) produced by Fay and Popper (1975). Thus, sounds intended to deflect *H. molitrix* and *A. nobilis* can be presented in such a way, as to be significantly less audible to *P. spathula* and *A. fulvescens*. Where the projectors are driven in phase, it is possible to create a region between them of high sound pressure, which is less audible to *P. spathula* and *A. fulvescens* than when the transducers are driven out of phase. This finding has considerable bearing on the efficiency and selectivity of bio-technological control systems that rely on acoustics, such as the AFD barrier introduced in this study.

The hearing thresholds from *P. spathula* and *A. fulvescens* in a sound field dominated by particle motion were found to be similar at all frequencies tested; in some cases (e.g. 250 Hz and 500 Hz) there was very little to distinguish between individuals. The lowest hearing thresholds were acquired from frequencies in a bandwidth of between 200 Hz to 300 Hz. This finding is in contrast with many generalist fish audiograms, which show the lowest thresholds are often obtained from frequencies at or below 100 Hz; such as the results of the ABR audiogram for the Italian freshwater gobies *Padogobius martensii* and *Gobius nigricans* (Lugli et al., 2003), or the behavioural audiogram for the cod (*Gadus morhua*) (Chapman and Hawkins, 1973). The lowest hearing thresholds with the sound field dominated by sound pressure (transducers driven in phase) was 131 dB (re 1 μPa) at 250 Hz for *P. spathula*, and 133 dB (re. 1 μPa) at 200 Hz for *A. fulvescens*. The lowest hearing thresholds with the sound field dominated by particle motion (transducers driven out of phase) was 119 dB (re 1 μPa) at 200 Hz for *P. spathula*, and 120 dB (re 1 μPa) at 250 Hz for *A. fulvescens*. However, Kenyon et al. (1998) found that ABR thresholds from the generalist oscar (*Astronotus ocellatus*) were significantly lower than behavioural thresholds, which occurred at sound pressures greater than 118 dB (re. 1 μPa). However,

the particle motion ABR audiograms obtained from both species examined in this study gave results that were similar, though slightly higher, than the behavioural audiogram for the oscar. In normally hearing humans, Gorga et al. (1988) found that ABR thresholds were higher than behavioural thresholds for all frequencies tested, especially from lower frequencies where intersubject variability was also greater. Worthy of note here, is the similarity of the sound pressure audiograms from both *P. spathula* and *A. fulvescens* to an ABR generated audiogram for the little skate *Leucoraja erinacea* by Casper et al., (2003).

As generalist fish are shown here to respond to the motion of the water particles in a sound field, rather than the sound pressure component, it would be prudent to measure the audiogram in units of particle velocity rather than sound pressure. However, for this study in particular, the use of a sound pressure in the audiogram is acceptable, as the target species for the AFD barrier are the pressure sensitive Asian carps *H. molitrix* and *A. nobilis*. The results of the auditory examination clearly show that *P. spathula* and *A. fulvescens* are not sensitive to sound pressure, and will therefore have a significantly higher deterrent threshold than *H. molitrix* and *A. nobilis* in a pressure dominated sound field. It is therefore concluded that an Acoustic Fish Deterrent (AFD) barrier generating a pressure dominated sound field of sufficient intensity to deter non-indigenous Asian carps from crossing, will be practicably inaudible to indigenous species and will thus have little or no influence on the ecology of paddlefish and sturgeon.

In most teleost fish the pars inferior comprises two fluid filled pouches, the saccule and lagena, though in *P. spathula* and *A. fulvescens*, there is no internal division between the two end organs. This feature is common to the ears of a number of non-teleost species, such as *S. platorynchus* (Popper, 1978) and the lungfish Protopterus (Platt et al., 2004). For fish to locate the source of a sound in both the horizontal and vertical planes, they rely on the stimulation of ciliary bundles oriented specifically along the sound propagation axis (Lu & Popper, 1998). In *P. spathula* and *A. fulvescens*, the saccule bears hair cells divided into two oppositely oriented groups, a feature also seen in *S. platorynchus* (Popper, 1978). The topographic data from the saccule shows that caudal hair cells are orientated on the dorsal and ventral axis, whereas the anterior hair cells are

orientated on the anterior posterior axis with respect to the fish. The shape and polarisation of the hair cells of the lagena and utricular macula in *P. spathula* and *A. fulvescens* are similar to the arrangement found in many fish (see Lovell et al., 2005 B and 2005 C; Popper & Fay, 1993).

Acknowledgments

The authors would like to acknowledge Dr Michael Fine of the Virginia Commonwealth University for his great assistance in the production of this manuscript, and Kevin Irons and all the staff at the Illinois River Biological Station for their hospitality and great expertise in the acquisition and maintenance of the fish studied in this work.

The authors also express gratitude to Dr J.R. Nedwell of Subacoustech Ltd for the provision of equipment and technical support

References

Casper, B.M., Lobel, P.S., Yan, H.Y., 2003. The hearing sensitivity of the little skate, *Raja erinacea*: A comparison of two methods. Environmental Biology of Fishes. 68, 371 – 379

Chapman, C.J. and Hawkins, A.D., 1973. A field study of hearing in the cod, *Gadus morhua*. Journal of comparative Physiology: 85, 147-167.

Corwin, J.T., 1981. Audition in elasmobranchs. In: W.N. Tavolga, A.N. Popper & R.R. Fay (eds.) Hearing and Sound Communication in Fishes, Springer-Verlag, New York. pp. 81 102.

Corwin, J.T., Bullock, T.H., & Schweitzer, J., 1982. The auditory brain stem response in five vertebrate classes. Electroencephalogr. Clin. Neurophysiol. 54, 629-641

Edds-Walton, P.L. & Fay, R.R., 2002. Directional auditory processing in the oyster toadfish (*Opsanus tau*). Bioacoustics, 12, 202-204.

Enger, P.S. & Anderson, R., 1967. An electrophysiological field study of hearing in fish. Comp Biochem Physiol 22, 517-525

Fay, R.R., & Edds-Walton PL., 1997. Directional response properties of saccular afferents of the toadfish, (*Opsanus tau*). Hearing Research 111, 1-21

Fay, R.R., & Popper, A.N., 1975. Modes of stimulation of the teleost ear. J. Exp. Biol 62, 370-387.

Fine, M.L., 1981. Mismatch between Sound Production and Hearing in the Oyster Toadfish. In: Hearing and Sound Communication in Fishes, Tavolga, W.N. et al (eds.), 257-263.

Gorga, M.P., Kaminski, J.R., Beauchaine, K.A., Jesteadt, W., 1988. Auditory brainstem responses to tone bursts in normally hearing subjects. J Speech Hear Res. 31, 87-97

Jacobson, J.T., 1985. An overview of the auditory brainstem response. In: Jacobson JT (ed) The auditory brainstem response. College-Hill Press, San Diego, 3-12

Jewett, D.L., 1970. Volume conducted potentials in response to auditory stimuli as detected by averaging in the cat. Electroencephalogr Clin Neurophysiol. 28, 609-618

Jewett, D.L. & Williston, J.S., 1971. Auditory evoked far fields averaged from the scalp of humans. Brain. 94, 681-696

Johnston, C.E. & Phillips, C.T., 2003. Sound production in sturgeon *Scaphirhynchrus albus* and *S. platyrynchus* (Acipenseridae). Env. Biol. Fish. 68, 59-64.

Kenyon, T.N., Ladich, F. & Yan, H.Y., 1998. A comparative study of the hearing ability in fishes: the auditory brainstem response approach". J. Comp. Physiol. A. 182, 307-318.

Lovell, J.M., Findlay, M.M., Moate, R.M., & Yan, H.Y., 2005 A. The hearing abilities of the prawn *Palaemon serratus*. Comp. Biochem. Physiol. A Mol. Integr. Physiol. 140, 89-100.

Lovell, J.M, Findlay, M.M., Moate, R.M., & Pilgrim, D.A., 2005 B. The polarization of inner ear ciliary bundles from a scorpaeniform fish. J. Fish. Biol. 66, 836-846

Lovell, J.M, Findlay, M.M, Harper, G, Moate, R.M & Pilgrim, D.A., 2005 C. The polarisation of hair cells from the ear of the European bass (*Dicentrarchus labrax*). Comp. Biochem. Physiol. A Mol. Integr. Physiol. 141, 116-121

Lovell, J.M., Findlay, M.M, Nedwell, J.R., Pegg, M.A., in prep. The hearing abilities of the silver carp *H. molitrix* and bighead carp *A. nobilis*

Lu, Z., & Popper, A.N., 1998. Morphological polarizations of sensory hair cells in the three otolithic organs of a teleost fish: fluorescent imaging of ciliary bundles. Hear. Res. 126, 47-57.

Lu, Z. & Popper, A.N., 2001. Neural response directionality correlates of hair cell orientation in a teleost fish. J. Comp. Physiol. A. 187, 453-465.

Lugli, M, Yan, H.Y, and Fine M.L., 2003. Acoustic communication in two freshwater gobies: the relationship between ambient noise, hearing thresholds and sound spectrum. J Comp Physiol A. 189, 309-320

Myrberg, A.A., 1981. Sound communication and interception in fishes. Hearing and Sound Communication in Fishes. Tavolga WN, Popper AN, and Fay RR, Eds. Springer-Verlag, New York.

Nordeide, J.T., & Kjellsby, E., 1999. Sound from spawning cod at their spawning grounds. ICES Journal of Marine Science. 56, 326-332.

Overbeck, G.W., & Church, M.W., 1992. Effects of tone burst frequency and intensity on the auditory brainstem response (ABR) from albino and pigmented rats. Hear Res. 59, 129-137

Platt, C., 1977. Hair cell distribution and orientation in goldfish otolith organs. J. Comp Neurol. 172, 283-297

Platt, C., Jorgensen, J.M., Popper, A.N., 2004. The inner ear of the lungfish Protopterus. J. Comp. Neurol. 471, 277-88

Popper, A.N., 1978. Scanning electron microscopic study of the otolithic organs in the bichir (*Polypterus bichir*) and shovel-nose sturgeon (*Scaphirhynchus platorynchus*). J Comp Neurol. 181, 117-28

Popper, A.N., & Fay, R.R., 1993. Sound detection and processing by fish: critical review and major research questions. Brain Behav Evol. 41, 14-38

Taylor, R.M., Pegg M.A., & Chick, J., In Press. Effectiveness of two bioacoustic behavioral fish guidance systems for preventing the spread of bighead carp to the Great Lakes. North American Journal of Fisheries Management.

Yan, H.Y., 1995. Investigations of fish hearing ability using an automated reward method. In: Methods in Comparative Psychophysics (eds) G. M. Klump, R. J. Dooling, R. R. Fay, and W. C. Stebbins. Birkhauser Verlag Basel/Switzerland. 263-276.

Yan, H.Y., Fine, M.L., Horn, N.S., Colon, W.E., 2000. Variability in the role of the gasbladder in fish audition. Journal of Comparative Physiology A. 186, 435-445.

Appendix ii

In review manuscripts

Lovell, J.M, Jepson, P.D, Moate, R.M & Sabin, R.C. Comparative Examination of the Inner Ear from the Common Dolphin (*Delphinus delphis*) and the Harbour Porpoise (*Phocoena phocoena*). Journal of Anatomy.

Lovell, JM, Christiansen, L, Findlay, MM & Moate, RM. The influence of body size on the form and function of the statocyst from the prawn (*Palaemon serratus*). Journal of Experimental Biology

Lovell, J.M, Findlay, M.M, Nedwell J.R, & Pegg M.A. The hearing abilities of the silver carp (*Hypopthalmichthys molitrix*) and bighead carp (*Aristichthysc nobilis*). Comp. Biochem. Physiol. A Mol. Integr. Physiol.

The morphology of the cetacean inner ear and methodology for viewing mammalian ultrastructural hair cells for environmental monitoring

J.M. Lovell[1], M.M. Findlay[1], P. D. Jepson[3], R.M. Moate[2] and R.C. Sabin[4]

[1]School of Earth, Ocean and Environmental Sciences j.lovell@plymouth.ac.uk, [2]Plymouth Electron Microscopy Centre, University of Plymouth, Drake Circus, Plymouth PL4 8AA. [3]Institute of Zoology, Zoological Society of London, Regents Park, London NW1 4RY [4]Department of Zoology, The Natural History Museum, Cromwell Road, South Kensington, London SW7 5BD. United Kingdom

Abstract

The morphology of the inner ear from the common dolphin (*Delphinus delphis*) and the harbour porpoise (*Phocoena phocoena*) are studied in conjunction with a Scanning Electron Microscope examination of the inner ear ultrastructure in the mammalian cochlea and vestibule. Concise physiological information on the hearing system of an animal is critical to the assessment of the potential effect of anthropogenic noise pollution in the marine environment, being especially relevant in cases where it is suspected that an animal has died as a consequence of intense noise exposure. In addition, we present a methodology for conducting non-invasive hearing tests on odontocetiformes by measuring the Auditory Brainstem Response, in order to objectively establish if hearing damage is a contributing factor in a live stranding event. The results of the anatomical investigation into the dimensions of the cochlea in *P. phocoena* and *D. delphis* showed similarities between these two animals. Both were shorter than the overall cochlea length reported for the bottlenose dolphin (*Tursiops truncatus*), indicating the possibility of differences in hearing ability between odontocetiformes; a finding that has fundamental implications in the assessment of anthropogenic noise pollution on marine mammals.

Key words

ABR; Cetacean; Dolphin; Inner ear; Cochlea; Electron microscopy; Noise Pollution

Introduction

The oceans are virtually transparent to sound, and opaque to light and radio waves. At a wavelength of 1 m (1,500 Hz), water is nearly 1,000,000 times more transparent to sound than to

radio signals (Pilgrim and Lovell, 2002). This fact underlies the intense interest currently being directed toward the acoustical exploration of the oceans. Naturally produced sounds arise from a number of sources, such as breaking waves, heavy rain, volcanic activity, or from marine animals (bio-acoustic sources). Vocalisations such as whale song, along with the grunts and whistles from sonic fish are especially relevant for communication purposes, and during predator prey interactions (Myrberg, 1981). There are several types of anthropogenic sources used routinely that produce intense levels of noise, from commercial shipping and powered leisure craft, to deliberately produced signals such as the Low Frequency Active Sonar (LFA) used by the military in anti-submarine warfare, or from the airgun arrays used during a seismic survey of the substrate beneath the seafloor by the petroleum industry. These activities can generate noise levels in excess of 253 dB (re 1 μPa at 1 m) (Engås et al., 1996) and are comparable to the noise levels generated by a seafloor volcanic eruption, which can produce a source level of in excess of 255 dB (re 1 μPa) (Northrop, 1974). Recent concerns regarding the impact of anthropogenic sounds on fish and other marine animals has prompted a number of studies into the effects of intense noise exposure on the hearing systems of marine mammals (e.g., Costa et al., 2003; Ketten, 1995; Richardson et al., 1995; Todd et al., 1996; Whitlow et al., 1997). Trauma to the auditory system can result in lesions developing along the VIII nerve pathway, or ruptures in the blood vessels surrounding the inner ear. Growing concern regarding the use of intense sources by the military and oil industry is stimulating considerable interest in the diagnosis of the existence and extent of hearing loss in marine animals. A number of techniques have been developed to investigate gross physiological damage, though concise evidence of raised hearing thresholds from odontocetiforms exposed to loud noise has as yet to be presented.

High intensity low frequency sounds such as LFA sonar may be particularly damaging to the vestibular (balance) organs of cetaceans and could account for the reported disorientation when these animals strand live; whereas loud midrange to high frequency sounds may damage the ultrastructure in the cochlea. Trauma to the auditory system can result in lesions developing along the VIII nerve pathway, or ruptures in the blood vessels surrounding the inner ear (Ketten, 1995). A number of techniques have been developed to study gross physiological damage to the inner ear, though these investigations do not necessarily verify the impairment of hearing and balance. In addition, the cause of an injury to the hearing system may be unrelated to loud noise exposure (e.g. André, et al., 2003) and sustained by a collision with a boat, or as the animal thrashes about on the shoreline. If caused by intense noise, signs of trauma (haematoma and nerve lesions) would probably manifest at the highest end of the impact scale, whereas more subtle damage to the ears

may only show in the ultrastructure and thus be missed when using conventional examination methodologies. Current literature shows a paucity of information on consistent and meticulous removal of inner ear parts necessary to identify damage to the ultrastructure symptomatic of hearing and balance loss. In addition, the fixing agent commonly used during autopsy is formalin, though this chemical does not bind the proteins in the ultrastructure and results in the rapid destruction of the cilia, making the sample unusable for SEM microscopy. It is therefore the purpose of this study to develop dissection and fixation methodologies relevant for the removal and SEM examination of the odontocetiform inner ear and ultrastructure. However, owing to the scarcity of cetacean inner ear samples suitable for SEM microscopy (due for the most part to the use of formalin in the fixation methodology), the inner ear of the domestic pig (*Sus scrofa*) is used to append the dissection and fixation methodologies required to view mammalian ultrastructural hair cells. The periotic bone containing the inner ear from *S. scrofa* is dimensionally similar (though slightly thinner) than the cetacean periotic, and has the considerable advantage of being easy to obtain fresh from commercial sources.

Materials and methods

Morphological examination of the cetacean inner ear

The common dolphin (*D. delphis*) examined in this study was recovered on the 2nd of February from Beacon Point in Devon (Ordnance Survey GB grid reading SX674406). The tagged carcass was not designated for collection (autopsy), due to its location at the foot of a steep cliff making access difficult. A brief inspection revealed that the animal was a mature male, approximately 2.4 meters in length, and estimated to have been dead for 10 to 12 days; injury to the front rows of teeth and the jaw indicate that it is highly possible that the animal died as a result of becoming entangled in fishing nets. The mature harbour porpoise (*P. phocoena*) was recovered on the 11th of February 2005 from Andurn Point, near Plymouth Sound, Ordnance Survey GB grid reading SX495492 (NHM reference SW.2005/30). The tagged carcass was 1.47 meters in length and approximately three years of age (Read, 1999) and was not designated for autopsy due to it being in an advanced state of decay.

Upon removal from the carcass, the periotic bone containing the inner ears from *D. delphis* and *P. phocoena* was separated from the petrous bone and washed in 70 % chilled ethanol. Removal of the inner ear from the encapsulating periotic bone required two cuts made using a fine cutting wheel, which was stopped short of penetrating to the inner ear canals by approximately 0.4 mm.

The weakness in the bone caused by the hemispherical cut allowed for the two halves of the periotic to be gently separated using minimal leverage, thus exposing the internal structure of the ear. A cast of the inner ear cavity was then made by injecting Silicone rubber into the cochlea duct and vestibule, and allowed to cure for 24 hours (Figures 1.a through c). The cast was removed by gently separating the three cut sections of the periotic and by easing the rubberised impression of the ear from the bone segments. The cast was then washed in 100 % ethanol and processed for a low powered Scanning Electron Microscope (SEM) examination of the surface features.

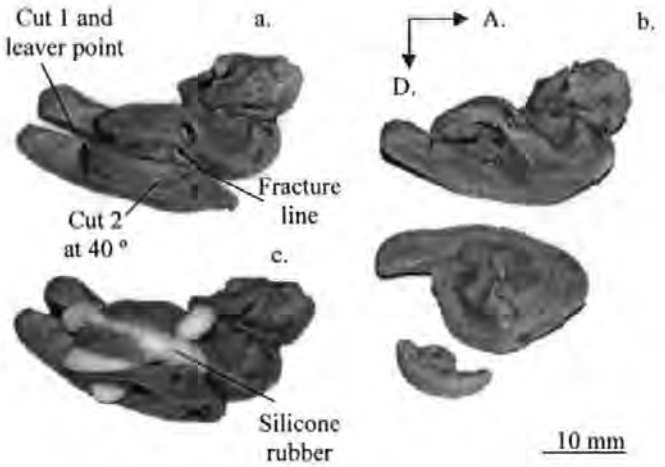

Fig. 1 a. Ventral view of the periotic from *P. phocoena* showing the position of the two cuts, **b.** the sections of periotic cut away to free the cochlea, and **c.** the periotic after the silicone injection moulding procedure. The annotations D. (Dorsal), and A. (Anterior) represent the orientation of the periotic in the skull

SEM examination of the mammalian inner ear ultrastructure

In total, 12 ears were removed from mature domestic pigs (*Sus scrofa*) during processing for the meat industry, within 1 hour of the animal's death, in order to assess the dissection and fixation methodologies required for an SEM examination of the inner ear ultrastructure from a large mammal. On removal from the cranium, the complete periotic bone containing the inner ear was immersed for 4 hours in a jar of chilled fixative (2.5% glutaraldehyde in 0.1 M cacodylate buffer) and taken to the Plymouth EM unit for processing. Samples selected for the examination of the vestibule were first immersed in a chilled aqueous solution of 2.5 % S-Carboxymethyl-L-Cysteine for 5 minutes prior to fixing, in order to hydrolyse the mucous binding the otoconia to the cilia. The periotic bone containing the inner ear was washed in a solution of 30 % ethanol, to remove excess fixative; then, using a fine electric cutting wheel, the outer bone layer covering the cochlea

and membranous labyrinth was removed, exposing the canals and pouches of the saccule, vestibule and cochlea. The opened periotic was then placed back into the fixative and refrigerated for a further 2 hours, to ensure that the fixative had fully penetrated the inner ear end organs. Working in 30 % ethanol, each of the end organs were dissected from the labyrinth using a fine scalpel, then dehydrated through a graded ethanol series ranging from 35% through 50%, 70% and 90% to absolute ethanol, prior to desiccation using the critical point drying method described by Platt (1977). The fully desiccated tissue was subsequently mounted on a specimen stub using a carbon tab, and coated with c. 8 nm of gold in an Emitech K 550 sputter coater (working at approximately 5×10^{-6} Torr). The processed specimens were investigated and photographed using a JEOL JSM 5600 scanning electron microscope operated at 15 kv and a 15 mm working distance.

Results

The ear cast from *D. delphis* and *P. phocoena*

Figures 2.a through 2.d presents SEM micrographs of the bony inner ear labyrinth cast from *D. delphis* and *P. phocoena* viewed laterally, toward and away from the mid sagittal plain of the brain. The length of the cochlea from the upper apical tip to the lower basal segment in *D. delphis* (2.a and 2.b) was calculated to be 30.1 mm, with the vestibule making up the remaining 3 mm of the inner ear (total ear length of 33.1 mm). In *P. phocoena* (Figures 2.c and 2.d), the cochlea was 21.8 mm in length and the vestibule was 2.7 mm (total ear length of 24.5 mm); the length of each semicircular canal was found to be around 3 mm in both animals.

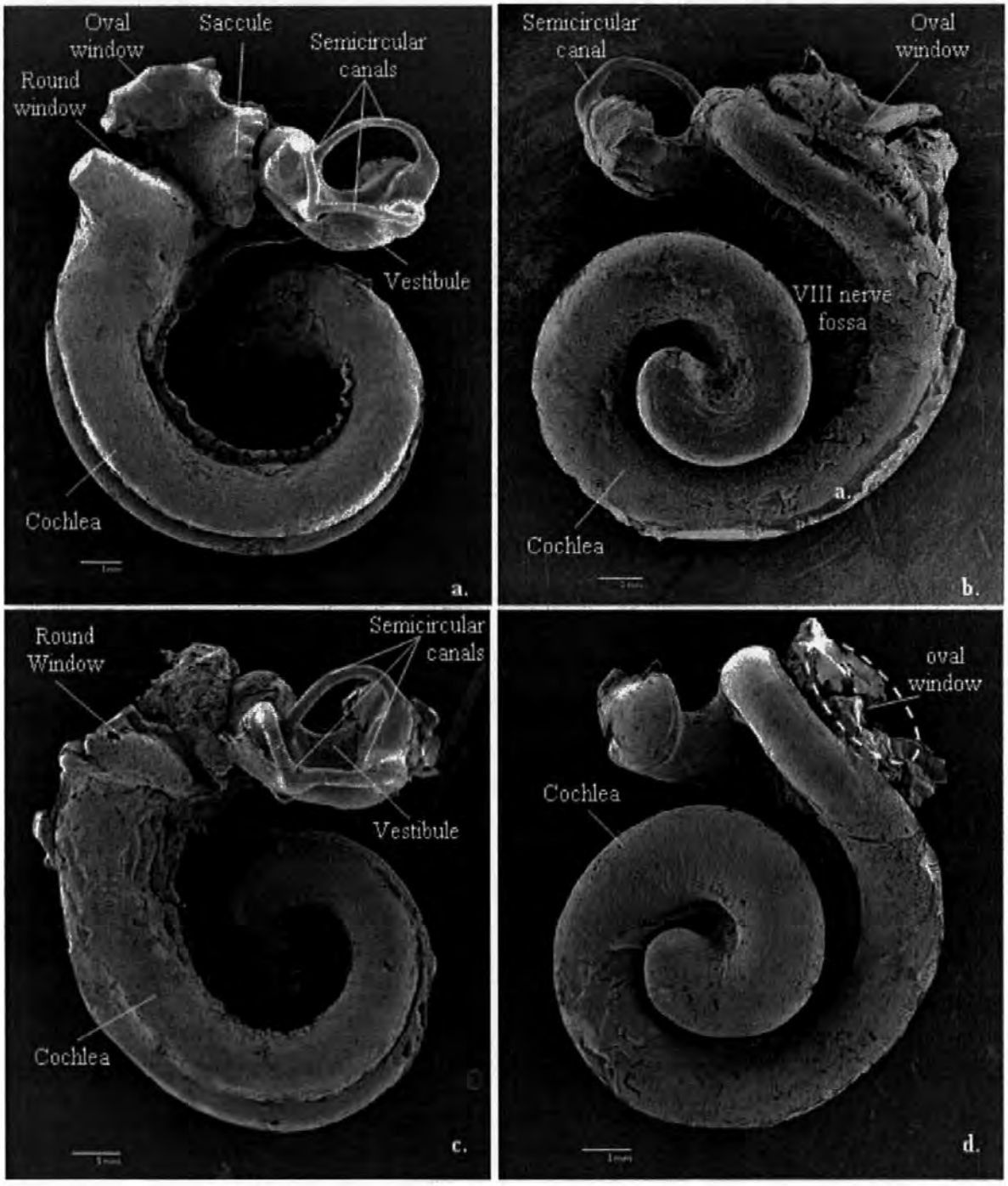

Figure 2.a. SEM micrograph of the left inner ear cast from *D. delphis* (lateral view away from the mid-sagittal plane of the brain). **2.b.** SEM micrograph of the left inner ear cast from *D. delphis* (lateral view toward the mid-sagittal plane of the brain). **2.c.** SEM micrograph of the left inner ear cast from *P. phocoena* (lateral view away from the mid-sagittal plane of the brain). **2.d.** SEM micrograph of the left inner ear cast from *P. phocoena* (lateral view toward the mid-sagittal plane of the brain)

SEM Examination of ultrastructure from the mammalian cochlea and vestibule

Partial removal of the bone covering the inner ear from *S. scrofa* (Figure 3.a) reveals the canals of cochlea surrounded by the dense auditory periotic bone. The anterior part of the capsule contains the cochlea (Figure 3.a); a spiral tube coiled approximately two and one-half turns around a hollow central pillar, the modiolus. Further removal of the remaining bone covering the posterior part of the inner ear reveals the membranous labyrinth of the vestibule, which contains the saccule, utricle and the semi-circular canals; each filled with endolymph, a substance possessing viscous and ionic properties that flows around the semicircular canals aiding the sense of balance.

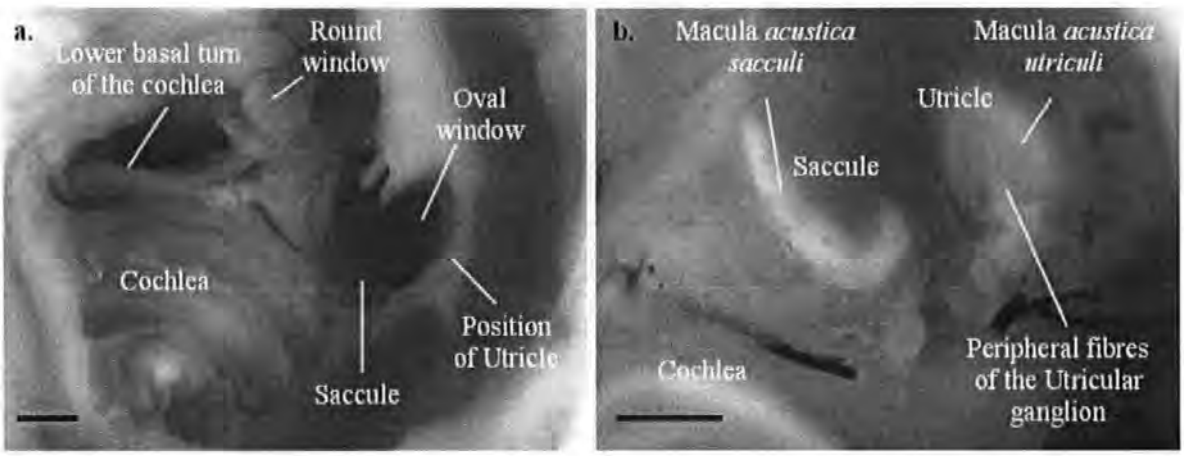

Figure 3.a. The labyrinth of the inner ear from *S. scrofa* with the covering periotic bone partially removed. **3.b.** the saccule and utricle with the covering bone fully removed prior to dissection and preparation for SEM microscopy (Bars = 1 mm) (total basilar membrane length = 32 mm)

Figures 4.a through 4.f shows ultrastructural hair cell proliferations from the upper apical tip to the lower basal region of the cochlea from *S. scrofa*. The Inner Hair Cells (IHC) afferents present in a single row arranged with longer (10 μm to 15 μm) cilia at the upper apical tip of the basilar membrane, and shorter hairs (2 μm to 3 μm) in the lower basal segment. The Outer Hair Cells (OHC) present in three ordered rows anchored to the basilar membrane outside of the reticular lamina. Each of the cells is orientated toward the outer wall of the cochlea, and contains over a hundred stereocilia, arranged in a crescent formed from three to four consecutively shorter rows.

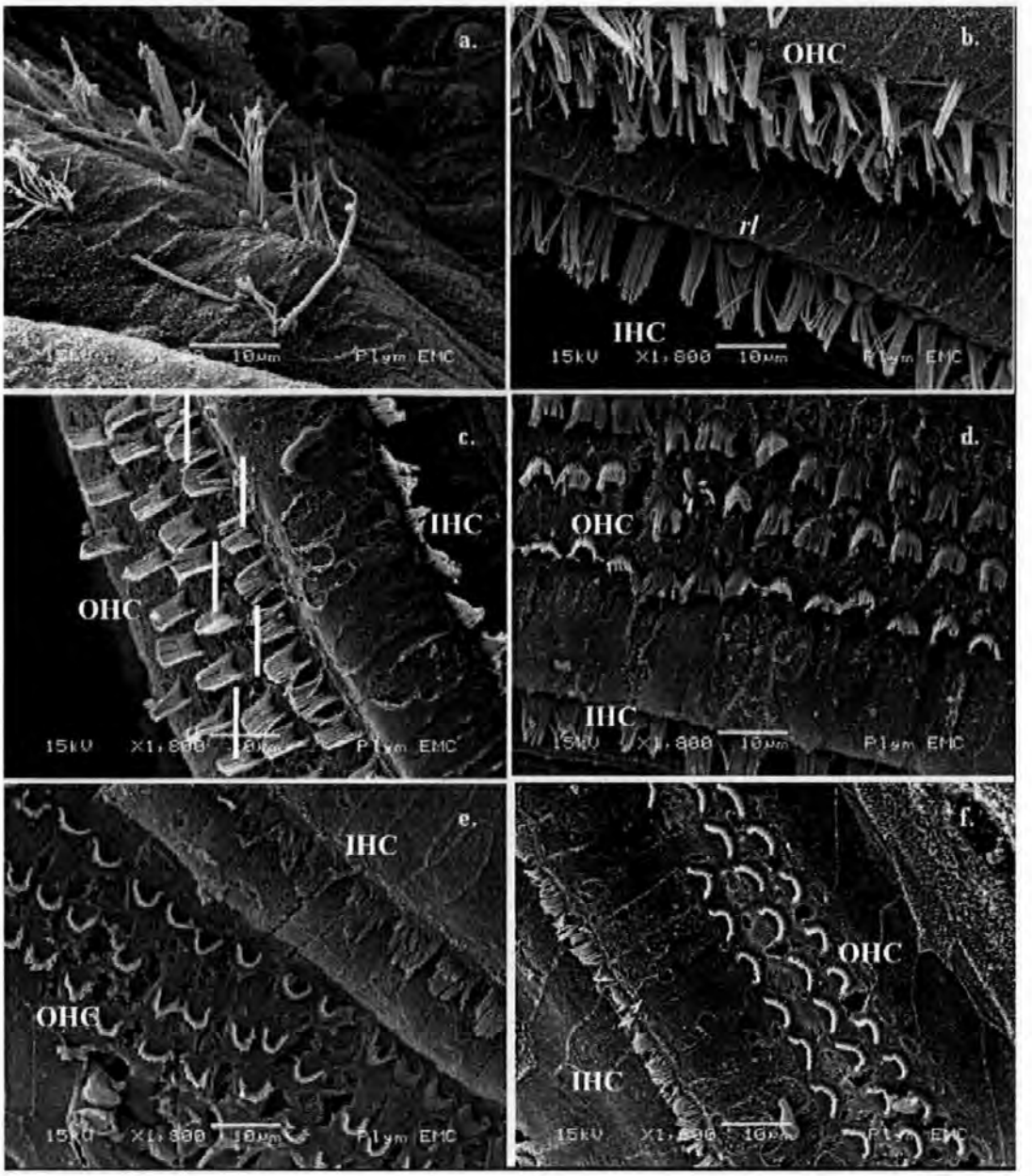

Figure 4.a. hair cells (10 to 15 µm) from the tip of the upper apical, **4.b** hair cells (8 to 10 µm) from the upper apical (*rl.* reticular lamina), **4.c** hair cells (6 µm) from the lower apical, **4.d** hair cells (6 µm) from the upper basal, **4.e** hair cells (4 µm) from the lower basal region, **4.f** hair cells (3 µm) close to the end of the lower basal region

The vestibular organs

The dissection vestibule (Figure 3.b) reveals the saccule and the utricle; the utricle is compressed transversely and occupies the upper and back part of the vestibule, lying in contact with the *recessus ellipticus* (Gray, 1918). The floor and anterior wall of the recess is thickened, forming the macula *acustica utriculi* and innervated by the utricular ganglion of the VIII nerve (Figure 3.b).

The posterior wall of the saccule forms the *ductus endolymphaticus*, which is joined by the *ductus utriculosaccularis* and passes along the *aquæductus vestibuli* ending in the *saccus endolymphaticus*. The cavity of the utricle communicates with the semicircular canal ducts by five orifices, which can be clearly seen in Figures 2.a and 2.c. The smaller of the two bulbous vestibular sacs is the saccule (Figure 3.b), which is fixed to the walls of the labyrinth near to the opening of the cochlea. The cavity is located adjacent to the upper basal turn of the cochlea in proximity to, but not in direct communication with the utricle, and presents with an oval thickening that forms the sensory macula (the *acustica sacculi*). The epithelial surface of the utricle (Figure 5.a) and the saccule (Figure 5.b), is covered with a thick layer of otoconia thought to function similarly to the teleost fish otolith in response to gravistatic and accelerational stimuli; in Figure 5.b, some of the otoconia has been removed revealing the underlying hair cells.

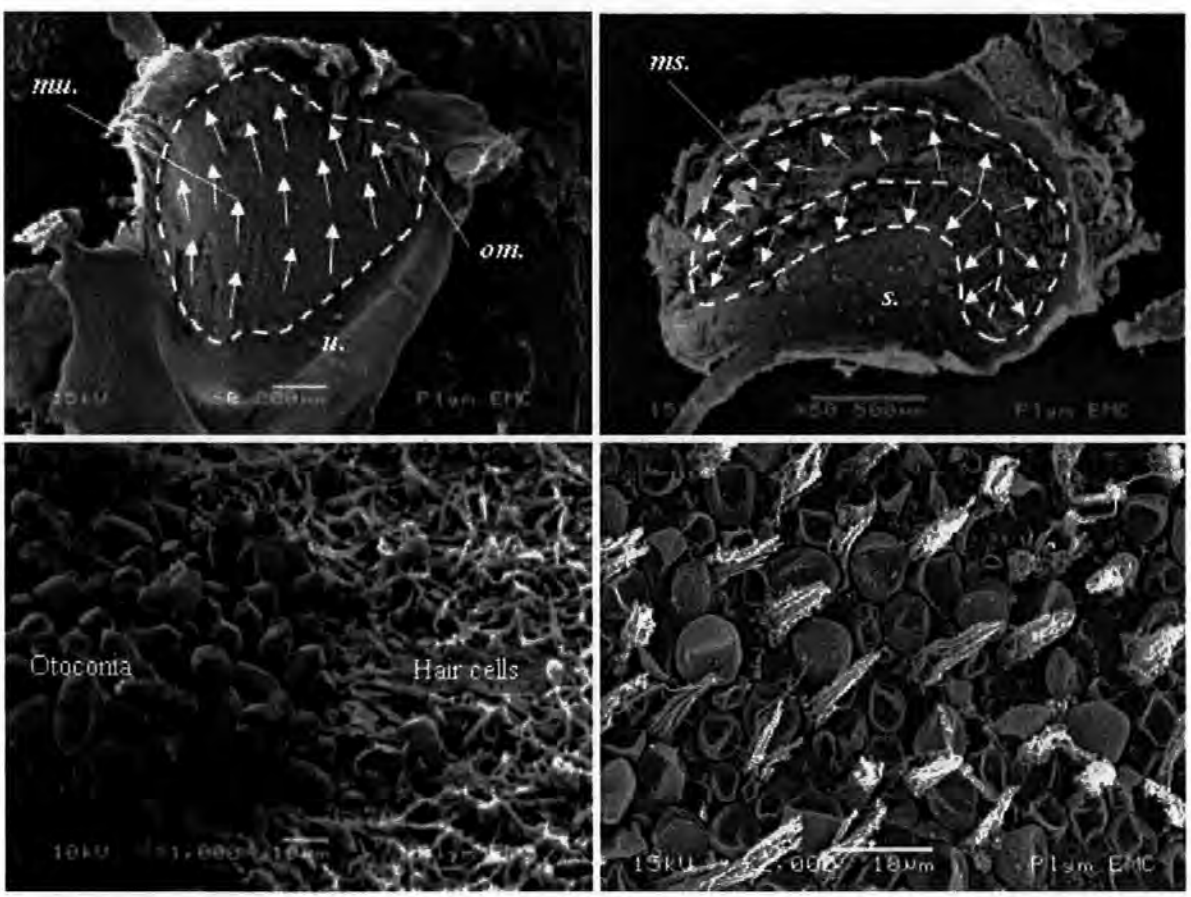

Figure 5.a SEM micrograph of the utricle from the domestic pig (*Sus scrofa*); the hatched line defines the perimeter of each sensory macula (*mu.*), **5.b.** the saccule (*s.*) and the sensory macula (ms.); the white arrows indicate the polarity of the hair cells across the surface of each macula, **5.c.** crystalline calcium carbonate otoconia overlaying the saccular hair cells, **5.d.** hair cells from the dorsal quadrant of the saccule after removal of the otoconia

Discussion

The use of the Scanning Electron Microscope (SEM) in the examination of the ultrastructure responsible for the mediation of auditory stimuli has been used to considerable effect on lower vertebrates such as fish (Platt 1977; Lovell et al., 2005b), and invertebrates (Lovell et al., 2005a), though no SEM examinations have, so far, been conducted on the inner ear ultrastructure from any of the cetacean species. However, the relative ease and speed in which the auditory periotic can be dissected from behind the mandible of *D. delphis* indicates that it should be possible to remove the complete inner ear for a Scanning Electron Microscope examination of the ultrastructural hair cells. A procedure for the fast removal of the complete cochlea and other end organs of the inner ear undamaged has been demonstrated here. However, as both cetacean carcass examined in this study were retrieved in an advanced state of decomposition, thus SEM examinations of the ultrastructure within the inner ear was not undertaken as inner ear hair cells are known to deteriorate within a short time after death. It is essential that the periotic is rapidly immersed in chilled fixative (2.5% glutaraldehyde in 0.1 M cacodylate buffer with 3.5% sodium chloride), then refrigerated to inhibit sample decomposition (the sample must not be frozen, as ice crystals will destroy the ultrastructure).

The saccule and utricle are sensitive to both angular accelerations and low frequency sounds (Popper and Fay, 1993). If either were to become damaged by anthropogenic noise pollution, it may contribute to the reported disorientation experienced by cetaceans which have become stranded live, yet do not present with any obvious signs of injury. The examination of both sensory maculae in the vestibule of *S. scrofa* reveals a thick blanket of otoconia which occludes the hair cells from view. The cilia are embedded in the otoconia and cohesion is provided by mucus (the remains of which is evident in Figures 5.c and 5.d). In order to remove the otoconia and mucus with as little disturbance to the hair cells beneath as possible, S-Carboxymethyl-L-Cysteine was employed to hydrolyse the mucus before fixing the sample. This procedure yielded best results when the solution was 'washed' through the vestibule using a pipette, prior to fixing the sample in the glutaraldehyde.

In *D. delphis* (2.a and 2.b) the length of the basilar membrane from the upper apical tip of the cochlea to the round window was calculated to be 30.1 mm, whilst the basilar membrane from *P. phocoena* (Figure 2.c and 2.d) had a length of 24.5 mm. Both the animals investigated in this study were mature individuals (see Read, 1999), thus it is tentatively concluded that the cochlea from *D. delphis* is 8 mm shorter, whilst *P. phocoena* is 16 mm shorter than the 38 mm reported for

T. truncatus (Wever et al., 1971). All mammalian cochleae appear to function according to the same basic principles; however, the effective frequency range differs between species (Fay, 1988). For example, the range of audible frequencies is about 20 Hz to 16 kHz in the human cochlea, about 300 Hz to 45 kHz in *S. scrofa* (Heffner and Heffner, 1990), about 100 Hz to 150 kHz in *T. truncates* (Johnson, 1966; 1967) and 300 Hz (Kastelein et al., 2002) up to as high as 190 kHz in *P. phocoena* (Bibikov, 1992; Popov, 1986; Kastelein et al., 2002). Table 1 presents the outlying frequencies audible to the marine and terrestrial mammals considered here, along with the cochlea length measurements.

Table 1. Comparison between cochlea length and audible frequency range

Species	Cochlea Length (mm)	Low (Hz)	High (Hz)
T. truncates	38	100	150000
P. phocoena	22	300	190000
Human	35	20	16000
S. scrofa	32	300	45000

The evidence presented in this study suggests that the audiogram for *D. delphis* may lie somewhere between the hearing range of *T. truncates* and *P. phocoena*; it is therefore concluded that their is considerable need for the production of an audiogram for *D. delphis*, being of importance for an accurate assessment of the impact of anthropogenic sounds on the inner ear physiology of this animal.

References

André, M., Supin, A., Delory, E., Kamminga, C., Degollada, E. M., Alonso J. (2003). Evidence of deafness in a striped dolphin, *Stenella coeruleoalba*. Aquatic Mammals, 29.1, 3–8

Bibikov, N.G. (1992). Auditory brainstem responses in the harbour porpoise (*Phocoena phocoena*). In: 'Marine Mammal Sensory Systems', 197-211. Thomas, J. *et al* (eds). Plenum Press, New York.

Costa, D.P., Crocker, D.E., Gedamke, J., Webb, P.M., Houser, D.S., Blackwell, S.B., Waples, D., Hayes, S.A., Le Boeuf, B.J. (2003). The effect of a low-frequency sound source (acoustic

thermometry of the ocean climate) on the diving behavior of juvenile northern elephant seals, *Mirounga angustirostris*. Journal of the Acoustical Society of America 113(2):1155-1165.

Engås, A., Løkkeborg, S., Ona, E., & Soldal, A.V. (1996). Effects of seismic shooting on local abundance and catch rates of cod (*Gadus Morhua*) and haddock (*Melanogrammus aeglefinus*). Canadian J. of Fisheries and Aquatic Sciences. 53, 2238 - 2249.

Fay R.R. (1988). Hearing in Vertebrates: a Psychophysics Databook. Hill-Fay Associates, Winnetka IL.

Gray, H. (1918). Anatomy of the Human Body. Lea & Febiger, Philadelphia: Bartleby.com, 2000. www.bartleby.com/107/. [15-02-05].

Heffner, R.S., and Heffner, H.E. (1990) Hearing in domestic pig (*Sus scrofa*) and goat (*Capra hircus*). Hearing Research, 48, 231-240

Johnson, C.S. (1966). Auditory thresholds of the bottlenosed porpoise (*Tursiops truncatus*). U.S. Naval Ord. Test Stn., Tech. Oubl., 4178: 1-28.

Johnson, C.S, (1967). Sound detection thresholds in marine mammals. In W.N. Tavolga (ed), Marine bio-acoustics, vol. 2. Pergamon, Oxford, U.K.

Kastelein, R.A., Bunskoek, P., Hagedoorn, M., Au, W.L.W. & de Haan, D. (2002). Audiogram of a harbor porpoise (Phocoena phocoena) measured with narrow-band frequency-modulated signals. JASA, 112(1), 334-344.

Ketten, D.R. (1995). Estimates of blast injury and acoustic trauma zones for marine mammals from underwater explosions. In: Sensory Systems of Aquatic Mammals, R. Kastelein, J. Thomas, and P. Nachtigall (eds.), DeSpil Publishers, pp. 391-408

Lovell, J.M., Findlay, M.M., Moate, R.M., & Yan, H.Y., 2005 A. The hearing abilities of the prawn *Palaemon serratus*. Comp. Biochem. Physiol. A Mol. Integr. Physiol. Jan;140(1):89-100.

Lovell, J.M., Findlay, M.M., Moate, R.M., Nedwell, J.R., & Pegg, M.A., (in review). The inner ear morphology and hearing abilities of the Paddlefish (*Polyodon spathula*) and the Lake Sturgeon (*Acipenser fulvescens*). Comp. Biochem. Physiol. A Mol. Integr. Physiol.

Myrberg, A.A. (1981). Sound communication and interception in fishes. Hearing and Sound Communication in Fishes. Tavolga WN, Popper AN, and Fay RR, Eds. Springer-Verlag, New York.

Northrup, J. (1974). Detection of low-frequency underwater sounds from a submarine volcano in the western Pacific. J. Acoust. Soc. Am. 56(3), 837-841.

Pilgrim, D.A. & Lovell, J.M., (2002). A review of current publications dealing with the impact of low frequency sounds upon fish. Report to Devon Sea Fishing Association.

Platt, C. (1977). Hair cell distribution and orientation in goldfish otolith organs. Journal of Comparative Neurology. 172, 283-297.

Popov, V.V., Ladygina, T.F. & Supin, A.Ya. (1986). Evoked potentials of the auditory cortex of the porpoise, *Phocoena phocoena*. J. Comp. Physiol., 158:705-711.

Popper, A.N., & Fay, R.R., 1993. Sound detection and processing by fish: critical review and major research questions. Brain Behav Evol, 41, 14-38

Read, A.J. (1999). Harbour porpoise (*Phocoena phocoena*). In S.H. Ridgeway & R. Harrison (eds.), Handbook of Marine Mammals, Volume 6: The Second Book of Dolphins and Porpoises. Academic Press. San Diego.

Richardson, W. J., Greene, C. R., Jr., Malme, C. I., & Thomson, D. H. (1995). Effects of Noise on Marine Mammals. Academic, San Diego pp 576.

Todd, S., S. Stevick, J. Lien, F. Marques, & D. Ketten (1996). Behavioural effects of exposure to underwater explosions in humpback whales (*Megaptera novaeangliae*). Canadian Journal of Zoology, 74(9):1661-1672.

Wever, E. G., McCormick, J. G., Palin, J. & Ridway, S. H. (1971). The Cochlea of the Dolphin, *Tursiops truncatus*: Hair Cells and Ganglion Cells. Proceedings of the National Academy of Sciences of the United States of America 68: 2908-2912.

Whitlow, W., Au, W., Nachtigall, P. & Pawloski, J. (1997). Acoutic effects of the ATOC signal (75Hz, 195 dB) on dolphins and whales. Journal of the Acoustical Society of America, 101(5) Pt1

Elsevier Editorial System(tm) for Insect Biochemistry and Molecular Biology

Manuscript Draft

Manuscript Number:

Title: The influence of body size on the form and function of the statocyst from the prawn Palaemon serratus

Article Type: Full Length Article

Keywords: Crustacean; Sensory system; Hair cell; Evoked potential; Ontogeny; Hearing; Palaemon serratus

Corresponding Author: Mr Jonathan Murray Lovell, Mphil/PhD

Corresponding Author's Institution: University of Plymouth

First Author: Jonathan Murray Lovell, Mphil/PhD

Order of Authors: Jonathan Murray Lovell, Mphil/PhD; Lee Christiansen, MSc; Malcolm M Findlay, Dr; Roy M Moate, Dr

The influence of body size on the form and function of the statocyst from the prawn *Palaemon serratus*

JM Lovell[1], L Christiansen[2], MM Findlay[1], RM Moate[2]

[1]School of Earth, Ocean and Environmental Sciences j.lovell@plymouth.ac.uk. [2]Plymouth Electron Microscopy Centre, University of Plymouth, Drake Circus, Plymouth PL4 8AA, United Kingdom.

Abstract

The organisation and function of the statocyst in the prawn (*Palaemon serratus*) from three body size classes have been studied using a combination of anatomical, electron microscopic and electrophysiological approaches. The statistical examination of the relationship between the sensory setae length and body size showed that small prawns had significantly smaller setae than medium and large prawns. In view of this finding, the electrophysiological response of the statocyst organ to sound stimuli was recorded from four specimens in each size class using two subcutaneous electrodes, positioned in the carapace close to the supraesophageal ganglion and statocyst. The results were analysed using a one way ANOVA, and the P value of 0.925 reveals that that body size has no significant impact on the amplitude of the electrophysiological response to tone bursts generated in an underwater sound field. The information provided by both SEM microscopy and ABR audiometry, shows that prawns are capable of hearing a 500 Hz tone with equal acuity regardless of body size, a finding that is of ecological importance when considering the effect of anthropogenic sound on crustaceans.

* Corresponding author. Tel.: +44 1752 232411; fax: +44 1752 232400.
E-mail address: j.lovell@plymouth.ac.uk (J.M. Lovell).

Key Words

Crustacean, Sensory system, Hair cell, Evoked potential, Ontogeny, Hearing, *Palaemon serratus*

1. Introduction

The ability of an organism to orientate itself in the 3-D marine environment requires the presence of a suitable gravity receptor. These receptors occur in many diverse organisms throughout the marine environment, and include cephalopods (Dilly et. al., 1975; Bettencourt & Guerra, 2000), crustaceans (Prentiss, 1901; Schöne, 1971; Rose & Stokes, 1981; Patton & Grove, 1992), and fish

(Popper & Platt, 1983; Bretschneider et al., 2001). In crustaceans the statocyst is located either at the anterior end of the animal in the basal segment of each antennule, or posteriorly within the uropods, abdomen or telson, (Farre, 1843; Cohen and Dijkgraaf, 1961; Finley and Macmillan, 2000). Several authors (e.g. Barber & Emerson, 1980; Popper, 1981; Yan et al., 1991) have studied the surface detail of the inner ear in vertebrate animals, employing a similar methodology to that used in the present study. Previous reports describe the statocyst as a fluid filled pouch formed internally by an infolding of the external epidermal layer. The chamber is never completely isolated from the external environment, and in some species the opening has become slit like, (Bate, 1858; Cohen and Dijkgraaf, 1961), or only exposed to the environment during the moulting phase (Prentiss, 1901). The epithelium of the statocyst contains a varying number of mechanosensory hairs or setae, which are primarily concentrated at the base or ventral area of the chamber (Hertwig, et.al., 1991; Sekiguchi and Terazawa, 1997).

The arrangement and number of setae within the statocyst varies greatly between species (Cohen, 1955; Budelmann, 1988; Kovalev and Kharkeevich, 1993), and in some species (e.g. *Cherax destructor*), different types of setae are present (Finley and Macmillan, 2000). The dense statolith structure within the statocyst is typically constructed from sand grains set in a gelatinous medium (Cohen and Dijkgraaf, 1961; Popper et al, 2001). The statolith may lie adjacent to the mechanosensory setae, in partial contact with, or cemented to them, (Cohen, 1955; Finley and Macmillan, 2000). The base of the setae is embedded in a highly innervated sensory epithelium or cushion (Prentiss, 1901), initiated by shear forces between the statolith and statocyst, which are determined by the animal's spatial movement in the environment (Cohen, 1955; Cate and Roye, 1997). It has been well established that the crustacean statocyst functions as an equilibrium organ by initiating corrective movements to maintain the animal's position in the water column, (Cohen and Dijkgraaf, 1961; Sekiguchi and Terazawa, 1997; Finley and Macmillan, 2000; Popper et al., 2001). However, few reports have examined the relationship between size and the fine structure of the crustacean statocyst, and none has examined the amplitude of the electrophysiological response of different sized afferents in an underwater sound field. In this work, we study the morphology of the statocyst receptors from three size classes of *P. serratus* using Scanning Electron Microscopy (SEM), and then test the amplitude of the electrophysiological response of the organ when stimulated with a 500 Hz tone, propagated in an underwater sound field. This information is of importance due to rising concerns regarding the impact of anthropogenic sounds on fish and other marine animals. These concerns have prompted a number of investigations into the effects of intense noise exposure on the hearing systems of marine mammals (e.g. Costa et al.,

2003; Richardson et al., 1995; Whitlow et al., 1997), and free living fish (Dalen and Knutsen, 1987; Engås et al., 1996; Pearson et al., 1992; Pickett et al., 1994). However, until recently, it has been generally assumed that crustaceans are only responsive to strong vibrations transmitted through a solid (see Cohen and Dijkgraaf, 1961). This is contrary to the findings of Lovell et al., (2005), which shows that prawns hear with an acuity and frequency range similar to that of generalist fish and have the potential to be equally affected by loud anthropogenic noise sources generated in the marine environment.

The Auditory Brainstem Response (ABR) recording technique was originally developed for use in clinical neurophysiology, and has been successfully applied in the auditory assessments of both mammalian and non-mammalian vertebrates (Corwin et al., 1982), and invertebrates (Lovell et al., 2005). The term ABR is used loosely in this study, as crustaceans and other invertebrates lack a brainstem, instead they present with clusters of neurons that belong to a central complex (Utting et al., 2000; Schmidt and Ache, 1996). However, the waveform of the response of the afferent neurones of the statocyst in a sound field is recorded using the electrophysiological technique, acquired by averaging conglomerate responses of peak potentials arising from nuclei in the auditory pathway during acoustic stimulation (Corwin et al., 1982; Overbeck and Church, 1992). The sweep records the generation of neural waveforms over a user-defined time span termed the sweep velocity, and measures activity prior to, during and after stimulation of the inner ear. Recordings have to be repeated over 1000 to 2000 presentations before clear results can be obtained, due to additional waveform generation by neural activities other than those associated with hearing, combined with muscular movements (Kenyon et al 1998; Yan et al 2000). The recorded waveforms resulting from each sweep are averaged together and produce a recognisable ABR waveform, which is then overlaid on the first run, to show that the evoked potentials are repeatable.

2. Materials and Methods

A total of one hundred common prawns, *Palaemon serratus* (Pennant), of mixed sex, and ranging in length from 27 mm (0.1 g) to 71 mm (1.9 g) were obtained from wild stock in the South West of England (ordnance survey GB grid reading SX483539) using a dip net. Once captured, the prawns were transferred to a marine tank divided by a fine mesh screen into four equal sized compartments of 50 litres each. An Eheim type 2013 biological filter with a flow rate of 390 litres per hour maintained water quality and provided aeration by spraying filtered seawater back into the tank via the filter outlet pipe located 60 mm above the water surface. The ambient noise

within the holding tank was measured using a hydrophone, and the sound pressure level was calculated to be 102 dB (re 1 µPa), with the Eheim pump active. In all of the experiments, and in the holding tank, the ambient water was kept at a temperature of 18° C and a salinity of 34 g/l. When not under experimental protocols, the prawns were provided with 14 hours of light per day from a fluorescent tube controlled by a mains timer switch. Prior to any experimentation the prawns were divided by size into three populations; each group was fed on a granulated feed at a daily rate of 6 g for the large prawns, 4 g for the medium and 2.5 g for the small.

12 specimens of *P. serratus* from each size class were dissected and the statocyst removed under seawater, and placed in a watch glass containing 2.5 ml of 0.9 % sodium chloride prior to micro-dissection. The capsules were opened by making a lateral incision around the statocyst chamber using a fine scalpel. Needlepoint tweezers were used to lift the upper section of the capsule, thus exposing the sand granules and ultrastructure. The sodium chloride solution was removed using a pipette and replaced with a solution of 2.5 % S-Carboxymethyl-L-Cysteine in sodium chloride, which was used to hydrolyse the mucus surrounding the statolith receptors. The contents of the dish were gently agitated for two minutes, after which the solution was removed and replaced with chilled fixative (2.5% glutaraldehyde in 0.1 M cacodylate buffer with 3.5% sodium chloride). The statolith capsules were then dehydrated through a graded ethanol series ranging from 35% through 50%, 70% and 90% to absolute ethanol, prior to desiccation using the critical point drying method described by Platt (1977). Fully desiccated statolith capsules were subsequently mounted on a specimen stub using a carbon tab, and coated with c. 8 nm of gold in an Emitech K 550 sputter coater. Finally, the processed specimens were investigated and imaged using a JEOL JSM 5600 scanning electron microscope operated at 15 kv, and a 15 mm working distance with the eucentric stage holding the specimen aligned for 'planar' image acquisition.

All measurements were carried out on a PC using the analySIS® (Soft Imaging System GmbH) program. The distance between bases of the closest neighbour was measured using arbitrary distance and the hair cell length was measured using polygon length, both measurements were recorded in micrometers. The hair cells were measured from their base to the point at which the delicate threads began to develop at the tip, and total sensory setae counts were all completed manually. Statistical calculations were carried out using Statgraphics plus 5.1 professional edition program. Analysis of variance (ANOVA) was used to test whether or not hair cell length and distance between neighbouring bases or the amplitude of the electrophysiological response

differed between small, medium and large individuals of *Palaemon serratus*. The program constructs various tests and graphs to compare the mean values for the three size categories. The F-test in the ANOVA assists in determining whether any significant differences are present between the means. Multiple range tests were incorporated into the analysis as it applies a multiple comparison analysis to the data to determine which means are significantly different from one another.

2.1. ABR methodology

The procedure used to acquire the acoustically evoked potentials was approved by the United Kingdom Home Office. The test subjects were placed into a flexible cradle formed from a soft nylon mesh rectangle saturated with seawater. Oxygenated water kept at a temperature of 18° C was gravity fed at an adjustable flow rate of 3 millilitres per second and directed toward the gills. The water was held in an aerated reservoir positioned in an adjacent room, and fed to the prawn through a 4 mm diameter plastic tube. The prawn was first placed lengthwise and centrally on an 80 mm x 60 mm rectangle of fine nylon netting, which was wrapped firmly around the cephalothorax and pleon, and the two sides of the net were held together using the clip shown in Fig. 1.b.

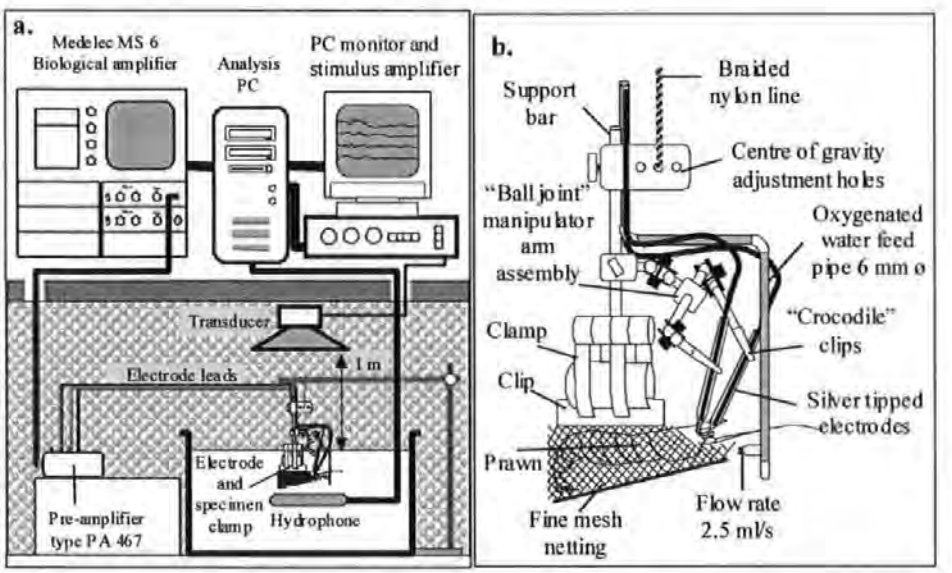

Fig. 1.a. Schematic of the ABR audiometry system, and **1.b.** the clamp used to hold the prawn in position, and manipulate the electrodes during the audiological test (from Lovell et al., 20005)

The clip was placed in a retort stand clamp fitted with ball joint electrode manipulator arms, and the aerated water pipe (detailed in Fig. 1.b). During the procedure to position the electrodes, the specimen and clamp were suspended over a plastic tray, and aerated water was supplied to the prawn. A retort stand and the experimental tank (L. 450 mm x W. 300 mm x D. 200 mm) were placed on an anti-vibration table, located in a concrete basement fitted with anechoic panelling L. 3 m x W. 2 m x H. 2m. A selection of 4 prawns from each size class ranging from 27 mm (0.1 g) to 35 mm (0.3 g) for the small, 50 mm (1.1 g) to 55 mm (1.4 g) for the medium, and 66 mm (1.8 g) to 71 mm (1.9 g) for the large, were tested with a 500 Hz, 4 cycle tone burst, presented at a sound pressure level of 125 dB (re 1 μPa at 1 m) from an air mounted speaker. Working under a MEIJI binocular microscope, two small holes were made in the cuticle layer using a lancet, penetrating the carapace to a maximum depth of 0.3 mm to facilitate electrode positioning. The reference electrode was located behind the supra-orbital spine, close to the neural complex associated with the antennule, and the record electrode was located in the peduncle close to the statocyst, at the junction between the lateral antennular and otic ganglia. The clamp assembly with the specimen and sited electrodes were then suspended from the retort stand positioned over the experimental tank, and the prawn stationed 5 mm below the surface of the water. After the hearing assessment, the prawns were relocated to a holding tank for observation, prior to being returned to the divided aquarium.

The evoked response was amplified and digitised to 12 bits resolution and recorded. This process was repeated 2000 times, and the response averaged to remove electrical interference caused by neural activities other than audition, and the myogenic noise generated by muscular activity. Each measurement was repeated twice, as this aids in separating the evoked response, which is the same from trace to trace, from the myogenic noise, which varies in two successive measurements. After the averaging process, the evoked potential could be detected, following the stimulus by a short latency period of 5 milliseconds. The latency is accounted for by the time it takes the sound in air to travel the 1 m to the prawn, plus 1 to 2 milliseconds response latency. Each prawn was tested twice to show that the Auditory Evoked Potential (AEP) was repeatable. In order to obtain a mean value for the EP, the μv value of the second peak of the response was calculated using the Root Mean Square method described in equation 1.

$$\sqrt{(1/T \int dt\, x^2\,(t))}$$

Equation 1. Definition of the Root-Mean-Square value, where $x(t)$ is the amplitude of the Evoked Potential, and T is the duration.

The RMS values of both runs from the same animal were then averaged together and entered into a one way ANOVA to test the correlation between body size and receptor length on the AEP. The response of the prawn was measured using a proprietary control and analysis programme which both generated the stimulus signals and captured and analysed the response, and was installed onto the PC shown in Fig. 1.a. Amplification of the sound was achieved using a Pioneer type SA-420 amplifier and a 200 mm Eagle L032 loudspeaker with a frequency response range of 40 Hz to 18000 Hz. Additionally, the loudspeaker was placed inside a Faraday cage and connected to a centralised earth point located in an adjacent room where the PC, amplification, and analysis equipment was set up. Connecting wires were fed through a 100 mm port in the partitioning wall.

2.2. The sound field

The properties of the sound field are especially relevant when comparing the audio capabilities of both pressure sensitive and motion sensitive fish in the near field. In a small laboratory set-up, the complexities associated with independently measuring sound pressure and particle motion are compounded by the reflectivity of the tank sides and base. For this reason, a number of experiments have used air-mounted transducers to successfully generate sounds underwater (e.g. Fay and Popper, 1975; Yan et al., 2000; Akamatsu et al., 2002). The principle advantage of such a system is that as the sound source is located at a distance of 1 m from the air/water interface, the moving part of the transducer does not contact the water and generate near-field displacements. In this situation the pressure and motion of the water adjacent to the fish ear can be considered as being equal (Hawkins 1981). The stimulus tone, presented from the loudspeaker to the prawn was calibrated using an insertion calibration. A calibrated Bruel and Kjaer Type 8106 hydrophone was placed in the tank and positioned adjacent to the shrimp cephalothorax region to record the intensity of the tone, relative to the position of the statocyst.

3. Results

The statocyst of *Palaemon serratus* is located in the basal segment of the left and right antennules (Fig. 2a and b), and are well developed and fluid filled in both male and female specimens from each of the size categories. The statocyst is oval in shape; being well rounded posteriorly and narrowing to a point anteriorly (Fig. 2c). The openings are protected by coarse setae and a thin layer of chitin that extends from the basal segment of the antennules, thus the statocyst is effectively closed to the external environment.

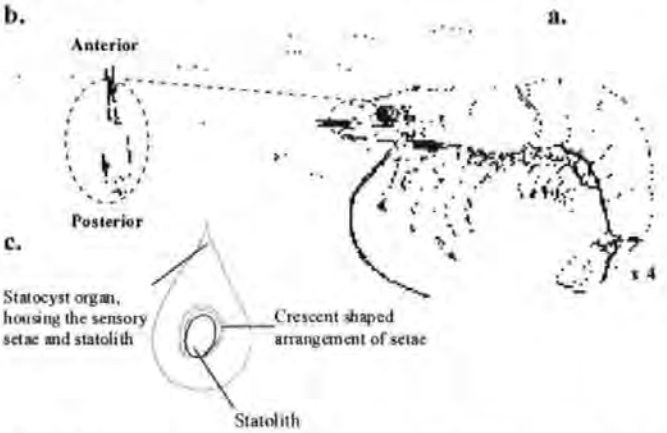

Fig. 2.a. Diagrammatic representation of a prawn showing all body segments and location of statocyst (circled area). **b.** Higher magnification of first antennule illustrating its segments and statocyst positioning (from Kavlekar, 1998) **c.** Sketch of the statocyst, showing the position of the sensory setae and statolith

The number of setae in the statocyst ranged from 30-38 from the small prawn, 56-73 from the medium, and 72-83 for the large. The statolith was primarily composed of sand grains; however other foreign material was regularly observed in many specimens throughout the samples. The sand is cemented to projections from the tips of the surrounding setae by mucus, forming a dense elliptical mass. A ring configuration, constructed by some of the projections from the tip of the sensory setae (*s*) connected the hairs together, creating an outline of the crescent shown in Fig. 3.a. Other projections from the tips of the setae interlaced and penetrated the centre of the statolith forming a supportive basket (Fig. 3.b). For the statistical interpretation of the data, the shape of the sample distributions has been ignored as the sample sizes are large so, the shape of the distribution of the individual samples is not important due to the central limit theorem (Fowler, 1998). The setae were positioned on the peak of the ridge circling the depression in a crescent shaped formation (Fig. 3.a and 3.b). The setae are slightly curved and orientate themselves towards the centre of the crescent, with an opening directed towards the posterior of the animal.

The setae were arranged in a regular row dividing further into two irregular rows at the base of the outer end of the crescent (*oc*), with a single sensory setae (*sss*) present just inside the aperture. Each seta was attached to the sensory cushion via a heavily ridged bulbous base constructed of chitin resembling sclerotised cuticle. The shortest hairs (< 120 μm) were found proliferating in a band running down the left side of the array, whilst the longest hairs (> 170 μm) were found in the right caudal quadrant. The satolith capsule is elliptical in shape, and the walls symmetrically curve inward toward the base, where the receptor cells are located on a mound rising 40 μm from the floor of the capsule. Observations of the sensory setae revealed that each hair was orientated towards the centre of the crescent (*cr*), and anchored by a bulbous ridged base (*rb*) to the statocyst floor. High Power magnification observations showed the presence of fine projections originating from the tip of the setae, which interlocked with one another to form the crescent shaped ring configuration.

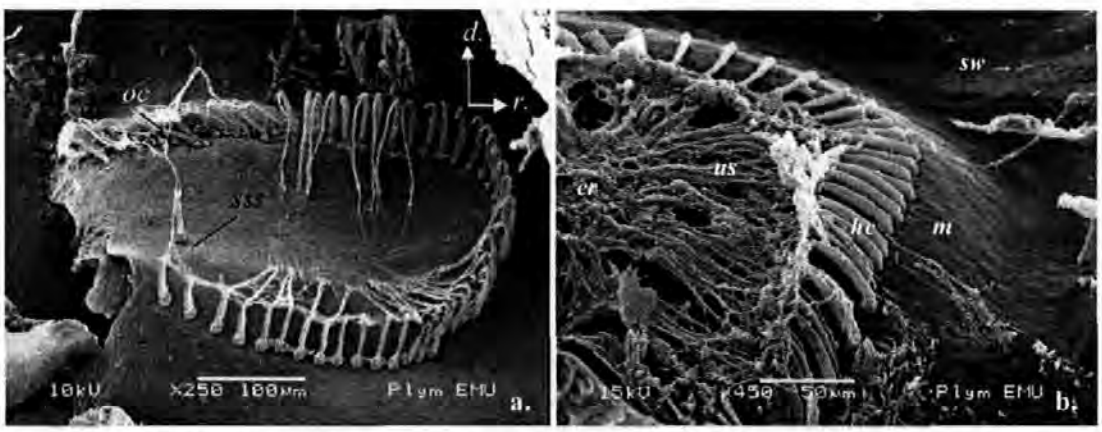

Fig. 3.a. SEM showing a solitary sensory setae positioned away from the setae row (*sss*). This feature has been demonstrated on each specimen examined, and is associated with the single row of setae inside the aperture of the crescent. **3.b.** Lateral view of the statocyst. *cr.* central region, *hc.* hair cell, *m.* mound, *sw.* statocyst wall, *us.* upper tapering section of hair cell (from Lovell et al. 2005)

Fig. 4.a shows an SEM of a typical row of sensory setae viewed from the front, and 4.b shows the row of setae (*s*) as viewed from above. The thread like projections (*tlp*) originate from the tip of the setae and range in number from 3 to 12, and are only found on the upper portion of the cell tip, and link with adjacent and neighbouring sensory setae to create the statolith net, which works in conjunction with the mucous to hold the sand granules in position.

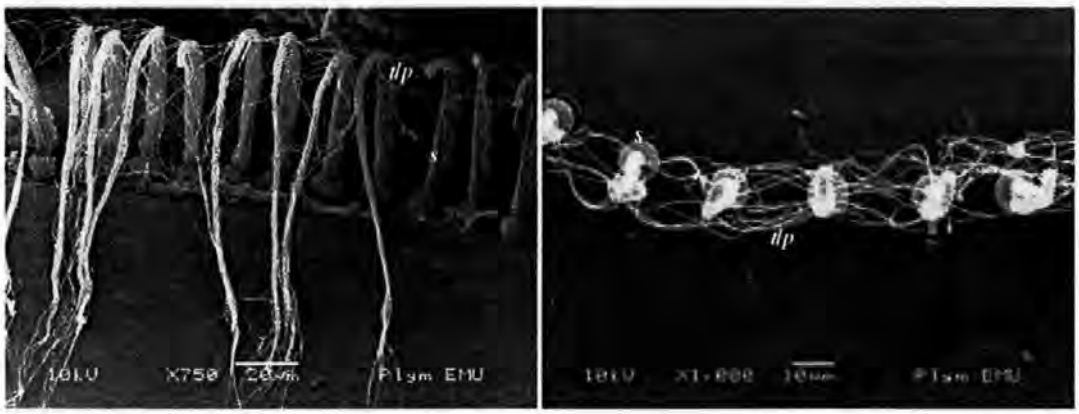

Fig. 4.a. SEM of a typical row of sensory setae present on all statocyst samples, viewed from the front, and **4.b**, the row of setae as viewed from above. Between 3 and 12 thread like projections (*tlp*) originate at the tip of the setae (*s*) and forms a web that secures the sand granules to the hair shaft

3.1. Relationship between body size and setae length

The lengths of setae were significantly different between the body sizes of *P. serratus* in the specimens examined, and the prawns in the small body size category had significantly smaller sensory setae compared to those of the medium and large prawns. The box and whisker plot (Fig. 5) shows similar mean setae lengths from both medium and large size categories. The data from the small prawns were positively skewed with the largest setae outlier overlapping the mean of the medium and large data. Medium body length was also positively skewed whilst the large body size category was negatively skewed; however, the deviation from the mean in both cases was considerably less. Differences were significant at the 5% level, and to determine how significant each sample is from one another a multiple range test was completed. This revealed that the hair cell length from the small body size category was significantly different from both medium and large categories which showed very little significant difference.

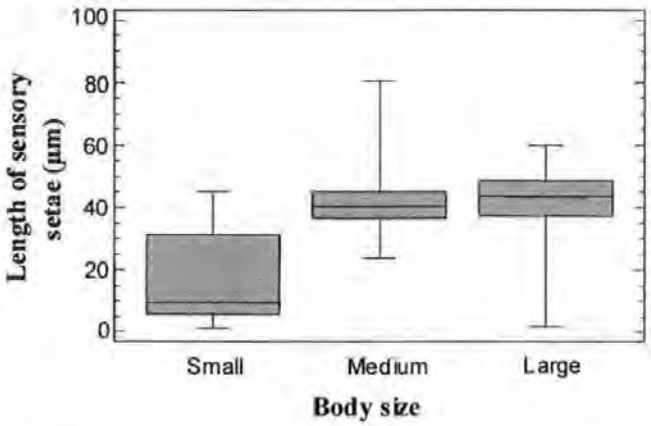

Fig. 5. Box and whisker plot displaying the relationship between setae length and body size in *P. serratus*. The grey boxes equal 50% of the overall data for that category and each error bar signifies 25% of the data. Black line in boxes specifies the median

3.2. Relationship between body size and distance between setae bases

Small body sized prawns had the largest distance between neighbouring setae bases, with medium sized prawns having the smallest distance. All three body size categories have similar outlying data, though the small body group data was negatively skewed whereas medium and large body groups were positively skewed. Comparing the medians allowed the differences to be accepted as being significant at the 5% limit. A multiple range test was conducted to determine which means were significantly different, resulting in one statistically significant difference, between that of small and medium size categories.

3.3. Electrophysiology

Twelve prawns from each size class were stimulated with a 500 Hz tone burst, presented at 125 dB (re 1 µPa at 1 m). The potential difference of the largest (second) sinusoid of the evoked response generated by the tone burst was calculated using the RMS equation. The Evoked potentials from a large medium and small prawn are presented in Fig. 6, which were averaged from 1000 repeat presentations of the stimulus sound.

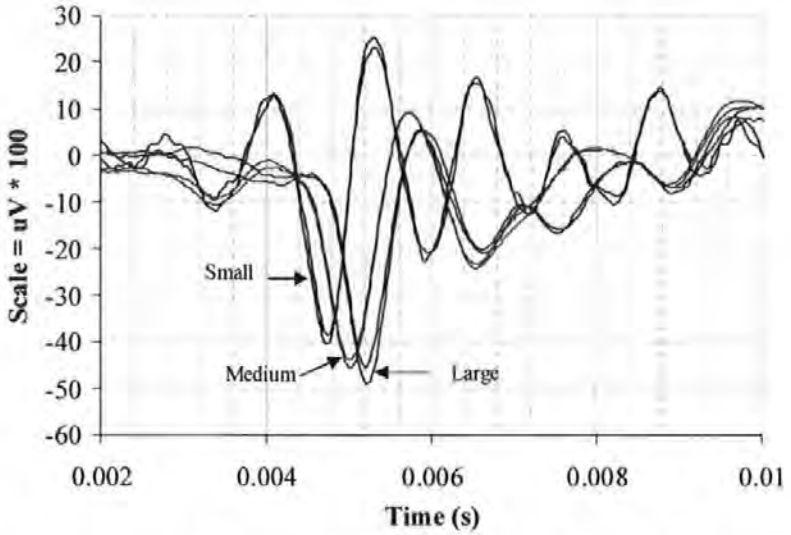

Fig. 6. Auditory evoked potentials from small, medium and large *P. serratus* in response to a 500 Hz tone burst presented at 125 dB, and averaged from 1000 iterations of the stimulus sound

The data were grouped into the 3 size-related populations and tested using a one way ANOVA, and the results presented in Table 1. This shows the mean AEP value of the three populations, and the *P* value gives the significance level of the AEP voltage difference between the populations. The results ($F = 0.08$, $P > 0.925$) indicates that AEP values are independent of body size which supports our null hypothesis that body size has no effect on the amplitude of AEP's at a frequency of 500 Hz.

Table 1. Comparison of hearing ability between three populations of *P. serratus* ranging in size from 27 mm to 71 mm. The *P* value gives the significance level of the AEP voltage

Source	DF	SS	MS	F	P
C1	2	0.00120	0.00060	0.08	0.925
Error	9	0.06891	0.00766		
Total	11	0.07011			

Level	N	Mean	StDev	Individual 95% CIs For Mean Based on Pooled StDev
1	12	0.57125	0.07057	(----------*----------)
2	12	0.54775	0.09006	(----------*----------)
3	12	0.55350	0.09939	(----------*----------)
Pooled StDev =		0.08750		0.480 0.540 0.600 0.660

One-way ANOVA

4. Discussion

The structure of the statocyst in Palaemon serratus, as detailed here, is similar to that described for other decapod crustaceans (Prentiss, 1901; Cohen, 1955; Budelmann, 1988; Schmitt, 1973; Sekiguchi and Terazawa, 1997; Finley and Macmillian, 2000; Popper et.al., 2001; Lovell et al., 2005). These authors found the sensory hairs or setae are positioned on a sensory epithelium or sensory cushion, encased in a fluid filled chamber. Previous reports (Sekiguchi and Terazawa, 1997; Finley and Macmillian, 2000) have shown the statocysts, if two were present, usually lie adjacent to one another and are located in the basal segments of the antennules with the exception of the Mysidacea family where the statocysts are located in the tail fan (Cohen and Dijkgraaf, 1961). The present study describes a similar arrangement of sensory setae in *P. serratus* to that reported in the Norway lobster *Nephrops norvegicus* (Neil and Wotherspoon, 1982); Australian crayfish *Cherax destructor* (Finley and Macmillan, 2000), prawns *Palaemonetes vulgaris* (Prentiss, 1901); *Palaemon antennarius* (Hensen, 1863 cited in Prentiss, 1901) and the crab *Callinectes sapidus* (Cate and Roye, 1997). The arrangement of the setae in prawns using, *Palaemonetes vulgaris*, has been described by Prentiss (1901) as being positioned in a "horse-shoe like curve". Detailed SEM observations in the present study revealed *Palaemon serratus* has one very orderly row of setae, which forms the crescent structure, with all of the setae directed inwards towards the centre of the statocyst. This organisation was seen in all the samples regardless of the setae being connected to the statolith or cemented with mucus to neighbouring seta, suggesting that all the setae are involved in the function of the statocyst. The two ends of the crescent are aimed towards the distal end of the statocyst whilst being angled centrally. Towards the inner end of the crescent the single orderly row of setae further separates into two irregular

rows. The Norway lobster, *Nephrops norvegicus*, has one prominent row of setae with the other hairs being smaller and less well organised, (Neil and Wotherspoon, 1982) in this respect its pattern is similar to that of *Palaemon serratus*, but not the same. The statocysts from *Palaemon serratus* had a solitary seta located just inside the aperture of the crescent positioned slightly closer to the single row of setae. It was typically of the same size as the other setae and orientated towards the centre of the sensory cushion; no previous studies have reported the presence of such a solitary seta for any other crustacean species.

A significant difference was seen between setae length and the body size of *Palaemon serratus*. After completion of multiple range tests the significant difference was found to be between the small and medium and the small and large category. No significant difference was found between medium and large. This was an expected result as the size of structures increase relative to the overall growth of the organism. As the size of the organism grows the effect of gravity will be increased on it thereby the need for a possibly larger statolith could result. As an organism approaches its maximum size the growth rate slowly levels off allowing less variation to occur within the data. Similarly, total setae number ranged from 30-38 in small specimens, 56-73 in medium and 72-83 in large; for the same reason mentioned previously this data couldn't be obtained for every sample so numerical data were averaged from at least two samples per group that allowed all the setae to be counted. The difference between the largest Fig. in the small group and the smallest Fig. in the middle group was 8, whereas the difference between medium and large was -1 (sample data overlapped) indicating that the need for both longer and more numerous setae in the medium and large categories are very similar and less varied. Again the larger the specimen the larger the statolith, therefore more setae are required to support the larger mass and cover more area around the sensory cushion. Finley and Macmillan (2000) carried out one recent investigation concerning statocyst structure and growth of the crayfish, *Cherax destructor*. They found that the total number of setae in large samples was significantly higher than those in the small samples, supporting the results found in this study.

In conclusion, this study directly compare the body size with the spatial arrangement and size of the sensory setae and amplitude of the electrophysiological response within the statocyst in crustacea. The statocyst morphology of *P. serratus* is similar to closely related species, however variation of the setae structure within the same genus was observed. The unique solitary seta found in all specimens was the first to be described from any crustacean species examined; however, the explanation put forth describing its function can apply to any crustacean statocyst

indicating that this seta may have been overlooked in earlier reports. Results of the electrophysiology experiment show the AEP voltage averages between 0.55 μv and 0.57 μv from each of the experimental populations when stimulated with a 500 Hz sound presented at 125 dB (ref 1 μPa at 1m). Given that a *P* value of 0.925 was obtained from the ANOVA, it is concluded that body size has no impact on hearing ability at 500 Hz, even though the length of setae altered with body size categories. An investigation into the ontogeny of the auditory system in zebrafish (*Danio rerio*) ranging in size from 10 to 45 mm total length, also found no difference in auditory sensitivity, response latency, or response amplitude with development (Higgs, et al., 2003). This information shows that crustaceans are potentially equally affected by anthropogenic noise, a finding that should be considered when assessing the impact of loud underwater noise on the ecology of marine animals.

References

Akamatsu, T., Okumura, T., Novarini, N. & Yan, H.Y., 2002. Empirical refinements applicable to the recording of fish sounds in small tanks. J. Acoust. Soc. Am. 112, 3073-3082.

Barber, V. C. & Emerson, C.J., 1980. Scanning electron microscopic observations on the inner ear of the skate, (Raja ocellata). Cell and Tissue Research 205, 199 215.

Bate, C.S., 1858. On the development of decapod Crustacea. Philosophical Transactions, 148, 589-605.

Bretschneider, F., van den Berg, A.V. & Peters, R.C., 2001. In: B.G. Kapoor and T.J. Hara (eds) Sensory Biology of Jawed Fishes. Science Publishers, Enfield NH, USA & Plymouth, UK. ISBN 1-57808-099-1.

Budelmann, B.U., 1988. Morphological diversity of equilibrium receptor systems in aquatic invertebrates. In Atema, J. Fay, R.R., Popper, A.N. and Tavolga, W.N. (Ed.) Sensory Biology of Aquatic Animals. Springer-Verlag, New York, pp.758-782.

Cate, H.S. & Roye, D.B., 1997. Ultrastructure and physiology of the outer row statolith sensilla of the Blue crab, *Callinectes sapidus*. Journal of Crustacean Biology, 17 (3), 398-411.

Cohen, M.J., 1955. The function of receptors in the statocyst of the lobster *Homarus Americanus*. Journal of Physiology. 130, 9-3.

Cohen, M.J. & Dijkgraaf, S., 1961. The Physiology of Crustaceans. Academic Press, London, pp. 65-108.

Corwin, J.T., Bullock, T.H., & Schweitzer, J., 1982. The auditory brain stem response in five vertebrate classes. Electroencephalogr. Clin. Neurophysiol. 54, 629-641

Costa, D.P, Crocker, D.E, Gedamke, J, Webb, P.M, Houser, D.S, Blackwell, S.B, Waples, D, Hayes, S.A. & Le Boeuf, B.J., 2003. The effect of a low-frequency sound source (acoustic thermometry of the ocean climate) on the diving behavior of juvenile northern elephant seals, *Mirounga angustirostris*. Journal of the Acoustical Society of America 113(2):1155-1165.

Dalen, J. & Knutsen, G.M., 1987. Scaring effects on fish and harmful effects on eggs, larvae and fry by offshore seismic exploration. In: Merklinger, H.M. (Ed.), Progress in Underwater Acoustics. Plenum Publishing Corp, pp. 93 - 102

Dilly, P.N., Stevens, P.R. & Young, J.Z., 1975. Receptors in the statocysts of squid. Journal of Physiology, 249, 59-61.

Engås, A., Løkkeborg, S., Ona, E., & Soldal, A.V., 1996. Effects of seismic shooting on local abundance and catch rates of cod (*Gadus Morhua*) and haddock (*Melanogrammus aeglefinus*). Canadian J. of Fisheries and Aquatic Sciences. 53, 2238 - 2249.

Farre, A., 1843. On the organ of hearing in crustaceans. Philosophical Transactions, 133, 233-242.

Finley, L. & Macmillan, D., 2000. The Structure and growth of the statocyst in the Australian crayfish *Cherax destructor*. Biological Bulletin, 199, 251-256.

Fowler, J., Cohen, L. & Jarvis, P., 1998. Practical Statistics for Field Biology. John Wiley & Sons Ltd., West Sussex

Hawkins, A. D., 1981. The hearing abilities of fish. In Hearing and Sound Communication in Fishes (Tavolga, W. N., Popper, A. N. & Fay, R. R., eds), Springer Verlag., New York 109 - 133.

Hensen, V., 1863. Studien über das Gehörorgan der Decapoden. Zeitschr. F. wiss. Zool., Bd. 13, 319-402, Taf. 19-22.

Hertwig, I., Schneider, H. & Hentschel, J., 1991. Light and electron microscopic analysis of the statocyst of the American crayfish *Orconectes limosus* (Crustacea, Decapoda). Zoomorphology, 110, 189-202.

Higgs, D. M., Rollo, A. K., Souza, M. J. & Popper, A. N., 2003. Development of form and function in peripheral auditory structures of the zebrafish (*Danio rerio*). J. Acoust. Soc. Am. 113, 1145 -1154.

Kavlekar, D., 1998. Morphology Goa, India: National Institute of Oceanography Available from http://www.indianocean.org/bioinformatics/prawns/GIF/ANATOMY/Penaei~1.htm [accessed 15 August 2003]

Kenyon, T.N., Ladich, F. & Yan, H.Y., 1998. A comparative study of the hearing ability in fishes: the auditory brainstem response approach". J. Comp. Physiol. A. 182, 307-318.

Kovalev, V.A. & Kharkeevich, T.A., 1993. Studies on morphological and functional organisms of the statocyst receptor macula in the crayfish *Procambrus cubensis*. Journal of Evolutionary Biochemical Physiology, 29, 117-119.

Lovell, J.M., Findlay, M.M., Moate, R.M., & Yan, H.Y., 2005 A. The hearing abilities of the prawn *Palaemon serratus*. Comp. Biochem. Physiol. A Mol. Integr. Physiol. 140, 89-100.

Neil, D.M. & Wotherspoon, R.M., 1982. Structural specialisations, fluid flow and angular sensitivity in the statocyst of the lobster, *Nephrops norvegicus*. Journal of Physiology (Lond.), 329, 26-27.

Overbeck, G.W., & Church, M.W., 1992. Effects of tone burst frequency and intensity on the auditory brainstem response (ABR) from albino and pigmented rats. Hear Res. 59, 129-137

Patton, M.L & Gove, R.F., 1992. The response of statocyst receptors of the lobster *Homarus americanus* to movements of statolith hairs. Comparative Biochemistry and Physiology, 101A, 249-257.

Pearson, W.H., Skalski, J.R. & Malme, C.I., 1992. Effects of sounds from a geophysical survey device on behavior of captive rockfish (*Sebastes spp*). Can. J. Fish. Aquat. Sci. 49, 1343 1356.

Pickett, G., Eaton, D., Seaby, R. & Arnold, G., 1994. Results of Bass tagging in Poole Bay during 1992, MAFF Laboratory Leaflet No 74. Lowestoft.

Popper, A.N. & Platt, C., 1993. In Evans, D.H. (Ed.) The Physiology of Fishes. CRC Press, Ann Arbor, pp. 99-136

Popper, A.N., 1981. Comparative scanning electron-microscopic investigations of the sensory epithelia in the teleost sacculus and lagena. Journal of Comparative Neurology. Wiley-Liss, New York 200 (3): 357-374 pp.

Popper, A.N., Salmon, M. & Horch, K.W., 2001. Acoustic detection and communication by decapod crustaceans. Journal of Comparative Physiology, 187, 83-89.

Prentiss, C.W., 1901. The otocyst of decapod Crustacea. Bulletin of the Museum of Comparative Zoology, 36, 167-251.

Richardson, W. J., Greene, C. R., Jr., Malme, C. I., & Thomson, D. H., 1995. Effects of Noise on Marine Mammals. Academic, San Diego pp 576.

Rose, R.D. & Stokes, D.R., 1981. A Crustacean statocyst with only three hairs: Light and scanning electron microscopy. Journal of Morphology, 169, 21-28.

Schmidt, M. and Ache, B.W., 1996. Processing of antennular input in the brain of the spiny lobster, *Panulirus argus*. 2. The olfactory pathway. J. Comp. Physiol. A 178: 605-628.

Schmitt, W.L., 1973. Crustaceans. Redwood Press Ltd., Newton Abbot

Schöne, H., 1971. Gravity receptors and gravity orientation in crustacea. In Gordon, S.A. and Cohen, M.J. (Ed.) Gravity and the organism. University of Chicago Press, Chicago, pp. 223-235.

Sekiguchi, H. & Terazawa, T., 1997. Statocyst of Jasus edwardsii, pueruli (*Crustacea, Palinuridae*), with a review of crustacean statocysts. Marine and Freshwater Research, 48, 715-719.

Utting M, Agricola H, Sandeman R, Sandeman D., 2000. Central complex in the brain of crayfish and its possible homology with that of insects. J Comp Neurol. 416, 245-61

Whitlow, W., Au, W., Nachtigall, P. & Pawloski, J., 1997. Acoutic effects of the ATOC signal (75Hz, 195 dB) on dolphins and whales. Journal of the Acoustical Society of America, 101(5) Pt1

Yan, H.Y., Fine, M.L., Horn, N.S. & Colon, W.E., 2000. Variability in the role of the gasbladder in fish audition. Journal of Comparative Physiology A. 186, 435-445.

Yan, H. Y., Saidel, W. M., Chang, J. S., Presson, J. C., & Popper, A. N., 1991. Sensory hair cells of fish ear: evidence of multiple types based on ototoxicity sensitivity. Proceedings of Royal Society London B. Biology. 245: 133-138.

ver Letter

Dear Dr Raikhel

I would like to submit the attached manuscript titled: "The influence of body size on the form and function of the statocyst from the prawn *Palaemon serratus*" for publication in the Journal of Insect Biochemistry and Molecular Biology.

The study uses a combination of electron microscopy and ABR audiometry to examine the form and function of the statocyst receptors in three size classes of prawn. This manuscript follows a previous paper that has been published in the Journal of Comparative Biochemistry and Physiology defining the hearing abilities of this crustacean.

Warmest regards

Jonathan

Joe Lovell
Bio-Acoustics
School of Earth, Ocean and Environmental Sciences
University Of Plymouth
Drake Circus
Plymouth
United Kingdom
PL4 8AA

Telephone: (01752) 232411

The hearing abilities of the silver carp (*Hypopthalmichthys molitrix*) and bighead carp (*Aristichthysc nobilis*)

J .M Lovell[1], M.M Findlay[1], J.R Nedwell[2] and M.A Pegg[3]

[1]School of Earth, Ocean and Environmental Sciences, University of Plymouth, Drake Circus, Plymouth PL4 8AA j.lovell@plymouth.ac.uk. [2] Subacoustech Ltd, Bishops Waltham, Hampshire, UK. [3]Illinois River Biological Station and Forbes Biological Station Illinois Natural History Survey 704 North Schrader Havana, Illinois 62644

Abstract

Concern regarding the spread of silver carp (*Hypopthalmichthys molitrix*) and bighead carp (*Aristichthysc nobilis*) through the Illinois River has prompted the development of an Acoustic Fish Deterrent (AFD) system. The application of this technology has resulted in a need to understand the auditory physiology of the target species, in order to maximise the effect of the AFD barrier in preventing the migration of the non-indigenous carp species into Lake Michigan, whilst minimising the effect on indigenous fish populations. Therefore, the hearing thresholds of twelve *H. molitrix* and twelve *A. nobilis* were defined using the Auditory Brainstem Response (ABR) technique, in a sound field generated by submerged transducers of the type used in the construction of the AFD barrier. The results clearly show that these fish are most sensitive to sounds in a frequency bandwidth of between 750 Hz to 1500 Hz, with higher thresholds below 300 Hz and above 2000 Hz.

* Corresponding author. Tel.: +44 1752 232411; fax: +44 1752 232400.
E-mail address: j.lovell@plymouth.ac.uk (J.M. Lovell).

Key words: Fish; Ear; Audiogram; Hearing; Asian carp; ABR; Evoked potential

1. Introduction

The spread of the Asian carp species, silver carp (*Hypopthalmichthys molitrix*) and bighead carp (*Aristichthysc nobilis*) through the Illinois River and into the man-made Chicago Canal is causing increasing concern as these non-indigenous species get closer to Lake Michigan. Trials conducted by the Illinois Natural History Survey (INHS, Havana, Illinois) have shown that 95% effectiveness can be achieved when preventing the migration of *A. nobilis* using an Acoustic Fish Deterrent (AFD) barrier (Taylor, Pegg and Chick, in press). While preventing the spread of these species is critical, it is also important that the noise generated by the AFD system does not affect

indigenous species where possible. Two species in particular, the paddlefish (*Polyodon spathula*) and the lake sturgeon (*Acipenser fulvescens*) from the subclass Chondrostei, in the order Acipenseriformes (sturgeons and paddlefishes) are of interest in this respect. An ideal acoustic barrier would appear "loud" to the alien carp species and "quiet" to the indigenous species, therefore having little or no influence on the behaviour of the paddlefish and sturgeon as they pass the barrier. To achieve this level of selectivity, it requires the definition of the potentially affected species hearing thresholds, which can ultimately be used to "fine tune" the sounds generated by the barrier. In a work that partners this study (Lovell et al., in press), the hearing abilities of *P. spathula* and *A. fulvescens* have been defined as a benchmark, using the equipment and methodology applied in this current study.

The hearing thresholds of any organism possessing the appropriate receptor mechanism are illustrated in an audiogram (Myrberg, 1981), which presents the lowest level of sound that a species can hear as a function of frequency. Auditory perception by fish varies between species (Popper and Fay, 1993; Yan et al., 2000), with most falling into the category of being either a hearing specialist or generalist. Specialists such as the carps and catfishes have a connection between the swim bladder and inner ear, making these fish sensitive to the sound pressure component of an acoustic signal, conventionally measured in units of dB (re. 1 μPa). However, generalists such as *P. spathula* and *A. fulvescens* lack this connection and rely on the motion of the water particles in a sound field to stimulate the sensory hairs of the ear (Hawkins and MacLennan, 1976; Yan et al., 2000). The volume of a swim bladder expands and contracts in a pressure field; in specialists, this motion is transmitted mechanically to the inner ear via the Weberian ossicles (von Frisch, 1938; Yan et al., 2000) and allows specialist fish to detect a wider bandwidth of frequency with greater sensitivity compared to generalist fish.

The techniques used to obtain fish audiograms may require a varying degree of time, surgical and technical expertise (e.g. Enger and Anderson 1967; Fay and Popper, 1975; Fine, 1981), or the use of behavioural paradigms to gain statistically sound data (e.g. Yan, 1995). The Auditory Brainstem Response (ABR) technique of measuring hearing thresholds has been successfully applied to both mammalian and non-mammalian vertebrates (Corwin et al., 1982), Elasmobranchs (Casper et al., 2003), and marine invertebrates (Lovell et al., 2005 A). The ABR is a non-invasive far-field recording of synchronous neural activity in the eighth nerve and auditory nuclei elicited by acoustic stimuli (Jewett, 1970; Jewett and Williston, 1971; Jacobson, 1985; Kenyon et al., 1998). Measurements of the ABR response are used routinely in the clinical

evaluation of human hearing (Jacobson, 1985) and allow for the determination of thresholds from uncooperative or inattentive subjects or in situations where behavioural methods cannot be readily applied. An ABR trace is formed by averaging conglomerate responses of peak potentials arising from centres in the auditory pathways extending from the periphery of the VIII nerve and reflects electrophysiological activity chiefly from the auditory nerve to the midbrain (Corwin et al., 1982; Overbeck and Church, 1992).

Several ABR studies have focused on measuring the hearing abilities of the specialist goldfish *Carrasius auratus*, stimulated with tone bursts presented through a transducer mounted in air above the holding tank (c.f. Kenyon, et al., 1998; Yan, et al., 2000). In addition, Fay and Popper (1975) recorded microphonic potentials from the saccule of the African mouthbreeders (*Tilapia macrocephala*) and the specialist catfish (*Ictalurus nebulosus*), using an air mounted transducer fixed below a 250 mm diameter PVC cylinder with a floor made from "Rho C" rubber. A loudspeaker with a diameter of 200 mm was suspended facing upwards 250 mm below the test tank in an airtight extension of the cylinder. In the present study, the hearing thresholds from *H. molitrix* and *A. nobilis* are acquired using submerged transducers (a setup not previously attempted in an ABR investigation of specialist fish hearing). An additional challenge was found when testing the hearing thresholds of *A. nobilis*, as some of the fish used in the experiment were approaching 750 mm in length, and weighing nearly 6.75 kg.

2. Materials and methods

Twelve specimens of *H. molitrix* ranging in length between 137 mm (25 g) to 392 mm (700 g) were kept in four 200 litre freshwater tanks, and twelve specimens of *A. nobilis* ranging in length between 545 mm (2.8 kg) to 740 mm (6.75 kg) were kept in two 2.5 m x 1 m x 0.5 m tanks. The water temperature in the holding tanks and test tank ranged between 18.2 and 18.6 ° C over a 24 hour period, and when not under experimental protocols, the fish were provided with 16 hours of light per day.

2.1. ABR Methodology

The ABR measurements of hearing thresholds were made using a proprietary control and analysis programme named "Brainwave", and written in LabView 7. A schematic of the equipment used to provide audiometric measurements from *H. molitrix* and *A. nobilis* is shown in Figure 1 (a more detailed description of the setup can be found in Lovell et al., in press). The

sound field in the experimental water tank holding *H. molitrix* and *A. nobilis* was generated by means of two Fish Guidance Systems Ltd. Mk II 15-100 Sound Projectors; with the stimulus sound amplified using a Tandy 250W power amplifier. These faced each other at a distance of 200 mm; the inner ear of the fish during the test was arranged on the axis connecting the centres of the two projectors.

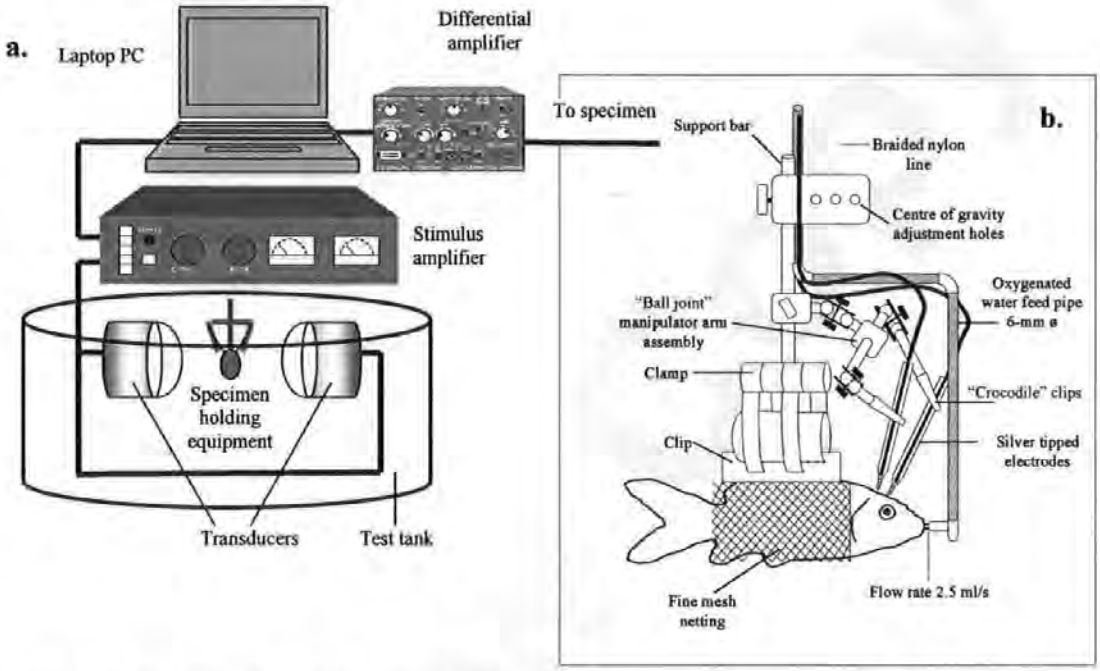

Figure 1.a Schematic of the ABR audiometry system and **Figure 1.b** schematic of the clamp assembly used to hold *H. molitrix* and position the electrodes

The procedure used to acquire the Auditory Evoked Potentials (AEPs) was approved by the University of Illinois, United States (Institutional Animal Care and Use Protocol #04271). The test subjects were placed into a flexible cradle formed from a soft nylon mesh rectangle saturated with freshwater for the small fish, or a clear rubber coated 1 mm gauge wire mesh for fish over 0.5 kg weight. Oxygenated water kept at a temperature of 18 °C was gravity fed at an adjustable flow rate of between 5 millilitres per second for the small fish, to 25 millilitres per second for the large, and directed toward the gills through a soft rubber mouth tube. The small fish were first placed lengthwise and centrally on a 160 mm x 120 mm rectangle of fine nylon netting, which was wrapped firmly around the body and tail, and the two sides of the net were held together using a clip. The clip was placed in a retort stand clamp fitted with ball joint electrode manipulator arms, and the aerated water pipe. During the procedure to position the electrodes the specimen and clamp were suspended over the test tank, and aerated water was supplied to the

fish. The electrophysiological response to acoustic stimulation was recorded using the two cutaneous electrodes positioned on the cranium of the fish adjacent to and spanning the VIII nerve, which were connected to the differential preamplifier by 1 m lengths of screened coaxial cable with an external diameter of 1.5 mm. The evoked response was amplified and digitised to 12 bits resolution and recorded. This process was repeated 2000 times and the response averaged to remove electrical interference caused by neural activities other than audition and the myogenic noise generated by muscular activity. Each measurement was repeated twice; this aids in separating the evoked response, which is the same from trace to trace, from the myogenic noise, which varies in two successive measurements. Tone bursts were presented to the fish at sound pressures not exceeding 134 dB (re. 1 μPa) and during the assessment, the projectors were driven with load resistors placed between the amplifier and projector. The reason for this was that due to the sensitive hearing of specialist fish, only relatively low levels of sound were required to evoke above threshold responses. The full output of the amplifier was only required when measuring the hearing of the less sensitive generalist fish such as *P. spathula* and *A. fulvescens* (see Lovell et al., in press).

The stimulus tones presented to *H. molitrix* and *A. nobilis* were calibrated using an insertion calibration, where the sound level is recorded in the absence of the fish, with the hydrophone stationed where the inner ear of the fish would be. The measurements were made using a Bruel & Kjaer Type 8104 Hydrophone (serial number 2225715) calibrated and traceable to International Standards, with the signal from the hydrophone amplified using a Bruel & Kjaer Type 2365 Charge Amplifier (Serial Number 1079556). In case there was any non-linearity of the signal, calibrations were made at every frequency and Sound Pressure Level (SPL) used during the test, totalling some 660 individual calibrations. These calibrated levels were then applied to the threshold defined by the ABR measurement to provide calibrated audiograms with pressure levels traceable to International Standards.

3. Results

Figure 2.a illustrates a typical set of acoustic brainstem responses from *H. molitrix* and Figure 2.b is from *A. nobilis* in response to tone bursts from 300 Hz to 3 kHz, acquired as the sound pressure level was successively reduced in steps of between 2 dB to 0.5 dB at threshold. In both Figures, above threshold EP waveforms are presented with a blue colour coding, whilst below threshold recordings are red.

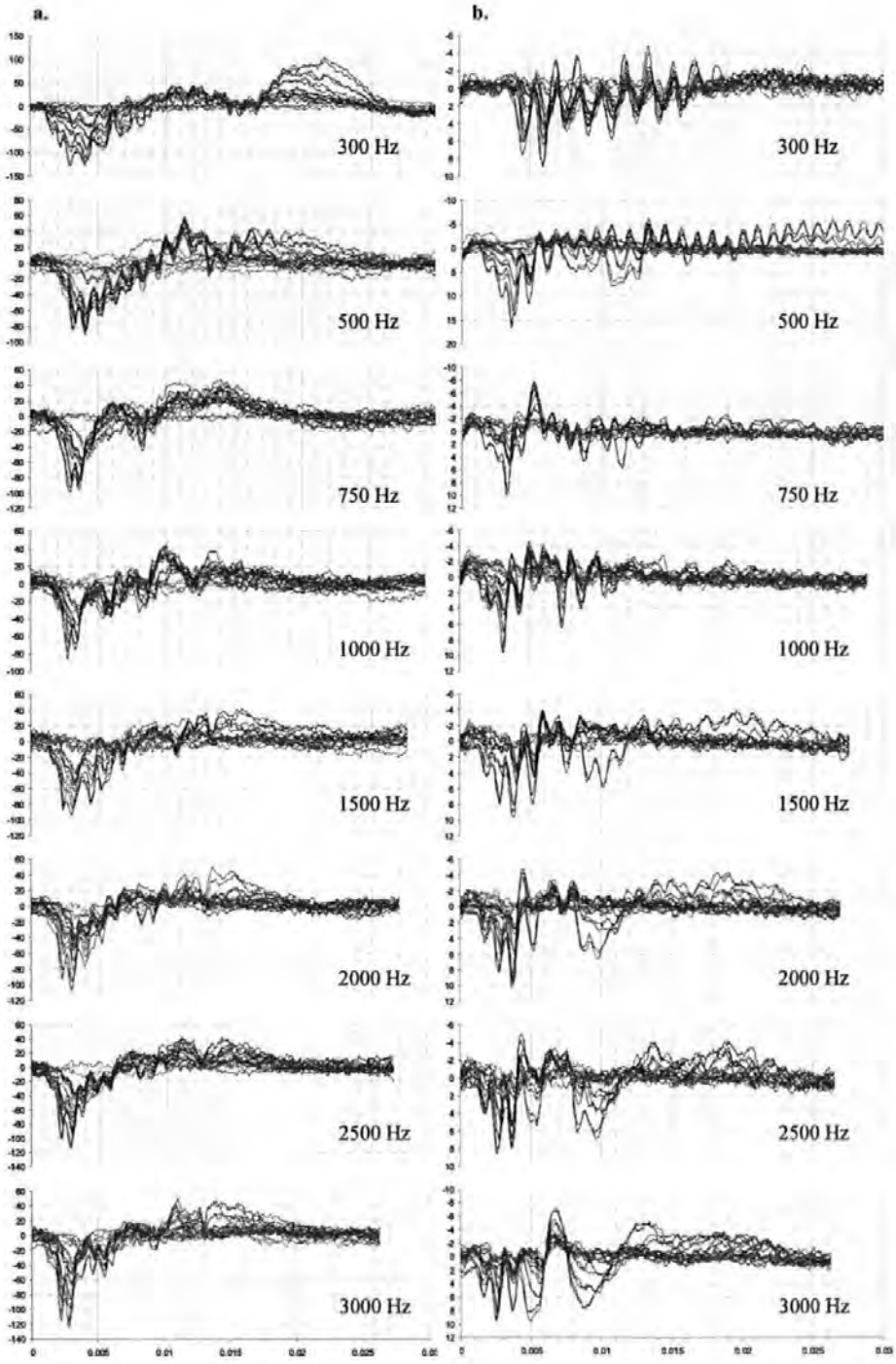

Figure 2.a Auditory Evoked Potentials from *H. molitrix* and **Figure 2.b** *A. nobilis*, recorded in a sound field dominated by sound pressure in response to four cycle tone bursts ranging in frequency from 300 Hz to 3000 Hz and attenuated in steps of 2 dB at high intensities to 0.5 dB as threshold is approached. The waveforms in blue show above threshold responses, whilst red represents below threshold myogenic noise (y axis scale = microvolts * 100 for Figure 2.a and microvolts * 10 for Figure 2.b, x axis scale = time (s))

At each frequency, the AEP waveforms from *H. molitrix* (Figure 2.a) evoked by the tone bursts typically consisted of a series of four to eight rapid negative peaks, followed by a slow positive deflection. Conversely, the waveforms recorded from *A. nobilis* (Figure 2.b) present with a series of four to eight rapid positive peaks, followed by a slow negative deflection (the AEP waveforms in Figure 2.b have been inverted to show consistency with Figure 2.a). Also, owing to the increase in myogenic noise from the larger bighead carp, the differential amplifier gain was reduced by a factor of 10.

The onset latency of the centre or largest sinusoid of the ABR response from *H. molitrix* varied with frequency, ranging from around 4 ms after stimulus onset at 100 Hz to 2.8 ms at 3000 Hz. As the sound pressure levels approached threshold, 2000 sweeps were required to distinguish ABRs from the background electronic noise. It is known that the frequency and intensity of a tone burst effects the latency of the evoked response (Corwin et al., 1982; Kenyon et al., 1998), as does the metabolic state of the organism (Corwin et al., 1982). The Inter-Peak Latency (IPL) of the evoked potentials from *A. nobilis* can be observed in Figure 3, and are in response to the second sinusoid of a 500 Hz tone burst.

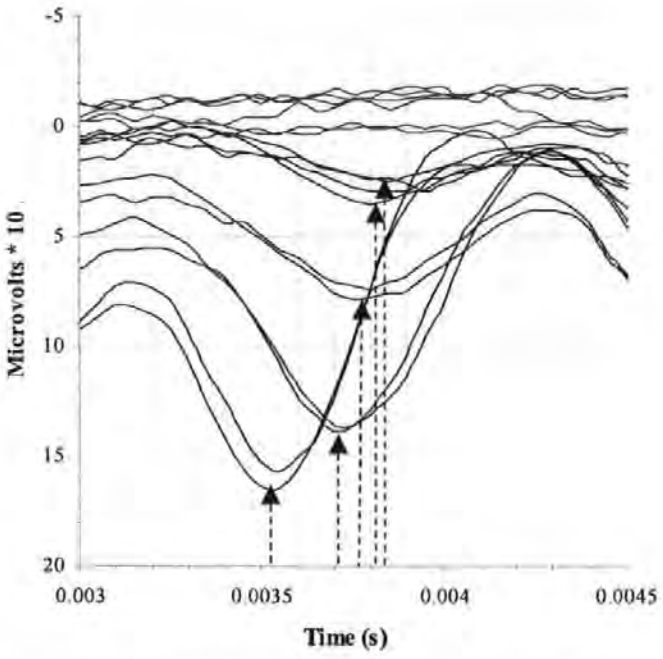

Figure 3. Auditory Evoked Potentials (AEPs) from *A. nobilis* in response to the second sinusoid of a 500 Hz 4 cycle tone burst presented initially at 116 dB (re 1 μPa), and attenuated in 2 dB steps to 108 dB (re 1 μPa). The arrows show the peak of the AEP, which occurs with an Inter-

Peak Latency (IPL) of between 0.1 to 0.2 ms for each of the amplitudes tested (averaged over 2000 iterations per waveform set)

The increase in the latency of the evoked potential in response to decreasing stimulus intensity is often used to verify that the averaged waveform is a product of auditory stimulation rather than a transient generated at the electrode tip (Kenyon et al., 1998). Thus, the Inter-Peak Latency (IPL) cannot be accounted for acoustically, as transients and other artefacts directly associated with the stimulus sound would occur at the same time regardless of sound amplitude.

Figure 4 presents the audiograms for both *H. molitrix* and *A. nobilis*, established by visual inspection of the ABR traces. Threshold was taken to be the lowest level of sound pressure (recorded using the B&K hydrophone and expressed in units of dB re. 1 μPa), that evoked a repeatable ABR response.

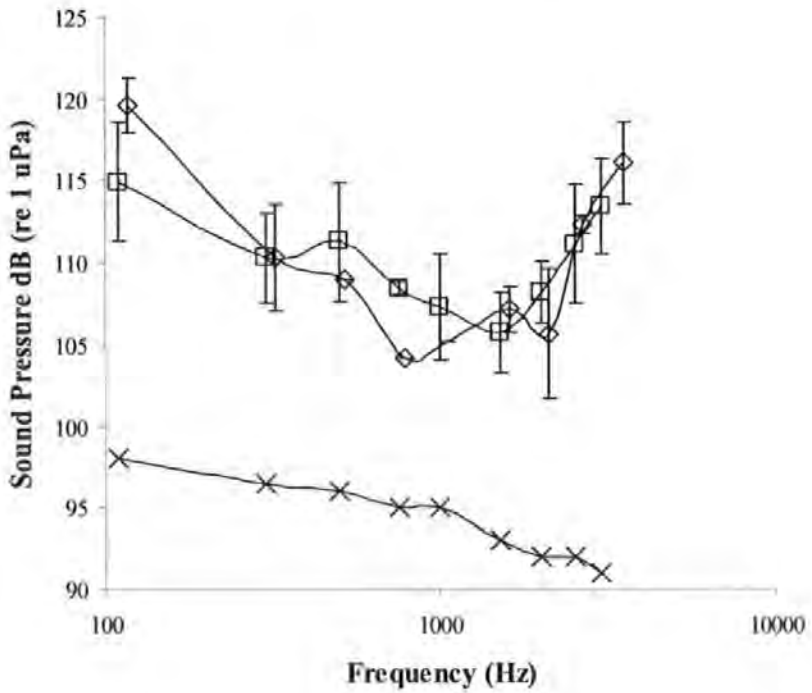

Figure 4. The audiograms for *H. molitrix* (diamonds) and *A. nobilis* (squares), Y axis error bars show the standard devotion of the data. The lowest curve (x) represents the ambient noise level in the test tank

It may be seen that the audiograms for both Asian carp species follow a similar Gaussian profile to each other, with the lowest thresholds occurring at frequencies of between 750 Hz to 1500 Hz.

At the higher frequencies, hearing sensitivity reduces sharply, whilst at the lower frequencies sensitivity reduces more gradually. It may be noted that the background noise level is lower than the recorded thresholds of hearing, and hence it may be concluded that the audiograms are uncontaminated by background noise. The lowest threshold recorded from *H. molitrix* was 104 dB (re. 1 μPa) at 750 Hz, whilst the lowest threshold from *A. nobilis* was 106 dB (re. 1 μPa) at 1500 Hz.

4. Discussion

The hearing thresholds of silver carp (*H. molitrix*) and bighead carp (*A. nobilis*) are presented in an audiogram as the lowest levels of sound pressure as a function of frequency that evoked a repeatable threshold response. The audiograms produced for the two Asian carp species is comparable in frequency bandwidth (though with slightly higher thresholds), to the audiogram for the specialist channel catfish (*I. punctatus*) produced by Fay and Popper (1975) in an electrophysiological study of fish audition using an air mounted transducer. Figure 5 presents the audiograms of both *H. molitrix* and *A. nobilis*, which are presented along with the audiogram for *I. punctatus* from Fay and Popper (1975) and the "benchmark" audiograms for *P. spathula* and *A. fulvescens* (from Lovell et al., in press). Figure 5 shows that the hearing thresholds from *H. molitrix* and *A. nobilis* are moderately higher than thresholds obtained from *I. punctatus*. It is probable that the higher thresholds recorded is, in part, due to the hearing of the two carp species being more acute than the lowest level of sound that the submerged transducers used in this study can consistently generate. In an attempt to stabilise the sound field at low intensities, the projectors were driven with load resistors placed between the amplifier and projector. To counter this problem, a number of published studies of specialist fish hearing (c.f. Fay and Popper, 1975, Kenyon et al., 1998), have used air mounted transducers to generate underwater sound fields below the threshold of hearing. However, in this instance, the use of submerged transducers is the most appropriate stimulus generating methodology (rather than air mounted transducers), as the sound field in the test tank is produced using the same type of transducer as is used in the AFD barrier. Thus, the sound transmission methodology is arguably closely representative of sources used in aquatic management strategies, thereby providing a more reliable approach to the acquisition of auditory information for practical "field" applications.

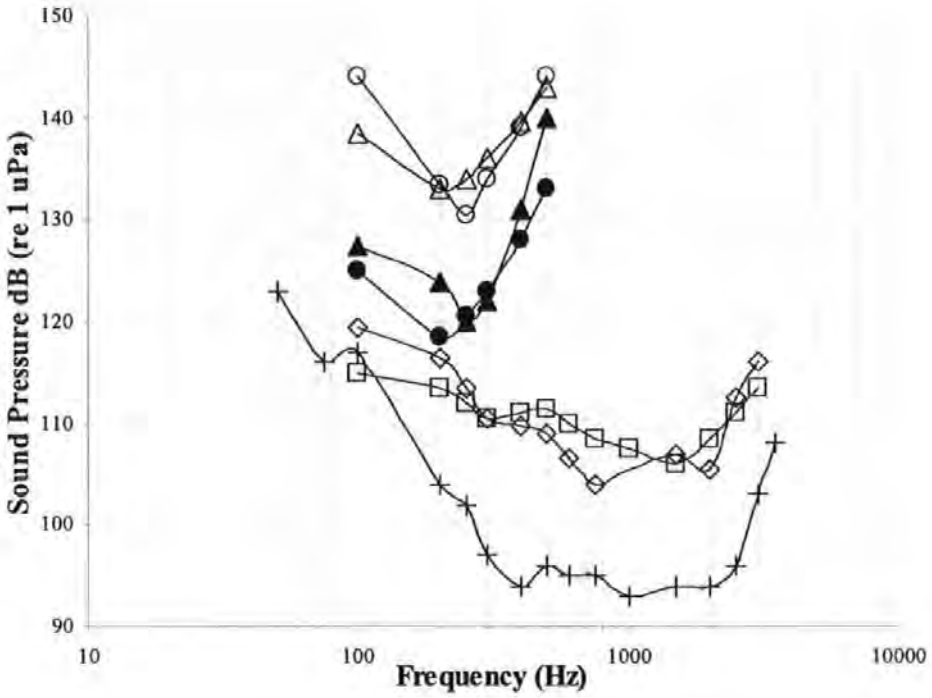

Figure 5. Comparison of the audiograms for *A. fulvescens* (closed circles = maximum sound pressure; open circles = maximum particle motion), and *P. spathula* (closed triangles = maximum sound pressure; open triangles = maximum particle motion) (from Lovell et al., in press), for *H. molitrix* (diamonds) and *A. nobilis* (squares) and for *I. punctatus* (Popper and Fay (1975) (crosses)

The results of the auditory examination of *H. molitrix* and *A. nobilis* (the target species for the AFD barrier) show that these fish are sensitive to sound pressure, whereas *P. spathula* and *A. fulvescens* (non-target indigenous species) are not (Lovell et al., in press). Thus, *P. spathula* and *A. fulvescens* will have a significantly higher deterrent threshold than *H. molitrix* and *A. nobilis* in a pressure dominated sound field. It is therefore concluded that an Acoustic Fish Deterrent (AFD) barrier generating a pressure dominated sound field of between 750 Hz to 2000 Hz and of sufficient intensity to deter non-indigenous Asian carps from crossing, will be practicably inaudible to *P. spathula* and *A. fulvescens*, having little or no influence on the ecology of these indigenous species.

Acknowledgments

The authors would like to acknowledge Kevin Irons and all the staff at the Illinois River Biological Station for their hospitality and great expertise in the acquisition and maintenance of

the fish studied in this work. The authors also express gratitude to Dr J.R. Nedwell of Subacoustech Ltd for the provision of equipment and technical support.

References

Casper, B.M., Lobel, P.S., Yan, H.Y., 2003. The hearing sensitivity of the little skate, *Raja erinacea*: A comparison of two methods. Environmental Biology of Fishes. 68, 371 – 379

Corwin, J.T., Bullock, T.H., & Schweitzer, J., 1982. The auditory brain stem response in five vertebrate classes. Electroencephalogr. Clin. Neurophysiol. 54: 629-641

Enger, P.S. & Anderson, R., 1967. An electrophysiological field study of hearing in fish. Comp Biochem Physiol 22, 517-525

Fay, R.R., & Popper, A.N., 1975. Modes of stimulation of the teleost ear. J. Exp. Biol., 62, 370-387.

Fine, M.L., 1981. Mismatch between Sound Production and Hearing in the Oyster Toadfish. In: Hearing and Sound Communication in Fishes, Tavolga, W.N. et al (eds.), 257-263.

Hawkins, A.D., & MacLennan, D.N., 1976. An acoustic tank for acoustic studies on fish. In A. Schuijf, and A.D. Hawkins (eds) Sound Reception in Fish. Elsevier, Amsterdam. pp 149 169

Jacobson, J.T., 1985. An overview of the auditory brainstem response. In: Jacobson JT (ed) The auditory brainstem response. College-Hill Press, San Diego, 3-12

Jewett, D.L., 1970. Volume conducted potentials in response to auditory stimuli as detected by averaging in the cat. Electroencephalogr Clin Neurophysiol. 28, 609-618

Jewett, D.L. & Williston, J.S., 1971. Auditory evoked far fields averaged from the scalp of humans. Brain. 94, 681-696

Kenyon, T.N., Ladich, F., & Yan, H.Y., 1998. A comparative study of the hearing ability in fishes: the auditory brainstem response approach". J. Comp. Physiol. A 182:307 318.

Lovell, J.M., Findlay, M.M., Moate, R.M., & Yan, H.Y., 2005 A. The hearing abilities of the prawn *Palaemon serratus*. Comp. Biochem. Physiol. A Mol. Integr. Physiol. Jan;140(1):89-100.

Lovell, J.M., Findlay, M.M, Nedwell, J.R., Pegg, M.A., in press. The inner ear morphology and hearing abilities of the Paddlefish (*Polyodon spathula*) and the Lake Sturgeon (*Acipenser fulvescens*). Comp. Biochem. Physiol. A Mol. Integr. Physiol.

Myrberg, A.A., 1981. Sound communication and interception in fishes. Hearing and Sound Communication in Fishes. Tavolga WN, Popper AN, and Fay RR, Eds. Springer-Verlag, New York.

Overbeck, G.W., & Church, M.W., 1992. Effects of tone burst frequency and intensity on the auditory brainstem response (ABR) from albino and pigmented rats". Hear Res 59: pp129-137

Popper, A.N., & Fay, R.R., 1993. Sound detection and processing by fish: critical review and major research questions. Brain Behav Evol, 41, 14-38

Taylor, R.M., Pegg M.A., & Chick, J., In Press. Effectiveness of two bioacoustic behavioral fish guidance systems for preventing the spread of bighead carp to the Great Lakes. North American Journal of Fisheries Management.

von Frisch K (1938). "The sense of hearing in fish". *Nature* 141, 8-11.

Yan, H.Y., 1995. Investigations of fish hearing ability using an automated reward method. In Methods in Comparative Psychophysics (eds) G. M. Klump, R. J. Dooling, R. R. Fay, and W. C. Stebbins. Birkhauser Verlag Basel/Switzerland. pp. 263-276.

Yan, H.Y., Fine, M.L., Horn, N.S., Colon, W.E., 2000. Variability in the role of the gasbladder in fish audition. Journal of Comparative Physiology A. 186, 435-445.

Appendix iii

Commissioned work

Nedwell, J.R., Turnpenny, A.W.H., Lovell, J.M., Langworthy J., Howell, D. & Edwards, B. (2003). The effects of underwater noise from coastal piling on salmon (*Salmo salar*) and brown trout (*Salmo trutta*). Report Reference: 576R0113.

Nedwell J.R; Lovell, J.M & Pegg, M.A (2005). The inner ear morphology and hearing abilities of the Paddlefish (*Polyodon spathula*) and the Lake Sturgeon (*Acipenser fulvescens*). Report reference: 611R0103

Nedwell J.R, Lovell, J.M, & Pegg M.A (2005) Mesurment of audiograms of silver carp (*Hypopthalmichthys molitrix*) and bighead carp (*Aristichthysc nobilis*) for Chicago Canal acoustic barrier optimisation. Report reference: 611R0205

The effects of underwater noise from coastal piling on salmon (*Salmo salar*) and brown trout (*Salmo trutta*)

Jeremy Nedwell, Andrew Turnpenny[1], Jonathan Lovell[2],
John Langworthy, Daren Howell & Bryan Edwards

[1] Fawley Aquatic Research Ltd, Fawley, UK.

[2] Institute of Marine Studies, University of Plymouth

Contents

Introduction.

This report presents monitoring measurements of waterborne noise taken at Town Quay, Southampton, during piling operations at Red Funnel's Southampton Terminal in September 2003, and interpretation of the effects of the noise on fish.

1.1. Background to the work.

The piling at the Southampton Terminal was required as part of a construction project installing improved loading facilities at the Red Funnel Southampton Terminal, illustrated in Figure 1. The project was required to provide infrastructure for improved ferry services, and in particular to allow twin-deck access to ferries. As part of this project piling in the water adjacent to the dock wall was required to provide foundations for the new structure. Existing ferries were also modified during the period of construction to allow twin deck access; during this period a temporary ferry was provided.

Driving of piles in water have been recorded as generating high levels of underwater noise (e.g. Abbott & Bing-Sawyer (2002)), and there was consequently concern by the Environment Agency (EA) and English Nature (EN), who have remits to control construction projects so as to mitigate adverse impacts on fish stocks. Their concern related to the possible effects construction noise might have on local fish populations, and in particular on migration of salmon.

A consent had initially been given by the Environment Agency for Red Funnel's contractors to undertake the piling between the 1st December 2003 and the 31st March 2004, during which period no significant impediment to the migration of salmon through the area and into the Test was expected. However, due to significant economic and commercial factors connected with the required timescales for withdrawing the ferries from service, and the need to accomplish the engineering work outside peak travel periods for passengers, a consent was sought from EA and EN to bring forward the piling project to commence on the 1st September.

Permission was subsequently given for the piling to be brought forward to September 2003, subject to two requirements, namely:

1. the mitigation of impact piling noise by use of bubble curtains as required, and
2. the work being monitored by means of measurements of underwater noise.

These measures were deemed sufficient to ensure there was no increased likelihood of salmon in Southampton Water and the River Test being affected by the piling.

Red Funnel additionally provided some funds for direct visual observation of a tethered cage of fish in order to make direct visual observations of any effect. Owing to the problems of obtaining salmon (*Salmo salar*) for testing, farmed brown trout (*Salmo trutta*) were used in the tests. It was thought that, as they were the most closely related species, they would have a similar hearing ability to *S. salar*, and hence would react to the sound in a similar way.

Shortly prior to the program commencing it was suggested to the Environment Agency that this programme would offer an opportunity to conduct fundamental research into the behavioural response of fish exposed to piling or other high-level noise sources. The EA made available sufficient funds to provide fish cages, and measurements of level, at four further ranges. Thus measurements were made from about 25 metres from the piling to 400 metres. The aim of this was to be able to measure the greatest range, and hence the threshold level of sound, at which behavioural effects of the noise occurred. It was thought

that such information would be valuable in predicting the environmental effects of future piling projects, and in monitoring noise levels.

The results of the monitoring programme funded by Red Funnel, which included observations of caged fish in a single cage at a range of 400 metres, were reported in Nedwell *et al* (2003b). This report subsumes those results, and includes the additional work undertaken on behalf of the EA.

1.2 Piling methods.

Two sorts of piling were undertaken on the site, namely vibropiling and impact piling.

Vibratory pile drivers are machines that install piling into the ground by applying a rapidly alternating force to the pile. This is generally accomplished by rotating eccentric weights about shafts. Each rotating eccentric produces a force acting in a single plane and directed toward the centreline of the shaft. Figure 2 shows the basic set-up for the rotating eccentric weights used in most current vibratory pile driving/extracting equipment. The weights are set off-centre of the axis of rotation by the eccentric arm. If only one eccentric is used, in one revolution a force will be exerted in all directions, giving the system a good deal of lateral whip. To avoid this problem the eccentrics are paired so the lateral forces cancel each other, leaving only axial force for the pile. Machines can also have several pairs of smaller, identical eccentrics synchronised to obtain the same effect as one larger pair.

Impact piling is performed using hammers which drive the pile by first inducing downward velocity in a metal ram, as shown in Figure 3. Upon impact with the pile accessory, the ram creates a force far larger than its weight, which moves the pile an increment into the ground. Most impact hammers have some kind of cushion under the end of the ram which receives the striking energy of the hammer. This cushion is necessary to protect the striking parts from damage; it also modulates the force-time curve of the striking impulse and can be used to match the impedance of the hammer to the pile, increasing the efficiency of the blow.

The sediments at the terminal were found to be relatively soft, such that nearly all the pile driving at the Red Funnel site was undertaken using vibropiling. This removed the need to impact pile at the site. However, since the instrumentation and fish cages were set up, and in view of the scientific importance of the measurements and observations, permission was given by the EA for a brief period of impact piling to be undertaken. This enabled the measurements of impact piling and observations of effect reported herein to be made.

2. The Measurements.

2.1. Philosophy of measurements; the dB_{ht} scale.

A brief description of the dB_{ht} scale used in this document, which is a method of rating noise in respect of its potential for behavioural effects and which incoporates species sensitivity to sound, is appropriate.

In man, a commonly used measure of the effect of sound is the Sound Level measured in dB(A). The human ear is most sensitive to sound at frequencies of the order of 1 to 4 kHz, and hence these frequencies are of greatest importance in determining the physical and psychological effects of sound for humans. At lower or higher frequencies the ear is much less sensitive, and humans are hence more tolerant of these frequencies. To reflect the importance of this effect a scale of sound, the dB(A), effectively allows for the frequency response of the human ear. The process can be thought of as measuring the level of sound after putting it through a filter which approximates the hearing ability as a function of frequency of the human ear. Measurements of sound level in dB(A) have been shown to relate well to the degree of both physical and behavioural effects of sound on humans. This approach has also been successfully extended (Parvin & Nedwell (1995)) to underwater human exposure to sound, despite human underwater hearing ability differing greatly from that of human hearing in air, yielding the dB(UW), which allows the effects of sound on submerged humans to be estimated.

The response of a living organism to a given sound is dependent on the particular species, since each species has its own range of frequencies over which it can hear and its own hearing sensitivity. Fish typically hear from a few Hz up to 1 kHz and above; marine mammals typically have peak hearing ability from about 1 kHz to 100 kHz. In the dB_{ht}(*Species*), (Nedwell, *et al* (2003)) a similar approach to the dB(A) is used to arrive at a number for the level of a given sound which is indicative of how much that species will be affected by that sound. In a similar fashion to the dB(A), a frequency dependent filter is used to weight the sound for a particular species; the suffix 'ht' relates to the fact that the sound is weighted by the hearing threshold of that given species. The process can be thought of as measuring the level of sound after putting it through a filter which approximates the hearing ability of the species; it hence corresponds to the likely perception of the sound by the species.. The level expressed in this scale is different for each species and hence the species must be appended. For instance, the dB_{ht}(*Salmo salar*) level of a sound (i.e. for a salmon) will be different from the dB_{ht}(*Phocena phocena*) level (for a seal). It is believed that the higher the number, *irrespective of the species*, the more likely it is that it will cause an effect. Initial research with fish indicates that at levels of 90 dB_{ht}(*Species*) or more, significant avoidance reaction occurs. This is also similar to sound levels on the dB(A) scale at which humans avoid sound.

It may be noted that the effective noise levels of sources measured in dB_{ht}(*Species*) are usually much lower than the unweighted levels, not only because the sound will contain frequency components that the species cannot detect, but also because most marine species are adapted to living in a noisy environment and hence have high thresholds of perception of (are insensitive to) sound.

2.2. Location of pile driving and measurement positions.

The piling was carried out at Red Funnel's terminal at Town Quay, at the southern end of Southampton High Street. The location of the site is illustrated in the sketch map in Figure 4. The monitoring measurements were taken at a number of locations, which are illustrated in

Figure 5. Locations R1 and R2 were at each end of a pontoon which was used for maintenance work on Red Funnel's vessels. R3 was at the side of a dolphin, access to which was via a ladder and walkway from the pontoon. R4 was at the 'knee' in Town Quay, and R5 was at the far end of the quay.

While the area of the piling looks from the sketch to be relatively confined, in fact since both Town Quay and Royal Pier are open piled structures they did not influence the sound field, and hence the propagation conditions approximated to open conditions.

In total 10 piles were driven at the site. Figure 6 is a sketch giving the locations of the individual piles on the site. It will be seen that two different diameter pile tubes were used, as indicated in the figure; a photograph of the piles is shown in Fig. 7. A photograph of site during piling operations can be seen in Figure 8. In the photograph, the two groups of four piles to one side of the linkspan can be seen. The other two piles (numbers 9 and 10) are obscured by the structure (pedestrian walkway) on the right of the photograph. One pile in each of the groups was left standing proud, for later dynamic testing purposes using the impact driver. The vibropiling was undertaken using a PVE 2316 VM driver; a picture of this driver is illustrated in Fig 9. Impact piling was performed using a BSP357/9 hydraulic drop hammer which is illustrated in Figure 10 and 11.

The distances between the piling and measurement locations were measured using a hand-held GPS receiver and display. The relevant distances (from a point on the quayside adjacent to the ferry's linkspan where the piling was undertaken) are given in Table 2.1.

Location	Distance (m)
R1	29.8
R2	54.2
R3	96.3
R4	233.8
R5	417.4

Table 2.1. Distances of measurement locations from piling site.

2.3. Instrumentation and measurement procedure.

Sound measurements were taken in two ways:

1) using a computerized data acquisition system, in which a hydrophone and its signal conditioning equipment was connected to a laptop computer to allow the on-line determination of dB_{ht}, and
2) using watertight boxes, each fitted with a hydrophone and containing signal conditioning equipment and a small DAT recorder, for later off-site study of the sound signal.

For the first (computerized) system, 1 of 3 types of Bruel & Kjaer hydrophone was used. The first was a Type 8104, serial number 2225716, the second was a Type 8105, serial number 1461320, and the third was a Type 8106, serial number 2256725. Details of the calibrations of these hydrophones and their traceability to International Standards are given in Appendix 1. Figure 12 is a block diagram of the instrumentation setup. The 8104 and 8105 hydrophones were connected to a Brüel & Kjær Type 2635 Charge Amplifier to condition the signal, and the output from this amplifier was fed to a Kemo filter, set to have a passband of

5 Hz to 20 kHz. The 8106 hydrophone, which has a built-in pre-amplifier adjacent to the pressure sensing element, was connected to a Subacoustech PE6 power supply/amplifier. The output from this was fed to the Kemo filter, set to have a lowpass cutoff frequency of 20 kHz. The output from the 2635 or PE6 amplifier was fed to a National Instruments 6062E DAQCard, an analogue-to-digital converter card, which was inserted in a PCMCIA slot in a Sony laptop computer. The computer ran a program, written using the National Instruments LabVIEW application, to digitize the signal and calculate a dB_{ht} (*Salmo salar*) value on one second noise segments.

For the second (recorded) measurements, four watertight boxes were fitted with Bruel & Kjaer Type 8103 hydrophones, serial numbers 2261918, 1785404, 1727543 and 1406215. The calibrations of these hydrophones are also given in Appendix 1. Each box also contained a Subacoustech CA01 charge amplifier, which conditioned the signal before it was recorded on a Sony TCD-D7 or TCD-D8 DAT recorder. The block diagram of this system is also given in Figure 12.

For the vibrodriving a total of nine sets of measurements was taken. For the impact driving three sets of measurements were taken. Table 2.2 lists the driving operations which were measured, and indicates the instrumentation which was used at each location.

Pile number	Pile diameter (mm)	Type of driving	Measurement position, and equipment used				
			R1	R2	R3	R4	R5
2	914	vibro	B	—	B	—	C-8104
3	914	vibro	—	B	—	—	C-8104
4	914	vibro	—	B	—	B	C-8104
5	508	vibro	—	—	—	—	C-8106
6	508	vibro	—	—	—	—	C-8106
7	508	vibro	B	B	—	—	C-8106
8	508	vibro	B	—	—	—	C-8106
9	508	vibro	—	—	—	C-8106	—
10	508	vibro	—	—	C-8105	—	—
1	914	impact	B	B	C-8105	B	—
6	508	impact	B	B	C-8105	B	—
9	508	impact	B	B	C-8105	B	—

B = watertight box; C-X = computerized capture, and hydrophone type.

Table 2.2. Details of measurements of pile driving.

For the measurements using the computer system the hydrophone was located at the measurement position by being taped to a rope which had a weight fixed at its end, and the rope and 'phone were lowered into the water until the hydrophone was 2.5 m below the water surface. For the measurements with the boxes, the box was held in a clamp to which a rope and weight were attached and lowered into the water. Again, the boxes were set so that the hydrophones were at a depth of 2.5 m, but, at positions R1 and R2, when the tide was out, water depth was less than 2.5 m and the boxes' depth was set at just above the sea bed. The ropes were adjusted at regular intervals to keep the hydrophones at the 2.5 m depth, where possible, as the tidal state varied.

After consultation with the Dean & Dyball operatives, and when the pile tube had been readied and it was clear that the driving operation was shortly to commence, the tape recorders in the boxes were started, and the boxes were closed and lowered into the water. Also, the computer program was started. On the computer data were captured continuously until the pile tube had been driven to depth, or there was a lengthy period when no driving was taking place because difficulties had been encountered. The boxes were left in place until driving stopped, when they were retrieved, opened and the tape recorders stopped.

3. Measurements of the hearing ability of brown trout (*Salmo trutta*).

As a consequence of the programme being conducted at short notice, and suitable farmed salmon being unavailable, readily available farmed brown trout (*Salmo trutta*) were used in the tests as a model for salmon (*Salmo salar*). During the programme, dB_{ht} (*Salmo salar*) levels were calculated. It would have been preferable to calculate actual dB_{ht} (*Salmo trutta*) levels, but at the time this was not possible due to the lack of an audiogram for the *S. trutta*. It was, however, thought that *S. trutta*, as the most closely related species to *S salar*, and having similar inner ear morphology, would have similar hearing ability. Discussions by the authors with fish and marine mammal biologists and bioacousticians have indicated a received wisdom which may be summarised as "species that are closely related and similar in their auditory morphology will have similar hearing abilities".

During the piling the dB_{ht} (*Salmo salar*) levels were therefore recorded and used as an estimate of the dB_{ht} (*Salmo trutta*) levels. The levels of sound were calculated from the measurements during the programme to be of the order of 70-80 dB_{ht} (*Salmo salar*). In general, at these levels medium to strong reaction to the sound would be expected (Nedwell *et al* (2003a)). There was, however, no apparent reaction from the fish.

This observation raised doubts as to whether the hearing of *S. trutta* was similar to that of *S. salar*. Consequently, a set of measurements of the hearing ability of the *S. trutta* used in the programme were made, and used the non-invasive Auditory Brainstem Response (ABR) method to gain the neurological data. The procedure used to acquire the evoked potentials was approved by the United Kingdom Home Office. The test subjects (*S. trutta*) were placed in a flexible cradle formed from a soft foam rectangle saturated with seawater. Figure 13 schematically illustrates the layout of the audiometric apparatus. Oxygenated water kept at a temperature of 18°C was gravity fed at an adjustable flow rate of 10 millilitres per second for the *S. trutta*, and 3 millilitres per second for the goldfish. The water was held in an aerated reservoir positioned in an adjacent room, and fed to the front of the foam "cradle" through a 6 mm diameter plastic tube. Water was able to flow around the fish and vent through an aperture positioned at the rear of the foam cradle; thus the fish was able to ventilate its gills by simply opening and closing its mouth. The foam cradle was placed in a second tank of length 450 mm, width 300 mm and depth 200 mm, and supported using a clamp to keep the nape of the fish's head 1 mm above the surface of the water. The experimental tank was placed on a table with vibration inhibiting properties, located in a quiet underground chamber 3 m length by 2 m width and 2 m height. After the hearing assessment the fish were relocated to a holding tank for observation, prior to being returned to a non-experimental aquarium.

The stimulus sound was generated by the PC shown in Figure 13, and presented to the fish at initial sound pressures not exceeding 145 dB re 1 µPa for *S. trutta*. Amplification of the sound was achieved using a Pioneer type SA-420 amplifier, and a 200 mm Eagle L032 loudspeaker with a frequency response range of 40 Hz to 18 kHz was used.

The stimulus tones presented from the loudspeaker to the fish were calibrated using an insertion calibration. A Bruel and Kjaer Type 8106 Hydrophone (Serial Number 2256725) was placed in the tank and positioned exactly in the position the fish would have been. The hydrophone was calibrated and traceable to International Standards; the calibration certificate is included in Appendix 1. The signal from the hydrophone was amplified using a Subacoustech PE6 preamplifier and digitised using a National Instruments DAQ-6062e interface card at a sample rate of 300 kS/s. In case of non-proportionality of the response of the loudspeaker, measurements of the sound pressure were taken for every amplitude and

frequency setting that could be used. Consequently, a total of 110 individual calibration measurements were taken in the calibration process. These calibrated levels were then applied to the threshold defined by ABR measurement to provide calibrated audiograms with pressure levels traceable to International Standards.

The loudspeaker was placed inside a Faraday cage and connected to a centralised earth point located in an adjacent room where the PC, amplification and analysis equipment were set up. Connecting wires were fed through a 100 mm port in the partitioning wall. The electrophysiological response of the fish to acoustic stimulation was recorded using two cutaneous electrodes. The reference electrode was positioned centrally on the head above the medulla, and the record electrode was located 5 mm anterior of this point; both electrodes were held in place using micromanipulators. The electrodes shown in Figure 14 were connected to the MS6 preamplifier by 1 m lengths of screened coaxial cable, with an external diameter of 1.5 mm. The outer insulating layer of the coax was removed 15 mm from the end where the electrode tip was to be fixed, and the screening layer removed 10 mm from the cable end. The inner insulating material was then trimmed by 2 mm, and the exposed inner wire (0.5 mm diameter) was tinned with silver solder and joined to a 10 mm length of 9 ct gold wire (0.25 mm diameter). The assemblage was pushed through a 100 mm length of plastic tubing with an internal diameter of 4 mm fixed to a fine pipette tip, until 0.4 mm of the gold wire was exposed. The electrode tip base, along with all the joints in the plastic tubing, were sealed using a clear epoxy resin, leaving 0.3 mm of exposed metal through which the EP could be conducted.

The ABR measurements of hearing threshold were made using a proprietary control and analysis programme, written in a LabView 7 environment. This programme both generated the stimulus signals and captured and analysed the response. The stimulus used was a sine train (sine wave pulse) which was presented to the fish at a given frequency and sound pressure level. The evoked potential was recorded by means of the electrodes, which were positioned on the cranium of the fish adjacent to and spanning the VIII nerve. The response was amplified and digitised to 12 bits resolution and recorded. This process was repeated 2000 times, and the response averaged; this was required to remove electrical interference caused by muscle movements. After the averaging process the evoked potential could be detected, following the stimulus by a short latency period of a millisecond or so. Each measurement was repeated twice; this aids in separating the evoked response, which is the same from trace to trace, from the noise, which varies in two successive measurements.

Figure 15 illustrates a typical result, in this instance for a frequency of 300 Hz. The trace at the bottom of the figure illustrates the waveform presented. The upper traces illustrate the evoked potential as a function of the level of the sound. At the highest level recorded, 130 dB re 1 μPa, it may be seen that there is a clear response, and hence this is above the threshold of hearing at this frequency. By comparison, at a level of 116 dB re 1 μPa, it may be seen that there is no significant similarity between the traces. A threshold response occurs at 118 dB re 1 μPa, which is just detectable, and this consequently defines the threshold of hearing at this frequency for this particular individual fish.

To ensure consistency with published work, and in order to validate the ABR system and software, measurements were initially made of the audiogram of the hearing specialist goldfish (*Carassius auratus*), thus repeating measurements previously made in the experiment conducted by Kenyon *et al* (1998). It may be seen from Figure 16 that the results from the present experiment closely agreed with these previously reported measurements in

the open literature. It was therefore felt that the ABR system was producing accurate and repeatable results to frequencies up to 5 kHz.

Measurements of the audiogram of *S. trutta* were made using this equipment, using four fish at all of the frequencies tested, and 24 fish at frequencies of between 300 and 1000 Hz. The *S. trutta* auditory threshold measured is illustrated in Figure 17. The *S. salar* audiogram, from Hawkins & Johnstone (1978), is also shown on the figure for comparison.

It may be seen that the hearing of the brown trout is significantly different from that of the salmon. The hearing of the brown trout is not only significantly less sensitive than that of the salmon, but also it is broader and flatter in frequency response, such that it is of significantly wider bandwidth, with effective hearing from 30 Hz to above 1 kHz. It is possible that this arises, in part, from the resonance of the swimbladder, which both species use to convert acoustic pressure in the water to movement of the hair cells, being less tuned in the trout than in the salmon. Recent work has shown that removal of gas from the swimbladder confirms its role in the enhancement of hearing, at least in terms of hearing threshold, though it does not necessary contribute to the enhancement of hearing frequency (Yan (2003)). Differences in the frequency response of the hearing system between *S. trutta* and *S. salar* may also be attributable to species-specific tuning of the VIII nerve, and discrete variations in lengths of hair cells in the inner ear. It is known that in lizards and birds regions having longer ciliary bundles detect lower-frequency signals, while shorter bundles detect higher frequencies (Popper & Fay (1993); Sugihara & Furukawa (1989)). Without further research it is not possible to determine the cause of the differences.

The audiogram of *S. trutta* became available about two weeks after the piling finished. It was then possible to retrospectively calculate the actual dB_{ht} (*Salmo trutta*) levels from the recorded raw data. It was found that, on average, the dB_{ht} (*Salmo trutta*) levels during piling were 15.9 dB lower than the dB_{ht} (*Salmo salar*) levels for the same data. This is of significance, because the highest levels of noise from the piling were only of the order of 60 dB_{ht} (*Salmo trutta*), and hence below the levels at which a reaction would be expected. This difference explained the lack of reaction of the caged *S. trutta* to the piling noise, and tends to confirm the hypothesis that strong reaction to noise occurs at levels of 90 dB_{ht} (*Species*) and above.

In summary, it was concluded that:

1. The audiometric apparatus, having been tested against a species with known hearing ability, was thought to be giving accurate and reproducible results.
2. The audiogram of the brown trout was found to be significantly different from that of the salmon, despite a common assumption that closely related species will have similar hearing ability.
3. It is not possible to infer the effects of noise from studies on a related species without knowledge of the hearing ability of both.

4. Analysis of piling noise measurements and results.

4.1. Vibro driver.

Part of a typical sound pressure level *vs.* time history obtained at position R5 (at the end of Town Quay, at 417.4 m from the piling) on the 18th September 2003 for the vibro driven pile case is shown in Figure 18. The figure illustrates the level of the sound in dB as a function of the time of day. The upper trace, in blue, indicates the unweighted sound level in dB re 1 μPa, and the lower trace the level in dB_{ht} (*Salmo salar*). Also marked on the figure are the periods during which vibropiling was undertaken.

First, looking at the unweighted sound pressure levels, it can be seen that there are periodic short but relatively large increases in level up to about 150 dB. These are associated with the passage of vessels along Southampton Water, which is a busy waterway, and the passage of ferries into the Red Funnel terminal. Most of these movements were noted at the time of the measurements, and have been noted on the figure. It is interesting to note that from about 15:00 hrs to the end of the recording at 17:00 hrs there is a significant and continuous increase in level over the earlier part of the recording from 14:00 hrs to 15:00 hrs. This is due to noise from the dredger *Bluefin,* which was removing silt from the waterway by suction dredging; a photograph of the vessel is illustrated in Figure 19. The dredger was at a distance of about 200 m from the measurement position.

In respect of the vibropiling, it may be seen that there is no discernible increase of the signal when the driving is taking place compared to when it is not; in fact the vibropiling could not be discerned audibly in the time history at 400 metres. It was apparent when listening to the recordings that the background noise was dominated by other man-made noise, and in particular by the movement of vessels.

It is interesting to note that there is little difference in the shape of the time histories (i.e. in the level variations over time between the dB_{ht} (*Salmo salar*) values and the unweighted dB levels), other than the dB_{ht} (*Salmo salar*) values being of much lower level. The lower level results from *S. salar* being relatively insensitive to sound, and to a lesser degree from their limited hearing bandwidth.

Similar results were noted for other recordings made during vibropiling, and in general there was no discernible difference between recordings of sound pressure level *vs.* time history made on days on which vibropiling was being conducted and those on which there was no vibropiling.

In summary, it may be concluded that in respect of the vibropiling, at the range at which monitoring was conducted of 417 m, there was no discernible contribution from the piling above the background noise. It was apparent when listening to the recordings that the vibropiling could not be heard above the background noise caused by the movement of vessels.

4.2. Impact driver.

4.2.1 Unweighted results.

Figure 20 is a plot of a typical pressure time history recorded at location R3 which illustrates the sound pressure in conventional unweighted units. A section of the recording having two pile driver strikes has been illustrated. It may be seen that there is a high level of impulsive sound as the pile is struck, having a peak-to-peak pressure of about 200 Pa and a roughly exponential decay, with a time constant of about 0.1 sec. There are two later arrivals, one

small arrival occurring at about 0.2 sec after the main arrival, and a further large arrival about 0.5 sec after the main arrival. These are thought to be seismic arrivals carried in the seabed.

Figure 21 illustrates the peak-to-peak Sound Pressure Level of the impact piling as a function of the range from the piling, for the case of the two 508 mm diameter piles and the single 914 mm diameter pile. These results have been averaged over all of the impacts at each of the ranges (typically 10 to 50 impacts). It may be seen that there is a significant scatter in the levels of noise recorded, and that although overall there was a general fall in noise level with range, there are some points where the noise was significantly higher or lower than the general trend. The reason for these is not known, but it is possible that it results from partial focussing or defocussing of noise during propagation through the water and sediments. There is also a significant variation in overall level between the three different piles driven.

In order to generalise measurements to provide an objective assessment of degree of any environmental effect and the range within which it will occur, it is normal to represent the sound in terms of two parameters. These are:-

1. The Source Level (i.e. level of sound) generated by the source, and the
2. Transmission Loss, i.e. the rate at which sound from the source is attenuated as it propagates.

If a given sound can be represented in terms of these two parameters it allows the sound level at all distances to be specified. Usually the decrease in sound pressure level (SPL) is modelled as being due to geometric losses, i.e. the sound mainly reduces as a result of being spread over an increasing area. Under these circumstances the (SPL) is modelled as

$$SPL = SL - N_g \log(R)$$

where SL is the source level of the noise source, N_g is a geometric attenuation constant and R is the range in metres from the source.

However, for the measurements of impact piling at the Red Funnel terminal, the losses in level with range were thought to be mainly due to absorption; consequently a reasonable fit for the case of the 508 mm diameter pile is given by the linear equation

$$SPL = SL - N_a (R)$$

where the Source Level is about 193 dB re 1 μPa @ 1 metre, and the Transmission Loss rate, N_a, is about 0.13 dB per metre. For the case of the 914 mm diameter pile, the Source Level is given by 201 dB re 1 μPa @ 1 metre, and the Transmission Loss by 0.13 dB per metre.

It is interesting to note that the Source Level of 193 dB is slightly higher than that measured during previous measurements at Littlehampton (Nedwell & Edwards (2002)) of 192 dB re 1 μPa. These levels are, however, very much lower than others obtained by the authors for underwater piling in deep water, where Source Levels in excess of 250 dB re 1 μPa @ 1 metre have been recorded, associated with propagation to large distances, albeit for larger diameter piles.

4.2.2 Results in dB_{ht} Levels.

Figure 22 presents the same data as figure 20, but this time weighted by the hearing ability of *S. salar*. The figure thus presents the pressure level of the noise from the piling in units of "salmon hearing thresholds" versus the time in seconds.

The *S. salar* weighted time history is generally similar in form to the unweighted time history. This is probably as a result of the majority of the energy from the piling being at the low frequencies at which fish can hear. It is interesting to note, however, that the seismic arrivals, which are at a frequency of about 10 Hz, have disappeared due to the relative insensitivity of *S. salar* to these frequencies of sound.

Figure 23 presents the dB_{ht} levels of the sound as a function of range. The figure presents two sets of data, one for the case of the two 508 mm diameter piles and one for the single 914 mm diameter pile. For each of these cases, two sets of data have been plotted, these are the dB_{ht} (*Salmo salar*) level, and the dB_{ht} (*Salmo trutta*) level.

For each set of results, a best fit of Source Level and Transmission Loss has been calculated and appended to the figure. These results are also tabulated as Table 4.2.

Species	Pile diameter (mm)	Source Level dB_{ht} (*Species*) @ 1metre	Transmission Loss dB_{ht} (*Species*) per metre
Salmon (*Salmo salar*)	508	85.4	0.16
Salmon (*Salmo salar*)	914	85.0	0.12
Brown Trout (*Salmo trutta*)	508	70.7	0.17
Brown Trout (*Salmo trutta*)	914	62.0	0.09

Table 4.1. Source Level and Transmission Loss for pile driving in dBht (Species) units.

In general, the dB_{ht} (*Salmo salar*) level levels are in general higher than the dB_{ht} (*Salmo trutta*) levels. This is to be expected, as the hearing of the salmon is more sensitive than that of the brown trout, as indicated by the audiogram measured and presented in Section 3. It is noticeable that there is a significant difference in Transmission Loss for the case of *S. trutta* for the two pile diameter cases. It is thought likely that this arises from the fit of Source Level and Transmission Loss to the data being poor in the case of the 914 mm diameter pile.

The thresholds at which a mild reaction, and a strong reaction, are expected to occur are illustrated on the figure, from Nedwell *et al* (2003a). In respect of the results for *S. trutta*, may be seen that both the actual measured levels and the estimated levels near to the piling are well below the levels at which a mild reaction would be expected to occur. In other words, no reaction would be expected by *S. trutta* at any range from the piling. By comparison, the results for *S. salar* would indicate that a mild reaction would be expected at a range of about 60 – 80 metres, and an increasingly stronger reaction as this range is reduced.

5. Observations of fish behaviour.

5.1. Source, preparation and examination of fish.

Owing to the problems of obtaining salmon for testing, it was decided that farmed brown trout (*Salmo trutta*) would be used in the tests, being the most closely related species. These were freshwater trout and were obtained from Itchen Valley Trout Farm at Alresford. The average size of fish was 25.4 cm (range 24.0-28.0 cm).

Prior to experimentation the fish were transported to Fawley Aquatic Research and acclimated to seawater. This process was carried out gradually over a period of five days or more without any apparent adverse effects on the fish. During this time they were fed pelleted food.

Fish were removed from the cages at the end of the trials and returned to the laboratory for further analysis. Five from each cage were transported to Plymouth for audiometric testing and ultrastructural examination of the hearing organs. The remaining fish were examined for signs of pressure-related injury (Turnpenny (1998)), e.g. externally for haemorrhaging of the eyes or gas embolisms in the eyes, and internally for swimbladder rupture.

5.2. Fish cage design and deployment.

Cages were purpose built for the project and were based on a nominal one-metre cube design. The cages are illustrated in Figure 26. The frames of the cages were made from mild steel angle and spray-painted. Plastic mesh of about 25 mm square aperture was fixed to the outside of the frames using plastic coated wire. A 20 cm-square flap opening was made in the top of the cage, the edges being reinforced with 25 mm plastic pipe attached to both the flap and the outer edges. These were used for introducing the fish and for removing them at the end of the trials. Cable-ties were used to close the openings during the tests.

During the trials the cages were taken to their respective positions suspended from 25 litre surface buoys by four ropes fixed to the top corners of the cage. The rope lengths were adjusted to put the centre of the cage 2.5 m below the water surface. Cage positions were at nominal distances of 25 m (cage 1), 50 m (cage 2), 100 m (cage 3), 200 m (cage 4) and 400 m (cage 5) from the piling operation; actual distances differed slightly according to which pile was being driven. A further, 'control', cage was located in the dock of Fawley Power Station, approximately 10 km from the piling site; this dock was not subject to boat traffic or other significant disturbance during the period when fish were held there.

5.3 Closed-Circuit Television Monitoring.

Behaviour of the fish was monitored via underwater closed-circuit television (CCTV) cameras fitted inside each of the fish cages. Aquacam® monochrome underwater cameras were used, these being waterproof to 10 m depth. Mountings for the cameras were fixed close to the top corner of the inside of the cage. The cameras were introduced via the openings and attached to the mountings. This allowed the cameras to be aimed across the long diagonal of the cage for maximum field of view.

Signals from the three nearest cameras (cages 1, 2 & 3) were fed into a 4-way multiplexer and thence into a time-lapse video cassette recorder (VCR) and video monitor located in a hut at a midway position on the Red Funnel pontoon. Cable lengths here were 50 m or less. Signals from the more distant cages 4 and 5 were fed to a similar multiplexer/VCR/monitor set-up located in a caravan on Town Quay. The longest cable run here was 180 m and a line amplifier was used to boost the signal and improve picture quality. The VCRs were run in 3-

hour mode (i.e. non-time-lapse) and tapes were changed every 3 hours during the working day. This meant that a considerable number of hours of 'control' records were made. Although no piling was being undertaken during these control periods, there were numerous other disturbances from boat traffic, including the regular arrivals and departures of the Red Funnel Isle of Wight ferries, small craft movements and the occasional ocean liner passing.

On completion of the field work, sequences of images were digitised and transferred to CD-ROMs using a WinTV® digital interface. A typical video frame from the monitoring equipment is shown in Figure 25.

5.4. Assessing fish behavioural reactions.

The video recordings were reviewed after the piling to identify any changes in behaviour that might have resulted from the piling noise or other local underwater noise events associated with ship movements in the locality. All reviewing was undertaken 'blind' by the operators, i.e. they were unaware of what sequences correlated with particular events, and this information was only later added by another operator.

Two types of behaviour were investigated:

Startle Reactions. For the purposes of this investigation a startle reaction was defined as the 'C-start' behaviour described by Blaxter and Hoss (1981) in response to an underwater sound stimulus, i.e. a sudden C-shaped flexure of the fish's body, which is quite clearly different from routine swimming activity.

Fish Activity Level. The second type of behaviour considered was a simple change in activity level of the fish. Captive fish that are exposed to irritating stimuli commonly show 'milling behaviour', in which the fish swim faster and make random turns. This type of behaviour is believed to provide a strategy for sampling the environment to expedite the fish's escape from potentially harmful conditions. In the present study the activity level was measured by counting the number of times a fish entered the camera's field of view within a two-minute observation period. This was possible because the field of view was limited by water clarity, so that the fish moved frequently in and out of vision. For each type of event investigated a two-minute 'control' period preceded each two-minute 'event' period. The control and event activity levels were compared using the non-parametric Mann-Whitney U-test (Campbell (1974)) with the null hypothesis that activity levels were not significantly different at the P=0.05 level.

5.5 Reactions during vibro-piling.

The initial cage placed at Location 5 (end of Town Quay, 400 m) to fulfil the Red Funnel monitoring obligations was put in position 24 h prior to the start of vibropiling but was raided overnight and the fish stolen. Since cages were in place at other, closer, locations, and fish in these showed no reaction to vibropiling, the cage at Location 5 was not replenished until 24 h before the start of impact piling. Observations are therefore presented here for the cages at Locations 1 and 2.

The analysis of the startle reactions was based on the of the VCR images at the start-up instant of each vibropiling session and for the next 5 seconds. No startle response was seen in any of the vibropiling sequences for any of the piles driven by this method.

Table 4.1 and Fig. 26 show the activity level observations (number of movements per 2-minute period) for the 2 minute period prior to piling and then for the first two minutes

during vibropiling. Activity levels are seen to have remained similar before and after the start of piling. The data shown combine the observations for all of the vibropiling operations. The Mann-Whitney U-test shows that there was no significant difference in activity level following the commencement of vibropiling (P=0.001).

Vibration Piling: Fish Activity Statistics (no. of movements per 2 min period)					
Mann-Whitney U test					
Location	Before	During	U	Z	P
1	147.5	152.5	69.5	0.1443	0.8852
2	150.5	149.5	71.5	-0.028	0.9769

Table 5.1. Comparison of fish activity levels prior to and during vibropiling (all vibropiling events combined): statistics shown for Mann-Whitney U-test

In summary, in the two cages nearest to the piling no startle response was seen for any of the piles driven by vibropiling, and no significant difference in activity level was detected

5.6 Reactions during impact piling

Impact piling was carried out on 24th September and data are reported here for all five monitoring locations. Table 4.2 shows that no startle reaction was recorded for the start of each of the three piling sessions that took place at any of the monitoring locations.

Pile	Start Time	Startle Reaction?				
		Cage 1	Cage 2	Cage 3	Cage 4	Cage 5
1 (914 mm)	08.41	no	no	no	n/a	no
2 (508 mm)	11.11	no	no	no	no	no
3 (505 mm)	11.54	no	no	no	no	no

Table 5.2. Startle reaction records for cages at Locations 1 to 5 during impact piling, 24th September (n/a = video record not available due to malfunction)

The activity levels recorded before and during the impact piling sessions are shown in Table 4.3 and Fig. 28. Fish activity is seen to have remained similar in most cases before and after the start of impact piling. The Mann-Whitney U-test shows that there was no significant difference in activity level following the commencement of pile driving (P=0.001) in cages at locations 1, 3, 4, & 5; a 36% increase in fish activity level was, however, observed at location 2, which was significant at the P=0.05 level.

Impact Pilings Statistics (no. of movements per 2 min period)					
Mann-Whitney U test					
Location	Before	After	U	Z	P
1	9	12	3	-0.654	0.512695
2	6	15	0	-1.96	0.0495
3	12	9	3	0.654	0.512
4	6.5	3.5	0.5	1.161	0.245
5	12	9	3	0.654	0.512

Table 4.3. Comparison of fish activity levels prior to and during impact piling (all impact piling events combined): statistics shown for Mann-Whitney U-test

In summary, no startle response was seen in any of the cages for any of the piles driven by impact piling. No significant difference in activity level was detected, other than an increase in fish activity in the cage at location 2, which was significant at the P=0.05 level.

5.7. Fish injuries.

Table 4.4 records fish injuries investigated.

Type of Injury	Fish Injury Frequency (sample size 10 fish per cage)					
	Location					
	1	2	3	4	5	Control (Fawley Dock)
Swimbladder rupture	0	0	0	0	0	0
Eye haemhorrage	0	0	0	0	0	0
Eye embolisms	0	0	0	0	0	0

Table 5.4. Records of fish injury inspection records for cages held at Town Quay and Fawley power station dock (control).

No evidence of fish injuries was seen in either the fish held at Locations 1 to 5 at Town Quay or in the Fawley controls.

5.8. Summary of observations on fish.

In summary, the caged trout monitoring revealed:

1. no evidence that trout reacted to vibropiling, even at close range (<50 m);
2. no evidence that trout reacted to impact piling, other than perhaps an increase in fish activity in the cage at location 2.
3. no evidence of gross physical injury to trout.

6. Electron microscope examination of the inner ear of the trout (*Salmo trutta*).

While as reported in Section 5 preceding no evidence of gross injury of fish was detected, damage to hearing is difficult to detect and yet may have long-term consequences for survival. For instance, Hastings *et al* (1996) found limited damage to regions of the inner ear of the oscar (*A. ocellatus*), 4 days after exposure to a continuous 300 Hz tone presented at 180 dB re 1 µPa.

As part of the investigation, five fish from each of the cages were examined for ultrastructural damage to the hearing organs.

6.1. General introduction.

The vertebrate inner ear is divided into two regions, known as the pars superior (semi-circular canals and the utriculus), and the pars inferior (the sacculus and lagena) (Retzius (1881)). In this study the sacculus was investigated for evidence of trauma to the inner ear ultrastructure as a result of exposure to the high intensity sound from the piling, as it is considered to be the primary auditory region of the fish ear (Popper & Fay (1993)). Examination of the polarisation of the ultrastructure from the sacculus of *S. trutta* undertaken for general familiarisation purposes revealed hair cells orientated in four diametrically opposed quadrants; a configuration common to fish with generalist hearing capabilities (Plat & Popper (1981)).

6.2. Preparation methodology.

Each sample was processed following the techniques described by Platt (1977). On arrival, the partially dissected cranium containing both ears was immersed in chilled fixative (2.5% glutaraldehyde in 0.1 M cacodylate buffer with 3.5% sodium chloride). Additional fixative was perfused into the sacculi prior to the dissection of the ears from the remaining cranium. The otolith capsules were then dehydrated through a graded ethanol series, prior to desiccation using the critical point drying method. Fully desiccated otolith capsules were subsequently mounted on a specimen stub using a carbon tab, and coated with c. 8 nm of gold in an Emitech K 550 sputter coater (working at approximately 5×10^{-6} Torr). Finally, the processed specimens were investigated and photographed using a JEOL JSM 5600 scanning electron microscope operated at 15 kV, and a 15 mm working distance.

The pouch containing the saccular otolith and macula, being very thin and membranous, does not always maintain its shape during the critical point drying process, and may become deformed. Much of this can be resolved when the sample is being mounted, though, if a significant fold runs through the macula, damage may still occur irrespective of delicate handling (this type of damage was found in around 10% of the samples). The hatched area in Figure 29 represents the location of the epithelia corresponding to the rosteral locus from one of the samples, which became detached during the drying process. Evidence of hair cell denudation from the hatched area and in similar regions from other affected specimens has been ignored.

6.3. Examination of the saccular hair cells from the six groups of *S. trutta*.

The hair cell proliferations in each quadrant of the macula from the six fish populations were examined at 100 µm intervals across the macula surface, using magnifications of x 1000 and x 5000. Damage to the ultrastructure is apparent in the form of breakages to the cilia at the base, close to where they contact the body of the receptor cell. Figure 30 shows two damaged and one undamaged hair cell from the sacculus of the bass (*Dicentrarchus labrax*), scanned at

a magnificeation of x 5000. These specimens serve to illustrate the effect of trauma on hair cells of the inner ear, and were not from this programme.

Figures 31 to 34 illustrate micrographs of the hair cells from the four quadrants illustrated in Figure 29.

Examination of the sacculus of *S. trutta* revealed no obvious signs of trauma to the cilia and macula which could be attributed to intense sound exposure; the examination was undertaken with the examiner unaware of which group the fish belonged to. The micrographs presented in Figures 35 to 41 were taken from comparable regions of the macula, located close to the central transect between all four quadrants. Comparable results were obtained from all six populations, though evidence of damage may not be immediately apparent.

While no trauma was detected, it should be noted that evidence of trauma to the hair cells may be apparent on other androgens of the inner ear (not studied in this work). Diagnosis would require further experimentation using larger population samples. In addition, a recent report by Popper (in press) indicates that the visible deterioration of peripheral cell structures can take in excess of a month.

In summary, no obvious signs were found of trauma to the cilia and macula which could be attributed to intense sound exposure.

7. Conclusions.

1. Monitoring of the effects of waterborne noise resulting from impact piling and vibropiling was undertaken at Town Quay, Southampton, during construction operations at Red Funnel's Southampton Terminal in September 2003. The noise levels were recorded, and because of interest in the potential effects of the noise on migration of salmon (*Salmo salar*), the reactions of the close relative brown trout (*Salmo trutta)* were observed in cages on CCTV equipment to determine whether there was any observable effect of the piling on their behaviour.
2. In respect of vibropiling, at the greatest range of 417 metres, the noise could not be detected above background noise, with any noise from the vibropiling being drowned by noise from the movement of vessels. The caged trout monitoring revealed no evidence that trout reacted to vibropiling even at the closest range of 29 m.
3. In respect of impact piling, no startle response was seen in any of the cages for any of the piles driven by impact piling. No significant difference in activity level was detected, other than an increase in fish activity in the cage at location 2. The results for dB_{ht} (*Salmo salar*) noise levels indicated that a mild reaction would be expected by salmon within ranges of 60 to 80 metres.
4. Consequently the audiogram of the brown trout was measured, and was found to be significantly different from that of the salmon, despite a common assumption that closely related species will have similar hearing ability. It was hence concluded that it is not possible to infer the effects of noise from studies on a related species without knowledge of the hearing ability of both.
5. The impact piling noise was retrospectively found to be below the levels at which a reaction would be expected. This difference explained the lack of reaction of the caged *S. trutta* to the piling noise, and tends to confirm that mild reaction to noise occurs at levels of about 75 dB_{ht} (*Species*) and above.
6. Micrographs of the sacculus of five brown trout from each cage were inspected. No signs were found of trauma to the cilia and macula which could be attributed to intense sound exposure.

References

Abbott, R. & Bing-Sawyer, E. (2002). *Assessment of pile driving impacts on the Sacramento blackfish (Othodon microlepidotus).* Draft report prepared for Caltrans District 4.

Blaxter, J.H.S. & Hoss, D.E. (1981). *Startle responses in herring: the effect of sound stimulus frequency, size of fish and selective interference with the acousto-lateralis system.* Journal of the Marine Bioacoustics Association, UK. 61: 871-9.

Campbell, R.C. (1974). *Statistics for Biologists.* Cambridge University Press, Cambridge.

Hastings M, Popper, A, Finneran, P & Lanford, P. (1996). *Effects of low frequency sound on the haircells of the inner ear and lateral line of teleost fish (Astronotus ocellatus).* J. Acoust. Soc. Am 99(3): pp 1759 – 1766.

Nedwell, J.R. & Turnpenny, A.W.H. (1998) *The use of a generic weighted frequency scale in estimating environmental effect.* Proceedings of the Workshop on Seismics and Marine Mammals, 23rd-25th June 1998, London. UK.

Nedwell, J.R. & Edwards, B. (2002). *Measurements of underwater noise in the Arun River during piling at County Wharf, Littlehampton.* Subacoustech Report Reference: 513 R 0104.

Nedwell, J.R, Turnpenny, A.W.H. & Lambert, D. (2003a). *Objective design of acoustic fish deflection systems.* US EPA Symposium on Cooling Water Intake Systems to Protect Aquatic Organisms.

Nedwell, J.R, Turnpenny, A.W.H, Langworthy, J & Edwards, B (2003b). *Measurements of underwater noise during piling at the Red Funnel Terminal, Southampton, and observations of its effect on caged fish.* Subacoustech Report Reference: 558 R 0207, 27 October 2003

Parvin, S.J & Nedwell, J,R. (1995). *Underwater sound perception and the development of an underwater noise weighting scale.* Journal of the Society for Underwater Technology, 21(1): 1.

Turnpenny, A.W.H. (1998). *Mechanisms of fish damage in low-head turbines: an experimental appraisal.* In: Fish Migration and Fish Bypasses (Ed. Jungwirth, M., Schmutz, S. and Weiss, S.). Fishing News Books, Oxford, Blackwell: 300-314.

Figures

Figure 1. Photograph taken from quayside with ferry docked at terminal, and vehicles disembarking along linkspan. Structure on left of photograph is covered walkway for pedestrian passengers, and the dolphin on which it rests can be seen.

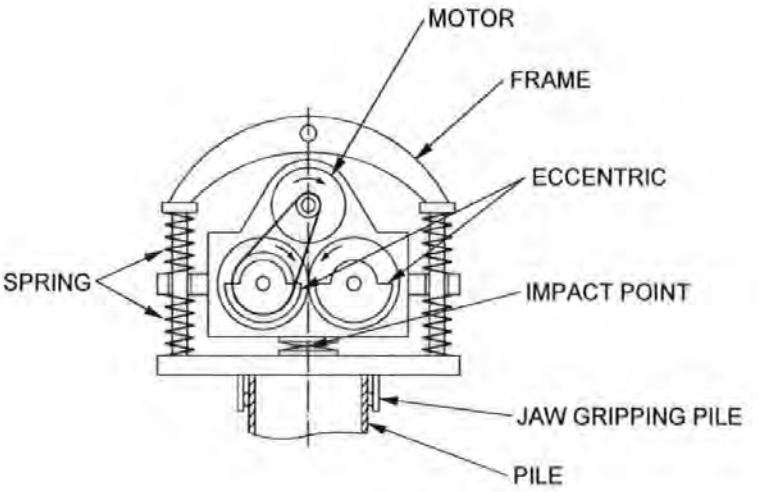

Figure 2. Sketch to illustrate principle of vibro pile driving.

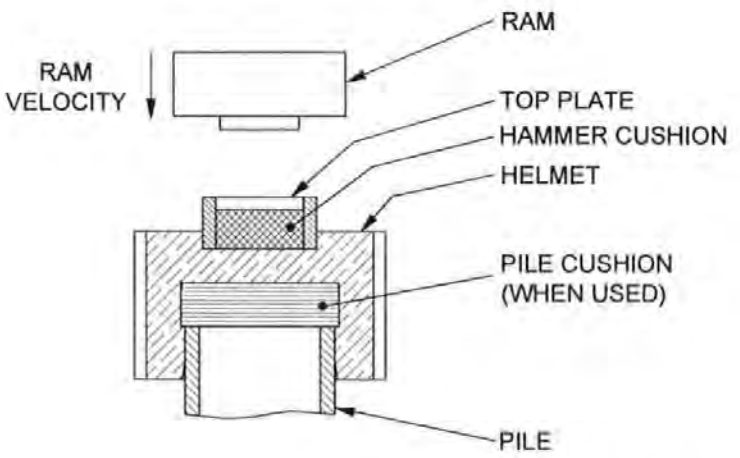

Figure 3. Sketch to illustrate principle of impact piling.

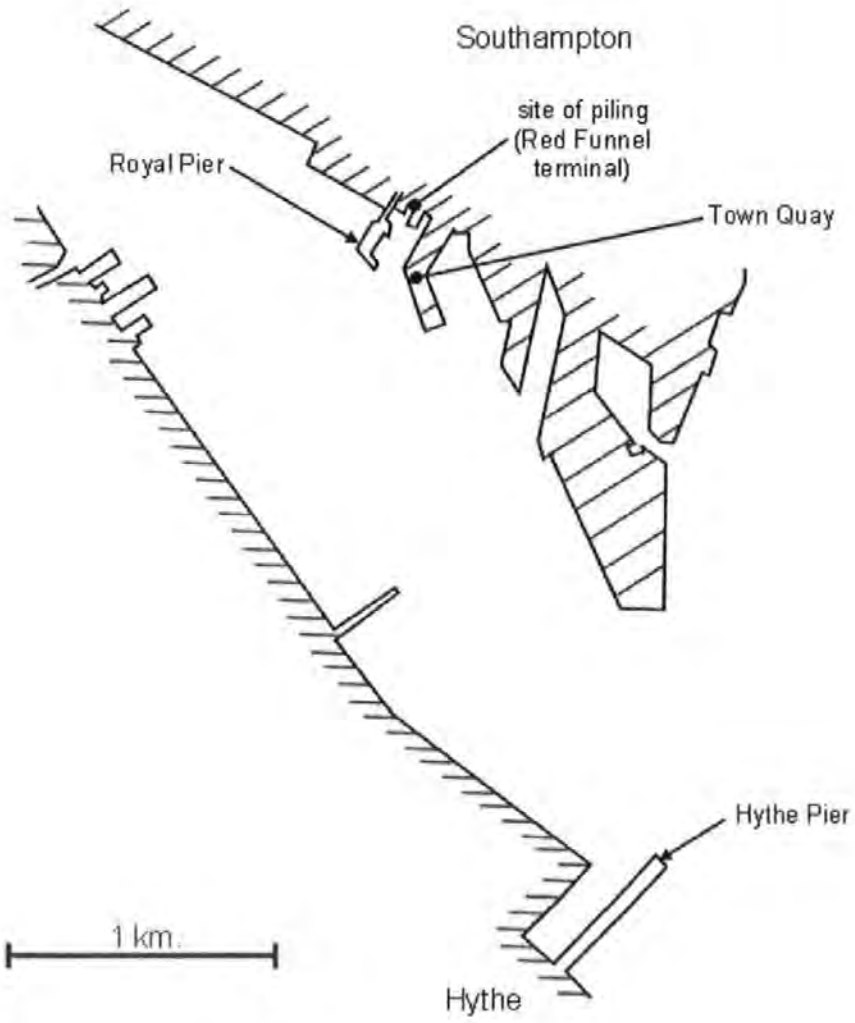

Figure 4. Sketch map showing location of site in Southampton

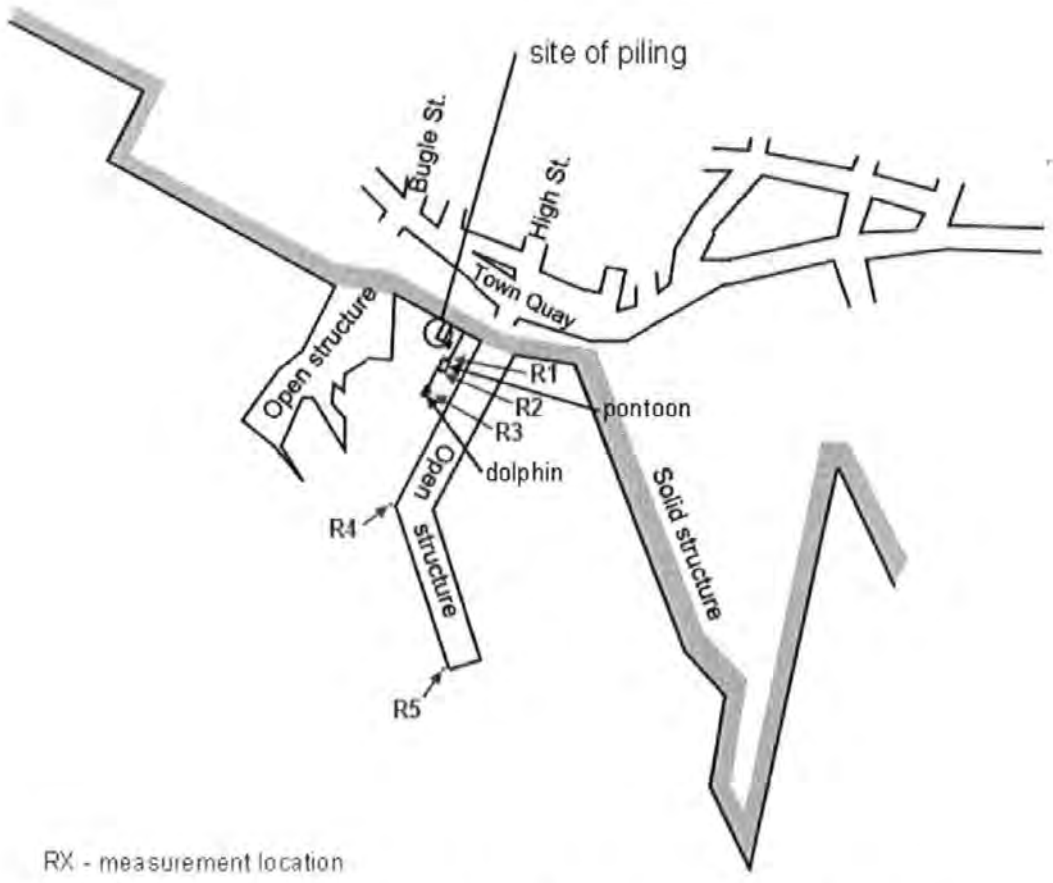

Figure 5. Sketch map showing piling and measurement locations.

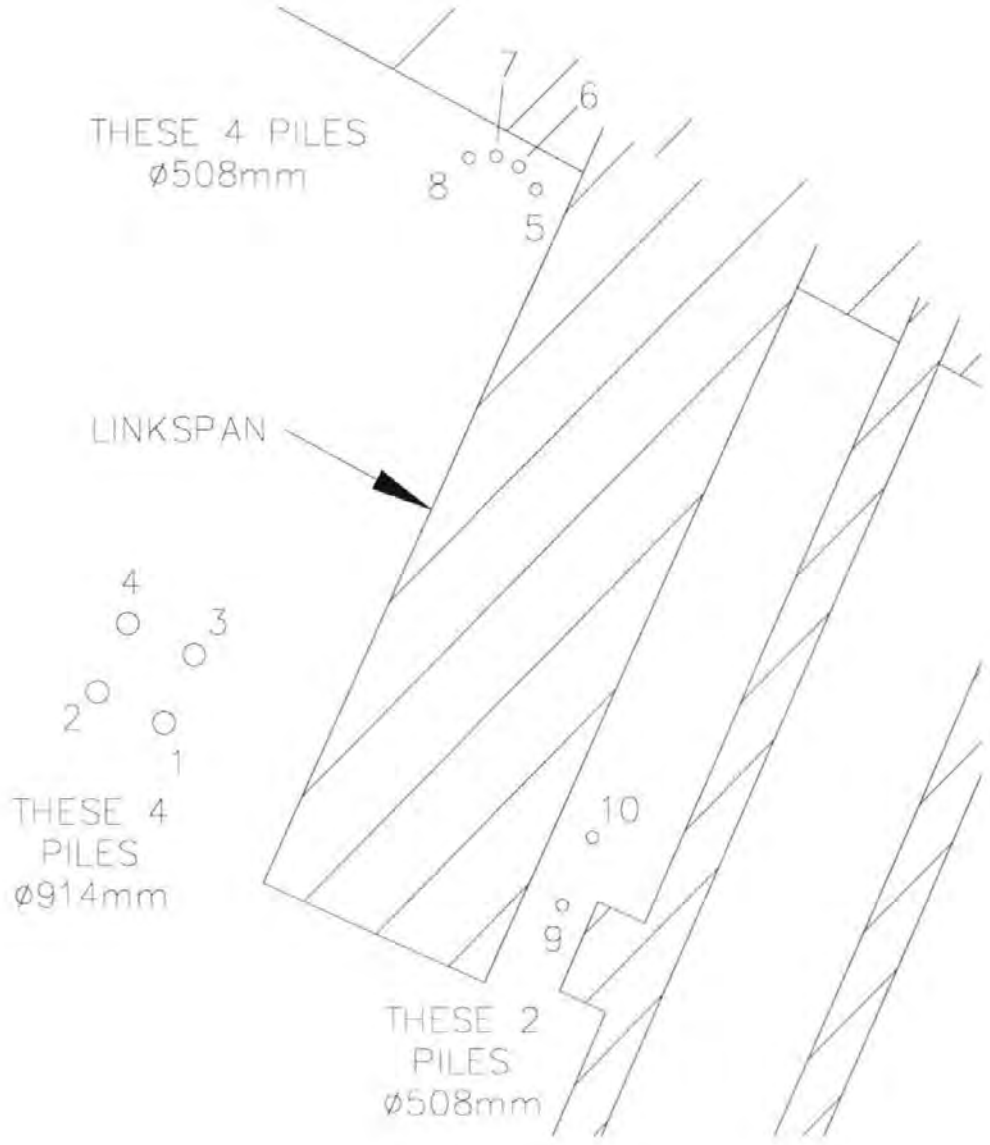

Figure 6. Details of pile locations.

Figure 7. Photograph of pile tubes being unloaded.

Figure 8. A photograph of site during piling operations.

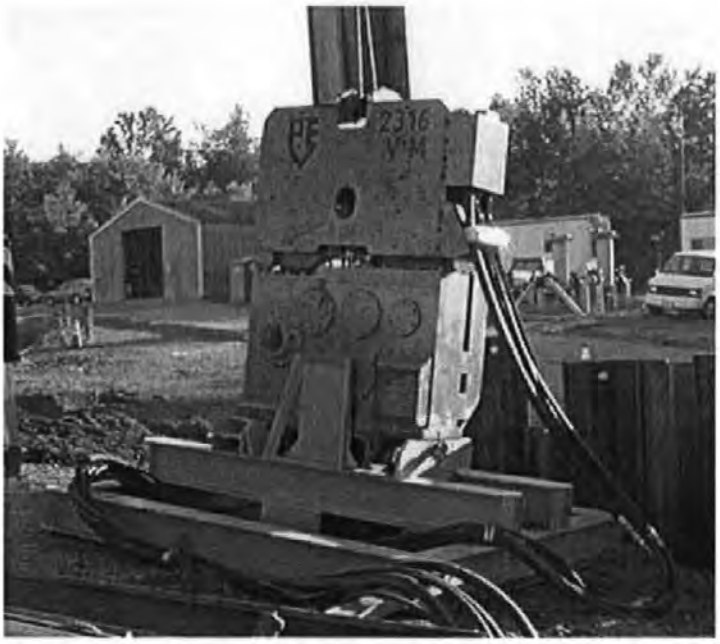

Figure 9. A PVE 2316 VM vibropiling driver. It is shown resting in a cradle made of I-section beams.

Figure 10. A view of the lower end of the BSP 357/9 Hydraulic Drop Hammer used for impact driving, while it was lying on a lorry.

Figure 11. The impact driver being held on the top of a pile for driving purposes.

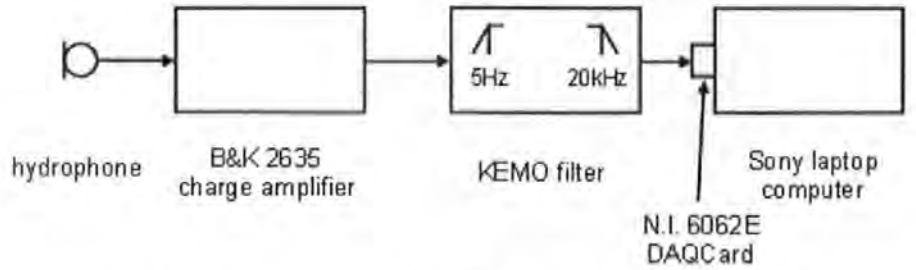

(a). set-up for 8104 and 8105 hydrophones, for vibrodriving.

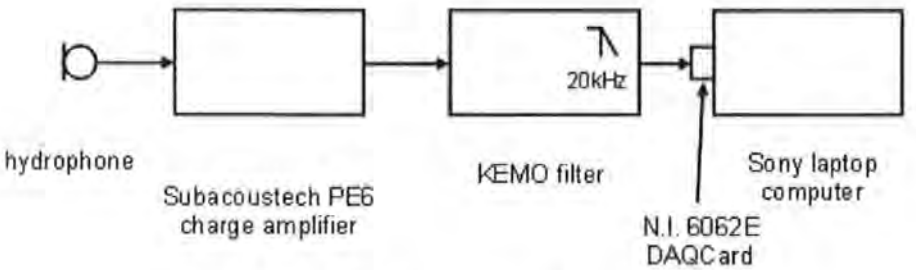

(b). set-up for 8106 hydrophone, for vibrodriving.

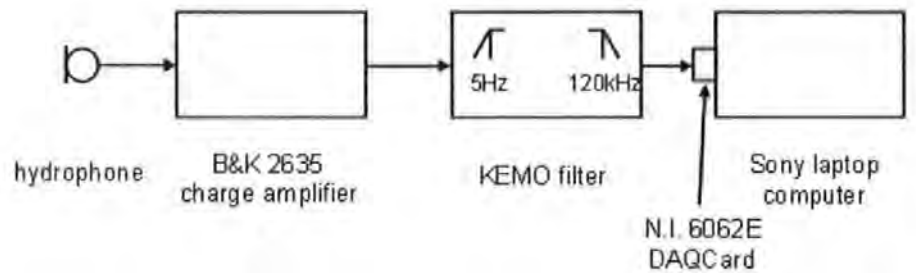

(c). set-up for 8105 hydrophone, for impact driving.

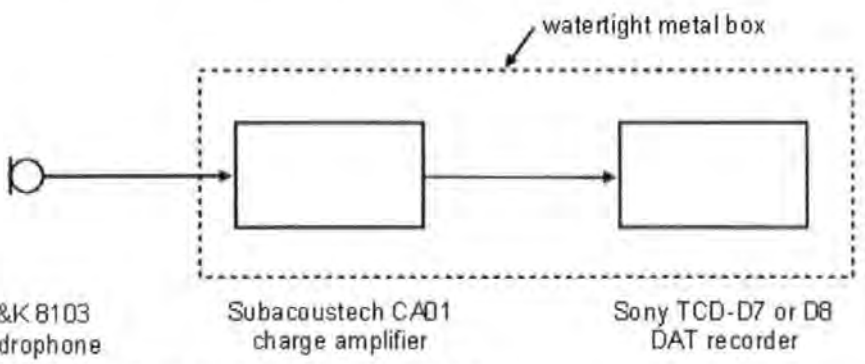

(d). equipment for watertight boxes.

Figure 12. Block diagrams of instrumentation.

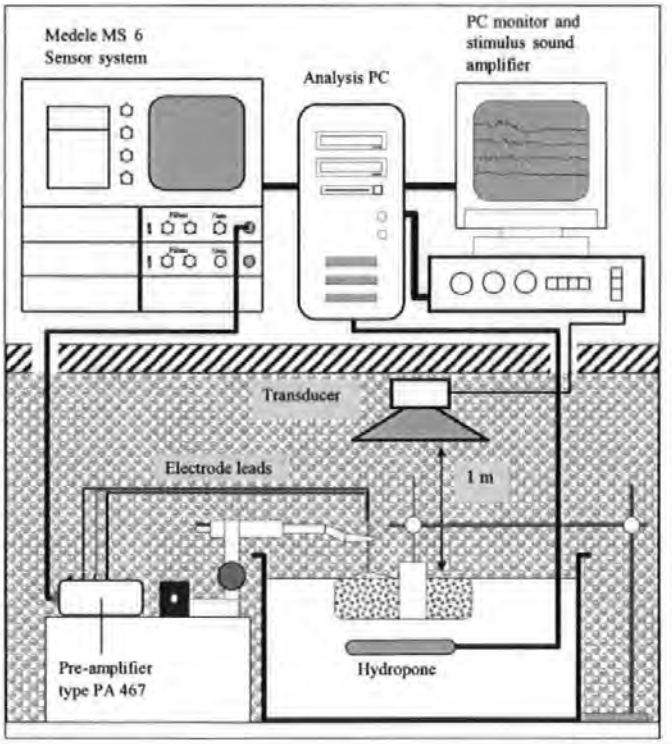

Figure 13. A schematic of the ABR audiometry system

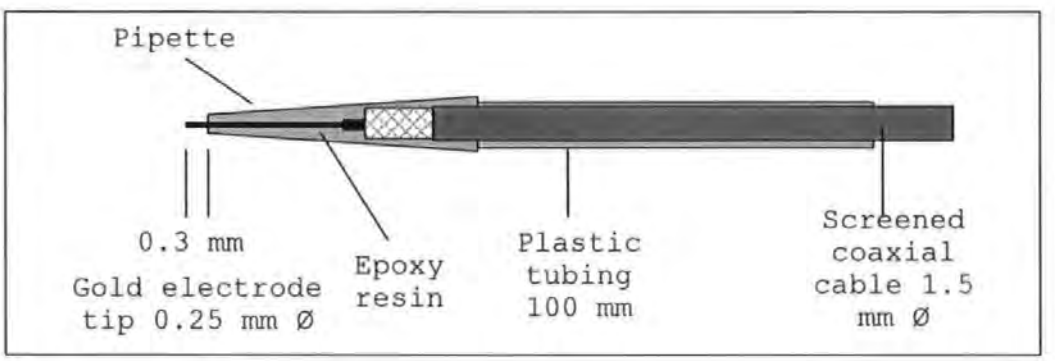

Figure 14. A schematic of the electrodes used to record the evoked potentials

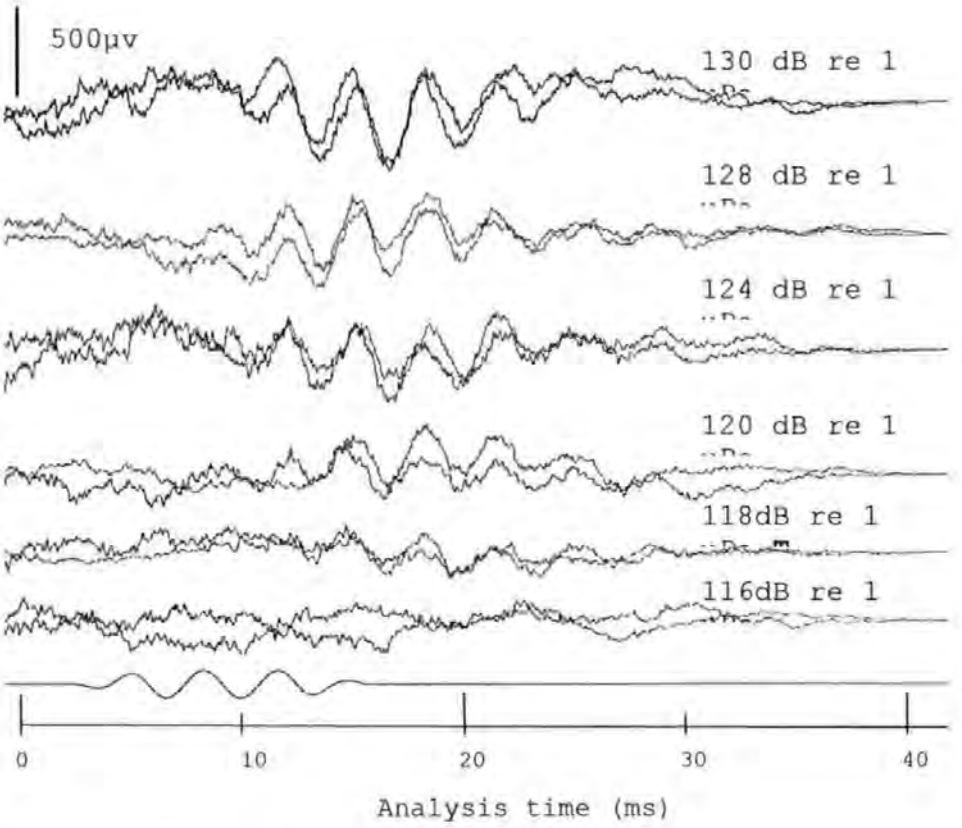

Figure 15. An example of evoked potentials from a naive *S. trutta* in response to a 300 Hz tone burst.

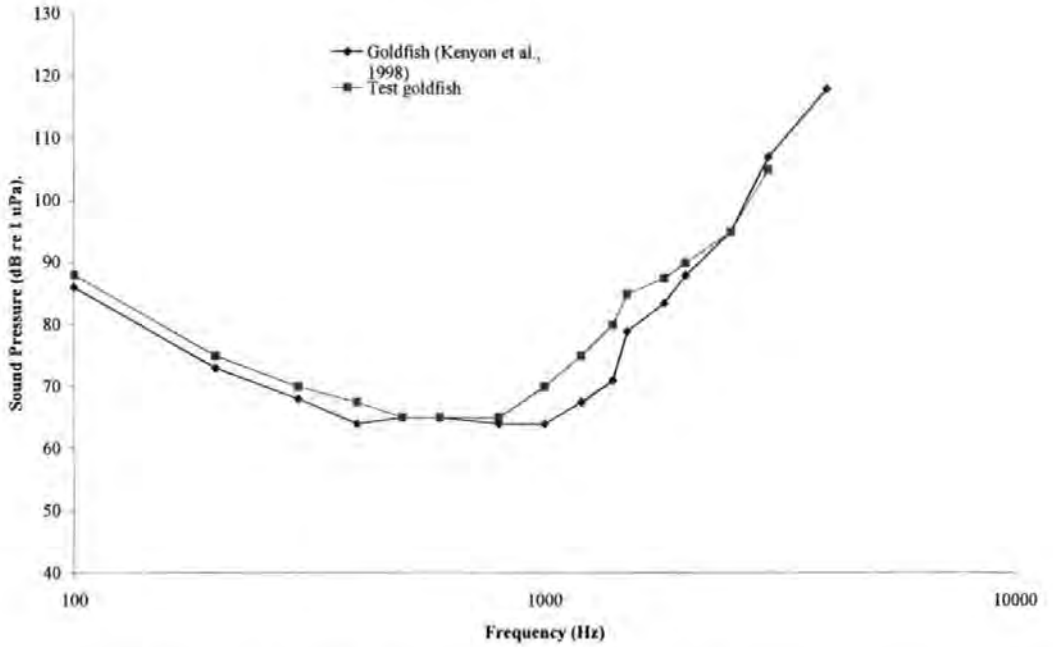

Figure 16. A comparison of the audiogram of a goldfish (*Carassius auratus*) made on the experimental apparatus, compared with the results of Kenyon *et al.* (1998).

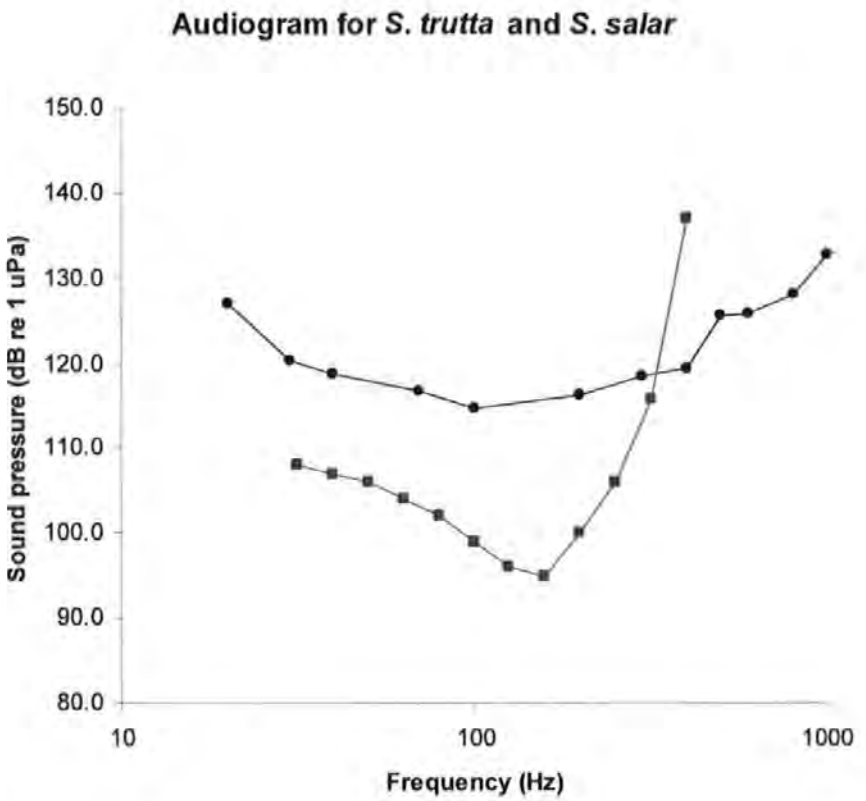

Figure 17. The measured auditory thresholds from the brown trout (*S. trutta*) compared with those of the salmon (*S. salar*) (from Hawkins & Johnstone (1978))

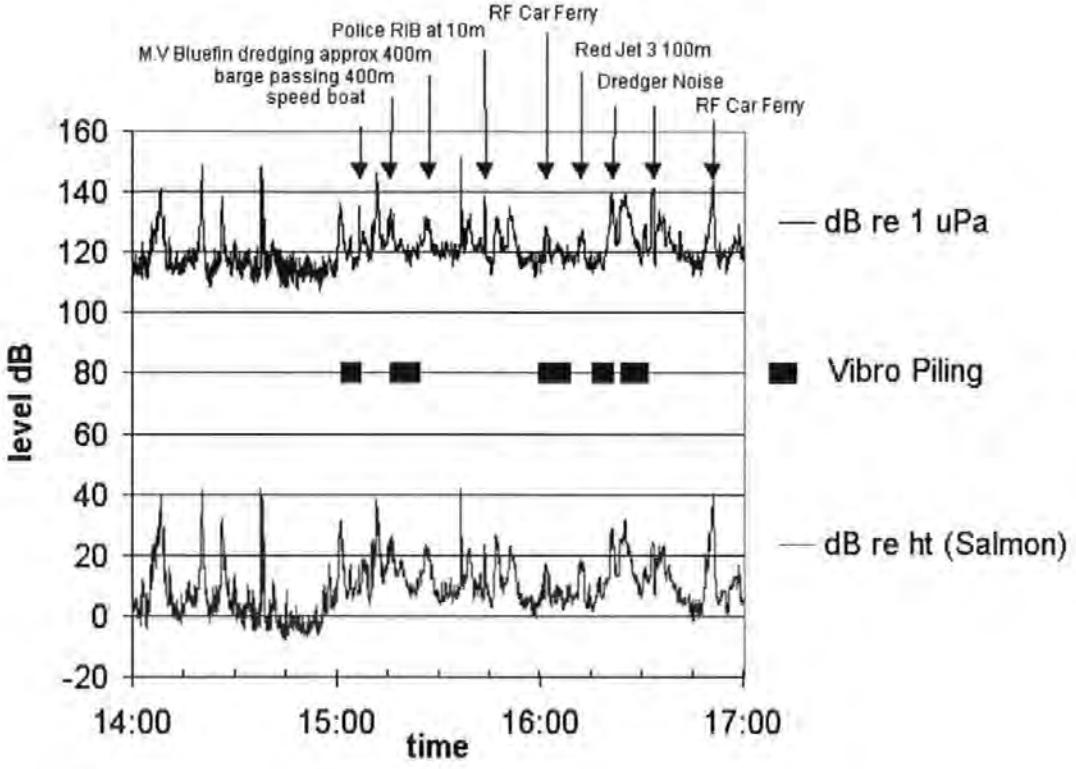

Figure 18. A typical sound pressure level *vs.* time history obtained at the end of Town Quay (location R5) for a vibro-driving case. The upper line illustrates the unweighted levels, and the lower line levels in dB_{ht} (*Salmo salar*).

Figure 18. The dredger *Bluefin*, noise from which dominated some of the monitoring measurements.

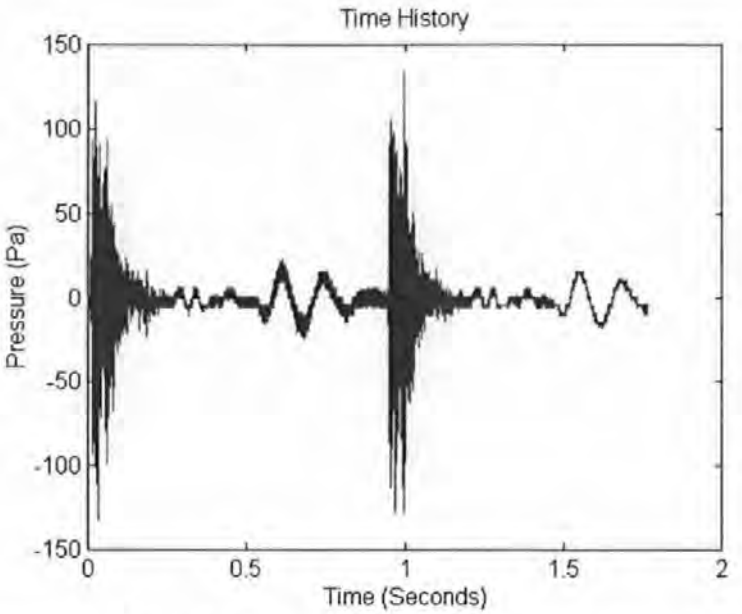

Figure 20: A typical time history for two impact pile driver strikes obtained from measurements at location R3.

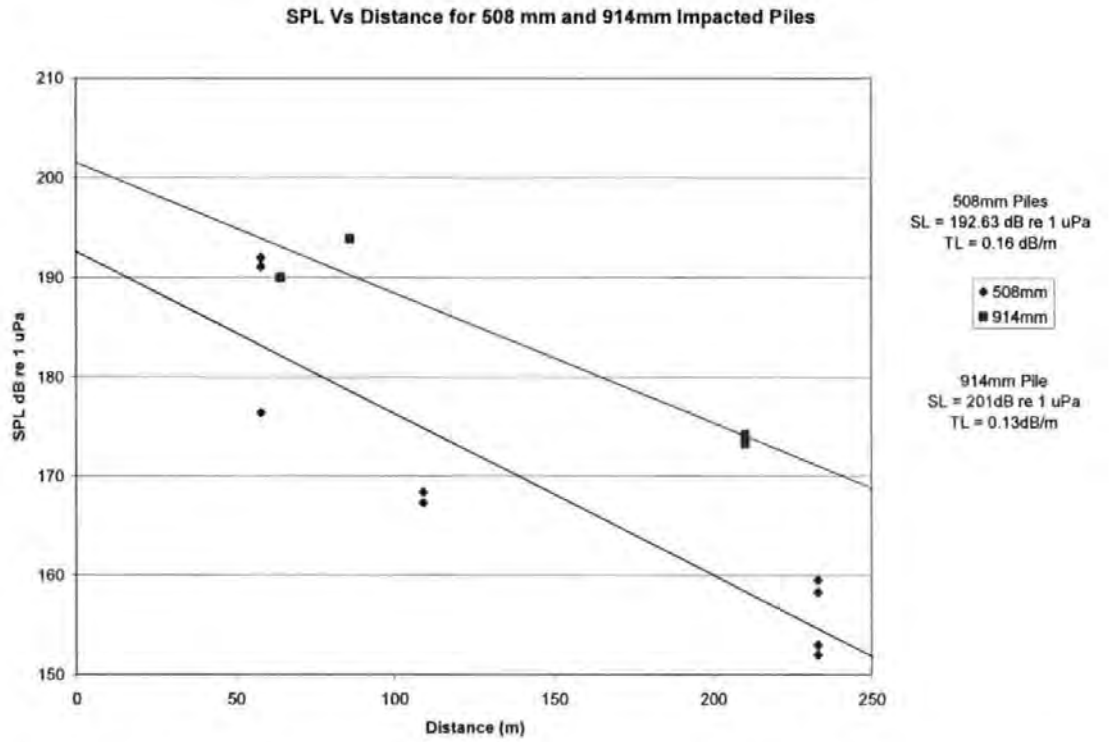

Figure 21: The average peak-to-peak Sound Pressure Level of the impact piling as a function of the range from the piling, for two 508 mm diameter piles and one 914 mm diameter pile.

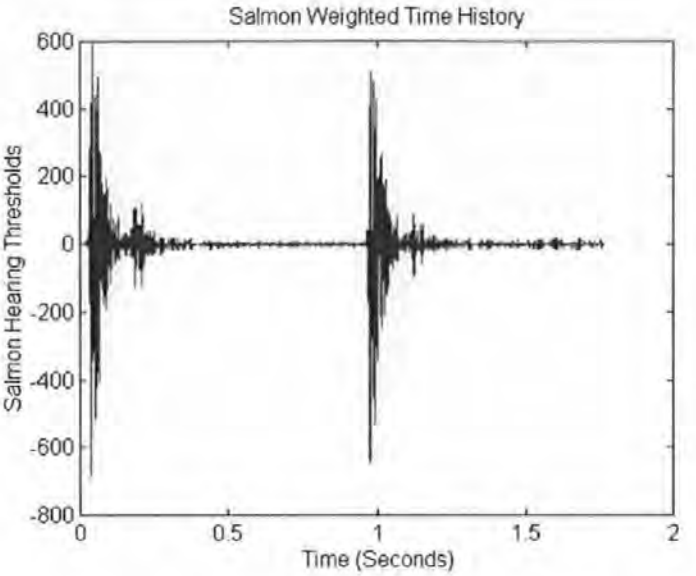

Figure 22. A pressure *vs.* time history for impact driving, *as per* Figure 20, but weighted by *S. salar* hearing.

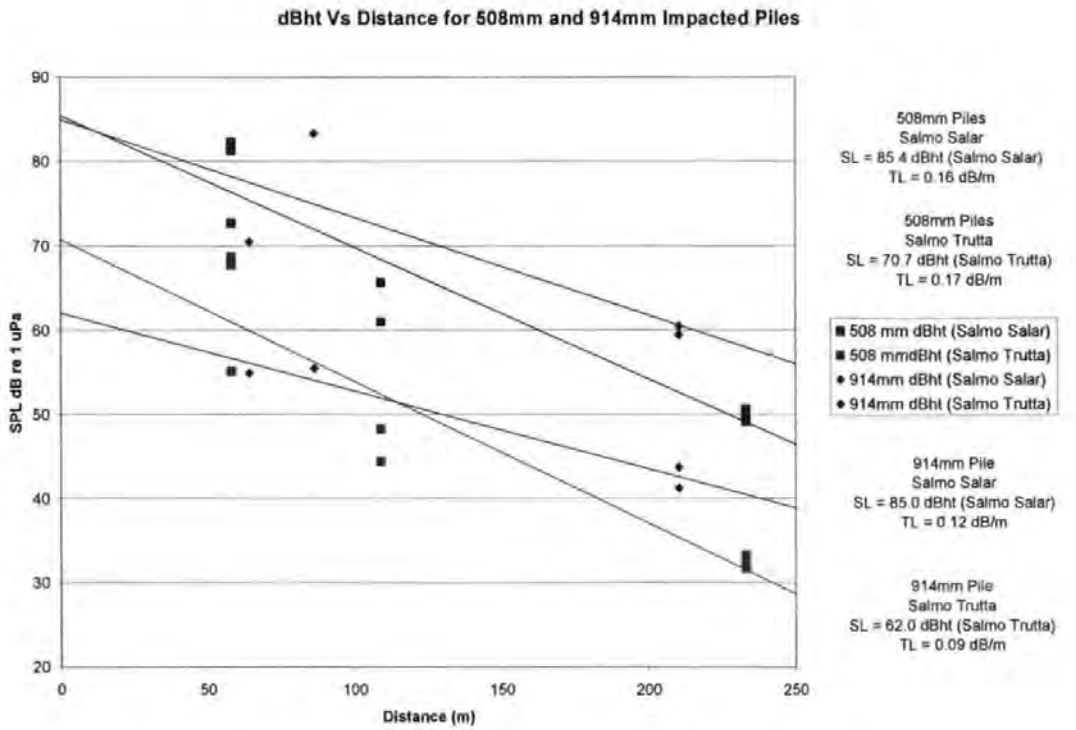

Figure 23: The average peak-to-peak Sound Pressure Level in dB_{ht} (*Species*) units of the impact piling as a function of the range from the piling, for two 508 mm diameter piles and one 914 mm diameter pile.

(a). A general view.

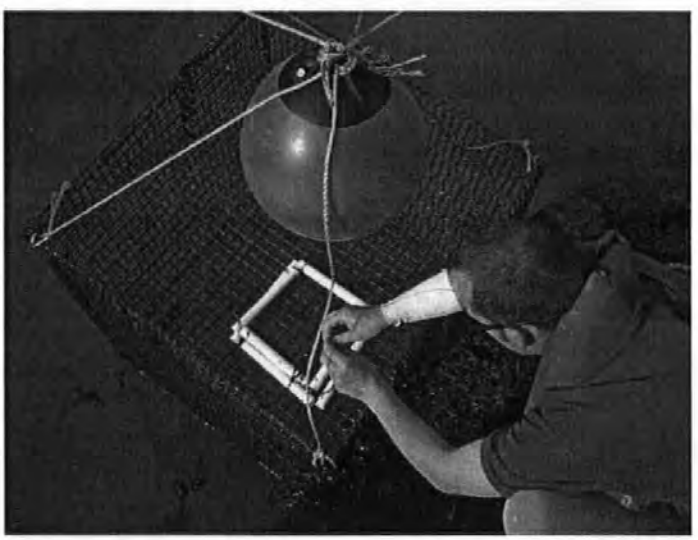

(b). View showing flap opening for introducing and removing the fish.

Figure 24. Photographs of the cages used for the fish monitoring.

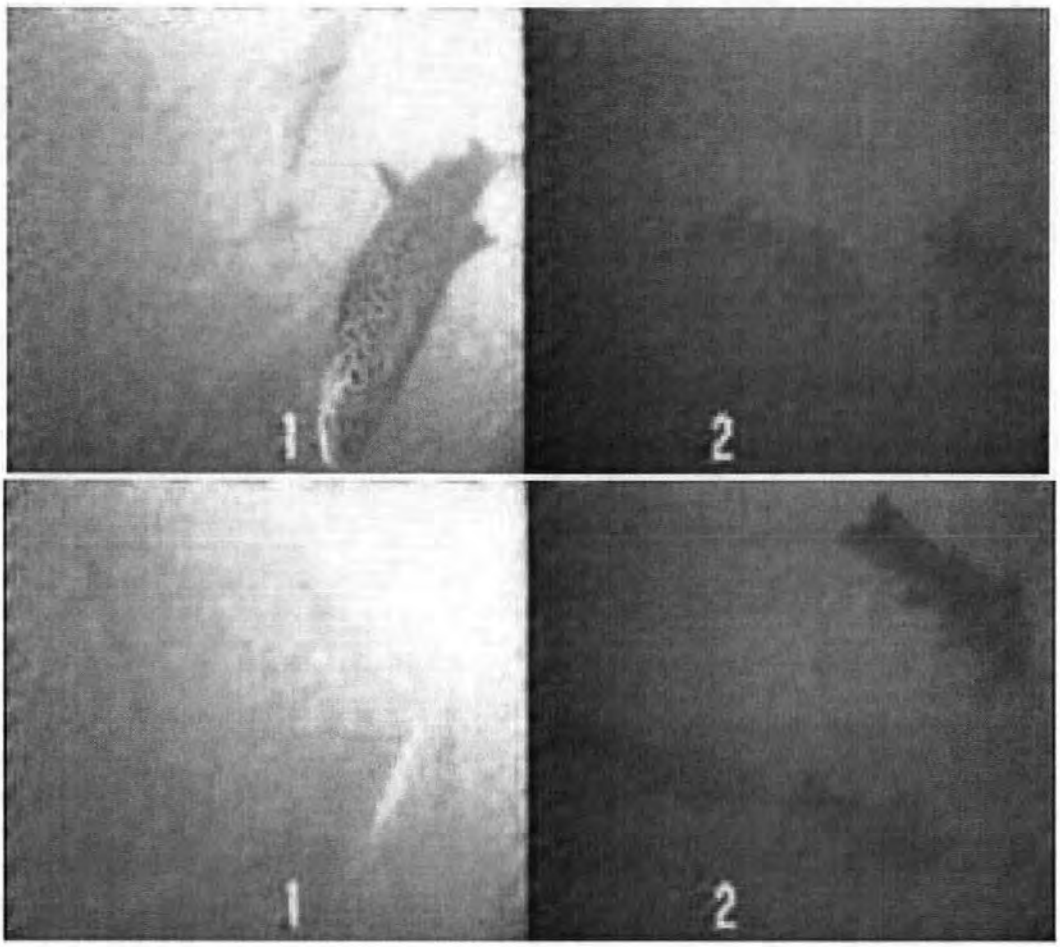

Figure 25. A still frame from the fish monitoring video.

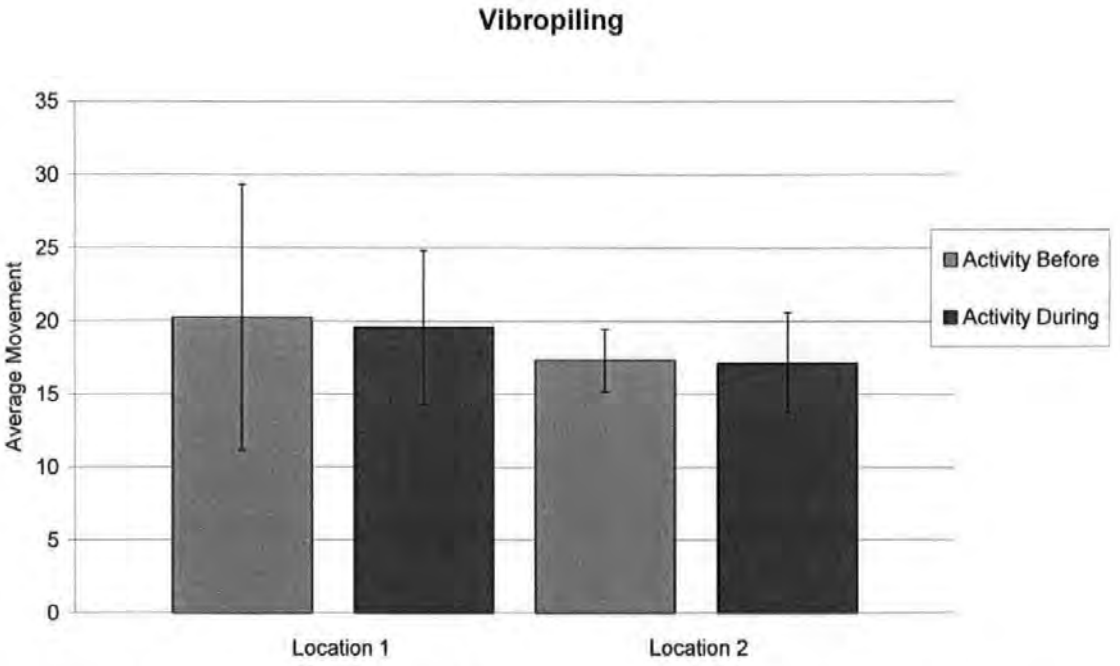

Figure 26. Comparison of fish activity levels before and during vibropiling (all data collected between 15-23 September), based on observed fish movements over 2 minutes before the start of piling and for 2 minutes from the start of driving each pile (mean & 95% confidence interval).

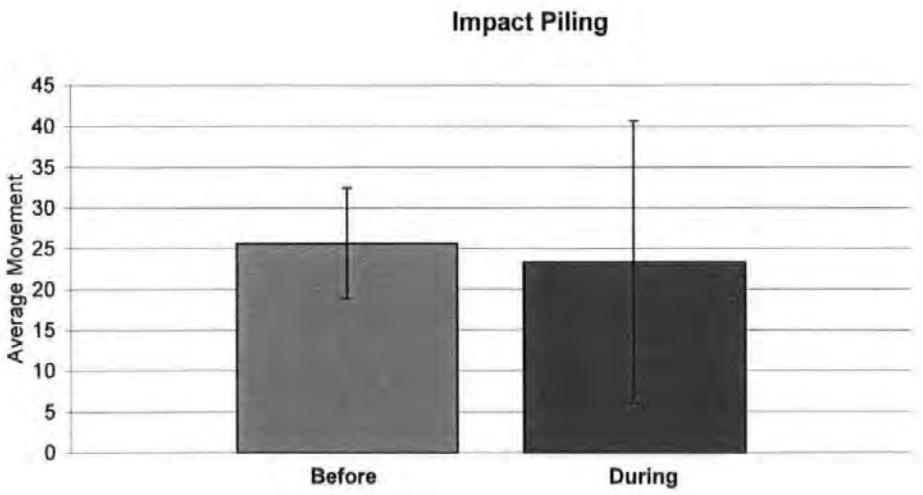

Figure 27. Comparison of fish activity levels before and during impact piling (piling on 24th September), based on observed fish movements over 2 minutes before the start of piling and for 2 minutes from the start of driving each pile (mean & 95% confidence interval).

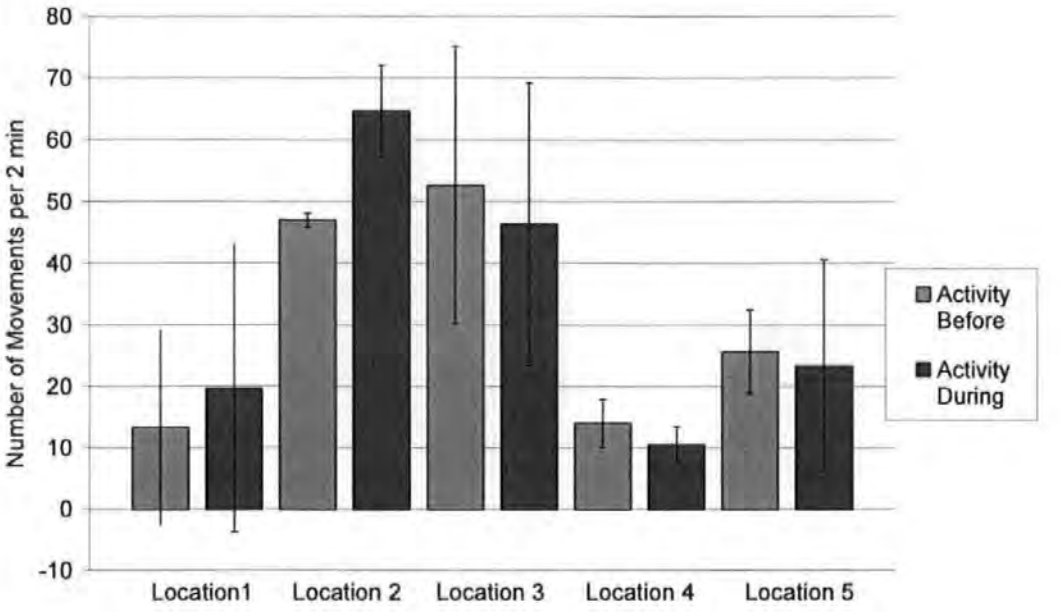

Figure 28 Comparison of fish activity levels before and during impact piling (24th September), based on observed fish movements over 2 minutes before the start of piling and for 2 minutes from the start of driving each pile.

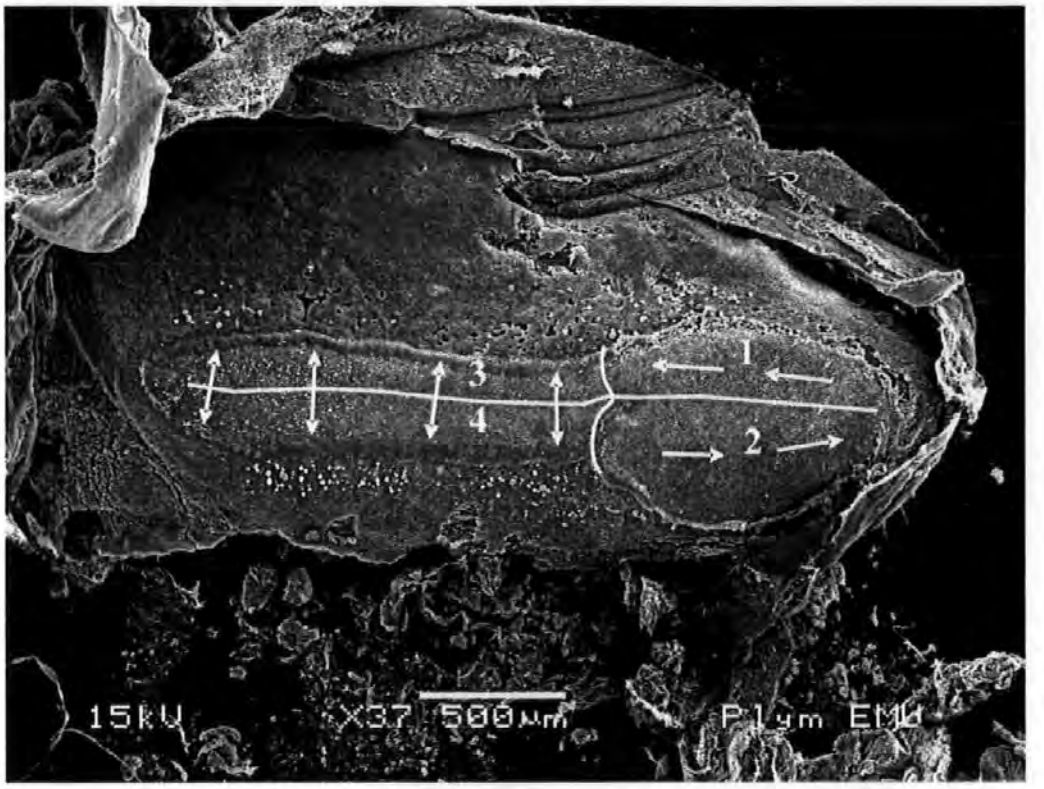

Figure 29. Hair cell polarisation patterns on the saccular epithelium from the left ear of *S. trutta* (arrows indicate a standard hair cell configuration)

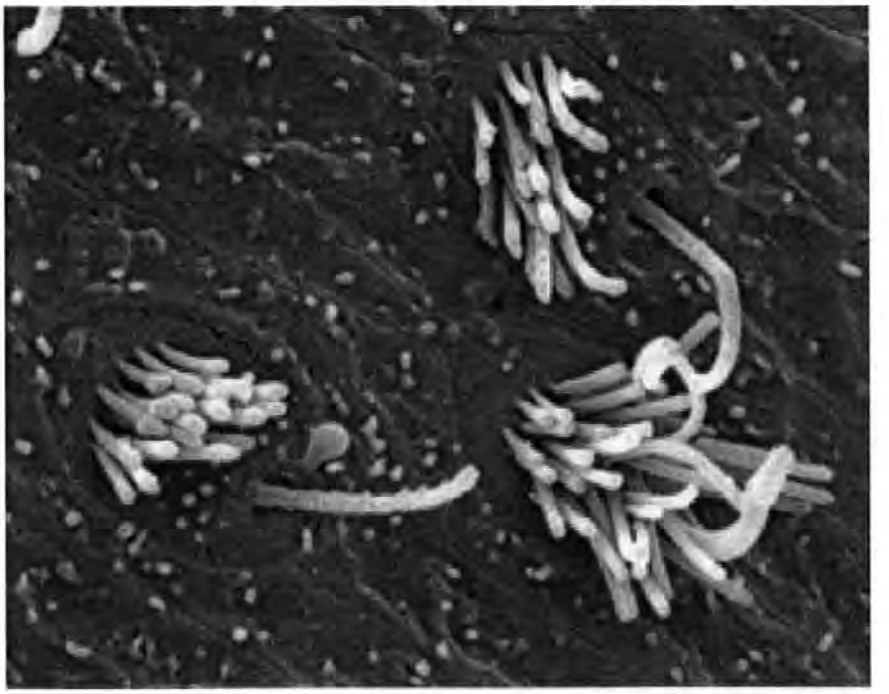

Figure 30. Example of damaged hair cell from the bass (*Dicentrarchus labrax*) (Lovell, unpublished). *Note:* the actual cause of the trauma shown here is not due to acoustic stimulation, though the effect (destruction of cilia) is similar in appearance

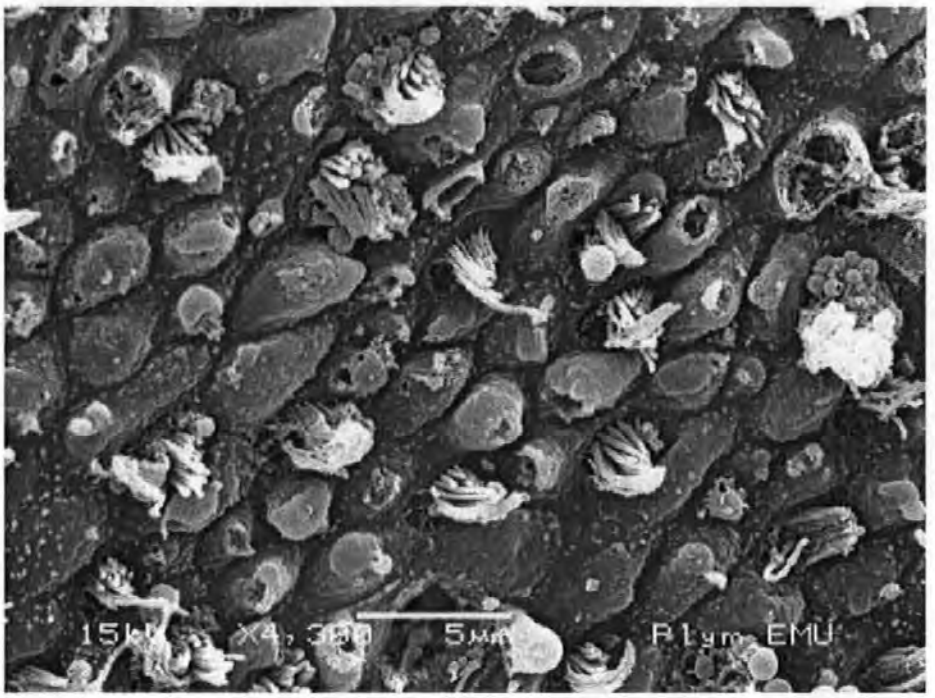

Figure 31. Micrograph of hair cells from quadrant 1 of the saccular epithelium

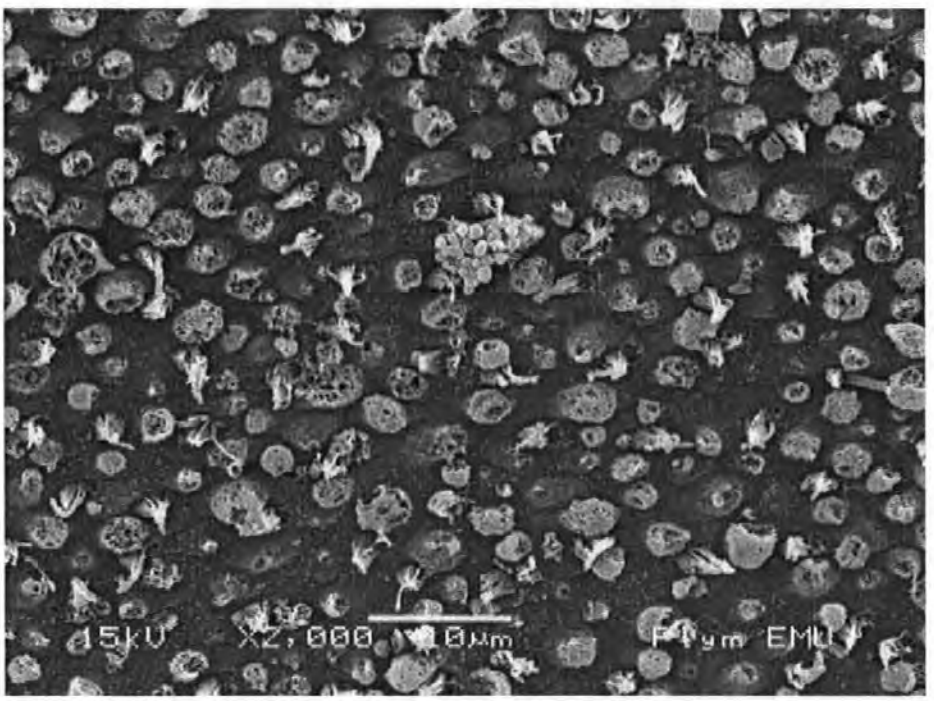

Figure 32. Micrograph of hair cells from quadrant 2

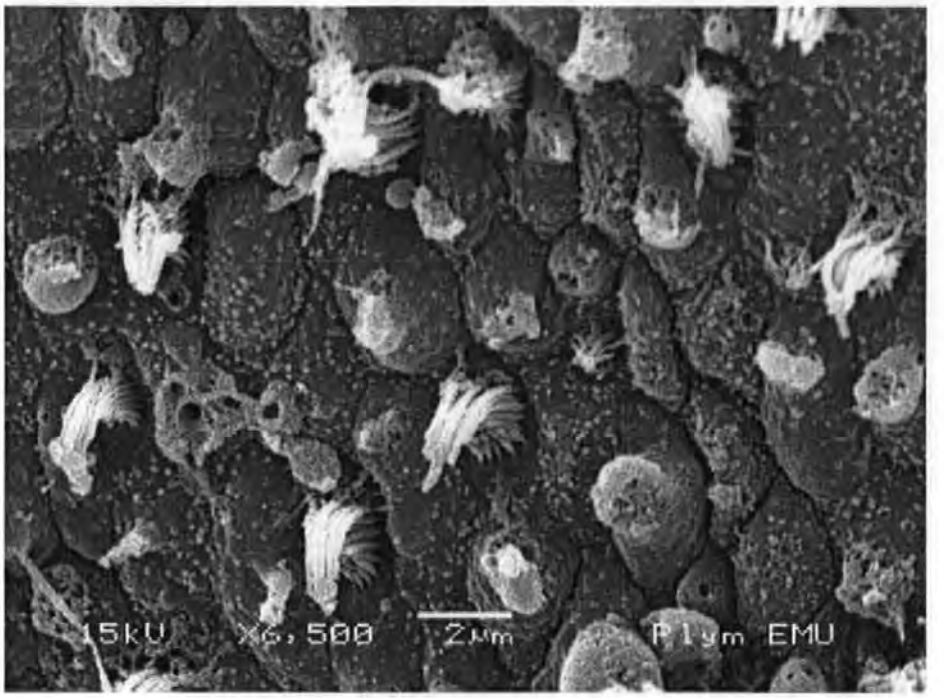

Figure 33. Micrograph of hair cells from quadrant 3

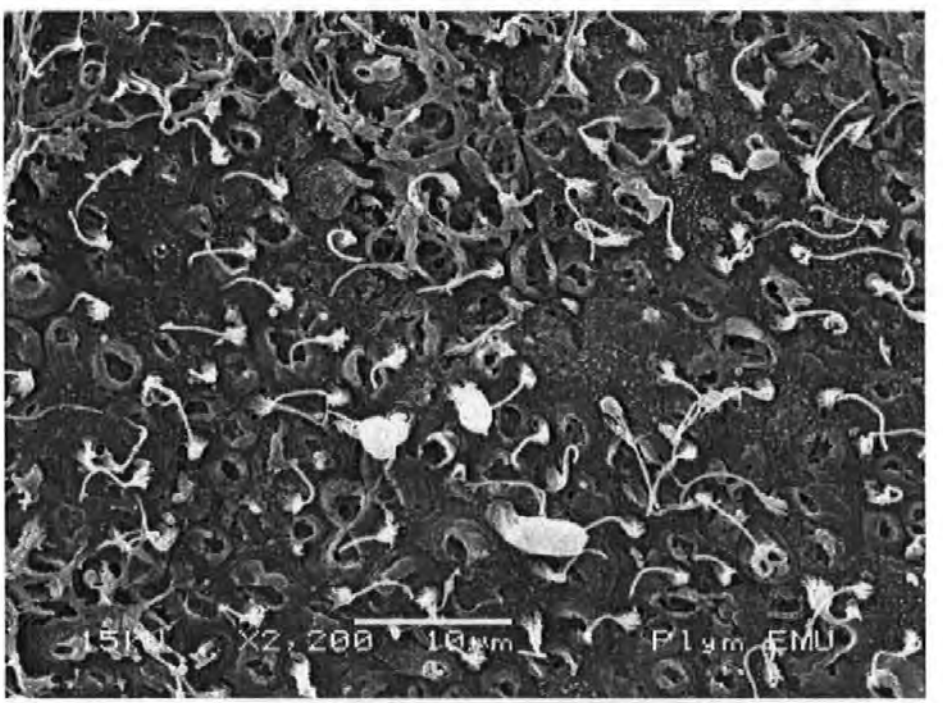

Figure 34. Micrograph of hair cells from quadrant 4

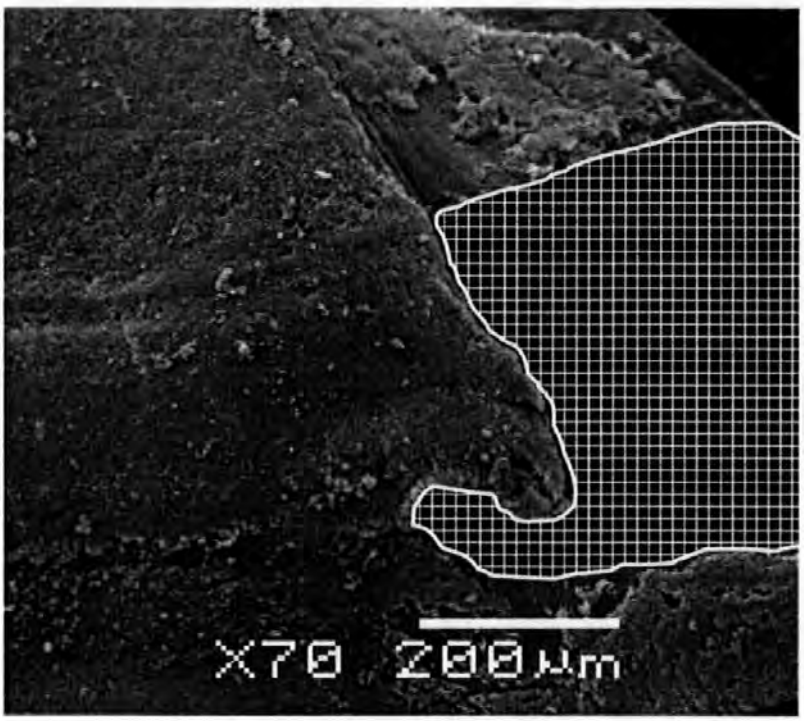

Figure 35. Large area of damage to the rosteral locus (hatched area) caused during the critical point drying process

Figure 36 Micrograph of macula (close to the central transect between all 4 quadrants), showing hair cells, for cage no. 1.

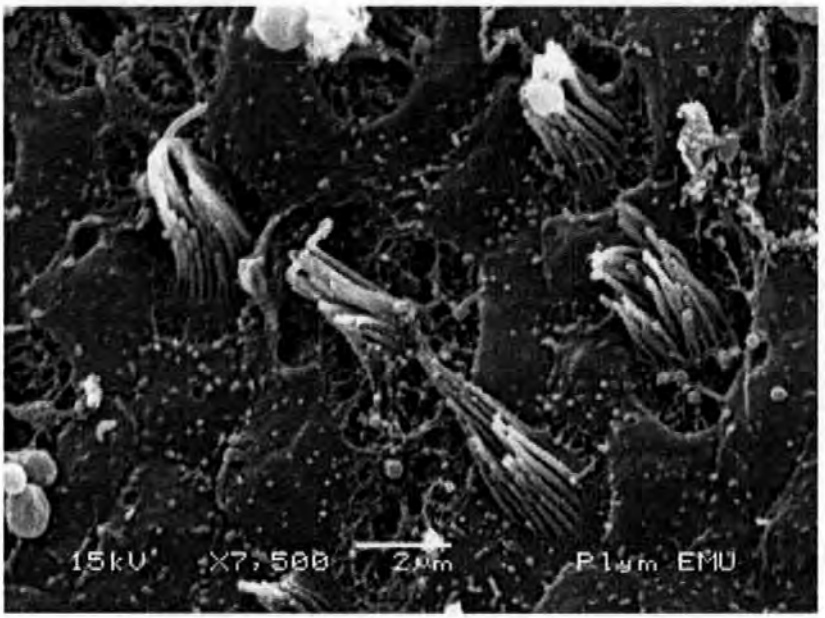

Figure 37 Micrograph of macula (close to the central transect between all 4 quadrants), showing hair cells, for cage no. 2.

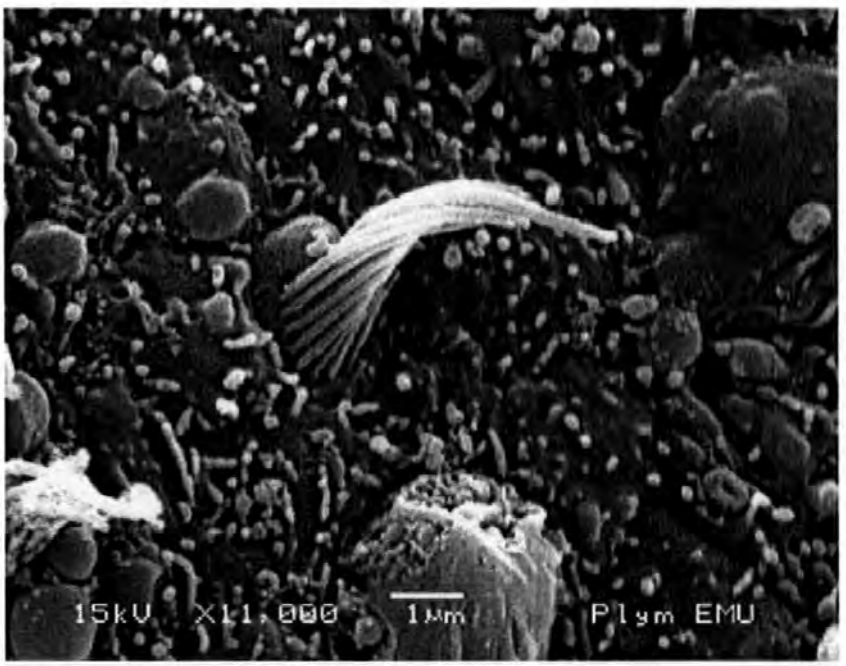

Figure 38 Micrograph of macula (close to the central transect between all 4 quadrants), showing hair cells, for cage no. 3.

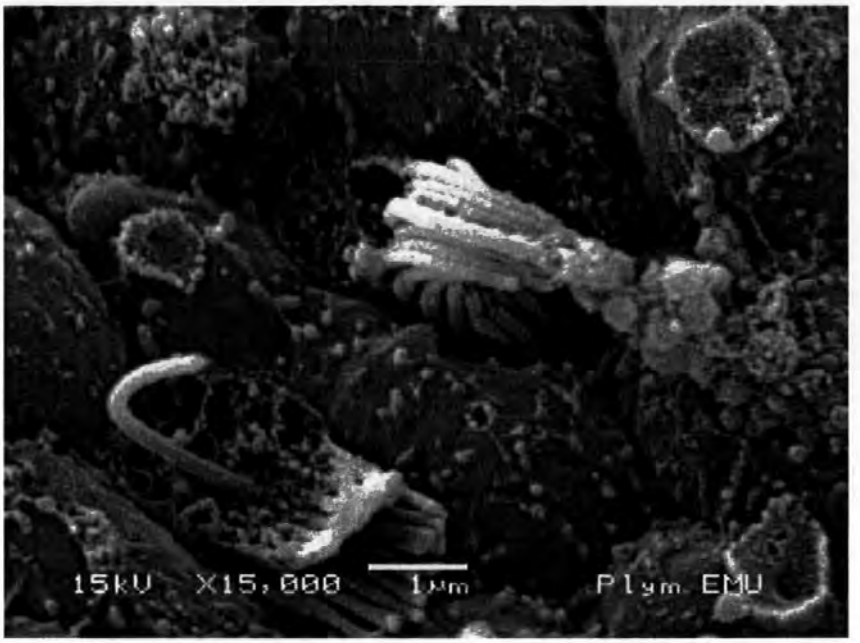

Figure 39 Micrograph of macula (close to the central transect between all 4 quadrants), showing hair cells, for cage no. 4.

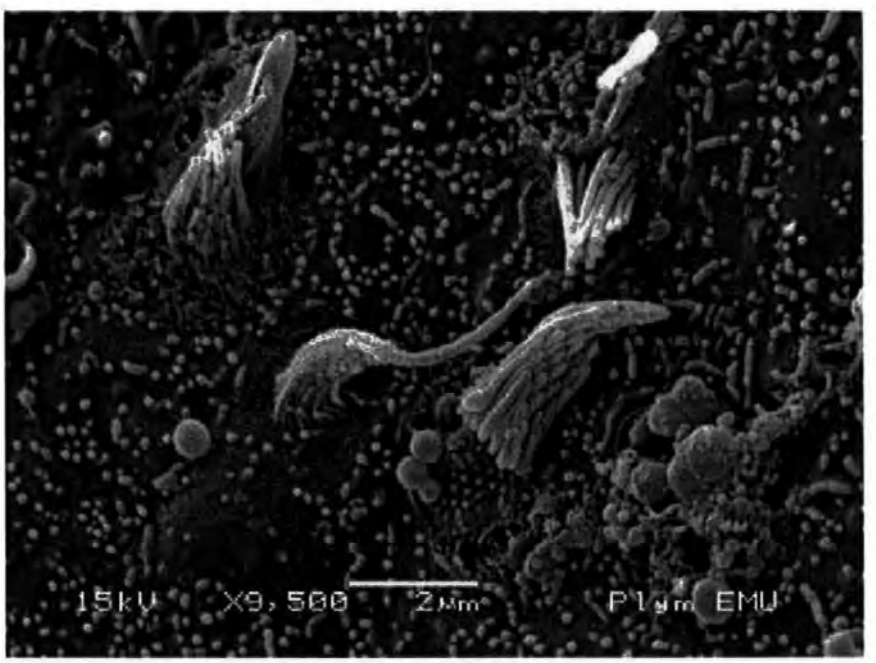

Figure 40 Micrograph of macula (close to the central transect between all 4 quadrants), showing hair cells, for cage no. 5.

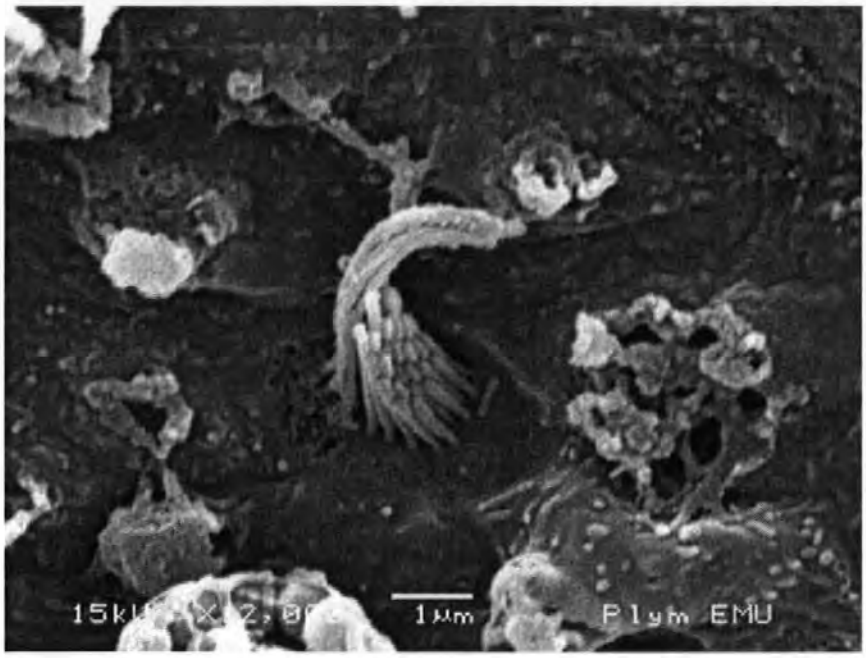

Figure 41 Micrograph of macula (close to the central transect between all 4 quadrants), showing hair cells, for the control cage.

Appendix 1: Hydrophone calibration certificates

Calibration Chart for Hydrophone Type 8104 Serial No.:2225716

Brüel & Kjær

Calibration Chart for Hydrophone Type 8104

Serial No.: 2225716

Reference Sensitivity at 250 Hz* ± 2 % at 23 °C including integral cable 10 m

Voltage Sensitivity (Open Circuit Sensitivity):

-206.1 dB ± 0.25 dB re 1 V/µPa** or 49.5 µV/Pa

Charge Sensitivity: 422.1 $\times 10^{-3}$ pC/Pa

Capacitance (including integral cable): 8520 pF

Cable Capacitance: 150 pF/m

Leakage Resistance >200 MΩ at 23 °C

Frequency Response (at ref. pos.): Individual Free Field Frequency Response Curve attached

Measuring Uncertainty (re 10 kHz):
10 to 80 kHz ± 1.5 dB
80 to 100 kHz ± 1.8 dB
100 to 200 kHz + 1.5 dB, - 3.5 dB

Summarized Specifications (re 250 Hz)

Frequency Response (tolerance field excluding measurement uncertainty):
0.1 Hz to 10 kHz ± 1.5 dB
0.1 Hz to 80 kHz ± 4 dB
0.1 Hz. to 120 kHz + 4 dB, -12 dB

Horizontal Directivity 100 kHz: (XY-plane) ±2 dB

Vertical Directivity 50 kHz: (XZ-plane) ±2 dB

Physical (mm)

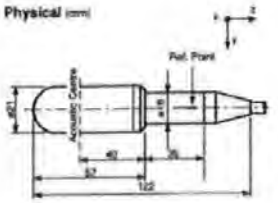

Cable: Shielded low noise with two conductors, waterblocked to MIL - C - 915

Weight (including 10 m cable): 1.6 kg

Environmental

Operating Temperature Range:
Short term -40° C to + 120° C
Continuous -40° C to + 80° C

Change of Sensitivity with Temperature:
Charge 0 to 0.03 dB/° C
Voltage 0 to - 0.04 dB/° C

Change of Sensitivity with Static Pressure:
0 to - 2 x 10^{-7} dB/Pa
0 to - 0.03 dB/atm

Temperature Transient Sensitivity: ≤ 70 Pa/° C (ANSI S12.11-1988); measured with Brüel & Kjær Charge Preamplifier Type 2626, LLF 3 Hz

Allowable Total Radiation Dose: 5 x 10^7 Rad

Maximum Operating Static Pressure: 4 x 10^7 Pa (40 atm)

Note: All values are typical at 25° C (77° F), unless measurement uncertainty or tolerance limit is specified. All uncertainty values are specified at 2 x the expanded uncertainty using a coverage factor of 2).

For further information see User Manual

Date 6.DEC.00 Signature AO

* Sensitivity Traceable to:
DPLA: Danish Primary Laboratory of Acoustics
NIST: National Institute of Standards and Technology, USA

** 1 Pa/pC = 1Nm^2 = 10 µbar

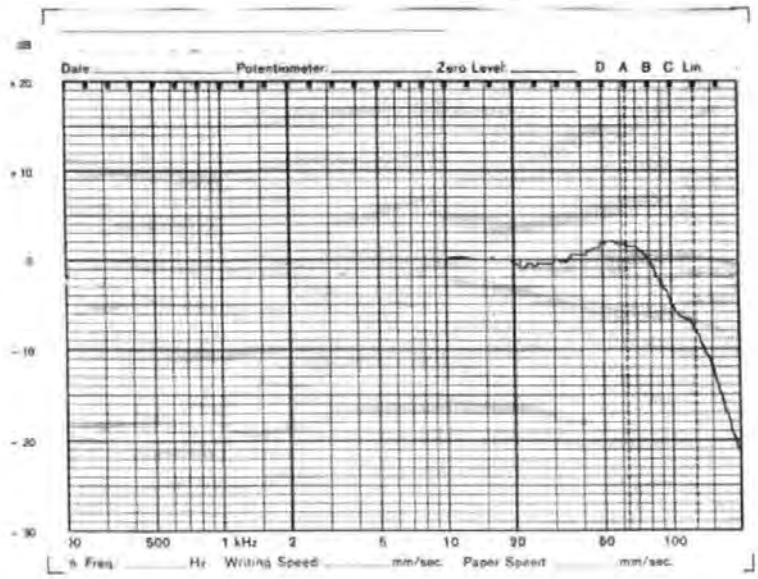

Brüel & Kjær

Calibration Chart for Hydrophone Type 8105

Serial No. 1961320

Reference Sensitivity at 250 Hz* at 23 °C
Including 10m integral cable

Cable Capacitance 150 pF/m typical

Open Circuit Sensitivity:

Voltage Sensitivity:
−208.0 dB re 1 V/µPa** or 562 µV/Pa

Charge Sensitivity: 407 · 10⁻³ pC/Pa

Capacitance (including 10m cable) 2250 pF

Leakage Resistance: 2 · 10⁹ MΩ at 23 °C

Frequency Response:
Individual Free Field Frequency Response Curve attached

Date 90-02-05 Signature O.M.

Summarized Specifications:

Usable Frequency Range: 0.1 Hz to 180 kHz +2 dB −10 dB

Linear Frequency Range: 0.1 Hz to 180 kHz ±0.5 dB −4 dB

Horizontal Directivity 100 kHz:
(XY-plane) typical ± 2 dB

Vertical Directivity 100 kHz (270°):
(XZ-plane) typical + 2 dB

8C 2170-12

Physical (mm)

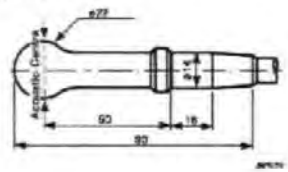

Operating Temperature Range:
Short term −40°C to +120°C
Continuous −40°C to + 80°C

Change of Sensitivity with Temperature:
Charge 0 to 0.05 dB/°C
Voltage 0 to −0.05 dB/°C

Change of Sensitivity with Static Pressure:
0 to −5 × 10⁻³ dB/kPa
(0 to −0.03 dB/atm)

Allowable Total Radiation Dose: 5 × 10⁷ Rad

Maximum Operating Static Pressure:
9.8 × 10⁶ Pa (100 atm)

Cable:
Two conductors shielded low noise
Waterblocked to MIL-C-915

Weight including 10m cable: 1.6 kg

For further information see instruction manual

* Traceable to NBS
** 1 Pascal = 1 N/m² = 10 µbar

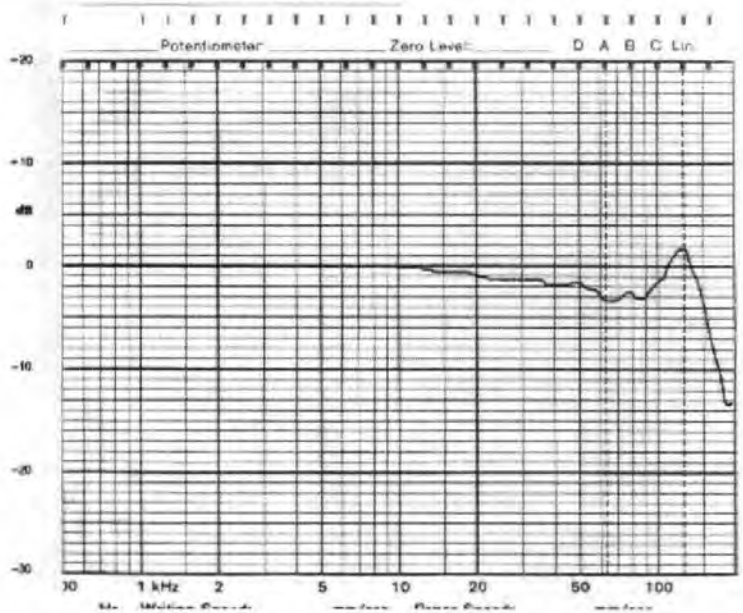

Calibration Chart for Hydrophone Type 8106 Serial No.:2256725

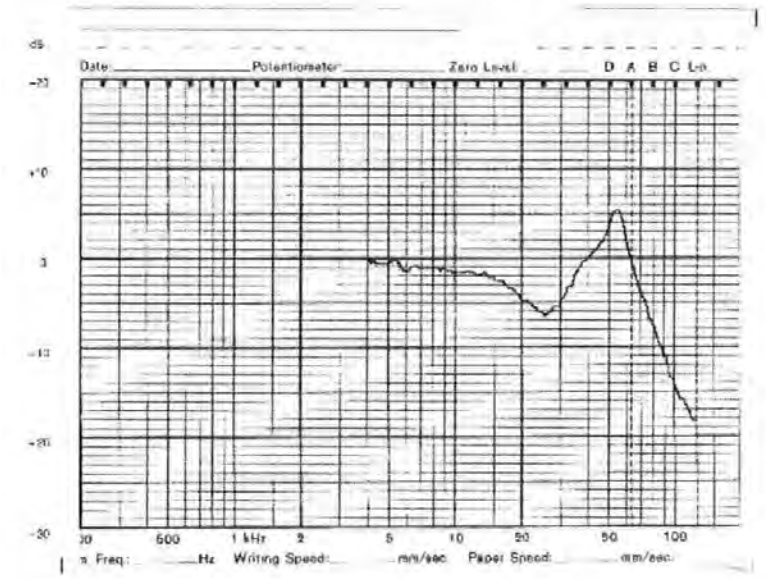

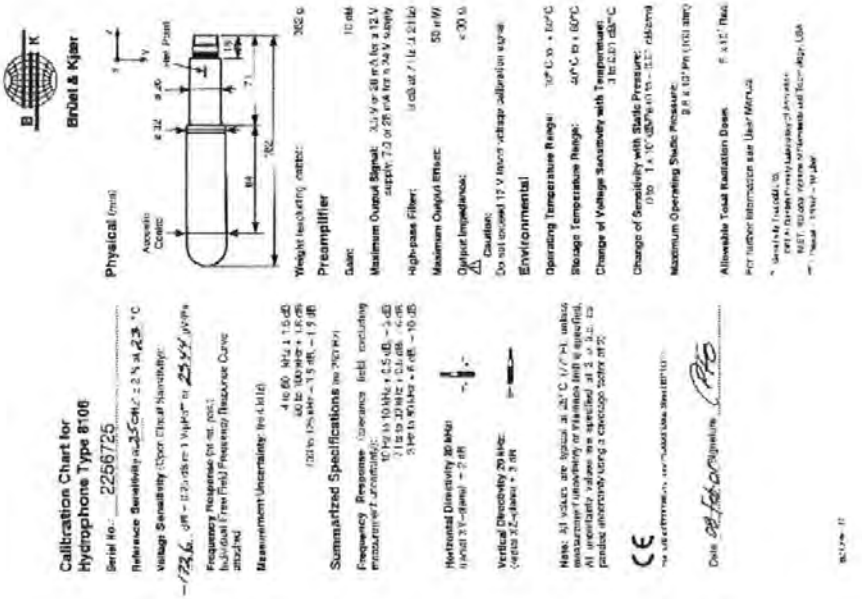

Submitted to:

Dr D Lambert
Fish Guidance Systems Ltd
Belmore Hill Court
Owslebury
Winchester
Hampshire SO21 1JW

Tel: +44 (0) 1962 777789
Fax: +44(0)1962 777 123
Email: info@fish-guide.com

Submitted by:

Dr Jeremy R Nedwell
Subacoustech Ltd
Chase Mill
Winchester Road
Bishop's Waltham
Hampshire SO32 1AH

Tel: +44 (0)1489 891849
Fax: +44 (0)8700 513060
email: subacoustech@subacoustech.com
website: www.subacoustech.com

The inner ear morphology and hearing abilities of the Mississippi Paddlefish (*Polyodon spathula*) and the Lake Sturgeon (*Acipenser fulvescens*)

J Nedwell, J M Lovell[1] and M. Pegg[2]

Report Reference: 611R0103

07 January 2005

1. **Plymouth Marine Laboratory**
2. **Illinois Natural History Survey**

Approved by .....

Contents

1. Background

The spread of Asian Carp, including Silver Carp (*Hypopthalmichthys molitrix*) and Bighead Carp (*Aristichthysc nobilis*), through the Upper Mississippi River Basin and towards Minnesota is causing increasing concern.

The Minnesota Department of Natural Resources (DNR) contracted FishPro, a firm of Consulting Engineers and Scientists, to review the available technologies that could be effective in limiting or stopping the northward movement of the carp into the Upper Mississippi River and adjacent tributaries. Their report 'Feasibility Study to Limit the Invasion of Asian Carp into the Upper Mississippi River Basin' was published on 15 March 2004. The BioAcoustic Fish Fence (BAFF), manufactured by Fish Guidance Systems Ltd (FGS), was identified as being the most appropriate technology.

The northward movement of the Asian Carp has also led to concern regarding their potential entry into the Great Lakes via the Chicago Shipping Canal and over the last few years there have been substantial resources committed to preventing this from occurring. This has included the installation of two Smith-Root Graduated Field Electric Fish Barriers, but due to limitations of the electric barriers there is a proposal to supplement the existing barriers by using an Acoustic Fish Deflection (AFD) System.

Trials conducted by the Illinois Natural History Survey (INHS, Havana, Illinois) have shown that 95% effectiveness can be achieved with Bighead Carp using a SPA driven BAFF system (Taylor, Pegg and Chick, in press) and further trials are underway with Silver Carp.

FGS was contracted by the Great Lakes Fishery Commission to measure the audiograms of two Asian Carp species, Silver Carp and Bighead Carp, as part of the preliminary works for a SPA driven BAFF system on the Chicago Canal. This would enable the SPA driven BAFF to be programmed with a specific signal tailored to the hearing ability of the Carp.

Following the FishPro report, FGS was requested by Minnesota DNR to extend the proposed measurements to included the Mississippi Paddlefish and Lake Sturgeon. This is because in the Upper Mississippi River Basin there is not only a requirement to prevent the spread of the Asian Carp, but it is also important that any AFD system installed does not affect indigenous species. The Mississippi Paddlefish (Polyodon spathula) and the Lake Sturgeon (Acipenser fulvescens) are two species that are of interest in this respect.

An ideal barrier would be 100% effective in blocking the non-indigenous species, while allowing indigenous species to pass. Ideally, the AFD system will generate sound which appears "unbearably loud" to the target species, that is, where most of the sound energy is at the optimum hearing frequencies of the species that is to be deterred and well above its threshold of hearing, but should appear "quiet" to species that should be allowed to pass. The auditory sensitivity is described by the species' audiogram, or plot of threshold of hearing of sound pressure versus sound frequency.

In order to achieve very highest possible levels of fish deflection for the non-indigenous carp species while causing as little disturbance as possible for the indigenous species, the structure and function of the hearing system of the Mississippi Paddlefish (*Polyodon spathula* Walbaum, 1792) and the Lake Sturgeon (*Acipenser fulvescens*) have been studied using ABR audiometry and scanning electron microscopy. The intention of the work reported herein was to compare this with measurements of hearing of the carp species to ascertain whether a suitable species-selective barrier could be specified.

2. Morphology

The fish inner ear is divided into two regions, the pars superior and the pars inferior (Retzius, 1881). The former responds primarily to movements of the body and postural changes, while the latter responds to both gravistatic and acoustic stimuli (Jenkins, 1981; Popper & Platt, 1993). The pars inferior comprises two fluid filled pouches, the saccule and lagena, with each pouch containing a crystalline calcium carbonate otolith (Carlström, 1963). However, *P. spathula* is from the subclass Chondrostei (cartilaginous bony fishes, Helfman et al.), in the order Acipenseriformes (sturgeons and paddlefishes), and indicates that the morphology of the inner ear, especially the otolithic organs may not follow the format of either the bony fishes or sharks. In order to investigate the mechanism of sound reception, the inner ear morphology of *P. spathula* has been investigated as part of this work. The saccule is considered to be the major auditory organ in most bony fish species, though there is evidence of a functional overlap between all three end organs (Popper & Fay 1993). For fish to locate the source of a sound in both the horizontal and vertical planes, they rely on the stimulation of ciliary bundles oriented specifically along the sound propagation axis (Lu & Popper, 1998). It is known (Enger et al., 1973; Hawkins & Sand, 1977; Fay, 1997) that the morphological polarities of sensory hair cells in the otolithic organs are fundamental to the directional hearing capabilities of fish. In general, azimuths of peak sensitivity tend to lie parallel to the plane of the otolith and sensory epithelium (Enger, et al. 1973; Sand & Hawkins, 1973; Fay, 1997). Examination of the orientation of the ciliary bundles provides evidence of a correlation between the morphological polarisation of receptor cells and the magnitude of an electrophysiological response to a sound (Popper & Fay, 1993). Excitation occurs when stereocilia are bent toward the kinocilium during the passage of a wave front, resulting in the cell becoming depolarised relative to its resting potential (Clegg & Mackean, 1994). Inhibition occurs when the bundle is deflected in the opposite direction, and results in the hyperpolarisation of the cell (Platt & Popper, 1981). The magnitude of both excitation and inhibition are a cosine function of the angle between the direction of the stimulus and the direction at which sensitivity is greatest (Enger, 1965; Popper, 1983). The detection and localisation of a sound source is of considerable biological importance to many fish species, and is often used to assess the suitability of a potential mate or during territorial displays (Nordeide & Kjellsby, 1999), and during predator prey interactions (Myrberg,1981).

2.1 Paddlefish

It is the first time that the hearing system of fish from the order Acipenseriformes has been studied. The inspection of the Paddlefish reveals that this fish is capable of detecting sound using arrays of sensory hairs located in three otolithic end organs in the inner ear.

Figure 1 illustrates a dissected paddlefish showing the internal organs and location of the brain. The dissection reveals that *P. spathula* possesses a well developed swim bladder, which is essential to its feeding habits (the paddlefish feeds on small planktonic organisms that abound at the water surface). As this fish lives in fresh water, it needs a well

developed swim bladder to achieve neutral buoyancy to aid in surface feeding. Figure 2 illustrates the left ear and VIII nerve; and the arrows D and A show the orientation of the ear in the fish. Figure 3 presents electron micrographs, this time from the right ear of *P. spathula*, and shows the saccule, lagena and the utricle. Also included are hair cells from the anterior-ventral region of the saccule, and hair cells from the anterior margin of the utricle. The configuration of the saccule is approaching standard (hair cells arranged in 4 almost dichotomous quadrants). This is common to a large proportion of non-specialist fish, though the ostium (the two anterior quadrants) has a number of hair cells orientated in the dorsal ventral plane, which follow the flow of hair cells proliferating in the adjacent quadrants, as well as hair cells orientated in the expected anterior posterior plane.

2.2 Lake Sturgeon

In addition to the paddlefish, this work looks at the hearing abilities of the Lake Sturgeon (*Acipenser fulvescens*) which is another cartilaginous fish in the same order as the paddlefish, but spends much of its time feeding in the benthos. Because of this demersal feeding habit, the sturgeon has no need for a well developed swim bladder, which was confirmed by an internal examination, which did not find obvious evidence of a swim bladder. However, an examination of the inner ear morphology revealed a similar configuration to the paddlefish. Both the size of the three otoliths, and the pathway taken by the VIII nerve was also found to be comparable within the order.

3. Audiograms

The techniques used to obtain fish audiograms require a varying degree of time, surgical and technical expertise, and many authors favour the use of operant reward based paradigms (behavioural methods) to gain statistically sound data (see, for instance, Yan 1995). There are two fundamental methods by which audiograms can be estimated.

3.1.1. The behavioural method. In this method, a species is trained to react in a specified and measurable way (e.g. a reward based method by seeking food) when a tone at a given frequency is played. The tone is gradually played at decreasing levels until no reaction occurs; this level is therefore taken as the threshold of hearing at that frequency for the species in question. In practice, the behavioural method is very time consuming and only effective with species that are easy to train, and therefore is not considered suitable for the measurements described herein.

3.1.2. The auditory evoked potential (AEP) method. Audiograms produced using the Auditory Brainstem Response (ABR) technique, are regarded as being the least time consuming and most reliable methodology for acquiring audiological data from fish and other animals. They are used for both mammalian and non-mammalian vertebrates (Corwin, Bullock and Schweitzer 1982), and marine invertebrates (Nedwell *et al* 2003, in press, Lovell *et al.*, in Press);

Additionally, ABR recordings require no invasive procedural work as measurements are taken in the electro-physiological far field using cutaneous electrodes, resulting in significant stress reduction during the hearing assessment (Kenyon et al 1998).

This approach relies on the fact that the electrical potential of the nervous impulse passing along the auditory nerve can be detected by electrodes placed in its vicinity. In practice, a pair of electrodes are applied to the species in a position spanning the auditory nerve. A sinusoidal tone at a given frequency is played to the species. An ABR trace is formed by averaging conglomerate responses of peak potentials arising from centres in the auditory pathways extending from the periphery of the VIII nerve, to the midbrain (Corwin et al 1982; Overbeck and Church 1992). The threshold of hearing is estimated by finding the level of sound at which the auditory response just appears above noise. One particular variety of the AEP method is to measure the auditory response at the brainstem; this approach is termed the Auditory Brainstem Response (ABR) method, and is the method that was chosen for the work presented herein.

The ABR measurements of hearing threshold were made using "BrainWave", a control and analysis program, written for the purpose by Subacoustech in a LabView 7 environment. This program both generates the stimulus signals and captures and analyses the response. The stimulus used was a sine train (sine wave pulse) which was presented to the fish at a given frequency and sound pressure level. The ABR response is readily dominated by responses caused by muscle movement and hence while undertaking the ABR measurements the fish are kept in dark and constrained conditions since many

species react to this by becoming passive. It is known that many fish species react to danger by hiding in weeds, and it is thought that this experimental environment mimics the natural environment, enabling the fish to feel protected, reducing avoidance behaviour. However, in addition to this BrainWave can detect ABR responses that are contaminated by muscle movement. The program ignores contaminated measurements when producing the averaged ABR response. The use of chilling as a muscle movement control measure has also been investigated. As cold-blooded animals, fish show a reduction in activity as their body temperature decreases, and this might in principle be used as a suitable control measure. However, chilling may have the effect of diminishing the auditory evoked potential from a fish (see for instance Corwin *et al*(1982); Stockard *et al* (1978)) and hence this approach has not been used.

A further refinement of the experimental measurements has been the use of submerged projectors (underwater sound transducers) to generate the insonification. Previous measurements, such as those by Yan, have used a domestic hi-fi loudspeaker above the experimental water tank to create the insonifying sound. The system has been calibrated by measuring the sound above the tank, and assuming that the sound pressure in the water is equal to the sound pressure in the air. This is unsatisfactory for two reasons. First, the walls of the tank may displace outwards under the influence of the waterborne sound, causing a "pressure release" effect and reduction in the waterborne pressure. Second, this method of insonification may set up complex pressure and particle velocity fields in the water tank, with the result that the condition of exposure is very difficult to specify.

In the experiment described herein, two identical projectors have been set up facing each other with the fish on the axis of symmetry between the two. Where the projectors are driven in phase, it is possible to create a region between them of high and even sound pressure, associated with a low level of particle velocity.

3.1 Method of recording audiograms

A block diagram of the equipment to provide audiometric measurements is shown in figure 4. The procedure used to acquire the acoustically evoked potentials was approved by the University of Illinois, United States 15.11.04. The sound signal was generated by a laptop computer running BrainWave, and amplified using a Tandy 250W power amplifier. The sound field in the experimental watertank was generated by means of two Fish Guidance Systems Ltd. Mk II 15-100 Sound Projectors. These faced each other at a distance of 200 mm; the inner ear of the fish during measurements was arranged on the axis connecting the centres of the two projectors.

During the measurements made on the Paddlefish and Sturgeon, the projectors were driven directly from the amplifier since due to the insensitivity of the fish meant that high levels of sound were required to cause an acoustic brainstem response. While provision had been made to reduce the output of the amplifier (by using load resistors placed

between the amplifier and projector) these were only required when measuring the hearing of more sensitive fish such as the carp species, where much lower levels of sound were required.

The stimulus tones presented from the loudspeaker to the fish were calibrated using an insertion calibration. In this method, the sound level is recorded in the absence of the fish, at the point where the inner ear of the fish would be. The measurements were made using a Bruel and Kjaer Type 8104 Hydrophone (serial number 2225715) calibrated and traceable to International Standards; the certificate of calibration is attached as appendix 1. The signal from the hydrophone was amplified by a Bruel and Kjaer Type 2365 Charge Amplifier (Serial Number 1079556). In case there was any non-linearity of the signal, calibrations were made at every frequency and every level used for a measurement, totaling some 660 individual calibrations. These calibrated levels were then applied to the threshold defined by ABR measurement to provide calibrated audiograms with pressure levels traceable to International Standards. In fact, no evidence of non-linearity was detected, other than at the very highest levels of sound, which was not required in any case for measuring audiograms.

The test subjects were placed into a flexible cradle formed from a soft nylon mesh rectangle saturated with freshwater for the small fish, and a rubber coated 1 mm gauge wire mesh for fish over 2 kg weight. This assembly is illustrated in figure 5. Oxygenated water kept at a temperature of 18° C was gravity fed at an adjustable flow rate of between 5 millilitres per second for the small fish, to 25 millilitres per second for the large, and directed toward the gills through a soft rubber mouth tube with a diameter of between 6 mm to 25 mm. The water was held in an aerated reservoir positioned 1 m from the water surface, and fed to the mouthpiece through a 6 mm to 25 mm diameter clear plastic tube. The small fish were first placed lengthwise and centrally on a 160 mm x 120 mm rectangle of fine nylon netting, which was wrapped firmly around the body and tail, and the two sides of the net were held together using the clip, which may be seen in the photograph of figure 6.

The clip was placed in a retort stand clamp fitted with ball joint electrode manipulator arms, and the aerated water pipe. During the procedure to position the electrodes the specimen and clamp were suspended over the test tank, and aerated water was supplied to the fish.

The electrophysiological response to acoustic stimulation was recorded using the two sub-cutaneous electrodes of figure 7, which were connected to the MS6 preamplifier by 1m lengths of screened coaxial cable with an external diameter of 1.5 mm. The outer insulating layer of the coax was removed 15 mm from the end where the electrode tip was to be fixed, and the screening layer removed 10 mm from the cable end. The inner insulating material was then trimmed by 2 mm, and the exposed inner wire (0.5 mm diameter) was tinned with silver solder and joined to a 10 mm length of silver wire (0.25 mm diameter), tapered to a fine point. The assemblage was pushed through a 100 mm

glass pipette with an internal diameter of 4 mm, until 0.4 mm of the silver wire was exposed. The remaining space inside the pipette was filled with a clear epoxy resin, and then trimmed to expose 0.3 mm of silver tip through which the AEP could be conducted. The impedance of the electrodes, both between the outer shielding and inner core, and the silver tip and MS 6, were tested using an M 205 precision digital multimeter. The impedance between the tip and pre-amplifier was found to be 0.2 Ω for both electrodes, and an open circuit was recorded between the outer shielding and inner core.

Stimulus sounds were presented to the fish at sound pressures initially not exceeding 145 dB re 1 µPa. The electrophysiological response of the fish to acoustic stimulation was recorded using two cutaneous electrodes, which were positioned on the cranium of the fish adjacent to and spanning the VIII nerve. The reference electrode was positioned centrally on the head above the medulla, and the record electrode was located 5 mm anterior of this point. The evoked response was amplified and digitised to 12 bits resolution and recorded. This process was repeated 2000 times and the response averaged to remove electrical interference caused by neural activities other than audition, and the myogenic noise generated by muscular activity. Each measurement was .repeated twice; this aids in separating the evoked response, which is the same from trace to trace, from the myogenic noise, which varies in two successive measurements. After the averaging process, the evoked potential could be detected, following the stimulus by a short latency period of about a millisecond.

3.2 The audiogram of the Paddlefish (*P. spathula*).

In order to concisely identify the frequency and intensity of sounds audible to paddlefish, twelve specimens of *P. spathula* were stimulated with sound ranging in the frequency domain between 100 Hz to 1500 Hz, presented in a sound field dominated by sound pressure at levels of between 150 dB to below 90 dB re 1 µPa. Figure 8 illustrates the auditory evoked potentials from *P. spathula* in response to tone bursts at frequencies of 100 Hz, 200 Hz, 250 Hz, 300 Hz, 500 Hz, 750 Hz, 1000 Hz, and 1500 Hz. Each waveform set from a particular frequency has been overlaid, and reveals a latency change in response to both the intensity and frequency of the sound. At each frequency, the ABR waveforms evoked by the tone bursts typically consisted of a series of four to eight rapid negative peaks, followed by a slow positive defection. The onset latency of the centre or largest sinusoid of the ABR response varied with frequency, ranging from 7.3 ms after stimulus onset at 100 Hz to 4 ms at 1500 Hz. As the sound pressure levels approached threshold, 2000 sweeps were required to distinguish ABR's from background noise.

It is known that the frequency and intensity of a tone burst effects the latency of the evoked response (Corwin et al 1982; Kenyon et al 1998), as does the metabolic state of the organism (Corwin et al 1982). The latency of the evoked potentials from *P. spathula* can be observed in Figure 9, and are in response to a 300 Hz tone burst, presented initially at 156 dB (re 1 µPa), and attenuated in 5 dB steps. The arrows positioned at 0.3 ms intervals represent vertex positive components issuing from the neural centres situated

along the auditory pathway to the midbrain (Overbeck and Church 1992). The increase in the latency of the evoked potential in response to decreasing stimulus intensity is often used to verify that the averaged waveform is a product of auditory stimulation rather than a transient generated at the electrode tip (Kenyon et, al., 1998), the Inter-Peak Latency (IPL) cannot be accounted for acoustically, as transients and other artefacts directly associated with the stimulus sound would occur at the same time regardless of sound amplitude.

Figure 10 shows ABR waveforms evoked from a 300 Hz tone burst, presented initially at 150 dB (re 1 µPa), and attenuated in steps of between 8 to 4 dB ordinarily, then in 2 dB steps as the hearing threshold was approached. When two replicates of waveforms showed opposite polarities, as seen in the traces for the results at 122 dB in Figure 10, the response was considered as being below threshold (cf. Kenyon et al. 1998).

All threshold responses were measured in this way, and the sound pressures at threshold were used to generate the audiogram shown in Figure 11. The audiogram was produced using the sequential ABR waveform data, acquired from frequencies of 100 Hz to 1500 Hz, presented in steps of between 200 Hz to 500 Hz. The audiogram follows Gaussian profile, determined by calculating the lowest intensity stimulus sounds (recorded underwater using the hydrophone located adjacent to the fish ear) that evoked a repeatable ABR response. The profile is centred at 300 Hz, which was found to be the "best" frequency for this species. The thresholds begin to rise slowly to 1000 Hz, and are substantially reduced at 1500 Hz, as the frequency goes out of the hearing range of the fish.

3.3 Audiogram for the Lake Sturgeon (*Acipenser fulvescens*)

The of head of *A. fulvescens* (detailed in Figure 3) was dissected to facilitate the correct positioning of the electrodes; using the anatomical information as a guide, the record electrode was placed 6 mm anterior of the reference electrode which was positioned centrally above the medulla. It was found that the hard bony structure of the head made electrophysiological recordings difficult, as there was no fleshy skin for the electrode to push into and create a good connection between the electrode tip and fish. This resulted in the 0.3 mm silver tip being almost entirely exposed to the ambient water, which can result in the substantial attenuation of the evoked potential. To resolve this issue, silicone tip insulators were used to create a seal around the electrode tip and fish, thus preventing the ambient water from contacting the electrodes. These adaptations can be clearly seen in Figure 6, which shows a specimen of *A. fulvescens* held in place during an audiological test.

Twelve specimens of *A. fulvescens* were stimulated with sound ranging in the frequency domain between 100 Hz to 1500 Hz, presented in a sound field dominated by sound pressure at levels of between 150 dB to below 120 dB re 1 µPa. Figure 12 illustrates the auditory evoked potentials from *A. fulvescens* in response to tone bursts at frequencies of 100 Hz, 200 Hz, 250 Hz, 300 Hz, 500 Hz, 750 Hz, 1000 Hz, and 1500 Hz. At each

frequency, the ABR waveforms evoked by the tone bursts typically consisted of a series of four to eight rapid negative peaks, followed by a slow positive defection, similar to those recorded from *P. spathula*. The audiogram in Figure 13 was produced using the same methodology as used for *P. spathula*; the curve follows a similar profile also centred at 300 Hz, indicating comparable frequency sensitivity and overall hearing abilities between these two members of the order Acipenseriformes.

4. Discussion.

Figure 14 illustrates the audiograms of both the Sturgeon and the Paddlefish. The audiograms of the Silver Carp and the Bighead Carp are also included on the figure for comparison. Also on the figure is the measured maximum level of background noise during the measurements.

It may be noted that the background noise levels were recorded on the identical apparatus used to measure the audiograms, and were found by reducing the signal from the system until no further reduction in level occurred. Hence the noise calibration process includes not only extraneous background noise, but also noise from the equipment used to generate the signal (such as noise from the power amplifier) and noise from the measuring equipment such as the hydrophone, charge amplifier and digitization equipment. It may be noted that the background noise level is of lower level than all of the recorded thresholds of hearing, and hence it may be concluded that the audiograms are uncontaminated by background noise.

It may be seen that the audiograms of the Paddlefish and the Sturgeon are similar. They indicate a peak sensitivity at about 250 Hz. However, the hearing of the Paddlefish is slightly more sensitive than that of the Sturgeon, having a minimum hearing threshold (*i.e.* maximum sensitivity to sound) of about 126 dB re 1 µPa, whereas the maximum sensitivity of the Sturgeon is about 134 dB re 1 µPa. Both of these fish are however highly insensitive to sound, with the audiograms placing them amongst the fish with the least sensitive hearing, comparable in hearing sensitivity with marine flatfish such as skate.

It may be seen by comparison that the hearing of the two carp species is much more sensitive, and extends to much higher frequencies than that of the Paddlefish and the Sturgeon.

This significant difference in hearing ability raises the possibility of a selective acoustic fish deflection (AFD) barrier, that might allow for instance such systems to selectively deter nonindigenous species while allowing indigenous species to pass. AFD systems comprise a set of underwater sound projectors and associated amplifiers; these are driven by a signal that has been developed to be unpleasant to the fish species that are the target of the system. It is apparent that a deterrent signal concentrated on frequencies of the order of 400 Hz to 2 kHz would probably achieve maximum deflection of the carp species, while effecting the Paddlefish and the Sturgeon to a much lower degree. Measurements by Taylor *et al* of the efficiency of a Fish Guidance Systems SPA/BAFF system have indicated that efficiencies of 95% or more are achievable for carp. Reductions in deflection efficiency of about 3% per dB_{ht} (that is, per dB of *perceived* level) have been recorded, and the audiograms indicate that it might be possible to achieve a signal with a dB_{ht} level for the Paddlefish and the Sturgeon at least 25 dB_{ht} lower than that for the carp species. This might therefore equate to a reduction in deflection efficiency of Paddlefish

and the Sturgeon of 75% or so, to say 20% or less for the same barrier. The results therefore indicate that a differential AFD barrier might be achievable.

A formal analysis of the system could be made using the dB_{ht} method, which would enable the probable efficiency of the barrier against various species to be determined and hence both the barrier and the deterrent signal to be designed for maximum deflection of nuisance species and minimum deflection of indigenous species.

It is interesting to compare acoustic fish deflection systems, which only work efficiently when carefully designed with the acoustics of the barrier and the hearing ability of the target species in mind, with electric fences which are "blunt instruments" which require no detailed design. While the lack of need for detailed preliminary design work is an apparent advantage of electric fences, this lack of selectivity is also a drawback when the fence blocks the passage of valuable species.

5. Summary

1) Audiograms have been measured for the Mississippi Paddlefish (*Polyodon spathula*) and the Lake Sturgeon (*Acipenser fulvescens*).
2) The audiograms of the Paddlefish and the Sturgeon are similar, with peak sensitivity at about 250 Hz. The hearing of the Paddlefish is slightly more sensitive than that of the Sturgeon, having a minimum hearing threshold (*i.e.* maximum sensitivity to sound) of about 126 dB re 1 µPa, whereas the maximum sensitivity of the Sturgeon is about 134 dB re 1 µPa. Both of these fish are however highly insensitive to sound.
3) By comparison, the hearing of the Bighead Carp and Silver Carp species is much more sensitive, and extends to much higher frequencies than that of the Paddlefish and the Sturgeon.
4) This significant difference in hearing ability raises the possibility of a selective acoustic fish deflection (AFD) barrier, that might allow Paddlefish and the Sturgeon to pass while barring the passage of non-indigenous carp species.
5) A formal analysis of a prospective AFD system could be made using the dB_{ht} method, which would enable the probable efficiency of the barrier against various species to be determined and hence both the barrier and the deterrent signal to be designed for maximum deflection of nuisance species and minimum deflection of indigenous species.

6. References

Carlström DA (1963) "Cystallographic study of vertebrate otoliths". Biol. Bull. 125, 441-463.

Clegg CJ and Mackean DG (1994) "Advanced Biology: principles and applications". John Murray, London, 448-461pp.

Corwin JT, Bullock TH, Schweitzer J. 1982. "The auditory brain stem response in five vertebrate classes". Electroencephalogr. Clin. Neurophysiol. 54: 629-641

Enger PS (1965). "Acoustic thresholds in goldfish and its relation to the sound source distance". Comp Biochem Physiol 18: 859-868

Enger PS, Hawkins AD, Sand O and Chapman CJ (1973). "Directional sensitivity of saccular microphonic potentials in the haddock". J. Exp. Biol., 59:425-433.

Fay RR (1997). "Directional response properties of saccular afferents of the toadfish, (Opsanus tau)". Ed. Walton PL. Hearing Research 111 (1-2): 1-21

Hawkins AD and Sand O (1977). "Directional hearing in the median vertical plane by the cod". Journal of Comparative Physiology. A. Vol. 122: page 1 - 8

Jenkins DB (1981). "The utricle in *Ictalurus punctatus*". *Hearing and Sound Communication in Fishes.* Tavolga, WN, Popper AN and Fay RR, Eds. Springer-Verlag, New York.

Kenyon, T.N., Ladich, F., Yan, H.Y. (1998) "A comparative study of the hearing ability in ? shes: the auditory brainstem response approach". *J Comp Physiol* A 182:307–318.

Lovell JM, Findlay MM, Moate RM and Yan HY (in press). "The hearing abilities of the prawn (*Palaemon serratus*)". Journal of Comparative Physiology and Biochemistry A.

Lu Z and Popper AN (1998). "Morphological polarizations of sensory hair cells in the three otolithic organs of a teleost fish: fluorescent imaging of ciliary bundles". Hear. Res. 126 (1-2): 47-57.

Myrberg AA (1981) "Sound communication and interception in fishes". *Hearing and Sound Communication in Fishes.* Tavolga WN, Popper AN, and Fay RR, Eds. Springer-Verlag, New York.

Nordeide JT and Kjellsby E (1999). "Sound from spawning cod at there spawning grounds". ICES Journal of Marine Science. 56: pp 326 – 332.

Overbeck GW, Church MW (1992) "Effects of tone burst frequency and intensity on the auditory brainstem response (ABR) from albino and pigmented rats". Hear Res 59: pp129-137

Popper AN and Platt C (1993). "Inner ear and lateral line". *The Physiology of Fishes.* Evans, D. H., Ed., CRC Press, Boca Raton.

Popper AN and Fay RR (1993) "Sound detection and processing by fish: critical review and major research questions". Brain Behav Evol, 41, 14-38

Popper AN (1983). "Organization of the ear and auditory processing". Fish Neurobiology 1st edition. Eds. Northcutt, R. G. and Davis, R. E., University of Michigan Press, Ann Arbor,

Retzius G (1881). "Das Gehörorgan der Wirbelthiere". Vol. 1, Das Gehörogan der Fische und Amphibien, Samson and Wallin, Stockholm.

Sand O and Hawkins AD (1973). "Acoustic properties of the cod swimbladder". J. Exp. Biol., 58:797-820.

Taylor, R.M., Pegg M.A. and Chick J.. "Effectiveness of two bioacoustic behavioral fish guidance systems for preventing the spread of bighead carp to the Great Lakes". North American Journal of Fisheries Management (in press).

Figures

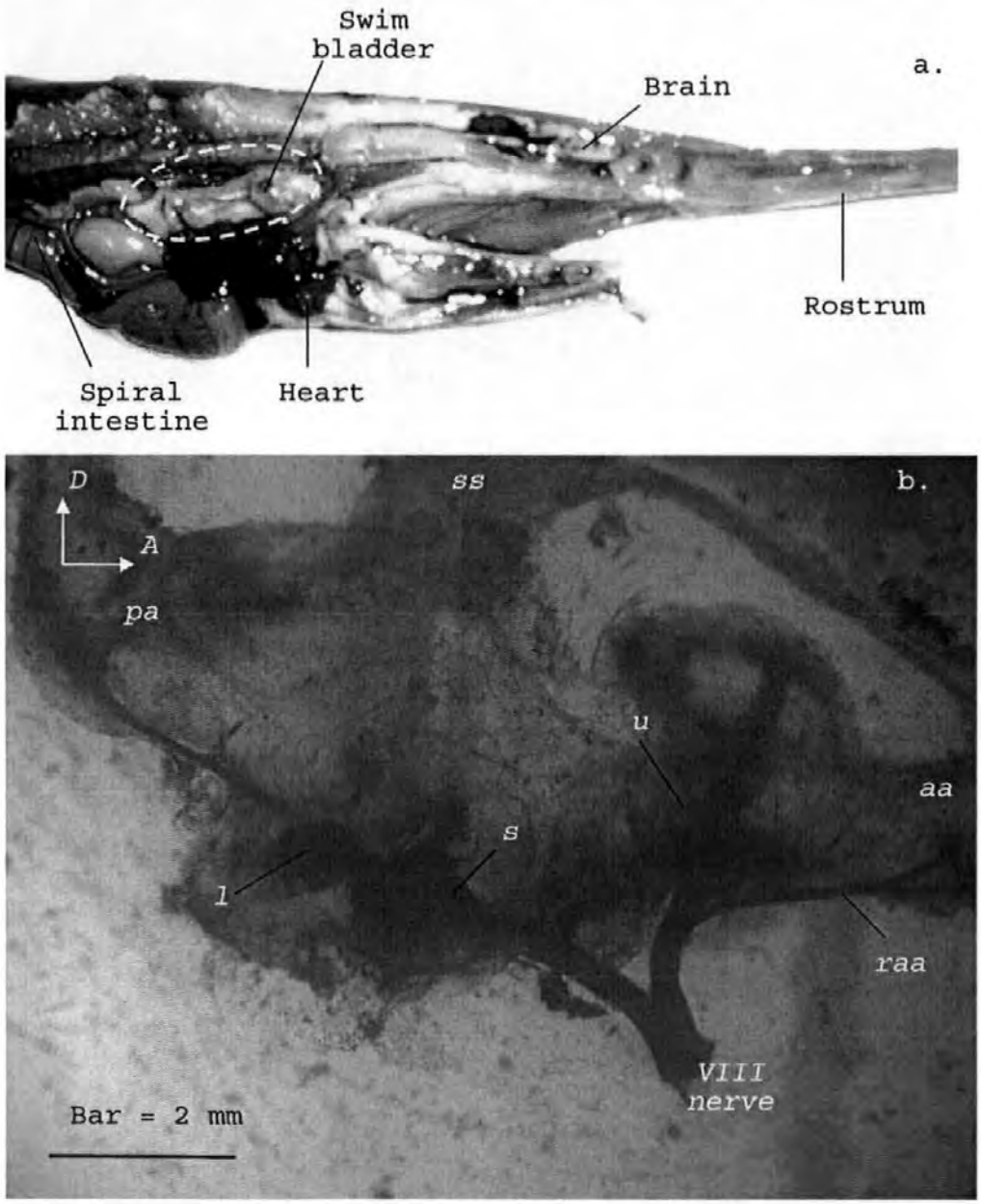

Figure 1. Upper: Dissected paddlefish showing the internal organs and location of the brain, revealing that *P. spathula* possesses a well developed swim bladder. Lower: The left ear and VIII nerve; *aa.* anterior ampulla , *pa.* posterior ampulla, *l.* lagena, *raa.* ramus anterior ampulla, , *s.* saccule, *ss.* sinus superior, *u.* utricle. The annotations D and A show the orientation of the ear in the fish. Bar = 2 mm

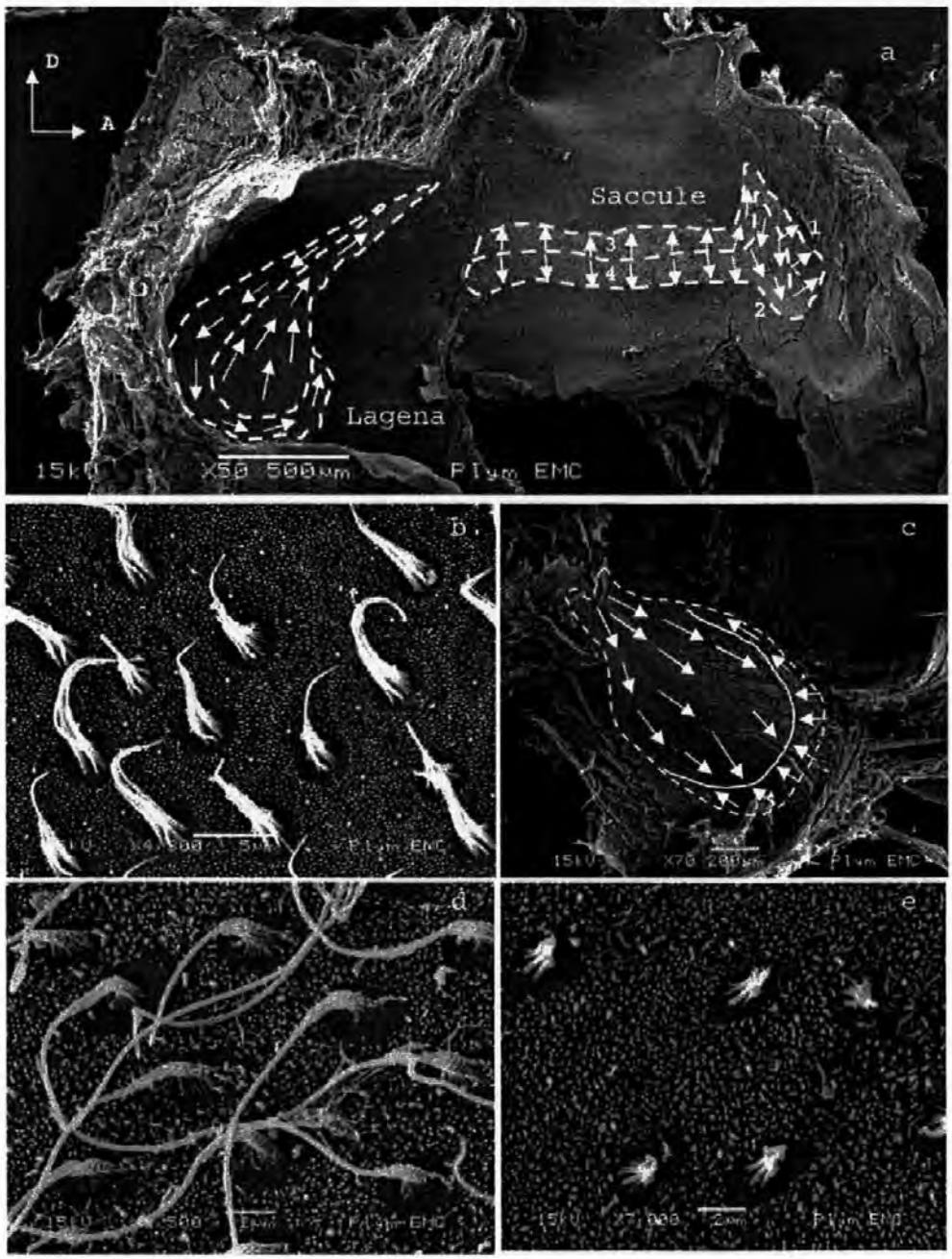

Figure 2. Electron micrographs of the right ear from *P. spathula*, showing the saccule and lagena (a), and the utricle (c). Also included are hair cells from the anterior-ventral region of the saccule (b), and hair cells from the anterior margin of the utricle (d and e).

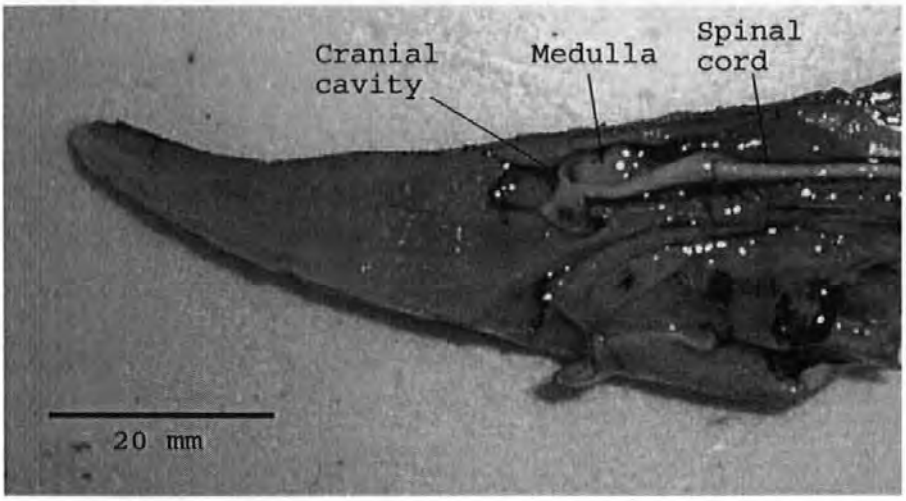

Figure 3. Dissected head of the sturgeon, showing the cranial cavity, brain and spinal cord (Bar = 20 mm)

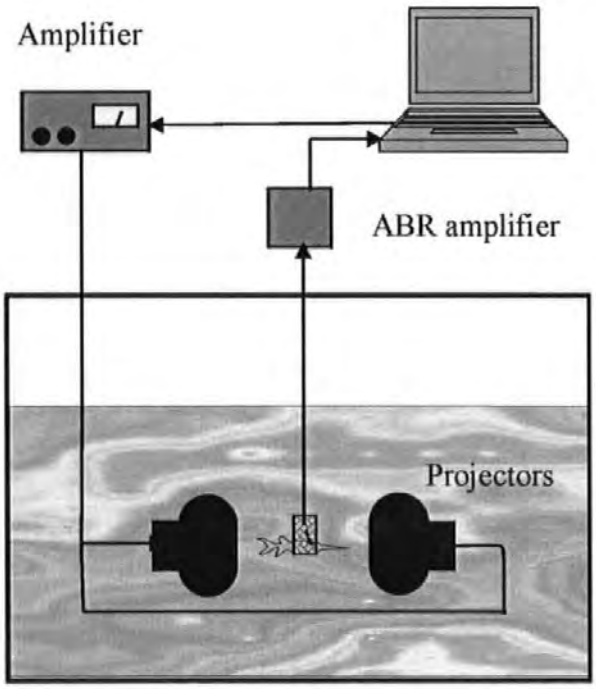

Figure 4. A block diagram of the experimental apparatus.

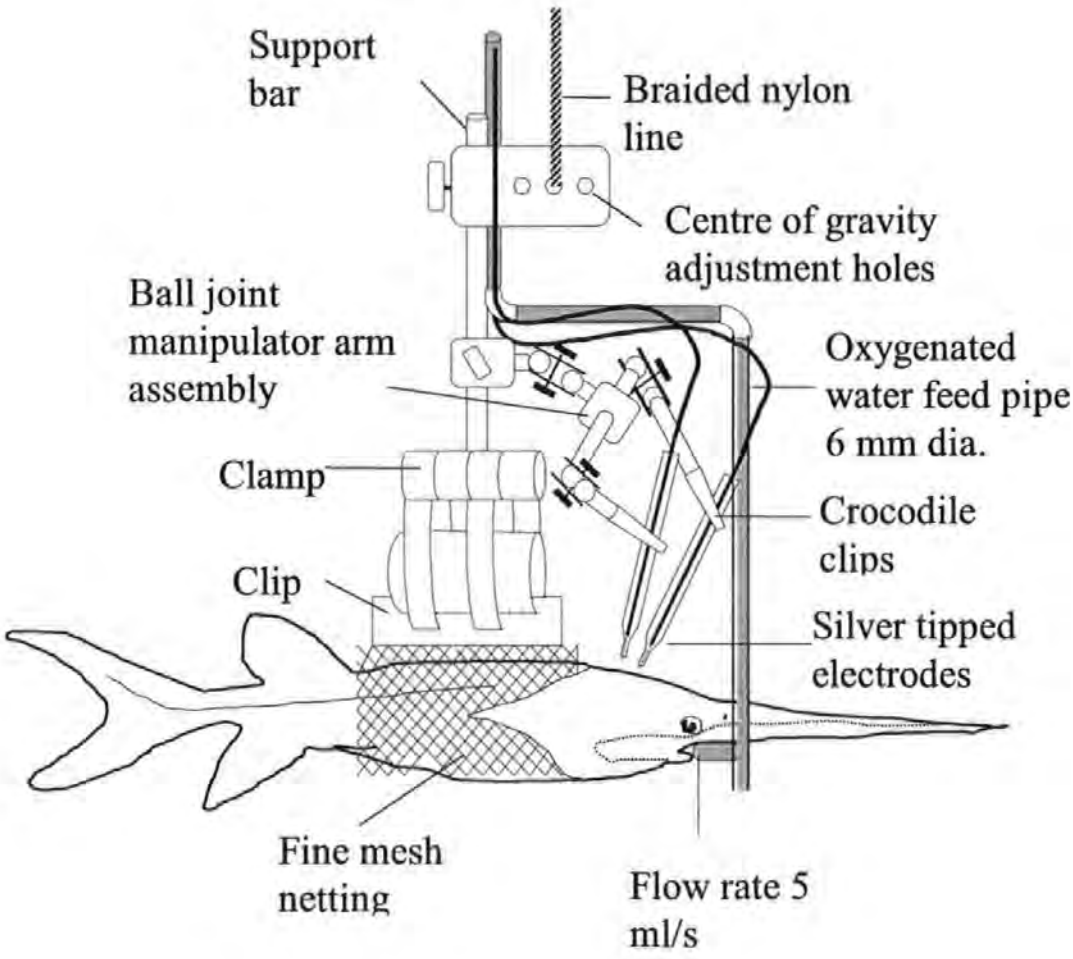

Figure 5. Schematic of the clamp used to hold the fish in position, and manipulate the electrodes during the audiological tests

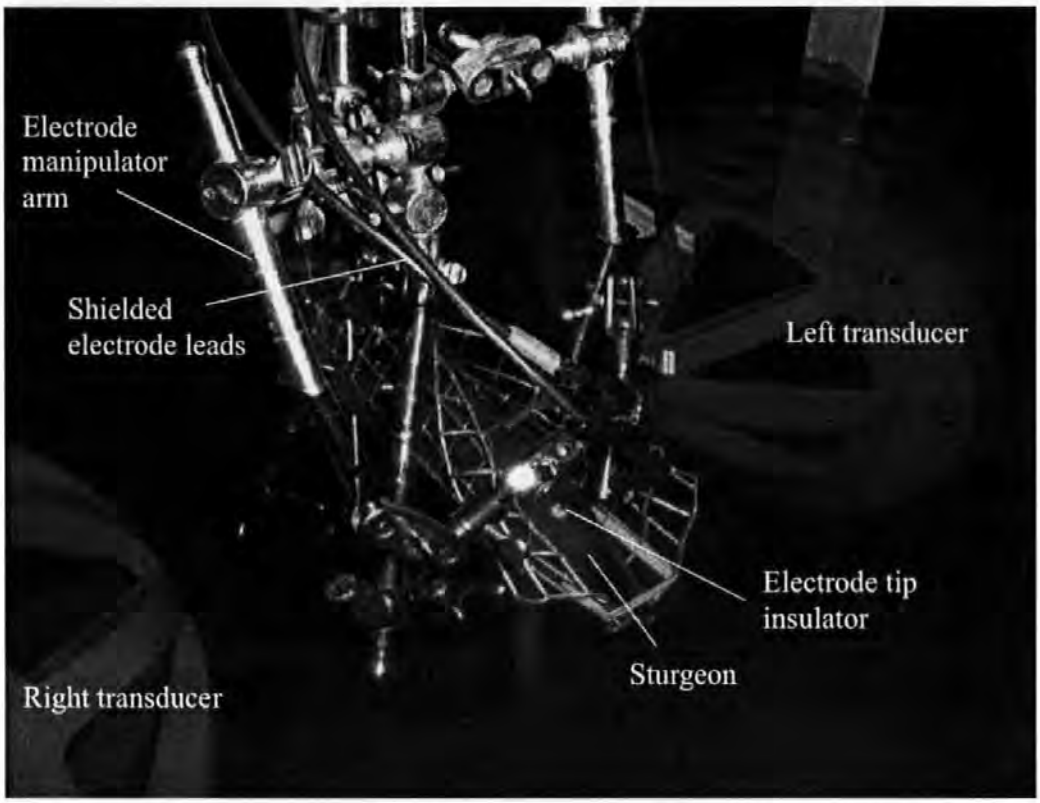

Figure 6. The transducers and the electrode holding and fish restraining device during the audiological examination, in this Figure, the subject is a sturgeon

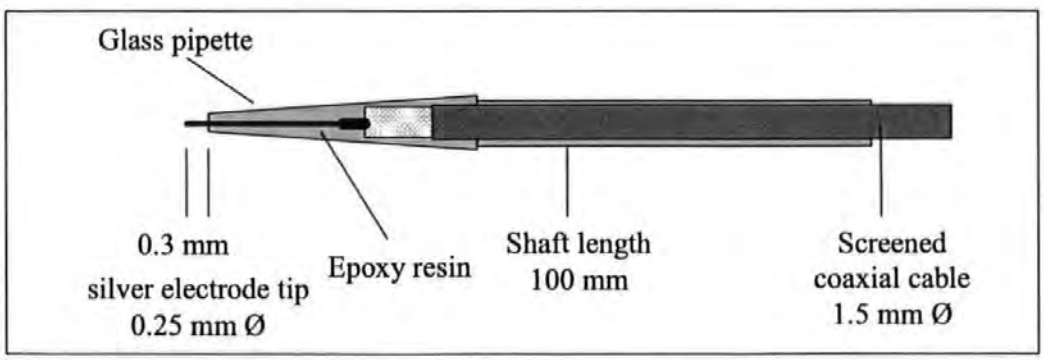

Figure 7. A schematic of the electrodes used to record the evoked potentials

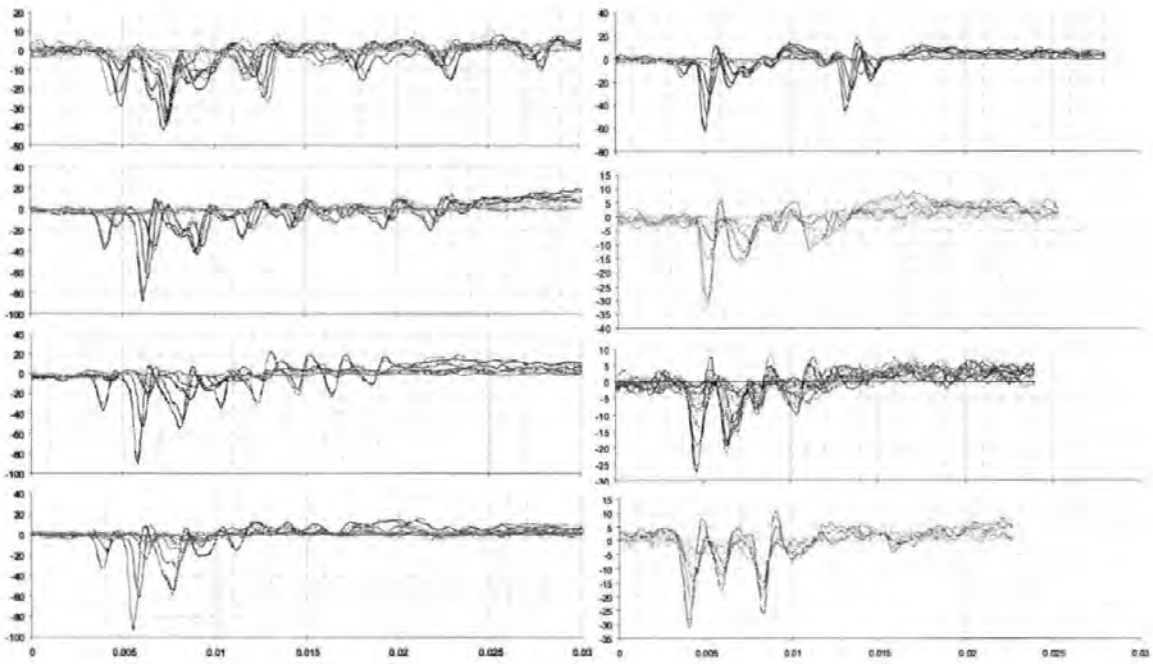

Figure 8. Auditory evoked potentials from *P. spathula* in response to a 100 Hz, 200 Hz, 250 Hz, 300 Hz, 500 Hz, 750 Hz, 1000 Hz, and 1500 Hz tone bursts. Y axis scale = microvolt * 100

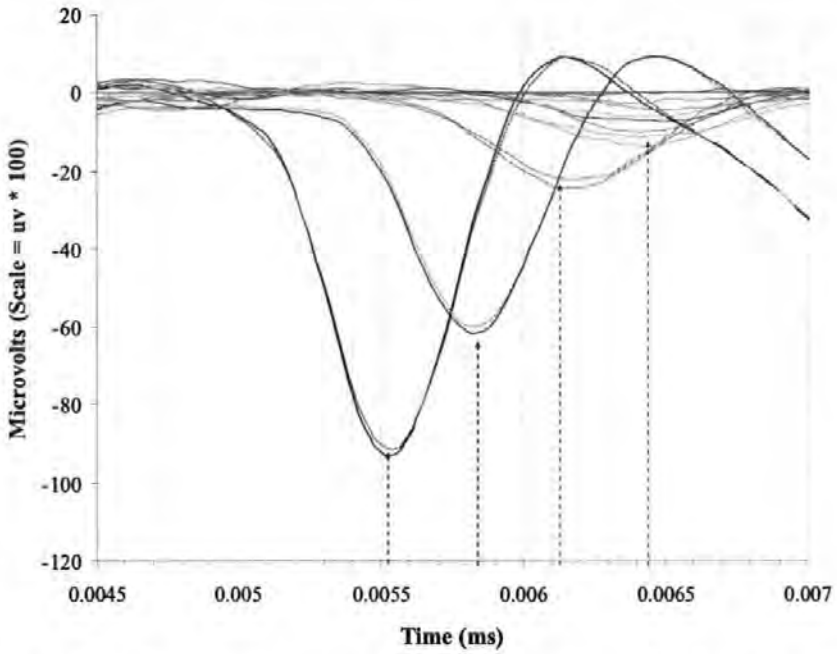

Figure 9. AEPs from *P. spathula* in response to the second sinusoid of a 300 Hz 4 cycle tone burst presented initially at 156 dB (re 1 µPa), and attenuated in steps of 5 dB. The arrows show the peak of the AEP, which occurs with an inter-peak latency (IPL) of approximately 0.3 ms for each of the amplitudes tested (averaged over 2000 iterations per waveform set)

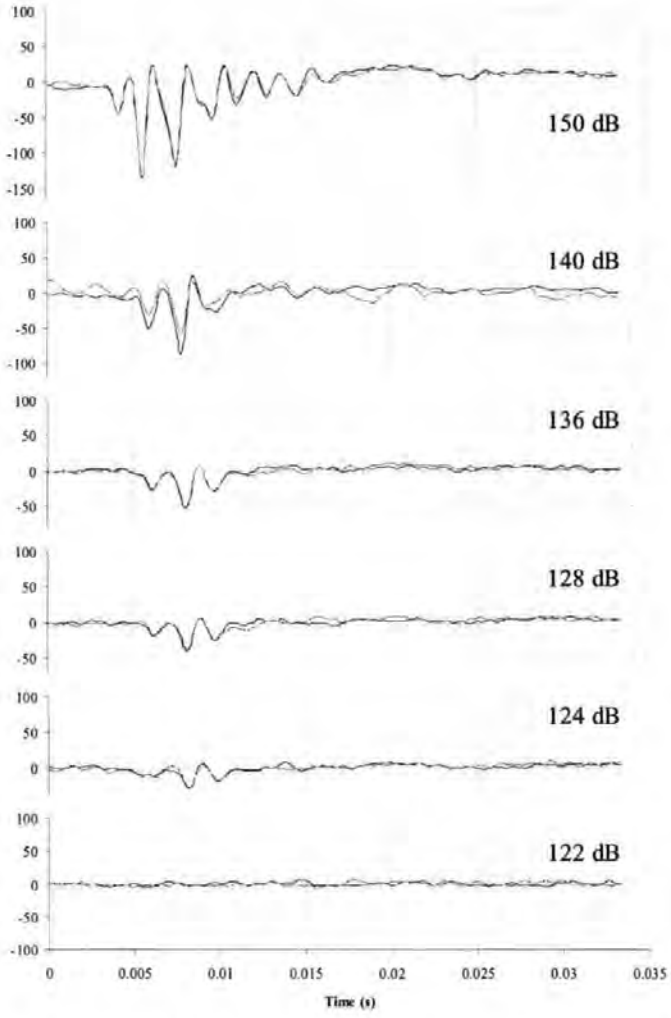

Figure 10. ABR waveforms from Paddlefish *P. spathula* in response to a 300 Hz tone burst attenuated in sequential steps. Averaged traces of two runs (2000 sweeps each), for each intensity are overlaid and arranged sequentially. Y axis scale = millivolts * 100

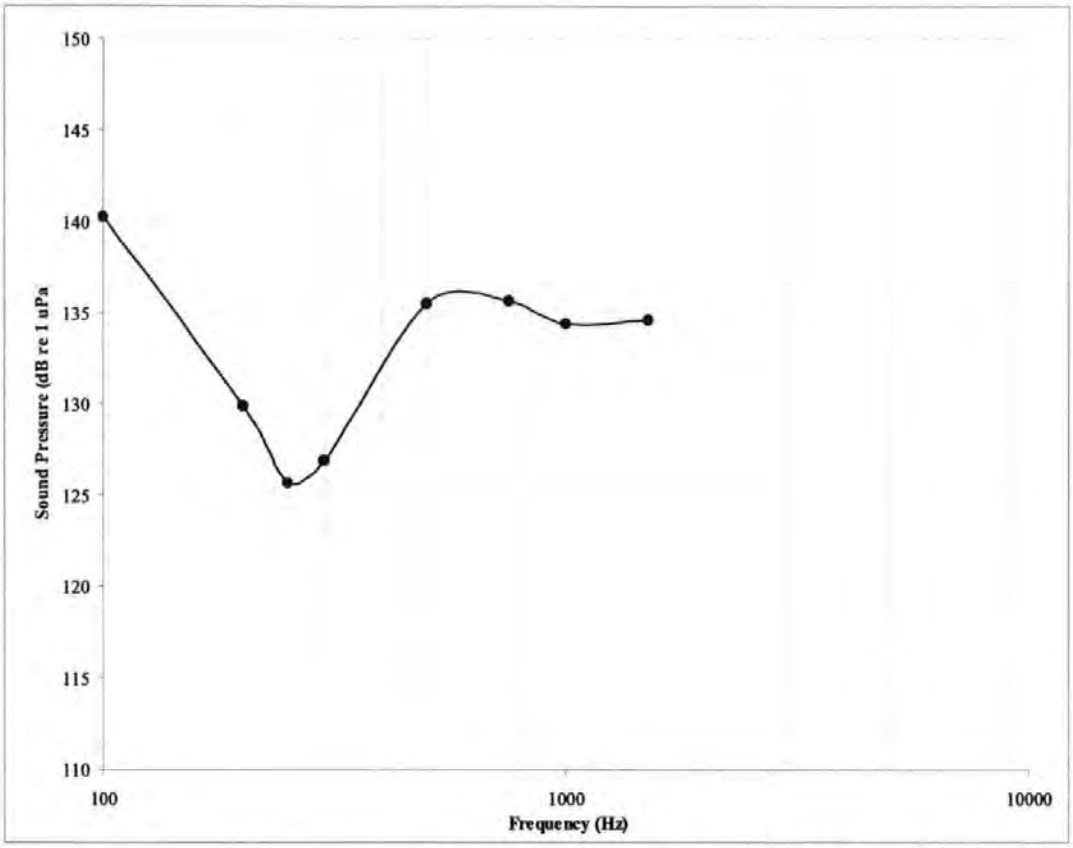

Figure 11. The audiogram (Averaged hearing thresholds) from 12 Paddlefish *P. spathula* in response to sound pressure.

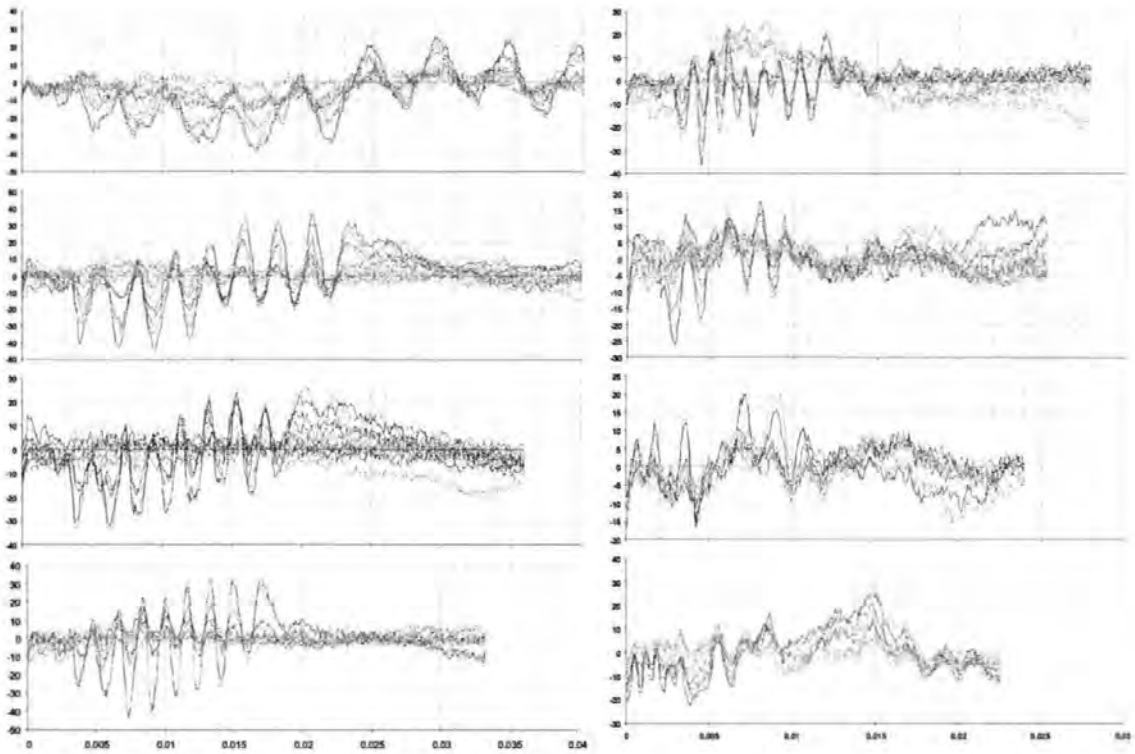

Figure 12. Auditory evoked potentials from sturgeon in response to a 100 Hz, 200 Hz, 250 Hz, 300 Hz, 500 Hz, 750 Hz, 1000 Hz, and 1500 Hz attenuated tone bursts. Y axis scale = millivolts * 100

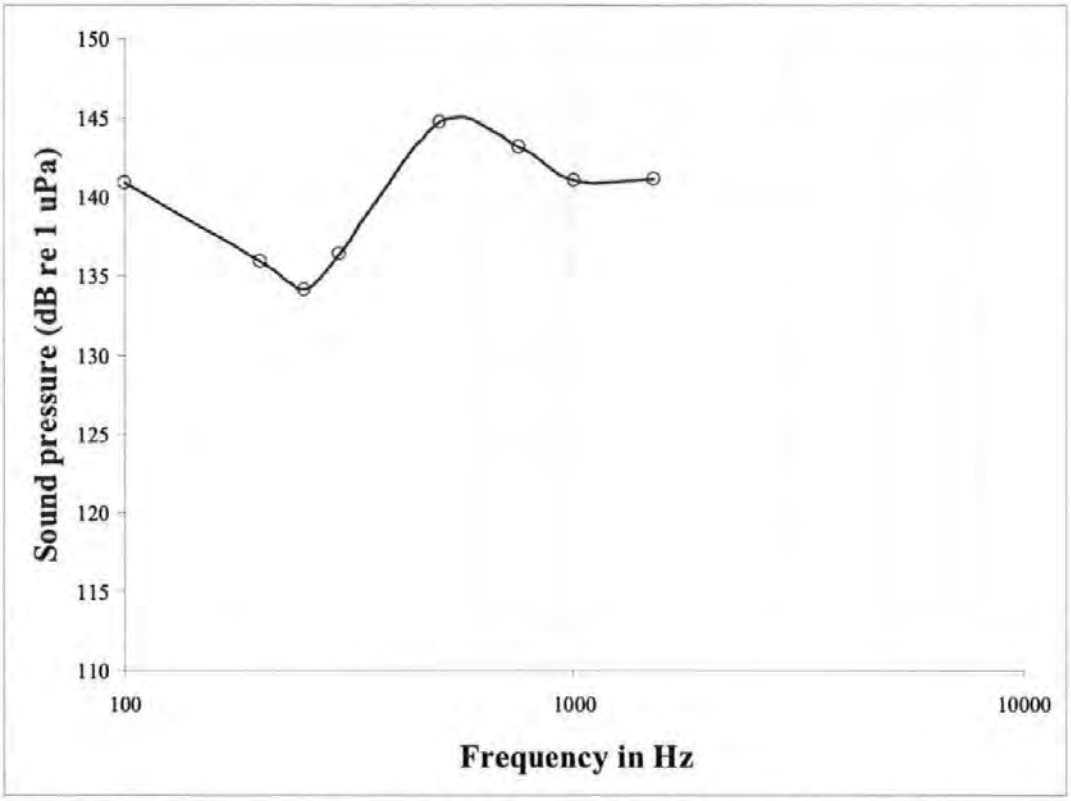

Figure 13. The audiogram (Averaged hearing thresholds) from Sturgeon *A. fulvescens* in response to sound pressure.

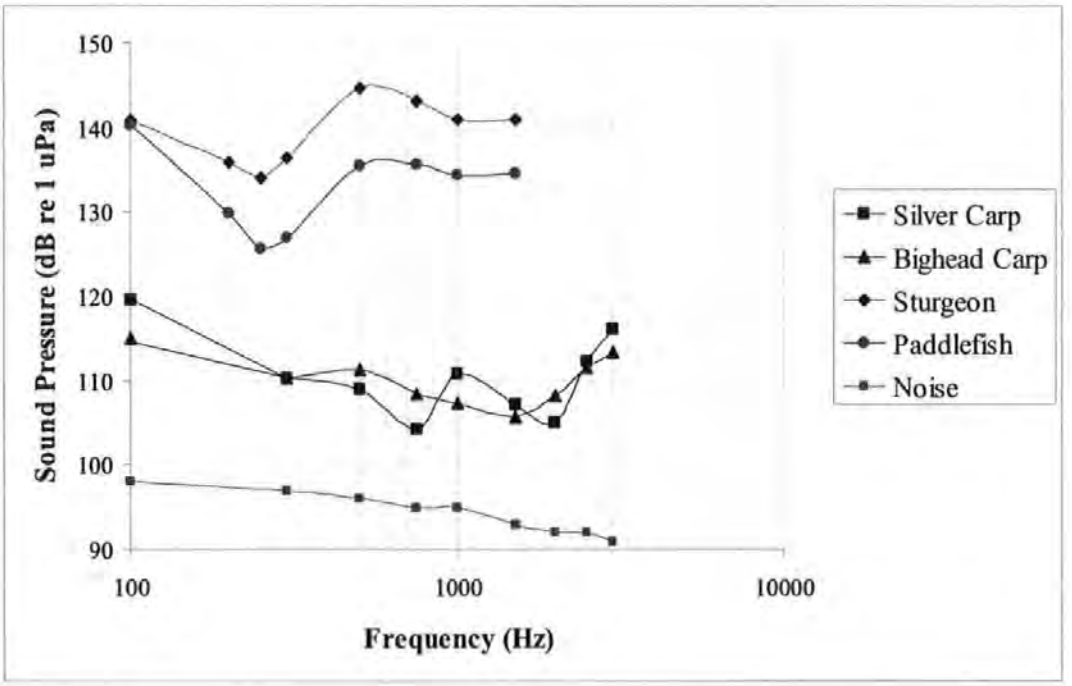

Figure 14. Summary of the audiograms of Sturgeon and Paddlefish in response to sound pressure, and comparison with Carp audiograms and background noise.

Calibration Chart for Hydrophone Type 8104 Serial No.:2225715

Brüel & Kjær

Calibration Chart for Hydrophone Type 8104

Serial No.: 2225715

Reference Sensitivity at 250 Hz* ± 2 % at 23 °C
Including integral cable 10 m

Voltage Sensitivity (Open Circuit Sensitivity)
-205.5 dB ± 0.25 dB re 1 V/µPa** or 427 µV/Pa

Charge Sensitivity: 401.10⁻³ pC/Pa

Capacitance (including integral cable): 8950 pF

Cable Capacitance: 150 pF/m

Leakage Resistance: > 2800 MΩ at 23 °C

Frequency Response (at ref. pos.):
Individual Free Field Frequency Response Curve attached

Measuring Uncertainty (re 10 kHz):
10 to 80 kHz ± 1.5 dB
80 to 100 kHz ± 1.8 dB
100 to 200 kHz + 1.5 dB, - 3.5 dB

Summarized Specifications (re 250 Hz)

Frequency Response (tolerance field excluding measurement uncertainty):
0.1 Hz to 10 kHz ± 1.5 dB
0.1 Hz to 80 kHz ± 4 dB
0.1 Hz. to 120 kHz + 4 dB, - 12 dB

Horizontal Directivity 100 kHz:
(XY–plane) ± 2 dB

Vertical Directivity 50 kHz:
(XZ–plane) ± 2 dB

Date 6.06.00 Signature

Physical (mm)

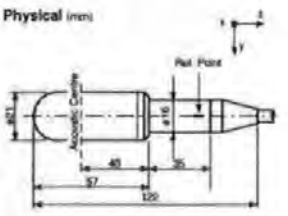

Cable: Shielded low noise with two conductors, waterblocked to MIL – C – 915

Weight (including 10 m cable): 1.6 kg

Environmental

Operating Temperature Range:
Short term –40° C to + 120° C
Continuous –40° C to +80° C

Change of Sensitivity with Temperature:
Charge 0 to 0.03 dB/° C
Voltage 0 to – 0.04 dB/° C

Change of Sensitivity with Static Pressure:
0 to – 3 x 10⁻⁷ dB/Pa
(0 to – 0.03 dB/atm)

Temperature Transient Sensitivity: ≤ 70 Pa/° C
(ANSI S 2.11–1969): measured with Brüel & Kjær Charge Preamplifier Type 2626, LLF 3 Hz

Allowable Total Radiation Dose: 5 x 10⁷ Rad

Maximum Operating Static Pressure:
4 x 10⁷ Pa (40 atm)

Note: All values are typical at 25° C (77° F), unless measurement uncertainty or tolerance limit is specified. All uncertainty values are specified at 2 σ (i.e. expanded uncertainty using a coverage factor of 2).

For further information see User Manual

* Sensitivity Traceable to:
DPLA: Danish Primary Laboratory of Acoustics
NIST: National Institute of Standards and Technology, USA

** 1 Pascal = 1 N/m² = 10 µbar

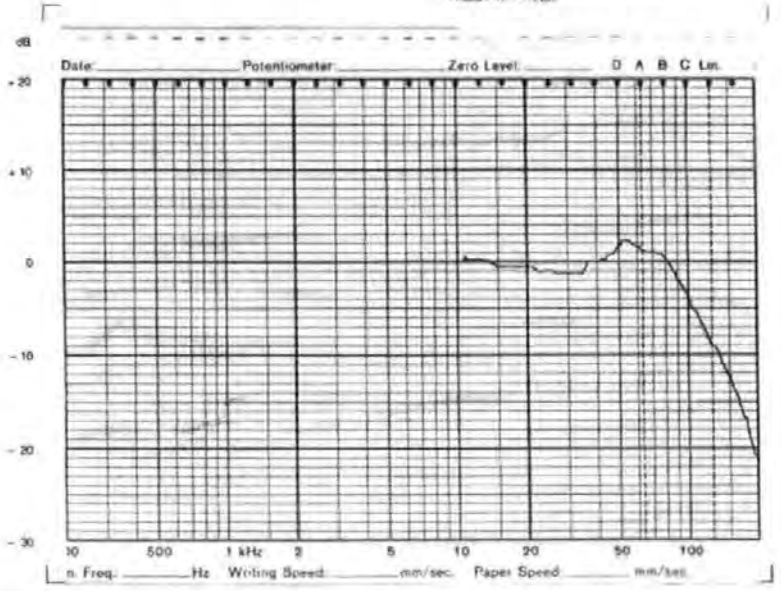

Submitted to:

Dr D Lambert
Fish Guidance Systems Ltd
Belmore Hill Court
Owslebury
Winchester
Hampshire SO21 1JW

Tel: +44 (0) 1962 777789
Fax: +44(0)1962 777 123
Email:info@fish-guide.com

Submitted by:

Dr Jeremy R Nedwell
Subacoustech Ltd
Chase Mill
Winchester Road
Bishop's Waltham
Hampshire SO32 1AH

Tel: +44 (0)1489 891849
Fax: +44 (0)8700 513060
email: subacoustech@subacoustech.com
website: www.subacoustech.com

Measurement of audiograms of Silver Carp (*Hypopthalmichthys molitrix*) and Bighead Carp (*Aristichthys nobilis*) for Chicago Canal acoustic barrier optimisation

J Nedwell, J M Lovell[1] and M. Pegg[2]

Report Reference: 611R0205

17 January 2006

1. **Plymouth Marine Laboratory**
2. **Illinois Natural History Survey**

Approved by .....

Contents

1. Background

The spread of the Asian carp species, silver carp (*Hypopthalmichthys molitrix*) and bighead carp (*Aristichthysc nobilis*) through the Illinois River and into the man-made Chicago Canal is causing increasing concern as these non-indigenous species get closer to Lake Michigan. There have been substantial resources committed to the prevention of this potentially serious environmental effect, with a number of parallel strategies having been developed. These include distribution monitoring, fish removal and creation of barriers to fish movement. A Smith-Root Graduated Field Electric Fish Barrier has already been installed in the Canal and a second electric barrier is under way. Electric barriers have proved highly effective at preventing passage of larger juveniles, as well as adult fish, but are less effective against small fish, owing to the lower potential difference they experience along the body compared with a larger fish in the same electric field. Thus, it is unlikely that a fully effective electric barrier could be used without using voltages that might be prejudicial to public safety.

The main alternative (supplementary) barrier method that has been identified as suitable for this application is through acoustic fish deterrent (AFD) systems. Trials conducted by the Illinois Natural History Survey (INHS, Havana, Illinois) have shown that 95% effectiveness can be achieved with bighead carp using a Fish Guidance Systems BioAcoustic Fish Fence (BAFF) system (Taylor, Pegg and Chick, in press) and further trials are underway with silver carp. During the experimental work associated with the efficiency testing, the signal was changed to include higher frequency components; a substantial increase in efficiency occurred. It was therefore suggested that, in order to achieve very highest possible levels of fish deflection for the non-indigenous carp species, further information concerning the structure and function of the hearing system of each species was required.

This study provides audiograms for the Silver Carp (*Hypopthalmichthys molitrix*) and Bighead Carp (*Aristichthys nobilis*) which have been measured using the Acoustic Evoked Potential (AEP) audiometry method. One particular variety of the AEP method is to measure the auditory response at the brainstem; this approach is termed the Auditory Brainstem Response (ABR) method, and is the method that was chosen for the work presented herein.

2. Fish hearing

The fish inner ear is divided into two regions, the pars superior and the pars inferior (Retzius, 1881). The former responds primarily to movements of the body and postural changes, while the latter responds to both gravistatic and acoustic stimuli (Jenkins, 1981; Popper & Platt, 1993). The pars inferior comprises two fluid filled pouches, the saccule and lagena, with each pouch containing a crystalline calcium carbonate otolith (Carlström, 1963). The saccule is considered to be the major auditory organ in most bony fish species, though there is evidence of a functional overlap between all three end organs (Popper & Fay 1993).

For fish to locate the source of a sound in both the horizontal and vertical planes, they rely on the stimulation of ciliary bundles oriented specifically along the sound propagation axis (Lu & Popper, 1998). It is known (Enger et al., 1973; Hawkins & Sand, 1977; Fay, 1997) that the morphological polarities of sensory hair cells in the otolithic organs are fundamental to the directional hearing capabilities of fish. In general, azimuths of peak sensitivity tend to lie parallel to the plane of the otolith and sensory epithelium (Enger, et al. 1973; Sand & Hawkins, 1973; Fay, 1997). Examination of the orientation of the ciliary bundles provides evidence of a correlation between the morphological polarisation of receptor cells and the magnitude of an electrophysiological response to a sound (Popper & Fay, 1993). Excitation occurs when stereocilia are bent toward the kinocilium during the passage of a wave front, resulting in the cell becoming depolarised relative to its resting potential (Clegg & Mackean, 1994). Inhibition occurs when the bundle is deflected in the opposite direction, and results in the hyperpolarisation of the cell (Platt & Popper, 1981). The magnitude of both excitation and inhibition are a cosine function of the angle between the direction of the stimulus and the direction at which sensitivity is greatest (Enger, 1965; Popper, 1983).

The detection and localisation of a sound source is of considerable biological importance to many fish species, and is often used to assess the suitability of a potential mate or during territorial displays (Nordeide & Kjellsby, 1999), and during predator prey interactions (Myrberg,1981).

3. Audiograms

The techniques used to obtain fish audiograms require a varying degree of time, surgical and technical expertise, and many authors favour the use of operant reward based paradigms (behavioural methods) to gain statistically sound data (see, for instance, Yan 1995). There are two fundamental methods by which audiograms can be estimated.

3.1.1. The behavioural method. In this method, a species is trained to react in a specified and measurable way (e.g. a reward based method by seeking food) when a tone at a given frequency is played. The tone is gradually played at decreasing levels until no reaction occurs; this level is therefore taken as the threshold of hearing at that frequency for the species in question. In practice, the behavioural method is very time consuming and only effective with species that are easy to train, and therefore is not considered suitable for the measurements described herein.

3.1.2. The auditory evoked potential (AEP) method. Audiograms produced using the Auditory Brainstem Response (ABR) technique, are regarded as being the least time consuming and most reliable methodology for acquiring audiological data from fish and other animals. They are used for both mammalian and non-mammalian vertebrates (Corwin, Bullock and Schweitzer 1982), and marine invertebrates (Lovell et al., in Press);

Additionally, ABR recordings require no invasive procedural work as measurements are taken in the electro-physiological far field using cutaneous electrodes, resulting in significant stress reduction during the hearing assessment (Kenyon et al 1998).

This approach relies on the fact that the electrical potential of the nervous impulse passing along the auditory nerve can be detected by electrodes placed in its vicinity. In practice, a pair of electrodes are applied to the species in a position spanning the auditory nerve. A sinusoidal tone at a given frequency is played to the species. An ABR trace is formed by averaging conglomerate responses of peak potentials arising from centres in the auditory pathways extending from the periphery of the VIII nerve, to the midbrain (Corwin et al 1982; Overbeck and Church 1992). The threshold of hearing is estimated by finding the level of sound at which the auditory response just appears above noise.

The ABR measurements of hearing threshold were made using "BrainWave", a control and analysis program, written for the purpose by Subacoustech in a LabView 7 environment. This program both generates the stimulus signals and captures and analyses the response. The stimulus used was a sine train (sine wave pulse) which was presented to the fish at a given frequency and sound pressure level. The ABR response is readily dominated by responses caused by muscle movement and hence while undertaking the ABR measurements the fish are kept in dark and constrained conditions since many species react to this by becoming passive. It is known that many fish species react to danger by hiding in weeds, and it is thought that this experimental environment mimics the natural environment, enabling the fish to feel protected, reducing avoidance behaviour. However, in addition to this BrainWave can detect ABR responses that are

contaminated by muscle movement. The program ignores contaminated measurements when producing the averaged ABR response. The use of chilling as a muscle movement control measure has also been investigated. As cold-blooded animals, fish show a reduction in activity as their body temperature decreases, and this might in principle be used as a suitable control measure. However, chilling may have the effect of diminishing the auditory evoked potential from a fish (see for instance Corwin *et al*(1982); Stockard *et al* (1978)) and hence this approach has not been used.

A further refinement of the experimental measurements has been the use of submerged projectors (underwater sound transducers) to generate the insonification. Previous measurements, such as those by Yan, have used a domestic hifi loudspeaker above the experimental watertank to create the insonifying sound. The system has been calibrated by measuring the sound above the tank, and assuming that the sound pressure in the water is equal to the sound pressure in the air. This is unsatisfactory for two reasons. First, the walls of the tank may displace outwards under the influence of the waterborne sound, causing a "pressure release" effect and reduction in the waterborne pressure. Second, this method of insonification may set up complex pressure and particle velocity fields in the watertank, with the result that the condition of exposure is very difficult to specify.

In the experiment described herein, two identical projectors have been set up facing each other with the fish on the axis of symmetry between the two. Where the projectors are driven in phase, it is possible to create a region between them of high and even sound pressure, associated with a low level of particle velocity. The measurements have been calibrated by directly measuring the sound at the position of the fish's inner ear by means of a hydrophone; they are consequently traceable to International Standards.

3.1 Method of recording audiograms

A block diagram of the equipment to provide audiometric measurements is shown in figure 1. The procedure used to acquire the acoustically evoked potentials was approved by the University of Illinois, United States (Institutional Animal Care and Use Protocol #04271). The sound signal was generated by a laptop computer running BrainWave, and amplified using a Tandy 250W power amplifier. The sound field in the experimental watertank was generated by means of two Fish Guidance Systems Ltd. Mk II 15-100 Sound Projectors. These faced each other at a distance of 200 mm; the inner ear of the fish during measurements was arranged on the axis connecting the centres of the two projectors.

During the measurements made on the two carp species the projectors were driven with load resistors placed between the amplifier and projector. The reason for this was that due to the sensitive hearing of carp only relatively low levels of sound were required to cause an acoustic brainstem response. The full output of the amplifier was only required when measuring the hearing of less sensitive fish such as the Paddlefish and Sturgeon.

The stimulus tones presented from the loudspeaker to the fish were calibrated using an insertion calibration. In this method, the sound level is recorded in the absence of the

fish, at the point where the inner ear of the fish would be. The measurements were made using a Bruel and Kjaer Type 8104 Hydrophone (serial number 2225715) calibrated and traceable to International Standards; the certificate of calibration is attached as appendix 1. The signal from the hydrophone was amplified by a Bruel and Kjaer Type 2365 Charge Amplifier (Serial Number 1079556). In case there was any non-linearity of the signal, calibrations were made at every frequency and every level used for a measurement, totaling some 660 individual calibrations. These calibrated levels were then applied to the threshold defined by the ABR measurement to provide calibrated audiograms with pressure levels traceable to International Standards. In fact, no evidence of non-linearity was detected, other than at the very highest levels of sound, which was not required in any case for measuring audiograms.

The test subjects were placed into a flexible cradle formed from a soft nylon mesh rectangle saturated with freshwater for the small fish, and a rubber coated 1 mm gauge wire mesh for fish over 2 kg weight. This assembly is illustrated in figure 2. Oxygenated water kept at a temperature of 18° C was gravity fed at an adjustable flow rate of between 5 millilitres per second for the small fish, to 25 millilitres per second for the large, and directed toward the gills through a soft rubber mouth tube. The small fish were first placed lengthwise and centrally on a 160 mm x 120 mm rectangle of fine nylon netting, which was wrapped firmly around the body and tail, and the two sides of the net were held together using the clip, which may be seen in the photograph of figure 3.

The clip was placed in a retort stand clamp fitted with ball joint electrode manipulator arms, and the aerated water pipe. During the procedure to position the electrodes the specimen and clamp were suspended over the test tank, and aerated water was supplied to the fish.

The electrophysiological response to acoustic stimulation was recorded using the two sub-cutaneous electrodes of figure 4, which were connected to the MS6 preamplifier by 1m lengths of screened coaxial cable with an external diameter of 1.5 mm. The outer insulating layer of the coax was removed 15 mm from the end where the electrode tip was to be fixed, and the screening layer removed 10 mm from the cable end. The inner insulating material was then trimmed by 2 mm, and the exposed inner wire (0.5 mm diameter) was tinned with silver solder and joined to a 10 mm length of silver wire (0.25 mm diameter), tapered to a fine point. The assemblage was pushed through a 100 mm glass pipette with an internal diameter of 4 mm, until 0.4 mm of the silver wire was exposed. The remaining space inside the pipette was filled with a clear epoxy resin, and then trimmed to expose 0.3 mm of silver tip through which the AEP could be conducted. The impedance of the electrodes, both between the outer shielding and inner core, and the silver tip and MS 6, were tested using an M 205 precision digital multimeter. The impedance between the tip and pre-amplifier was found to be 0.2 Ω for both electrodes, and an open circuit was recorded between the outer shielding and inner core.

Stimulus sound was presented to the fish at sound pressures initially not exceeding 145 dB re 1 µPa. The electrophysiological response of the fish to acoustic stimulation was

recorded using two cutaneous electrodes, which were positioned on the cranium of the fish adjacent to and spanning the VIII nerve. The reference electrode was positioned centrally on the head above the medulla, and the record electrode was located 5 mm anterior of this point. The evoked response was amplified and digitised to 12 bits resolution and recorded. This process was repeated 2000 times and the response averaged to remove electrical interference caused by neural activities other than audition, and the myogenic noise generated by muscular activity. Each measurement was .repeated twice; this aids in separating the evoked response, which is the same from trace to trace, from the myogenic noise, which varies in two successive measurements. After the averaging process, the evoked potential could be detected, following the stimulus by a short latency period of about one millisecond.

3.2 The audiogram of the Silver Carp (*Hypopthalmichthys molitrix*)

Figure 5 illustrates a typical set of acoustic brainstem responses to sound pressure for the Silver Carp at an insonification frequency of 500 Hz. The figure presents traces acquired as the sound pressure level was successively reduced; it may be seen that the responses vary from strong response to the sound to no discernible response. The highest pressure of sound at which no response occurred was taken to be the auditory threshold.

Figure 6 presents the audiogram found by inspection of the ABR traces of the Silver Carp. The audiogram indicates the sound pressure level in dB re 1 µPa at the threshold of hearing.

It may be seen that the hearing is most sensitive (has the lowest threshold of hearing) at frequencies between about 500 Hz and 3 kHz, where the maximum hearing sensitivity is of the order of 105 dB re 1 µPa.. At the higher frequencies, the hearing reduces sharply in sensitivity; the sensitivity also reduces more gradually for lower frequencies.

3.3 The audiogram of the Bighead Carp (*Aristichthys nobilis*)

Figure 7 illustrates a typical set of acoustic brainstem responses to sound pressure for the Bighead Carp at an insonification frequency of 500 Hz. The form of the traces is similar to that of the Silver Carp, however the threshold of hearing was found to be at generally slightly lower levels of sound.

Figure 8 presents the audiogram found by inspection of the ABR traces of the Bighead Carp, again as the sound pressure level in dB re 1 µPa at the threshold of hearing.

The hearing peaks in sensitivity at a frequency of about 1500 Hz, where it has its lowest threshold of hearing at a sound pressure level of about 106 dB re 1 µPa. The region of peak sensitivity is, however, apparently rather narrower than for the Silver Carp. As for the Silver Carp, the hearing reduces sharply in sensitivity at the higher frequencies and more gradually for the lower frequencies.

4. Discussion.

Figure 9 illustrates the audiograms of both the Silver Carp and the Bighead Carp for comparison. Also indicated on the figure is the measured maximum level of background noise during the measurements.

It may be noted that the background noise levels were recorded on the identical apparatus used to measure the audiograms, and were found by reducing the signal from the system until no further reduction in level occurred. Hence the noise calibration process includes not only extraneous background noise, but also noise from the equipment used to generate the signal (such as noise from the power amplifier) and noise from the measuring equipment such as the hydrophone, charge amplifier and digitization equipment. It may be noted that the background noise level is of lower level than the recorded thresholds of hearing, and hence it may be concluded that the audiograms are uncontaminated by background noise.

It may be noted that the hearing of the Bighead Carp is generally similar to that of the Silver Carp. The shape of the audiograms of both species are similar, and the maximum sensitivity, and the frequency at which it occurs, is also similar. While it is tempting to conclude that "closely related species will have similar hearing ability", this has been shown by Nedwell *et al* (2003) to be untrue for the related species Atlantic Salmon *Salmo salar* and Brown Trout *Salmo trutta*, and hence this generalisation is unsafe.

The results throw an interesting light on the previous measurements of the efficiency of Fish Guidance SPA/BAFF system mentioned in the introduction and reported by Taylor *et al*. It was found in initial measurements that the efficiency of the system using frequencies ranging between 20 Hz and 500 Hz was poor, achieving only 50% effectiveness or so. Such systems comprise a set of underwater sound projectors and associated amplifiers; these are driven by a signal that has been developed to be unpleasant to the fish species that are the target of the system. At the time of the initial measurements an existing acoustic signal that had been developed for causing efficient deflection of fish at estuarine power stations was used. However, this signal had been developed for deflecting different target species, mainly species such as herring, whiting and sprat. These are non-specialist species (*i.e.* those which do not use sound to explore their environment) which typically have hearing ranges up to a few hundred Hz only. The signal was therefore tailored to this hearing range, which explains why despite a typical estuarine system being found by Maas *et al* to achieve efficiencies of 95% or so against these species, it was found to be ineffective against carp.

Subsequently, an alternative signal was used to drive the system, which had an extended frequency range with frequency components up to 2 kHz. A much higher efficiency was reported for the system using this second signal, of some 95%. Clearly, the reason for this increased efficiency is the fact that, as seen from figure 9, the two carp species have relatively high-frequency hearing and hence the second signal would have fallen in their peak hearing range. The extended hearing range of the audiograms also indicates that

further improvements in efficiency might be made by extending the frequency range of the deterrent signal still further.

The results indicate the importance of matching the sound generated by an acoustic fish deflection system to the hearing range of the target species if high efficiency is to be achieved. While the requirement for such preliminary work is a disadvantage of acoustic fish deflection systems when compared with unselective electric fences, it offers a prospective advantage that it may be possible to tailor the sound generated by such systems to selectively deter nonindigenous species while allowing indigenous species to pass.

5. Summary

1) Measurements of the audiograms of the Silver Carp (*Hypopthalmichthys molitrix*) and Bighead Carp (*Aristichthys nobilis*) have been made. The audiograms are presented as the lowest detectable levels of sound in dB re 1 µPa as a function of frequency.
2) The hearing of both species is similar. Silver Carp have hearing which is most sensitive between about 500 Hz and 3 kHz, where the maximum hearing sensitivity is of the order of 105 dB re 1 µPa.. Bighead Carp hearing peaks in sensitivity at a frequency of about 1500 Hz, where is has its lowest threshold of hearing at a sound pressure level of about 106 dB re 1 µPa. The region of peak sensitivity is, however, apparently rather narrower for the Bighead Carp than for the Silver Carp. For both species of carp, the hearing reduces sharply in sensitivity at the higher frequencies and more gradually for the lower frequencies.
3) The results explain the reason for the inefficiency of the first acoustic fish deflection barrier (about 50%), and the efficiency of the second (about 95%), which lies in the greater proportion of higher frequencies generated by the second barrier which were better matched to the hearing of the carp.
4) The results indicate the importance of matching the sound generated by an acoustic fish deflection system to the hearing range of the target species if high efficiency is to be achieved.
5) While the requirement for such preliminary work is a disadvantage of acoustic fish deflection systems when compared with unselective electric fences, it offers a prospective advantage that it may be possible to tailor the sound generated by such systems to selectively deter nonindigenous species while allowing indigenous species to pass.

6. References

Carlström DA (1963) "Cystallographic study of vertebrate otoliths". Biol. Bull. 125, 441-463.

Clegg CJ and Mackean DG (1994) "Advanced Biology: principles and applications". John Murray, London, 448-461pp.

Corwin JT, Bullock TH, Schweitzer J. 1982. "The auditory brain stem response in five vertebrate classes". Electroencephalogr. Clin. Neurophysiol. 54: 629-641

Enger PS (1965). "Acoustic thresholds in goldfish and its relation to the sound source distance". Comp Biochem Physiol 18: 859-868

Enger PS, Hawkins AD, Sand O and Chapman CJ (1973). "Directional sensitivity of saccular microphonic potentials in the haddock". J. Exp. Biol., 59:425-433.

Fay RR (1997). "Directional response properties of saccular afferents of the toadfish, (Opsanus tau)". Ed. Walton PL. Hearing Research 111 (1-2): 1-21

Hawkins AD and Sand O (1977). "Directional hearing in the median vertical plane by the cod". Journal of Comparative Physiology. A. Vol. 122: page 1 - 8

Jenkins DB (1981). "The utricle in *Ictalurus punctatus*". *Hearing and Sound Communication in Fishes.* Tavolga, WN, Popper AN and Fay RR, Eds. Springer-Verlag, New York.

Kenyon, T.N., Ladich, F., Yan, H.Y. (1998) "A comparative study of the hearing ability in fishes: the auditory brainstem response approach". *J Comp Physiol* A 182:307–318.

Lovell JM, Findlay MM, Moate RM and Yan HY (in press). "The hearing abilities of the prawn (*Palaemon serratus*)". Journal of Comparative Physiology and Biochemistry A.

Lu Z and Popper AN (1998). "Morphological polarizations of sensory hair cells in the three otolithic organs of a teleost fish: fluorescent imaging of ciliary bundles". Hear. Res. 126 (1-2): 47-57.

Myrberg AA (1981) "Sound communication and interception in fishes". *Hearing and Sound Communication in Fishes.* Tavolga WN, Popper AN, and Fay RR, Eds. Springer-Verlag, New York.

Nedwell J R, Turnpenny AW H, Lovell J, Langworthy J, Howell D & Edwards B "The effects of underwater noise from coastal piling on salmon (*Salmo salar*) and brown trout (*Salmo trutta*)". Subacoustech Report Reference: 576R0113, 17/12/2003.

Nordeide JT and Kjellsby E (1999). "Sound from spawning cod at there spawning grounds". ICES Journal of Marine Science. 56: pp 326 – 332.

Overbeck GW, Church MW (1992) "Effects of tone burst frequency and intensity on the auditory brainstem response (ABR) from albino and pigmented rats". Hear Res 59: pp129-137

Popper AN and Platt C (1993). "Inner ear and lateral line". *The Physiology of Fishes*. Evans, D. H., Ed., CRC Press, Boca Raton.

Popper AN and Fay RR (1993) "Sound detection and processing by fish: critical review and major research questions". Brain Behav Evol, 41, 14-38

Popper AN (1983). "Organization of the ear and auditory processing". Fish Neurobiology 1st edition. Eds. Northcutt, R. G. and Davis, R. E., University of Michigan Press, Ann Arbor,

Retzius G (1881). "Das Gehörorgan der Wirbelthiere". Vol. 1, Das Gehörogan der Fische und Amphibien, Samson and Wallin, Stockholm.

Sand O and Hawkins AD (1973). "Acoustic properties of the cod swimbladder". J. Exp. Biol., 58:797-820.

Taylor, R.M., Pegg M.A. and Chick J.. "Effectiveness of two bioacoustic behavioral fish guidance systems for preventing the spread of bighead carp to the Great Lakes". North American Journal of Fisheries Management (in press).

Figures.

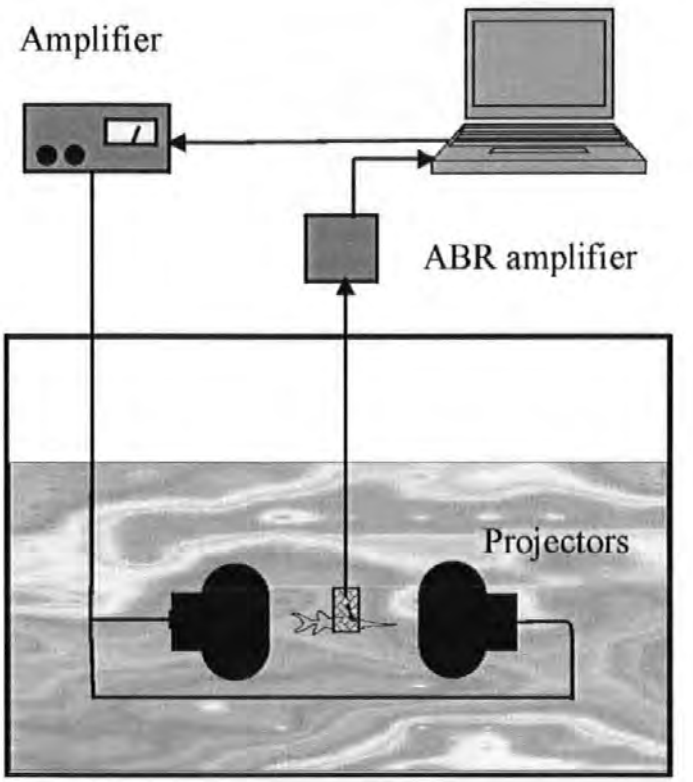

Figure 1. A block diagram of the experimental apparatus.

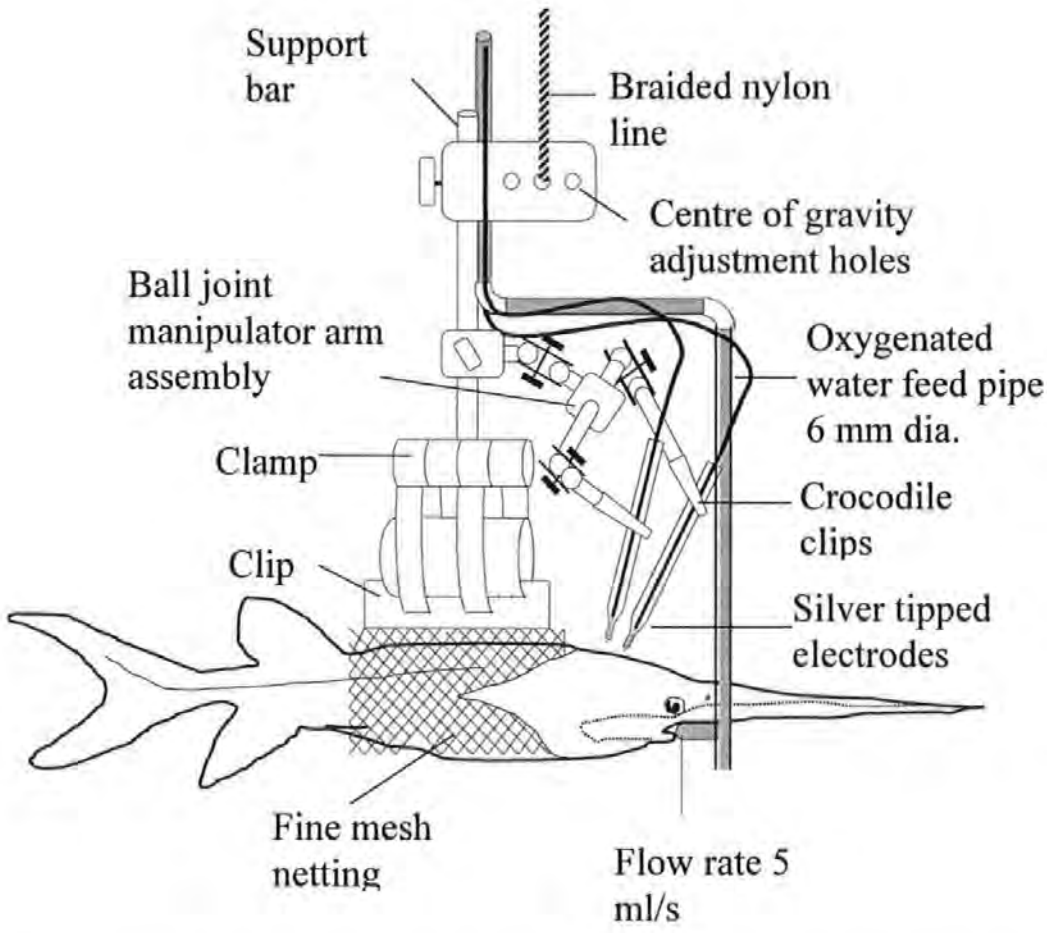

Figure 2. Schematic of the clamp used to hold the fish in position, and manipulate the electrodes during the audiological tests

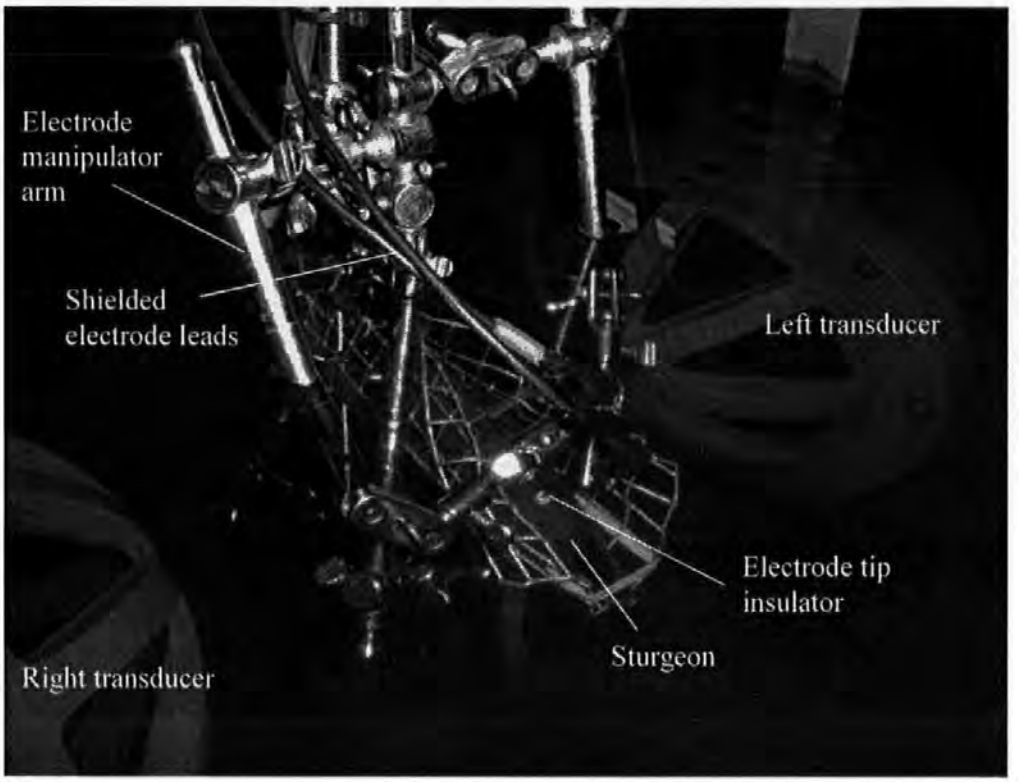

Figure 3. The transducers and fish restraining device, which is used to position the fish and hold electrodes during the audiological examination (the subject illustrated is a sturgeon).

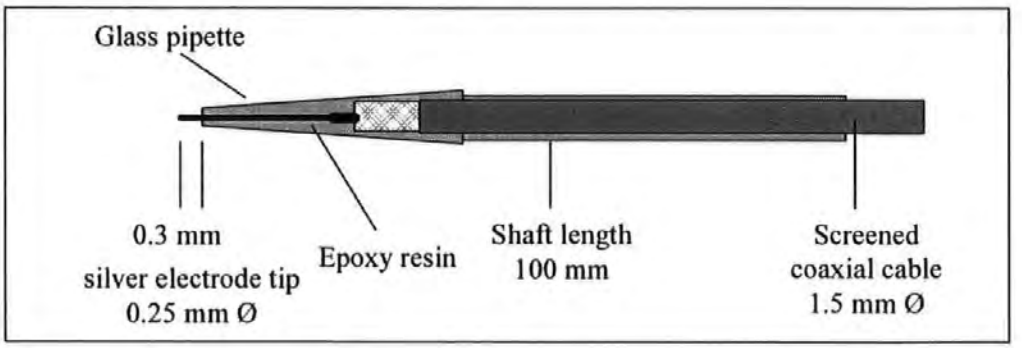

Figure 4. A schematic of the electrodes used to record the evoked potentials

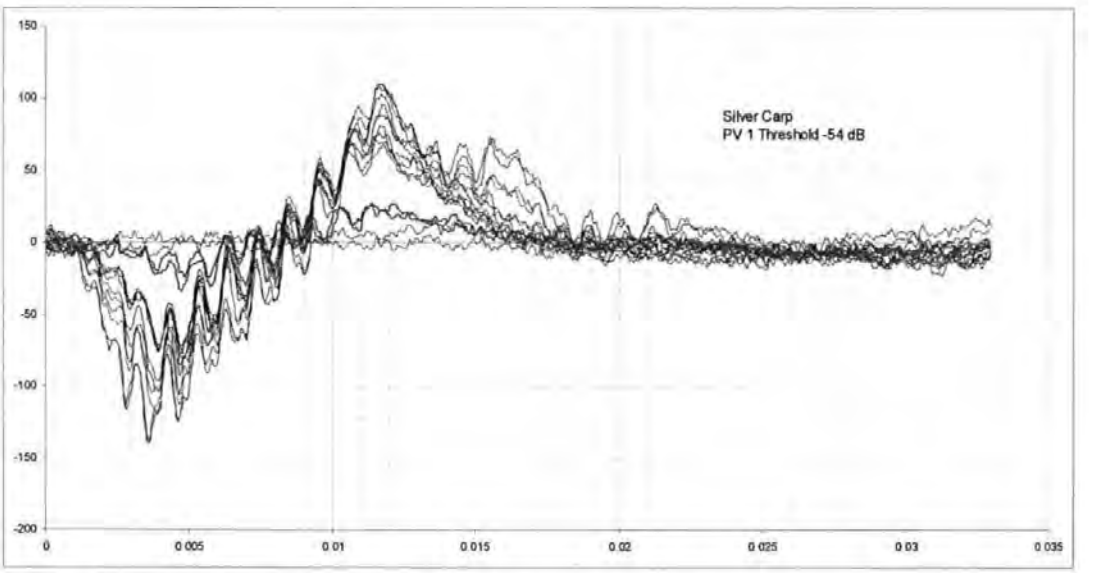

Figure 5. A typical set of acoustic brainstem responses to sound pressure for the Silver Carp at an insonification frequency of 500 Hz.

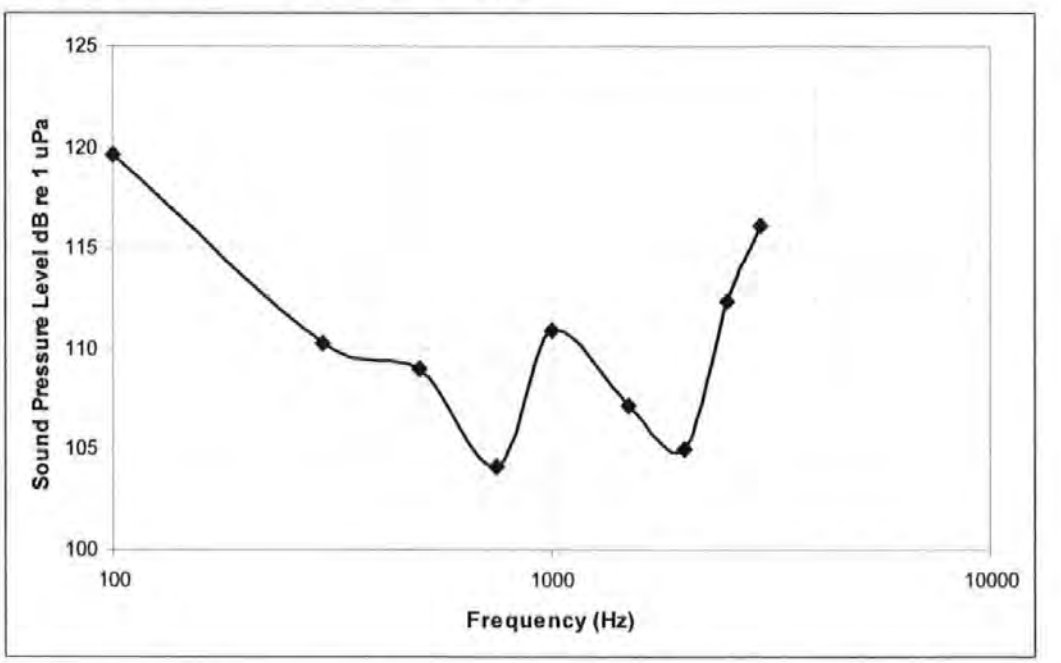

Figure 6. The audiogram (sound pressure level at threshold of hearing in dB re 1 µPa) of the Silver Carp.

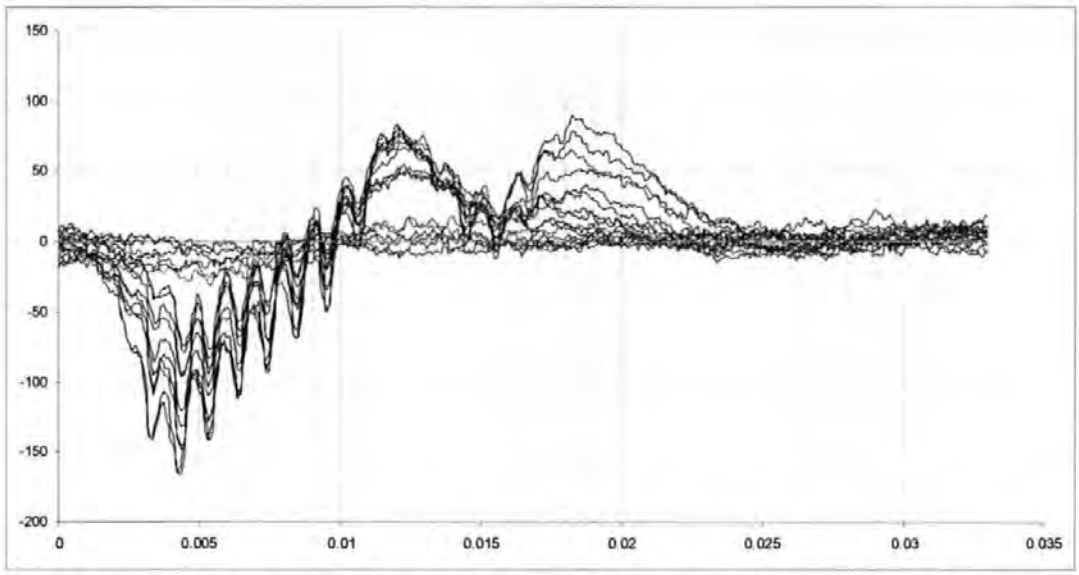

Figures 7. A typical set of acoustic brainstem responses to sound pressure for the Bighead Carp at an insonification frequency of 500 Hz

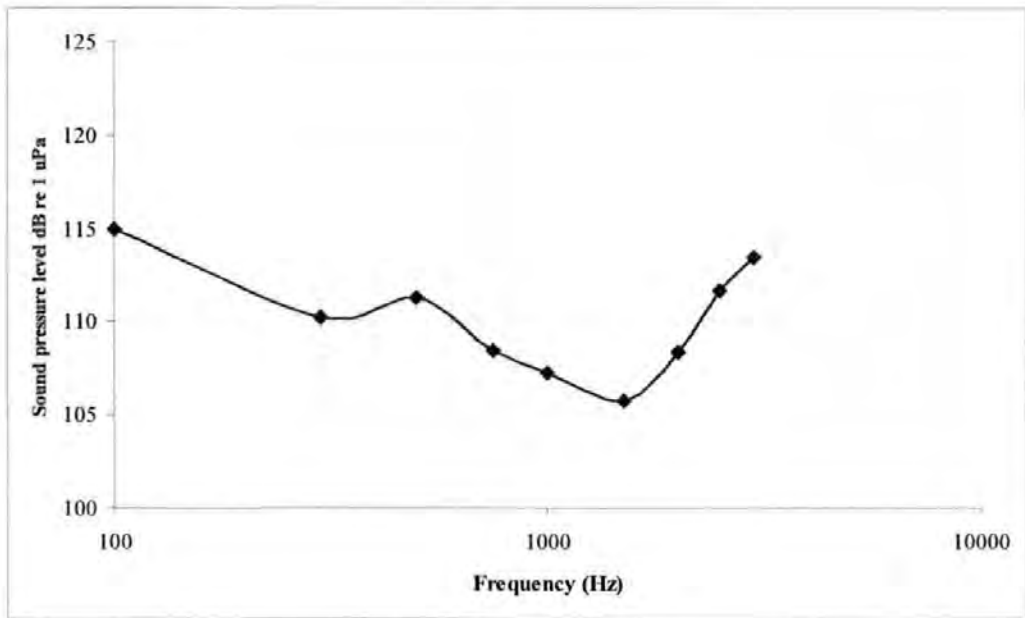

Figure 8. The audiogram (sound pressure level at threshold of hearing in dB re 1 μPa) of the Bighead Carp.

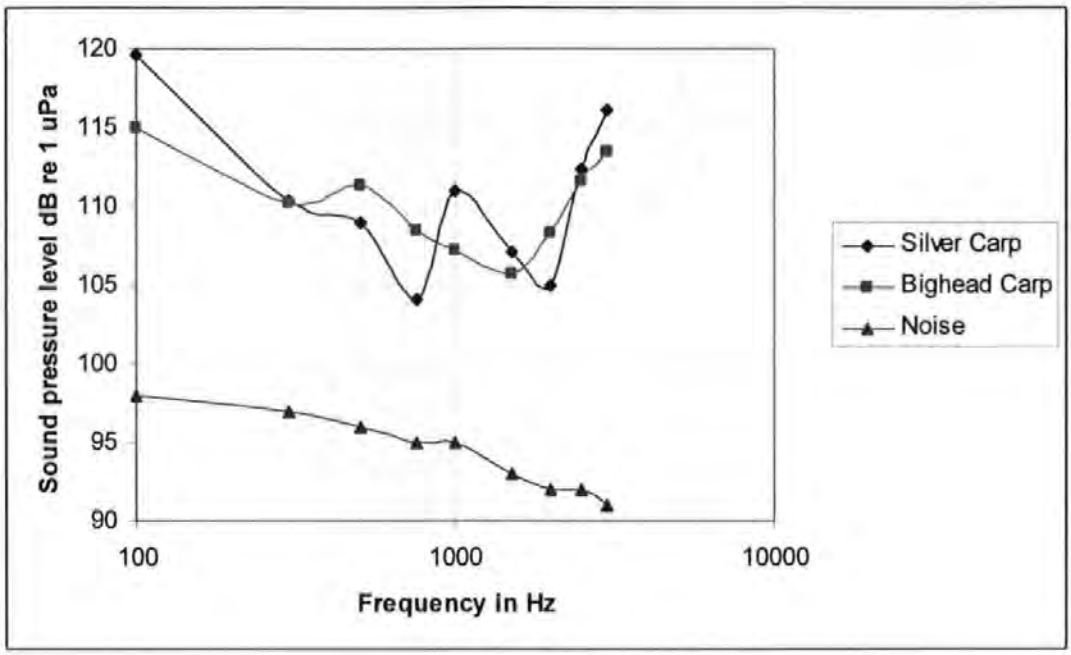

Figure 9. Comparison of the audiograms of both the Silver Carp and the Bighead Carp, and the level of background noise during measurement.